Studien zur anodischen Kupplung von Anilinderivaten und verwandten Substraten

Dissertation zur Erlangung des akademischen Grades

„Doktor der Naturwissenschaften“

im Promotionsfach Chemie

am Fachbereich Chemie, Pharmazie, Geographie und Geowissenschaften

der Johannes Gutenberg-Universität in Mainz

vorgelegt von

LARA SCHULZ

Geboren in Frankenthal (Pfalz)

Mainz, September 2019

Dekan:

Erster Gutachter:

Zweiter Gutachter:

Datum der mündlichen Prüfung:

Die vorliegende Arbeit wurde in der Zeit von Mai 2016 bis September 2019 am Institut für Organische Chemie der Johannes Gutenberg-Universität Mainz unter Anleitung von Prof. Dr. Siegfried R. Waldvogel angefertigt.

Hiermit versichere ich, dass die vorliegende Arbeit eigenständig und mit keinen anderen als den angegebenen Hilfsmitteln (Literatur, Apparaturen, Materialien) angefertigt wurde. Alle wörtlichen oder dem Inhalt nach ähnlichen Stellen aus fremden Arbeiten und Publikationen sowie adaptierte Abbildungen und Schemata wurden als solche eindeutig gekennzeichnet.

_____

M. Sc. Lara Schulz

Meiner Familie

Es ist schwieriger, eine vorgefasste Meinung zu zertrümmern, als ein Atom.

Albert Einstein (1879–1955)

Inhaltsverzeichnis

1 Einleitung und Überblick

In Zeiten des fortschreitenden Klimawandels und knapper werdenden Ressourcen, vor allem zur Energiegewinnung, wird es immer wichtiger, dass Wissenschaftler, Industrie und Politik vereint nach Alternativen für bestehende, oft umweltschädigende und veraltete Prozesse streben, die einen nachhaltigeren Umgang der vorhandenen Ressourcen erlauben und gleichzeitig umweltschonender sind. Die Dekarbonisierung des Energiesystems spielt hierbei eine zentrale Rolle. Doch erneuerbare Energiegewinnung durch Windkraft- oder Solaranlagen erzeugt oft starke Stromüberschüsse, die gespeichert werden müssen, um sie später an wind- oder sonnenärmeren Tagen wieder nutzbar zu machen. Dies bedarf effizienter Energiespeicher, um das zeitlich versetzte Angebot und die Nachfrage an elektrischer Energie zu decken. Neben mechanischen Großspeichern wie z.B. Pumpspeicherkraftwerken, ist auch die Speicherung elektrischer Energie in chemischen Bindungen möglich (Abbildung 1). Die Energie wird also in Substanzen gespeichert, die später als Energieträger oder Chemikalien verwendet werden können. In diesem Zusammenhang wird oft die Elektrolyse von Wasser zu Wasserstoff und Sauerstoff genannt. Aber auch die direkte Verwendung der Stromüberschüsse zur Darstellung von Basis- oder Feinchemikalien ist eine attraktive Methode zur Energiespeicherung.[1] Vor allem die elektrochemische C,C-Bindungsknüpfung zwischen Aromaten stellt eine attraktive Methode zur Darstellung wertvoller Feinchemikalien dar.

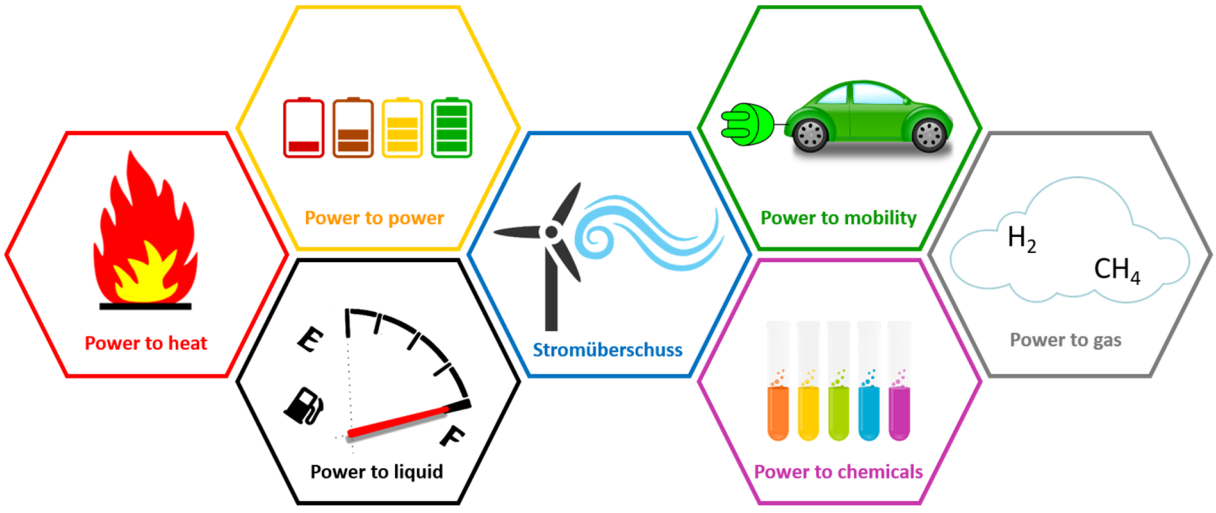

Abbildung 1: Übersicht der Energiespeichersysteme für Stromüberschüsse.

1.1 Kreuzkupplung von Aromaten

Die selektive Knüpfung aromatischer C,C-Bindungen ist eine der wichtigsten Reaktionen im Bereich der Organischen Chemie. Vor allem Biarylmotive finden Anwendung in vielfältigen Bereichen der Naturstoffsynthese,[2–4] den Materialwissenschaften[5] sowie der Katalyse.[6] Grundsätzlich kann hier zwischen zwei Reaktionstypen unterschieden werden – der reduktiven und der oxidativen Kupplung (Abbildung 2). Bei der reduktiven Kupplung werden präfunktionalisierte Aromaten mittels Übergangsmetallkatalysatoren zu den gewünschten Biarylen umgesetzt. Auf diese Weise kann ein breites Produktspektrum in hoher Selektivität und hervorragenden Ausbeuten erhalten werden.[7] Der herausragende Einfluss dieser Reaktionen auf die moderne organische Synthesechemie wird durch die Verleihung des Nobelpreises in Chemie 2010 an RICHARD HECK, AKIRA SUZUKI sowie EI-ICHI NEGISHI hervorgehoben.[8]

Die genannten präfunktionalisierten Edukte sowie die Verwendung von meist toxischen Katalysatoren auf Basis seltener Übergangsmetalle bergen allerdings auch erhebliche Nachteile. Die metall- (M) oder (pseudo-)halogensubstituierten (X) Substrate müssen oft in mehrstufigen Prozessen hergestellt werden, was hohe Kosten und große Mengen Abfall verursacht.[9] Als Abgangsgruppen werden meistens toxische Metallorganyle verwendet, welche vor allem im Bereich der Wirkstoffsynthese vermieden werden sollten.[10]

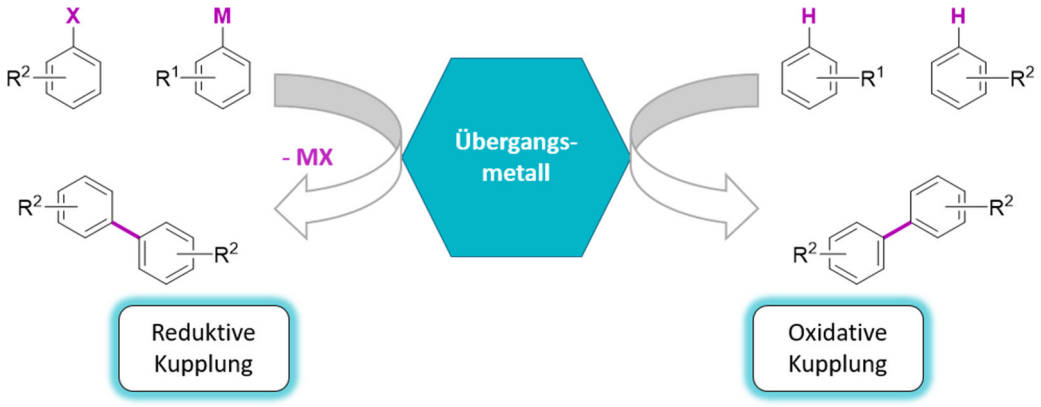

Abbildung 2: Schematische Darstellung der reduktiven und oxidativen Kupplung.

Im Gegensatz hierzu findet bei den oxidativen Kupplungen eine direkte C,H-Aktivierung statt. Allerdings werden hier oft (über-)stöchiometrische Mengen eines Oxidations-mittels oder einer Lewis-/Brønsted-Säure verwendet.[11] Somit fällt eine große Menge an

Reagenzabfall an, insgesamt ist die Atomökonomie allerdings oft besser als bei den vorher genannten reduktiven Kupplungen, da eine aufwendige Eduktsynthese entfällt.[12]

Aktuelle Forschungen beschäftigen sich vor allem mit dem Aspekt der Nachhaltigkeit, um die Atomökonomie der genannten Reaktionen zu verbessern. Ein vielversprechendes und stark untersuchtes Gebiet ist hierbei die Elektrochemie. Diese versucht, Kupplungsreagenzien durch elektrischen Strom zu ersetzen, worum es auch im Folgenden gehen soll.[13]

1.1.1 Direkte elektrochemische Kreuzkupplung

Elektrochemische dehydrierende Kupplungsreaktionen durch direkte oxidative C,H- und N,H-Aktivierung stellen eine große Herausforderung dar. Oft treten Oligomerisierung oder sogar Mineralisation der Substrate oder der gebildeten Produkte auf. Insbesondere C,H–C,H-Kreuzkupplungen zwei unterschiedlicher Arene sind anspruchsvoll, da einer der Kupplungspartner selektiv oxidiert werden muss. Andernfalls werden überwiegend Homokupplungs- und Überoxidationsprodukte gebildet (Schema 1).

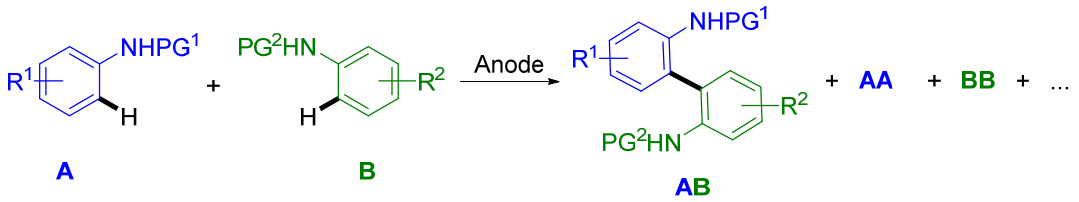

Schema 1: Die direkte C,C-Kupplung zweier Aniline ohne Abgangsgruppen führt normalerweise überwiegend zur Bildung von Homokupplungs- und Überoxidationsprodukten.

Verschiedene Vorgehensweisen versuchen, die Reaktion in die gewünschte Richtung zu lenken, so z.B. die „radical cation pool method“ von YOSHIDA und Mitarbeitern.[14–16] Hierbei sind die Oxidation und die eigentliche Kupplung zeitlich und räumlich getrennt, um Homokupplung und Überoxidation zu vermeiden. Allerdings werden hierfür meist niedrige Temperaturen benötigt und die Reaktionen sind nur schwer skalierbar. Die einfachste Möglichkeit, eine solche Kupplung zu beeinflussen, wäre die Verwendung eines Elektrolytsystems, das sowohl Oxidationspotential als auch Nukleophilie der jeweiligen Kupplungspartner so beeinflussen kann, dass selektiv eines der Arene oxidiert wird und es zur Kreuzkupplung kommen kann. Mit 1,1,1,3,3,3-Hexafluorisopropanol (im

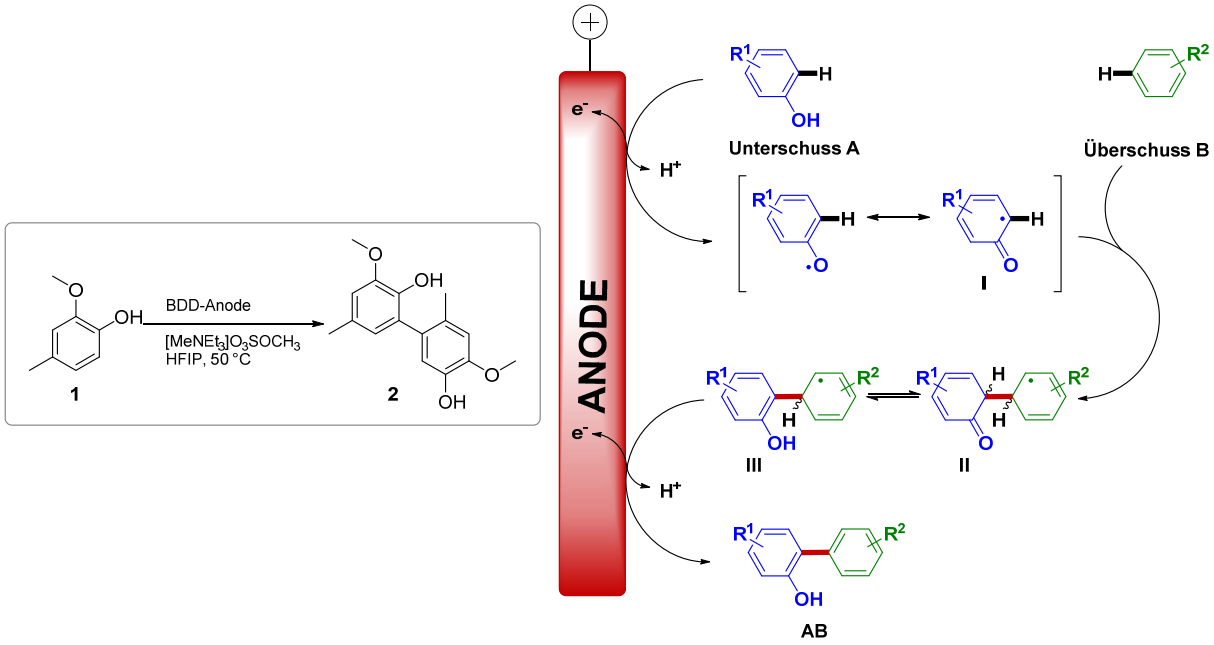

Schema 2: Links: Unerwartete *ortho-meta*-Kupplung von 4-Methylguajakol. Rechts: Vorgeschlagener Mechanismus für die anodische Phenol-Aren-Keuzkupplung.[17]

Folgenden als HFIP abgekürzt) wurde ein solches Lösungsmittel gefunden (mehr zu HFIP als Lösungsmittel in Kapitel 1.2).[18]

Um die bei der direkten elektrochemischen Umsetzung von 2,4-Dimethylphenol entstehenden Nebenprodukte[19] zu vermindern, wurde zunächst eine borbasierte Templatstrategie entwickelt[20] und später die Selektivität durch Zugabe fluorierter Alkohole deutlich erhöht.[21] Die optimierten Elektrolysebedingungen konnten anschließend auf Guajakolderivate ausgeweitet werden. Die direkte anodische Umsetzung von 4-Methylguajakol **1** ergab allerdings nicht wie erwartet das symmetrische *ortho-ortho*-Kupplungsprodukt, sondern ein unsymmetrisches *ortho-meta*-gekuppeltes Biphenol **2** (Schema 2, links).[22] Dies führte zu der Annahme, dass das Biphenol nicht durch eine radikalische Rekombination gebildet wird, sondern über eine Oxidation des Phenols, an welche sich ein nukleophiler Angriff eines zweiten Phenols (oder Arens) anschließt und letztendlich das Produkt in einem zweiten Oxidationsschritt gebildet wird (vgl. Schema 2, rechts).[17] Daraufhin wurde dieses außergewöhnliche Konzept auf weitere Phenol-Phenol-, sowie Phenol-Aren-Kreuzkupplungen ausgeweitet und weiter optimiert.[17,23] Seitdem konnten viele verschiedene Produktklassen auf einfache Art zugänglich gemacht werden, da für dieses einfache elektrochemische Verfahren weder Abgangsfunktionalitäten noch Oxidationsmittel oder Katalysatoren

benötigt werden. Außerdem können die beschriebenen Transformationen einfach bei gleicher Ausbeute und Selektivität hochskaliert werden.[24,25] Auch eine Verwendung sehr hoher Stromdichten bis zu 100 mA/cm^2 ist möglich, dies zeigt die außergewöhnliche Robustheit dieser Reaktion.[26] Dadurch ergibt sich eine deutliche technische Relevanz.

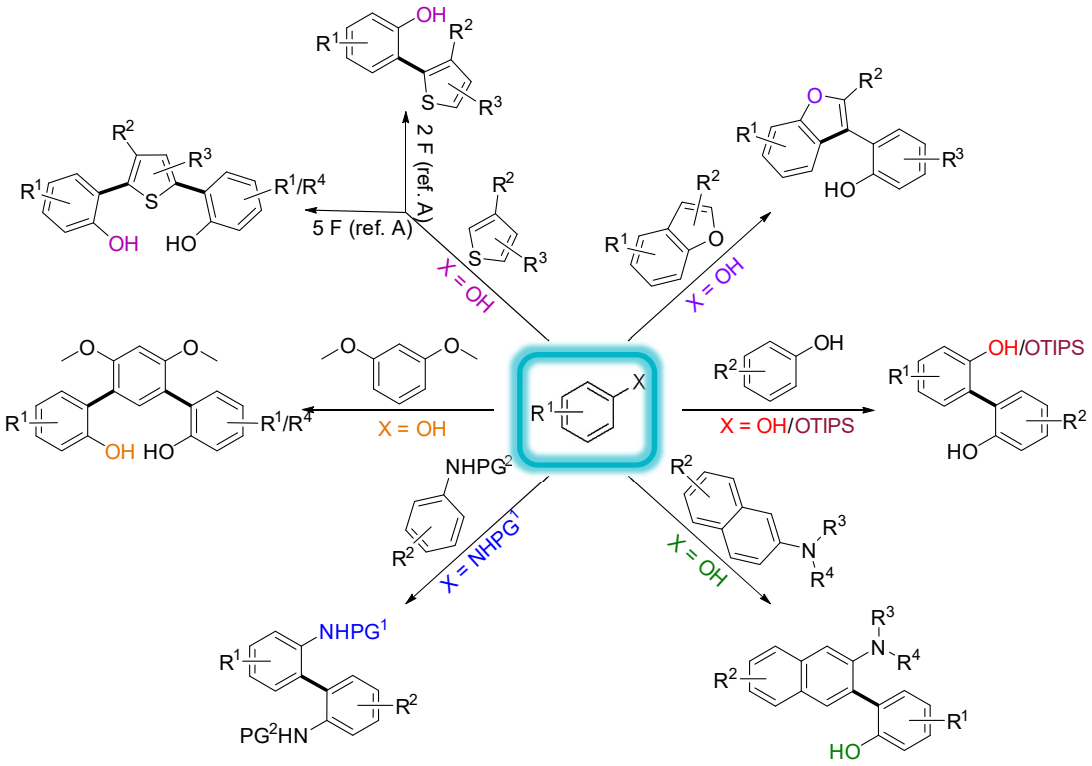

Schema 3: Auswahl anodischer Kupplungsreaktionen von Arenen, entwickelt im Arbeitskreis WALDVOGEL.[24,25,27–31]

Zu den synthetisierten Produktklassen gehören unter anderem teilgeschützte 2,2‘-Biphenole,[24] 4,4‘-Biphenole,[32] symmetrische und unsymmetrische 2,2‘-Diaminobiaryle,[27,28] *N,O*-Biarylstrukturen durch die Kupplung von Naphthylaminen mit Phenolen,[31] (2-Hydroxyphenyl)benzofurane,[30] *meta*-Terphenyl-2,2‘‘-diole[29] und 2-Hydroxy-*p*-terphenyle,[33] oder auch *N,N*-Diarylamide.[34] Des Weiteren konnten verschiedene Phenole mit Thiophenen[25] und Benzothiophenen[35] gekuppelt werden, genauso wie mit Natriumsulfinaten.[36] Schema 3 zeigt eine Auswahl dieser Kreuzkupplungsreaktionen.

1.2 1,1,1,3,3,3-Hexafluorisopropanol (HFIP)

Das verwendete Lösungsmittel ist ein oft vernachlässigter Parameter in der elektrochemischen Synthese. Bei der richtigen Wahl eines geeigneten Elektrolyten, ist es möglich den Ausgang der durchgeführten Reaktion positiv zu beeinflussen. Elektrolyte können Einfluss auf die Nukleophilie und das Oxidationspotential der Substrate haben, während der Elektrolyse gebildete, geladene Intermediate stabilisieren und sogar entstehende Produkte vor einer Überkonversion schützen (Abbildung 3).[18]

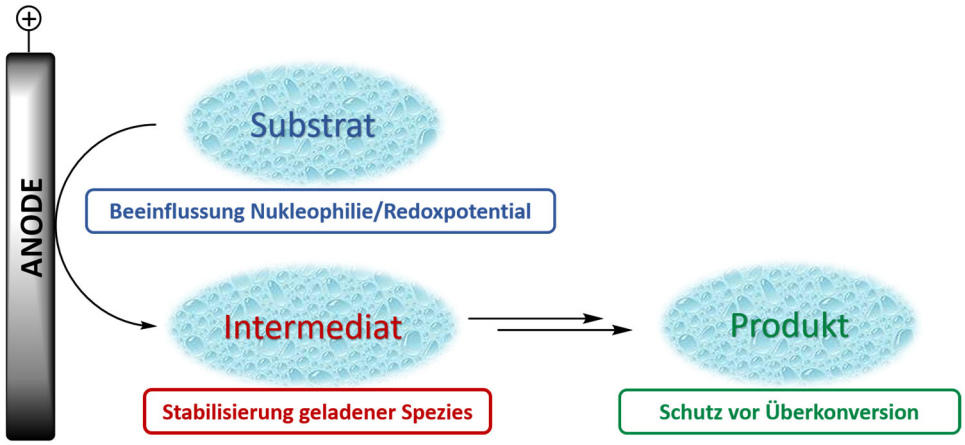

Abbildung 3: Schematische Darstellung, wie Solvenseffekte eine elektrochemische Reaktion beeinflussen können.[18]

Bedeutende Studien wurden durch den späten EBERSON durchgeführt, in denen eine starke Erhöhung der Stabilität von Radikalkationen in HFIP im Vergleich zu Trifluoressigsäure beobachtet wurde.[37,38] Diese nützlichen Effekte wurden auch in zahlreichen Metallkatalysen und Oxidationsreaktionen beobachtet.[39,40] Bis vor kurzem konnte dieser besondere Einfluss von HFIP als Lösungsmittel allerdings noch nicht erklärt werden. Erst 2017 hat die Gruppe um B. KIRCHNER in Zusammenarbeit mit dem Arbeitskreis WALDVOGEL näher das katalytische Verhalten von HFIP-H_2O_2-Mischungen mittels spezifischer Molekulardynamik-Simulationen untersucht.[39] Hierbei ist aufgefallen, dass HFIP eine mikroheterogene Struktur ausbildet, welche aus der Separation der polaren Hydroxygruppen von den fluorierten Alkylfunktionen resultiert. Auf diese Weise werden Domänen geformt, die große Bereiche des Systems einnehmen, wohingegen HFIP makroskopisch homogen bleibt. Anschließende Studien zeigten außerdem, dass diese Domänenbildung die Adsorption der Substrate an die

Elektrodenoberfläche beeinflusst. Die Adsorption der Substrate ist zum Teil durch attraktive lipophile-lipophile Wechselwirkungen zwischen Substraten und Elektrode bedingt, zum anderen durch die Minimierung der abstoßenden Wechselwirkung zwischen lipophilen Bereichen der Substrate sowie Elektrode und den fluorhaltigen Bereichen von HFIP (Abbildung 4). Dies führt zu einer Anreicherung der Substrate an der Elektrode, wo die elektronenreichere Komponente **A** oxidiert wird. Durch die höhere Konzentration der anderen Arylderivate an der Anodenoberfläche kann es leicht zur Kupplungsreaktion kommen. Dies ist von Vorteil, da die Zeitspanne des freien Phenoxyl-Radikals verkürzt wird und somit ungewollte Nebenreaktionen vermindert werden können.[41] Vor allem in Kombination mit Bor-dotierten Diamantelektroden (BDD), aber auch mit anderen Elektrodenmaterialien, wie z.B. Glaskohlenstoff, ergibt sich in HFIP ein für protische Lösungsmittel sehr großes Potentialfenster (ca. 5.2 V an BDD, 4.6 V an Glaskohlenstoff).[42] Diese herausragenden Kombinationen ermöglichen eine Vielzahl elektrochemischer Umsetzungen.

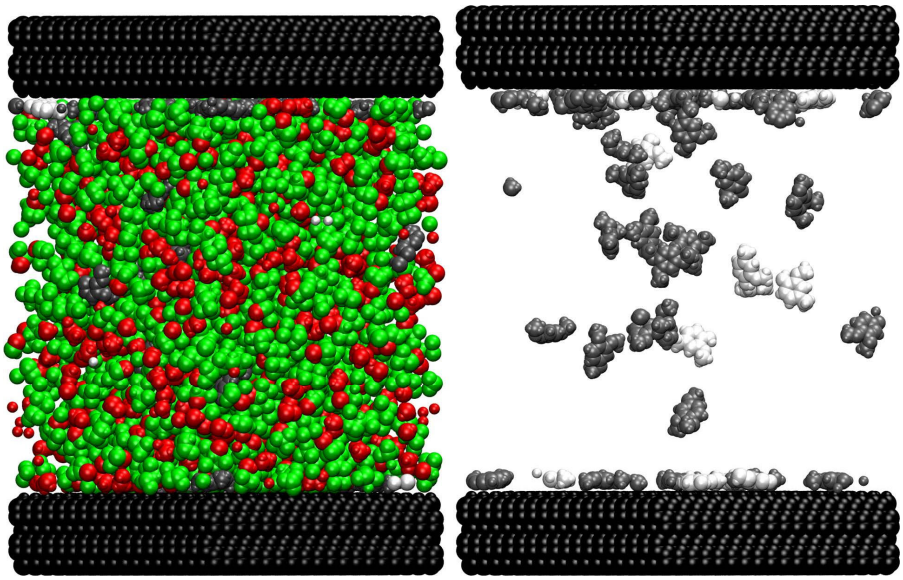

Abbildung 4: Schnappschuss der Simulation mit folgenden Komponenten: Links: BDD-Elektrode (schwarz), Methanol (rot), Hydroxygruppen von HFIP (rot), CF_3–CH–CF_3-Gruppe von HFIP (grün), Komponente A (hellgrau), Komponente B (dunkelgrau). Rechts: nur die Substrate A und B sind dargestellt.[41] Nachgedruckt mit Erlaubnis von [42]. Copyright 2019 American Chemical Society.

Weitere Arbeiten aus dem Arbeitskreis WALDVOGEL haben zudem gezeigt, dass die Zugabe protischer Additive wie Wasser oder Methanol positiven Einfluss auf Selektivität und Ausbeute einer Kupplungsreaktion haben kann. Der größte Einfluss war bei 18 vol-%. MeOH bzw. 9 vol-%. H_2O zu beobachten.[17] In Abbildung 5 ist schematisch dargestellt,

wie HFIP die Oxidationspotentiale und Nukleophilie der Substrate bei der Kreuzkupplung von Phenolen, Arenen und Anilinen beeinflussen kann.

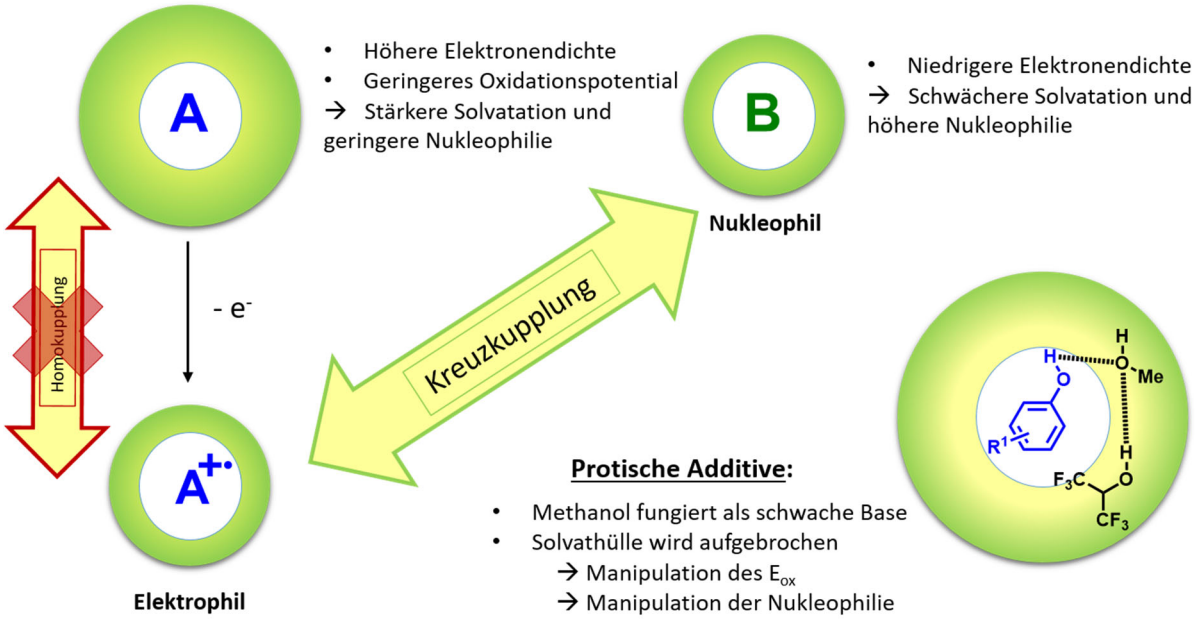

Abbildung 5: Quelle der Selektivität in der anodischen Kreuzkupplung von Phenolen und Anilinen.[17]

Komponente **A** besitzt hierbei ein niedrigeres Oxidationspotential als **B** und ist dadurch stärker von HFIP solvatisiert. Komponente **B** ist elektronenärmer als **A** und somit schwächer solvatisiert. Dies hat zur Folge, dass das eigentlich elektronenreichere **A** aufgrund der stärkeren Solvatation eine geringere Nukleophilie aufweist. Aufgrund des niedrigeren Oxidationspotentials wird **A** an der Anode oxidiert und durch einen nukleophilen Angriff der Komponente **B** wird das Kreuzkupplungsprodukt **AB** gebildet. Die Homokupplung zwischen zwei **A**-Komponenten ist weitestgehend unterdrückt, da **A** keine ausreichende Nukleophilie aufweist. Auf diese Weise kann das gewünschte Kreuzkupplungsprodukt in hoher Selektivität und sehr guten Ausbeuten erhalten werden.

Zu diesem Kapitel wurde ein Übersichtsartikel veröffentlicht:

L. Schulz, S. R. Waldvogel, *Solvent Control in Electro-Organic Synthesis, Synlett* **2019**, *30*, 275–286.

1.3 2,2‘-Diaminobiaryle

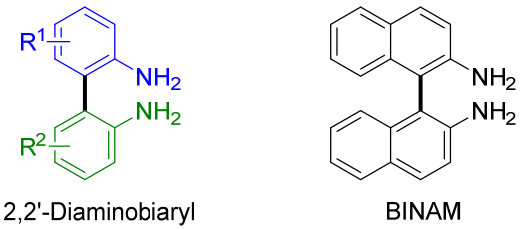

Abbildung 6: Gewünschte Struktureinheit unsymmetrischer 2,2‘-Diaminobiaryle (links) und BINAM als wichtiger Ligand in der Übergangsmetallchemie (rechts).

Symmetrische 2,2‘-Diaminobiaryle, wie das oben gezeigte BINAM, wurden bereits eingehend auf ihr Potenzial als Liganden untersucht.[43,44,45] Unter anderem konnten asymmetrische MICHAEL-Additionen,[45] Hydrierungen[44] oder Ringöffnungen von 3,4-Epoxyalkoholen[46] erolgreich unter Verwendung von BINAM oder Derivaten davon realisiert werden. Unsymmetrische Bisanilide (Abbildung 6, links) hingegen finden bis heute kaum Anwendung. Dies liegt vor allem an der aufwendigen Synthese und der damit verbundenen schlechten Verfügbarkeit solcher Verbindungen.

1.3.1 Bedeutung von 2,2‘-Diaminobiarylderivaten

Unsymmetrische Biaryle spielen in Naturstoffen und in der Katalyse eine wichtige Rolle.[4] In der asymmetrischen Hydrierung nach ROCAMORA wird ein Rhodium(I)-Katalysator mit Bis(diamidophosphit)-Liganden, der das BINAM-Grundgerüst beinhaltet, verwendet (Abbildung 7, links).[47]

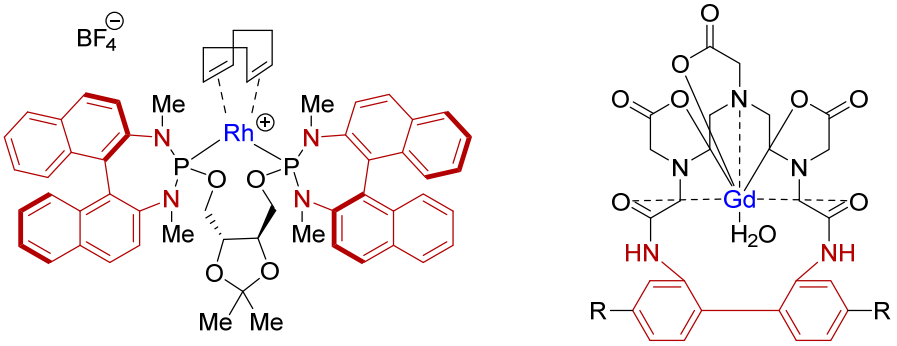

Abbildung 7: Rhodium-Komplex mit BINAM-Derivat als Ligand zur asymmetrischen Hydrierung nach ROCAMORA (links); Gadolinium-Komplex nach CHANG und KIM für die Verwendung als Kontrastmittel im MRT (rechts).

Aber auch abseits der Katalyse finden 2,2‘-Diaminobiaryle Verwendung. So zum Beispiel als Ligand eines neuartigen Gadolinium-Komplexes, wie er in Abbildung 7, rechts dargestellt ist. Der gezeigte Gadolinium-Komplex findet Anwendung in der Forschung für neuartige Kontrastmittel für die Magnetresonanztomographie (MRT). Die Verwendung von Kontrastmitteln auf Gd-Basis führt aufgrund der paramagnetischen Eigenschaften zu kürzeren Relaxationszeiten und somit zu einer helleren, d.h. signalreicheren Darstellung des untersuchten Gewebes.[48] Diese und viele andere Beispiele zeigen, dass die angestrebten Diaminobiaryle nicht nur im Labor eine wichtige Substanzklasse darstellen, sondern auch als Intermediate technische und medizinische Relevanz besitzen.[49]

1.3.2 Klassische Synthese von 2,2‘-Diaminobiarylderivaten

Der Zugang zu dieser Substanzklasse mittels klassischer Synthese ist begrenzt, da Aniline sehr leicht zu Polyanilin polymerisieren (Bildung von „Anilinschwarz“).[50] Eine Möglichkeit, symmetrische Biarylderivate darzustellen, bietet die kupfer-katalysierte ULLMANN-Reaktion.[51] Eine direkte oxidative Kreuzkupplung von Anilinderivaten mittels anorganischer Oxidationsmittel wie z.B. Cu(II)-Salzen verläuft komplett unselektiv und wurde lediglich für Naphthylamine beschrieben (Schema 4).[52]

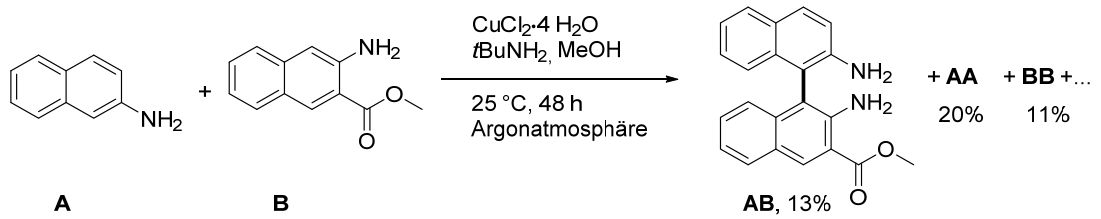

Schema 4: Direkte oxidative Kreuzkupplung mittels Cu(II)-Salzen.[52]

Sigmatrope Umlagerungen von Diarylhydrazinen mittels katalytischer Mengen Säure liefern symmetrische 2,2‘-Diaminobiaryle in guten Ausbeuten, unsymmetrische Produkte sind jedoch eine Herausforderung. Außerdem sind mehrere Syntheseschritte notwendig, um die kanzerogenen Hydrazinderivate herzustellen (Schema 5).[53,54,55] Unter Verwendung einer axial chiralen Phosphorsäure können über die genannte Umlagerung BINAM-Derivate atropselektiv hergestellt werden.[55]

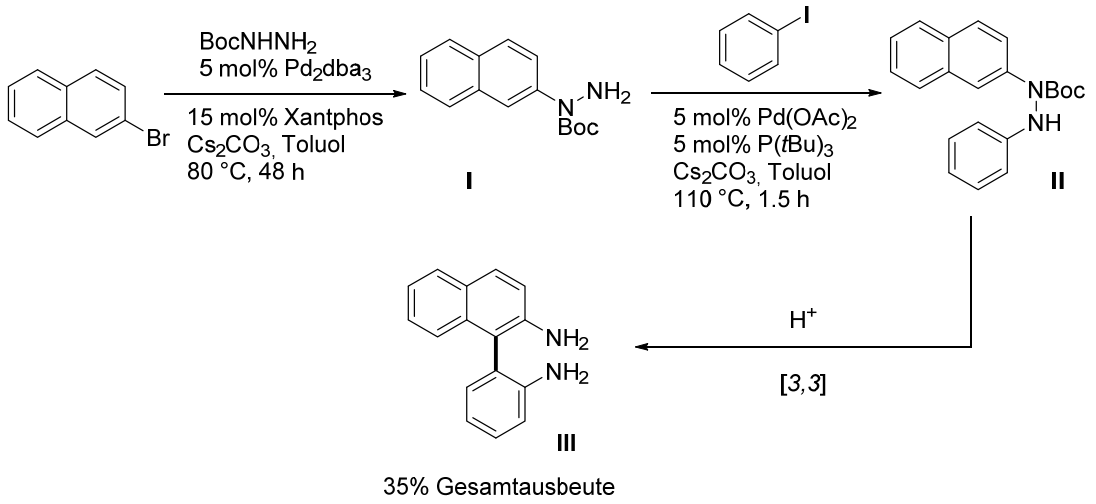

Schema 5: Synthese unsymmetrischer 2,2'-Diaminobiaryle über eine Pd-katalysierte Synthse gemischter Hydrazine und anschließender [3,3]-sigmatroper Umlagerung.[54]

Kürzlich berichteten MEI und LU von einer Palladium-katalysierten oxidativen Kupplung pivaloylgeschützter Aniline. Auf diese Weise sind symmetrische, aber auch unsymmetrische, geschützte 2,2'-Diaminobiaryle zugänglich (Schema 6).[56] Verschieden substituierte Anilinderivate konnten erfolgreich eingesetzt werden und ergaben die Kupplungsprodukte in guten bis exzellenten Ausbeuten. Allerdings wird eine große Menge des Palladiumkatalysators benötigt (8–16 mol%) und bei Kreuzkupplungen wird die **B**-Komponente in einem bis zu 30-fachen Überschuss eingesetzt. Des Weiteren wurden die Reaktionen nur im unteren Millimol-Maßstab durchgeführt, eine einfache Hochskalierung bei den gegebenen Bedingungen ist nicht möglich.

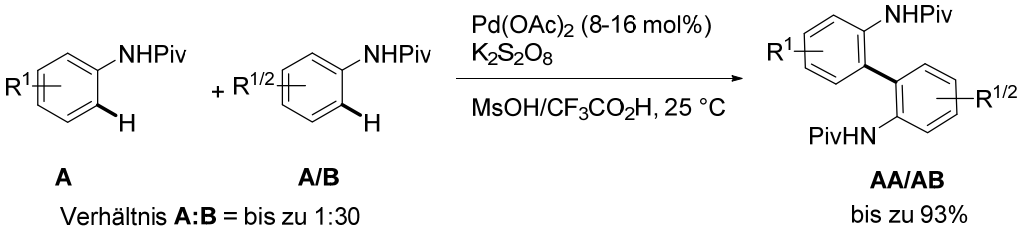

Schema 6: Pd-katalysierte Homo- und Kreuzkupplung pivaloylgeschützter Anilinderivate.[56]

Alle bisher bekannten Möglichkeiten, Diaminobiaryle klassisch darzustellen, haben viele Nachteile gemeinsam. Die meisten benötigen zeit- und kostenintensive Mehrstufensynthesen mit schlechter Atomökonomie. Dies führt zu großen Mengen oft toxischen Abfalls und somit zu ineffizienten Reaktionsbedingungen.

2 Aufgabenstellung

Die Verwendung stöchiometrischer Mengen Oxidationsmittel, die Notwendigkeit von Abgangsgruppen und Katalysatoren sowie eine schlechte Atomökonomie und große Mengen Abfall machen die vorgestellten Synthesen unattraktiv und stehen im Widerspruch zur heutzutage angestrebten „grünen Chemie“. Besonders für technische Anwendungen, wie die Speicherung von Energieüberschüssen in Form von chemischer Energie, sind günstige Reaktionsbedingungen, eine leichte Aufarbeitung sowie eine gute Skalierbarkeit von Nöten.

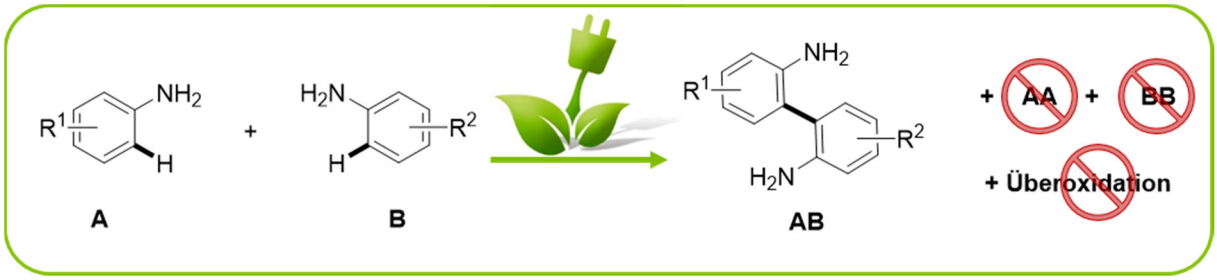

Schema 7: Allgemeines Schema der direkten elektrochemischen Kreuzkupplung.

In dieser Arbeit soll eine nachhaltige und einfach durchzuführende elektrochemische Synthese (un-)symmetrischer 2,2‘-Diaminobiaryle ausgehend von Anilinderivaten entwickelt werden. Die besondere Schwierigkeit liegt darin, die anodische Polymerisation der eingesetzten Aniline zu „Anilinschwarz“ zu vermeiden. Auch die entstehenden Produkte besitzen ein niedriges Oxidationspotential und neigen somit zur Überoxidation. Deshalb soll ein Verfahren entwickelt werden, das sowohl die eingesetzten Edukte, als auch die Produkte während der Elektrolyse vor ungewollten Nebenreaktionen schützt. Die Synthese soll zudem ohne Abgangsfunktionalitäten auskommen, aber trotzdem eine hohe Selektivität hin zum Kreuzkupplungsprodukt aufweisen. Durch die Verwendung von elektrischem Strom als Reagenz sollen nicht nur Reagenzabfälle vermieden, sondern auch die Reaktionsbedingungen sowie die Aufarbeitung des Reaktionsgemischs stark vereinfacht und somit eine nachhaltige Reaktionssequenz kreiert werden.

3 Ergebnisse und Diskussion

3.1 Anodische C,C-Kreuzkupplung geschützter Anilinderivate mit anschließender selektiver Entschützung

In diesem Projekt wurde eine metall- und reagensfreie Syntheseroute zur direkten elektrochemischen Darstellung unsymmetrischer 2,2‘-Diaminobiaryle entwickelt. Schema 8 zeigt die optimierten Bedingungen für die Anilin-Anilin-Kreuzkupplung.

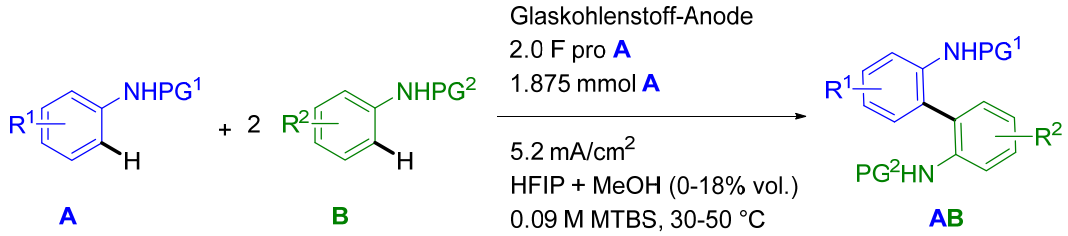

Schema 8: Direkte anodische C,C-Kreuzkupplung geschützter Anilinderivate (PG = Schutzgruppe).

Einfache Anilinderivate neigen aufgrund ihrer niedrigen Oxidationspotentiale zur Überoxidation. Durch die Schützung der Aminofunktion können allerdings nicht nur oligo- oder polymere Nebenprodukte vermindert werden, sondern auch die Einbettung der Anilide in das Wasserstoffbrückennetzwerk von HFIP verbessert werden. Durch die Verwendung verschiedener Schutzgruppen können die Oxidationspotentiale der Aniline zu einem gewissen Grad angepasst werden, um eine ideale Oxidationspotential-Differenz für die Kupplung zu erreichen (Abbildung 8). Auch durch die Verwendung von Glaskohlenstoff-Elektroden können Nebenreaktionen wie Elektropolymerisation und Homokupplung unterdrückt werden. Außerdem ist eine Stabilisierung der entstehenden reaktiven Radikale essenziell, um unerwünschte Nebenreaktionen zu vermeiden. Dies wird durch die Verwendung des einzigartigen Lösungsmittels 1,1,1,3,3,3-Hexafluor-isopropanol (HFIP) erreicht. Um eine effiziente Durchführung vieler Testreaktionen zu gewährleisten, werden in unserem Arbeitskreis entwickelte Screening-Apparaturen verwendet.[57] Auf diese Weise können bis zu acht verschiedene Elektrolyse-Ansätze im 5 mL-Maßstab (0.375 mmol **A**) gleichzeitig durchgeführt werden. Wurden geeignete Parameter oder Substratkombinationen gefunden, werden die Reaktionen in einem größeren Maßstab (1.875 mmol **A** in 25 mL) wiederholt und die Produkte isoliert.

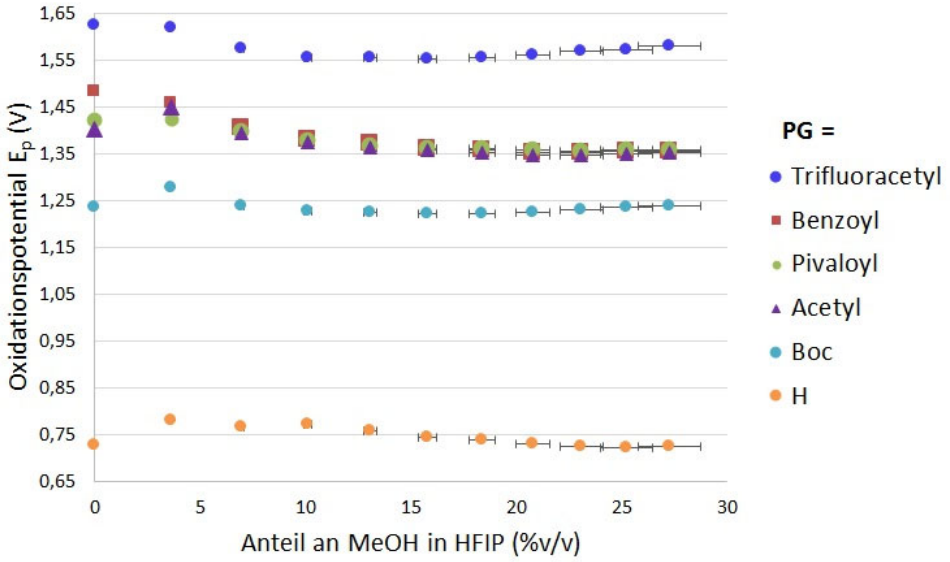

Abbildung 8: Verschiebung der Oxidationspotentiale unter Verwendung verschiedener Schutzgruppen; PG=Schutzgruppe.

Auf diese Weise konnten viele verschiedene 2,2‘-Diaminobiaryle in guten Ausbeuten synthetisiert werden (Abbildung 9). Es ist anzumerken, dass keine der Schutzgruppen während der Elektrolyse abgespalten wurde. Die Elektrolysebedingungen sind sehr mild, weshalb sogar halogenierte Substrate toleriert werden (Abbildung 9, Molekül **6**). Auch sehr elektronenreiche Derivate wie 3,4-Dimethoxyanilin konnten erfolgreich gekuppelt werden (z.B. Moleküle **4**–**6**). In allen Fällen wurde das Kreuzkupplungsprodukt selektiv erhalten, d.h. es wurde kein Homokupplungsprodukt gebildet. Der Anteil an nicht umgesetzter **A**-Komponente lag bei 2–24%. Generell werden nicht umgesetzte Substrate und vor allem das Lösungsmittel HFIP nach der Elektrolyse wieder gewonnen und auch wieder verwendet.

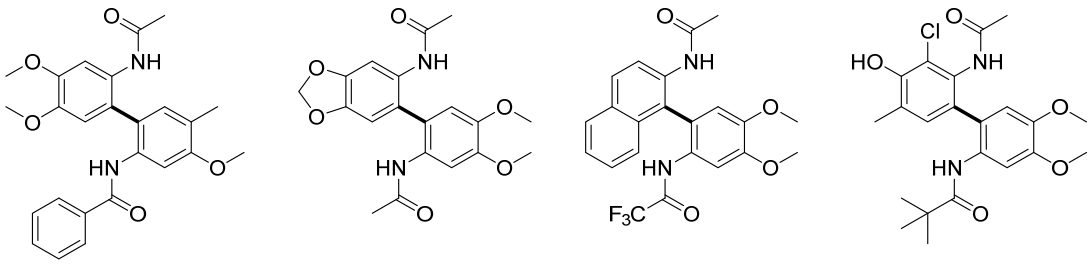

Abbildung 9: Ausgewählte unsymmetrische 2,2'-Diaminobiaryle, die über die anodische Kreuzkupplung dargestellt werden konnten.

Um eine spätere Anwendung der Diaminobiaryle in Liganden oder funktionalisierten Materialien zu ermöglichen, ist es unverzichtbar, die Aminofunktion effizient entschützen zu können. Die genutzten carbonylbasierten Schutzgruppen können einfach durch Standardmethoden entfernt werden.[58] Durch die Anwendung orthogonaler Schutzgruppen sind beide Aminofunktionen zudem unabhängig voneinander zugänglich, was eine weitere chemo- sowie regioselektive Umsetzung ermöglicht (Abbildung 10).

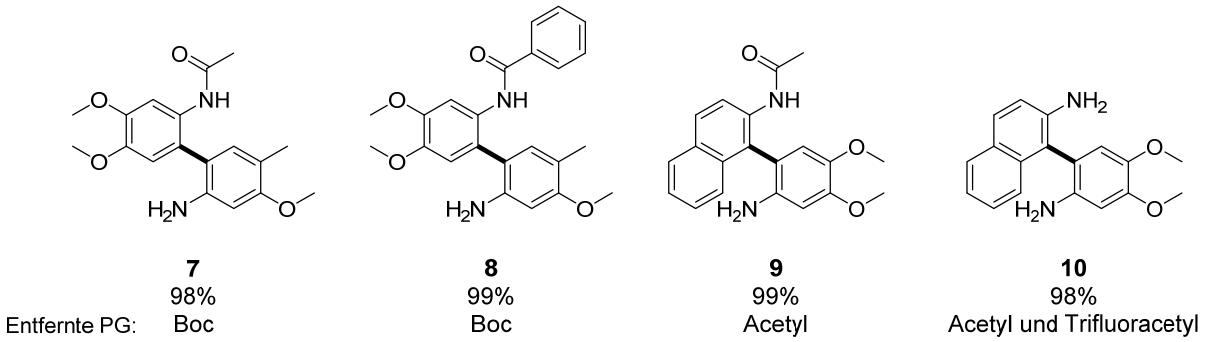

Abbildung 10: Teilweise und komplette Entschützung verschiedener 2,2'-Diaminobiaryle.

Aufgrund der außergewöhnlichen stabilisierenden Eigenschaften von HFIP und der Beeinflussung der Oxidationspotentiale durch verschiedene Schutzgruppen kann diese einzigartige Reaktion galvanostatisch, d.h. bei konstantem Strom in einer ungeteilten Becherglas-Zelle durchgeführt werden. Somit kann ein sehr einfacher Zwei-Elektroden-Aufbau verwendet werden. Das vorgestellte Verfahren erlaubt erstmalig die einfache und selektive anodische Synthese geschützter 2,2‘-Diaminobiaryle in Ausbeuten bis zu 74%. Die Substratbreite deckt verschieden substituierte und geschützte Anilinderivate ab. Auf diese Weise wird eine effiziente, metall- und reagensfreie und somit äußerst nachhaltige Reaktionssequenz kreiert.[27]

Zu diesem Kapitel wurde ein Manuskript veröffentlicht:

L. Schulz, M. Enders, B. Elsler, D. Schollmeyer, K. M. Dyballa, R. Franke, S. R. Waldvogel,

(a) *Reagent- and Metal-Free Anodic C-C Cross-Coupling of Aniline Derivatives, Angew. Chem. Int. Ed.* **2017**, *56*, 4877–4881;

(b) *Reagens- und metallfreie anodische C-C-Kreuzkupplung von Anilinderivaten, Angew. Chem.* **2017**, *129*, 4955–4959.

3.2 Direkte anodische Kreuz- und Homokupplung von Formaniliden

Neben den bereits in Kapitel 3.1 vorgestellten Schutzgruppen konnte auch die Formylgruppe erfolgreich in der anodischen Umsetzung von Anilinderivaten verwendet werden. Formamide repräsentieren eine außergewöhnliche Substanzklasse, die häufig in der organischen und medizinischen Chemie anzutreffen ist.[59,60] Außerdem ist die Formylgruppe eine unentbehrliche und sehr atomökonomische Art, Aminofunktionen zu schützen.[61] Darüber hinaus stellen Formamide wichtige Intermediate in der (technischen) Synthese von Isocyanaten,[62] Nitrilen,[63] Carbamaten,[64] aber auch von verschiedenen Fungiziden[59,65] und pharmazeutisch relevanten Strukturen dar (Schema 9).[59,60,66]

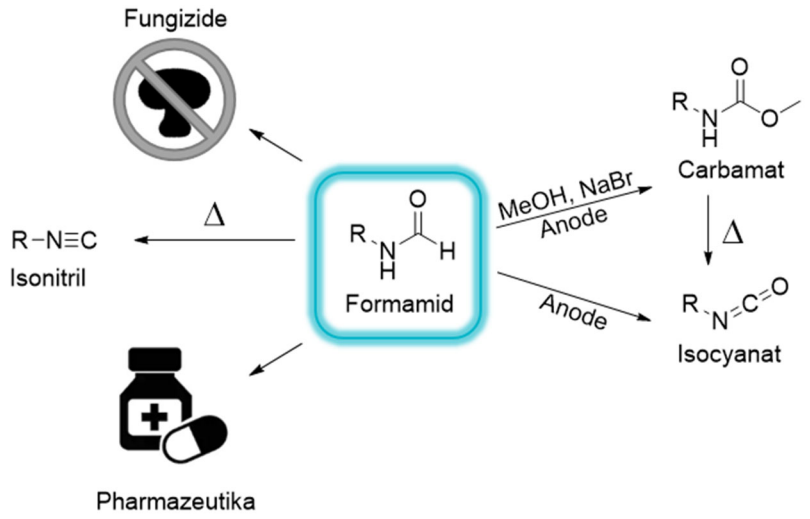

Schema 9: Verwendung von Formamiden in Fungiziden, Pharmazeutika und anderen technisch relevanten Syntesen.

Durch anodische Homo- und Kreuzkupplung von Formaniliden wurden erstmals symmetrische und nicht-symmetrische 2,2‘-Diformamidbiphenyle und 2-Formamid-2‘-amidbiphenyle auf einfache Weise zugänglich. Schema 10 zeigt eine Auswahl der dargestellten Kreuz- und Homokupplungsprodukte. Bei der Umsetzung von Formaniliden konnten erstmals iodsubstituierte Anilinderivate erfolgreich eingesetzt (**15**) und weniger elektronenreiche Derivate wie 3,4-Dimethylanilin erfolgreich zu **16** umgesetzt werden. Eine Dehalogenierung wurde dabei nicht beobachtet.

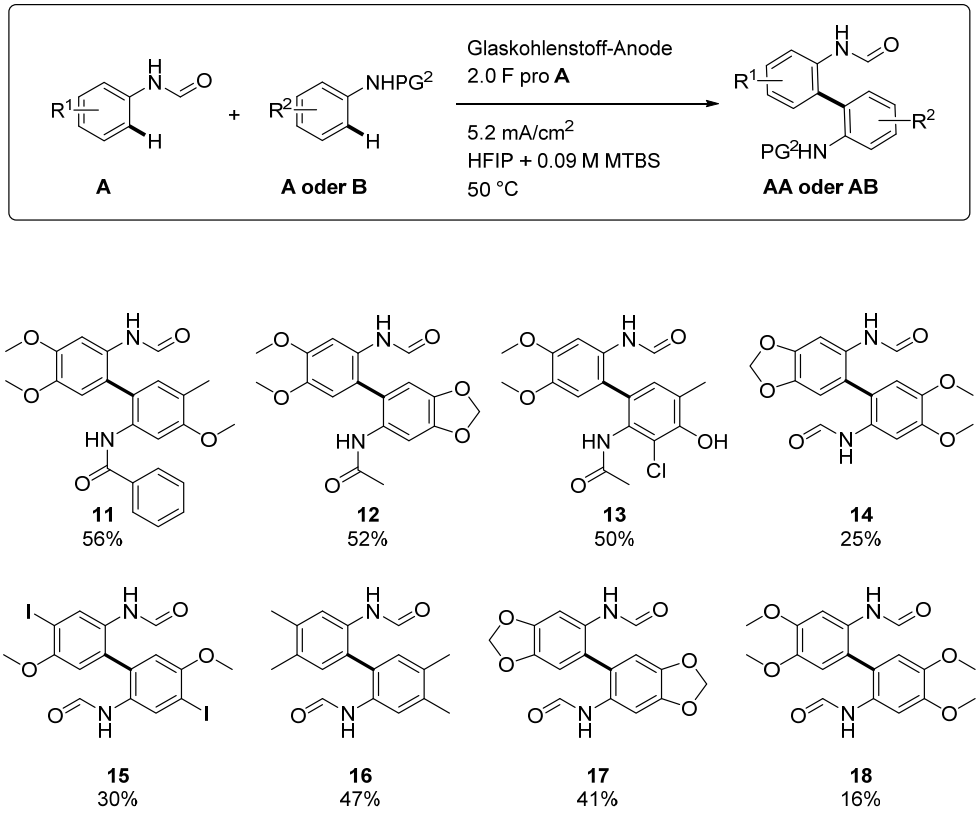

Schema 10: Auswahl unsymmetrischer (oben) und symmetrischer (unten) formylgeschützter 2,2'-Diaminobiaryle.

Die Kreuzkupplungsprodukte **11**–**13** wurden in exzellenter Selektivität erhalten, bei **14** wurde jedoch auch das Homokupplungsprodukt des Benzodioxolderivats erhalten. Generell wurden bei den Kupplungen zwischen einem Formamid und einem anderen Amid bessere Ergebnisse erhalten als in der Kupplung zwei verschiedener Formamide.

Die vorgestellte anodische Umsetzung von Formaniliden verläuft unter sehr einfachen und milden Bedingungen, sodass sogar Substrate mit labilen Iodgruppen erfolgreich eingesetzt werden können. Die direkte elektrochemische Synthese stellt somit eine attraktive Alternative zu den klassischen Darstellungsmöglichkeiten dar.[28]

Zu diesem Kapitel wurde ein Manuskript veröffentlicht:

L. Schulz, R. Franke, S. R. Waldvogel, *Direct Anodic Dehydrogenative Cross- and Homo-Coupling of Formanilides, ChemElectroChem* **2018**, *5*, 2069–2072.

3.3 Außergewöhnliche Robustheit der anodischen Anilin-Kupplung

Die oxidative Umsetzung von Anilinen führt üblicherweise zur Entstehung schwarzer Polymere, die oft als „Anilinschwarz“ bezeichnet werden. Diese Überoxidation ist nur schwer zu kontrollieren und auch in der anodischen Umsetzung eine große Herausforderung. Deshalb ist es umso bemerkenswerter, wie robust die vorgestellte anodische Kupplung von Anilinderivaten ist.

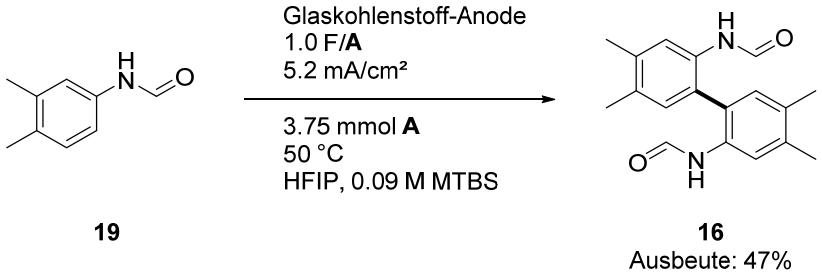

Schema 11: Standardbedingungen der Homokupplung geschützter Anilinderivate.[28]

In Schema 11 sind die bisher verwendeten Standardbedingungen der Homokupplung geschützter Aniline angegeben, unter denen das Homokupplungsprodukt in 47% Ausbeute erhalten werden konnte.[28] Aufgrund der vergleichsweise niedrigen Elektronendichte von *N*-(3,4-Dimethylphenyl)formamid ergibt sich ein größerer Spielraum, in dem die Elektrolyseparameter variiert und optimiert werden können.

Tabelle 1: Variierte Parameter der Homokupplung von *N*-(3,4-Dimethylphenyl)formamid 19.

Parameter	Untersuchter Bereich
Konzentration Substrat	0.15–0.6 mol/L
Ladungsmenge	1.0–2.0 F/**A**
Stromdichte	3.9–100 mA/cm²
Additive	MeOH, H_2O
Temperatur	30–50 °C
Elektrodenmaterial	Glaskohlenstoff, Graphit, BDD, Platin

In Tabelle 1 sind die untersuchten Parameter zusammengefasst. Im Folgenden werden exemplarisch der Einfluss des verwendeten Elektrodenmaterials, der Ladungsmenge und Stromdichte, welche den größten Einfluss auf die Ausbeute hatten, näher diskutiert. Die Verwendung protischer Additive führte in allen Fällen zu einer schlechteren Ausbeute. Auch die Erhöhung der verwendeten Stoffmenge hatte nur wenig Einfluss.

Besonders die applizierte Ladungsmenge ist ein wichtiger Faktor in elektrosynthetischen Prozessen. Die theoretisch benötigte Ladungsmenge für einen vollständigen Umsatz der eingesetzten Edukte beträgt 1.0 F/**A**. Durch stattfindende Nebenreaktionen, wie Oligomerisierung und Überoxidation, kann es jedoch zu einem unvollständigen Umsatz kommen. Eine Erhöhung der applizierten Ladungsmenge kann demnach in einem höheren Umsatz resultieren. Allerdings können gleichzeitig auch die genannten Nebenreaktionen begünstigt werden. Der Einfluss der Ladungsmenge wurde in einem Bereich von 1.0–2.0 F/**A** untersucht (Abbildung 11).

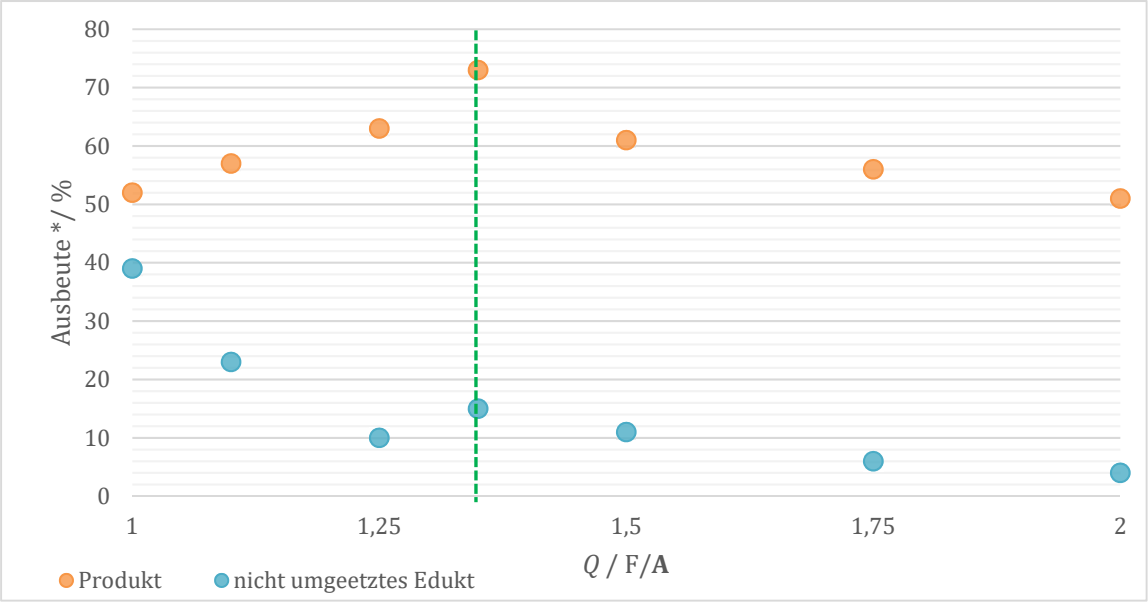

Abbildung 11: Einfluss der applizierten Ladungsmenge *Q*. Elektroden: Glaskohlenstoff, *j*=7.2 mA/cm², 0.75 mmol A, T=50 °C, Lösungsmittel: 5 mL HFIP + 0.09 M MTBS. * GC-Ausbeute, bestimmt unter Verwendung von 3,3‘,5,5‘-Tetramethyl-2,2’-biphenol als internen Standard.

Eine leicht erhöhte Ladungsmenge von 1.25–1.5 F/**A** führt zu einer verbesserten Ausbeute, wobei das Optimum bei 1.35 F/**A** liegt. Eine weitere Erhöhung resultiert allerdings wieder in einer Abnahme der Ausbeuten und auch die Menge an nicht umgesetztem Edukt verringert sich. Dies spricht für ein vermehrtes Auftreten von Überoxidation als Nebenreaktion.

Ein weiterer sehr wichtiger Faktor bei galvanostatischen Elektrolysen ist die verwendete Stromdichte. Hohe Stromdichten führen zu einer besseren Raum-Zeit-Ausbeute und sind somit sehr interessant für technische Anwendungen. Allerdings sind hohe Stromdichten mit einer erhöhten Rate des heterogenen Elektronentransfers an den Elektroden verbunden, wodurch auch Nebenreaktionen begünstigt werden können. Anhand verschiedener Phenol-Kupplungen konnte bereits gezeigt werden, dass das Verfahren der anodischen Kupplung in einem sehr breiten Stromdichtebereich durchgeführt werden kann.[26] Aufgrund der hohen Anfälligkeit von Anilinen für Überoxidation und Polymerisation, ist der Einsatz hoher Stromdichten sehr ungewöhnlich.[2,50] Der Einfluss der Stromdichte auf die Homokupplung von **19** wurde im Bereich von 3.9–100 mA/cm^2 untersucht (Abbildung 12).

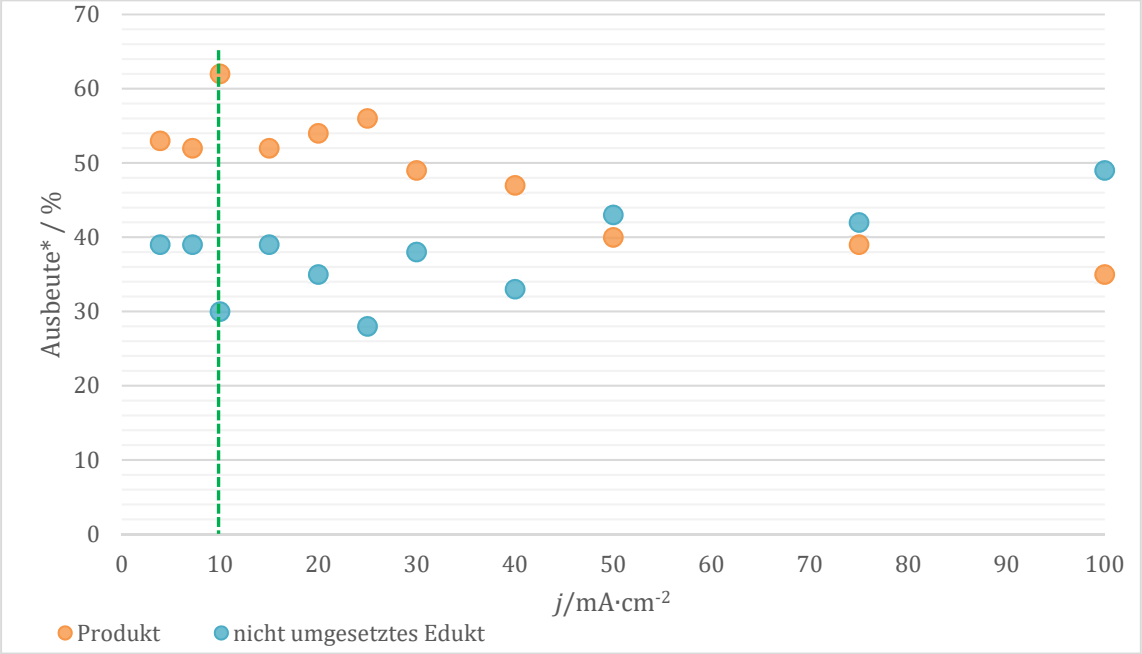

Abbildung 12: Einfluss der verwendeten Stromdichte *j*. Elektroden: Glaskohlenstoff, *Q*=1.0 F/A, 0.75 mmol A, *T*=50 °C, Lösungsmittel: 5 mL HFIP + 0.09 M MTBS. * GC-Ausbeute, bestimmt unter Verwendung von 3,3‘,5,5‘-Tetramethyl-2,2’-biphenol als internen Standard.

Sehr hohe Stromdichten von 250 mA/cm^2 und mehr werden üblicherweise nur für die KOLBE-Elektrolyse verwendet. Hier wird eine hohe Radikaldichte benötigt, um die Rekombination zweier Alkylradikale zu begünstigen.[67] Elektrochemische Reaktionen, wie die hier beschriebene Anilin-Kupplung, die eine höhere Selektivität erfordern und nicht auf der Rekombination zweier Radikale beruhen, werden in der Regel bei wesentlich geringeren Stromdichten unter 10 mA/cm^2 durchgeführt.[27,28] Deshalb ist es

umso erstaunlicher, dass die hier untersuchte Anilin-Homokupplung auch bei hohen Stromdichten von 50–100 mA/cm² das gewünschte Produkt in guten Ausbeuten ergibt. Schlüssel zu dieser ungewöhnlichen Robustheit ist das verwendete Lösungsmittel HFIP. Das Maximum der Ausbeute wird allerdings bei einer Stromdichte von 10 mA/cm² erreicht (Eintrag 3). Die Menge an nicht umgesetztem Edukt nimmt mit steigender Stromdichte zu und kann somit nach der Reaktion recyclisiert werden. Abbildung 13veranschaulicht, dass die Reaktion über einen sehr breiten Stromdichtebereich stabil ist. Wird die Screeningreaktion bei einer Stromdichte von 100 mA/cm² durchgeführt statt bei den bisher genutzten 7.2 mA/cm², so verkürzt sich die Reaktionsdauer von 1.5 h auf weniger als 7 min.

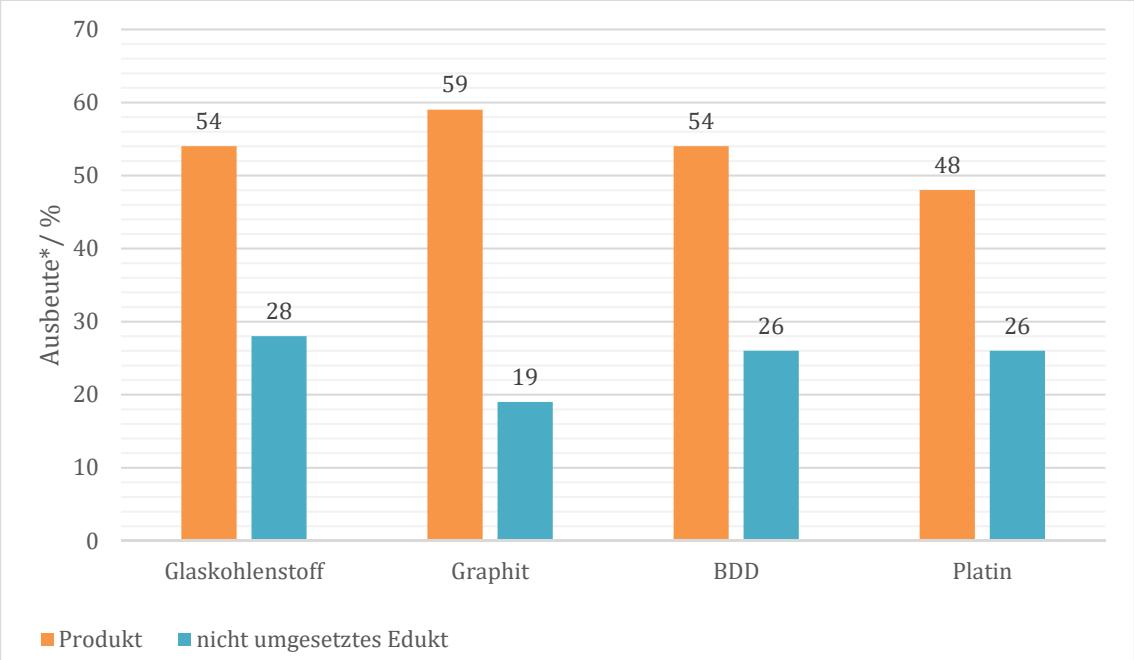

Abbildung 13: Einfluss des verwendeten Elektrodenmaterials.

Auch das Elektrodenmaterial kann einen wesentlichen Einfluss auf elektrochemische Umsetzungen haben (Abbildung 13). Bor-dotierte Diamantelektroden (BDD) haben sich vor allem in der anodischen Phenol-Phenol- und Phenol-Aren-Kupplung als Erfolg versprechender Faktor gezeigt.[68] Neben BDD und Glaskohlenstoff wurden die gängigsten Elektrodenmaterialien Graphit und Platin getestet. Wie in Abbildung 13 zu sehen, werden an allen Elektrodenmaterialien vergleichbare Ergebnisse erhalten. Vor allem Graphit als sehr günstiges und leicht verfügbares Material wird gerne bei technischen Prozessen eingesetzt. Aber auch im Labormaßstab ist es sehr nützlich, dass

alle Standard-Elektrodenmaterialien verwendet werden können. So kann eine große Breite an elektrochemischen Reaktionen mit einer kleinen, standardmäßigen Ausstattung durchgeführt werden.

Anschließend wurden einige der optimierten Parameter in weiteren Screening-reaktionen miteinander kombiniert, die erfolgreichsten Versuche hochskaliert und die Produkte anschließend isoliert. Im Zuge der Optimierung der Homokupplung von *N*-(3,4-Dimethylphenyl)formamid konnte die Ausbeute von 47% auf 64% erhöht werden (Schema 12). Unter Verwendung einer Stromdichte von 100 mA/cm^2 konnte das Produkt immer noch in 29% isoliert werden.

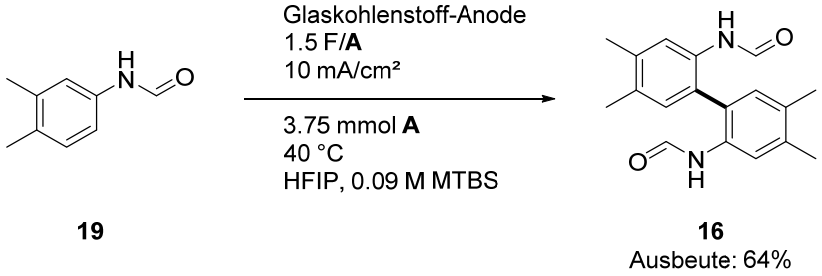

Schema 12: Optimierte Parameter der Homokupplung.

Dank der herausragenden Lösungsmitteleigenschaften von HFIP ist die Umsetzung von Anilinderivaten in einem großen Stromdichtebereich durchführbar und daher eine Anpassung an eventuelle Stromüberschüsse, bedingt durch erneuerbare Energiequellen, möglich. Die Elektrolysen können bei Bedarf einfach abgeschaltet und später fortgesetzt werden. Durch die Verwendung hoher Stromdichten kann die Reaktionszeit enorm verkürzt oder der verwendete Elektrolyse-Aufbau verkleinert werden. Somit ist die vorgestellte elektrochemische Umsetzung nahezu unabhängig von der verwendeten Ausrüstung und daher sowohl für Akademiker, als auch für die Industrie leicht realisierbar.

Zu den Kapiteln 3.3 und 3.4 wurde ein gemeinsames Manuskript vorbereitet:

L. Schulz, Jan-Åke Husmann, S. R. Waldvogel, *Outstandingly Robust Anodic Dehydrogenative Aniline Coupling Reaction, Manuskript in Fertigstellung.*

3.4 Doppelte Kreuzkupplung von Anilinen und Benzidinderivaten

Neben den bereits erfolgreich durchgeführten einfachen Kreuz- und Homokupplungen geschützter Anilinderivate ist auch eine doppelte Kreuzkupplung interessant, ähnlich wie sie bereits bei der Kupplung von Phenolen mit Arenen zu *meta*- oder *para*-Terphenylen oder auch bei der der doppelten Kupplung von Phenolen mit Thiophenen beobachtet werden konnte.[25,29] Auf diese Weise könnten amino-substituierte Terphenyl-Analoga hergestellt werden. *Meta*-Terphenylamine wurden bereits auf ihre Anwendbarkeit als Cyclooxygenase-Inhibitoren getestet[69] und amino-subistuierte *para*-Terphenylderivate können als α-Helix-Mimetika eingesetzt werden.[70]

Ein sehr interessantes Substrat für eine doppelte Kreuzkupplung ist Benzidin. Aufgrund der nachgewiesenen Kanzerogenität und der daraus resultierenden schlechten Verfügbarkeit von Benzidin wurde zunächst 4-Phenylanilin als Modellsubstrat verwendet. Dieses zeigte allerdings weder in Homo- noch in Kreuzkupplungsreaktionen eine erfolgreiche Umsetzung. Da diese und andere Vorarbeiten bereits gezeigt haben, dass Methoxygruppen *para* zur gewünschten Kupplungsstelle von Vorteil sind, wurde **23** über drei Stufen ausgehend von 2-Methoxy-4-nitroanilin hergestellt und mit verschiedenen Schutzgruppen als Testsubstrat verwendet (Schema 13).

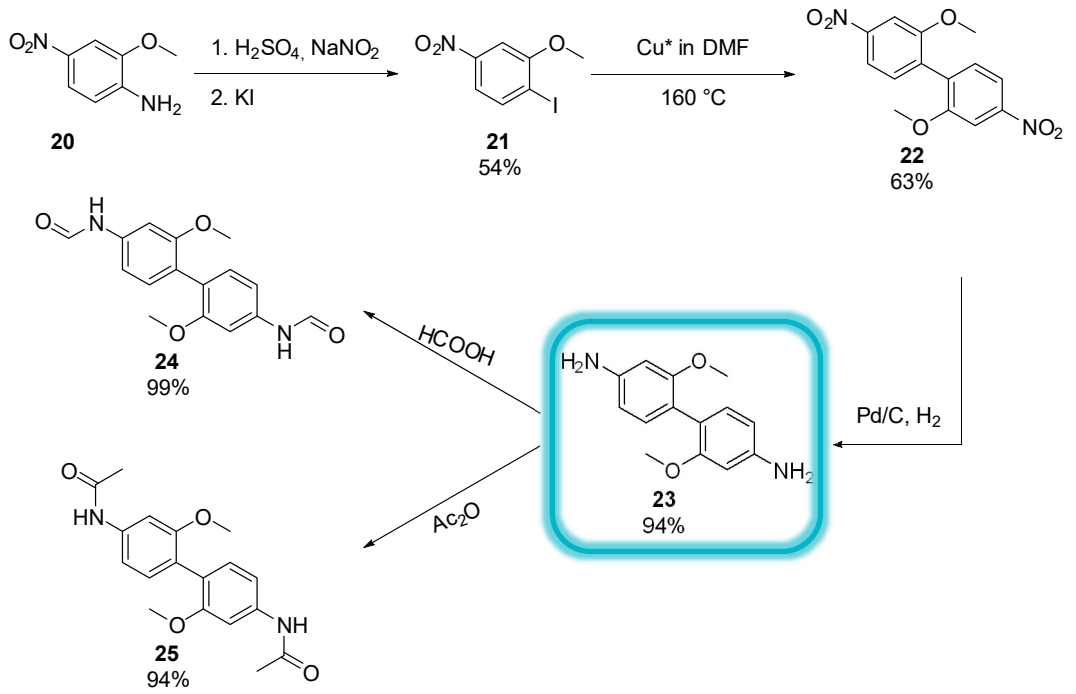

Schema 13: Synthese und Schützung des Benzidinderivats 23. Cu*: aktiviertes Kupfer.

Anschließend wurden die formyl- bzw. acetylgeschützten Benzidinderivate **24** und **25** mit verschieden substituierten und geschützten Anilinderivaten in Screeningreaktionen umgesetzt. Bisher konnte hierbei lediglich eine einfache Kreuzkupplung beobachtet werden. Abbildung 14 zeigt die isolierten einfachen Kreuzkupplungsprodukte **26** und **27**, wobei letzteres bisher nur über HRMS nachgewiesen wurde. Als Nebenprodukte wurden jeweils die Homokupplungsprodukte der Überschusskomponente erhalten.

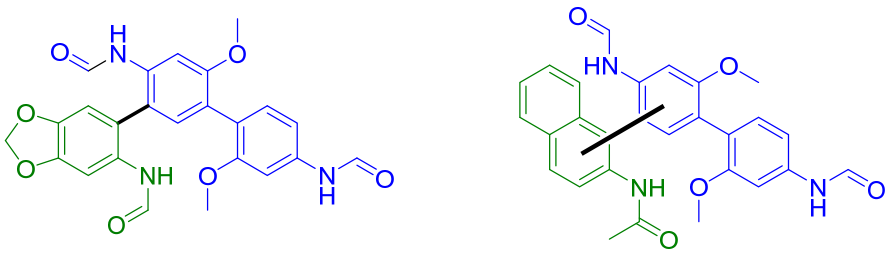

26
41%

27

Abbildung 14: Isolierte Produkte aus den Kreuzkupplungen von Benzidin- mit geschützten Anilinderivaten.

Die erste Kreuzkupplung von Benzidin- und Anilinderivaten konnte erfolgreich durchgeführt werden. Das methoxysubstituierte Benzidinderivat **23** hat sich hierbei als geeignetes Substrat herausgestellt. Bisher konnte allerdings nur eine einfache Kreuzkupplung von **23** mit verschiedenen geschützten Anilinderivaten beobachtet werden. Durch weitere Optimierung der Reaktionsbedingungen ist aber auch eine doppelte Kreuzkupplung denkbar.

Zu den Kapiteln 3.3 und 3.4 wurde ein gemeinsames Manuskript verfasst:

L. Schulz, Jan-Åke Husmann, S. R. Waldvogel, *Outstandingly Robust Anodic Dehydrogenative Aniline Coupling Reaction, Manuskript in Fertigstellung.*

3.5 Anodische Kupplungsreaktionen von Arenen an neuartigen aktiven Nickelelektroden

Während der Untersuchungen zu molybdänbasierten Elektroden in HFIP wurden auch andere Übergangsmetalle auf ihre Eignung als aktive Elektroden hin untersucht.[71] Unter anderem wurden Nickel und Blei mit den für die Molybdän-Elektrode optimierten Bedingungen an 4-Bromveratrol als Modellsubstrat getestet (Schema 14). An der bereits etablierten aktiven Molybdän-Elektrode in HFIP wurde **29** in 75% und an Nickel in 87% Ausbeute erhalten. An der Blei-Anode wurden lediglich Nebenprodukte erhalten.

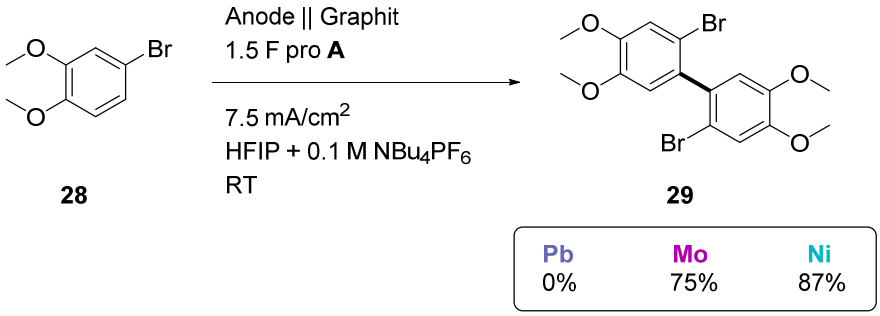

Schema 14: Vergleich verschiedener aktiver Elektrodenmaterialien in der anodischen Kupplung von 28.

Diese Resultate inspirierten zu weiteren Untersuchungen zur Verwendung von Nickelelektroden. Hierbei ist aufgefallen, dass es in einigen Fällen von Vorteil sein kann, wenn das Reaktionsgemisch während der Elektrolyse nicht gerührt wird. Vor allem im Fall des 4-Fluorveratrols wurde dadurch eine drastische Ausbeutensteigerung von 16% auf 42% erreicht (Abbildung 15, Molekül **30**). Es wird die Bildung einer aktiven Schicht auf der Elektrode vermutet, die als eine Art Redoxfilter agiert.

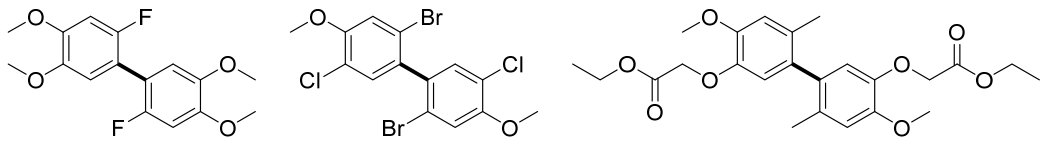

Abbildung 15: Auswahl an Kupplungsprodukten, die an einer Nickel-Anode erhalten wurden. Ausbeuten beziehen sich auf die isolierten Produkte.

Bei der Kupplung eines 2-Arylacetonitrilderivats wurde nicht wie erwartet, das C_{Ar}–C_{Ar}-gekuppelte Produkt erhalten, sondern es fand eine Benzyl-Aryl-Kupplung statt. Es gibt nur wenige Beispiele, die eine solche direkte Synthese von α-Aryl-Benzylnitrilen beschreiben.[72] Solche hochfunktionalisierten Nitrile sind oft in Pharmazeutika wie Anastrozol oder Verapamil zu finden, oder in Naturstoffen wie Cheryllindimethyl-ether.[73] Mehrere benzylische Kreuzkupplungen konnten erfolgreich durchgeführt werden. Anisole oder Biphenyle sind mögliche Kupplungspartner und die entsprechenden Kupplungsprodukte (Abbildung 16, Moleküle **34** und **35** bzw. **33**) konnten in guten Ausbeuten bis 41% erhalten werden. Im Gegensatz zu den in Abbildung 15 gezeigten Transformationen war hier Rühren allerdings unerlässlich. Als Neben-produkte wurden teilweise die entsprechenden HFIP-Ether erhalten.

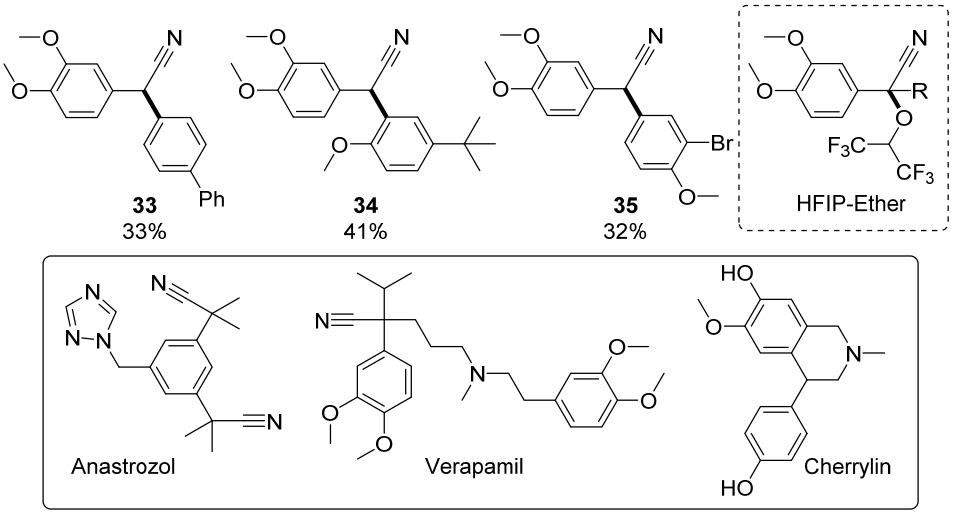

Abbildung 16: Produkte der benzylischen Kreuzkupplung von 2-Arylacetonitril.

Die erste anodische Umsetzung an aktiven Nickel-Anoden in HFIP wurde entwickelt und erfolgreich für die Homokupplung verschiedener Arene sowie für die Benzyl-Aryl-Kreuzkupplung von 2-Arylacetonitril mit verschiedenen Arenen verwendet.

Zu diesem Kapitel wurde ein Manuskript verfasst:

S. B. Beil, **L. Schulz**, M. Breiner, A. Schüll, T. Müller, N. Beiser, D. Schollmeyer, A. Bomm, M. Holtkamp, U. Karst, W. Schade, S. R. Waldvogel, *Active Nickel Electrodes for Anodic Dehydrogenative Arylation Reaction in HFIP and their Unusual Behavior, Manuskript in Fertigstellung.*

4 Unveröffentlichte Ergebnisse

4.1 Verwendung aktiver Nickelelektroden zur Kupplung geschützter Anilinderivate

Im Zuge der Untersuchungen zur Verwendung aktiver Nickelelektroden wurde auch die Kupplung von Anilinderivaten an diesen getestet. Es wurden sowohl Homo- als auch Kreuzkupplungen durchgeführt und der Einfluss des Rührens überprüft (Schema 15).

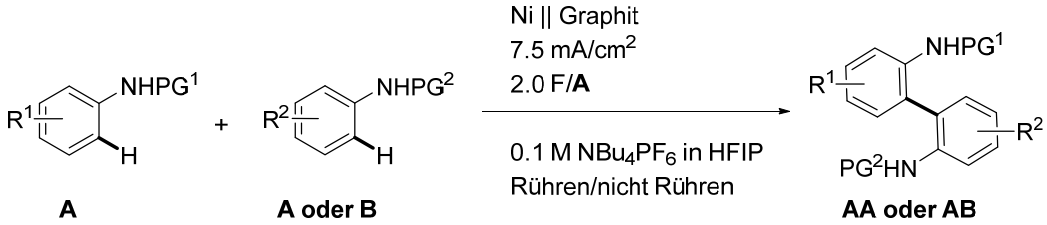

Schema 15: Allgemeines Schema der anodischen Kreuz- und Homokupplung geschützter Anilinderivate an Nickel-Anoden.

Tabelle 2 zeigt exemplarisch zwei der isolierten Produkte, die an Nickel-Anoden erhalten werden konnten. In allen Fällen waren die Ausbeuten wesentlich geringer als die zuvor an Glaskohlenstoff erhaltenen.[27,28] Für die Anilin-Kupplung stellt Nickel somit kein geeignetes Anodenmaterial dar.

Tabelle 2: Vergleich Nickel- und Glaskohlenstoff-Anode.

Eintrag	Produkt	Ausbeute (Nickel-Anode)	Ausbeute (Glaskohlenstoff-Anode)
1	 **36**	10%	46%
2	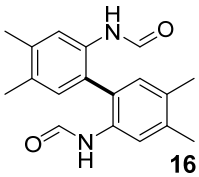 **16**	8%	47%

4.2 Anodische Biarylethersynthese durch C,O-Kupplung von Phenolen

Ein weiteres Thema meiner Doktorarbeit, mit dem ich mich während meines viermonatigen Aufenthalts am Centro Conjunto de Investigación en Química Sustentable UAEM/UNAM in Toluca, Mexiko beschäftigt habe, ist die anodische Biarylethersynthese durch C,O-Kupplung von Phenolen. Biarylether sind wichtige Strukturmotive in vielen Pharmazeutika[74] und Naturstoffen.[75] Beispiele hierfür sind Pierazinomycin, Obovatol oder Thyroxin, aber auch potentielle neue Tumor-Therapeutika beinhalten solche Strukturen.[74] Deshalb ist die Entwicklung einer neuen, einfacheren und „grüneren" Methode, solche Biarylether herzustellen, von großem Interesse. Bisher können solche Strukturen über die kupfermediierte ULLMANN-Ethersynthese[76] oder kupferkatalysierte CHAN-LAM-EVANS-Kupplungen von Arylboranen mit Phenolen erhalten werden.[77] Kürzlich wurde eine Methode veröffentlicht, die solche Biarylether durch radikalische C,O-Kupplung zugänglich macht.[78] Viele klassische Methoden haben die Verwendung von Metallsalzen oder aufwendigen Reaktionsbedingungen gemeinsam. Mildere Bedingungen werden bei der nukleophilen aromatischen Substitution zur Zyklisierung verwendet.[79] Allerdings werden hier hochfunktionalisierte Edukte benötigt, welche über mehrere Stufen hergestellt werden müssen. Auch eine elektrochemische Variante zur Darstellung von Biarylethern ist bereits bekannt.[80] Ein großer Nachteil ist jedoch, dass nur Phenole mit Chlor- oder Bromsubstituenten in beiden *ortho*-Positionen gekuppelt werden können. Dadurch sind die möglichen Kupplungen stark limitiert und die Edukte müssen vorher aufwendig hergestellt werden.

Während Untersuchungen zur anodischen Benzofuran-Phenol-Kreuzkupplung[30] in unserer Gruppe wurde die Bildung eines Biarylethers beobachtet (Schema 16).

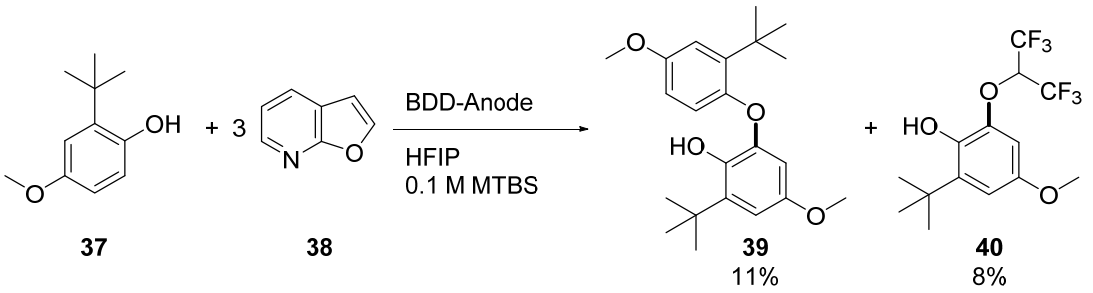

Schema 16: Erste elektrochemische Biarylethersynthese in HFIP.

Statt des gewünschten substituierten Benzofurans wurden der Biarylether **39** sowie der HFIP-Ether **40** erhalten. Frühere Umsetzungen von Phenolen in HFIP ergaben immer das C,C-Kupplungsprodukt,[81] warum wurden hier also plötzlich Ether gebildet? Testreaktionen ohne **38** zeigten, dass das Pyridinderivat nötig ist, um die Ether **39** und **40** zu bilden. Es wurden systematisch weitere Pyridinderivate sowie andere Basen als Additiv getestet. Die Verwendung eines Äquivalents Pyridin als Additiv stellte sich hierbei als am geeignetsten heraus, nach weiterer Optimierung der Parameter konnte der Biarylether **39** in einer Ausbeute von 50% isoliert werden (Schema 17).

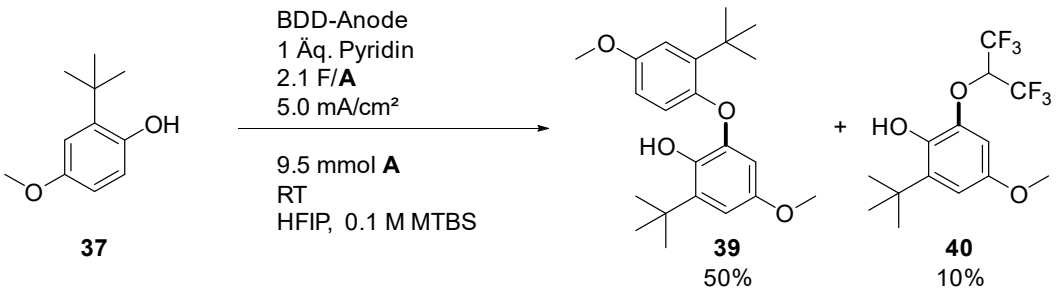

Schema 17: Optimierte Parameter der anodischen C,O-Kupplung.

Erste cyclovoltammetrische Untersuchungen zeigen eine Verschiebung des Oxidationspotentials des Phenols zu niedrigeren Werten bei Zugabe von Pyridin (Abbildung 17).

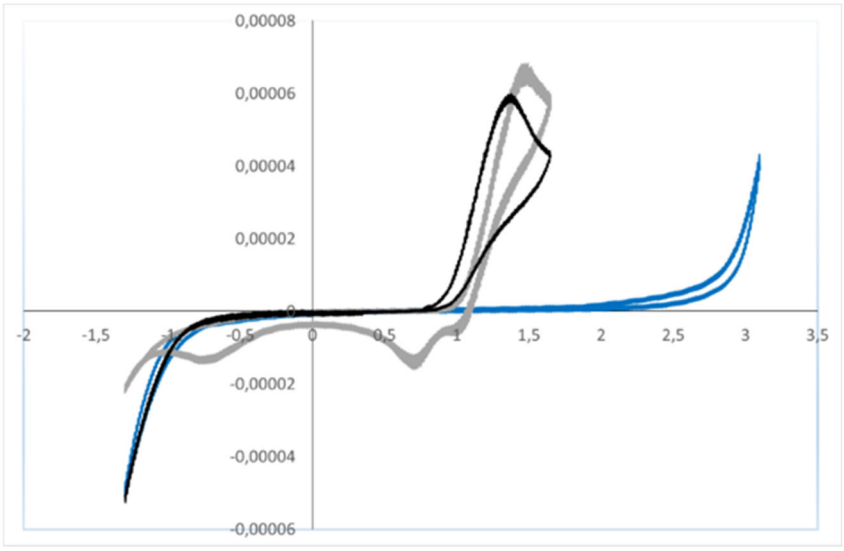

Abbildung 17: Cyclovoltammogramm von 37. WE: BDD, CE: Glaskohlenstoff, RE: Ag/AgCl (LiCl ges. in EtOH), ν=100 mV/s. Blau: Elektrolyt (HFIP + 0.1 M MTBS); grau: 37 in HFIP + 0.1 M MTBS; schwarz: 37 in HFIP + 0.1 M MTBS + 1 Äq. Pyridin.

Bei der Umsetzung von 3,4,5-Trimethoxyphenol **41** entstand nicht der gewünschte Biarylether, sondern ein Tricyclus, der Ähnlichkeiten zum Pummerer-Keton aufweist. Produkt **42** konnte in einer Ausbeute von 51% isoliert werden (Schema 18).

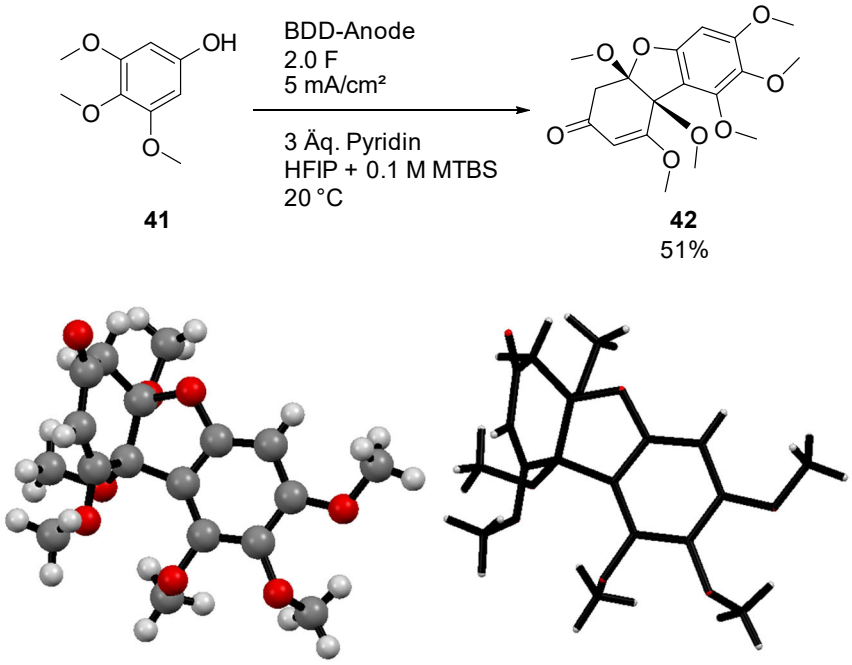

Schema 18: Oben: Anodische Umsetzung von 3,4,5-Trimethoxyphenol; unten: Molekülstruktur von 42.

Auch bei der Umsetzung von **43** wurde nicht der gewünschte Biarylether erhalten, sondern das symmetrische C,C-Kupplungsprodukt **46** als Hauptprodukt, der Tricyclus **44**, sowie **45** (Schema 19).

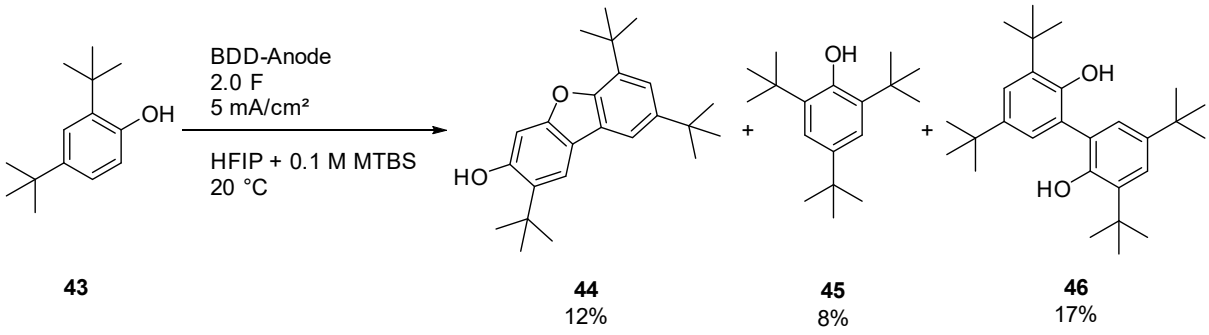

Schema 19: Anodische Umsetzung von 43.

Aufbauend auf diesen Ergebnissen wurden auch Kreuzkupplungen durchgeführt, um hochfunktionalisierte Tricyclen zu erhalten. Die Kreuzkupplung von **37** und **41** ergab den Tricyclus **47** (Schema 20).

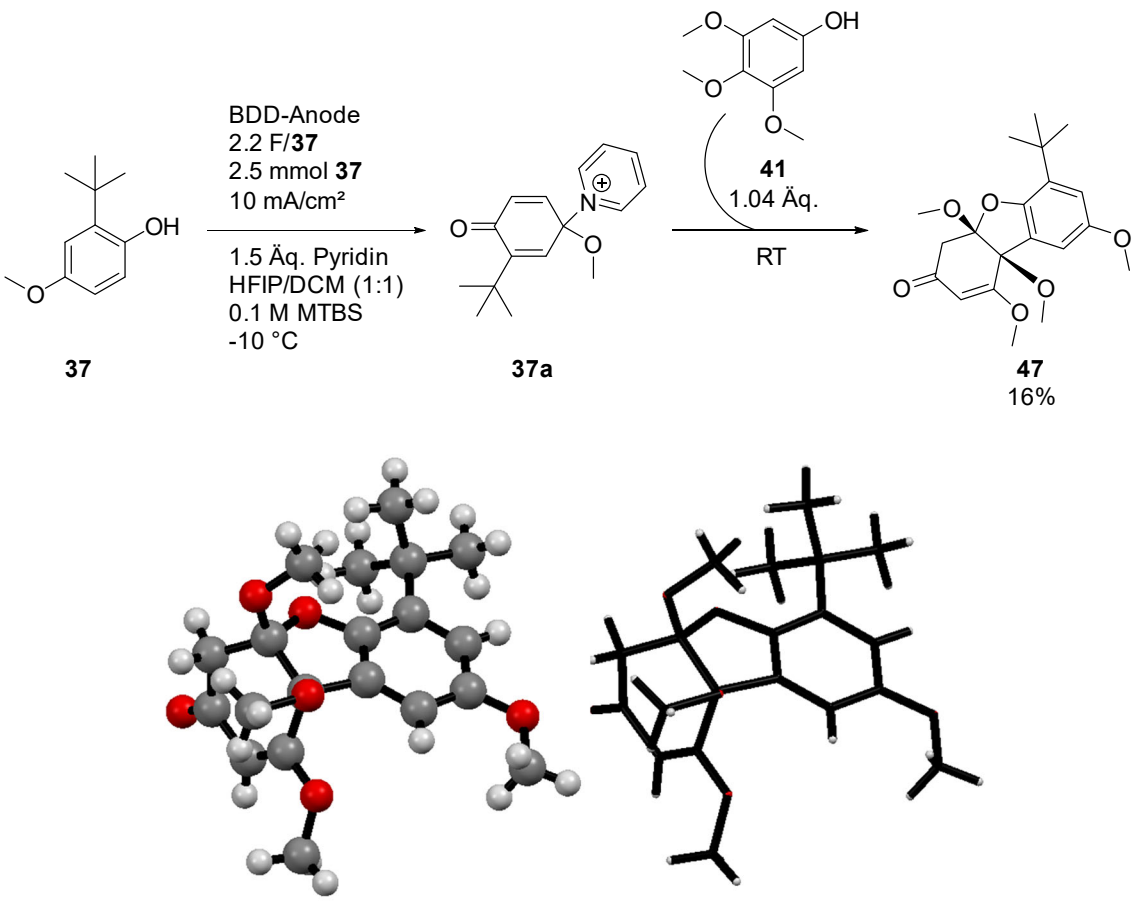

Schema 20: Oben: Kupplungsreaktion zwei verschiedener Phenole zum Tricyclus 47; unten: Molekülstruktur von 47.

Für die Kreuzkupplung wurde ein Vorgehen, ähnlich der „cation pool method“ von YOSHIDA gewählt.[14–16] Hierfür wurde zunächst Phenol **37** bei –10 °C elektrolysiert, nach beendeter Elektrolyse **41** zugegeben und anschließend ohne Kühlung 0.5 h gerührt. Versuche, die bei Zimmertemperatur durchgeführt wurden, ergaben nicht das gewünschte Kreuzkupplungsprodukt. Dies spricht dafür, dass das Intermediat **37a** ausschließlich bei niedrigeren Temperaturen eine ausreichend lange Lebenszeit hat, damit es nach Zugabe der **B**-Komponente zu einer Kreuzkupplung kommen kann. Bei Raumtemperatur wird ausschließlich das C,O-Homokupplungsprodukt von **37** erhalten. HFIP besitzt einen Schmelzpunkt von –4 °C,[37] weshalb für Elektrolysen bei tieferen Temperaturen eine 1:1-Mischung aus HFIP und Dichlormethan (DCM) als Lösungsmittel verwendet wurde.

5 Zusammenfassung

Im Rahmen der vorliegenden Arbeit konnte das Spektrum elektrochemisch zugänglicher Kupplungsprodukte um die Synthese verschiedener symmetrischer sowie unsymmetrischer Biaryle erweitert werden. Der Fokus lag vor allem auf der elektrochemischen Synthese unsymmetrischer 2,2‘-Diaminobiaryle, welche eine deutliche Vereinfachung zu bisher genutzten klassischen Synthesen darstellt. Die Schützung der Aminofunktion, um eine anodische Polymerisation zu verhindern und die Einbettung in das HFIP-Wasserstoffbrückenbindungsnetzwerk zu verbessern, ist hierbei essentiell. Die Verwendung unterschiedlicher, carbonylbasierter Schutzgruppen erlaubt eine sehr leichte und selektive Freisetzung der Aminofunktionen nach der Elektrolyse. Durch die Verwendung formylgeschützter Aniline konnten erstmals auch elektronenärmere Derivate erfolgreich gekuppelt werden. Aufgrund der milden Reaktionsbedingungen werden auch Halogensubstituenten wie Chlor oder Iod toleriert, was eine spätere Weiterfunktionalisierung der Biaryle erlaubt. So konnten sowohl unsymmetrische, als auch symmetrische 2,2‘-Diaminobiaryle auf einfache Weise durch eine direkte anodische C,C-Kupplung ausgehend von geschützten Anilinderivaten hergestellt werden (Abbildung 18).[27,28] Durch die selektiv freisetzbaren Aminofunktionen stellen die gezeigten 2,2‘-Diaminobiaryle interessante Bausteine für Liganden, Organokatalysatoren oder funktionalisierte Materialien dar.[82]

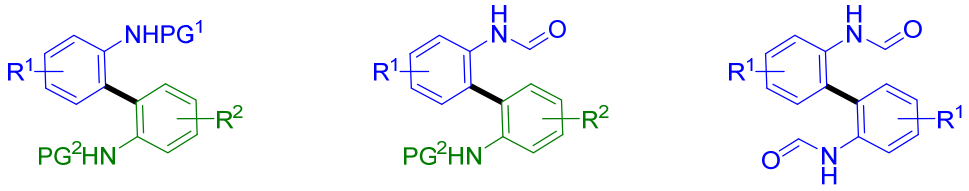

Abbildung 18: Übersicht elektrochemisch dargestellter, geschützter 2,2‘-Diaminobiaryle.[27,28]

Am Beispiel von *N*-(3,4-Dimethylphenyl)formamid wurde die Homokupplung von weniger elektronenreichen Anilinen optimiert, die Ausbeute konnte von 47% auf 64% gesteigert werden. Während der Optimierung zeigte sich, dass auch sehr hohe Stromdichten von bis zu 100 mA/cm^2 erfolgreich verwendet werden können.

Aufbauend auf diesen Ergebnissen wurden erste Studien zur doppelten Kreuzkupplung von Anilinen und Benzidinderivaten durchgeführt. Bisher konnte jeweils die einfache Kupplung zwischen dem Benzidinderivat und Anilinen beobachtet werden (Abbildung 19).

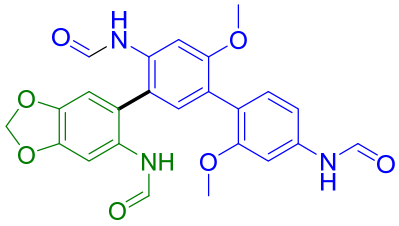

26
41%

Abbildung 19: Anodische Kreuzkupplung geschützter Benzidinderivate mit Anilinen.

Darüber hinaus wurde Nickel als neuartiges, aktives Elektrodenmaterial auf seine Anwendbarkeit in anodischen Anilin- und Aren-Kupplungen getestet. Verschieden substituierte Arene konnten damit in Ausbeuten bis 76% erfolgreich gekuppelt werden. Für die Anilin-Kupplung ist Nickel hingegen kein geeignetes Elektrodenmaterial.

Es konnte zudem ein Verfahren zur anodischen C,O-Kupplung von Phenolen erarbeitet und optimiert werden, mit welchem sowohl Homokupplungen, als auch eine erste Kreuzkupplung realisiert werden konnten. In den meisten Fällen wird allerdings nicht wie gewünscht der Biarylether erhalten, sondern tricyclische Systeme (Abbildung 20).

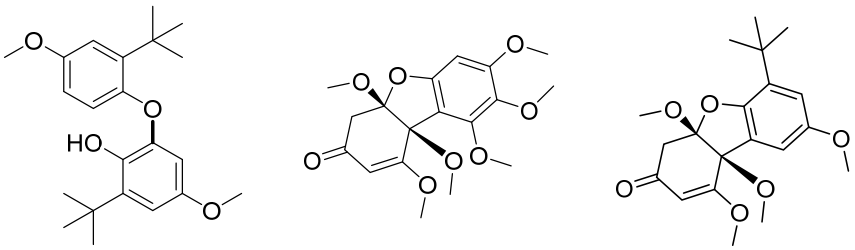

39
50%

42
51%

47
16%

Abbildung 20: Biphenolether 39 (links) und tricyclische Systeme 42 und 47, die durch Pyridinzugabe zur Elektrolyse erhalten wurden.

Abschließend wurden in dieser Arbeit nachhaltige und einfach durchzuführende, elektrochemische Synthesen verschiedener Biarylderivate entwickelt, die ohne Abgangsfunktionalitäten oder Oxidationsmittel auskommen und eine deutliche Verbesserung zu bisher bekannten klassischen organischen Synthesen darstellen.

6 *Ausblick*

Aufbauend auf den in dieser Arbeit gewonnenen Erkenntnissen ergeben sich eine Vielzahl interessanter Möglichkeiten, die auf den jeweiligen Themengebieten noch untersucht werden können:

Erste Versuche zu einer doppelten anodischen Kreuzkupplung von Anilinderivaten haben bisher lediglich die einfach gekuppelten Produkte ergeben. Durch weitere Optimierung der Reaktionsparameter sowie cyclovoltammetrische Studien und geschickter Wahl der Schutzgruppen sollte auch eine doppelte Kupplung am Benzidinderivat **23** möglich sein. Denkbar wäre auch eine zweistufige Synthese ähnlich der *meta*-Terphenylsynthese von LIPS *et al.*,[29] in der zunächst das **AB**-System hergestellt und isoliert wird und anschließend in einer zweiten Elektrolyse ein weiteres Anilin **C** an das **AB**-System gekuppelt wird (Schema 21). Denkbar wäre neben Anilinen auch die Verwendung von Phenolen oder anderen Aromaten als **C**-Komponente. Ebenfalls interessant wäre die elektrochemische Generierung von Benzidinderivaten durch eine selektive Kupplung *para* zur Aminofunktion.

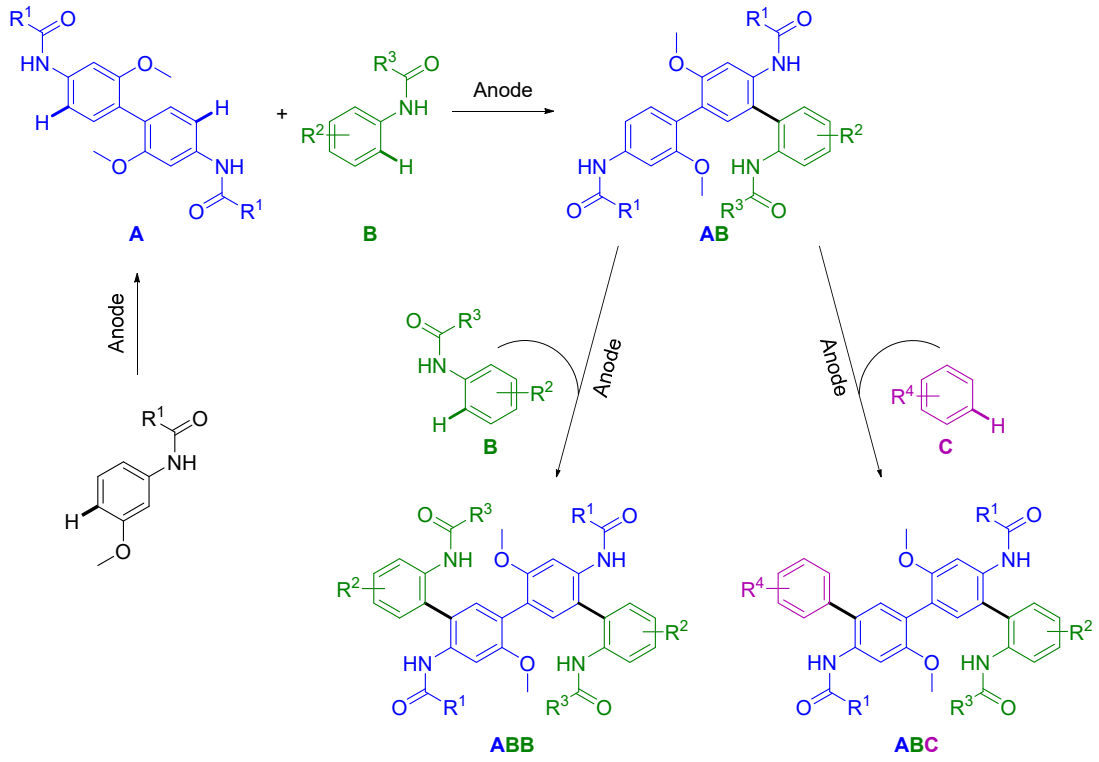

Schema 21: Mögliche zweistufige Synthese von Quarterarylderivate.

Erste Studien zur anodischen C,O-Kupplung ergaben größtenteils dem Pummerer-Keton ähnelnde Tricyclen. Diese Tatsache könnte man nutzen, um weitere Tetrahydrodibenzofurane herzustellen, welche unter anderem als Morphinanaloga auf ihre Wirksamkeit als Antitussiva getestet wurden.[83] Des Weiteren kann eine Optimierung der Reaktionsparameter durchgeführt werden, um statt der genannten Tricyclen selektiv das C,O-gekuppelte Produkt zu erhalten. In der Kreuzkupplung könnten statt eines weiteren Phenols als **B**-Komponente auch andere Arene, wie z.B. Aniline eingesetzt werden (Schema 22). Biarylether sind ein häufiges Strukturmotiv in Naturstoffen und biologisch aktiven Substanzen, deshalb könnte der Einsatz der gezeigten Methode in der Synthese solcher Wirkstoffe von großem Nutzen sein.[74,75]

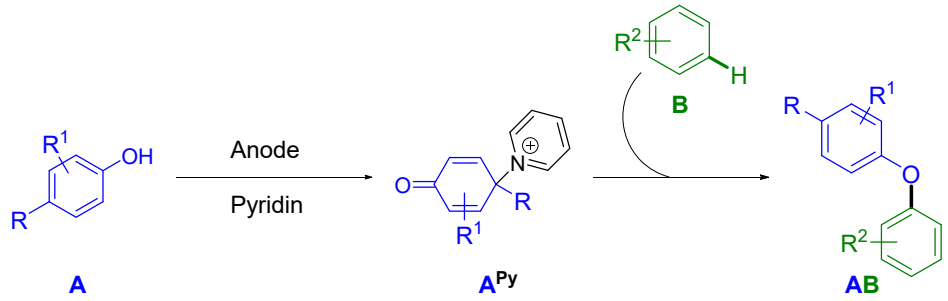

Schema 22: Vorschlag zur anodischen C,O-Kreuzkupplung von Phenolen mit Arenen. Denkbare B-Komponenten sind Phenole, Aniline, Arene oder Thiophene.

Neben der anodischen C,C- sowie C,O-Kupplung sind auch C,N- oder N,N-Kupplungen von großem Interesse. Vor allem die Steuerung der Verknüpfungsstelle allein durch die Wahl des Elektrolyten und der Elektrolyseparameter wäre äußerst attraktiv. V. BREISING arbeitet derzeit vor allem an der anodischen N,N-Kupplung acetylgeschützter Aniline (Schema 23).

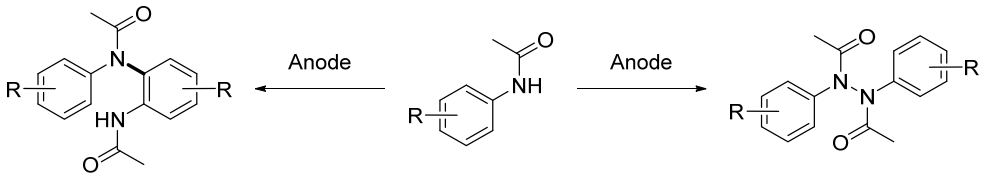

Schema 23: Anodische C,N- bzw. N,N-Kupplung acetylgeschützter Anilinderivate.

Auch dieser Reaktionstyp kann Anwendung in der Synthese biologisch aktiver Moleküle finden, wie die Gruppe um BARAN bereits in der Totalsynthese von Dixiamycin B zeigen konnte.[84]

7 Experimenteller Teil

Alle Reagenzien wurden ohne weitere Aufreinigung verwendet. Als Leitsalz wurde *N*-Methyl-*N,N,N*-tributylammoniummethylsulfat (MTBS, freundlicherweise zur Verfügung gestellt von BASF SE, Ludwigshafen, Deutschland) verwendet. Für die elektrochemischen Reaktionen wurden Elektroden aus Glaskohlenstoff (SIGRADUR® G; von HTW Hochtemperaturwerkstoffe GmbH, Thierhaupten, Deutschland), Bor-dotiertem Diamant (DIACHEM®, 15 µm Bor-dotierte Diamantschicht auf 3 mm Silizium als Trägermaterial; von CONDIAS GmbH, Itzehoe, Deutschland), isostatischem Graphit (SIGRAFINE® V2100; von SGL Carbon, Bonn-Bad Godesberg, Deutschland) oder Platin (99.9% Pt; ÖGUSSA GES.mbH, Wien, Österreich) verwendet.

Chromatographie: Die präparativen flüssigkeitschromatographischen Trennungen via „Flashchromatographie“ wurden an Kieselgel 60 M (0.04–0.063 mm) der Firma MACHEREY-NAGEL GMBH & CO KG, Düren, durchgeführt. Hierfür wurde ein modulares Chromatographie-System der Firma BÜCHI LABORTECHNIK AG, Flawil, Schweiz, mit einer Kontrolleinheit C-620, einem Fraktionssammler C-660, einem UV-Photometer C-635 und zwei Pumpenmodulen C-605 verwendet. Als Säulen dienten die Kartuschen PP 12/150 oder PP 40/150 der Firma BÜCHI LABORTECHNIK AG, Flawil, Schweiz. Die als Eluenten verwendeten Lösungsmittel (Essigsäureethylester (technisch), Cyclohexan (technisch)) wurden zuvor destillativ am Rotationsverdampfer gereinigt. Verhältnisangaben zum Lösungsmittelgemisch beziehen sich auf Volumenverhältnisse.

Zur Dünnschichtchromatographie (DC) wurden Aluminium-Fertigplatten Kieselgel 60 F254 der Firma MERCK KGAA, Darmstadt, verwendet. Die R_f-Werte sind in Abhängigkeit vom verwendeten Laufmittelgemisch angegeben. Die Substanzen wurden unter UV-Licht (λ = 254 nm) nachgewiesen.

Gaschromatographie (GC/GCMS): Die gaschromatographische Untersuchung (GC) von Produktgemischen und Reinsubstanzen erfolgte mit Hilfe des Gaschromatographen GC-2025 der Firma SHIMADZU, Japan. Es wurde an einer Quarzkapillarsäule ZB-5 der Firma PHENOMENEX, USA (Länge: 30 m; Innendurchmesser: 0.25 mm; Filmdicke der kovalent gebundenen stationären Phase: 0.25 µm; Trägergas: Wasserstoff; Injektortemperatur: 250 °C; Detektortemperatur 310 °C) gemessen. Es wurde die Methode „hart“ mit 50 °C

Starttemperatur für 1 min, einer Heizrate von 15 °C/min und 290 °C Endtemperatur für 8 min verwendet. Gaschromatographische Massenspektren (GC-MS) von Produktgemischen und Reinsubstanzen wurden mit Hilfe des Gaschromatographen GC-2010 kombiniert mit dem Massendetektor GCMS-QP2010 der Firma SHIMADZU, Japan aufgenommen. Es wurde an einer Quarzkapillarsäule ZB-5 der Firma PHENOMENEX, USA (Länge: 30 m; Innendurchmesser: 0.25 mm; Filmdicke der kovalent gebundenen stationären Phase: 0.25 µm Trägergas: Wasserstoff; Injektortemperatur: 250 °C; Detektortemperatur 310 °C) gemessen. Es wurde die Methode „hart" mit 50 °C Starttemperatur für 1 min, einer Heizrate von 15 °C/min, einer Endtemperatur von 290 °C für 8 min und einer Temperatur der Ionenquelle von 200 °C verwendet.

Schmelzpunkte: Schmelzpunkte wurden mit Hilfe des Schmelzpunktbestimmungsgeräts M-565 der Firma BÜCHI, Schweiz gemessen und sind unkorrigiert. Heizrate: 2 °C/min.

Massenspektrometrie: Alle Elektrosprayionisations-Messungen (ESI+) wurden an einem QTof Ultima 3 der Firma WATERS MICROMASSES, Milford, Massachusetts durchgeführt. EI-Massenspektren sowie die hochaufgelösten EI-Spektren wurden an einem Gerät des Typs MAT 95 XL Sektorfeldgerät der Firma THERMO FINNIGAN, Bremen, gemessen.

NMR-Spektroskopie: Die NMR-spektroskopischen Untersuchungen wurden an einem Multikernresonanzspektrometer des Typs Avance II 400 der Firma BRUKER, Analytische Messtechnik, Karlsruhe, durchgeführt. Als Lösungsmittel wurde $CDCl_3$, d_6-DMSO oder d_6-Aceton verwendet. Die ^1H- und ^{13}C-Spektren wurden gemäß dem Restgehalt an nicht deuteriertem Lösungsmittel nach der NMR Solvent Data Chart der Firma CAMBRIDGE ISOTOPES LABORATORIES, USA, kalibriert. Die chemischen Verschiebungen sind als δ-Werte in ppm angegeben. Für die Multiplizitäten der NMR-Signale wurden folgende Abkürzungen verwendet: s (Singulett), bs (breites Singulett), d (Dublett), t (Triplett), q (Quartett), m (Multiplett), dd (Dublett von Dublett), dt (Dublett von Triplett), tq (Triplett von Quartett). Alle Kopplungskonstanten *J* wurden in Hertz (Hz) angegeben.

Einkristall-Röntgenstrukturanalysen wurden an einem STOE IPDS-2T-Diffraktometer der Firma STOE&CIE GMBH, Darmstadt, Deutschland, unter Verwendung eines Mo-K_α-Graphitmonochromators (λ = 0.71073 Å) angefertigt. Die Auswertung erfolgte mit den

Programmen SIR-2004 (Direkte Methoden) oder SHELXT-2014, die Verfeinerung mit dem Programm SHELXL-2014 (Vollmatrixverfahren).

7.1 Allgemeine Arbeitsvorschriften

AAV1: Arbeitsvorschrift zur elektrochemischen C,C-Kreuzkupplung im Screeningmaßstab

In einer ungeteilten Screeningzelle wird eine Lösung aus geschützter Anilinkomponente **A** (0.375 mmol, 1.0 Äq.) und geschützter Anilinkomponente **B** (0.75 mmol, 2.0 Äq.) in 5 mL HFIP bzw. HFIP + 18% vol. MeOH angesetzt. Als Leitsalz wird Methyltributylammoniummethylsulfat (MTBS) mit einer Konzentration von 0.09 mol/L verwendet. Die Elektrolyse wird in einer Teflonzelle, die in einem Stahlsockel befestigt ist, unter galvanostatischen Bedingungen durchgeführt. Nach beendeter Elektrolyse werden ca. 100 µL der abgekühlten Reaktionslösung entnommen und über 0.4 g Kieselgel 60 mit ca. 2.5 mL Ethylacetat als Eluenten filtriert. Das erhaltene Filtrat wird mittels GC auf entstandene Kreuzkupplungsprodukte untersucht. Die Aufreinigung erfolgt säulenchromatographisch. Folgende Standardbedingungen werden für die Elektrolyse verwendet:

Elektrodenmaterial:

Anode: Glaskohlenstoff (SIGRADUR® G)

Kathode: Glaskohlenstoff (SIGRADUR® G)

Elektrolysebedingungen:

Temperatur [T]: 50 °C

Stromdichte [j]: 7.2 mA·cm^{-2}

Ladungsmenge [Q]: 72.4 C (2.0 F bezogen auf die Unterschusskomponente **A**)

AAV2: Arbeitsvorschrift zur elektrochemischen C,C-Homokupplung im Screeningmaßstab

In einer ungeteilten Screeningzelle wird eine Lösung aus geschützter Anilinkomponente **A** (0.75 mmol, 2.0 Äq.) in 5 mL HFIP bzw. HFIP + 18% vol. MeOH angesetzt. Als Leitsalz wird Methyltributylammoniummethylsulfat (MTBS) mit einer Konzentration von 0.09 mol/L verwendet. Die Elektrolyse wird in einer Teflonzelle, die in einem Stahlsockel befestigt ist, unter galvanostatischen Bedingungen durchgeführt. Nach beendeter Elektrolyse werden ca. 100 µL der abgekühlten Reaktionslösung entnommen und über 0.4 g Kieselgel 60 mit ca. 2.5 mL Ethylacetat als Eluenten filtriert. Das erhaltene Filtrat wird mittels GC auf entstandene Homokupplungsprodukte untersucht. Die Aufreinigung erfolgt säulenchromatographisch. Folgende Standardbedingungen werden für die Elektrolyse verwendet:

Elektrodenmaterial:

Anode: Glaskohlenstoff (SIGRADUR® G)

Kathode: Glaskohlenstoff (SIGRADUR® G)

Elektrolysebedingungen:

Temperatur [T]: 50 °C

Stromdichte [j]: 7.2 mA·cm^{-2}

Ladungsmenge [Q]: 72.4 C (1.0 F bezogen auf die Komponente **A**)

AAV3: Arbeitsvorschrift zur doppelten elektrochemischen C,C-Kreuzkupplung im Screeningmaßstab

In einer ungeteilten Screeningzelle wird eine Lösung aus geschützter Benzidinkomponente **A** (0.375 mmol, 1.0 Äq.) und geschützter Anilinkomponente **B** (1.125 mmol, 3.0 Äq.) in 5 mL HFIP bzw. HFIP + 18% vol. MeOH angesetzt. Als Leitsalz wird Methyltributylammoniummethylsulfat (MTBS) mit einer Konzentration von 0.09 mol/L verwendet. Die Elektrolyse wird in einer Teflonzelle, die in einem Stahlsockel befestigt ist, unter galvanostatischen Bedingungen durchgeführt. Nach beendeter Elektrolyse werden ca. 100 µL der abgekühlten Reaktionslösung entnommen und über

0.4 g Kieselgel 60 mit ca. 2.5 mL Ethylacetat als Eluenten filtriert. Das erhaltene Filtrat wird mittels GC auf entstandene Kreuzkupplungsprodukte untersucht. Die Aufreinigung erfolgt säulenchromatographisch. Folgende Standardbedingungen werden für die Elektrolyse verwendet:

Elektrodenmaterial:

Anode: Glaskohlenstoff (SIGRADUR® G)

Kathode: Glaskohlenstoff (SIGRADUR® G)

Elektrolysebedingungen:

Temperatur [*T*]: 50 °C

Stromdichte [*j*]: 7.2 mA·cm^{-2}

Ladungsmenge [*Q*]: 72.4 C (4.0 F bezogen auf die Unterschusskomponente **A**)

AAV4: Arbeitsvorschrift für elektrochemische C,O-Homokupplungen im Screeningmaßstab

In einer ungeteilten Screeningzelle wird eine Lösung aus einem Phenol (0.38 mmol, 1.0 Äq.) und Pyridin (1.0–3.0 Äq.) in 5 mL HFIP angesetzt. Als Leitsalz wird Methyltributylammoniummethylsulfat (MTBS) mit einer Konzentration von 0.1 mol/L verwendet. Die Elektrolyse wird in einer Teflonzelle, die in einem Stahlsockel befestigt ist, unter galvanostatischen Bedingungen durchgeführt. Nach beendeter Reaktion werden ca. 100 µL der Reaktionslösung entnommen und über 0.4 g Kieselgel 60 mit ca. 2.5 mL Ethylacetat als Eluenten filtriert. Das erhaltene Filtrat wird mittels GC auf entstandene Kupplungsprodukte untersucht. Die Aufreinigung erfolgt säulenchromatographisch. Folgende Standardbedingungen werden für die Elektrolyse verwendet:

Elektrodenmaterial:

Anode: Bor-dotierter Diamant (15 µm auf Silicium)

Kathode: Bor-dotierter Diamant (15 µm auf Silicium)

Elektrolysebedingungen:

Temperatur [*T*]: 20 °C

Stromdichte [*j*]: 5.0 mA·cm^{-2}

Ladungsmenge [*Q*]: 73 C (1.0 F bezogen auf die Phenolkomponente)

AAV5: Arbeitsvorschrift für elektrochemische C,O-Homokupplungen im mittelgroßen Maßstab

In einer ungeteilten Becherglaszelle wird eine Lösung aus einem Phenol (9.5 mmol, 1.0 Äq.) und Pyridin (1.0–3.0 Äq.) in 30 mL HFIP angesetzt. Als Leitsalz wird Methyltributylammoniummethylsulfat (MTBS) mit einer Konzentration von 0.1 mol/L verwendet. Die Elektrolyse wird unter galvanostatischen Bedingungen durchgeführt. Die Aufreinigung erfolgt säulenchromatographisch. Folgende Standardbedingungen werden für die Elektrolyse verwendet:

Elektrodenmaterial:

Anode: Bor-dotierter Diamant (15 µm auf Silicium)

Kathode: Bor-dotierter Diamant (15 µm auf Silicium)

Elektrolysebedingungen:

Temperatur [*T*]: 20 °C

Stromdichte [*j*]: 5.0 mA·cm^{-2}

Ladungsmenge [*Q*]: 1833.2 C (1.0 F bezogen auf die Phenolkomponente)

AAV6: Arbeitsvorschrift für elektrochemische C,O-Kreuzkupplungen im Screeningmaßstab

In einer ungeteilten Screeningzelle wird eine Lösung aus Phenol **A** (0.38 mmol, 1.0 Äq.) und Pyridin (1.0–1.5 Äq.) in 5 mL HFIP/DCM (1:1) angesetzt. Als Leitsalz wird Methyltributylammoniummethylsulfat (MTBS) mit einer Konzentration von 0.1 mol/L verwendet. Die Elektrolyse wird in einer Teflonzelle, die in einem Stahlsockel befestigt ist, unter galvanostatischen Bedingungen durchgeführt. Nach beendeter Elektrolyse wird die Phenolkomponente **B** (0.4 mmol, 1.05 Äq.) zu der Reaktionsmischung gegeben und

bei 20 °C für 0.5 h gerührt. Nach beendeter Reaktion werden ca. 100 µL der Reaktionslösung entnommen und über 0.4 g Kieselgel 60 mit ca. 2.5 mL Ethylacetat als Eluenten filtriert. Das erhaltene Filtrat wird mittels GC auf entstandene Kupplungsprodukte untersucht. Die Aufreinigung erfolgt säulenchromatographisch. Folgende Standardbedingungen werden für die Elektrolyse verwendet:

Elektrodenmaterial:

Anode: Bor-dotierter Diamant (15 µm auf Silicium)

Kathode: Bor-dotierter Diamant (15 µm auf Silicium)

Elektrolysebedingungen:

Temperatur [*T*]: -10 °C

Stromdichte [*j*]: 5.0 mA·cm^{-2}

Ladungsmenge [*Q*]: 73 C (2.0 F bezogen auf Komponente **A**)

AAV7: Darstellung *N*-formylgeschützter Aniline

Das zu schützende Anilin (1.0 Äq,) wird in Ameisensäure (98%, 3.0–10.0 Äq.) gelöst und bei 90 °C im Druckrohr über Nacht gerührt. Nach beendeter Reaktion wird das Lösungsmittel unter vermindertem Druck entfernt. Die erhaltenen Formamide können ohne weitere Aufarbeitung eingesetzt werden.

AAV8: Darstellung *N*-acetyl- oder *N*-trifluoracetylgeschützter Aniline

Das zu schützende Anilin (1.0 Äq.) wird in einem Rundkolben in Dichlormethan gelöst. Unter Eiskühlung wird Essigsäureanhydrid bzw. Trifluoressigsäureanhydrid (1.2 Äq.) unter starkem Rühren zugetropft und anschließend bei 20 °C über Nacht gerührt. Nach beendeter Reaktion wird das Lösungsmittel unter vermindertem Druck entfernt. Die erhaltenen Acetamide bzw. Trifluoracetamide können ohne weitere Aufarbeitung eingesetzt werden.

7.2 Doppelte Kreuzkupplung von Anilin- und Benzidinderivaten

4,4‘-Diacetamido-2,2‘-dimethoxybiphenyl (25)

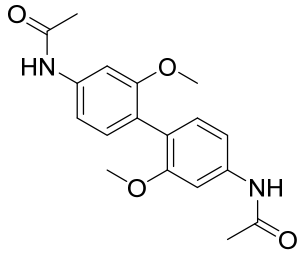

Gemäß *AAV8* werden 1.0 g (4.1 mmol, 1.0 Äq.) 2,2‘-Dimethoxy-4,4‘-diaminobiphenyl in 30 mL DCM gelöst. Unter starkem Rühren und Eiskühlung werden 1.3 mL (12.3 mmol, 3.0 Äq.) Essigsäureanhydrid zugetropft. Das Reaktionsgemisch wird über Nacht bei 25 °C gerührt und anschließend das Lösungsmittel unter vermindertem Druck entfernt.

Ausbeute: 99% (4.05 mmol, 1.33 g), gelbliches Pulver.

Charakterisierung:

R_f (CH:EE = 0:1): 0.31.

Schmelzpunkt: Zersetzung oberhalb 300 °C.

^{1}H-NMR (400 MHz, d_6-DMSO): δ (ppm) = 9.97 (s, 2H), 7.35 (d, J=2.0 Hz, 2H), 7.13 (dd, *J*=8.2, 2.0 Hz), 7.0 (d, J=8.2 Hz, 2H), 3.64 (s, 6H), 2.05 (s, 6H).

^{13}C-NMR (101 MHz, d_6-DMSO): δ (ppm) = 24.54, 55.68, 102.99, 111.07, 122.32, 131.52, 140.01, 157.22, 168.72.

HRMS für $C_{18}H_{20}N_2O_4$ (ESI+) $[M+H]^+$: ber.: 329,1496; gef.: 329,1502.

HRMS für $C_{24}H_{21}N_3O_7$ (ESI+) $[M+Na]^+$: ber.: 486.1277; gef.: 486.1268.

Molekül (27)

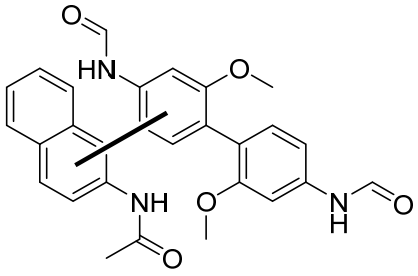

In einer Screeningzelle werden gemäß *AAV3* 112 mg (0.375 mmol, 1.0 Äq.) 4,4‘-Diformamido-2,2‘-dimethoxybiphenyl **24** zusammen mit 208 mg (1.125 mmol, 3.0 Äq.) 2-Acetamidonaphthalin in 5 mL HFIP + MTBS (0.09 M) gelöst und bei einer Temperatur von 50 °C mit einer Ladungsmenge von 146 C (4.0 F bezogen auf die Biphenylkomponente) elektrochemisch umgesetzt.

Die Aufreinigung des Produktgemisches erfolgt säulenchromatographisch (Eluent: CH:EE = 8:2 → 0:1).

Ausbeute: 2% (0.008 mmol, 4 mg), farbloses Pulver.

Charakterisierung:

R_f (CH:EE = 0:1): 0.2.

HRMS für $C_{28}H_{25}N_3O_5$ (ESI+) $[M+Na]^+$: ber.: 506.1692; gef.: 506.1678.

7.3 Biarylethersynthese durch anodische C,O-Kupplung

2-(1,1-Dimethylethyl)-6-(2'-(1,1-dimethylethyl)-4'-methoxyphenoxy-4-methoxyphenol (39)

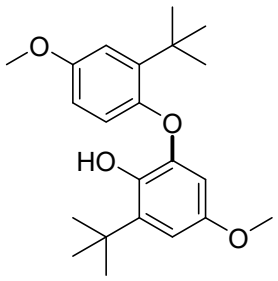

In einer Becherglaszelle werden gemäß *AAV5* 1.71 g (9.5 mmol, 1.0 Äq.) 2-(1,1-Dimethylethyl)-4-methoxyphenol zusammen mit 0.81 mL (10.0 mmol, 1.05 Äq.) Pyridin in 30 mL HFIP + MTBS (0.1 M) gelöst und bei einer Temperatur von 20 °C mit einer Ladungsmenge von 1930 C (1.05 F bezogen auf die Phenolkomponente) elektrochemisch umgesetzt.

Die Aufreinigung des Produktgemisches erfolgt säulenchromatographisch (Eluent: CH:EE = 1:0 → 99:1).

Ausbeute: 50% (2.38 mmol, 0.85 g), farbloser Feststoff.

Charakterisierung:

^{1}H-NMR (400 MHz, d_6-DMSO): δ (ppm) = 7.00 (d, *J* = 3.0 Hz, 1H), 6.79 (d, *J* = 8.8 Hz, 1H), 6.69 (dd, *J* = 8.8, 3.0 Hz, 1H), 6.63 (d, *J* = 2.9 Hz, 1H), 6.22 (d, *J* = 2.9 Hz, 1H), 5.68 (s, 1H), 3.82 (s, 3H), 3.67 (s, 3H), 1.48 (s, 9H), 1.45 (s, 9H).

^{13}C-NMR (101 MHz, d_6-DMSO): δ (ppm) = 155.67, 152.26, 149.04, 145.39, 142.39, 140.18, 137.42, 120.76, 114.05, 111.06, 107.30, 101.09, 55.81, 55.70, 35.19, 35.06, 3x30.40, 3x29.53.

(4aS, 9bS)-4*H*-1,4a,7,8,9,9b-Hexamethoxy-4a,9b-dihydrodibenzo[*b,d*]furan-3-on (42)

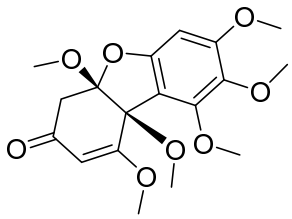

In einer Becherglaszelle werden gemäß *AAV5* 0.46 g (2.5 mmol, 1.0 Äq.) 3,4,5-Trimethoxyphenol zusammen mit 0.20 mL (2.5 mmol, 1.0 Äq.) Pyridin in 30 mL HFIP + MTBS (0.1 M) gelöst und bei einer Temperatur von 20 °C mit einer Ladungsmenge von 507 C (1.05 F bezogen auf die Phenolkomponente) und einer Stromdichte von 4 mA/cm^2 elektrochemisch umgesetzt.

Die Aufreinigung des Produktgemisches erfolgt säulenchromatographisch (Eluent: CH:EE = 9:1 → 7:3).

Ausbeute: 33% (0.41 mmol, 0.15 g), farbloser Feststoff.

Charakterisierung:

^{1}H-NMR (400 MHz, d$_6$-Aceton): δ (ppm) = 6.31 (s, 1H), 5.52 (s, 1H), 3.91 (s, 3H), 3.81 (s, 3H), 3.78 (s, 3H), 3.70 (s, 3H), 3.46 (s, 3H), 3.36 (s, 3H), 3.07 (d, *J* = 16.7, 1H), 2.85 (d, , *J* = 16.7, 1H).

^{13}C-NMR (101 MHz, d$_6$-Aceton): δ (ppm) = 192.35, 172.53, 157.06, 154.72, 153.40, 138.62, 111.38, 109.54, 104.66, 91.82, 86.61, 61.57, 60.72, 56.97, 56.36, 54.42, 50.80, 43.52.

2,6,8-Tri(1,1,-dimethylethyl)dibenzo[*b,d*]furan-3-ol (44)

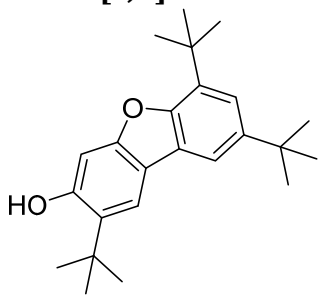

In einer Becherglaszelle werden gemäß *AAV5* 0.206 g (1.0 mmol, 1.0 Äq.) 2,4-(1,1-Dimethylethyl)phenol in 30 mL HFIP + MTBS (0.1 M) gelöst und bei einer Temperatur von 20 °C mit einer Ladungsmenge von 241 C (2.5 F bezogen auf die Phenolkomponente) elektrochemisch umgesetzt.

Die Aufreinigung des Produktgemisches erfolgt säulenchromatographisch (Eluent: CH:EE = 1:0 → 98:2).

Ausbeute: 17% (0.09 mmol, 30 mg), farbloser Feststoff.

Charakterisierung:

^{1}H-NMR (400 MHz, $CDCl_3$): δ (ppm) = 7.82 (d, *J* = 2.0 Hz, 1H), 7.55 (d, *J* = 1.7 Hz, 1H), 7.44 (d, *J* = 2.0 Hz, 1H), 7.11 (d, *J* = 1.8 Hz, 1H), 5.44 (s, 1H), 1.59 (s, 9H), 1.47 (s, 9H), 1.44 (s, 9H).

^{13}C-NMR (101 MHz, $CDCl_3$): δ (ppm) = 153.10, 147.32, 145.79, 142.15, 140.18, 134.31, 125.68, 124.90, 121.71, 114.92, 111.29, 108.86, 35.12, 35.05, 34.81, 3x32.10, 3x32.02, 3x30.08.

(4aS, 9bS)-4*H*-6-(1,1-Dimethylethyl)-1,4a,8,9b-tetramethoxy-4a,9b-dihydrodibenzo[*b,d*]furan-3-on (47)

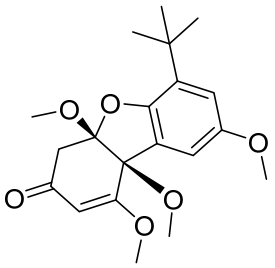

In einer Becherglaszelle werden gemäß *AAV6* 0.451 g (2.5 mmol, 1.0 Äq.) 2-(1,1-Dimethylethyl)-4-methoxyphenol zusammen mit 0.30 mL (3.75 mmol, 1.5 Äq.) Pyridin in 30 mL HFIP + MTBS (0.1 M) gelöst und bei einer Temperatur von -10 °C mit einer Ladungsmenge von 531 C (2.2 F bezogen auf die Phenolkomponente) elektrochemisch umgesetzt. Anschließend wurden 0.479 g (2.6 mmol, 1.04 Äq.) 3,4,5-Trimethoxyphenol dazugegeben und 0.5 h bei 20 °C gerührt.

Die Aufreinigung des Produktgemisches erfolgt säulenchromatographisch (Eluent: CH:EE = 9:1 → 7:3).

Ausbeute: 16% (0.39 mmol, 0.127 g), farbloser Feststoff.

Charakterisierung:

^{1}H-NMR (400 MHz, d_6-Aceton): δ (ppm) = 6.84 (d, *J* = 2.7 Hz, 1H), 6.74 (d, *J* = 2.7 Hz, 1H), 5.59 (s, 1H), 3.78 (s, 3H), 3.75 (s, 3H), 3.45 (s, 3H), 3.38 (s, 3H), 3.19 (dd, *J* = 16.7 Hz, 1H), 2.92 (s, 1H), 1.31 (s, 9H).

^{13}C-NMR (101 MHz, d_6-Aceton): δ (ppm) = 192.36, 171.43, 2x155.63, 149.55, 134.37, 129.95, 114.86, 108.59, 108.39, 106.00, 84.30, 56.99, 55.92, 53.81, 51.45, 3x45.02, 34.64.

HRMS für $C_{20}H_{26}O_6$ (ESI+) $[M+H]^+$: ber.: 363.1808; gef.: 363.1807.

7.4 Spektrenanhang

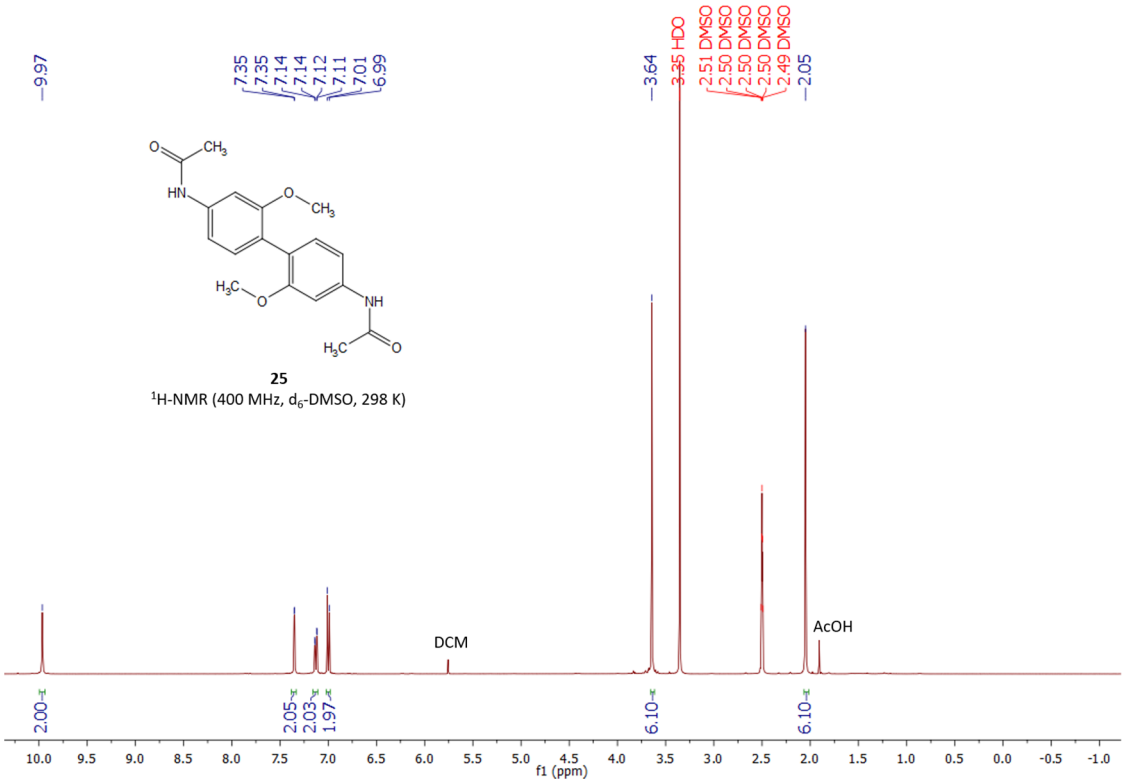

25

^{1}H-NMR (400 MHz, d_6-DMSO, 298 K)

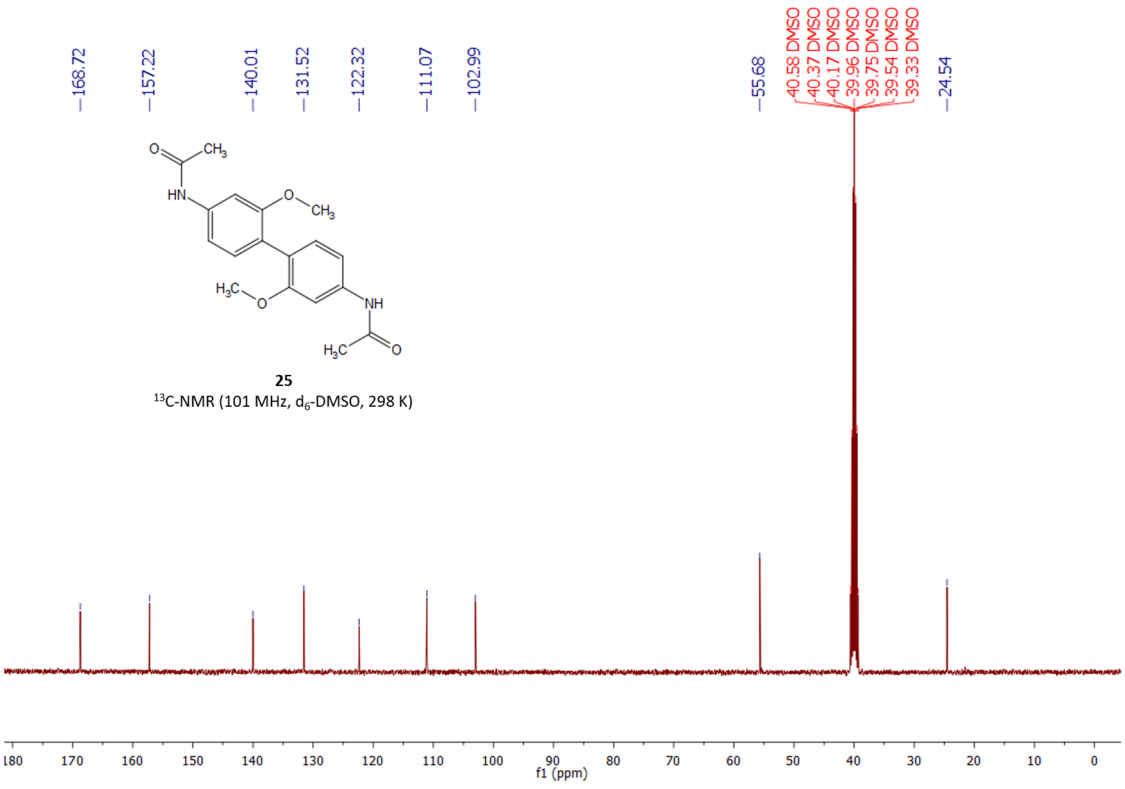

25

^{13}C-NMR (101 MHz, d_6-DMSO, 298 K)

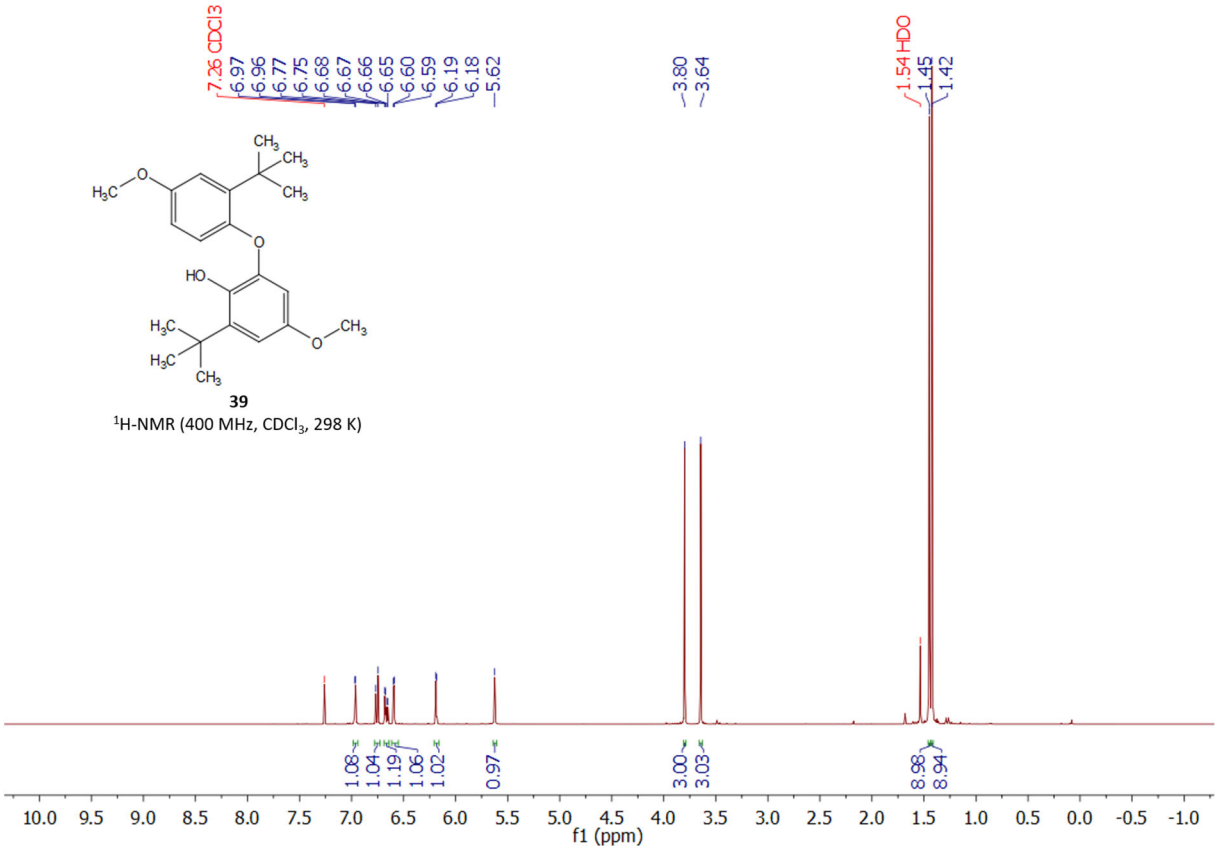

39

^{1}H-NMR (400 MHz, $CDCl_3$, 298 K)

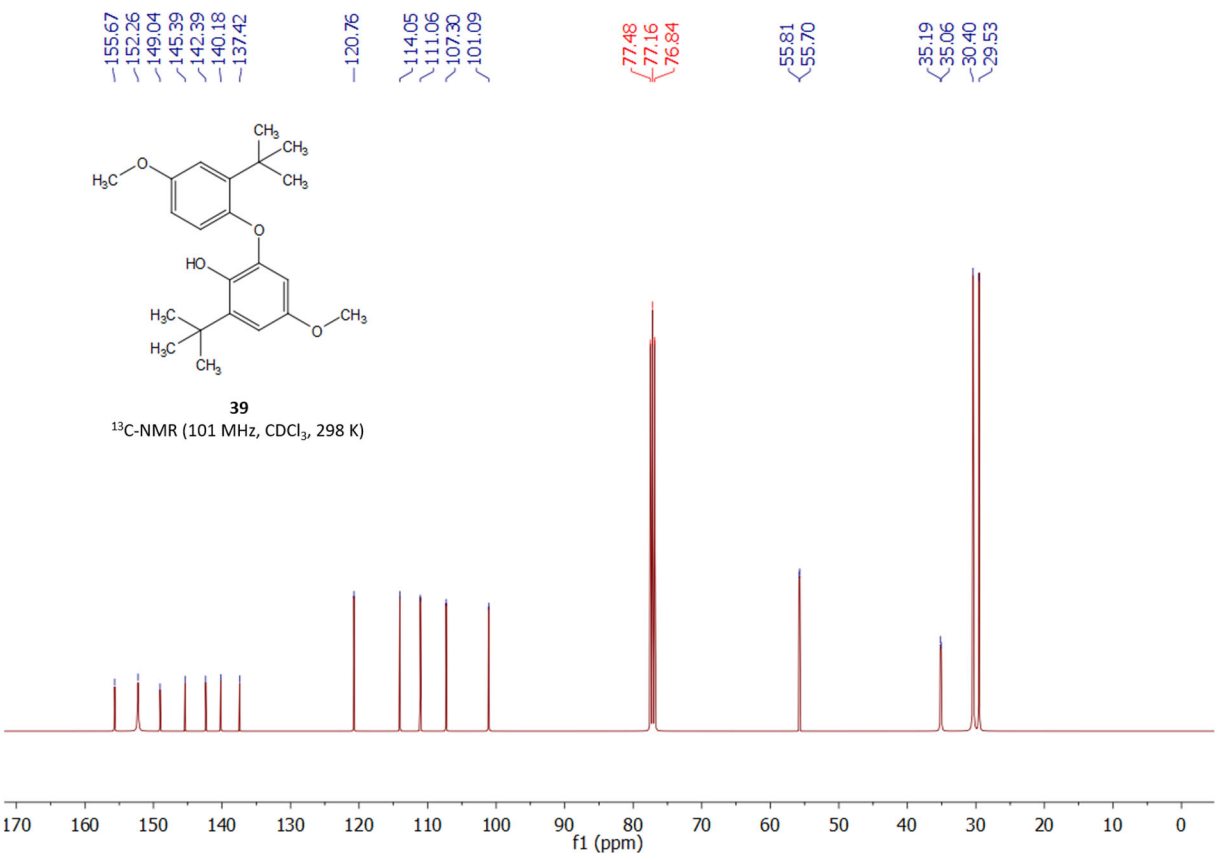

39

^{13}C-NMR (101 MHz, $CDCl_3$, 298 K)

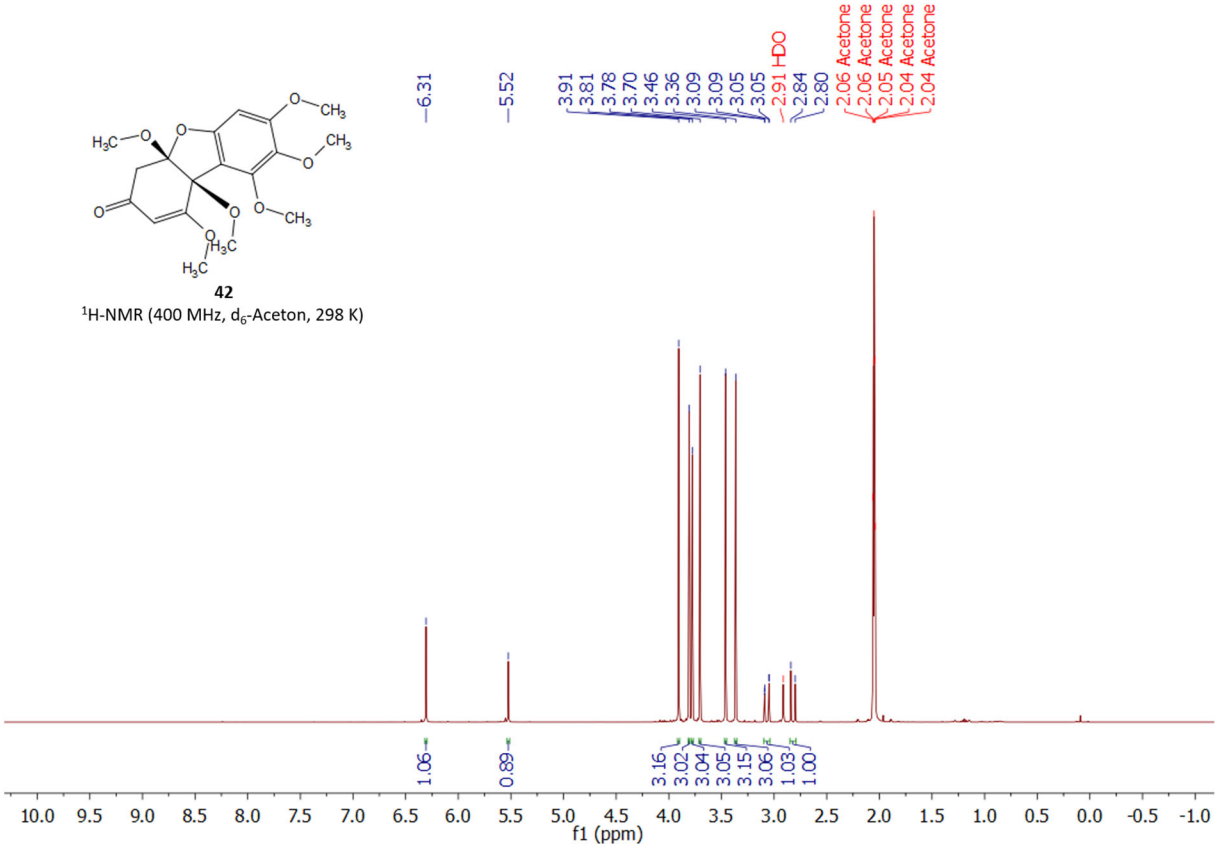

42

^{1}H-NMR (400 MHz, d_6-Aceton, 298 K)

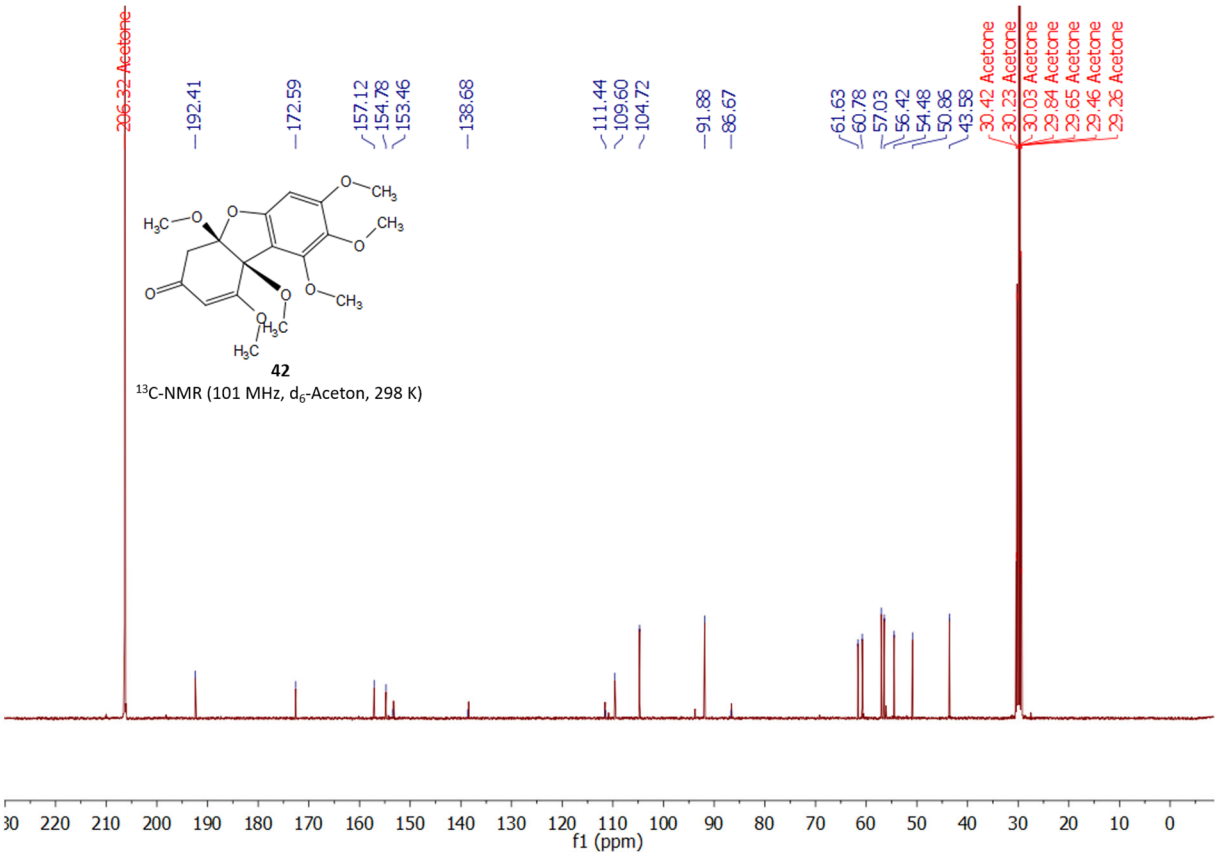

42

^{13}C-NMR (101 MHz, d_6-Aceton, 298 K)

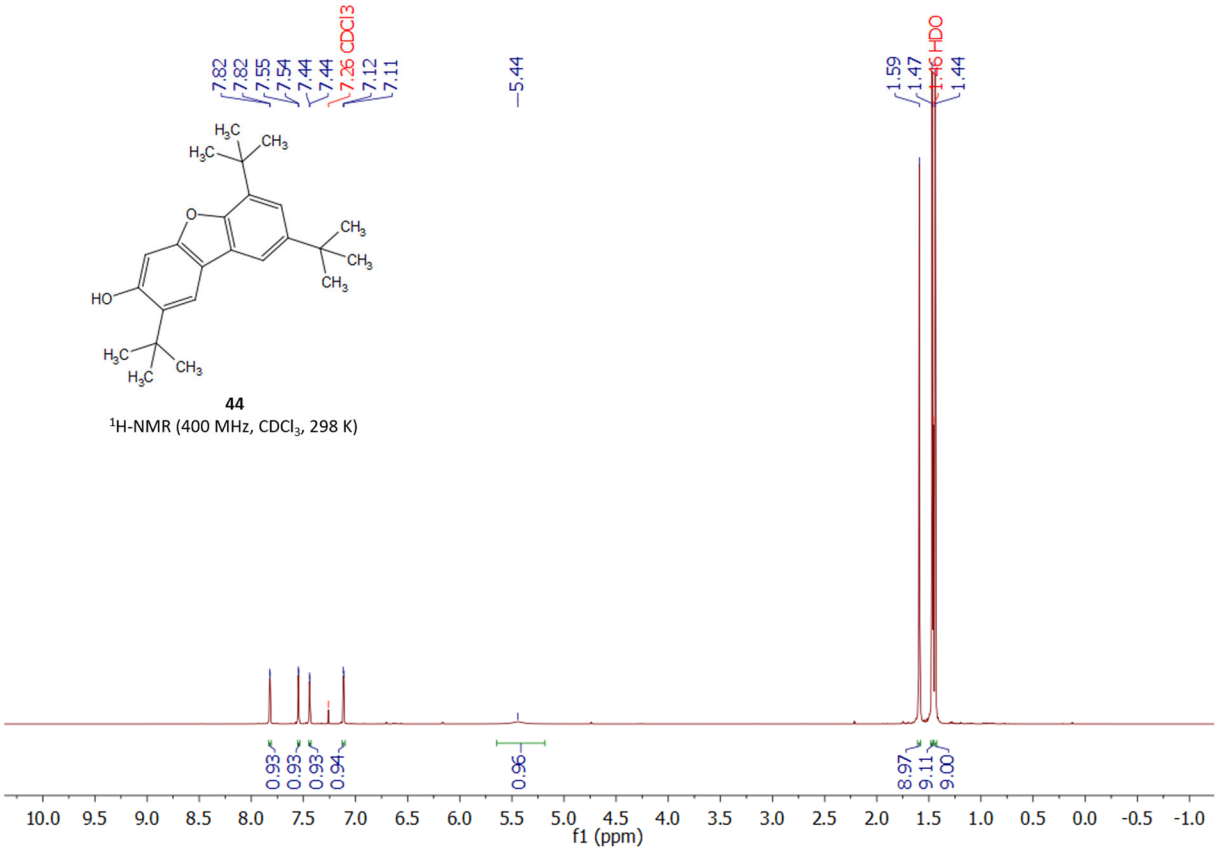

44

^{1}H-NMR (400 MHz, $CDCl_3$, 298 K)

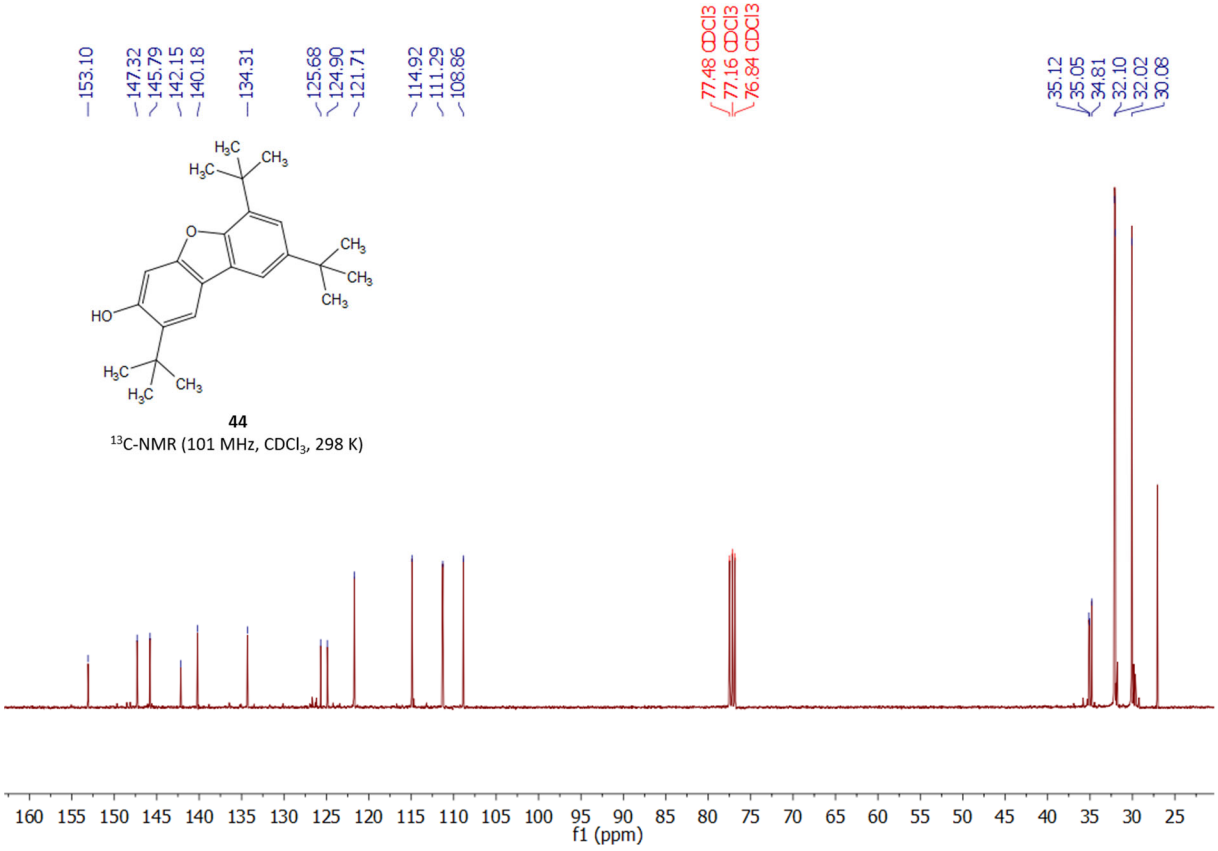

44

^{13}C-NMR (101 MHz, $CDCl_3$, 298 K)

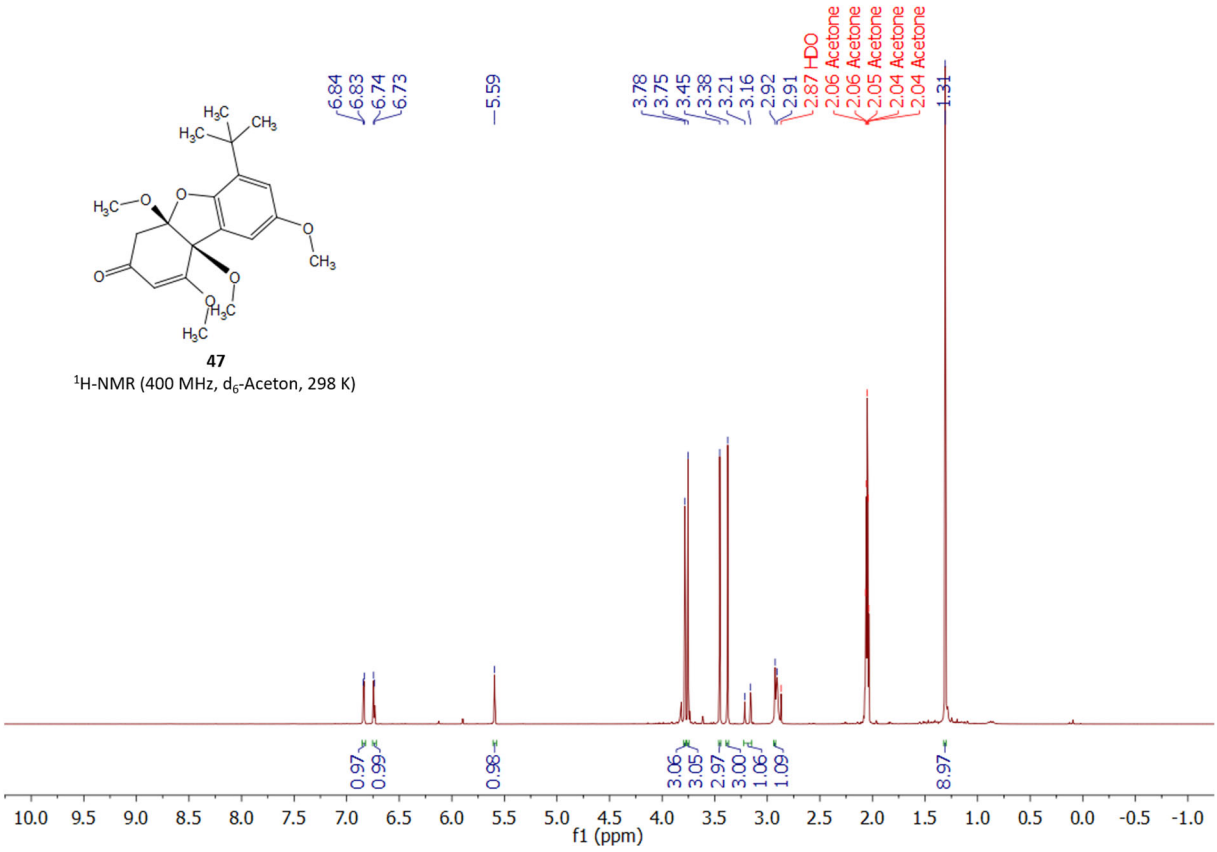

47

^{1}H-NMR (400 MHz, d_6-Aceton, 298 K)

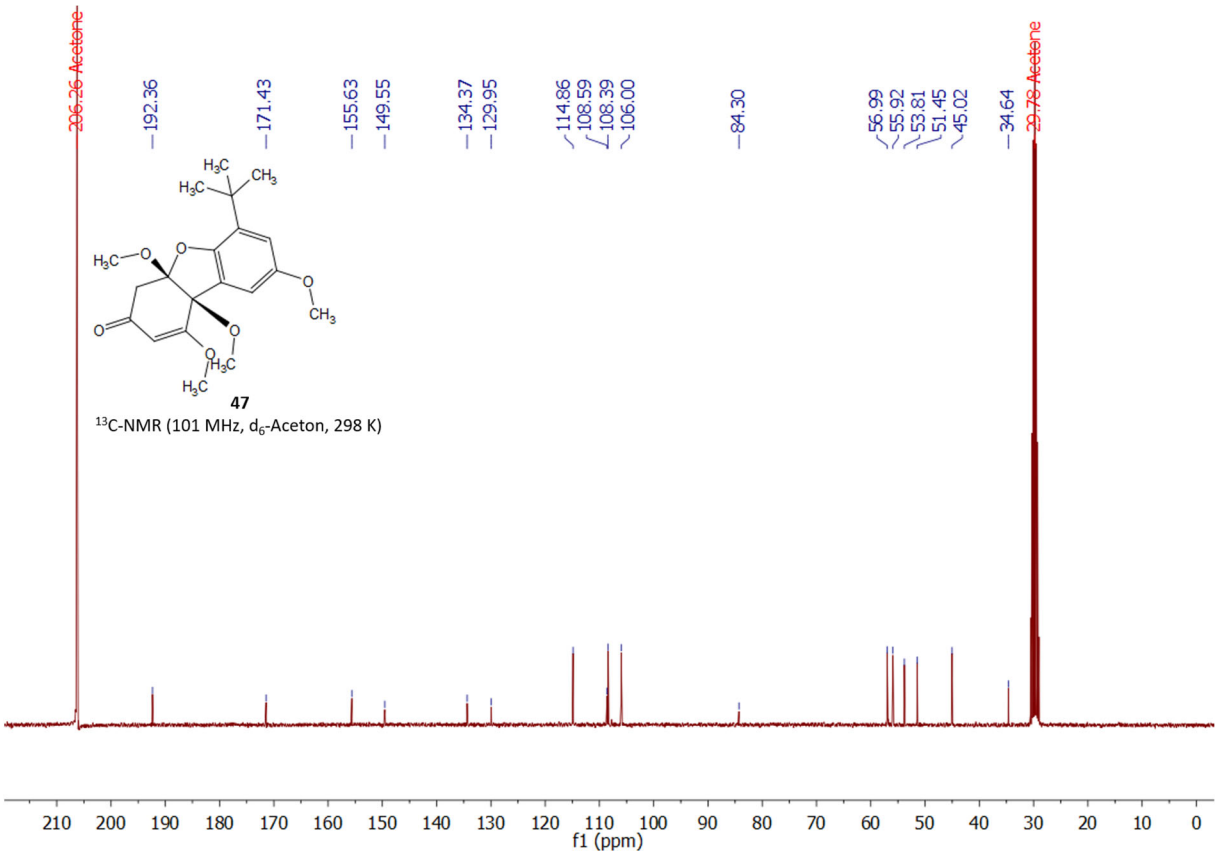

47

^{13}C-NMR (101 MHz, d_6-Aceton, 298 K)

8 Literaturverzeichnis

[1] a) F. Ausfelder, C. Beilmann, M. Bertau, S. Bräuninger, A. Heinzel, R. Hoer, W. Koch, F. Mahlendorf, A. Metzelthin, M. Peuckert et al., *Chem. Ing. Tech.* **2015**, *87*, 17–89; b) A. Sternberg, A. Bardow, *Energy Environ. Sci.* **2015**, *8*, 389–400; c) https://uk.reuters.com/article/uk-germany-powertochemicals/chemical-industry-in-bid-to-harness-germanys-green-power-overload-idUKKBN1F72AG; (Aufgerufen am 14.08.2019).

[2] D. M. Mohilner, R. N. Adams, W. J. Argersinger, *J. Am. Chem. Soc.* **1962**, *84*, 3618–3622.

[3] K. C. Nicolaou, P. G. Bulger, D. Sarlah, *Angew. Chem. Int. Ed.* **2005**, *44*, 4442–4489; *Angew. Chem.* **2005**, *117*, 4516–4563.

[4] G. Bringmann, T. Gulder, T. A. M. Gulder, M. Breuning, *Chem. Rev.* **2011**, *111*, 563–639.

[5] a) A. C. Grimsdale, K. L. Chan, R. E. Martin, P. G. Jokisz, A. B. Holmes, *Chem. Rev.* **2009**, *109*, 897–1091; b) Y.-Y. Noh, R. Azumi, M. Goto, B.-J. Jung, E. Lim, H.-K. Shim, Y. Yoshida, K. Yase, D.-Y. Kim, *Chem. Mater.* **2005**, *17*, 3861–3870.

[6] J. M. Brunel, *Chem. Rev.* **2005**, *105*, 857–897.

[7] a) E. Negishi, *Acc. Chem. Res.* **1982**, *15*, 340–348; b) J. Magano, J. R. Dunetz, *Chem. Rev.* **2011**, *111*, 2177–2250; c) N. Miyaura, A. Suzuki, *Chem. Rev.* **1995**, *95*, 2457–2483.

[8] a) E.-i. Negishi, *Angew. Chem. Int. Ed.* **2011**, *50*, 6738–6764; b) A. Suzuki, *Angew. Chem. Int. Ed.* **2011**, *50*, 6722–6737.

[9] J. D. Hayler, D. K. Leahy, E. M. Simmons, *Organometallics* **2019**, *38*, 36–46.

[10] K. S. Egorova, V. P. Ananikov, *Organometallics* **2017**, *36*, 4071–4090.

[11] A. A. O. Sarhan, C. Bolm, *Chem. Soc. Rev.* **2009**, *38*, 2730–2744.

[12] a) J. A. Ashenhurst, *Chem. Soc. Rev.* **2010**, *39*, 540–548; b) S. R. Waldvogel, S. Trosien, *Chem. Commun.* **2012**, *48*, 9109–9119.

[13] a) A. Wiebe, T. Gieshoff, S. Möhle, E. Rodrigo, M. Zirbes, S. R. Waldvogel, *Angew. Chem. Int. Ed.* **2018**, *57*, 5594–5619; *Angew. Chem*. **2018**, *130*, 5694–5721.; b) S. Möhle, M. Zirbes, E. Rodrigo, T. Gieshoff, A. Wiebe, S. R. Waldvogel, *Angew. Chem. Int. Ed.* **2018**, *57*, 6018–6041; *Angew. Chem*. **2018**, *130*, 6124–6149.; c) E. J. Horn, B. R. Rosen, P. S. Baran, *ACS Cent. Sci.* **2016**, *2*, 302–308; d) H. Yi, G. Zhang, H. Wang, Z. Huang, J. Wang, A. K. Singh, A. Lei, *Chem. Rev.* **2017**, *117*, 9016–9085.

[14] T. Morofuji, A. Shimizu, J.-i. Yoshida, *Angew. Chem. Int. Ed.* **2012**, *51*, 7259–7262; *Angew. Chem*. **2012**, *124*, 7371–7374.

[15] K. Mitsudo, J. Yamamoto, T. Akagi, A. Yamashita, M. Haisa, K. Yoshioka, H. Mandai, K. Ueoka, C. Hempel, J.-i. Yoshida et al., *Beilstein J. Org. Chem.* **2018**, *14*, 1192–1202.

[16] A. Shimizu, S. Horiuchi, R. Hayashi, K. Matsumoto, Y. Miyamoto, Y. Morisawa, T. Wakabayashi, J.-i. Yoshida, *Arkivoc* **2018**, *2018*, 97–113.

[17] B. Elsler, A. Wiebe, D. Schollmeyer, K. M. Dyballa, R. Franke, S. R. Waldvogel, *Chem. Eur. J.* **2015**, *21*, 12321–12325.

[18] L. Schulz, S. Waldvogel, *Synlett* **2019**, *30*, 275–286.

[19] a) J. Barjau, P. Königs, O. Kataeva, S. Waldvogel, *Synlett* **2008**, 2309–2312; b) J. Barjau, G. Schnakenburg, S. R. Waldvogel, *Angew. Chem. Int. Ed.* **2011**, *50*, 1415–1419; *Angew. Chem*. **2011**, *123*, 1451–1455.; c) I. M. Malkowsky, C. E. Rommel, K. Wedeking, R. Fröhlich, K. Bergander, M. Nieger, C. Quaiser, U. Griesbach, H. Pütter, S. R. Waldvogel, *Eur. J. Org. Chem.* **2006**, 241–245.

[20] I. M. Malkowsky, C. E. Rommel, R. Fröhlich, U. Griesbach, H. Pütter, S. R. Waldvogel, *Chem. Eur. J.* **2006**, *12*, 7482–7488.

[21] A. Kirste, M. Nieger, I. M. Malkowsky, F. Stecker, A. Fischer, S. R. Waldvogel, *Chem. Eur. J.* **2009**, *15*, 2273–2277.

[22] A. Kirste, G. Schnakenburg, S. R. Waldvogel, *Org. Lett.* **2011**, *13*, 3126–3129.

[23] a) A. Kirste, G. Schnakenburg, F. Stecker, A. Fischer, S. R. Waldvogel, *Angew. Chem. Int. Ed.* **2010**, *49*, 971–975; Angew. Chem. **2010**, *122*, 983–987.; b) A. Kirste, B. Elsler, G. Schnakenburg, S. R. Waldvogel, *J. Am. Chem. Soc.* **2012**, *134*, 3571–3576.

[24] A. Wiebe, D. Schollmeyer, K. M. Dyballa, R. Franke, S. R. Waldvogel, *Angew. Chem. Int. Ed.* **2016**, *55*, 11801–11805; Angew. Chem. **2016**, *128*, 11979–11983.

[25] A. Wiebe, S. Lips, D. Schollmeyer, R. Franke, S. R. Waldvogel, *Angew. Chem. Int. Ed.* **2017**, *56*, 14727–14731; Angew. Chem. **2017**, *129*, 14920–14925.

[26] A. Wiebe, B. Riehl, S. Lips, R. Franke, S. R. Waldvogel, *Sci. Adv.* **2017**, *3*, eaao3920/1-7.

[27] L. Schulz, M. Enders, B. Elsler, D. Schollmeyer, K. M. Dyballa, R. Franke, S. R. Waldvogel, *Angew. Chem. Int. Ed.* **2017**, *56*, 4877–4881; Angew. Chem. **2017**, *129*, 4955–4959.

[28] L. Schulz, R. Franke, S. R. Waldvogel, *ChemElectroChem* **2018**, *5*, 2069–2072.

[29] S. Lips, A. Wiebe, B. Elsler, D. Schollmeyer, K. M. Dyballa, R. Franke, S. R. Waldvogel, *Angew. Chem. Int. Ed.* **2016**, *55*, 10872–10876; Angew. Chem. **2016**, *128*, 11031–11035.

[30] S. Lips, B. A. Frontana-Uribe, M. Dörr, D. Schollmeyer, R. Franke, S. R. Waldvogel, *Chem. Eur. J.* **2018**, *24*, 6057–6061.

[31] B. Dahms, R. Franke, S. R. Waldvogel, *ChemElectroChem* **2018**, 1249–1252.

[32] B. Dahms, P. J. Kohlpaintner, A. Wiebe, R. Breinbauer, D. Schollmeyer, S. R. Waldvogel, *Chem. Eur. J.* **2019**, *25*, 2713–2716.

[33] S. Lips, R. Franke, S. R. Waldvogel, *Synlett* **2019**, *30*, 1174–1177.

[34] M. Dörr, S. Lips, C. A. Martínez-Huitle, D. Schollmeyer, R. Franke, S. R. Waldvogel, *Chem. Eur. J.* **2019**, *25*, 7835–7838.

[35] S. Lips, D. Schollmeyer, R. Franke, S. R. Waldvogel, *Angew. Chem. Int. Ed.* **2018**, *57*, 13325–13329; *Angew. Chem.* **2018**, *130*, 13509–13513.

[36] J. Nikl, S. Lips, D. Schollmeyer, R. Franke, S. R. Waldvogel, *Chem. Eur. J.* **2019**, *25*, 6891–6895.

[37] L. Eberson, M. P. Hartshorn, O. Persson, *J. Chem. Soc., Chem. Commun.* **1995**, 1131.

[38] L. Eberson, O. Persson, M. P. Hartshorn, *Angew. Chem. Int. Ed.* **1995**, *34*, 2268–2269; *Angew. Chem*. **1995**, *107*, 2417–2418.

[39] O. Hollóczki, A. Berkessel, J. Mars, M. Mezger, A. Wiebe, S. R. Waldvogel, B. Kirchner, *ACS Catal.* **2017**, *7*, 1846–1852.

[40] a) A. Berkessel, J. A. Adrio, D. Hüttenhain, J. M. Neudörfl, *J. Am. Chem. Soc.* **2006**, *128*, 8421–8426; b) A. Berkessel, J. A. Adrio, *J. Am. Chem. Soc.* **2006**, *128*, 13412–13420; c) I. Shuklov, N. Dubrovina, A. Börner, *Synthesis* **2007**, 2925–2943.

[41] O. Hollóczki, R. Macchieraldo, B. Gleede, S. R. Waldvogel, B. Kirchner, *J. Phys. Chem. Lett.* **2019**, *10*, 1192–1197.

[42] R. Francke, D. Cericola, R. Kötz, D. Weingarth, S. R. Waldvogel, *Electrochim. Acta* **2012**, *62*, 372–380.

[43] a) S. Guizzetti, M. Benaglia, G. Celentano, *Eur. J. Org. Chem.* **2009**, 3683–3687; b) T. Kano, Y. Tanaka, K. Osawa, T. Yurino, K. Maruoka, *J. Org. Chem.* **2008**, *73*, 7387–7389; c) A. Sakakura, K. Suzuki, K. Ishihara, *Adv. Synth. Catal.* **2006**, *348*, 2457–2465.

[44] H. Huang, T. Okuno, K. Tsuda, M. Yoshimura, M. Kitamura, *J. Am. Chem. Soc.* **2006**, *128*, 8716–8717.

[45] J. Wang, H. Li, W. Duan, L. Zu, W. Wang, *Org. Lett.* **2005**, *7*, 4713–4716.

[46] C. Wang, H. Yamamoto, *J. Am. Chem. Soc.* **2015**, *137*, 4308–4311.

[47] M. J. Bravo, R. M. Ceder, G. Muller, M. Rocamora, *Organometallics* **2013**, *32*, 2632–2642.

[48] K.-H. Jung, H.-K. Kim, G. H. Lee, D.-S. Kang, J.-A. Park, K. M. Kim, Y. Chang, T.-J. Kim, *J. Med. Chem.* **2011**, *54*, 5385–5394.

[49] a) K.-H. Jung, H.-K. Kim, J.-A. Park, K. S. Nam, G. H. Lee, Y. Chang, T.-J. Kim, *ACS Med. Chem. Lett.* **2012**, *3*, 1003–1007; b) H. Toyama, M. Nakamura, Y. Hashimoto, S. Fujii, *Bioorg. Med. Chem.* **2015**, *23*, 2982–2988.

[50] H. Letheby, *J. Chem. Soc.* **1862**, *15*, 161–163.

[51] W. Kalk, H.-S. Bien, K.-H. Schündehütte, *Liebigs Ann. Chem.* **1977**, 329–337.

[52] M. Smrcina, S. Vyskocil, B. Maca, M. Polasek, T. A. Claxton, A. P. Abbott, P. Kocovsky, *J. Org. Chem.* **1994**, *59*, 2156–2163.

[53] a) B.-Y. Lim, M.-K. Choi, C.-G. Cho, *Tetrahedron Lett.* **2011**, *52*, 6015–6017; b) H.-Y. Kim, W.-J. Lee, H.-M. Kang, C.-G. Cho, *Org. Lett.* **2007**, *9*, 3185–3186; c) H.-M. Kang, Y.-K. Lim, I.-J. Shin, H.-Y. Kim, C.-G. Cho, *Org. Lett.* **2006**, *8*, 2047–2050; d) S.-E. Suh, I.-K. Park, B.-Y. Lim, C.-G. Cho, *Eur. J. Org. Chem.* **2011**, 455–457.

[54] Y.-K. Lim, J.-W. Jung, H. Lee, C.-G. Cho, *J. Org. Chem.* **2004**, *69*, 5778–5781.

[55] G.-Q. Li, H. Gao, C. Keene, M. Devonas, D. H. Ess, L. Kürti, *J. Am. Chem. Soc.* **2013**, *135*, 7414–7417.

[56] C. Mei, W. Lu, *J. Org. Chem.* **2018**, *83*, 4812–4823.

[57] C. Gütz, B. Klöckner, S. R. Waldvogel, *Org. Process Res. Dev.* **2015**, *20*, 26–32.

[58] P. G. M. Wuts, T. W. Greene, *Greene's Protective Groups in Organic Synthesis*, John Wiley & Sons, Inc, Hoboken, NJ, USA.

[59] B.-C. Chen, M. S. Bednarz, R. Zhao, J. E. Sundeen, P. Chen, Z. Shen, A. P. Skoumbourdis, J. C. Barrish, *Tetrahedron Lett.* **2000**, *41*, 5453–5456.

[60] K. Kobayashi, S. Nagato, M. Kawakita, O. Morikawa, H. Konishi, *Chem. Lett.* **1995**, *24*, 575–576.

[61] J. Martinez, J. Laur, *Synthesis* **1982**, *1982*, 979–981.

[62] a) M. K. Faraj, US5686645A; b) U. Griesbach, L. Wittenbecher, H. Puetter, WO2009010420 A1.

[63] a) D. Arlt, G. Klein, US4419297A; b) F. Becke, P. Paessler, DE1908967 A1.

[64] a) D. Degner, H. Hannebaum, DE3606478 A1; b) D. Degner, H. Hannebaum, M. Steiniger, DE3529531 A1.

[65] H. G. Grant, L. A. Summers, *Aust. J. Chem.* **1980**, *33*, 613–617.

[66] a) A. Jackson, O. Meth-Cohn, *J. Chem. Soc., Chem. Commun.* **1995**, 1319; b) G. Pettit, M. Kalnins, T. Liu, E. Thomas, K. Parent, *J. Org. Chem.* **1961**, *26*, 2563–2566.

[67] J. Heinze, E. Steckhan (Eds.) *Electrochemistry IV*, *Topics in current chemistry*, *152*, **1990**, Springer, Berlin.

[68] S. Lips, S. R. Waldvogel, *ChemElectroChem* **2019**, *6*, 1649–1660.

[69] J. D. Bauer, M. S. Foster, J. D. Hugdahl, K. L. Burns, S. W. May, S. H. Pollock, H. G. Cutler, S. J. Cutler, *Med. Chem. Res.* **2007**, *16*, 119–129.

[70] M. Peters, M. Trobe, H. Tan, R. Kleineweischede, R. Breinbauer, *Chem. Eur. J.* **2013**, *19*, 2442–2449.

[71] a) S. B. Beil, P. Franzmann, T. Müller, M. M. Hielscher, T. Prenzel, D. Pollok, N. Beiser, D. Schollmeyer, S. R. Waldvogel, *Electrochim. Acta* **2019**, *302*, 310–315; b) S. B. Beil, T. Müller, S. B. Sillart, P. Franzmann, A. Bomm, M. Holtkamp, U. Karst, W. Schade, S. R. Waldvogel, *Angew. Chem. Int. Ed.* **2018**, *57*, 2450–2454; *Angew. Chem*. **2018**, *130*, 2475–2479.

[72] a) A. V. Aksenov, N. A. Aksenov, Z. V. Dzhandigova, D. A. Aksenov, M. Rubin, *RSC Adv.* **2015**, *5*, 106492–106497; b) M. H. Al-Huniti, Z. B. Sullivan, J. L. Stanley, J. A. Carson, I. F. D. Hyatt, A. C. Hairston, M. P. Croatt, *J. Org. Chem.* **2017**, *82*, 11772–11780; c) D. K. Singh, S. S. Prasad, J. Kim, I. Kim, *Org. Chem. Front.* **2019**, *6*, 669–673.

[73] a) R. Shang, *Dissertation*, Hefei, China, University of Science and Technology of China; b) A. S. Kumar, S. Ghosh, K. Bhima, G. N. Mehta, *J. Chem. Res.* **2009**, 482–484.

[74] F. Bedos-Belval, A. Rouch, C. Vanucci-Bacqué, M. Baltas, *Med. Chem. Commun.* **2012**, *3*, 1356–1372.

[75] E. N. Pitsinos, V. P. Vidali, E. A. Couladouros, *Eur. J. Org. Chem.* **2011**, 1207–1222.

[76] a) F. Ullmann, *Ber. dtsch. Chem. Ges.* **1904**, *37*, 853–854; b) G. Evano, N. Blanchard, M. Toumi, *Chem. Rev.* **2008**, *108*, 3054–3131.

[77] D. M.T. Chan, K. L. Monaco, R.-P. Wang, M. P. Winters, *Tetrahedron Lett.* **1998**, *39*, 2933–2936.

[78] K. Tanaka, H. Gotoh, *Tetrahedron* **2019**, *75*, 3875–3885.

[79] a) J. Zhu, *Synlett* **1997**, 133–144; b) J. Qiao, P. Lam, *Synthesis* **2011**, 829–856.

[80] a) S. Nishiyama, M. H. Kim, S. Yamamura, *Tetrahedron Lett.* **1994**, *35*, 8397–8400; b) S. Yamamura, S. Nishiyama, *Synlett* **2002**, 533–543; c) Y. Naito, T. Tanabe, Y. Kawabata, Y. Ishikawa, S. Nishiyama, *Tetrahedron Lett.* **2010**, *51*, 4776–4778.

[81] B. Elsler, D. Schollmeyer, K. M. Dyballa, R. Franke, S. R. Waldvogel, *Angew. Chem. Int. Ed.* **2014**, *53*, 5210–5213; *Angew. Chem.* **2014**, *126*, 5311–5314.

[82] a) T. Kinzel, Y. Zhang, S. L. Buchwald, *J. Am. Chem. Soc.* **2010**, *132*, 14073–14075; b) Y. Yang, S. K. Seidlits, M. M. Adams, V. M. Lynch, C. E. Schmidt, E. V. Anslyn, J. B. Shear, *J. Am. Chem. Soc.* **2010**, *132*, 13114–13116; c) S. Handa, L. M. Slaughter, *Angew. Chem. Int. Ed.* **2012**, *51*, 2912–2915; *Angew. Chem*. **2012**, *124,* 2966–2969.

[83] S. S. Matharu, D. A. Rowlands, J. B. Taylor, R. Westwood, *J. Med. Chem.* **1977**, *20*, 197–204.

[84] B. R. Rosen, E. W. Werner, A. G. O'Brien, P. S. Baran, *J. Am. Chem. Soc.* **2014**, *136*, 5571–5574.

9 Publikationen und Konferenzbeiträge

Publikationen

1. **L. Schulz**, M. Enders, B. Elsler, D. Schollmeyer, K. M. Dyballa, R. Franke, S. R. Waldvogel,

a) *Reagent- and Metal-free Anodic C-C Cross-Coupling of Aniline Derivatives, Angew. Chem. Int. Ed.* **2017**, *56*, 4877–4881;

b) *Reagens- und Metallfreie Anodische C-C-Kreuzkupplung von Anilinderivaten, Angew. Chem.* **2017**, *129*, 4955–4959.
Hervorgehoben in *Chemical and Engineering News* und *ChemistryViews.*

2. **L. Schulz**, R. Franke, S. R. Waldvogel, *Direct Anodic Dehydrogenative Cross- and Homo-Coupling of Formanilides, ChemElectroChem* **2018**, *5*, 2069–2072.
3. **L. Schulz**, S. R. Waldvogel, *Solvent Control in Electro-Organic Synthesis, Synlett* **2019**, *30*, 275–286.
4. **L. Schulz**, J.-Å. Husmann, S. R. Waldvogel, *Outstandingly Robust Anodic Dehydrogenative Aniline Coupling Reaction, Manuskript in Fertigstellung.*
5. S. B. Beil, **L. Schulz**, M. Breiner, A. Schüll, T. Müller, A. Bomm, M. Holtkamp, U. Karst, W. Schade, S. R. Waldvogel, *Active Nickel Electrodes for Anodic Dehydrogenative Arylation Reaction in HFIP and their Unusual Behavior*, *Manuskript in Fertistellung.*

Wissenschaftliche Vorträge und Poster

09/2018 **Electrochemistry 2018, Ulm**

Vortrag: Reagent- and Metal-free Anodic C,C Coupling of Aniline Derivatives

Poster: Reagent and Metal-free Anodic Cross- and Homo-Coupling of Formanilides

09/2017 **7th German-Japanese Symposium on Electrosynthesis, Mainz**

Poster: Reagent and Metal-free Anodic C,C Cross-Coupling of Protected Aniline Derivatives and Subsequent Selective Deblocking.

09/2017 **GDCh-Wissenschaftsforum Chemie, Berlin**

Poster: Reagent and Metal-free Anodic C,C Cross-Coupling of Protected Aniline Derivatives and Subsequent Selective Deblocking.

04/2017 **Hausvortrag im Rahmen des Organisch-Chemischen Kolloquiums, Uni Mainz**

Thema: Reagens- und Metallfreie Anodische C,C-Kreuzkupplung von Anilinderivaten

09/2017 **Electrochemistry 2016, Goslar**

Poster: Selective Synthesis of Protected Non-Symmetric 2,2‘-Diaminobiaryls by Anodic Aniline-Aniline-Cross-Coupling Reactions

Stipendien und Auszeichnungen

02/2019–05/2019 **DAAD-Kurzstipendium für Doktoranden**

Forschungsaufenthalt in Toluca, Mexiko

09/2016 **Metrohm Posterpreis Electrochemistry 2016, Goslar**

Thema: Selective Synthesis of Protected Non-Symmetric 2,2‘-Diaminobiaryls by Anodic Aniline-Aniline-Cross-Coupling Reactions

10 Appendix

Inhaltsverzeichnis – Appendix

A Journal of the Gesellschaft Deutscher Chemiker

Angewandte International Edition Chemie

GDCh

www.angewandte.org

2017–56/17

The formation of polyanilines ...

… is avoided in an anodic coupling of anilines with simple and easily removable carbonyl-based protecting groups. In their Communication on page 4877 ff., S. R. Waldvogel and co-workers present a facile method for the electrolytic synthesis of protected 2,2′-diaminobiaryl derivatives in high yield and excellent selectivity by oxidative cross-coupling. The use of 1,1,1,3,3,3-hexafluoro-2-propanol as the solvent allows for clean electrochemical conversion.

150 Years GDCh

WILEY-VCH

Appendix Seite A69

VIP Electrosynthesis Very Important Paper

International Edition: DOI: 10.1002/anie.201612613
German Edition: DOI: 10.1002/ange.201612613

Reagent- and Metal-Free Anodic C–C Cross-Coupling of Aniline Derivatives

*Lara Schulz, Mathias Enders, Bernd Elsler, Dieter Schollmeyer, Katrin M. Dyballa, Robert Franke, and Siegfried R. Waldvogel**

Abstract: *The dehydrogenative cross-coupling of aniline derivatives to 2,2′-diaminobiaryls is reported. The oxidation is carried out electrochemically, which avoids the use of metals and reagents. A large variety of biphenyldiamines were thus prepared. The best results were obtained when glassy carbon was used as the anode material. The electrosynthetic reaction is easily performed in an undivided cell at slightly elevated temperature. In addition, common amine protecting groups based on carboxylic acids were employed that can be selectively removed under mild conditions after the cross-coupling, which provides quick and efficient access to important building blocks featuring free amine moieties.*

Nonsymmetric biaryls are very important structural motifs in natural products and in catalysis.[1] In particular, 1,1′-binaphthyl-2,2′-diamine (BINAM) is a promising ligand system and has already been studied in detail. Asymmetric Michael additions,[2] indole N arylation reactions,[3] as well as hydrogenations of ketones and olefins[4] have been realized using BINAM or derivatives thereof as a ligand in transition-metal catalysis. Moreover, new ligands for contrast agents in magnetic resonance imaging also feature 2,2′-diaminobiaryls as structural motifs.[5] However, access to these substrates by classical synthetic means is limited because anilines easily undergo oxidative polymerization to polyaniline, which is also known as aniline black.[6] Symmetric 2,2′-diaminobiaryls are accessible by copper-catalyzed Ullmann reactions, for example.[7] Direct oxidative cross-couplings with stoichiometric amounts of inorganic reagents such as Cu^{II} salts have only been reported for naphthylamines and provided the desired compounds in rather poor yields.[8] Sigmatropic rearrangements of diaryl hydrazines in the presence of catalytic amounts of an acid provide symmetric 2,2′-diaminobiaryls in good yields while the synthesis of nonsymmetric derivatives is still challenging.[9] Furthermore, several steps are required for synthesizing those starting materials.[9,10] Applying these strategies requires much effort and complicated reaction conditions. Such approaches often lead to complex reaction mixtures and low yields of the desired products. In contrast, oxidative coupling reactions by direct C–H activation are of great interest as a sustainable method.[11,12] Recently, an oxidative conversion of diaryl amines in the presence of a highly fluorinated iron phthalocyanine catalyst was reported that enabled C–C as well as N–N bond formation.[13]

In particular, electrochemical techniques are remarkably advanced in terms of avoiding the formation of waste products because no leaving groups or oxidants are required.[14] The generation of reactive intermediates by electrochemical means is a highly attractive pathway in terms of atom economy and cost efficiency.[15] In our group, anodic phenol–phenol[12,16,17] and phenol–arene cross-couplings have been developed.[18] The best results for the direct oxidative cross-coupling of aryl compounds were attained in stabilizing media such as 1,1,1,3,3,3-hexafluoro-2-propanol (HFIP), which is frequently used in reactions that involve hypervalent iodine.[19,20] This unique solvent can form strong hydrogen bonds,[21] which results in a significantly different solvation of the individual coupling partners, and the oxidation potential is thus decoupled from its nucleophilicity.[22]

Herein, we present a selective method for the synthesis of nonsymmetric 2,2′-diaminobiaryls by anodic cross-coupling (Scheme 1). The electrochemical synthesis of nonsymmetric 2,2′-diaminobiaryls is very easy to conduct as only a simple two-electrode arrangement in an undivided beaker-type cell is required. In addition, the electrolysis is performed in a constant-current mode, which immensely simplifies the equipment needed. To efficiently find suitable coupling partners, several screening experiments were performed.[23] Usually, component **A** has a lower oxidation potential than aniline **B**, and is therefore preferentially oxidized at the anode. To statistically favor the cross-coupling over the homocoupling product, the aniline with the higher oxidation potential, that

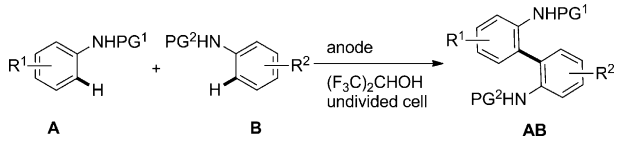

Scheme 1. Direct anodic C–C cross-coupling of protected aniline derivatives. PG = protecting group.

[*] L. Schulz, M. Enders, Dr. B. Elsler, Dr. D. Schollmeyer, Prof. Dr. S. R. Waldvogel
Institut für Organische Chemie
Johannes Gutenberg-Universität Mainz
Duesbergweg 10–14, 55128 Mainz (Germany)
E-mail: waldvogel@uni-mainz.de
Homepage: http://www.chemie.uni-mainz.de/OC/AK-Waldvogel/
Dr. K. M. Dyballa, Prof. Dr. R. Franke
Evonik Performance Materials GmbH
Paul-Baumann-Strasse 1, 45772 Marl (Germany)
Prof. Dr. R. Franke
Lehrstuhl für Theoretische Chemie
Ruhr-Universität Bochum
44780 Bochum (Germany)
Supporting information and the ORCID identification number(s) for the author(s) of this article can be found under: http://dx.doi.org/10.1002/anie.201612613.

is, **B**, was applied in slight excess. It was essential to stabilize the reactive radical intermediates during the electrolysis to avoid undesired oligomerization or even mineralization. The favorable effects of HFIP and protic additives such as methanol or water on yield and selectivity were recently described.[12,18,22] Unfortunately, simple aniline derivatives are prone to overoxidation because of their electron-rich nature and the resulting low oxidation potentials. Polymerization is a serious problem in anodic reactions of anilines.[24] Organocatalytic reactions currently use nitrogen protecting groups to prevent the formation of undesired side products.[19] N-Mesyl-protected anilines were converted in good yields in a hypervalent iodine mediated coupling but the desired aminobiphenyls were only obtained after waste-intensive and time-consuming deprotection.[19] Recently, Muñiz and co-workers used a hypervalent iodine reagent in a diamination reaction generating tosyl-protected diamines.[25] However, in our work, various easily removable protecting groups were used for the aniline derivatives (Figure 1).

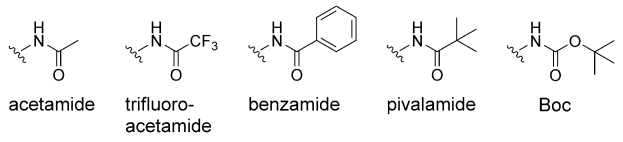

Figure 1. Common and easily removable carbonyl-based protecting groups for anilines.

Amides and carbamates proved to be suitable groups for N protection and exhibited sufficient stability during the electrolysis. In addition, cyclic voltammetry (CV) studies indicated that the protecting groups have a significant influence on the oxidation potential (which correlates with the pK_a values of the anilides)[26] as well as on the potential interaction between substrate and solvent by hydrogen bonding (Figure 2).

Electron-rich anilines, such as 3,4-dimethoxyaniline, have low oxidation potentials (832 mV in pure HFIP; p$K_{a(anilinium)}$ = 4.6 in DMSO)[26] and are therefore prone to anodic over-

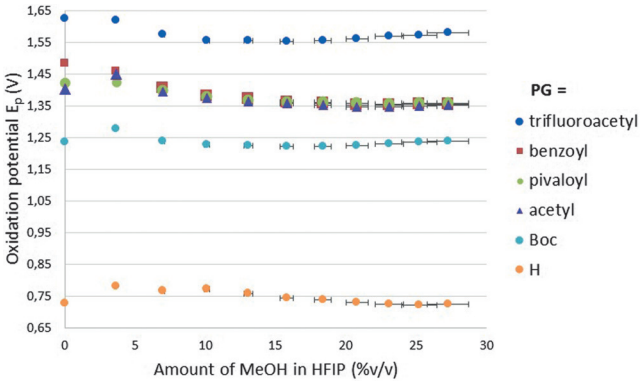

Figure 2. Changes in the oxidation potentials of various protected 3,4-dimethoxyanilines with increasing MeOH concentration in HFIP. WE: glassy carbon electrode tip, 2 mm diameter; CE: glassy carbon rod; RE: Ag/AgCl in saturated LiCl/EtOH; solvent: HFIP with 0–27% v/v MeOH; supporting electrolyte: 0.09 M Bu_3NMeO_3SOMe.

oxidation. The oxidation potential can be increased to 1.39 V or even 1.57 V, respectively, through the installation of an acetyl or trifluoroacetyl group (p$K_{a(acetanilide)}$ = 18.8, p$K_{a(trifluoroacetanilide)}$ = 12.6 in DMSO).[26] Owing to the ability of the amide functional group to participate in hydrogen bonding as a donor as well as an acceptor, the protected anilines experience strong solvation by HFIP. CV investigations of differently protected 3,4-dimethoxyanilines revealed a clear shift of the oxidation potentials to lower values with an increasing concentration of methanol in HFIP. Methanol acts as a weak base when added to the electrolyte and thus weakens the solvation of the amides. The oxidation potentials of anilines can be adjusted to some extent by using different protecting groups (Figure 2). This benefits the anodic cross-coupling of anilides as there seems to be an ideal difference for the oxidation potentials of the coupling partners.[22] In general, CV helps to indicate the correct stoichiometry for the anodic cross-coupling as component **A** should exhibit a lower oxidation potential than component **B** and thus be preferably oxidized at the anode to initiate the cross-coupling sequence (Scheme 1).

Usually, the electrode material has a crucial influence on electrochemical conversions as different reaction pathways and adsorption characteristics often result. However, in this system, the electrolyte system was found to be the key. Interestingly, the investigated reaction of anilides **1** and **2** (Scheme 2) gave consistent results when performed at different electrode materials, such as platinum, boron-doped diamond, graphite, or glassy carbon (Table 1).

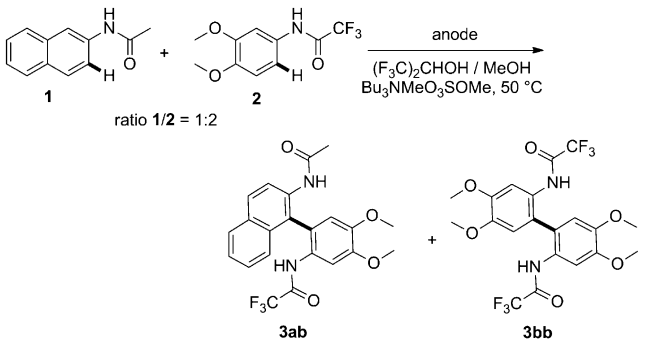

Scheme 2. The influence of methanol and different electrode materials on the anodic cross-coupling of anilines. 2-Acetamidonaphthalene (**1**) was used as component **A**, compound **2** as component **B**.

Considering the selectivity in HFIP, all electrode materials gave similar results but the best yields were achieved on graphite and platinum. The addition of methanol to the solvent led to significantly improved selectivity, and the cross-coupling product was exclusively obtained on glassy carbon (Table 1, entry 2). In addition, significantly less oligomerization was observed on glassy carbon than on the other electrode materials. This is important for two reasons: First, it simplifies the work-up tremendously, and second, non-converted starting materials can be easily recovered. Furthermore, glassy carbon shows excellent chemical stability even after long-term use whereas graphite undergoes signifi-

Table 1: Influence of the electrode material on the aniline–aniline cross-coupling.[a]

Entry[b]	Electrode material	Additive	Yield [%][c]	**3 ab**/**3 bb**[c]
1	glassy carbon	–	51	6:1
2	glassy carbon	MeOH	20	>100:1[d]
3	boron-doped diamond	–	48	3:1
4	boron-doped diamond	MeOH	34	34:1
5	graphite	–	60[e]	6:1
6	graphite	MeOH	28[e]	28:1
7	platinum	–	60[e]	7:1
8	platinum	MeOH	29[e]	29:1

[a] 2-Acetamidonaphthalene **1** was used as component **A**, compound **2** as component **B**. [b] Electrolysis conditions: 50 °C, constant current ($j = 5.2$ mA cm^{-2}), undivided screening cell, $Q = 2$ F (aniline **A**), solvent: HFIP or HFIP/MeOH (18% v/v), supporting electrolyte: 0.09 M Bu_3NMeO_3SOMe, **A**/**B** = 1:2. [c] Determined by GC analysis. [d] The homocoupling product **3 bb** was not detected. [e] Increased formation of oligomeric side products.

cant erosion. When taking into account the selectivity, electrochemical stability, and cost, glassy carbon is the electrode material of choice.

During this aniline cross-coupling, the new C–C bond is formed exclusively *ortho* to the amine moiety, and 2,2′-diaminobiaryl derivatives are obtained. Aniline derivatives with electron-releasing moieties such as methoxy groups in the *para* position to the newly formed C–C bond seem to particularly favor the coupling reaction. The scope of protected, nonsymmetric 2,2′-diaminobiaryl derivatives obtained by electrolysis is shown in Figure 3. It should be noted that none of the protecting groups was removed during electrolysis.

Oligomerization is still the predominant side reaction decreasing the yields of the cross-coupling products. Nevertheless, N-Boc-protected 3-methoxy-4-methylaniline provided the mixed 2,2′-diaminobiaryl derivatives **4**, **5**, **6**, and **7** in good yields of 40 to 51%. The highest yield of 74% was achieved for the coupling of *N*-(3,4-dimethoxyphenyl)acetamide with *N*-(3-methoxy-4-methylphenyl)benzamide (**8**). In the cross-coupling of *N*-(3,4-dimethoxyphenyl)acetamide with a benzodioxole derivative, the yield was slightly inferior (38%, **12**). 2-Acetamidonaphthalene (**1**) was also cross-coupled with trifluoroacetamide **2** to provide **3** in 59% yield. Accordingly, anilines with electron-releasing or alkyl moieties in the 3- and 4-position turned out to be suitable coupling partners. The coupling of anilines with chloro substituents was also possible (56%, **10** and 51%, **11**). The amount of unconverted component **A** was about 2–24%. Increasing the applied charge could, in some cases, improve the yields.

During the initial optimization of the electrolysis conditions, the influence of temperature on the yields of the cross-coupling products was evaluated (Table 2). These studies revealed that an electrolysis temperature of 30 °C seems to be advantageous (entries 3 and 6).

To enable the later use of such protected 2,2′-diaminobiaryls in organocatalysts, ligands, or functionalized materials,[27] it is vital to efficiently deprotect the amino moiety. The applied protecting groups are based on common carboxylic

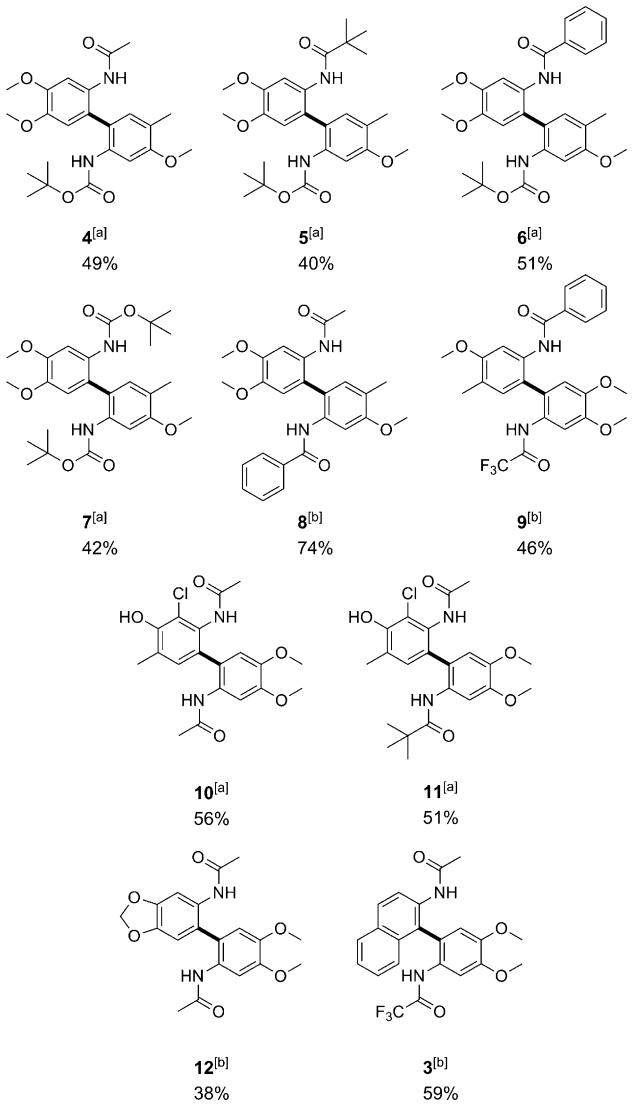

Figure 3. Scope of protected nonsymmetric 2,2′-diaminobiaryls. Yields of isolated products are given. [a] Electrolysis conditions: 50 °C, constant current ($j = 5.2$ mA cm^{-2}), glassy carbon anode, glassy carbon cathode, undivided beaker-type cell, $Q = 2$ F (aniline **A**), solvent: HFIP/MeOH (18% v/v), supporting electrolyte: 0.09 M Bu_3NMeO_3SOMe, **A**/**B** = 1:2. [b] Electrolysis conditions as in [a], solvent: HFIP.

acids and are thus easily removed by standard procedures.[28] By employing orthogonal protecting groups, the two amino groups can be independently deprotected, which allows for further chemo- and regioselective transformations (Table 3). These partially protected cross-coupling products had previously not been described and can be considered as congeners to the recently reported partially protected biphenol derivatives.[16]

A Boc group could be selectively removed with water without the need for additional acid,[29] whereas the acetyl and benzoyl groups in substrates **4** and **6**, respectively, remained unaffected (Table 3, entries 1 and 2). A trifluoroacetyl group could be selectively removed with potassium carbonate in the presence of an acetamide (entry 3). Both protecting groups in **3**, an acetyl and a trifluoroacetyl moiety, could be simulta-

Table 2: Temperature dependence of the anodic cross-coupling of aniline derivatives.[a]

Entry	Product	*T* [°C]	Yield [%][b]
1	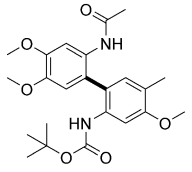	50	49
2		40	46
3		*30*	*59*
4		20	49
	4[c]		
5	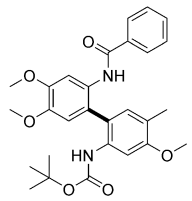	50	51
6		*30*	*59*
7		20	54
	6[c]		

[a] Electrolysis conditions: 20–50 °C, constant current ($j = 5.2$ mA cm^{-2}), glassy carbon anode, glassy carbon cathode, undivided beaker-type cell, $Q = 2$ F (aniline **A**), HFIP/MeOH (18% v/v), supporting electrolyte: 0.09 M Bu_3NMeO_3SOMe, **A**/**B** = 1:2. [b] Yields of isolated products. [c] Acetyl- and benzoyl-protected 3,4-dimethoxyaniline was used as component **A** for the synthesis of **4** and **6**, respectively.

Table 3: Partial and complete deprotection of differently protected 2,2′-diaminobiaryl derivatives.

Entry	Substrate	Removed PG	Product	Yield [%]
1	**4**	Boc[a]	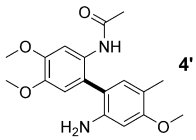 **4'**	98[d]
2	**6**	Boc[a]	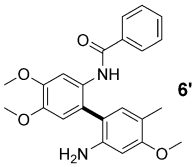 **6'**	99
3	**3**	trifluoroacetyl[b]	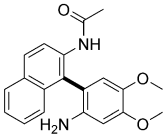 **3'**	99
4	**3**	acetyl and trifluoroacetyl[c]	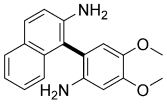 **3''**	98

[a] Reaction conditions: Substrate (0.20 mmol), 100 °C, H_2O/MeOH (2:1 v/v), 24 h. [b] Substrate (1.50 mmol), 20 °C, MeOH/H_2O (2:1 v/v), K_2CO_3 (10 equiv), 4 days. [c] Substrate (0.7 mmol), 120 °C, hydrazine hydrate (80% in H_2O), 4 days. [d] Migration of the remaining acetyl moiety can occur after work-up (see the Supporting Information).

neously cleaved with hydrazine hydrate (entry 4). These facile and efficient methods for deprotecting the cross-coupling products highlight once more the effectiveness of our method in generating precursors for relevant building blocks.

In conclusion, an innovative and facile method to obtain 2,2′-diaminobiaryls by electrochemical C–C cross-coupling has been established. The scope includes differently substituted and protected aniline derivatives. The HFIP solvent effect is essential for the high selectivity while no leaving groups are required. This highly fluorinated alcohol allows the oxidation potential to be decoupled from the nucleophilicity of the coupling partners. The protecting groups are based on common carboxylic acids and therefore easily removable. When a set of different protecting groups is applied, they can be selectively removed, and thus liberate the respective amino groups, with different nucleophiles. The use of electric current to drive this conversion leads to an exceptionally sustainable metal- and reagent-free reaction sequence. Moreover, the electrolysis protocol is very easy to conduct because an undivided cell and a two-electrode arrangement are employed.

Acknowledgments

S.R.W. thanks the DFG (Wa1278/14-1) for funding. We highly appreciate support by BMBF-EPSYLON (FKZ 12XP2016D).

Conflict of interest

The authors declare no conflict of interest.

Keywords: biaryls · C–H activation · cross-coupling · electrochemistry · protecting groups

How to cite: *Angew. Chem. Int. Ed.* **2017**, *56*, 4877–4881
Angew. Chem. **2017**, *129*, 4955–4959

[1] a) G. Bringmann, A. J. Mortimer, P. A. Keller, M. J. Gresser, J. Garner, M. Breuning, *Angew. Chem. Int. Ed.* **2005**, *44*, 5384–5427; *Angew. Chem.* **2005**, *117*, 5518–5563; b) K. C. Nicolaou, P. G. Bulger, D. Sarlah, *Angew. Chem. Int. Ed.* **2005**, *44*, 4442–4489; *Angew. Chem.* **2005**, *117*, 4516–4563; c) A. Zapf, M. Beller, *Top. Catal.* **2002**, *19*, 101–109.
[2] J. Wang, H. Li, W. Duan, L. Zu, W. Wang, *Org. Lett.* **2005**, *7*, 4713–4716.
[3] R. K. Rao, A. B. Naidu, E. A. Jaseer, G. Sekar, *Tetrahedron* **2009**, *65*, 4619–4624.
[4] a) K. Kabuto, T. Yoshida, S. Yamaguchi, S. Miyano, H. Hashimoto, *J. Org. Chem.* **1985**, *50*, 3013–3015; b) F.-Y. Zhang, C.-C. Pai, A. S. C. Chan, *J. Am. Chem. Soc.* **1998**, *120*, 5808–5809.
[5] K.-H. Jung, H.-K. Kim, G. H. Lee, D.-S. Kang, J.-A. Park, K. M. Kim, Y. Chang, T.-J. Kim, *J. Med. Chem.* **2011**, *54*, 5385–5394.
[6] H. Letheby, *J. Chem. Soc.* **1862**, *15*, 161.
[7] W. Kalk, H.-S. Bien, K.-H. Schündehütte, *Justus Liebigs Ann. Chem.* **1977**, 329–337.
[8] M. Smrcina, S. Vyskocil, B. Maca, M. Polasek, T. A. Claxton, A. P. Abbott, P. Kocovsky, *J. Org. Chem.* **1994**, *59*, 2156–2163.
[9] a) B.-Y. Lim, M.-K. Choi, C.-G. Cho, *Tetrahedron Lett.* **2011**, *52*, 6015–6017; b) H.-Y. Kim, W.-J. Lee, H.-M. Kang, C.-G. Cho, *Org. Lett.* **2007**, *9*, 3185–3186; c) H.-M. Kang, Y.-K. Lim, I.-J. Shin, H.-Y. Kim, C.-G. Cho, *Org. Lett.* **2006**, *8*, 2047–2050; d) S. E. Suh, I.-K. Park, B.-Y. Lim, C.-G. Cho, *Eur. J. Org. Chem.*

2011, 455 – 457; e) Y.-K. Lim, J.-W. Jung, H. Lee, C.-G. Cho, *J. Org. Chem.* **2004**, *69*, 5778 – 5781; f) G.-Q. Li, H. Gao, C. Keene, M. Devonas, D. H. Ess, L. Kürti, *J. Am. Chem. Soc.* **2013**, *135*, 7414 – 7417.

[10] T. Gieshoff, D. Schollmeyer, S. R. Waldvogel, *Angew. Chem. Int. Ed.* **2016**, *55*, 9437 – 9440; *Angew. Chem.* **2016**, *128*, 9587 – 9590.

[11] a) S. Lips, A. Wiebe, B. Elsler, D. Schollmeyer, K. M. Dyballa, R. Franke, S. R. Waldvogel, *Angew. Chem. Int. Ed.* **2016**, *55*, 10872 – 10876; *Angew. Chem.* **2016**, *128*, 11031 – 11035; b) N. Y. More, M. Jeganmohan, *Org. Lett.* **2015**, *17*, 3042 – 3045; c) T. Morofuji, A. Shimizu, J.-i. Yoshida, *Angew. Chem. Int. Ed.* **2012**, *51*, 7259 – 7262; *Angew. Chem.* **2012**, *124*, 7371 – 7374; d) A. Libman, H. Shalit, Y. Vainer, S. Narute, S. Kozuch, D. Pappo, *J. Am. Chem. Soc.* **2015**, *137*, 11453 – 11460; e) Y. E. Lee, T. Cao, C. Torruellas, M. C. Kozlowski, *J. Am. Chem. Soc.* **2014**, *136*, 6782 – 6785.

[12] B. Elsler, D. Schollmeyer, K. M. Dyballa, R. Franke, S. R. Waldvogel, *Angew. Chem. Int. Ed.* **2014**, *53*, 5210 – 5213; *Angew. Chem.* **2014**, *126*, 5311 – 5314.

[13] R. F. Fritsche, G. Theumer, O. Kataeva, H.-J. Knölker, *Angew. Chem. Int. Ed.* **2017**, *56*, 553 – 557; *Angew. Chem.* **2017**, *129*, 564 – 568.

[14] E. J. Horn, B. R. Rosen, P. S. Baran, *ACS Cent. Sci.* **2016**, *2*, 302 – 308.

[15] H. J. Schäfer, *C. R. Chim.* **2011**, *14*, 745 – 765.

[16] A. Wiebe, D. Schollmeyer, K. M. Dyballa, R. Franke, S. R. Waldvogel, *Angew. Chem. Int. Ed.* **2016**, *55*, 11801 – 11805; *Angew. Chem.* **2016**, *128*, 11979 – 11983.

[17] B. Riehl, K. M. Dyballa, R. Franke, S. R. Waldvogel, *Synthesis* **2017**, 252 – 259.

[18] A. Kirste, B. Elsler, G. Schnakenburg, S. R. Waldvogel, *J. Am. Chem. Soc.* **2012**, *134*, 3571 – 3576.

[19] M. Ito, H. Kubo, I. Itani, K. Morimoto, T. Dohi, Y. Kita, *J. Am. Chem. Soc.* **2013**, *135*, 14078 – 14081.

[20] a) K. Morimoto, K. Sakamoto, Y. Ohnishi, T. Miyamoto, M. Ito, T. Dohi, Y. Kita, *Chem. Eur. J.* **2013**, *19*, 8726 – 8731; b) R. Samanta, J. Lategahn, A. P. Antonchick, *Chem. Commun.* **2012**, *48*, 3194 – 3196.

[21] a) R. Francke, D. Cericola, R. Kötz, D. Weingarth, S. R. Waldvogel, *Electrochim. Acta* **2012**, *62*, 372 – 380; b) O. Hollóczki, A. Berkessel, J. Mars, M. Mezger, A. Wiebe, S. R. Waldvogel, B. Kirchner, *ACS Catal.* **2017**, *7*, 1846 – 1852.

[22] B. Elsler, A. Wiebe, D. Schollmeyer, K. M. Dyballa, R. Franke, S. R. Waldvogel, *Chem. Eur. J.* **2015**, *21*, 12321 – 12325.

[23] C. Gütz, B. Klöckner, S. R. Waldvogel, *Org. Process Res. Dev.* **2016**, *20*, 26 – 32.

[24] D. M. Mohilner, R. N. Adams, W. J. Argersinger, *J. Am. Chem. Soc.* **1962**, *84*, 3618 – 3622.

[25] J. A. Souto, C. Martínez, I. Velilla, K. Muñiz, *Angew. Chem. Int. Ed.* **2013**, *52*, 1324 – 1328; *Angew. Chem.* **2013**, *125*, 1363 – 1367.

[26] F. G. Bordwell, D. J. Algrim, *J. Org. Chem.* **1976**, *41*, 2507 – 2508.

[27] a) T. Kinzel, Y. Zhang, S. I. Buchwald, *J. Am. Chem. Soc.* **2010**, *132*, 14073 – 14075; b) Y. Yang, S. K. Seidlits, M. M. Adams, V. M. Lynch, C. E. Schmidt, E. V. Anslyn, J. B. Shear, *J. Am. Chem. Soc.* **2010**, *132*, 13114 – 13116; c) S. Handa, L. M. Slaughter, *Angew. Chem. Int. Ed.* **2012**, *51*, 2912 – 2915; *Angew. Chem.* **2012**, *124*, 2966 – 2969.

[28] P. G. M. Wuts, T. W. Greene, *Protective Groups in Organic Synthesis*, 4th ed., Wiley, Hoboken, **2007**.

[29] C. Zinelaabidine, O. Souad, J. Zoubir, B. Malika, A. Nour-Eddine, *Int. J. Chem.* **2012**, *4*, 73 – 79.

Manuscript received: December 29, 2016
Final Article published: March 2, 2017

Angewandte Chemie

GDCh

Eine Zeitschrift der Gesellschaft Deutscher Chemiker

www.angewandte.de

2017–129/17

Die Bildung von Polyanilinen ...

… lässt sich durch anodische Kupplung von Anilinen mit einfachen carbonylbasierten und leicht entfernbaren Schutzgruppen vermeiden. In der Zuschrift auf S. 4955 ff. präsentieren S. R. Waldvogel et al. eine leicht durchführbare elektrolytische Synthese geschützter 2,2′-Diaminobiaryl-Derivate in hoher Ausbeute und mit exzellenter Selektivität über oxidative Kreuzkupplung. Mit 1,1,1,3,3,3-Hexafluor-2-propanol als Lösungsmittel gelingt eine saubere elektrochemische Umsetzung.

Appendix Seite A75

150 Jahre GDCh

WILEY-VCH

VIP Elektrosynthese Very Important Paper

Deutsche Ausgabe: DOI: 10.1002/ange.201612613
Internationale Ausgabe: DOI: 10.1002/anie.201612613

Reagens- und metallfreie anodische C-C-Kreuzkupplung von Anilinderivaten

*Lara Schulz, Mathias Enders, Bernd Elsler, Dieter Schollmeyer, Katrin M. Dyballa, Robert Franke und Siegfried R. Waldvogel**

Abstract: *Vorgestellt wird die oxidative Kreuzkupplung von Anilinderivaten zu 2,2′-Diaminobiarylen. Der Oxidationsschritt wird elektrochemisch durchgeführt, ohne die Notwendigkeit von Metallen und Reagenzien. Ein breites Spektrum an Biphenyldiaminen konnte hergestellt werden. Die besten Resultate wurden mit Glaskohlenstoff als Anodenmaterial erhalten. Die elektrochemische Umsetzung kann problemlos in einer ungeteilten Zelle bei leicht erhöhten Temperaturen durchgeführt werden. Außerdem wurden gebräuchliche, auf Carbonsäuren basierende, Schutzgruppen verwendet, die nach der Kreuzkupplung unter milden Bedingungen selektiv abgespalten werden können. Auf diese Weise erhält man schnell und effizient Zugang zu äußerst wichtigen Bausteinen.*

Unsymmetrische Biaryle sind bedeutende Strukturmotive in Naturstoffen und in der Katalyse.[1] Besonders 1,1′-Binaphthyl-2,2′-diamin (BINAM) ist ein vielversprechender Ligand und wurde bereits eingehend erforscht: Asymmetrische Michael-Additionen,[2] N-Arylierungen von Indolen[3] und Hydrierungen von Ketonen und Olefinen[4] wurden unter der Verwendung von BINAM oder Derivaten davon als Liganden in Übergangsmetallkatalysen durchgeführt. Darüber hinaus beinhalten auch neuartige Liganden für Kontrastmittel in der Magnetresonanztomographie 2,2′-Diaminobiaryle als Strukturmotiv.[5] Jedoch ist der Zugang zu diesen Substanzen über klassische Synthesen begrenzt, da Aniline sehr leicht zu Polyanilin polymerisieren (Bildung von „Anilinschwarz“).[6] Symmetrische 2,2′-Diaminobiaryle sind z. B. über eine kupferkatalysierte Ullmann-Kupplung zugänglich.[7] Direkte oxidative Kreuzkupplungen mit stöchiometrischen Mengen anorganischer Reagenzien wie Cu^{II}-Salze wurden bisher nur mit Naphthylaminen realisiert und führen zu eher schlechten Ausbeuten.[8] Sigmatrope Umlagerungen von Diarylhydrazinen mittels katalytischer Mengen an Säure liefern symmetrische 2,2′-Diaminobiaryle in guten Ausbeuten, unsymmetrische Produkte sind jedoch immer noch eine Herausforderung.[9] Zusätzlich sind mehrere Syntheseschritte notwendig, um die Ausgangsverbindungen herzustellen.[9,10] Die Anwendung dieser Strategien ist oft mit großem Aufwand und komplizierten Reaktionsbedingungen verbunden. Solche Herangehensweisen führen oft zu komplexen Reaktionsgemischen und geringen Ausbeuten des gewünschten Produktes. Dagegen sind oxidative Kupplungsreaktionen mit direkter C-H-Aktivierung als nachhaltige Methoden von großem Interesse.[11,12] Kürzlich wurde eine Arbeit über die oxidative Umsetzung von Diarylaminen mittels eines hochfluorierten Eisen-Phthalocyanin-Katalysators, der sowohl C-C- als auch N-N-Kupplungen ermöglicht, veröffentlicht.[13]

Elektrochemische Methoden sind bemerkenswert fortschrittlich in der Abfallvermeidung, da weder Abgangsgruppen noch Oxidationsmittel benötigt werden.[14] Die elektrochemische Erzeugung reaktiver Intermediate ist höchst interessant hinsichtlich der Atomökonomie und Kosteneffizienz.[15] In unserer Gruppe wurden die anodische Phenol-Phenol-[12,16,17] sowie die Phenol-Aren-Kreuzkupplung entwickelt.[18] Die besten Resultate bei direkten oxidativen Kreuzkupplungen von Arylen werden in stabilisierenden Medien wie 1,1,1,3,3,3-Hexafluor-2-propanol (HFIP) erhalten, das auch häufig in Reaktionen mit hypervalentem Iod eingesetzt wird.[19,20] Dieses einzigartige Lösungsmittel ist in der Lage, starke Wasserstoffbrücken zu bilden.[21] Dies führt zu signifikanten Änderungen in der Solvatation der einzelnen Kupplungspartner und somit zu einer Entkopplung des Oxidationspotentials von der Nukleophilie.[22]

Nachfolgend wird ein selektiver Zugang zu unsymmetrischen 2,2′-Diaminobiarylen mittels anodischer Kreuzkupplung vorgestellt (Schema 1). Die elektrochemische Synthese unsymmetrischer 2,2′-Diaminobiaryle ist apparativ sehr einfach, da lediglich ein Zwei-Elektroden-Aufbau in einer ungeteilten Becherglaszelle benötigt wird. Außerdem wird die Elektrolyse bei konstantem Strom durchgeführt, was die benötigte Ausstattung stark vereinfacht. Um geeignete Kupplungspartner zu finden, wurde eine Reihe von Screening-

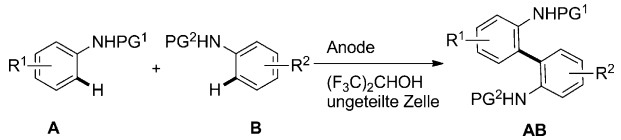

Schema 1. Direkte anodische C-C-Kreuzkupplung zweier geschützter Anilinderivate (PG = Schutzgruppe).

[*] L. Schulz, M. Enders, Dr. B. Elsler, Dr. D. Schollmeyer, Prof. Dr. S. R. Waldvogel
Institut für Organische Chemie
Johannes Gutenberg-Universität Mainz
Duesbergweg 10–14, 55128 Mainz (Deutschland)
E-Mail: waldvogel@uni-mainz.de
Homepage: http://www.chemie.uni-mainz.de/OC/AK-Waldvogel/
Dr. K. M. Dyballa, Prof. Dr. R. Franke
Evonik Performance Materials GmbH
Paul-Baumann-Straße 1, 45772 Marl (Deutschland)
Prof. Dr. R. Franke
Lehrstuhl für Theoretische Chemie, Ruhr-Universität Bochum
44780 Bochum (Deutschland)
Hintergrundinformationen und die Identifikationsnummer (ORCID) eines Autors sind unter:
http://dx.doi.org/10.1002/ange.201612613 zu finden.

Experimenten durchgeführt.[23] Üblicherweise hat die Komponente **A** ein niedrigeres Oxidationspotential als das Anilin **B** und wird damit bevorzugt an der Anode oxidiert. Um die Bildung des Kreuzkupplungsprodukts gegenüber dem Homokupplungsprodukt statistisch zu begünstigen, wird das Anilin mit dem höheren Oxidationspotential **B** in einem leichten Überschuss eingesetzt. Die Stabilisierung der reaktiven Radikale während der Elektrolyse ist essenziell, um unerwünschte Oligomerisierung oder sogar Mineralisierung zu vermeiden. Die positiven Einflüsse auf die Ausbeute und die Selektivität von HFIP und protischen Additiven wie Methanol oder Wasser wurden kürzlich beschrieben.[12,18,22] Einfache Anilinderivate sind elektronenreich und neigen wegen der daraus resultierenden niedrigen Oxidationspotentiale zu Überoxidation. Polymerisation ist ein ernsthaftes Problem in anodischen Umsetzungen von Anilinen.[24] In organokatalytischen Reaktionen werden derzeit N-Schützungen genutzt, um die Entstehung unerwünschter Nebenprodukte zu verhindern.[19] N-Mesyl-geschützte Aniline liefern gute Ausbeuten in durch hypervalente Iodreagentien vermittelten Kupplungen, allerdings ist eine abfall- und zeitintensive Entschützung notwendig, um die gewünschten Aminobiphenyle zu erhalten.[19] Muñiz et al. nutzten kürzlich ein hypervalentes Iodreagens, um durch Diaminierung Tosyl-geschützte Diamine zu erhalten.[25] Dahingegen wurden in dieser Arbeit verschiedene leicht abspaltbare Schutzgruppen für die Anilinderivate genutzt (Abbildung 1).

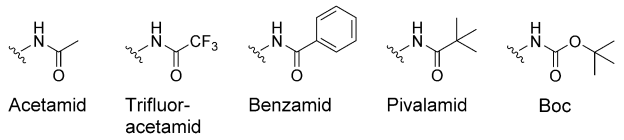

Abbildung 1. Weitverbreitete und einfach abspaltbare carbonylbasierte Schutzgruppen für Aniline.

Es hat sich herausgestellt, dass Amide und Carbamate geeignet sind, um die Aminofunktion zu schützen und dass diese Gruppen während der Elektrolyse stabil sind. Cyclovoltammetrische Untersuchungen haben zudem sowohl einen deutlichen Einfluss der Schutzgruppen auf das Oxidationspotential (das mit den pK_S-Werten der Anilide korreliert)[26] als auch auf die möglichen Wechselwirkungen zwischen Substrat und Lösungsmittel durch Wasserstoffbrücken gezeigt (Abbildung 2).

Elektronenreiche Aniline wie 3,4-Dimethoxyanilin haben niedrige Oxidationspotentiale (832 mV in reinem HFIP; vgl. $pK_{S(Anilinium)} = 4.6$ in DMSO[26]) und tendieren deshalb zur Überoxidation. Durch Einführen einer Acetyl- oder einer Trifluoracetylgruppe kann das Oxidationspotential auf 1.39 V bzw. 1.57 V angehoben werden (vgl. $pK_{S(Acetanilid)} = 18.8$; $pK_{S(Trifluoracetanilid)} = 12.6$ in DMSO).[26] Aufgrund der Fähigkeit der Amidfunktion, an Wasserstoffbrücken sowohl als Donor als auch als Akzeptor teilzunehmen, erfahren die geschützten Aniline eine starke Solvatation durch HFIP. Cyclovoltammetrische Untersuchungen von unterschiedlich geschütztem 3,4-Dimethoxyanilin zeigen eine deutliche Verschiebung der Oxidationspotentiale zu niedrigeren Werten bei steigender

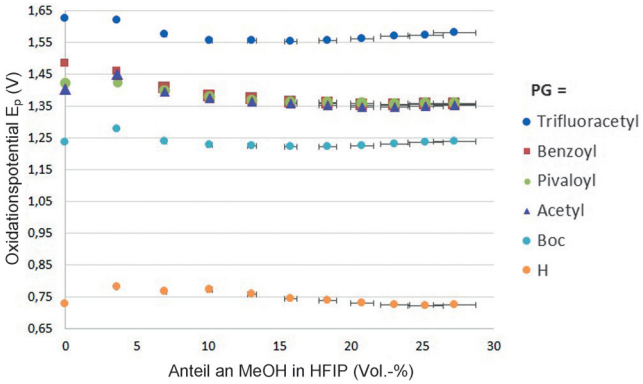

Abbildung 2. Verschiebungen des Oxidationspotentials von unterschiedlich geschütztem 3,4-Dimethoxyanilin mit zunehmendem MeOH-Anteil in HFIP. AE: Glaskohlenstoff-Elektrodenspitze, 2 mm Durchmesser; GE: Glaskohlenstoffstab; RE: Ag/AgCl in ges. LiCl/EtOH, Lösungsmittel: HFIP + 0–27 Vol.-% MeOH, Leitsalz: 0.09 M Bu_3NMeO_3SOMe.

Konzentration von Methanol in HFIP. Methanol wirkt im Elektrolyten als schwache Base und verringert somit die Solvatation der Amide. Abbildung 2 zeigt, dass die Oxidationspotentiale von Anilinen durch verschiedene Schutzgruppen zu einem gewissen Grad angepasst werden können. Diese Tatsache begünstigt die anodische Kreuzkupplung von Aniliden, da es eine optimale Differenz zwischen den Oxidationspotentialen der Kupplungspartner zu geben scheint.[22] Im Allgemeinen helfen CV-Messungen dabei, die korrekte Stöchiometrie für die anodische Kreuzkupplung zu bestimmen, da Komponente **A** ein niedrigeres Oxidationspotential als Komponente **B** aufweisen sollte und somit bevorzugt an der Anode oxidiert wird, um somit die Kreuzkupplungssequenz einzuleiten (Schema 1).

Üblicherweise hat das Elektrodenmaterial einen entscheidenden Einfluss auf elektrochemische Umsetzungen, da oft verschiedene Reaktionswege und Adsorptionscharakteristiken auftreten können. In dieser Arbeit jedoch stellte sich heraus, dass das gewählte Elektrolytsystem der ausschlaggebende Faktor zu sein scheint. Interessanterweise wurden bei der untersuchten Umsetzung der Anilide **1** und **2** (Schema 2) an verschiedenen Elektrodenmaterialien wie

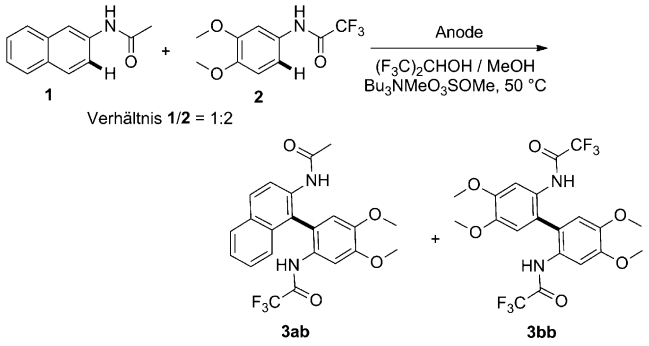

Schema 2. Einfluss von Methanol und verschiedenen Elektrodenmaterialien auf die anodische Kreuzkupplung von Anilinen. 2-Acetamidonaphthalin (**1**) wurde als **A**-Komponente verwendet, **2** als **B**-Komponente.

Platin, Bor-dotierter Diamant, Graphit und Glaskohlenstoff konsistente Ergebnisse erhalten (Tabelle 1).

Angesichts der Selektivität in HFIP führen alle Elektrodenmaterialien zu ähnlichen Ergebnissen, die besten Ausbeuten jedoch wurden an Graphit und Platin erhalten. Durch Zugabe von Methanol zum Lösungsmittel stieg die Selektivität signifikant an, und an Glaskohlenstoff wurde ausschließlich das Kreuzkupplungsprodukt erhalten (Nr. 2, Tabelle 1). Außerdem wurde an Glaskohlenstoff wesentlich weniger Oligomerisierung beobachtet als an den anderen Materialien. Dieser Fakt ist in zweierlei Hinsicht wichtig: Erstens, wird die Aufreinigung wesentlich erleichtert, und zweitens können nicht umgesetzte Ausgangsverbindungen einfach zurückgewonnen werden. Darüber hinaus ist Glaskohlenstoff auch bei Langzeitnutzung chemisch hoch stabil, während Graphit deutliche Abnutzung zeigt. Wägt man Selektivität, elektrochemische Stabilität und Kosten ab, so ist Glaskohlenstoff das Elektrodenmaterial der Wahl.

Tabelle 1: Einfluss des Elektrodenmaterials auf die Anilin-Anilin-Kreuzkupplung.[a]

Nr.	Elektrodenmaterial	Additiv[b]	Ausbeute [%][c]	**3ab/3bb**[c]
1	Glaskohlenstoff	–	51	6:1
2	Glaskohlenstoff	MeOH	20	>100:1[d]
3	Bor-dotierter Diamant	–	48	3:1
4	Bor-dotierter Diamant	MeOH	34	34:1
5	Graphit	–	60[e]	6:1
6	Graphit	MeOH	28[e]	28:1
7	Platin	–	60[e]	7:1
8	Platin	MeOH	29[e]	29:1

[a] 2-Acetamidonaphthalin (**1**) wurde als **A**-Komponente verwendet, **2** als Komponente **B**. [b] Elektrolysebedingungen: 50 °C, galvanostatisch ($j = 5.2$ mA cm^{-2}), ungeteilte Screening-Zelle, $Q = 2$ F (Anilin **A**), Lösungsmittel: HFIP oder HFIP + MeOH (18 Vol.-%), Leitsalz: 0.09 M Bu_3NMeO_3SOMe, Verhältnis **A**/**B** = 1:2. [c] Bestimmt mittels GC. [d] Homokupplungsprodukt **3bb** wurde mittels GC nicht detektiert. [e] Vermehrte Bildung von oligomeren Nebenprodukten.

In der Kreuzkupplung von Anilinen wird die neue C-C-Bindung ausschließlich in *ortho*-Stellung zur Aminofunktion gebildet, wodurch 2,2′-Diaminobiaryl-Derivate erhalten werden. Vor allem Anilinderivate mit elektronenschiebenden Gruppen, z. B. Methoxygruppen, in *para*-Position zur neu gebildeten C-C-Bindung, scheinen die Kupplungsreaktion zu begünstigen. Die Vielfalt der elektrochemisch hergestellten geschützten unsymmetrischen 2,2′-Diaminobiaryle ist in Abbildung 3 gezeigt. Es ist anzumerken, dass keine der Schutzgruppen während der Elektrolyse abgespalten wurde.

Oligomerisierung ist weiterhin die vorherrschende Nebenreaktion, durch die die Ausbeuten der Kreuzkupplungsprodukte verringert werden. Trotzdem konnten durch Umsetzung von N-Boc-geschütztem 3-Methoxy-4-methylanilin die gemischten 2,2′-Diaminobiaryle **4**, **5**, **6** und **7** in guten Ausbeuten von 40 % bis 51 % erhalten werden. Die höchste Ausbeute von 74 % wurde bei der Kupplung von *N*-(3,4-Dimethoxyphenyl)acetamid mit *N*-(3-Methoxy-4-methylphenyl)benzamid erhalten (**8**). Bei der Kreuzkupplung von *N*-(3,4-Dimethoxyphenyl)acetamid mit einem Benzodioxolderivat wurden leicht geringere Ausbeuten erhalten (38 %, **12**). Außerdem konnte 2-Acetamidonaphthalin (**1**) in einer Kreuzkupplung mit einem Trifluoracetamid **2** umgesetzt werden, um **3** in 59 % Ausbeute zu erhalten. Folglich hat sich gezeigt, dass Aniline mit elektronenschiebenden Gruppen oder Alkylgruppen in 3- und 4-Position geeignete Kupplungspartner sind. Die Kreuzkupplung von Anilinen mit Chlorsubstituenten war ebenfalls möglich (56 %, **10** und 51 %, **11**). Der Anteil an nicht umgesetzter **A**-Komponente liegt bei ca. 2–24 %. Eine Erhöhung der Ladungsmenge könnte also in manchen Fällen eine Ausbeutensteigerung bewirken.

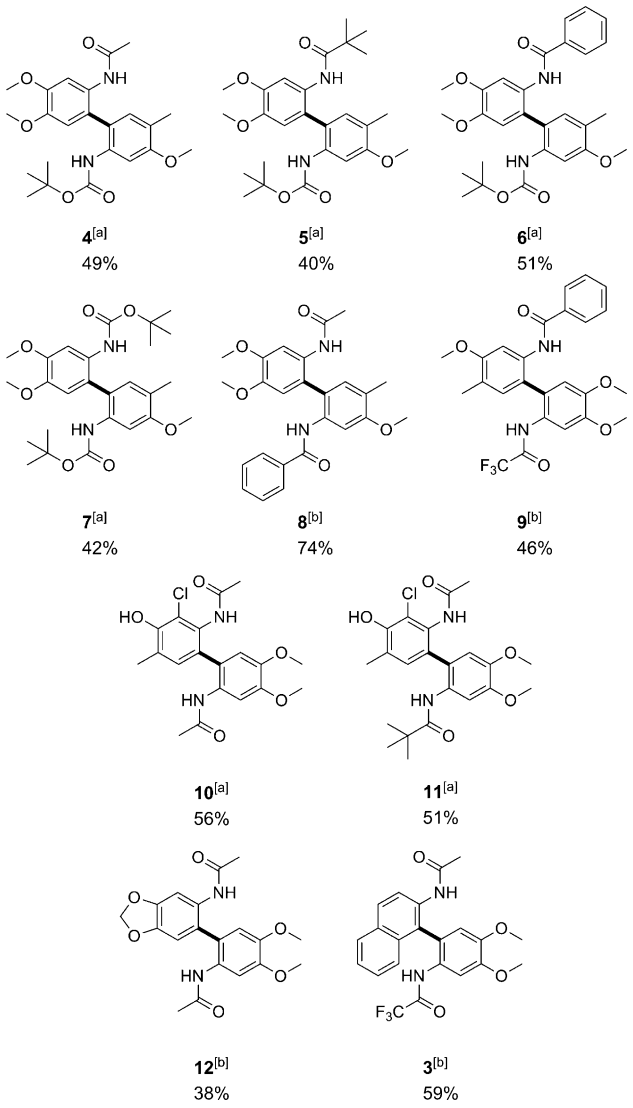

Abbildung 3. Substratbreite der geschützten unsymmetrischen 2,2′-Diaminobiaryle. [a] Elektrolysebedingungen: 50 °C, galvanostatisch ($j = 5.2$ mA cm^{-2}), Glaskohlenstoff-Anode, Glaskohlenstoff-Kathode, ungeteilte Becherglaszelle, $Q = 2$ F (Anilin **A**), Lösungsmittel: HFIP + MeOH (18 Vol.-%), Leitsalz: 0.09 M Bu_3NMeO_3SOMe, Verhältnis **A**/**B** = 1:2. [b] Elektrolysebedingungen wie in [a], Lösungsmittel: HFIP. [c] Die angegebenen Ausbeuten beziehen sich auf isolierte Produkte.

Im Verlauf erster Optimierungen der Elektrolysebedingungen wurde der Einfluss der Temperatur auf die Ausbeuten der jeweiligen Kreuzkupplungsprodukte untersucht (Tabelle 2). Diese Untersuchungen haben gezeigt, dass eine Elektrolysetemperatur von 30 °C vorteilhaft ist (Nr. 3 und 6).

Tabelle 2: Einfluss der Temperatur auf die anodische Kreuzkupplung von Anilinderivaten.

Nr.	Produkt[a]	*T* [°C]	Ausbeute[b] [%]
1	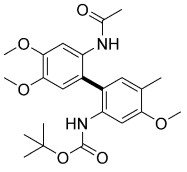	50	49
2		40	46
3		*30*	*59*
4		20	49
	4[c]		
5	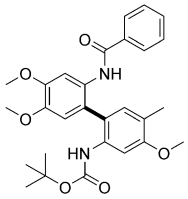	50	51
6		*30*	*59*
7		20	54
	6[c]		

[a] Elektrolysebedingungen: 20–50 °C, galvanostatisch ($j = 5.2$ mA cm^{-2}), Glaskohlenstoff-Anode, Glaskohlenstoff-Kathode, ungeteilte Becherglaszelle, $Q = 2$ F (Anilin **A**), Lösungsmittel: HFIP + MeOH (18 Vol.-%), Leitsalz: 0.09 M Bu_3NMeO_3SOMe, Verhältnis **A**/**B** = 1:2. [b] Ausbeute an isoliertem Produkt. [c] Acetyl- bzw. Benzoyl-geschütztes 3,4-Dimethoxyanilin wurde als Komponente **A** verwendet.

Tabelle 3: Teilweise und komplette Entschützung unterschiedlicher, geschützter 2,2′-Diaminobiaryle.

Nr.	Substrat	Entfernte PG	Produkt	Ausbeute [%]
1	**4**	Boc[a]	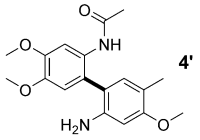 **4'**	98[d]
2	**6**	Boc[a]	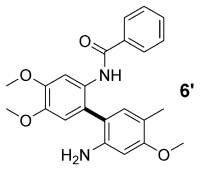 **6'**	99
3	**3**	Trifluoracetyl[b]	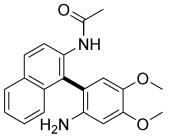 **3'**	99
4	**3**	Acetyl und Trifluoracetyl[c]	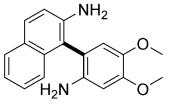 **3''**	98

[a] Reaktionsbedingungen: 0.20 mmol Substrat, 100 °C, Lösungsmittel: H_2O/MeOH (2:1 v/v), 24 h. [b] 1.50 mmol Substrat, 20 °C, Lösungsmittel: MeOH/H_2O (2:1 v/v), 10 Äquiv. K_2CO_3, 4 d. [c] 0.7 mmol Substrat, 120 °C, Lösungsmittel: Hydrazinhydrat (80 % in H_2O), 4 d. [d] Verschiebung der verbleibenden Acetylgruppe nach der Aufreinigung (siehe die Hintergrundinformationen).

Um eine spätere Anwendung solch geschützter 2,2′-Diaminobiaryle in Liganden oder funktionalisierten Materialien zu ermöglichen,[27] ist es unverzichtbar, die Aminofunktion effizient entschützen zu können. Die genutzten Schutzgruppen basieren auf gebräuchlichen Carbonsäuren und können daher einfach durch Standardmethoden entfernt werden.[28] Durch die Anwendung orthogonaler Schutzgruppen sind die beiden Aminofunktionen voneinander unabhängig zugänglich, was eine weitere chemo- und regioselektive Umsetzung ermöglicht (Tabelle 3). Diese teilgeschützten Kreuzkupplungsprodukte wurden bisher nicht beschrieben und repräsentieren das Pendant zu den kürzlich vorgestellten teilgeschützten Biphenolen.[16]

Wir erreichten die selektive Abspaltung einer Boc-Gruppe durch Wasser ohne die Notwendigkeit zusätzlicher Säure,[29] während die Acetyl- bzw. Benzoylgruppe in den Substraten **4** und **6** verblieben (Tabelle 3, Nr. 1 und 2). Eine Trifluoracetylgruppe konnte mittels Kaliumcarbonat selektiv in Gegenwart einer Acetylgruppe entfernt werden (Nr. 3). Beide Schutzgruppen in **3**, eine Acetyl- sowie eine Trifluoracetylgruppe, konnten gleichzeitig durch Hydrazinhydrat abgespalten werden (Nr. 4). Diese einfachen und effizienten Möglichkeiten, die Kreuzkupplungsprodukte zu entschützen, zeigen einmal mehr die Leistungsfähigkeit dieser Methode, Vorstufen für relevante Bausteine herzustellen.

Abschließend lässt sich hervorheben, dass ein hoch innovatives und einfach durchzuführendes Versuchsprotokoll zur Synthese von 2,2′-Diaminobiarylen durch elektrochemische C-C-Kreuzkupplung etabliert werden konnte. Die Substratbreite deckt verschieden substituierte und geschützte Anilinderivate ab. Essenziell für die hohe Selektivität ohne die Notwendigkeit von Abgangsgruppen ist der Lösungsmitteleffekt von HFIP. Dieser hochfluorierte Alkohol ermöglicht eine Entkopplung des Oxidationspotentials von der Nukleophilie der Kupplungspartner. Die Schutzgruppen basieren auf gebräuchlichen Carbonsäuren und sind daher einfach abzuspalten. Werden verschiedene Schutzgruppen verwendet, so ist eine selektive Freisetzung der einzelnen Aminofunktionen durch Nukleophile möglich. Durch die Nutzung von elektrischem Strom für diese Umsetzung wird eine metall- und reagensfreie und somit äußerst nachhaltige Reaktionssequenz kreiert. Außerdem ist das Elektrolyseprotokoll sehr einfach durchzuführen, da lediglich eine ungeteilte Zelle und ein Zwei-Elektroden-Arrangement benötigt werden.

Danksagung

S.R.W. dankt der DFG (Wa1278/14-1) für die Förderung. Wir sind für die finanzielle Unterstützung durch BMBF-EPSYLON (FKZ 12XP2016D) sehr dankbar.

Interessenkonflikt

Die Autoren erklären, dass keine Interessenkonflikte vorliegen.

Stichwörter: Biaryle · C-H-Aktivierung · Elektrochemie · Kreuzkupplungen · Schutzgruppen

Zitierweise: *Angew. Chem. Int. Ed.* **2017**, *56*, 4877 – 4881
Angew. Chem. **2017**, *129*, 4955 – 4959

[1] a) G. Bringmann, A. J. Mortimer, P. A. Keller, M. J. Gresser, J. Garner, M. Breuning, *Angew. Chem. Int. Ed.* **2005**, *44*, 5384 – 5427; *Angew. Chem.* **2005**, *117*, 5518 – 5563; b) K. C. Nicolaou, P. G. Bulger, D. Sarlah, *Angew. Chem. Int. Ed.* **2005**, *44*, 4442 – 4489; *Angew. Chem.* **2005**, *117*, 4516 – 4563; c) A. Zapf, M. Beller, *Top. Catal.* **2002**, *19*, 101 – 109.
[2] J. Wang, H. Li, W. Duan, L. Zu, W. Wang, *Org. Lett.* **2005**, *7*, 4713 – 4716.
[3] R. K. Rao, A. B. Naidu, E. A. Jaseer, G. Sekar, *Tetrahedron* **2009**, *65*, 4619 – 4624.
[4] a) K. Kabuto, T. Yoshida, S. Yamaguchi, S. Miyano, H. Hashimoto, *J. Org. Chem.* **1985**, *50*, 3013 – 3015; b) F.-Y. Zhang, C.-C. Pai, A. S. C. Chan, *J. Am. Chem. Soc.* **1998**, *120*, 5808 – 5809.
[5] K.-H. Jung, H.-K. Kim, G. H. Lee, D.-S. Kang, J.-A. Park, K. M. Kim, Y. Chang, T.-J. Kim, *J. Med. Chem.* **2011**, *54*, 5385 – 5394.
[6] H. Letheby, *J. Chem. Soc.* **1862**, *15*, 161.
[7] W. Kalk, H.-S. Bien, K.-H. Schündehütte, *Justus Liebigs Ann. Chem.* **1977**, 329 – 337.
[8] M. Smrcina, S. Vyskocil, B. Maca, M. Polasek, T. A. Claxton, A. P. Abbott, P. Kocovsky, *J. Org. Chem.* **1994**, *59*, 2156 – 2163.
[9] a) B.-Y. Lim, M.-K. Choi, C.-G. Cho, *Tetrahedron Lett.* **2011**, *52*, 6015 – 6017; b) H.-Y. Kim, W.-J. Lee, H.-M. Kang, C.-G. Cho, *Org. Lett.* **2007**, *9*, 3185 – 3186; c) H.-M. Kang, Y.-K. Lim, I.-J. Shin, H.-Y. Kim, C.-G. Cho, *Org. Lett.* **2006**, *8*, 2047 – 2050; d) S. E. Suh, I.-K. Park, B.-Y. Lim, C.-G. Cho, *Eur. J. Org. Chem.* **2011**, 455 – 457; e) Y.-K. Lim, J.-W. Jung, H. Lee, C.-G. Cho, *J. Org. Chem.* **2004**, *69*, 5778 – 5781; f) G.-Q. Li, H. Gao, C. Keene, M. Devonas, D. H. Ess, L. Kürti, *J. Am. Chem. Soc.* **2013**, *135*, 7414 – 7417.
[10] T. Gieshoff, D. Schollmeyer, S. R. Waldvogel, *Angew. Chem. Int. Ed.* **2016**, *55*, 9437 – 9440; *Angew. Chem.* **2016**, *128*, 9587 – 9590.
[11] a) S. Lips, A. Wiebe, B. Elsler, D. Schollmeyer, K. M. Dyballa, R. Franke, S. R. Waldvogel, *Angew. Chem. Int. Ed.* **2016**, *55*, 10872 – 10876; *Angew. Chem.* **2016**, *128*, 11031 – 11035; b) N. Y. More, M. Jeganmohan, *Org. Lett.* **2015**, *17*, 3042 – 3045; c) T. Morofuji, A. Shimizu, J.-i. Yoshida, *Angew. Chem. Int. Ed.* **2012**, *51*, 7259 – 7262; *Angew. Chem.* **2012**, *124*, 7371 – 7374; d) A. Libman, H. Shalit, Y. Vainer, S. Narute, S. Kozuch, D. Pappo, *J. Am. Chem. Soc.* **2015**, *137*, 11453 – 11460; e) Y. E. Lee, T. Cao, C. Torruellas, M. C. Kozlowski, *J. Am. Chem. Soc.* **2014**, *136*, 6782 – 6785.
[12] B. Elsler, D. Schollmeyer, K. M. Dyballa, R. Franke, S. R. Waldvogel, *Angew. Chem. Int. Ed.* **2014**, *53*, 5210 – 5213; *Angew. Chem.* **2014**, *126*, 5311 – 5314.
[13] R. F. Fritsche, G. Theumer, O. Kataeva, H.-J. Knölker, *Angew. Chem. Int. Ed.* **2017**, *56*, 553 – 557; *Angew. Chem.* **2017**, *129*, 564 – 568.
[14] E. J. Horn, B. R. Rosen, P. S. Baran, *ACS Cent. Sci.* **2016**, *2*, 302 – 308.
[15] H. J. Schäfer, *C. R. Chim.* **2011**, *14*, 745 – 765.
[16] A. Wiebe, D. Schollmeyer, K. M. Dyballa, R. Franke, S. R. Waldvogel, *Angew. Chem. Int. Ed.* **2016**, *55*, 11801 – 11805; *Angew. Chem.* **2016**, *128*, 11979 – 11983.
[17] B. Riehl, K. M. Dyballa, R. Franke, S. R. Waldvogel, *Synthesis* **2017**, 252 – 259.
[18] A. Kirste, B. Elsler, G. Schnakenburg, S. R. Waldvogel, *J. Am. Chem. Soc.* **2012**, *134*, 3571 – 3576.
[19] M. Ito, H. Kubo, I. Itani, K. Morimoto, T. Dohi, Y. Kita, *J. Am. Chem. Soc.* **2013**, *135*, 14078 – 14081.
[20] a) K. Morimoto, K. Sakamoto, Y. Ohnishi, T. Miyamoto, M. Ito, T. Dohi, Y. Kita, *Chem. Eur. J.* **2013**, *19*, 8726 – 8731; b) R. Samanta, J. Lategahn, A. P. Antonchick, *Chem. Commun.* **2012**, *48*, 3194 – 3196.
[21] a) R. Francke, D. Cericola, R. Kötz, D. Weingarth, S. R. Waldvogel, *Electrochim. Acta* **2012**, *62*, 372 – 380; b) O. Hollóczki, A. Berkessel, J. Mars, M. Mezger, A. Wiebe, S. R. Waldvogel, B. Kirchner, *ACS Catal.* **2017**, *7*, 1846 – 1852.
[22] B. Elsler, A. Wiebe, D. Schollmeyer, K. M. Dyballa, R. Franke, S. R. Waldvogel, *Chem. Eur. J.* **2015**, *21*, 12321 – 12325.
[23] C. Gütz, B. Klöckner, S. R. Waldvogel, *Org. Process Res. Dev.* **2016**, *20*, 26 – 32.
[24] D. M. Mohilner, R. N. Adams, W. J. Argersinger, *J. Am. Chem. Soc.* **1962**, *84*, 3618 – 3622.
[25] J. A. Souto, C. Martínez, I. Velilla, K. Muñiz, *Angew. Chem. Int. Ed.* **2013**, *52*, 1324 – 1328; *Angew. Chem.* **2013**, *125*, 1363 – 1367.
[26] F. G. Bordwell, D. J. Algrim, *J. Org. Chem.* **1976**, *41*, 2507 – 2508.
[27] a) T. Kinzel, Y. Zhang, S. I. Buchwald, *J. Am. Chem. Soc.* **2010**, *132*, 14073 – 14075; b) Y. Yang, S. K. Seidlits, M. M. Adams, V. M. Lynch, C. E. Schmidt, E. V. Anslyn, J. B. Shear, *J. Am. Chem. Soc.* **2010**, *132*, 13114 – 13116; c) S. Handa, L. M. Slaughter, *Angew. Chem. Int. Ed.* **2012**, *51*, 2912 – 2915; *Angew. Chem.* **2012**, *124*, 2966 – 2969.
[28] P. G. M. Wuts, T. W. Greene, *Protective Groups in Organic Synthesis*, 4. Aufl., Wiley-VCH, Hoboken, **2007**.
[29] C. Zinelaabidine, O. Souad, J. Zoubir, B. Malika, A. Nour-Eddine, *Int. J. Chem.* **2012**, *4*, 73 – 79.

Eingegangen am 29. Dezember 2016
endgültige Fassung veröffentlicht am 2. März 2017

Appendix Seite A80

Angewandte Chemie
Eine Zeitschrift der Gesellschaft Deutscher Chemiker

Supporting Information

Reagent- and Metal-Free Anodic C–C Cross-Coupling of Aniline Derivatives

*Lara Schulz, Mathias Enders, Bernd Elsler, Dieter Schollmeyer, Katrin M. Dyballa, Robert Franke, and Siegfried R. Waldvogel**

ange_201612613_sm_miscellaneous_information.pdf

Table of Contents

General Remarks

All reagents were used in analytical grades without further purification. Solvents were purified by standard methods.[1] As supporting electrolyte *N*-methyl-*N,N,N*-tributylammonium methylsulfate was used (MTBS, kindly provided by BASF SE, Ludwigshafen, Germany). For electrochemical reactions glassy carbon (SIGRADUR® G, obtained from HTW, Thierhaupten, Germany), boron-doped diamond (DIACHEM®, 15 µm boron-doped diamond layer on 3 mm silicon support; obtained from CONDIAS GmbH, Itzehoe, Germany), graphite (SGL Carbon, Wiesbaden, Germany) and platinum electrodes (ÖGUSSA GES.M.B.H, Wien, Austria) were applied.

Column chromatography was performed on silica gel 60 M (0.040–0.063 mm, Macherey-Nagel GmbH & Co, Düren, Germany) with a maximum pressure of 1.6 bar. As eluents mixtures of cyclohexane and ethyl acetate were used. Silica gel 60 sheets on aluminum (F254, Merck, Darmstadt, Germany) were employed for thin layer chromatography.

Gas chromatography was performed with a Shimadzu GC-2010 (Shimadzu, Japan) using a HP 5 column (Agilent Technologies, USA; length: 30 m, inner diameter: 0.25 mm, film: 0.25 µm, carrier gas: hydrogen, injection temperature: 250 °C, detection temperature: 310 °C, program: method *hart*: 50 °C starting temperature for 1 min, heating rate: 15 °C/min, 290 °C final temperature for 8 min). GC-MS measurements were carried out on a Shimadzu GC-2010 (Shimadzu, Japan) using a ZB-5 column (Phenomenex, USA; length: 30 m, inner diameter: 0.25 mm, film: 0.25 mm, carrier gas: hydrogen, method *hart*: 50 °C starting temperature for 1 min, heating rate: 15 °C/min, 290 °C final temperature for 8 min). The method was coupled with mass spectrometry on a Shimadzu GCMS-QP2010 (ion source's temperature: 200 °C).

Microanalysis was performed with a VarioMICRO cube (Elementar Analysesysteme, Hanau, Germany).

Melting points were determined with a Melting Point Apparatus SMP3 (Stuart Scientific, Staffordshire, U.K.) and are uncorrected. Heating rate: 2 °C/min.

Spectroscopy and spectrometry: ^{1}H NMR, ^{13}C NMR and ^{19}F NMR spectra were recorded at 25 °C by using a Bruker Avance II 400 (Analytische Messtechnik, Karlsruhe, Germany) or a Bruker Avance III HD 300, respectively. Chemical shifts (δ) are reported in parts per million (ppm) relative to TMS as internal standard or traces of $CHCl_3$ or d_5-DMSO in the corresponding deuterated solvent. High resolution mass spectra were obtained by using a QTof Ultima 3 (Waters, Milford, Massachusetts) apparatus employing ESI+.

Cyclic voltammetry was performed with a Metrohm 663 VA Stand equipped with a µAutolab type III potentiostat (Metrohm AG, Herisau, Switzerland). *WE*: glassy carbon electrode tip, 2 mm diameter; *CE*: glassy carbon rod; *RE*: Ag/AgCl in saturated LiCl/EtOH. Solvent: 1,1,1,3,3,3-hexafluoroisopropanol (HFIP) + 0–27% v/v methanol supporting electrolyte: 0.09 M Bu_3NMeO_3SOMe (MTBS); scan rate: 50 mV/s.

X-ray analysis: All data were collected on a STOE IPDS2T diffractometer (Oxford Cryostream 700er series, Oxford Cryosystems, Oxford, United Kingdom) using graphite monochromated Mo K_α radiation (λ = 0.71073 Å). Intensities were measured using fine-slicing ω and φ-scans and corrected for background, polarization and Lorentz effects. The structures were solved by direct methods and refined anisotropically by the least-squares procedure implemented in the SHELX program system.[2]

Synthesis of Substrates

A: General protocol for *N*-acetylation:

In a round-bottom flask the aniline (32–55 mmol, 1.0 eq.) was dissolved in anhydrous dichloromethane (90–130 mL). It was sealed by a septum and acetic anhydride (38–66 mmol, 1.2 eq.) was added to the chilled solution (0 °C) by a syringe, allowing pressure equilibration through a second cannula within the septum. The reaction mixture was stirred overnight at room temperature (23 °C) and the solvent was removed at reduced pressure. If necessary, a recrystallization from boiling cyclohexane/ethyl acetate (ca. 25 mL/g product) is possible.

B: General protocol for synthesis of benzamides:

In a round-bottom flask the aniline (22–33 mmol, 1.0 eq.) and triethylamine (24–36 mmol, 1.1 eq.) were dissolved in anhydrous dichloromethane (50–100 mL). It was sealed by a septum and benzoyl chloride (24–36 mmol, 1.1 eq.) was added by a syringe, allowing pressure equilibration through a second cannula within the septum. This reaction mixture was stirred overnight at room temperature (23 °C). The reaction mixture was washed with water (2x 30 mL) and the organic layer was dried with sodium sulfate. The solvent was removed at reduced pressure. If necessary, a recrystallization from boiling cyclohexane/ethyl acetate (ca. 25 mL/g product) is possible.

C: General protocol for *N*-2,2,2-trifluoroacetylation:

In a round-bottom flask the aniline (24 mmol, 1.0 eq.) was dissolved in anhydrous dichloromethane (60 mL). It was sealed by a septum and trifluoroacetic anhydride (29 mmol, 1.2 eq.) was added to the chilled solution by a syringe, allowing pressure equilibration through a second cannula within the septum. The reaction mixture was stirred overnight at room temperature (23 °C) and the solvent was removed at reduced pressure. If necessary, a recrystallization from boiling cyclohexane/ethyl acetate (ca. 25 mL/g product) is possible.

D: General protocol for synthesis of pivalamides:

In a round-bottom flask the aniline (20 mmol, 1.0 eq.) and triethylamine (26 mmol, 1.3 eq.) were dissolved in anhydrous dichloromethane (40 mL). It was sealed by a septum and pivaloyl chloride (26 mmol, 1.3 eq.) was added to the chilled solution (0 °C) by a syringe, allowing pressure equilibration through a second cannula within the septum. This reaction mixture was boiled under reflux (4 h). The reaction mixture was washed with water (2x 30 mL) and the organic layer was dried with sodium sulfate. The solvent was removed at reduced pressure. If necessary, a recrystallization from boiling cyclohexane/ethyl acetate (ca. 25 mL/g product) is possible.

E: General protocol for synthesis of Boc-protected anilines:

In a round-bottom flask the aniline (35 mmol, 1.0 eq.) was dissolved in anhydrous ethanol (200 mL). It was sealed by a septum and di-*tert*-butyl dicarbonate (54 mmol, 1.5 eq.) was added by a syringe, allowing pressure equilibration through a second cannula within the septum. This reaction mixture was stirred at room temperature (23 °C, 2 h). The solvent was removed at reduced pressure. If necessary, a recrystallization from boiling cyclohexane/ethyl acetate (ca. 25 mL/g product) is possible**.**

F: General protocol for aniline-aniline cross-coupling reactions:

Beaker-type Teflon cells and beaker-type glass cells were home-made by the local mechanical shop at the university. The undivided cells are briefly described here, whereas more details are reported in literature.[3,4] They are equipped with glassy carbon electrodes. Due to over-oxidation of desired 2,2‘-diaminobiaryls, electrolysis was stopped after applying 2 F per mol aniline **A** and using the optimized current density.[4]

Screening experiments (beaker-type)

A solution of protected aniline component **A** (0.4 mmol, 1.0 eq), protected aniline component **B** (0.8 mmol, 2.0 eq) and *N*-methyl-*N*,*N*,*N*-tributylammonium methylsulfate (MTBS) (0.14 g, 0.45 mmol) in 5 mL 1,1,1,3,3,3-hexafluoroisopropanol (HFIP) and/or 4.1 mL HFIP + 0.9 mL methanol (18% v/v), respectively, was transferred into a screening cell equipped with glassy carbon electrodes. A constant current electrolysis with a current density of 7.2 mA/cm^2 was performed at 50°C. After application of 73 C (2.0 F per aniline **A**) the electrolysis was stopped and the solvent mixture was recovered *in vacuo* (50 °C, 200–70 mbar). The residual mixture was analyzed by GC or GC/MS.

Recently, the set-up for screening was reported in detail.[3] Dimensions of glassy carbon electrodes are 7.0 x 1.0 x 0.3 cm. Using a 5 mL reaction mixture, electrodes immerse 1.8 cm into solution. This gives an active surface of 1.8 cm².

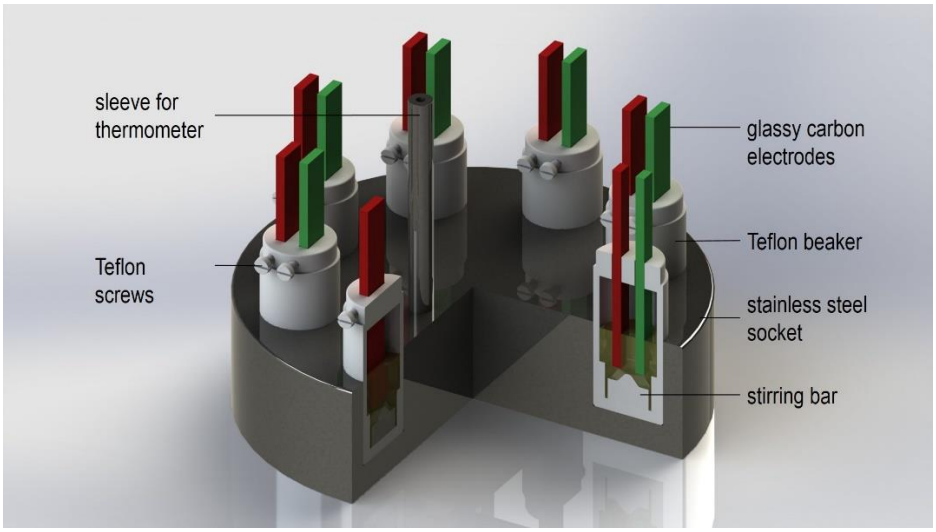

Figure S1: Schematic view of undivided screening cells in a screening arrangement.[3]

Beaker-type cell (25 mL)

A solution of protected aniline component **A** (1.9 mmol, 1.0 eq.), protected aniline component **B** (3.8 mmol, 2.0 eq.) and *N*-methyl-*N,N,N*-tributylammonium methylsulfate (MTBS) (0.70 g, 2.3 mmol, 1.2 eq.) in 25 mL 1,1,1,3,3,3-hexafluoroisopropanol (HFIP) or 20.5 mL HFIP + 4.5 mL methanol (18% v/v), respectively, was transferred into an undivided beaker-type electrolysis cell equipped with glassy carbon electrodes. A constant current electrolysis with a current density of 5.2 mA/cm² was performed at 30–50 °C. After application of 363 C (2.0 F per aniline **A**) the electrolysis was stopped and the solvent mixture was recovered *in vacuo* (50 °C, 200–70 mbar). The crude coupling products were purified by column chromatography (SiO_2, cyclohexane/ethyl acetate).

The beaker-type cell (25 mL) consists of a simple glass beaker with cooling jacket, covered with a Teflon plug. This cap allows precise location of the glassy carbon electrodes. Usually, a single glassy carbon electrode has upon immersion into the electrolyte an active surface of 9.0 cm^2 (2.0 cm x 4.5 cm).

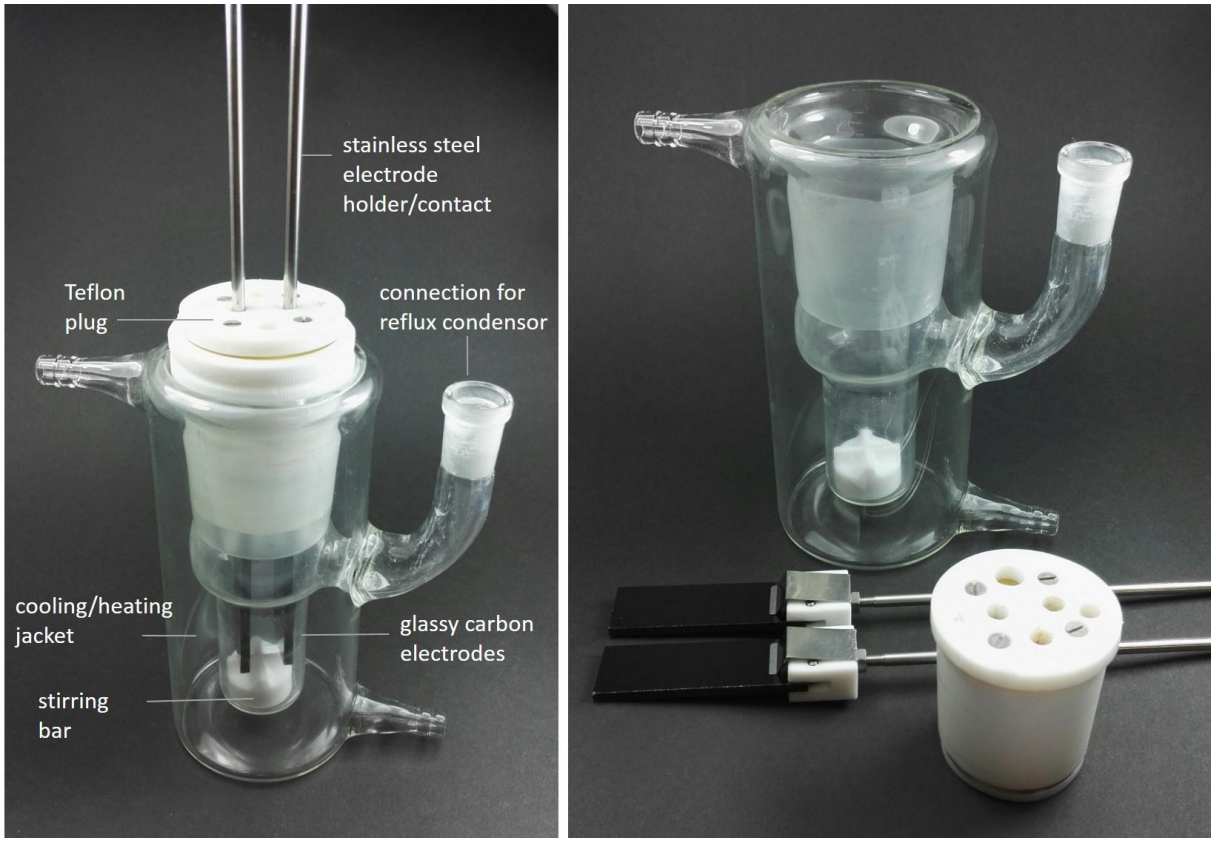

Figure S2: Pictures of an undivided beaker-type electrolysis cell. Essential parts are labeled.

Synthesis of Protected Non-symmetric 2,2'-Diaminobiaryls

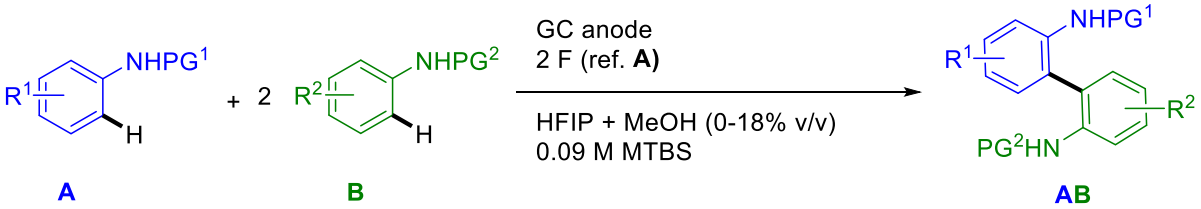

2-Acetamido-1-(4',5'-dimethoxy-2'-trifluoroacetamidophenyl)naphthalene (3)

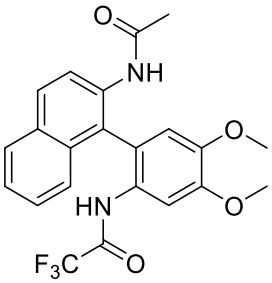

According to the general protocol **F**, 345 mg (1.9 mmol, 1.0 eq.) 2-acetamidonaphthalene **1**, 934 mg (3.8 mmol, 2.0 eq.) *N*-(3,4-dimethoxyphenyl)trifluoroacetamide **2** and 0.70 g MTBS were dissolved in 25 mL HFIP. After electrolysis, the solvent was recovered by distillation. Column chromatography of the residue (cyclohexane/ethyl acetate = 1:1 → 0:1) yielded the desired product as an off-white powder (yield: 59%, 474 mg, 1.1 mmol).

R_f (cyclohexane/ethyl acetate = 1:1) = 0.2; m.p. 179–180 °C; ^{1}H NMR (400 MHz, $CDCl_3$): δ (ppm) = 1.98 (s, 3 H), 3.83 (s, 3 H), 3.99 (s, 3 H), 6.72 (s, 1 H), 7.20 (bs, 1 H), 7.26 (d, *J* = 8.4 Hz, 1 H), 7.37–7.49 (m, 2 H), 7.64 (s, 1 H), 7.87–7.93 (m, 2 H), 7.99 (bs, 1 H), 8.07 (d, *J* = 8.9 Hz, 1 H); ^{13}C NMR (101 MHz, $CDCl_3$): δ (ppm) = 24.05, 56.19, 56.24, 107.68, 113.05, 115.43 (d, *J* = 288.4 Hz), 120.82, 122.50, 124.63, 124.78, 125.83, 126.91, 127.39, 128.33, 129.91, 131.40, 132.25, 133.84, 147.99, 149.39, 155.56 (d, *J* = 37.4 Hz), 169.38; ^{19}F NMR (282 MHz, $CDCl_3$): δ (ppm) = -77.43; HRMS for $C_{22}H_{19}F_3N_2O_4$ (ESI+) $[M+H]^+$: calc.: 433.1375; found: 433.1376; Elemental anal. for $C_{22}H_{19}F_3N_2O_4$ calc.: C: 61.11%, H: 4.43%, N: 6.48%, found: C: 60.87%, H: 4.39%, N: 6.39%.

Crystal structure determination of **3**: $C_{22}H_{19}F_3N_2O_4$, M_r = 432.39 gmol^{-1}; colorless block-like crystal (0.08x0.27x0.85 mm^3), triclinic space group P -1, a = 9.2354(5) Å, α = 97.624(2)°, b = 11.4079(5) Å, β = 99.191(2)°, c = 12.0960(9) Å, γ = 104.992(2)°, V = 1194.8(2) Å^3, z = 2, F(000) = 448, $\rho_{calc.}$ = 1.202 gcm^{-3}, μ = 0.107 mm^{-1}, λ(MoK$_\alpha$) = 0.71073 Å, T = 173 K, $2\theta_{max}$ = 56°, no. of measured reflections = 23892, no. of independent reflections = 5616 (R_{int} = 0.042), no. of independent reflections = 4482 (|F|/σ(F) > 4.0), R_1 = 0.0493 (observed reflections), R_1 = 0.0612 (all reflections), wR_2 = 0.1379, corrections = Lorentz- and polarization correction, solution = SIR-2004 (direct methods), refinement = SHELDL-2014 w=1/[$\sigma^2(F_o^2)$ + (0.0565*P)^2+0.03*P] while P = (Max(F_o^2,0)+2*F_c^2)/3, CCDC deposition number = CCDC-1517624.

The crystal structure consists of only one independent molecule within the unit cell. It is connected to two other molecules by two hydrogen bonds for each neighboring molecule. This results in an infinite chain of dimeric units (Fig. S3).

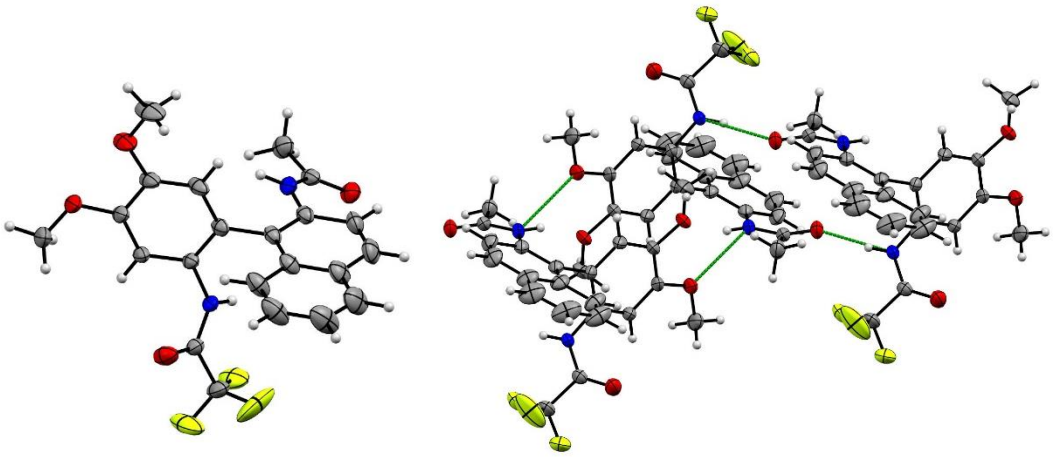

Figure S3: Molecular structure of **3**, hydrogen bonding is indicated in green.

2'-Acetamido-2-(1,1-dimethylethyl)oxycarbonylamido-5-methyl-4,4',5'-trimethoxy-biphenyl (4)

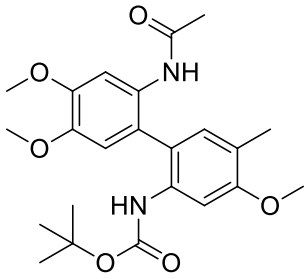

According to the general protocol **F**, 374 mg (1.9 mmol, 1.0 eq.) *N*-(3,4-dimethoxyphenyl)acetamide **16**, 899 mg (3.8 mmol, 2.0 eq.) *N*-(1,1-dimethyl-ethyl)oxycarbonyl)-3-methoxy-4-methylaniline **15** and 0.70 g MTBS were dissolved in 20.5 mL HFIP + 4.5 mL methanol (18% v/v). After electrolysis, the solvent was recovered by distillation. Column chromatography of the residue (cyclohexane/ethyl acetate = 9:1 → 1:1) yielded the desired product as an off-white powder (yield: 49%, 405 mg, 0.9 mmol).

R_f (cyclohexane/ethyl acetate = 7:3) = 0.1; m.p. 163–164 °C; ^{1}H NMR (300 MHz, $CDCl_3$): δ (ppm) = 1.45 (s, 9 H), 1.97 (s, 3 H), 2.19 (s, 3 H), 3.84 (s, 3 H), 3.91 (s, 3 H), 3.95 (s, 3 H), 6.17 (s, 1 H), 6.63 (s, 1 H), 6.87 (bs, 1 H), 6.89 (s, 1 H), 7.68 (s, 1 H), 8.02 (s, 1 H); ^{13}C NMR (75 MHz, $CDCl_3$): δ (ppm) = 15.80, 24.77, 28.40, 55.69, 56.16, 56.27, 80.85, 102.94, 105.63, 113.21, 117.98, 118.87, 122.10, 129.95, 132.27, 135.27, 145.63, 148.94, 153.25, 158.31, 168.40; HRMS for $C_{23}H_{30}N_2O_6$ (ESI+) $[M+Na]^+$: calc.: 453.2002; found: 453.1992; Elemental anal. for $C_{23}H_{30}N_2O_6$ calc.: C: 64.17%, H: 7.02%, N: 6.51%, found: C: 64.07%, H: 6.97%, N: 6.51%.

2-(1,1-Dimethylethyl)oxycarbonylamido-5-methyl-2'-pivalamido-4,4',5'-trimethoxybiphenyl (5)

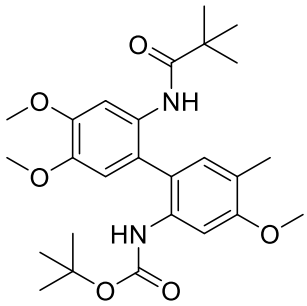

According to the general protocol **F**, 450 mg (1.9 mmol, 1.0 eq.) *N*-(3,4-dimethylphenyl)pivalamide **18**, 911 mg (3.8 mmol, 2.0 eq.) *N*-(1,1-dimethyl-ethyl)oxycarbonyl)-3-methoxy-4-methylaniline **15** and 0.70 g MTBS were dissolved in a mixture of 20.5 mL HFIP + 4.5 mL methanol (18% v/v). After electrolysis, the solvent was recovered by distillation. Column chromatography of the residue (cyclohexane/ethyl acetate = 7:3 → 0:1) yielded the desired product as an off-white powder (yield: 40%, 355 mg, 0.8 mmol).

R_f (cyclohexane/ethyl acetate = 7:3) = 0.5; m.p. 69–71 °C; ^{1}H NMR (300 MHz, $CDCl_3$): δ (ppm) = 1.05 (s, 9 H), 1.43 (s, 9 H), 2.17 (s, 3 H), 3.84 (s, 3 H), 3.91 (s, 3 H), 3.96 (s, 3 H), 6.21 (s, 1 H), 6.66 (s, 1 H), 6.89 (s, 1 H), 7.24 (s, 1 H), 7.83 (s, 1 H), 8.14 (s, 1 H); ^{13}C NMR (75 MHz, $CDCl_3$): δ (ppm) = 15.66, 27.40, 28.41, 39.85, 55.68, 56.11, 56.25, 80.84, 101.79, 104.98, 113.08, 116.81, 118.45, 121.53, 130.26, 132.22, 135.50, 145.38, 149.06, 152.80, 158.35, 176.60; HRMS for $C_{26}H_{36}N_2O_6$ (ESI+) $[M+Na]^+$: calc.: 495.2471; found: 495.2472; Elemental anal. for $C_{63}H_{36}N_2O_6$ calc.: C: 66.08%, H: 7.68, N: 5.93%, found: C: 66.10%, H: 7.62%, N: 5.91%.

2'-Benzamido-2-(1,1-dimethylethyl)oxycarbonylamido-5-methyl-4,4'-5'-trimethoxybiphenyl (6)

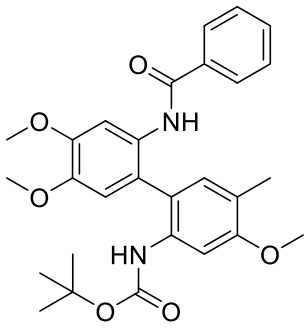

According to the general protocol **F**, 490 mg (1.9 mmol, 1.0 eq.) *N*-(3,4-dimethoxyphenyl)benzamide **17**, 890 mg (3.8 mmol, 2.0 eq.) *N*-(1,1-dimethyl-ethyl)oxycarbonyl)-3-methoxy-4-methylaniline **15** and 0.70 g MTBS were dissolved in a mixture of 20.5 mL HFIP + 4.5 mL methanol (18% v/v). After electrolysis, the solvent was recovered by distillation. Column chromatography of the residue (cyclohexane/ethyl acetate = 9:1 → 7:3) yielded the desired product as an off-white powder (yield: 51%, 479 mg, 1.0 mmol).

R_f (cyclohexane/ethyl acetate = 7:3) = 0.5; m.p. 136–138 °C; ^{1}H NMR (400 MHz, $CDCl_3$): δ (ppm) = 1.37 (s, 9 H), 2.20 (s, 3 H), 3.87 (s, 3 H), 3.93 (s, 3 H), 4.01 (s, 3 H), 6.29 (s, 1 H), 6.71 (s, 1 H), 6.98 (s, 1 H), 7.36–7.40 (m, 2 H), 7.45–7.49 (m, 1 H), 7.56–7.58 (m, 2 H), 7.80 (d, *J* = 8.4 Hz, 2 H), 8.32 (s, 1 H); ^{13}C NMR (101 MHz, $CDCl_3$): δ (ppm) = 15.74, 28.31, 55.74, 56.21, 56.30, 80.87, 102.33, 105.28, 113.32, 117.15, 118.95, 121.88, 126.88, 128.89, 130.06,

131.88, 132.34, 134.71, 135.50, 145.76, 149.10, 152.92, 158.47, 165.06; HRMS for $C_{28}H_{32}N_2O_6$ (ESI+) $[M+Na]^+$: calc.: 515.2158; found: 515.2161; Elemental anal. for $C_{28}H_{32}N_2O_6$ calc.: C: 68.28%, H: 6.55%, N: 5.69%, found: C: 67.96%, H: 6.53%, N: 5.65%.

2,2'-Bis(1,1-dimethylethyl)oxycarbonylamido-5-methyl-4,4',5'-trimethoxybiphenyl (7)

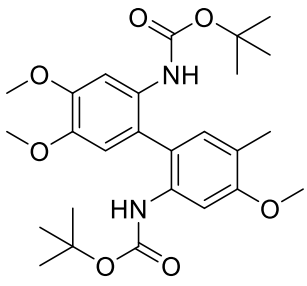

According to the general protocol **F**, 335 mg (1.3 mmol, 1.0 eq.) *N*-(1,1-dimethylethyl)oxycarbonyl)-3,4-dimethoxyaniline **19**, 626 mg (2.6 mmol, 2.0 eq.) *N*-(1,1-dimethylethyl)oxycarbonyl)-3-methoxy-4-methylaniline **15** and 0.70 g MTBS were dissolved in a mixture of 20.5 mL HFIP + 4.5 mL methanol (18% v/v). After electrolysis, the solvent was recovered by distillation. Column chromatography of the residue (cyclohexane/ethyl acetate = 9:1 → 7:3) yielded the desired product as an off-white powder (yield: 42%, 268 mg, 0.6 mmol).

R_f (cyclohexane/ethyl acetate = 7:3) = 0.6; m.p. 152–153 °C; ^{1}H NMR (300 MHz, $CDCl_3$): δ (ppm) = 1.44 (s, 18 H), 2.17 (s, 3 H), 3.81 (s, 3 H), 3.90 (s, 3 H), 3.96 (s, 3 H), 6.14 (s, 1 H), 6.22 (s, 1 H), 6.59 (s, 1 H), 6.86 (s, 1 H), 7.81 (bs, 1 H), 7.83 (bs, 1 H); ^{13}C NMR (75 MHz, $CDCl_3$): δ (ppm) = 15.72, 2x 28.40, 55.60, 56.07, 56.24, 80.55, 80.64, 101.85, 104.15, 113.50, 117.18, 117.69, 121.28, 130.46, 132.20, 135.59, 144.77, 149.12, 152.88, 153.08, 158.19; HRMS for $C_{26}H_{36}N_2O_7$ (ESI+) $[M+Na]^+$: calc.: 511.2420; found: 511.2434.

2'-Acetamido-2-benzamido-5-methyl-4,4',5'-trimethoxybiphenyl (8)

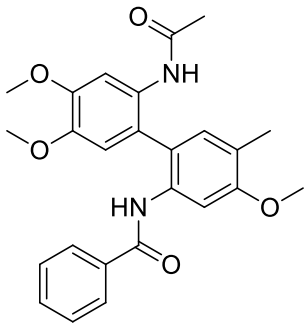

According to the general protocol **F**, 372 mg (1.9 mmol, 1.0 eq.) *N*-(3,4-dimethoxyphenyl)acetamide **16**, 920 mg (3.8 mmol, 2.0 eq.) *N*-(3-methoxy-4-methyl-phenyl)benzamide **14** and 0.70 g MTBS were dissolved in 25 mL HFIP. After electrolysis, the solvent was recovered by distillation. Column chromatography of the residue (cyclohexane/ethyl acetate = 9:1 → 3:7) yielded the desired product as an off-white powder (yield: 74%, 616 mg, 1.4 mmol).

R_f (cyclohexane/ethyl acetate = 1:1) = 0.2; m.p. 103–105 °C; ^{1}H NMR (400 MHz, $CDCl_3$): δ (ppm) = 1.93 (s, 3 H), 2.23 (s, 3 H), 3.80 (s, 3 H), 3.93 (s, 6 H), 6.70 (s, 1 H), 6.98 (s, 1 H), 6.99 (bs, 1 H), 7.35–7.40 (m, 2 H), 7.46–7.49 (m, 1 H), 7.57–7.59 (m, 2 H), 7.84 (bs, 1 H), 7.91 (s, 1 H) 8.00 (s, 1 H); ^{13}C NMR (101 MHz, $CDCl_3$): δ (ppm) = 16.00, 24.49, 55.70, 56.18, 56.21, 104.63, 106.32, 113.11, 119.78, 119.80, 123.63, 126.90, 128.97, 129.70, 132.10, 132.12,

134.28, 134.78, 146.01, 149.06, 158.16, 165.76, 168.79; HRMS for $C_{25}H_{26}N_2O_5$ (ESI+) $[M+H]^+$: calc.: 435.1920; found: 435.1909.

2'-Benzamido-5'-methyl-2-trifluoroacetamido-4,5,4'-trimethoxybiphenyl (9)

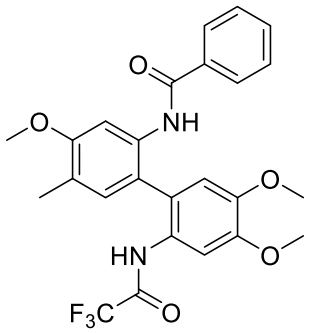

According to the general protocol **F**, 454 mg (1.9 mmol, 1.0 eq.) *N*-(3-methoxy-4-methylphenyl)benzamide **14**, 937 mg (3.8 mmol, 2.0 eq.) *N*-(3,4-dimethoxyphenyl)-trifluoroacetamide **2** and 0.70 g MTBS were dissolved in 25 mL HFIP. After electrolysis, the solvent was recovered by distillation. Column chromatography of the residue (cyclohexane/ethyl acetate = 9:1 → 1:1) yielded the desired product as an off-white powder (yield: 46%, 427 mg, 0.9 mmol).

R_f (cyclohexane/ethyl acetate = 1:1) = 0.6; m.p. 91–92 °C; ^{1}H NMR (400 MHz, $CDCl_3$): δ (ppm) = 2.23 (s, 3 H), 3.83 (s, 3 H), 3.93 (s, 3 H), 3.95 (s, 3 H), 6.78 (s, 1 H), 6.97 (s, 1 H), 7.36–7.40 (m, 2 H), 7.47–7.50 (m, 1 H), 7.50–7.56 (m, 2 H), 7.70 (bs, 1 H), 7.81 (s, 1 H), 8.00 (s, 2 H); ^{13}C NMR (101 MHz, $CDCl_3$): δ (ppm) = 15.90, 55.72, 56.30, 56.32, 104.85, 106.30, 113.09, 114.27, 115.71 (d, *J* = 288.6 Hz), 118.62, 121.49, 124.12, 126.80, 129.02, 131.79, 132.19, 134.24, 134.78, 147.41, 149.25, 155.07 (d, *J* = 37.3 Hz), 158.60, 165.70; ^{19}F NMR (282 MHz, $CDCl_3$): δ (ppm) = -77.18; HRMS for $C_{25}H_{23}F_3N_2O_5$ (ESI+) $[M+Na]^+$: calc.: 511.1457; found: 511.1459; Elemental anal. for $C_{25}H_{23}F_3N_2O_5$ calc.: C: 61.47%, H: 4.75%, N: 5.74%, found: C: 61.67%, H: 4.86%, N: 5.71%.

3'-Chloro-2,2'-diacetamido-4,5-dimethoxy-4'-hydroxy-5'-methylbiphenyl (10)

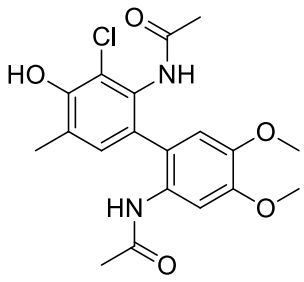

According to the general protocol **F**, 384 mg (1.9 mmol, 1.0 eq.) *N*-(2-chloro-3-hydroxy-4-methylphenyl)acetamide **19**, 746 mg (3.8 mmol, 2.0 eq.) *N*-(3,4-dimethoxyphenyl)acetamide **16** and 0.70 g MTBS were dissolved in a mixture of 20.5 mL HFIP + 4.5 mL methanol (18% v/v). After electrolysis, the solvent was recovered by distillation. Column chromatography of the residue (cyclohexane/ethyl acetate = 8:2 → 0:1) yielded the desired product as an off-white powder (yield: 51%, 387 mg, 1.0 mmol).

R_f (cyclohexane/ethyl acetate = 0:1) = 0.5; m.p. 238–240 °C; ^{1}H NMR (300 MHz, d_6-DMSO): δ (ppm) = 1.83 (s, 6 H), 2.21 (s, 3 H), 3.67 (s, 3 H), 3.74 (s, 3 H), 6.61 (s, 1 H), 6.87 (s, 1H), 7.28 (bs, 1 H), 8.40 (bs, 1 H), 9.19 (bs, 1 H), 9.24 (s, 1 H); ^{13}C NMR (75 MHz, d_6-DMSO): δ (ppm) = 16.65, 2x 22.37, 23.36, 55.52, 55.57, 113.46, 120.52, 125.11, 128.95, 129.25, 130.18, 132.11, 145.31, 147.60, 150.81, 168.42, 169.56; HRMS for $C_{19}H_{21}{}^{35}ClN_2O_5$ (ESI+) $[M+H]^+$: calc.: 393.1217; found: 393.1205.

2'-Acetamido-3'-chloro-4,5-dimethoxy-4'-hydroxy-5'-methyl-2-pivalamidobiphenyl (11)

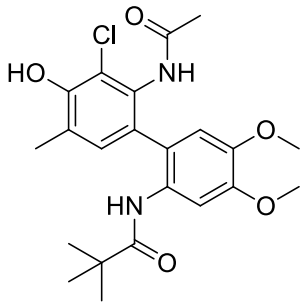

According to the general protocol **F**, 374 mg (1.9 mmol, 1.0 eq.) *N*-(2-chloro-3-hydroxy-4-methylphenyl)acetamide **19**, 893 mg (3.8 mmol, 2.0 eq.) *N*-(3,4-dimethoxyphenyl)pivalamide **18** and 0.70 g MTBS were dissolved in a mixture of 20.5 mL HFIP + 4.5 mL methanol (18% v/v). After electrolysis, the solvent was recovered by distillation. Column chromatography of the residue (cyclohexane/ethyl acetate = 8:2 → 0:1) yielded the desired product as an off-white powder (yield: 56%, 457 mg, 1.1 mmol).

R_f (cyclohexane/ethyl acetate = 0:1) = 0.4; m.p. 149–150 °C; ^{1}H NMR (300 MHz, d_6-DMSO): δ (ppm) = 0.95 (s, 9 H), 1.78 (s, 3 H), 2.17 (s, 3 H), 3.68 (s, 3 H), 3.75 (s, 3 H), 6.61 (s, 1 H), 6.79 (s, 1 H), 7.13 (s, 1 H), 8.06 (bs, 1 H), 9.27 (1 H); ^{13}C NMR (75 MHz, d_6-DMSO): δ (ppm) = 16.43, 22.28, 26.99, 38.50, 55.51, 55.60, 109.42, 109.55, 112.86, 120.17, 125.10, 129.04, 129.88, 129.97, 132.12, 145.48, 147.69, 150.72, 169.71, 175.95; HRMS for $C_{22}H_{27}{}^{35}ClN_2O_5$ (ESI+) $[M+Na]^+$: calc.: 457.1506; found: 457.1489; Elemental anal. for $C_{22}H_{27}ClN_2O_5$ calc.: C: 60.76%, H: 6.26%, N: 6.44%, found: C: 60.43%, H: 6.03%, N: 6.36%.

5-Acetamido-6-(2'-acetamido-4',5'-dimethoxyphenyl)benzo-1,3-dioxol (12)

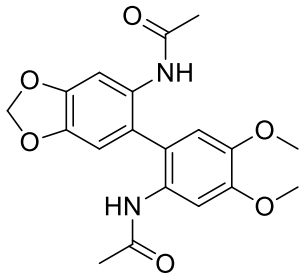

According to the general protocol **F**, 339 mg (1.9 mmol, 1.0 eq.) 5-acetylaminobenzo-1,3-dioxol **20**, 734 mg (3.8 mmol, 2.0 eq.) *N*-(3,4-dimethoxyphenyl)-acetamide **16** and 0.70 g MTBS were dissolved in 25 mL HFIP. After electrolysis, the solvent was recovered by distillation. Column chromatography of the residue (cyclohexane/ethyl acetate = 1:1 → 0:1) yielded the desired product as an off-white powder (yield: 38%, 271 mg, 0.7 mmol).

R_f (cyclohexane/ethyl acetate = 0:1) = 0.1; m.p. 155–156 °C; ^{1}H NMR (300 MHz, $CDCl_3$): δ (ppm) = 1.95 (s, 3 H), 1.99 (s, 3 H), 3.83 (s, 3 H), 3.92 (s, 3 H), 6.01 (dd, *J* = 3.8, 1.4 Hz, 2 H), 6.63 (d, *J* = 4.5 Hz, 2 H), 6.91 (bs, 2 H), 7.53 (s, 1 H), 7.65 (s, 1 H); ^{13}C NMR (75 MHz, $CDCl_3$): δ (ppm) = 24.13, 24.24, 56.15, 56.28, 101.82, 105.49, 107.36, 109.93, 110.12, 113.00, 121.10, 122.54, 129.13, 129.90, 145.17, 146.41, 148.00, 149.14, 169.35; HRMS for $C_{19}H_{20}N_2O_6$ (ESI+) $[M+Na]^+$: calc.: 395.1219; found: 395.1222.

Crystal structure determination of **12**: $2(C_{19}H_{20}N_2O_6)$, H_2O, M_r = 762.76 gmol^{-1}; colorless block-like crystal (0.1x0.18x0.49 mm^3), triclinic space group P -1, a = 11.2663(6) Å, α = 76.237(4)°, b = 11.6003(6) Å, β = 75.580(4)°, c =14.6526(8)Å, γ = 88.344(4)°, V = 1800.5(2) Å^3, z = 2, F(000) = 804, $\rho_{calc.}$ = 1.407 gcm^{-3}, μ = 0.107 mm^{-1}, λ(MoK_α) = 0.71073 Å, T = 193 K, $2\theta_{max}$ =

56°, no. of measured reflections = 27039, no. of independent reflections = 8831 (R_{int} = 0.042), no. of independent reflections = 5912 (|F|/σ(F) > 4.0), R_1 = 0.0412 (observed reflections), R_1 = 0.0724 (all reflections), wR_2 = 0.1084, corrections = Lorentz- and polarization correction, solution = SIR-2004 (direct methods), refinement = SHELDL-2014 $w=1/[\sigma^2(F_o^2) + (0.0565*P)^2+0.03*P]$ while $P=(Max(F_o^2,0)+2*F_c^2)/3$, CCDC deposition number = CCDC-1517625.

The crystal structure consists oft wo independent molecules A and B which only slightly differ in their geometry. The two molecules of A or B are connected by hydrogen bonds to form dimers A-A and B-B. Two dimers of each species are again linked by hydrogen bonding. The unit cell contains one molecule H_2O which additionally interconnects these molecules (Fig. S4).

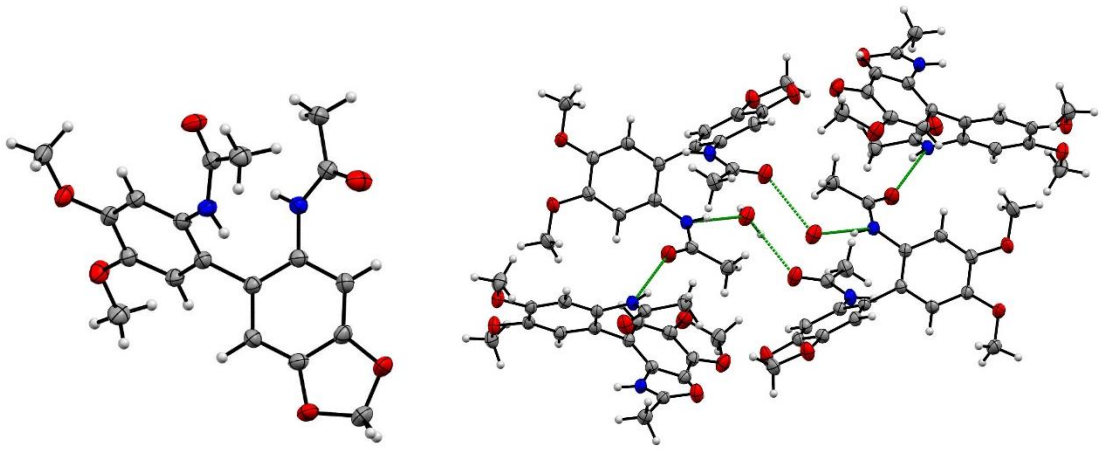

Figure S4: Molecular structure of **12**, hydrogen bonding is indicated in green.

Deblocking of Cross-Coupling Products

2'-Acetamido-2-amino-5-methyl-4,4',5'-trimethoxy-biphenyl (4')

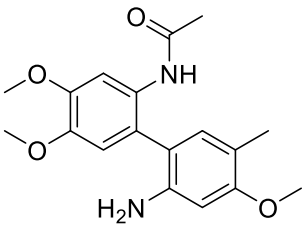

2'-Acetamido-2-(1,1-dimethylethyl)oxycarbonylamido-5-methyl-4,4',5'-trimethoxy-biphenyl **4** (97 mg, 0.22 mmol, 1 eq.) was dissolved in 10 mL H_2O + 5 mL methanol and stirred 24 h at 100 °C. The solvent was removed at reduced pressure. Column chromatography of the residue (cyclohexane/ethyl acetate = 1:1→0:1) gave the desired product as a light brown oil (yield: 98%, 74 mg, 0.22 mmol). Note: migration of the acetyl moiety can occur later to work-up (see ^{1}H NMR of **4'** immediately after work-up and after one week, p. S30).

R_f (cyclohexane/ethyl acetate = 0:1) = 0.3; ^{1}H NMR (300 MHz, $CDCl_3$): δ (ppm) = 2.01 (s, 3 H), 2.14 (s, 3 H), 3.83 (s, 3 H), 3.84 (s, 3 H), 3.91 (s, 3 H), 6.34 (s, 1 H), 6.70 (s, 1 H), 6.84 (s, 1 H), 7.51 (bs, 1 H), 7.80 (s, 1 H); ^{13}C NMR (75 MHz, $CDCl_3$): δ (ppm) = 15.43, 24.76, 55.45, 56.11, 56.19, 98.58, 106.31, 113.48, 115.42, 117.80, 121.20, 129.38, 133.06, 142.23, 145.83, 148.50, 158.53, 168.66; HRMS for $C_{18}H_{22}N_2O_4$ (ESI+) $[M+H]^+$: calc.: 331.1658; found: 331.1652.

2-Amino-2’-benzamido-5-methyl-4,4’-5’-trimethoxybiphenyl (6’)

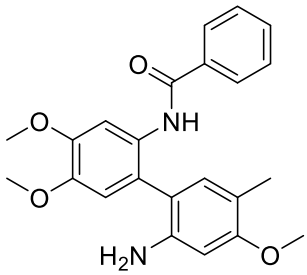

2’-Benzamido-2-(1,1-dimethylethyl)oxycarbonylamido-5-methyl-4,4’,5’-trimethoxy-biphenyl **6** (99 mg, 0.20 mmol, 1 eq.) was dissolved in 10 mL H_2O + 5 mL methanol and the mixture was stirred 24 h at 100 °C (the substrate was just soluble in hot H_2O/methanol). The solvent was removed at reduced pressure. Column chromatography of the residue (cyclohexane/ethyl acetate = 8:2→1:1) gave the desired product as a light yellow oil (yield: 99%, 78 mg, 0.20 mmol).

R_f (cyclohexane/ethyl acetate = 0:1) = 0.4; ^{1}H NMR (300 MHz, $CDCl_3$): δ (ppm) = 2.14 (s, 3 H), 3.83 (s, 3 H), 3.87 (s, 3 H), 3.96 (s, 3 H), 6.38 (s, 1 H), 6.78 (s, 1 H), 6.91 (s, 1 H), 7.36–7.50 (m, 3 H), 7.70–7.73 (m, 2 H), 8.08 (bs, 1 H), 8.52 (bs, 1 H); ^{13}C NMR (75 MHz, $CDCl_3$): δ (ppm) = 15.43, 55.52, 56.15, 56.23, 98.66, 106.07, 113.56, 115.62, 118.18, 121.47, 2x127.06, 2x128.75, 129.50, 131.64, 133.24, 135.11, 141.96, 145.92, 148.59, 158.66, 165.24; HRMS for $C_{23}H_{24}N_2O_4$ (ESI+) $[M+H]^+$: calc.: 393.1814; found: 393.1828.

2-Acetamido-1-(2’-amino-4’,5’-dimethoxyphenyl)naphthalene (3’)

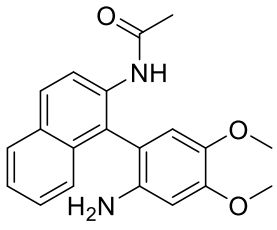

To a solution of 650 mg 2-acetamido-1-(4’,5’-dimethoxy-2’-trifluoroacetamidophenyl)naphthalene **3** (1.50 mmol, 1 eq.) in 120 mL of a methanol/water mixture (2:1 v/v), 2.07 g (15.01 mmol, 10 eq.) potassium carbonate were added. This solution was stirred 4 d at room temperature (23 °C). Subsequently, the solvent was removed at reduced pressure, 100 mL H_2O were added and the deprotected product **3‘** was extracted with dichloromethane (3x30 mL) to yield **3‘** as a light brown oil (yield: 99%, 500 mg, 1.49 mmol).

R_f (cyclohexane/ethyl acetate = 1:2) = 0.5; ^{1}H NMR (400 MHz, $CDCl_3$): δ (ppm) = 2.04 (s, 3 H), 3.08 (bs, 2 H), 3.77 (s, 3H), 3.94 (s, 3 H), 6.53 (s, 1H), 6.61 (s, 1H), 7.38–7.46 (m, 4 H), 7.87 (dd, J = 13.8 Hz, J = 8.1 Hz,2 H), 8.42 (d, J = 9.0 Hz, 1 H); ^{13}C NMR (101 MHz, $CDCl_3$): δ (ppm) = 24.87, 56.02, 56.58, 101.21, 111.55, 114.60, 121.36, 123.50, 125.18, 125.61, 126.81, 128.25, 129.01, 131.28, 132.77, 134.48, 137.70, 143.04, 150.28, 168.96; HRMS for $C_{20}H_{20}N_2O_3$ (ESI+) $[M+H]^+$: calc.: 337.1552; found: 337.1552.

2-Amino-1-(2’-amino-4’,5’-dimethoxyphenyl)naphthalene (3’’)

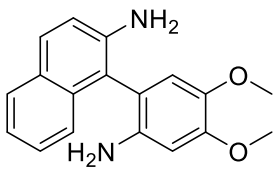

A solution of 300 mg (0.69 mmol, 1 eq.) 2-acetamido-1-(4’,5’-dimethoxy-2’-trifluoroacetamidophenyl)naphthalene in 80 mL hydrazine hydrate (80% v/v in H_2O) was

stirred for 4 d at 120 °C. After cooling down, the deprotected product was extracted with dichloromethane (3x20 mL) to yield **3‘‘** as a light brown oil (yield: 90%, 200 mg, 0.68 mmol).

R_f (cyclohexane/ethyl acetate = 1:2) = 0.4; ^{1}H NMR (300 MHz, d_6-DMSO): δ (ppm) = 3.61 (s, 3 H), 3.78 (s, 3 H), 4.01 (bs, 2 H), 4.77 (bs, 2 H), 6.50 (s, 1 H), 6.58 (s, 1 H), 7.09–7.25 (m, 4 H), 7.67 (dd, *J* = 11.4 Hz, 8.6 Hz, 2 H); ^{13}C NMR (75 MHz, $CDCl_3$): δ (ppm) = 55.25, 56.37, 100.60, 111.34, 113.66, 116.07, 118.46, 120.99, 123.45, 125.97, 127.07, 127.88, 128.19, 133.70, 140.43, 140.84, 143.58, 149.32; HRMS for $C_{18}H_{18}N_2O2$ (ESI+) $[M+H]^+$: calc.: 295.1447; found: 295.1458.

Preparation of Protected Aniline Derivatives

2-Acetamidonaphthalene (1)

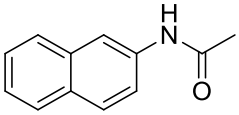

2-Acetamidonaphthalene was prepared as described by *Waldvogel et al.*[5] (yield: 81%, 2.09 g, 11 mmol).

M.p. 132–133 °C (recrystallized from EtOH/H_2O); ^{1}H NMR (300 MHz, $CDCl_3$): δ (ppm) = 2.23 (s, 3 H), 7.37–7.50 (m, 4 H), 7.76 (s, 2 H), 7.79 (s, 1 H), 8.18 (bs, 1 H).

All analytic data are in agreement with reported data.[6]

N-(3,4-Dimethoxyphenyl)-2,2,2-trifluoroacetamide (2)

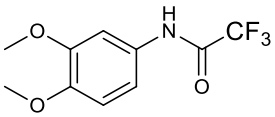

N-(3,4-Dimethoxyphenyl)trifluoroacetamide was prepared as described by *Umezawa et al.* with a slight variation:[7] According to the general protocol **C**, 3.72 g (24 mmol, 1.0 eq.) 3,4-dimethoxyaniline were dissolved in 60 mL anhydrous dichloromethane. It was sealed by a septum and 4.1 mL (29 mmol, 1.2 eq.) of trifluoroacetic anhydride were added to the chilled solution (0 °C) by a syringe. This reaction mixture was stirred overnight at room temperature (23 °C). Subsequently, the reaction mixture was washed with water (2x 30 mL) and the organic layer was dried with sodium sulfate. The solvent was removed at reduced pressure. Recrystallization from cyclohexane (100 mL, reflux) gave the trifluoroacetamide as a light purple powder (yield: 71%, 4.23 g, 17 mmol).

M.p. 103–104 °C (recrystallized from cyclohexane); ^{1}H NMR (300 MHz, $CDCl_3$): δ (ppm) = 3.88 (s, 3 H), 3.89 (s, 3 H), 6.85 (d, *J* = 8.6 Hz, 1 H), 6.99 (dd, *J* = 8.6, 2.5 Hz, 1 H), 7.29 (d, *J* = 2.5 Hz, 1 H), 7.89 (bs, 1 H).

All analytic data are in agreement with reported data.[7]

3-Methoxy-4-methylaniline (13)

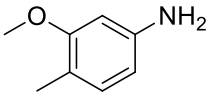

3-Methoxy-4-methylaniline was prepared as described by *Knoelker et al.*[8] (yield: 99%, 10.82 g, 79 mmol).

M.p. 57–58 °C; ^{1}H NMR (300 MHz, $CDCl_3$): δ (ppm) = 2.20 (s, 3 H), 3,84 (s, 3 H), 6.91 (dd, *J* = 8.0, 2.0 Hz, 1 H), 7.08 (d, *J* = 8.0 Hz, 1 H), 7.44–7.57 (m, 4 H), 7.85–7.88 (m, 2 H), 7.92 (bs, 1 H).

All analytic data are in agreement with reported data.[8]

N-(3-Methoxy-4-methylphenyl)benzamide (14)

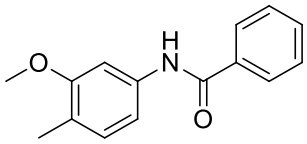

N-(3-Methoxy-4-methylphenyl)benzamide was prepared as described by *Taha et al.* with a slight variation:[9] According to the general protocol **B**, 2.98 g (22 mmol, 1.0 eq.) 3-methoxy-4-methylaniline and 3.4 mL (24 mmol, 1.1 eq.) triethylamine were dissolved in 50 mL anhydrous dichloromethane. It was sealed with a septum and 2.8 mL (24 mmol, 1.1 eq.) of benzoyl chloride were added by a syringe. This reaction mixture was stirred overnight at room temperature (23 °C). Subsequently the reaction mixture was washed with water (2x30 mL) and the organic layer was dried with sodium sulfate. The solvent was removed at reduced pressure. Recrystallization from cyclohexane/ethyl acetate (120 mL, reflux) gave the benzamide as colorless crystals (yield: 83%, 4.36 g, 18 mmol).

M.p. 130–131 °C (recrystallized from cyclohexane/ethyl acetate); ^{1}H NMR (300 MHz, $CDCl_3$): δ (ppm) = 2.20 (s, 3 H), 3,84 (s, 3 H), 6.91 (dd, *J* = 8.0, 2.0 Hz, 1 H), 7.08 (d, *J* = 8.0 Hz, 1 H), 7.44–7.57 (m, 4 H), 7.85–7.88 (m, 2 H), 7.92 (bs, 1 H).

All analytic data are in agreement with reported data.[9]

N-(1,1-Dimethylethyloxycarbonyl)-3-methoxy-4-methylaniline (15)

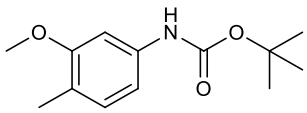

According to the general protocol **E**, 4.74 g (35 mmol, 1.0 eq.) 3-methoxy-3-methylaniline were dissolved in 200 mL anhydrous ethanol. It was sealed by a septum and 11.5 mL (54 mmol, 1.5 eq.) of di-*tert*-butyl dicarbonate were added to the solution by a syringe. This reaction mixture was stirred for 2.5 h at room temperature (23 °C). Subsequently, the solvent was removed at reduced pressure. Recrystallization from cyclohexane (200 mL, reflux) gave the carbamate as colorless crystals (yield: 94%, 7.75 g, 33 mmol).

M.p. 122–123 °C (recrystallized from cyclohexane); ^{1}H NMR (300 MHz, $CDCl_3$): δ (ppm) = 1.52 (s, 9 H), 2.15 (s, 3 H), 3.83 (s, 3 H), 6.45 (bs, 1 H), 6.64 (dd, *J* = 8.0, 2.1 Hz, 1 H), 7.00 (d, *J* = 8.0 Hz, 1 H), 7.14 (bs, 1 H); ^{13}C NMR (75 MHz, $CDCl_3$): δ (ppm) = 15.77, 28.51, 55.45, 80.44, 101.53, 110.05, 121.19, 130.51, 137.44, 152.93, 158.12; HRMS for $C_{13}H_{19}NO_3$ (ESI+) $[M+Na]^+$: calc.: 260.1263; found: 260.1256.

N-(3,4-Dimethoxyphenyl)acetamide (16)

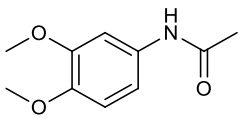

According to the general protocol **A**, 5.00 g (33 mmol, 1.0 eq.) 3,4-dimethoxyaniline were dissolved in 100 mL anhydrous dichloromethane. It was sealed by a septum and 3.7 mL (39 mmol, 1.2 eq.) of acetic anhydride were added to the chilled solution

by a syringe. This reaction mixture was stirred overnight at room temperature (23 °C). Subsequently, the solvent was removed at reduced pressure to give the acetamide as a purple powder (yield: 95%, 6.05 g, 31 mmol).

M.p. 126–128 °C; ^{1}H NMR (300 MHz, $CDCl_3$): δ (ppm) = 2.13 (s, 3 H), 3.83 (6 H), 6.77 (d, *J* = 8.6 Hz, 1 H), 6.86 (dd, *J* = 8.6, 2.4 Hz, 1 H), 7.28 (d, *J* = 2.4 Hz, 1 H), 7.51 (bs, 1 H).

All analytic data are in agreement with reported data.[10]

N-(3,4-Dimethoxyphenyl)benzamide (17)

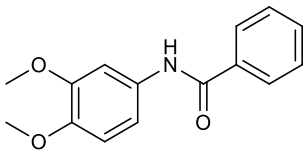

N-(3,4-Dimethoxyphenyl)benzamide was prepared as described by *Domínguez et al.* with a slight variation:[11] According to the general protocol **B**, 5.12 g (33 mmol, 1.0 eq.) 3,4-dimethoxyaniline and 5.0 mL (36 mmol, 1.1 eq.) triethylamine were dissolved in 100 mL anhydrous dichloromethane. It was sealed by a septum and 4.2 mL (36 mmol, 1.1 eq.) of benzoyl chloride were added by a syringe. The reaction mixture was stirred overnight at room temperature (23 °C). Subsequently, the reaction mixture was washed with water (2x50 mL) and the organic layer was dried with sodium sulfate. The solvent was removed at reduced pressure. Recrystallization from cyclohexane/ethyl acetate (120 mL, reflux) gave the benzamide as colorless crystals (yield: 95%, 8.07 g, 31 mmol).

M.p. 171–173 °C (recrystallized from cyclohexane/ethyl acetate); ^{1}H NMR (300 MHz, $CDCl_3$): δ (ppm) = 3.86 (s, 3 H), 3.88 (s, 3 H), 6.82 (d, *J* = 8.6 Hz, 1 H), 7.00 (dd, *J* = 8.6, 2.4 Hz, 1 H), 7.43–7.56 (m, 4 H), 7.84–7.87 (m, 2 H), 7.92 (bs, 1 H).

All analytic data are in agreement with reported data.[11]

N-(3,4-Dimethoxyphenyl)pivalamide (18)

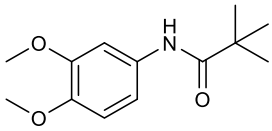

According to the general protocol **D**, 3.04 g (20 mmol, 1.0 eq.) 3,4-dimethoxyaniline and 3.6 mL (26 mmol, 1.3 eq.) triethylamine were dissolved in 40 mL anhydrous dichloromethane. It was sealed by a septum and 3.2 mL (26 mmol, 1.3 eq.) of pivaloyl chloride were added to the chilled solution (0 °C) by a syringe. This reaction mixture was stirred 4 h under reflux and the solvent was removed at reduced pressure. Column chromatography of the residue (cyclohexane/ethyl acetate = 1:1) provided the pivalamide as light purple crystals (yield: 70%, 3.00 g, 13 mmol).

M.p. 127–128 °C; ^{1}H NMR (300 MHz, $CDCl_3$): δ (ppm) = 1.30 (s, 9 H), 3.84 (s, 3 H), 3.87 (s, 3 H), 6.78 (d, *J* = 8.6 Hz, 1 H), 6.82 (dd, *J* = 8.6, 2.2 Hz, 1 H), 7.29 (bs, 1 H), 7.45 (d, *J* = 2.2 Hz, 1 H).

All analytic data are in agreement with reported data.[12]

N-(2-Chloro-3-hydroxy-4-methylphenyl)acetamide (19)

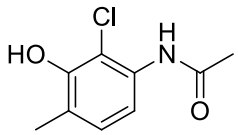

According to the general protocol A, 5.00 g (32 mmol, 1.0 eq.) 3-amino-2-chloro-6-methylphenol were dissolved in 130 mL anhydrous dichloromethane. It was sealed by a septum and 3.6 mL (38 mmol, 1.2 eq.) of acetic anhydride were added to the chilled solution by a syringe. This reaction mixture was stirred overnight at room temperature (23 °C). Subsequently, the reaction mixture was washed with water (2x30 mL) and the organic layer was dried with sodium sulfate. The solvent was removed at reduced pressure to give the acetamide as a red powder (yield: 95%, 6.05 g, 31 mmol).

M.p. 147–148 °C; ^{1}H NMR (300 MHz, d_6-DMSO): δ (ppm) = 2.05 (s, 3 H), 2.17 (s, 1 H), 6.98–7.08 (m, 2 H), 9.10 (bs, 1 H), 9.32 (bs, 1 H); ^{13}C NMR (75 MHz, d_6-DMSO): δ (ppm) = 16.54, 23.39, 115.31, 116.85, 123.01, 128.09, 133.68, 151.14, 168.55; HRMS for $C_9H_{10}{}^{35}ClNO_2$ (ESI+) $[M+Na]^+$: calc.: 222.0298; found: 222.0296.

5-Acetamidobenzo-1,3-dioxole (20)

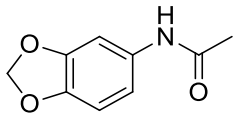

5-Acetamidobenzo-1,3-dioxol was prepared as described by *Hecht et al.* with a slight variation:[14] According to the general protocol A, 7.50 g (55 mmol, 1.0 eq.) 5-aminobenzo-1,3-dioxol were dissolved in 90 mL anhydrous dichloromethane. It was sealed by a septum and 6.2 mL (66 mmol, 1.2 eq.) of acetic anhydride were added to the chilled solution (0 °C) by a syringe. This reaction mixture was stirred overnight at 40 °C. The solvent was removed at reduced pressure. Column chromatography of the residue (cyclohexane/ethyl acetate = 4:1 → 1:1) gave the acetamide as purple crystals (yield: 66%, 6.45 g, 36 mmol).

M.p. 133–134 °C; ^{1}H NMR (300 MHz, $CDCl_3$): δ (ppm) = 2.12 (s, 3 H), 5.92 (s, 2 H), 6.70 (d, *J* = 8.3 Hz, 1 H), 6.77 (dd, *J* = 8.3 Hz, 2.0 Hz, 1 H), 7.17 (d, *J* = 2.0 Hz, 1 H), 7.65 (bs, 1 H).

All analytic data are in agreement with reported data.[13]

NMR Spectra

2-Acetamido-1-(4',5'-dimethoxy-2'-trifluoroacetamidophenyl)naphthalene (3)

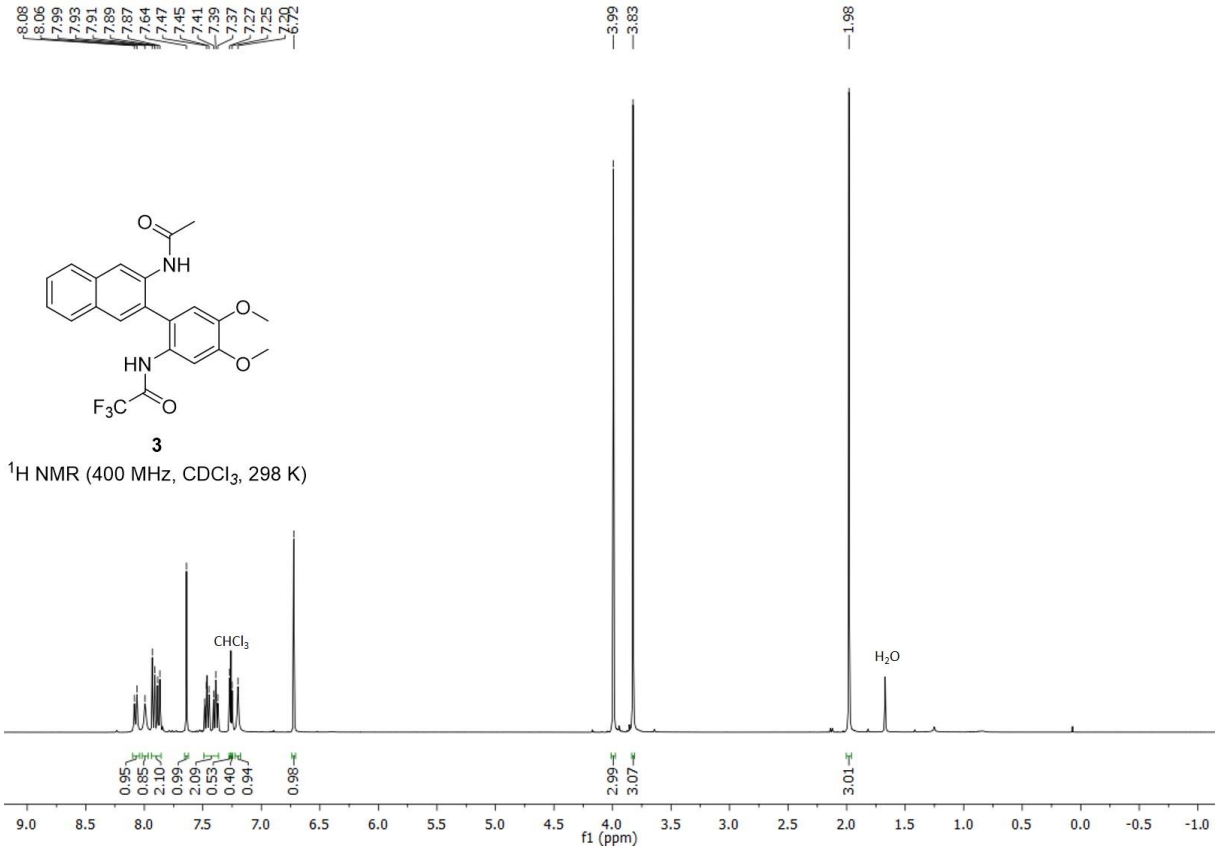

3

^{1}H NMR (400 MHz, $CDCl_3$, 298 K)

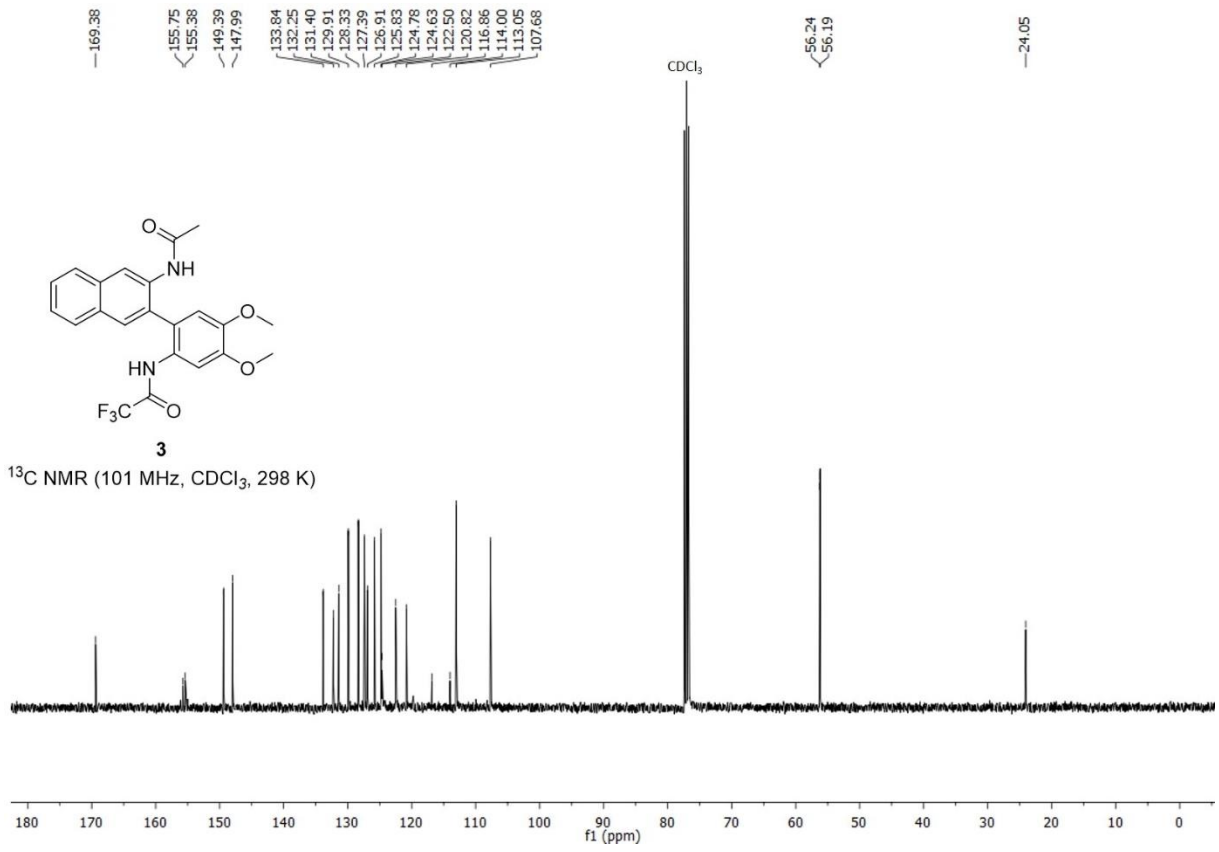

3

^{13}C NMR (101 MHz, $CDCl_3$, 298 K)

2’-Acetamido-2-(1,1-dimethylethyl)oxycarbonylamido-5-methyl-4,4’,5’-trimethoxy-biphenyl (4)

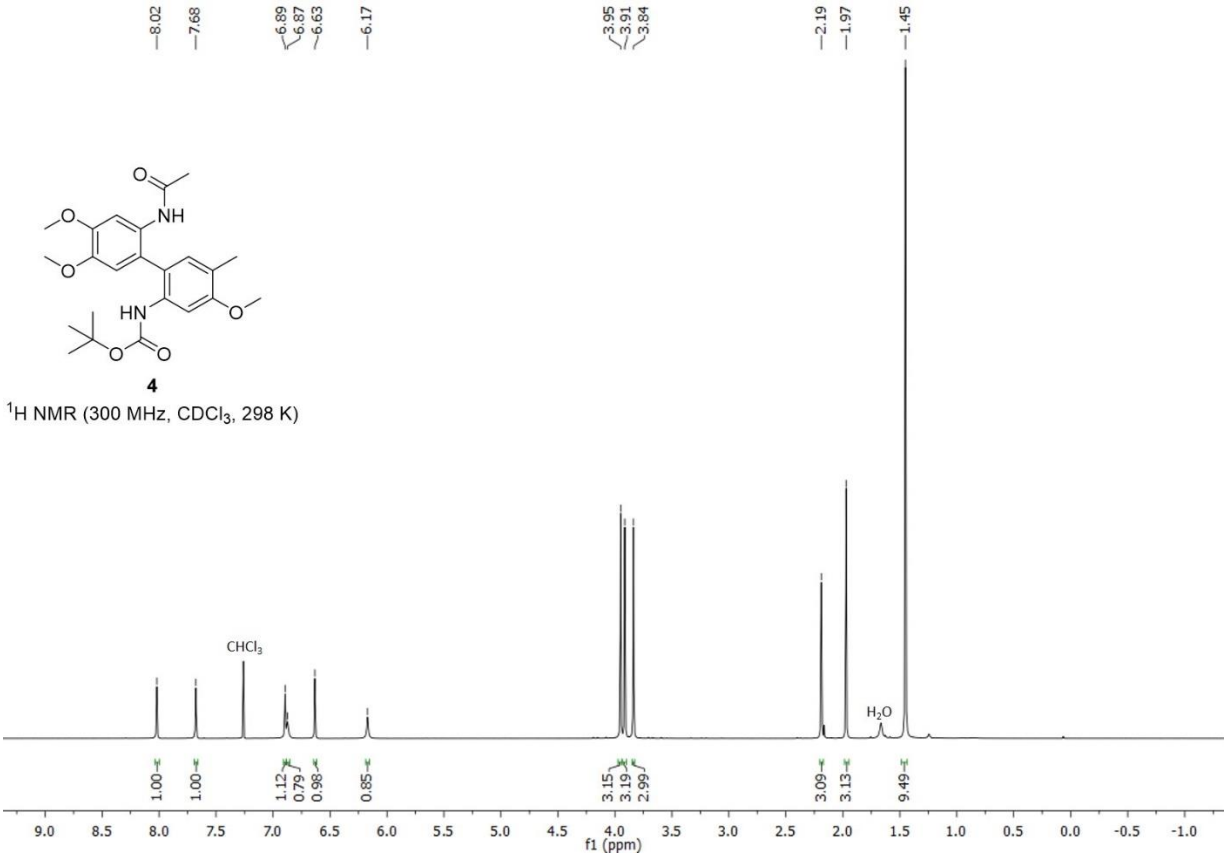

4

^{1}H NMR (300 MHz, $CDCl_3$, 298 K)

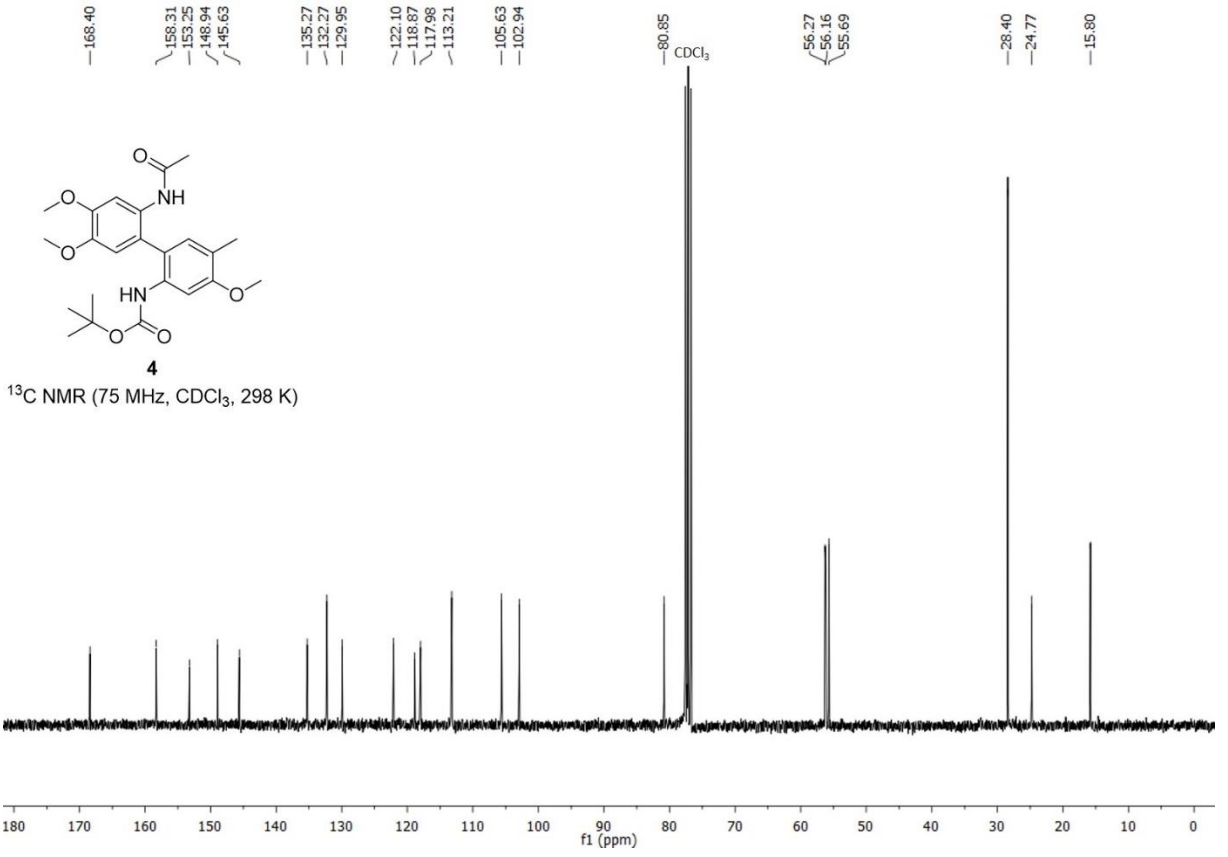

4

^{13}C NMR (75 MHz, $CDCl_3$, 298 K)

2-(1,1-Dimethylethyl)oxycarbonylamido-5-methyl-2'-pivalamido-4,4',5'-trimethoxy-biphenyl (5)

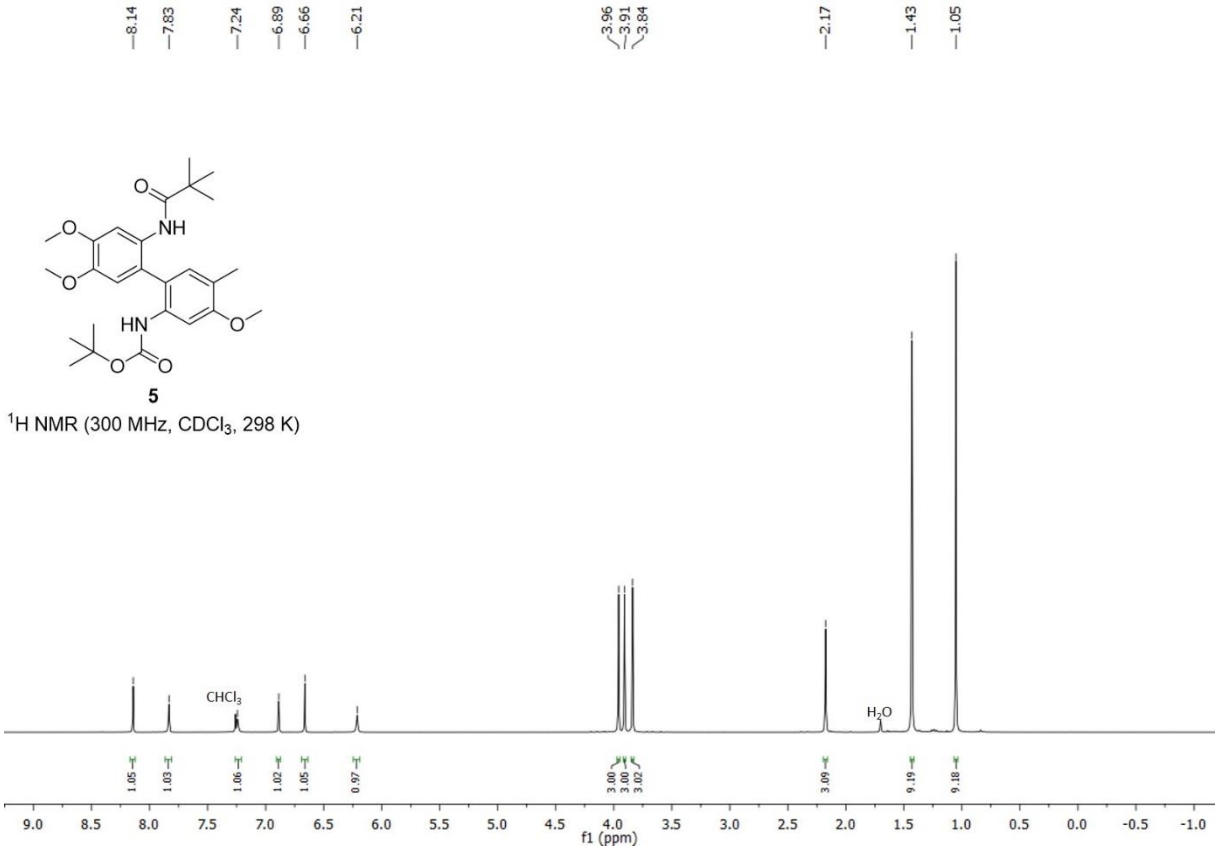

5

^{1}H NMR (300 MHz, $CDCl_3$, 298 K)

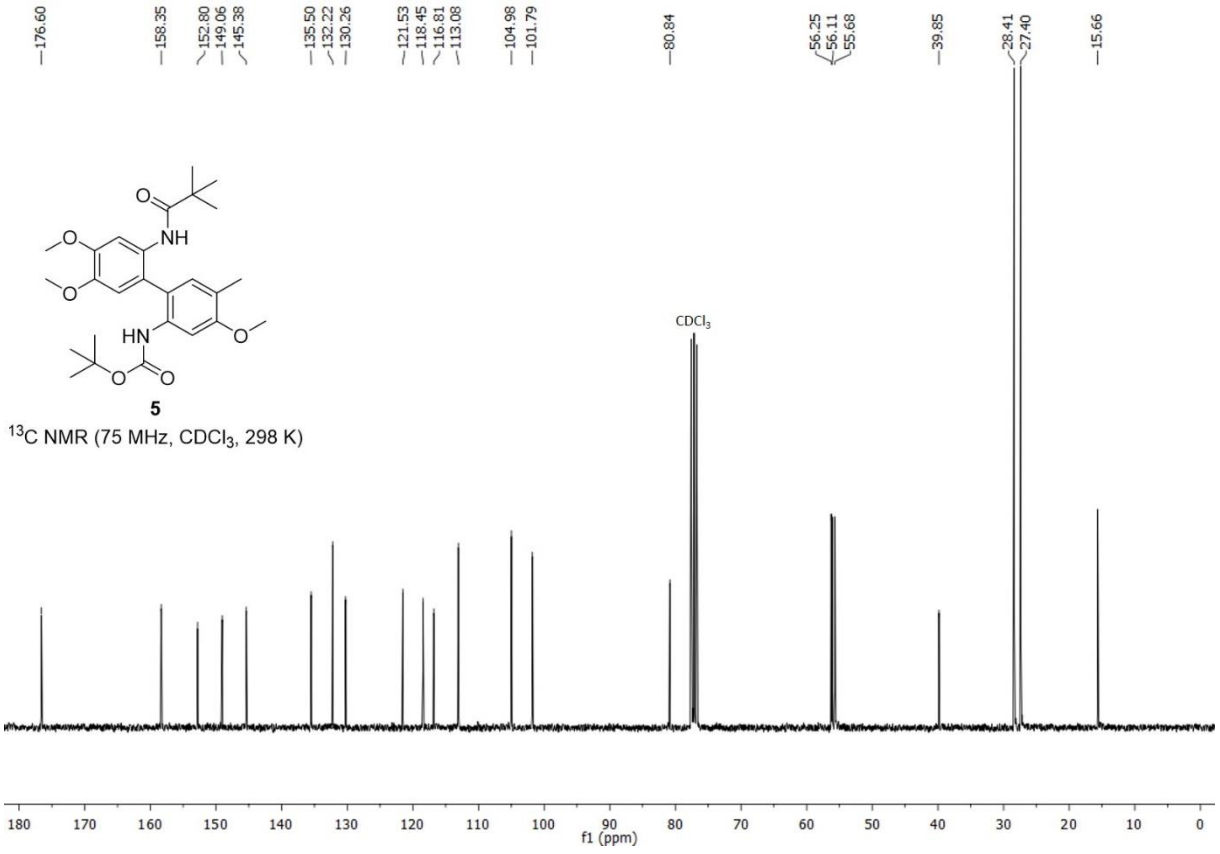

5

^{13}C NMR (75 MHz, $CDCl_3$, 298 K)

2’-Benzamido-2-(1,1-dimethylethyl)oxycarbonylamido-5-methyl-4,4’-5’-trimethoxy-biphenyl (6)

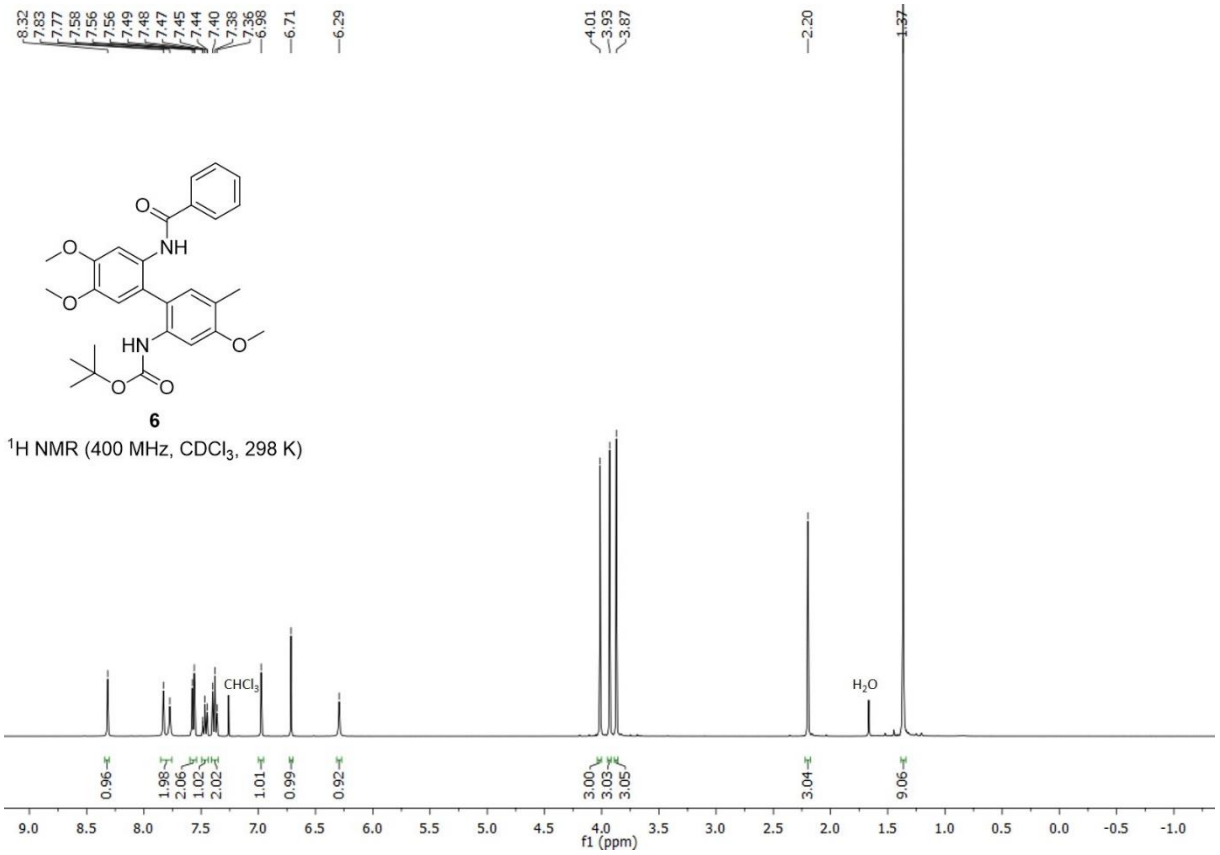

6

^{1}H NMR (400 MHz, $CDCl_3$, 298 K)

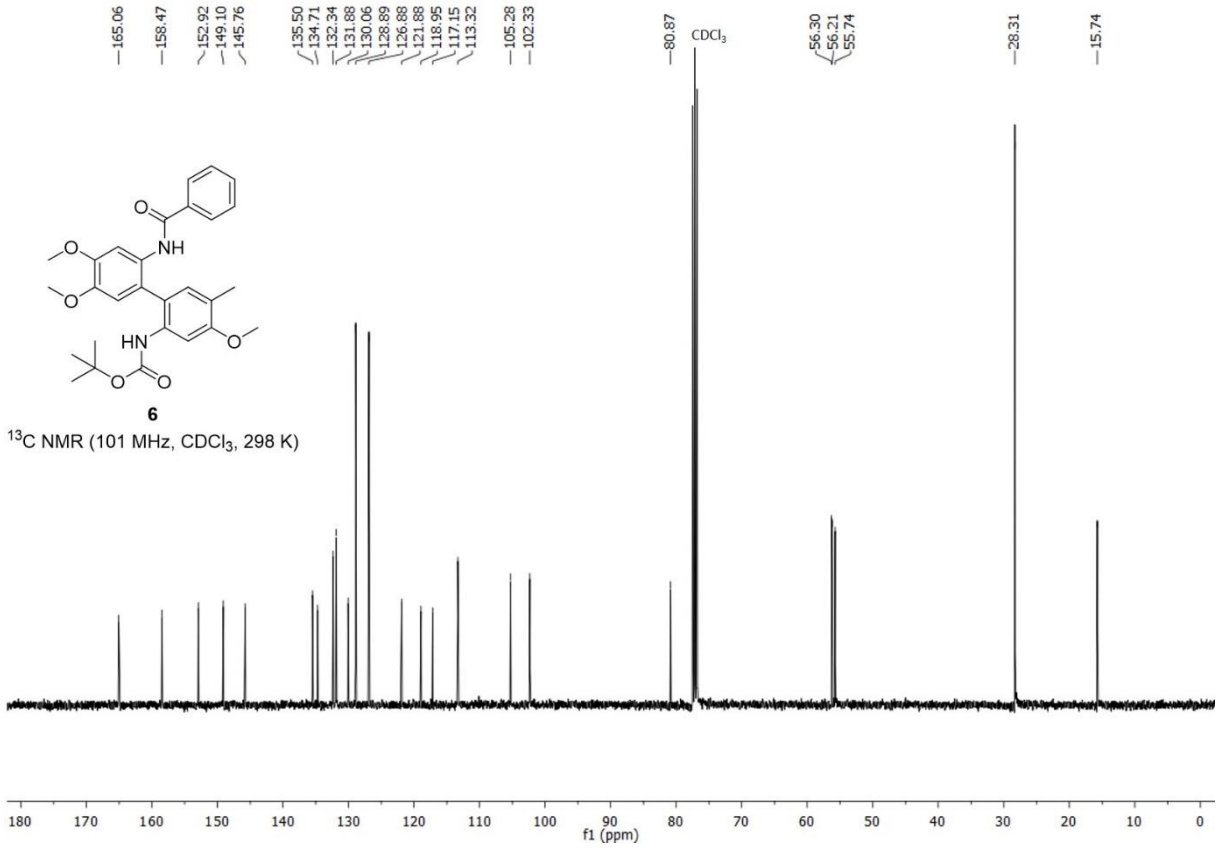

6

^{13}C NMR (101 MHz, $CDCl_3$, 298 K)

2,2'-Bis(1,1-dimethylethyl)oxycarbonylamido-5-methyl-4,4',5'-trimethoxybiphenyl (7)

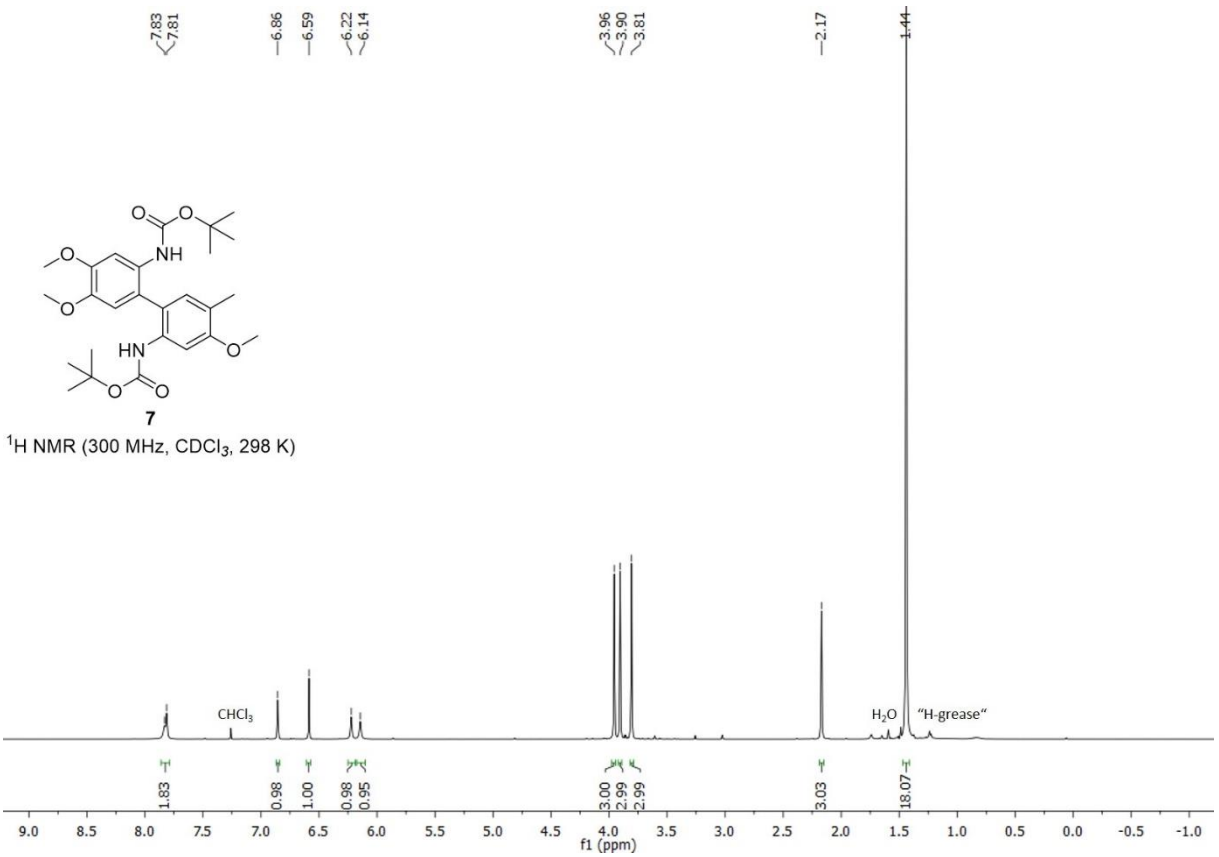

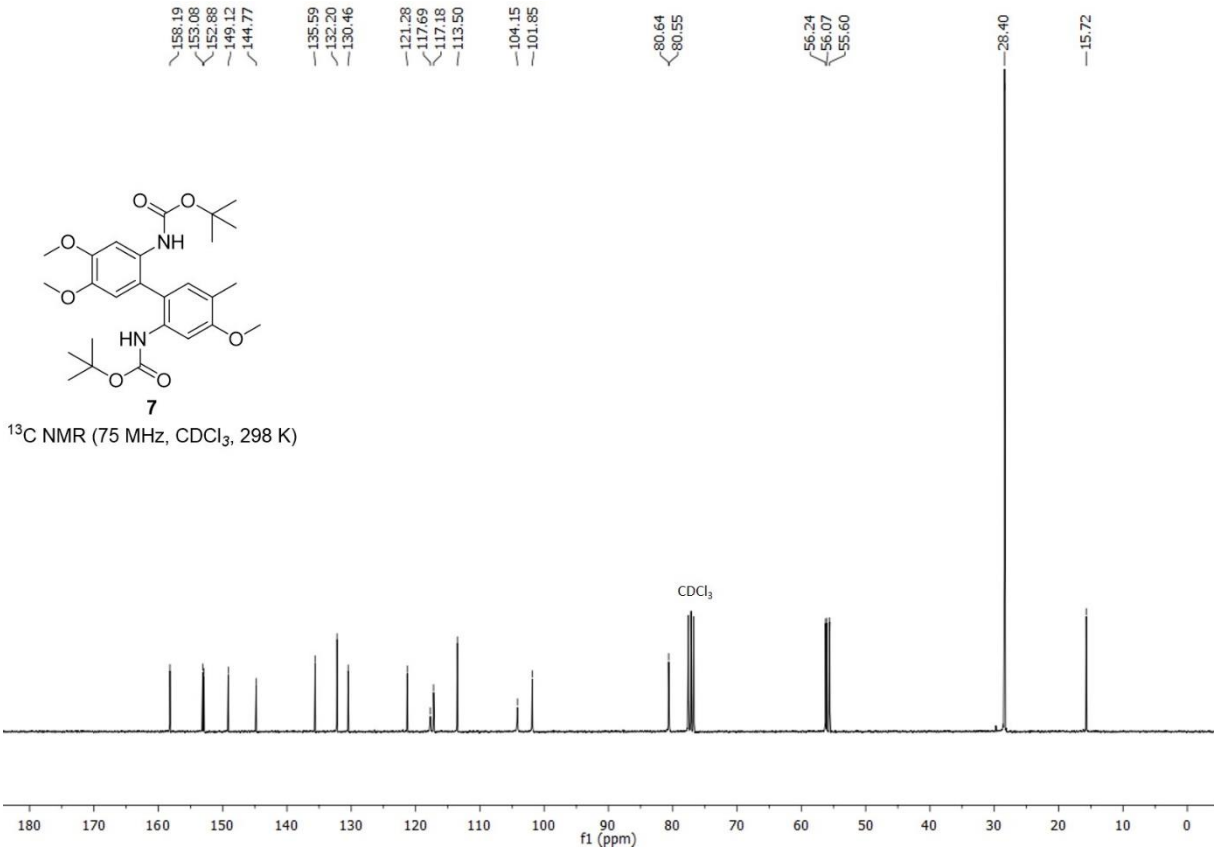

2’-Acetamido-2-benzamido-5-methyl-4,4’,5’-trimethoxybiphenyl (8)

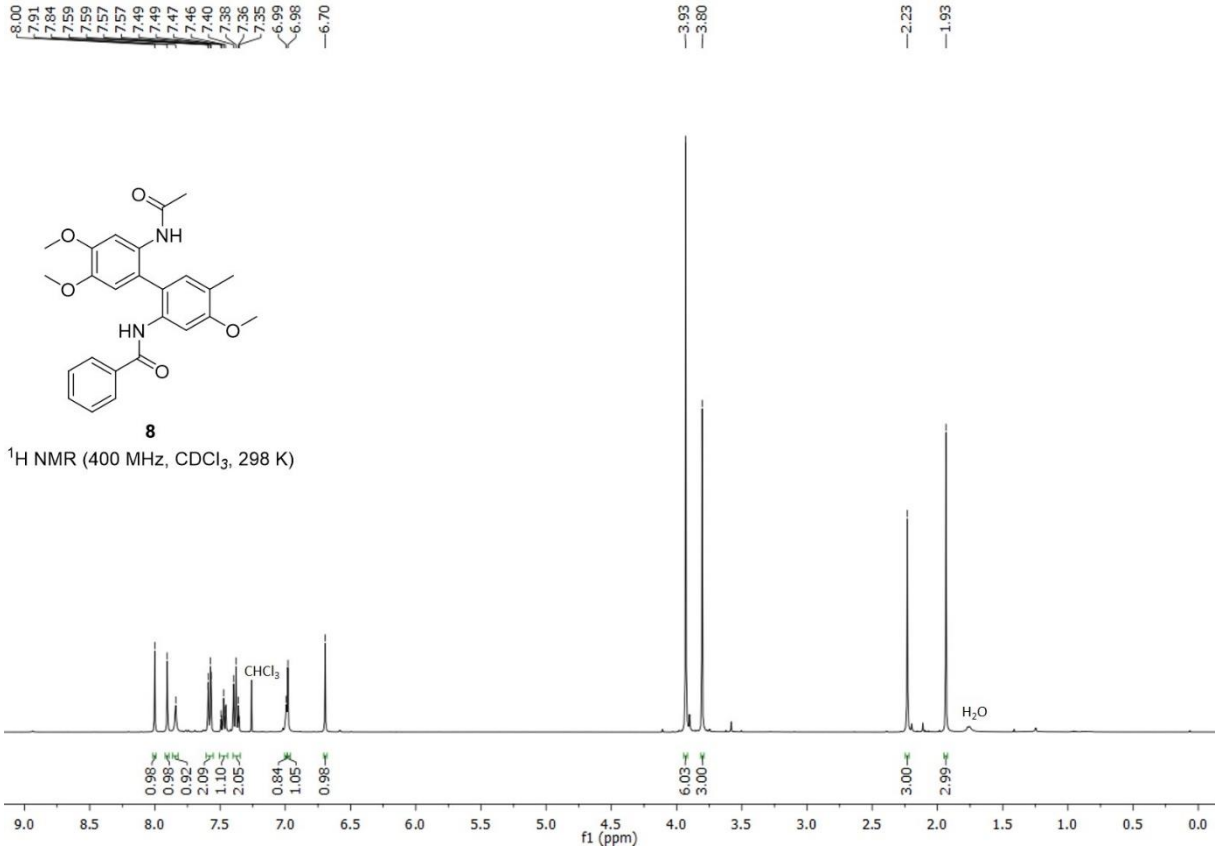

8

^{1}H NMR (400 MHz, $CDCl_3$, 298 K)

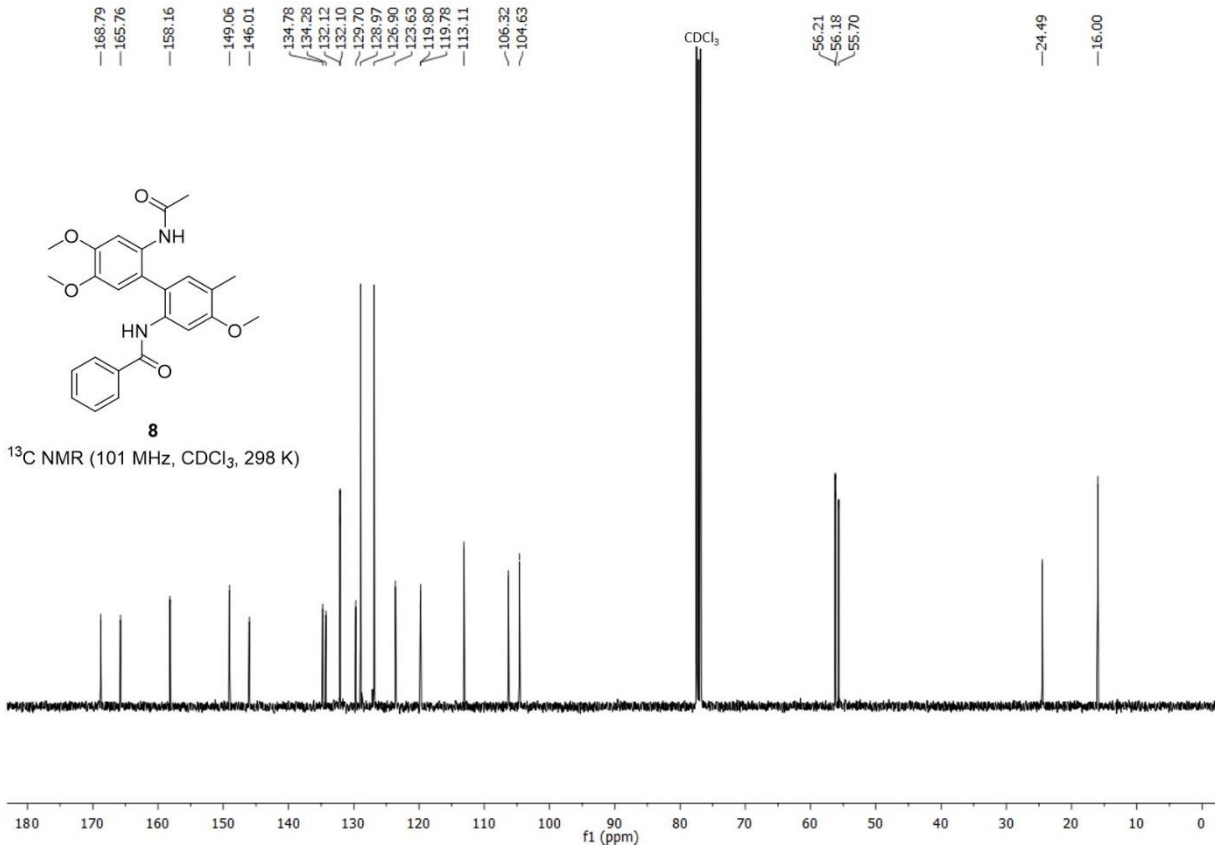

8

^{13}C NMR (101 MHz, $CDCl_3$, 298 K)

2’-Benzamido-5’-methyl-2-trifluoroacetamido-4,5,4’-trimethoxybiphenyl (9)

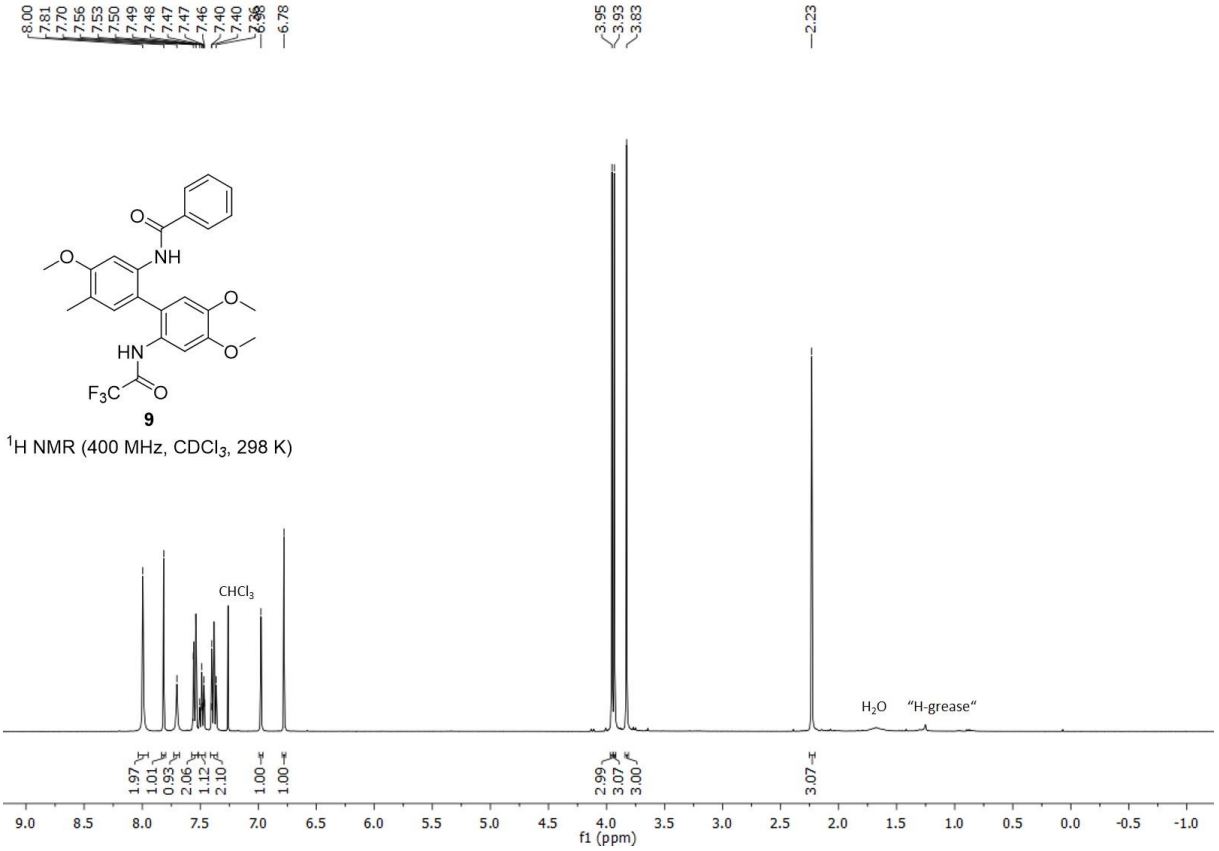

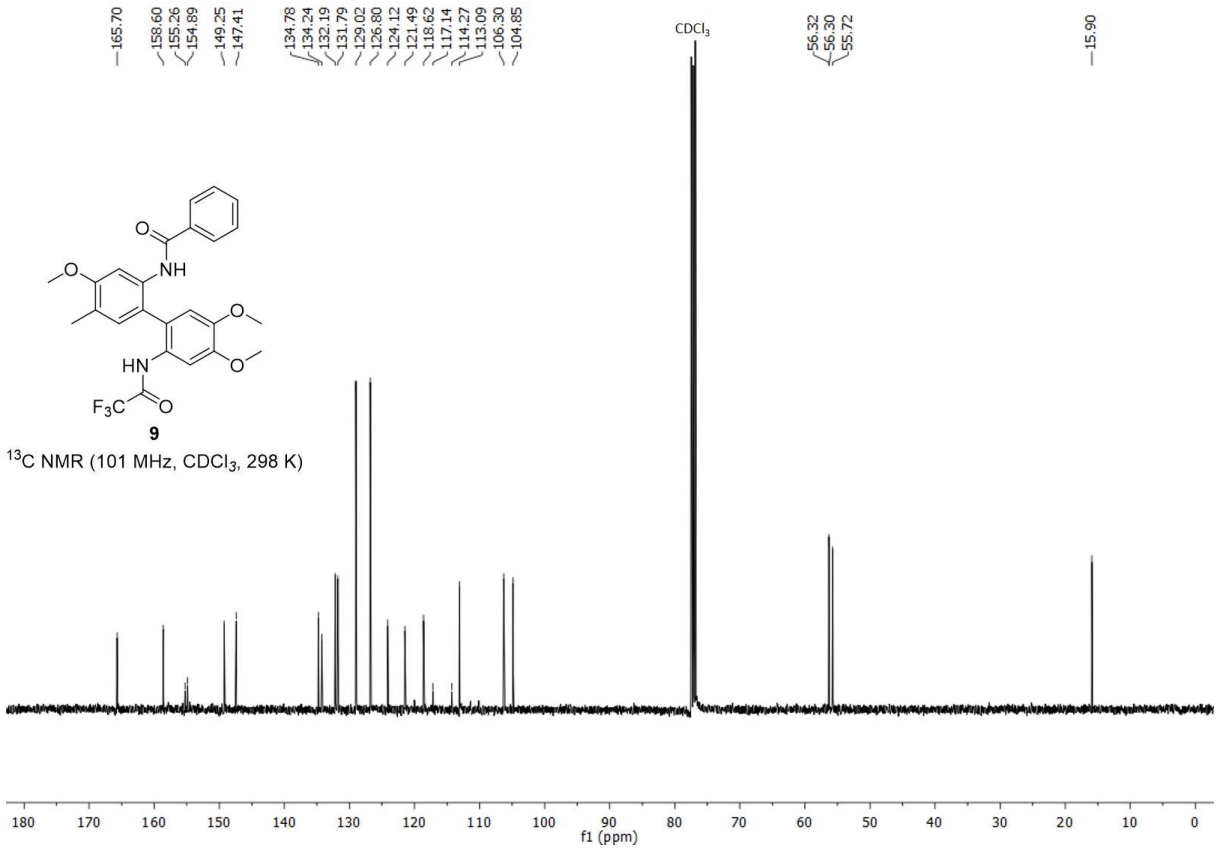

2’-Acetamido-3’-chloro-4,5-dimethoxy-4’-hydroxy-5’-methyl-2-pivalamidobiphenyl (10)

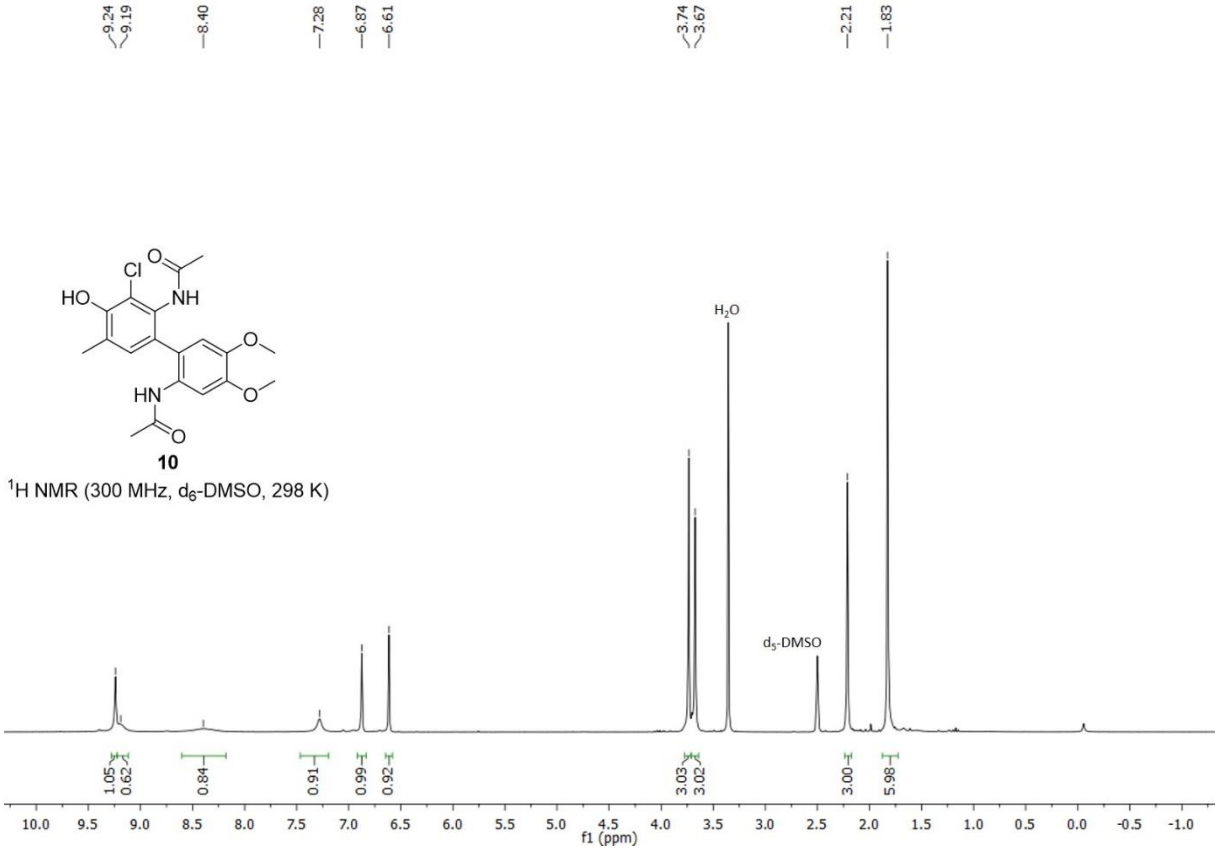

10

^{1}H NMR (300 MHz, d_6-DMSO, 298 K)

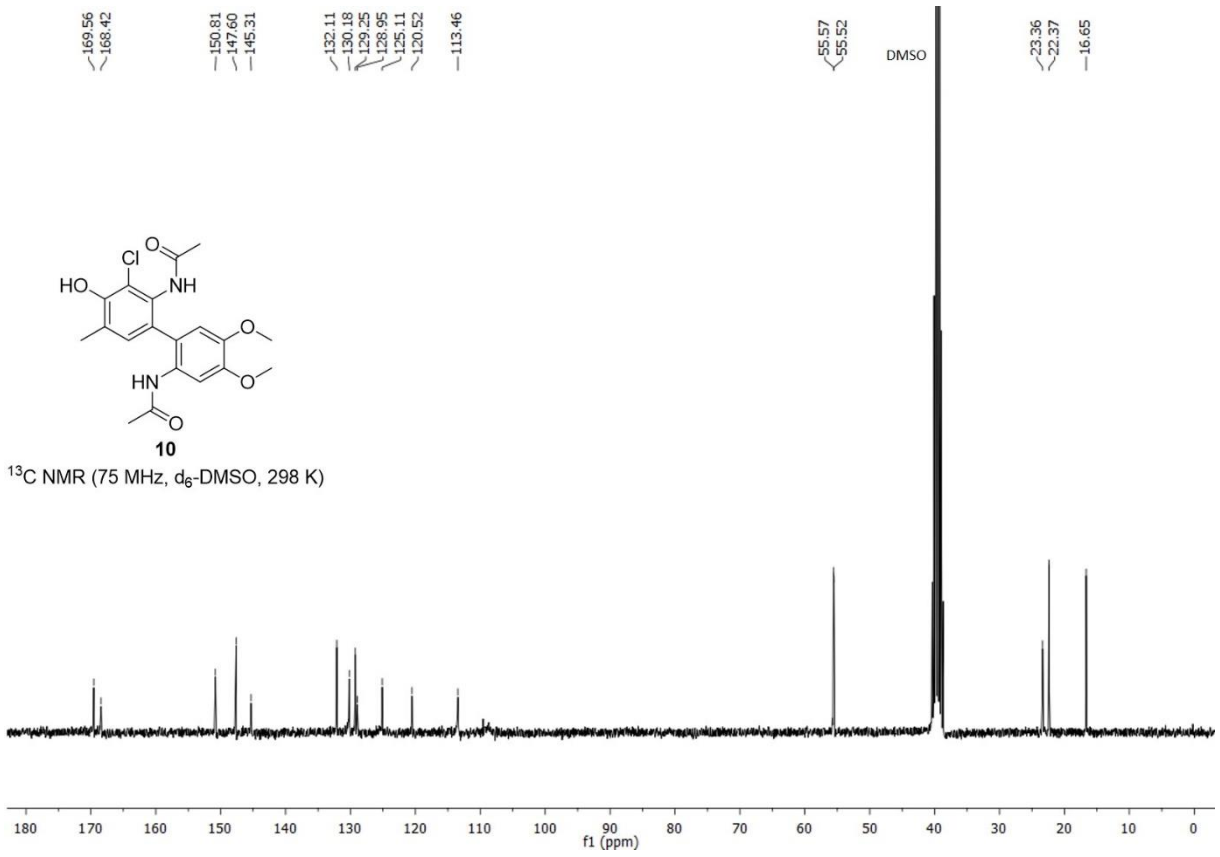

10

^{13}C NMR (75 MHz, d_6-DMSO, 298 K)

2,2'-Bisacetamido-3'-chloro-4,5-dimethoxy-4'-hydroxy-5'-methylbiphenyl (11)

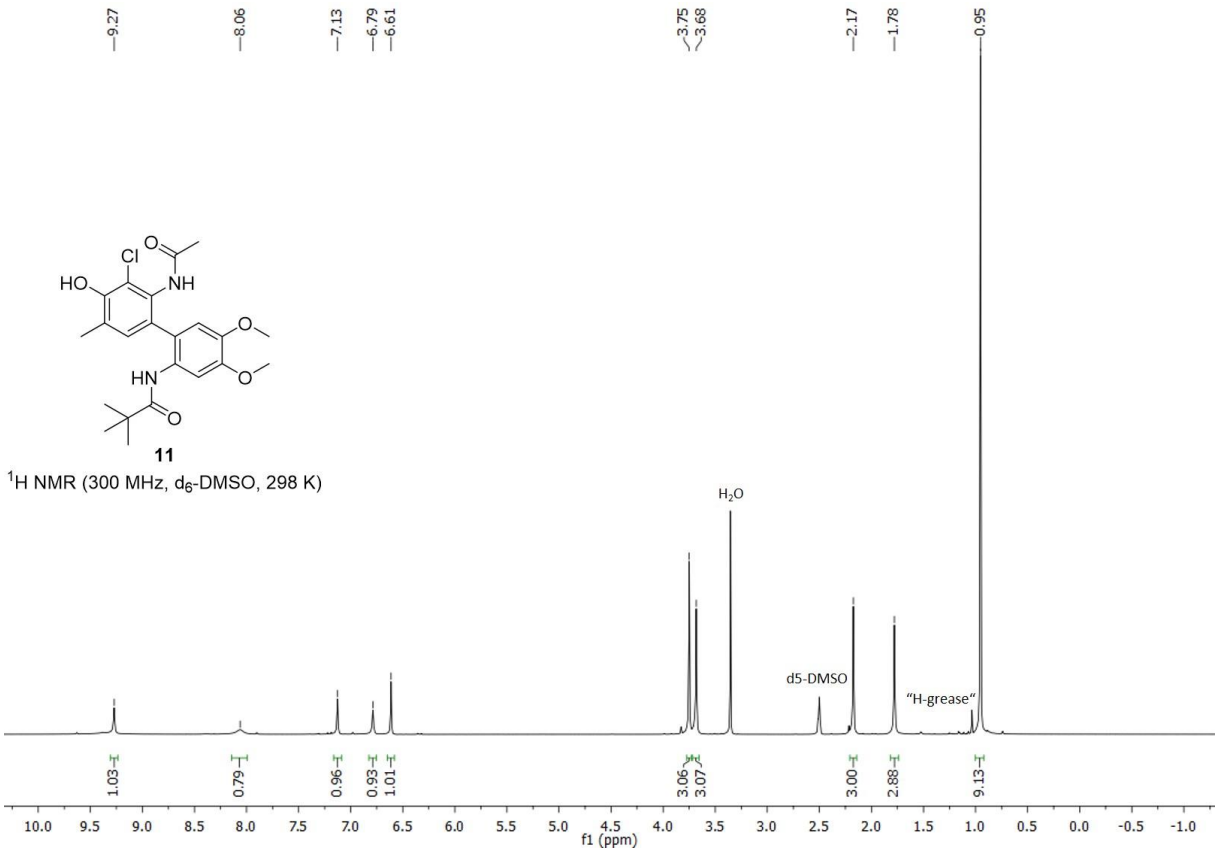

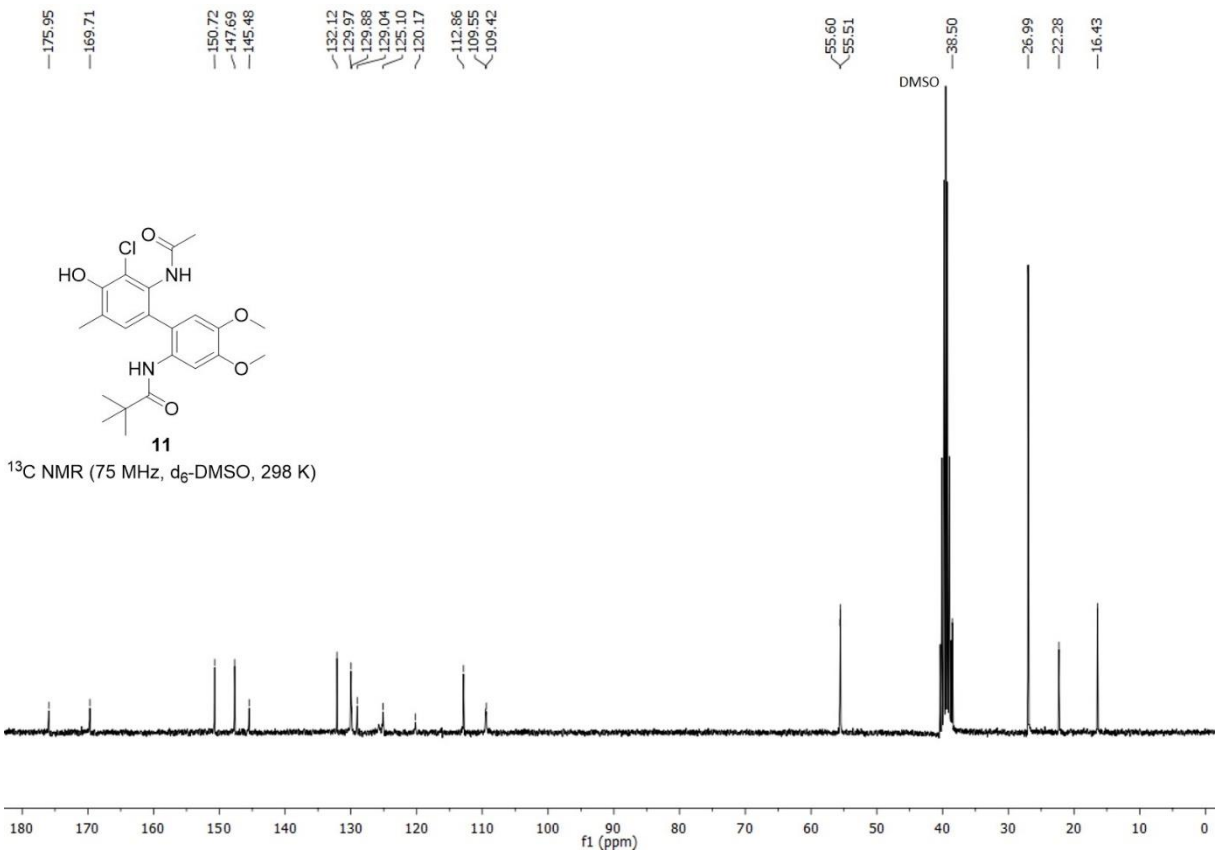

5-Acetamido-6-(2’-acetamido-4’,5’-dimethoxyphenyl)benzo-1,3-dioxol (12)

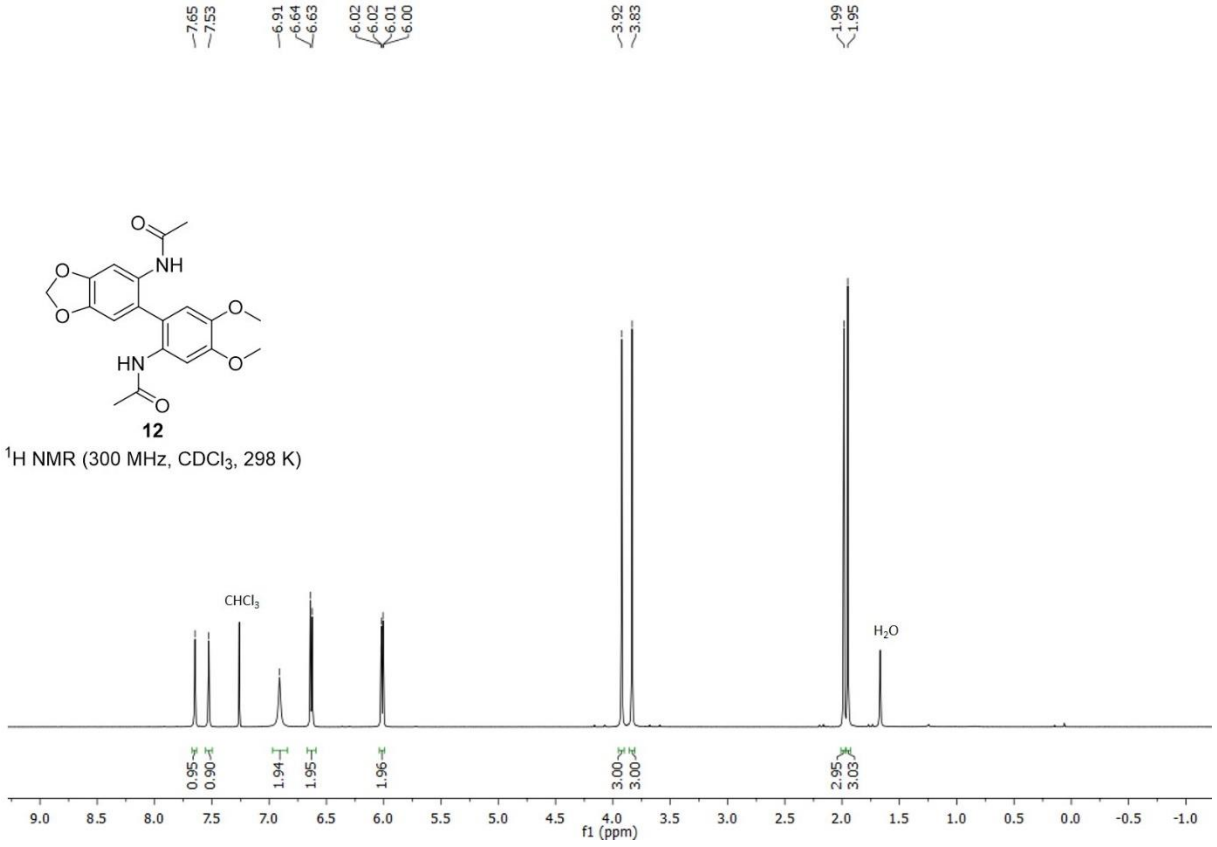

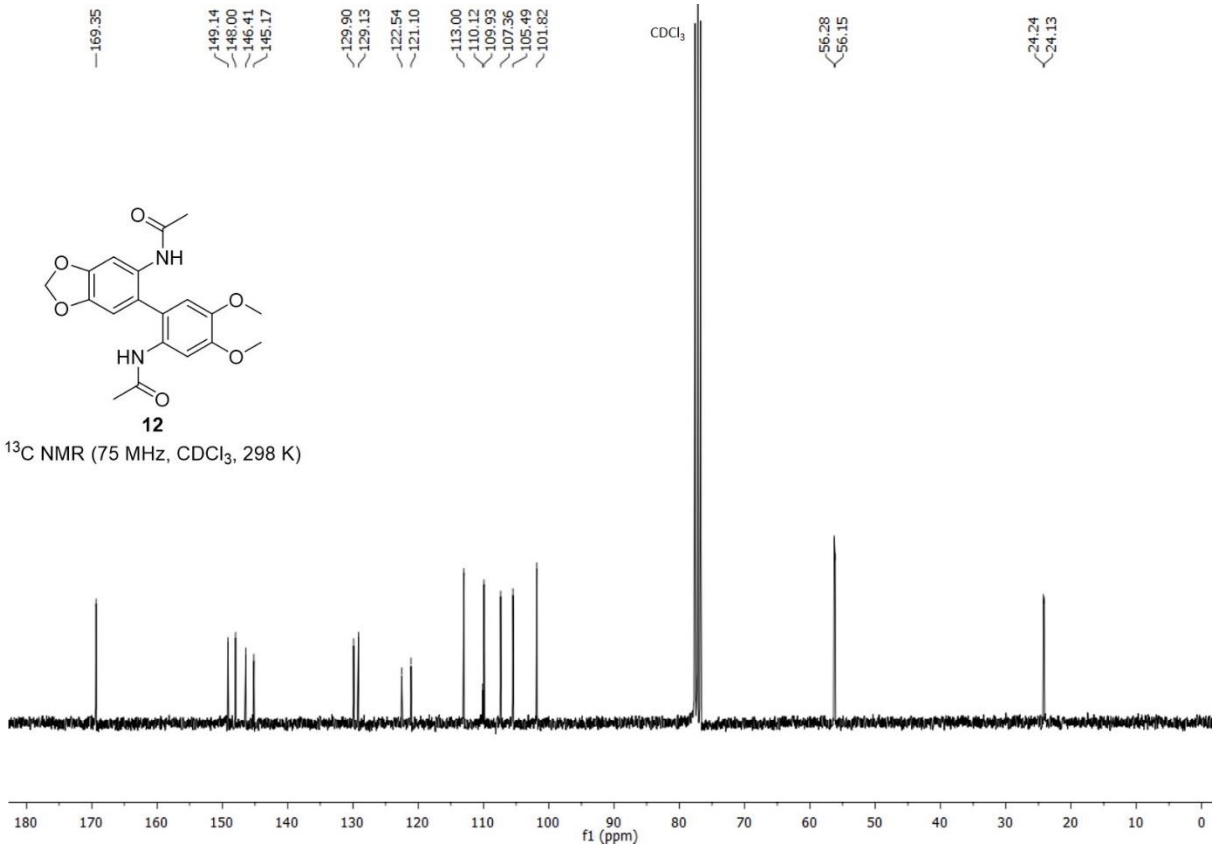

2'-Acetamido-2-amino-5-methyl-4,4',5'-trimethoxy-biphenyl (4')

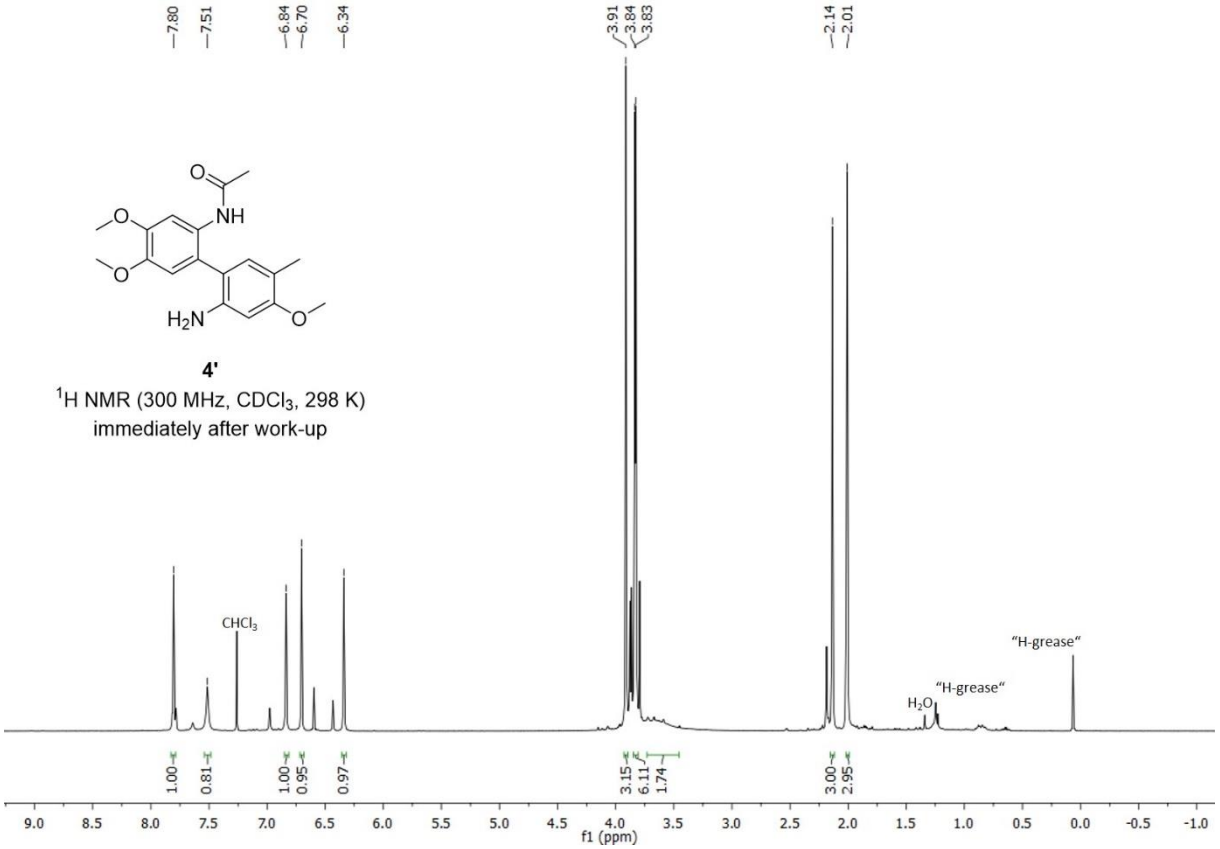

4'

^{1}H NMR (300 MHz, $CDCl_3$, 298 K)
immediately after work-up

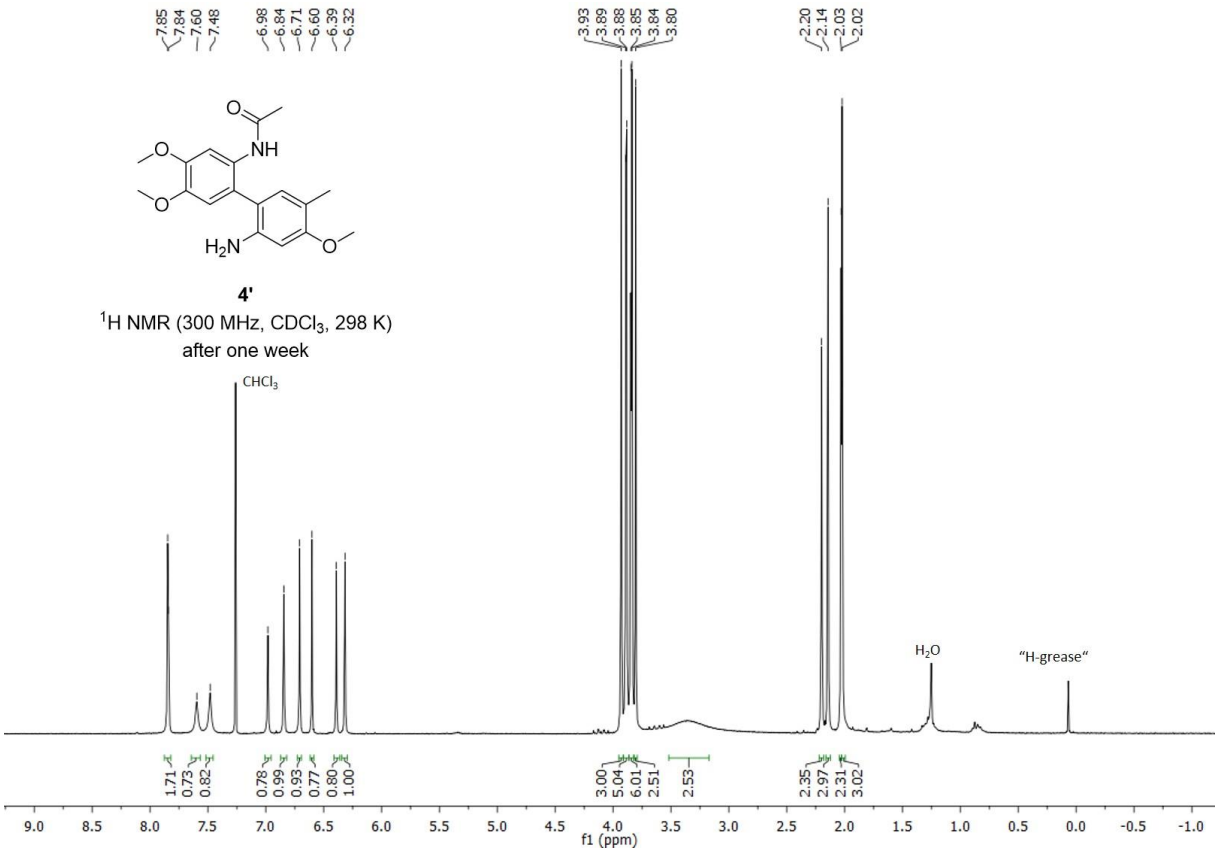

4'

^{1}H NMR (300 MHz, $CDCl_3$, 298 K)
after one week

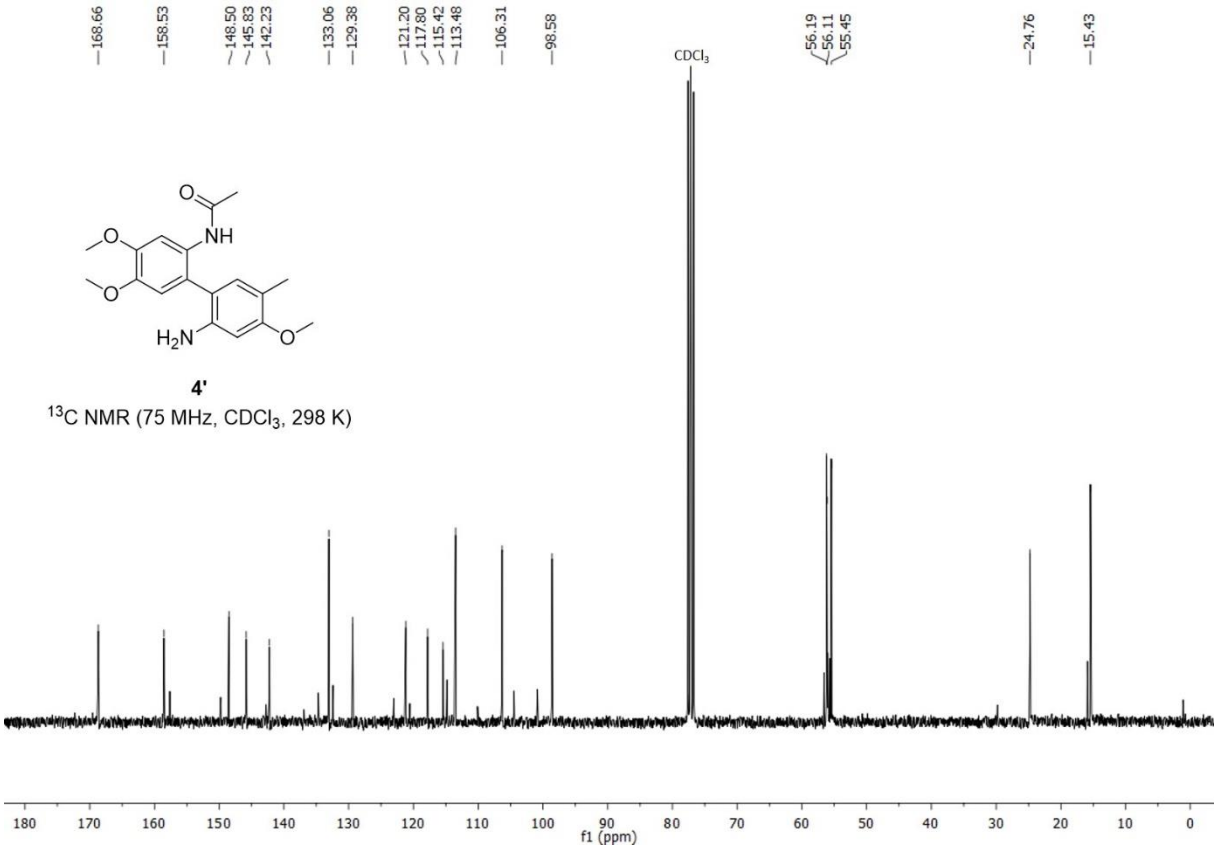

4'

^{13}C NMR (75 MHz, $CDCl_3$, 298 K)

2-Amino-2'-benzamido-5-methyl-4,4'-5'-trimethoxybiphenyl (6')

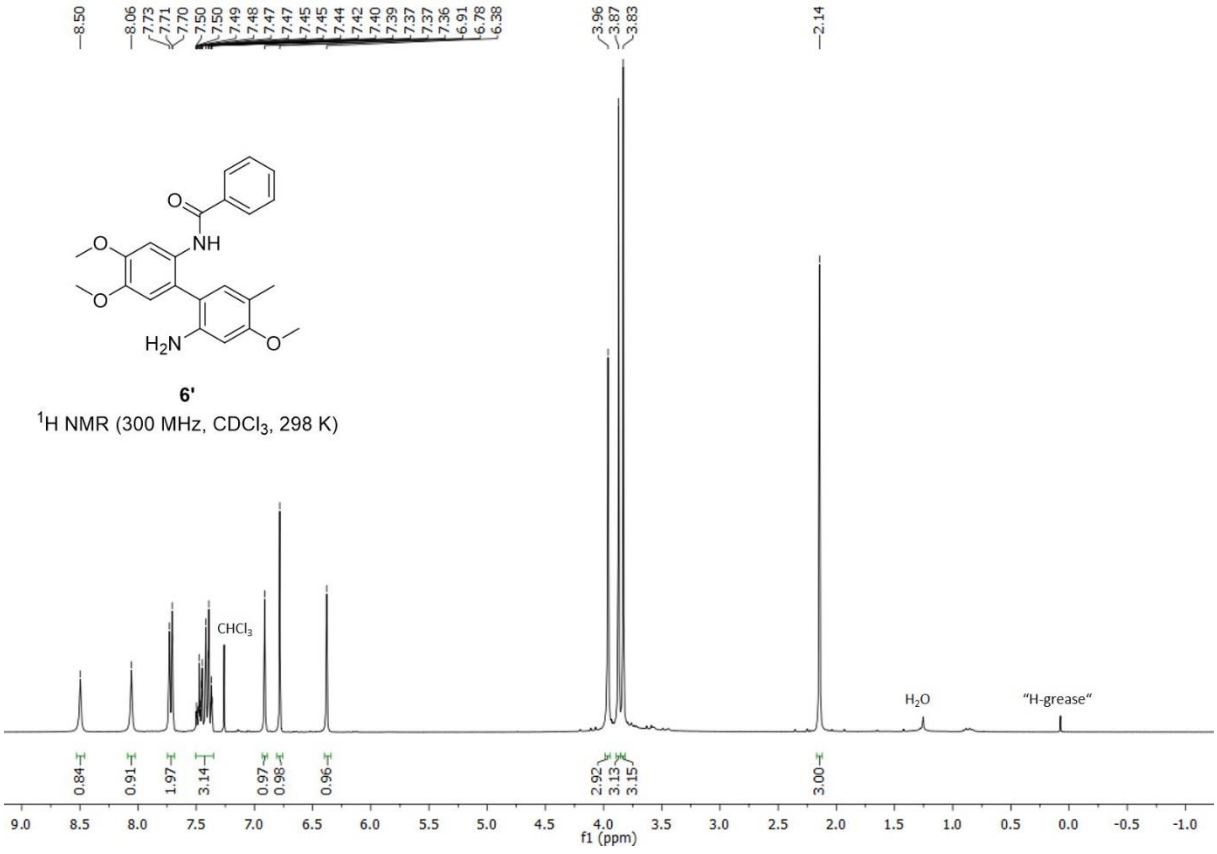

6'

^{1}H NMR (300 MHz, $CDCl_3$, 298 K)

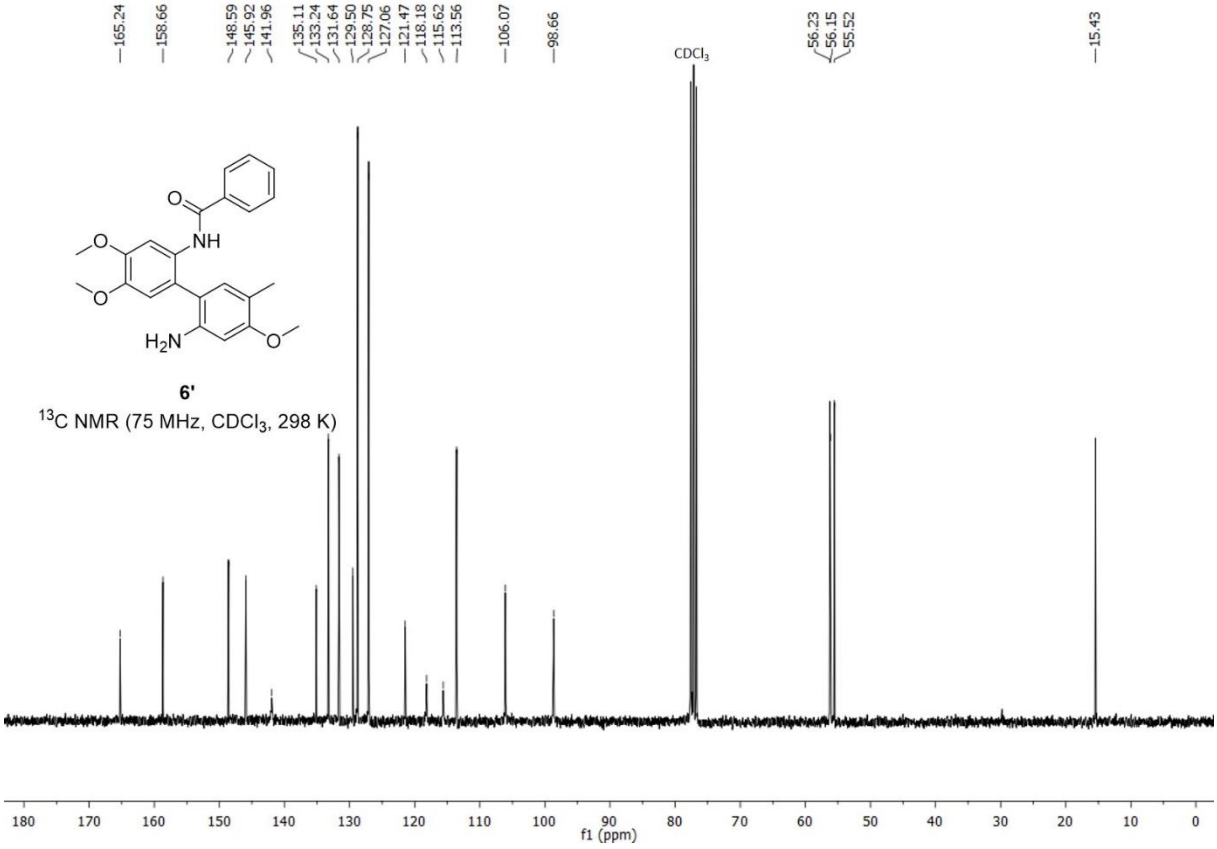

6'

^{13}C NMR (75 MHz, $CDCl_3$, 298 K)

2-Acetamido-1-(2'-amino-4',5'-dimethoxyphenyl)naphthalene (3')

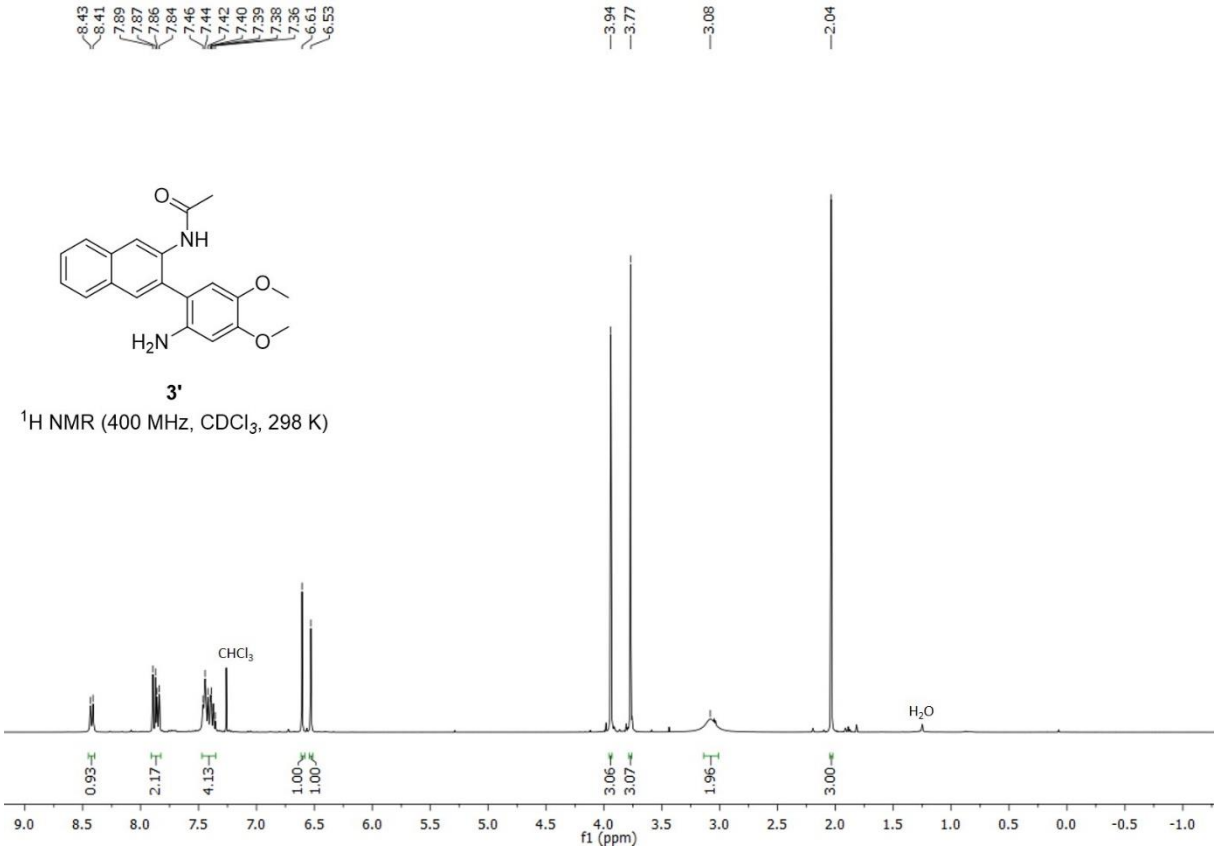

3'

^{1}H NMR (400 MHz, $CDCl_3$, 298 K)

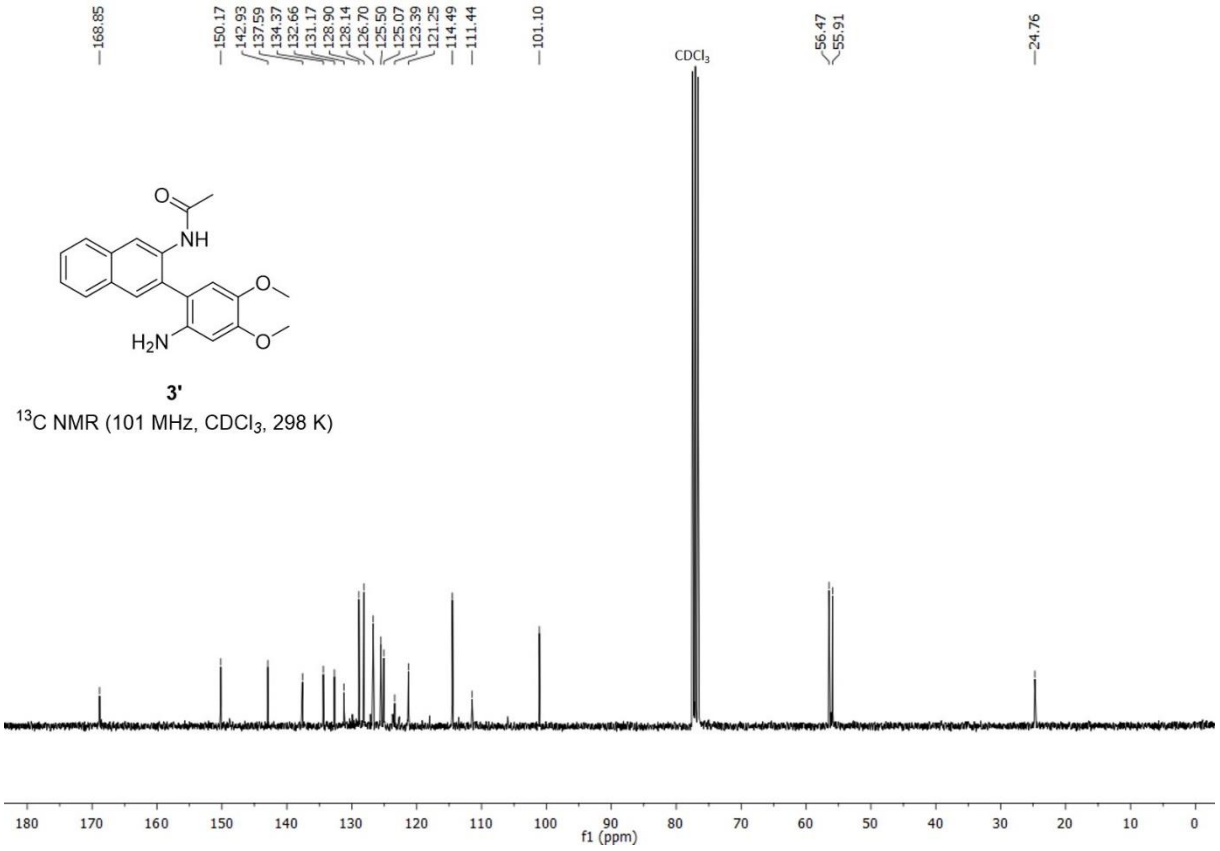

3'

^{13}C NMR (101 MHz, $CDCl_3$, 298 K)

2,2'-Diamino-1-(4',5'-dimethoxyphenyl)naphthalene (3'')

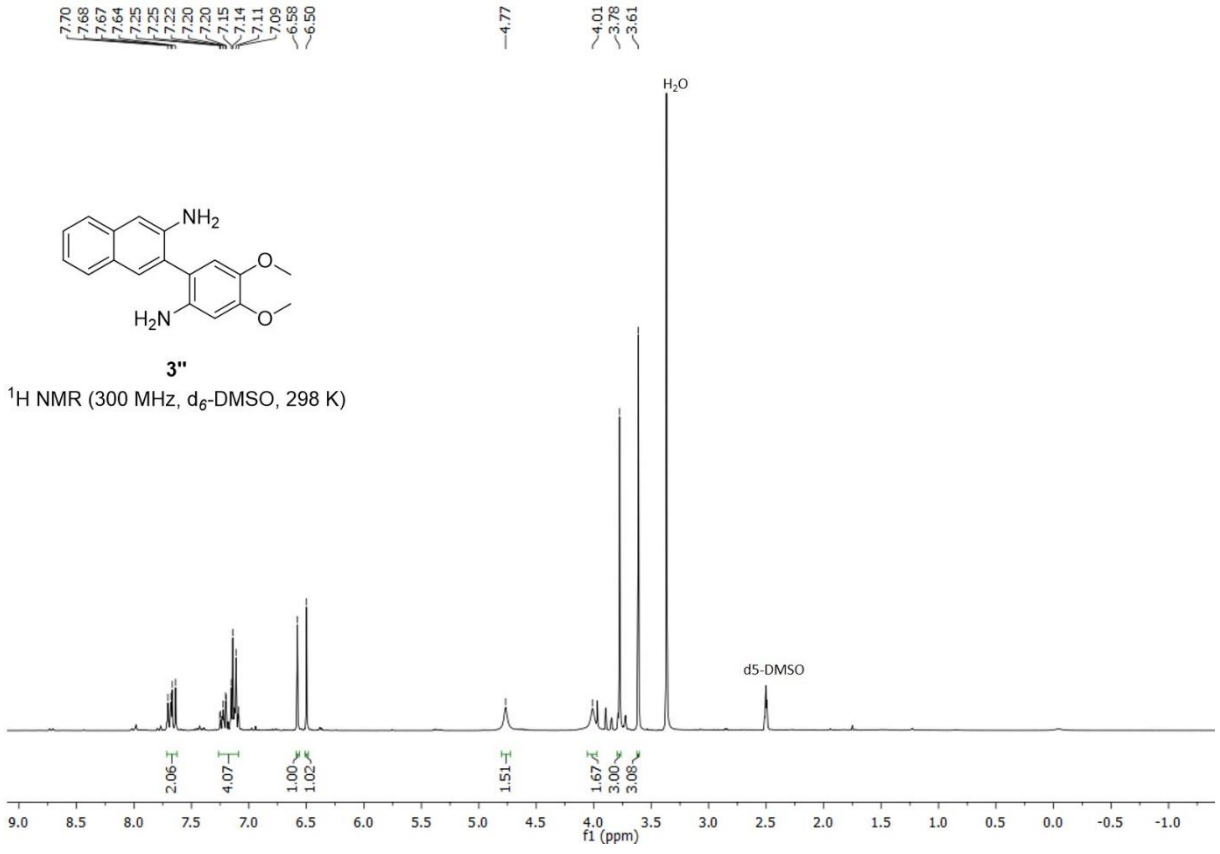

3''

^{1}H NMR (300 MHz, d_6-DMSO, 298 K)

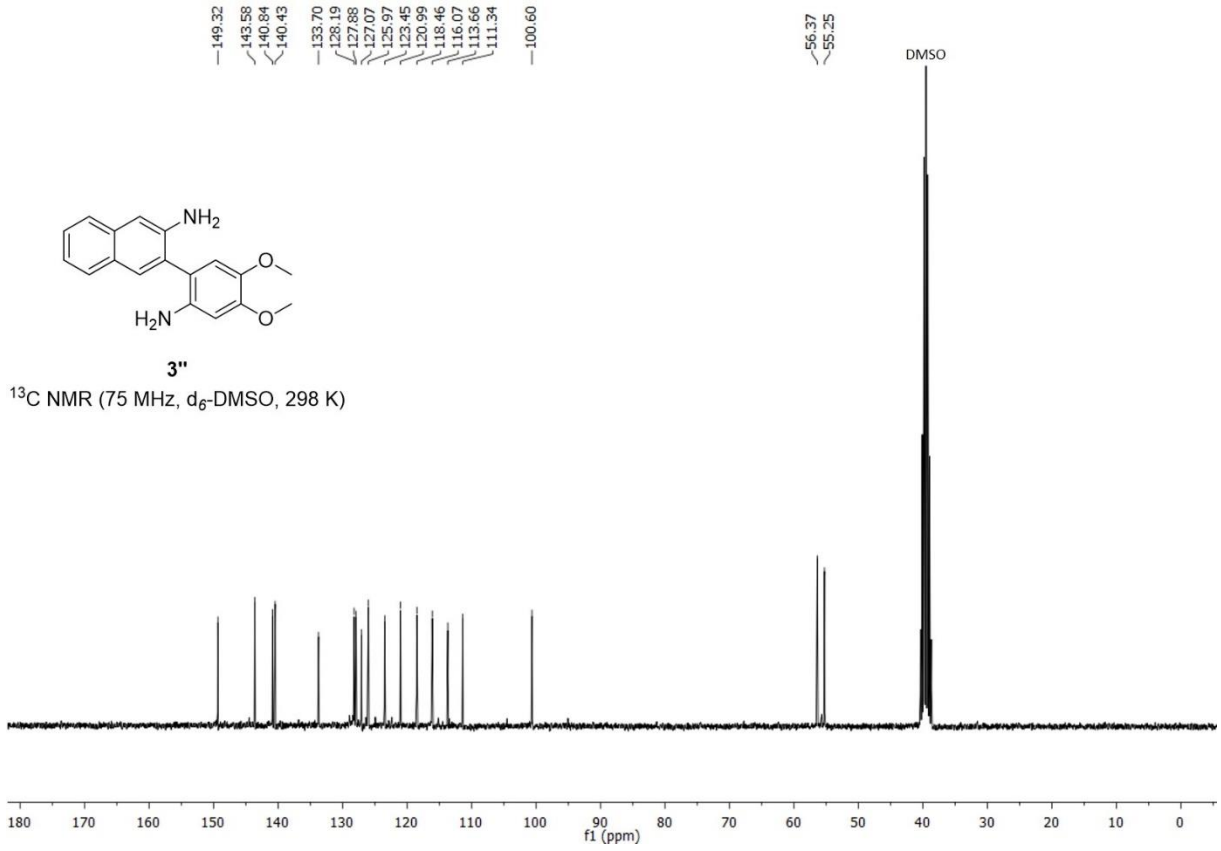

3''

^{13}C NMR (75 MHz, d_6-DMSO, 298 K)

References

[1] W. L. F. Armarego, C. L. L. Chai, *Purification of Laboratory Chemicals*, 7th ed., Elsevier Ltd., Oxford, **2012**.

[2] Sheldrick, G.M. *SHELXS97* and *SHELXL97*: *Program for the Refinement of Crystal Structures;* Dept. of Structural Chemistry, University of Göttingen: Germany, 1997.

[3] C. Gütz, B. Klöckner, S. R. Waldvogel, *Org. Process Res. Dev.* **2016**, *20*, 26–32.

[4] A. Kirste, G. Schnakenburg, F. Stecker, A. Fischer, S. R. Waldvogel, *Angew. Chem. Int. Ed*. **2010**, *49*, 971–975; *Angew. Chem.* **2010**, *122*, 983–987.

[5] N. Kamimoto, D. Schollmeyer, K. Mitsudo, S. Suga, S. R. Waldvogel, *Chem. Eur. J.* **2015**, *21*, 8257–8261.

[6] G. E. M. Crisenza, O. O. Sokolova, J. F. Bower, *Angew. Chem. Int. Ed.* **2015**, *54*, 14866–14870; *Angew. Chem.* **2015**, *127*, 15079–15083.

[7] T. Watanabe, T. Takeuchi, M. Otsuka, S.-I. Tanaka, K. Umezawa, *Jpn. J. Antibiot.* **1995**, *48*, 1460–1466.

[8] M. P. Krahl. O. Kataeva, A. W. Schmidt, H.-J. Knölker, *Eur. J. Org. Chem.* **2013**, 59–64.

[9] J. D. Al-Shawabkeh, A. H. Al-Nadaf, L. A. Dahabiyeh, M. O. Taha, *Med. Chem. Res.* **2014**, *23*, 127–145.

[10] A. Aksenov, N. Aksenov, O. Nadein, I. Aksenova, *Synlett* **2010**, *2010*, 2628–2630.

[11] I. Moreno, I. Tellitu, J. Etayo, R. SanMartín, E. Domínguez, *Tetrahedron* **2001**, 57, 5403–5411.

[12] J. M. Fourquez, A. Godard, F. Marsais, G. Quéguiner, *J. Heterocyclic Chem.* **1995**, *32*, 1165–1170.

[13] M. A. Elban, W. Sun, B. M. Eisenhauer, R. Gao, S. M. Hecht, *Org. Lett.* **2006**, *8*, 3513–3516.

ChemPubSoc Europe

DOI: 10.1002/celc.201800422

CHEMELECTROCHEM Communications

Direct Anodic Dehydrogenative Cross- and Homo-Coupling of Formanilides

Lara Schulz,[a] Robert Franke,[b, c] and Siegfried R. Waldvogel*[a]

The direct anodic dehydrogenative C–C cross- and homo-coupling of formanilides is reported. This exceptional electrochemical synthesis allows one to prepare a broad variety of non-symmetrical and symmetrical 2,2′-diformamidobiphenyls as well as 2-formamido-2′-amidobiphenyls. By applying an easy and simple to perform metal- and oxidizer-free electrochemical protocol, and the formyl group as a highly atom-economic amino-protecting group, an important contribution to a sustainable and green-minded chemistry was achieved.

Formamides are considered as an outstanding class of compounds in organic and medicinal chemistry.[1,2] Furthermore, the formyl group represents an essential and highly atom-economic amino-protecting group.[3] In particular, formamides represent central intermediates in the preparation of isocyanates,[4] nitriles,[5] formamidines,[6] carbamates,[7] as well as of various fungicides[1,8] and pharmaceutically relevant structures[1,2,9] (Scheme 1).

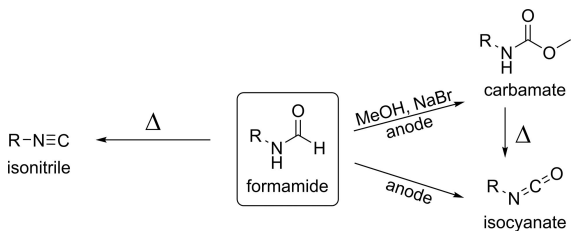

Scheme 1. Application of formamides in different important technical syntheses.

In particular, 2,2′-diformamidobiphenyl is of significant interest in the synthesis of diaryl based ligands[10] or in cyclization reactions for the construction of diazapyrenes.[11] Despite the wide interest in such structural features, synthesizing 2,2′-diformamidobiphenyls and 2,2′-diaminobiaryls in general, is still a challenging task since anilines severely suffer from oxidative polymerization to polyaniline, also known as aniline black.[12] A commonly used classical approach to symmetrical 2,2′-diaminobiaryls is the copper-mediated Ullmann reaction,[13] whereas direct oxidative cross-coupling reactions using stoichiometric amounts of Cu^{II} salts have only been reported for a few naphthylamines and provided the desired biaryls in fairly low yield.[14] An organocatalytic approach uses sigmatropic rearrangements of diaryl hydrazines in the presence of catalytic amounts of an acid to provide symmetrical 2,2′-diaminobiaryls in good yield. However, the access to non-symmetrical derivatives is still challenging.[15] Overall, many conventional approaches require several steps and often lead to complex reaction mixtures and thus low yield of the desired product. Recently, many efforts were made to develop oxidative coupling reactions by direct C–H activation.[16] The oxidative conversion of diaryl amines in the presence of a highly fluorinated iron phthalocyanine catalyst enabling C–C as well as N–N bond formation can be considered as a seminal example.[17]

However, many outstanding syntheses involve electrochemical techniques, which are exceptionally advanced in terms of avoiding the generation of waste because no leaving groups or oxidizers are required.[18] Moreover, electro-organic syntheses often need fewer steps, exploit electric current as inexpensive reagent and allow an easier scale-up than conventional protocols.[19] The anodic cross-coupling of different substrates in 1,1,1,3,3,3-hexafluoropropan-2-ol (HFIP) was developed including cross-coupling of phenols with arenes,[20] heterocycles[21] or other phenols,[22] as well as cross-couplings of protected aniline derivatives[23] and naphthylamines with phenols or naphthols.[24] Furthermore, recent studies pointed out the robustness of such electrochemical conversions.[25] Using an undivided cell, an unique solvent effect of HFIP is crucial for achieving high yield and selectivity.[26] This exceptional solvent forms strong hydrogen bonds,[27] which results in a distinct solvation of the individual coupling partners, and thus a decoupling of their oxidation potentials from nucleophilicity.[26] In several cases, addition of methanol or water could increase the yield and selectivity by manipulating the solvation properties.[26]

Here, for the first time an easy to conduct electrosynthetic approach to 2,2′-diformamidobiphenyls and 2-formamido-2′-amidobiphenyls is reported, using the highly atom-economic formyl group as nitrogen protecting group (Scheme 2). This electro-conversion is performed in a constant current mode, which allows the use of a very simple two-electrode arrangement in a common undivided beaker-type cell. Furthermore, employing glassy carbon as electrode material leads to a

[a] L. Schulz, Prof. Dr. S. R. Waldvogel
Institut für Organische Chemie
Johannes Gutenberg-Universität Mainz
Duesbergweg 10–14,
55128 Mainz (Germany)
E-mail: waldvogel@uni-mainz.de
[b] Prof. Dr. R. Franke
Evonik Performance Materials GmbH
Paul-Baumann-Straße 1
45772 Marl (Germany)
[c] Prof. Dr. R. Franke
Lehrstuhl für Theoretische Chemie
Ruhr-Universität Bochum
44780 Bochum (Germany)

Supporting information for this article is available on the WWW under https://doi.org/10.1002/celc.201800422

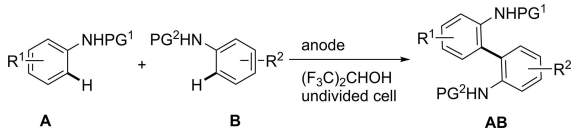

Scheme 2. Direct anodic C–C cross-coupling of formanilides. PG = formyl, acetyl or benzoyl group.

superior performance in aniline cross-coupling reaction because side reactions like electro-polymerization and homo-coupling can be diminished.[23]

In the electrochemical oxidation of anilines, it is essential to stabilize the reactive radical intermediates during the electrolysis to inhibit undesired oligomerization. Because of their electron-rich nature and resulting lower oxidation potentials, the parent aniline is very prone to over-oxidation. Thus the anodic polymerization of aniline derivatives is well-known.[28] Current organocatalytic approaches using nitrogen protecting groups in a hypervalent iodine-mediated coupling reaction can inhibit emerging side reactions. In this manner, *N*-mesyl-anilines could be converted in good yield. However, the desired aminobiphenyls could only be obtained after a wasteful and time-consuming deblocking protocol.[29]

As outlined in our previous work, oxidation potentials of anilines can be distinctly increased and to some extent adjusted by employing different protecting groups.[23] Here, we show for the first time, that the formyl group can effectively protect the amino moieties. This highly atom-economic protecting group exhibits sufficient stability during the electrochemical coupling and many of the desired non-symmetrical biaryls could be exclusively obtained in isolated yield up to 56% (Figure 1, compounds **1**, **2**, and **6**). Still, oligomerization and homo-coupling are the significant side reactions decreasing the yield of the cross-coupling reaction.

It was possible to couple different formyl-protected anilines like *N*-(3,4-dimethoxyphenyl)formamide with either benz- and acetamides (**1**, **2**, and **7**) in up to 56% yield or further formanilides (**4** and **8**) in up to 25% yield. C–C coupling reaction of a benzodioxole derivative was also successful with both, formamides (**4**, 25%) and acetamides (**3** and **5**, 17% and 51%, respectively). Even a chloro-substituted formanilide derivative could successfully be converted to biaryls **6**–**8** in up to 50% yield. Overall, the cross-coupling of one formamide with another amide (e.g. **1**, **2**, and **5**) often provides slightly better yield compared to the coupling of two formyl-protected amides (**4**, **8**). The amount of non-converted and recycled component **A** was up to 25%. However, increasing the applied charge is concomitant with an increase of oligomerization and therefore complicates the work-up.

Since formamides represent a highly interesting and widely used class of compounds, the homo-coupling reaction of formanilides was additionally investigated to broaden the scope. Former anodic aniline couplings revealed a distinct

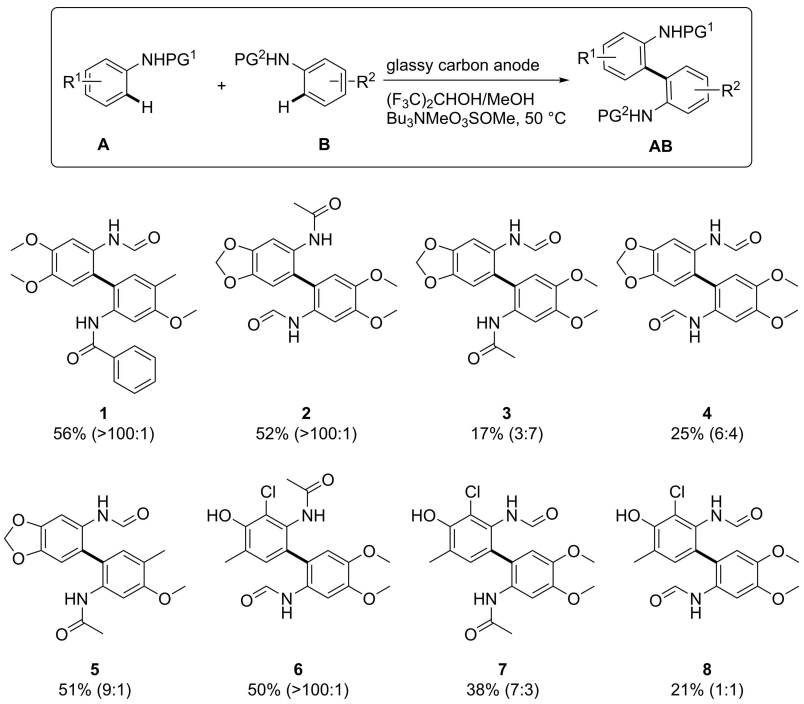

Figure 1. Scope of fully or partly formyl-protected non-symmetrical 2,2′-diaminobiaryls. Isolated yield are given; ratio of cross-coupling product **AB** to homo-coupling product **BB** is given in parentheses. [a] Electrolytic conditions: 1.875 mmol **A**, 50 °C, constant current ($j = 5.2$ mA cm^{-2}), glassy carbon anode, glassy carbon cathode, undivided beaker-type cell, $Q = 2$ F (aniline **A**), solvent: HFIP, supporting electrolyte: 0.09M Bu_3NMeO_3SOMe, **A**/**B** = 1:2. [b] Electrolytic conditions as in [a], solvent: HFIP/MeOH (18% v/v).

Table 1. Temperature dependence of the anodic homo-coupling of formanilide derivatives.[a]

Entry	Aniline **A**	Product **AB**	*T* [°C]	Yield [%][b]
1	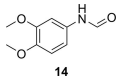 **14**	**12**	50	16%
2			30	11%
3	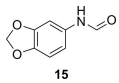 **15**	**11**	50	41%
4			**30**	36%

[a] Electrolytic conditions: 3.75 mmol **A**, constant current ($j = 5.2$ mA cm^{-2}), glassy carbon anode, glassy carbon cathode, undivided beaker-type cell, $Q = 2$ F (aniline **A**/2//), solvent: HFIP, supporting electrolyte: 0.09M Bu_3NMeO_3SOMe. [b] Yield of isolated products.

temperature dependence,[23] thus initial optimization of the homo-coupling conditions included evaluation of the temperature on the yield of the homo-coupling products (Table 1). In contrast to cross-couplings with Boc-protected anilines,[23] the coupling of formanilides seems to be preferred at slightly elevated temperatures (Table 1, entries 1 and 3).

For the homo-coupling of formyl-protected anilines, the same electrolytic conditions of the cross-coupling could be successfully applied (Figure 2). By this means, formyl-protected anilines that could already be successfully used in the cross-coupling, could similarly be converted in the homo-coupling. *N*-(3,4-dimethoxyphenyl)formamide gave biaryl **12** in 16% yield and the benzodioxole derivative gave **11** in 41% yield. Additionally, for the first time it was possible to use less electron-rich anilines like 3,4-dimethylaniline in the anodic coupling reaction, which gave the best yield of 47% (**10**). Besides, *N*-(3,5-dimethylphenyl)formamide was the first aniline derivative to be coupled with a free position *para* to the amide moiety. Interestingly, all three potential biaryls with different connectivity occurred, which are *ortho-ortho* (**13a**), *ortho-para* (**13b**) and *para-para* (**13c**) linked biaryls. Even formanilides containing labile but very valuable iodo moieties could be converted to the homo-coupling product **9** in 30% yield. Dehalogenation was not observed as a potential side reaction. The amount of non-converted and recycled aniline **A** was up to 38%, but again, increasing the applied charge leads to increased oligomerization and therefore challenges the work-up.

It is noteworthy that all of the coupling products showed a doubling of the signals in the ^{1}H and ^{13}C NMR spectra, caused by hindered rotation of the *N*-formyl group. If the diaminobiaryls contain two *N*-formyl groups, there were up to four different rotamers visible in the NMR spectra. NMR measurements of compounds **1**, **4**, **6**, **8** and **11** at higher temperatures showed coalescence of the formyl proton resonances at 353 K and 373 K, respectively (see Supporting Information).

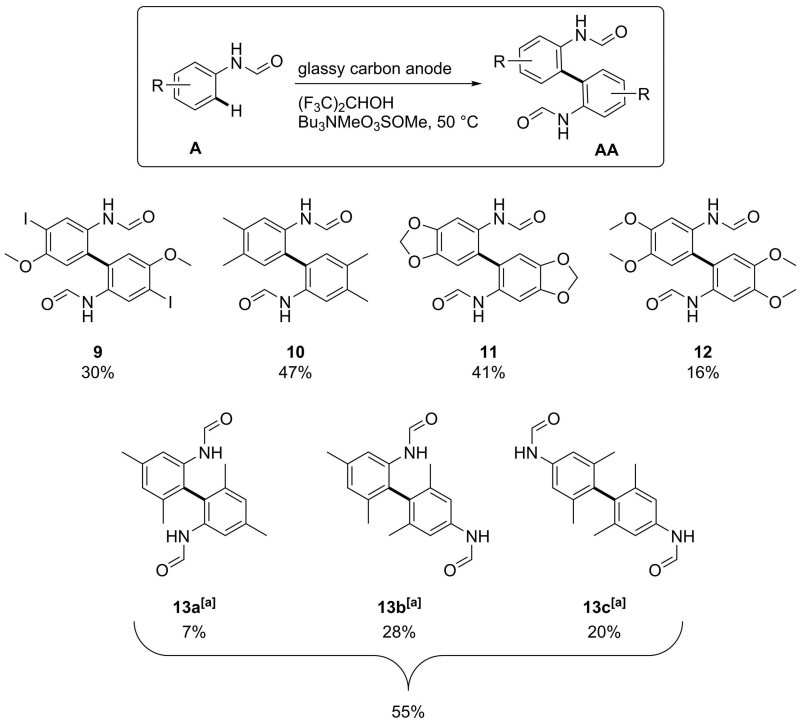

Figure 2. Scope of symmetrical 2,2′-diformamidobiphenyls. Yield of isolated products are given. Electrolytic conditions: 3.75 mmol **A**, 50 °C, constant current ($j = 5.2$ mA cm^{-2}), glassy carbon anode, glassy carbon cathode, undivided beaker-type cell, $Q = 2$ F (aniline **A**/2), solvent: HFIP, supporting electrolyte: 0.09M Bu_3NMeO_3SOMe. [a] Three different products arose from the homo-coupling of 3,5-dimethylformanilide due to a free position para to the amide function. The products are linked *ortho-ortho* (**13a**), *ortho-para* (**13b**) and *para-para* (**13b**), respectively.

In conclusion, the first electrochemical pathway to symmetrical and non-symmetrical formamidobiphenyls by anodic cross- and homo-coupling of formanilides was established. Using HFIP as solvent and the mild reaction conditions seem to be the key to diminish electro-polymerization of the electrochemically labile starting materials and thus promoting the cross- or homo-coupling reaction.

This electrosynthesis is easy to conduct, since only a very easy two-electrode arrangement and a common non-divided electrolysis cell are employed. No leaving functionalities or complicated reaction conditions are required, which makes this conversion much more efficient than conventional approaches. And by using electric current to drive this conversion, an easy and extraordinarily sustainable metal- and reagent-free path to formamidobiphenyls is created.

Experimental Section

The detailed description of electrolytic conversions, the products and their characterization are provided within the Supporting Information.

Acknowledgements

We highly appreciate support by BMBF-EPSYLON (FKZ 12XP2016D). The authors thank the DFG (Wa 1276/17-1) for financial support. Support by the Advanced Lab of Electrochemistry and Electrosynthesis – ELYSION (Carl Zeiss Stiftung) is gratefully acknowledged. The authors highly appreciate the financial support by the Center for INnovative and Emerging MAterials (CINEMA).

Conflict of Interest

The authors declare no conflict of interest.

Keywords: biaryls · C–H activation · electrosynthesis · formamides · green chemistry

[1] B.-C. Chen, M. S. Bednarz, R. Zhao, J. E. Sundeen, P. Chen, Z. Shen, A. P. Skoumbourdis, J. C. Barrish, *Tetrahedron Lett.* **2000**, *41*, 5453–5456.
[2] K. Kobayashi, S. Nagato, M. Kawakita, O. Morikawa, H. Konishi, *Chem. Lett.* **1995**, *24*, 575–576.
[3] J. Martinez, J. Laur, *Synthesis* **1982**, *1982*, 979–981.
[4] a) M. K. Faraj, US5686645 A, **1992**; b) U. Griesbach, L. Wittenbecher, H. Puetter, WO2009010420 A1, **2008**.
[5] a) D. Arlt, G. Klein, US4419297A, **1982**; b) F. Becke, P. Paessler, DE1908967A1, **1969**.
[6] Y. Han, L. Cai, *Tetrahedron Lett.* **1997**, *38*, 5423–5426.
[7] a) D. Degner, H. Hannebaum, M. Steiniger, DE3529531A1, **1995**; b) D. Degner, H. Hannebaum, DE3606478A1, **1986**.
[8] H. G. Grant, L. A. Summers, *Aust. J. Chem.* **1980**, *33*, 613–617.
[9] a) A. Jackson, O. Meth-Cohn, *J. Chem. Soc. Chem. Commun.* **1995**, 1319; b) G. Pettit, M. Kalnins, T. Liu, E. Thomas, K. Parent, *J. Org. Chem.* **1961**, *26*, 2563–2566.
[10] Z. Jin, Y.-J. Li, Y.-Q. Ma, L.-L. Qiu, J.-X. Fang, *Chem. Eur. J.* **2012**, *18*, 446–450.
[11] a) W. L. Mosby, *J. Org. Chem.* **1957**, *22*, 671–673; b) G. M. Badger, W. F. H. Sasse, *J. Chem. Soc.* **1957**, *0*, 4–8.
[12] H. Letheby, *J. Chem. Soc.* **1862**, *15*, 161–163.
[13] W. Kalk, H.-S. Bien, K.-H. Schündehütte, *Liebigs Ann. Chem.* **1977**, 329–337.
[14] M. Smrcina, S. Vyskocil, B. Maca, M. Polasek, T. A. Claxton, A. P. Abbott, P. Kocovsky, *J. Org. Chem.* **1994**, *59*, 2156–2163.
[15] a) H.-M. Kang, Y.-K. Lim, I.-J. Shin, H.-Y. Kim, C.-G. Cho, *Org. Lett.* **2006**, *8*, 2047–2050; b) H.-Y. Kim, W.-J. Lee, H.-M. Kang, C.-G. Cho, *Org. Lett.* **2007**, *9*, 3185–3186; c) B.-Y. Lim, M.-K. Choi, C.-G. Cho, *Tetrahedron Lett.* **2011**, *52*, 6015–6017; d) Y.-K. Lim, J.-W. Jung, H. Lee, C.-G. Cho, *J. Org. Chem.* **2004**, *69*, 5778–578; e) S.-E. Suh, I.-K. Park, B.-Y. Lim, C.-G. Cho, *Eur. J. Org. Chem.* **2011**, 455–457; f) G.-Q. Li, H. Gao, C. Keene, M. Devonas, D. H. Ess, L. Kürti, *J. Am. Chem. Soc.* **2013**, *135*, 7414–7417.
[16] a) N. Y. More, M. Jeganmohan, *Org. Lett.* **2015**, *17*, 3042–3045; b) T. Morofuji, A. Shimizu, J.-i. Yoshida, *Angew. Chem. Int. Ed.* **2012**, *51*, 7259–7262; *Angew. Chem.* **2012**, *124*, 7371–7374; c) A. Libman, H. Shalit, Y. Vainer, S. Narute, S. Kozuch, D. Pappo, *J. Am. Chem. Soc.* **2015**, *137*, 11453–11460; d) Y. E. Lee, T. Cao, C. Torruellas, M. C. Kozlowski, *J. Am. Chem. Soc.* **2014**, *136*, 6782–6785; e) S. Tang, Y. Liu, A. Lei, *Chem* **2018**, *4*, 27–45.
[17] R. F. Fritsche, G. Theumer, O. Kataeva, H.-J. Knölker, *Angew. Chem. Int. Ed.* **2017**, *56*, 549–553; *Angew. Chem.* **2017**, *129*, 564–568.
[18] E. J. Horn, B. R. Rosen, P. S. Baran, *ACS Cent. Sci.* **2016**, *2*, 302–308.
[19] a) H. J. Schäfer, *C. R. Chim.* **2011**, *14*, 745–765; b) S. Möhle, M. Zirbes, E. Rodrigo, T. Gieshoff, A. Wiebe, S. R. Waldvogel, *Angew. Chem. Int. Ed.* **2018**; *in press* (DOI: 10.1002/anie.201712732); c) A. Wiebe, T. Gieshoff, S. Möhle, E. Rodrigo, M. Zirbes, S. R. Waldvogel, *Angew. Chem. Int. Ed.* **2018**; *in press* (DOI: 10.1002/anie.201711060); d) M. Yan, Y. Kawamata, P. S. Baran, *Chem. Rev.* **2017**, *117*, 13230–13319.
[20] A. Kirste, B. Elsler, G. Schnakenburg, S. R. Waldvogel, *J. Am. Chem. Soc.* **2012**, *134*, 3571–3576.
[21] A. Wiebe, S. Lips, D. Schollmeyer, R. Franke, S. R. Waldvogel, *Angew. Chem. Int. Ed.* **2017**, *56*, 14727–14731; *Angew. Chem.* **2017**, *129*, 14920–14925.
[22] a) B. Elsler, D. Schollmeyer, K. M. Dyballa, R. Franke, S. R. Waldvogel, *Angew. Chem. Int. Ed.* **2014**, *53*, 5210–5213; *Angew. Chem.* **2014**, *126*, 5311–5314; b) A. Wiebe, D. Schollmeyer, K. M. Dyballa, R. Franke, S. R. Waldvogel, *Angew. Chem. Int. Ed.* **2016**, *55*, 11801–11805; *Angew. Chem.* **2016**, *128*, 11979–11983; c) B. Riehl, K. Dyballa, R. Franke, S. R. Waldvogel, *Synthesis* **2016**, *49*, 252–259.
[23] L. Schulz, M. Enders, B. Elsler, D. Schollmeyer, K. M. Dyballa, R. Franke, S. R. Waldvogel, *Angew. Chem. Int. Ed.* **2017**, *56*, 4877–4881; Angew. Chem. **2017**, 129, 4955–4959.
[24] B. Dahms, R. Franke, S. R. Waldvogel, *ChemElectroChem* **2018**; *in press* (DOI: 10.1002/celc.201800050).
[25] A. Wiebe, B. Riehl, S. Lips, R. Franke, S. R. Waldvogel, *Sci. Adv.* **2017**, *3*, eaao3920/1-7.
[26] B. Elsler, A. Wiebe, D. Schollmeyer, K. M. Dyballa, R. Franke, S. R. Waldvogel, *Chem. Eur. J.* **2015**, *21*, 12321–12325.
[27] a) R. Francke, D. Cericola, R. Kötz, D. Weingarth, S. R. Waldvogel, *Electrochim. Acta* **2012**, *62*, 372–380; b) O. Hollóczki, A. Berkessel, J. Mars, M. Mezger, A. Wiebe, S. R. Waldvogel, B. Kirchner, *ACS Catal.* **2017**, *7*, 1846–1852.
[28] D. M. Mohilner, R. N. Adams, W. J. Argersinger, *J. Am. Chem. Soc.* **1962**, *84*, 3618–3622.
[29] M. Ito, H. Kubo, I. Itani, K. Morimoto, T. Dohi, Y. Kita, *J. Am. Chem. Soc.* **2013**, *135*, 14078–14081.

Manuscript received: March 31, 2018
Version of record online: May 23, 2018

Supporting Information

Direct Anodic Dehydrogenative Cross- and Homo-Coupling of Formanilides

Lara Schulz, Robert Franke, and Siegfried R. Waldvogel*

Table of Contents

General Remarks

All reagents were used in analytical grades without further purification. Solvents were purified by standard methods.[1] As supporting electrolyte *N*-methyl-*N,N,N*-tributylammonium methylsulfate was used (MTBS, kindly provided by BASF SE, Ludwigshafen, Germany). For electrochemical reactions glassy carbon (SIGRADUR® G, obtained from HTW Hochtemperatur Werkstoffe GmbH, Thierhaupten, Germany) was applied.

Column chromatography was performed on silica gel 60 M (0.040–0.063 mm, Macherey-Nagel GmbH & Co, Düren, Germany) with a maximum pressure of 1.6 bar. In addition, a preparative chromatography system (Büchi Labortechnik GmbH, Essen, Germany) was used with a büchi control Unit C-620, an UV detector Büchi UV photometer C-635, Büchi fraction collector C-660 and two pump modules C-605 for adjusting the solvent mixtures. As eluents mixtures of cyclohexane and ethyl acetate were used. Silica gel 60 sheets on aluminum (F254, Merck, Darmstadt, Germany) were employed for thin layer chromatography.

Gas chromatography was performed on a Shimadzu GC-2010 (Shimadzu, Japan) using a ZB-5 column (Phenomenex, USA; length: 30 m, inner diameter: 0.25 mm, film: 0.25 µm, carrier gas: hydrogen. GC-MS measurements were carried out on a Shimadzu GC-2010 (Shimadzu, Japan) using a ZB-5 column (Phenomenex, USA; length: 30 m, inner diameter: 0.25 mm, film: 0.25 mm, carrier gas: helium). The chromatograph was coupled to a mass spectrometer (Shimadzu GCMS-QP2010; ion source's temperature: 200 °C).

Microanalysis was performed with a VarioMICRO cube (Elementar Analysesysteme, Hanau, Germany).

Melting points were determined with a Melting Point Apparatus B-545 (Büchi, Flawil, Switzerland) and are uncorrected. Heating rate: 2 °C/min.

Spectroscopy and spectrometry: ^{1}H NMR and ^{13}C NMR spectra were recorded at 298 K, 353 K or 373 K by using a Bruker Avance III HD 400 (400 MHz; Analytische Messtechnik, Karlsruhe, Germany) or a Bruker Avance II 400 (400 MHz), respectively. Chemical shifts (δ) are reported in parts per million (ppm) relative to traces of d_5-DMSO in the corresponding deuterated solvent. High resolution mass spectra were obtained by using a QTof Ultima 3 (Waters, Milford, Massachusetts) apparatus employing ESI^+.

Synthesis of Substrates

A: General protocol for *N*-formylation of anilines:

The aniline (4–46 mmol, 1.0 eq) was dissolved in formic acid (98%, 3.0–10.0 eq, depending on the solubility of the aniline) and heated at 80–90 °C overnight in a pressure tube. The mixture was chilled to room temperature and excess solvent was removed at reduced pressure. The formanilides were used without further purification.

B: General protocol for aniline-aniline coupling reactions:

Beaker-type Teflon cells and beaker-type glass cells were home-made by the local mechanical shop at the university. The undivided cells are briefly described here, whereas more details are found in literature.[2,3]They are equipped with glassy carbon electrodes. Due to over-oxidation of desired 2,2'-diaminobiaryls, electrolysis was stopped after applying 2 F per mol aniline **A** and using the optimized current density.[3]

B1: Screening experiments, cross-coupling reactions (beaker-type)

A solution of protected aniline component **A** (0.4 mmol, 1.0 eq), protected aniline component **B** (0.8 mmol, 2.0 eq) and *N*-methyl-*N*,*N*,*N*-tributylammonium methylsulfate (MTBS) (0.14 g, 0.45 mmol) in 5 mL 1,1,1,3,3,3-hexafluoroisopropanol (HFIP) and/or 4.1 mL HFIP + 0.9 mL methanol (18% v/v), respectively, was transferred into a screening cell equipped with glassy carbon electrodes. A constant current electrolysis with a current density of 5.2 mA/cm^2 was performed at 50°C. After application of 73 C (2.0 F per aniline **A**) the electrolysis was stopped and the solvent mixture was recovered *in vacuo* (50 °C, 200–70 mbar). The residual mixture was analyzed by GC or GC/MS, and TLC.

B2: Screening experiments, homo-coupling reactions (beaker-type)

A solution of protected aniline component **A** (0.75 mmol, 2.0 eq) and *N*-methyl-*N*,*N*,*N*-tributylammonium methylsulfate (MTBS) (0.14 g, 0.45 mmol) in 5 mL 1,1,1,3,3,3-hexafluoroisopropanol (HFIP) and/or 4.1 mL HFIP + 0.9 mL methanol (18% v/v), respectively, was transferred into a screening cell equipped with glassy carbon electrodes. A constant current electrolysis with a current density of 5.2 mA/cm^2 was performed at 50°C. After application of 73 C (1.0 F per aniline **A**) the electrolysis was stopped and the solvent mixture was recovered *in vacuo* (50 °C, 200–70 mbar). The residual mixture was analyzed by GC or GC/MS and TLC.

Recently, the set-up for screening was reported in detail.[2] Dimensions of glassy carbon electrodes are 7.0 x 1.0 x 0.3 cm. Using a 5 mL reaction mixture, electrodes immerse 1.8 cm into solution. This gives an active surface of 1.8 cm².

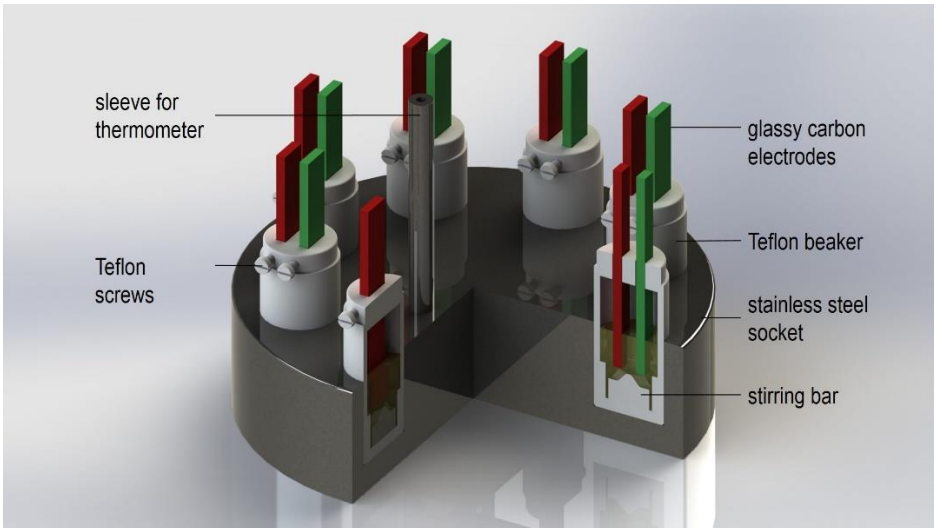

Figure S1: Schematic view of undivided screening cells in a screening arrangement.[2]

B3: Beaker-type cell, cross-coupling reactions (25 mL)

A solution of protected aniline component **A** (1.9 mmol, 1.0 eq), protected aniline component **B** (3.8 mmol, 2.0 eq) and *N*-methyl-*N,N,N*-tributylammonium methylsulfate (MTBS) (770 mg, 2.3 mmol, 1.2 eq) in 25 mL 1,1,1,3,3,3-hexafluoroisopropanol (HFIP) or 20.5 mL HFIP + 4.5 mL methanol (18% v/v), respectively, was transferred into an undivided beaker-type electrolytic cell equipped with glassy carbon electrodes. A constant current electrolysis with a current density of 5.2 mA/cm² was performed at 50 °C. After application of 363 C (2.0 F per aniline **A**) the electrolysis was stopped and the solvent mixture was recovered *in vacuo* (50 °C, 200–70 mbar). The crude coupling products were purified by column chromatography (SiO_2, cyclohexane/ethyl acetate).

B4: Beaker-type cell, homo-coupling reactions (25 mL)

A solution of protected aniline component **A** (3.8 mmol, 2.0 eq) and *N*-methyl-*N,N,N*-tributylammonium methylsulfate (MTBS) (770 mg, 2.3 mmol, 1.2 eq) in 25 mL 1,1,1,3,3,3-hexafluoroisopropanol (HFIP) was transferred into an undivided beaker-type electrolysis cell equipped with glassy carbon electrodes. A constant current electrolysis with a current density of 5.2 mA/cm² was performed at 50 °C. After application of 363 C (1.0 F per aniline **A**) the electrolysis was stopped and the solvent mixture was recovered *in vacuo* (50 °C, 200–70 mbar). The crude coupling products were purified by column chromatography (SiO_2, cyclohexane/ethyl acetate).

The beaker-type cell (25 mL) consists of a simple glass beaker with cooling jacket, covered with a Teflon plug. This cap allows precise location of the glassy carbon electrodes. Usually, a single glassy carbon electrode has upon immersion into the electrolyte an active surface of 9.0 cm^2 (2.0 cm x 4.5 cm).

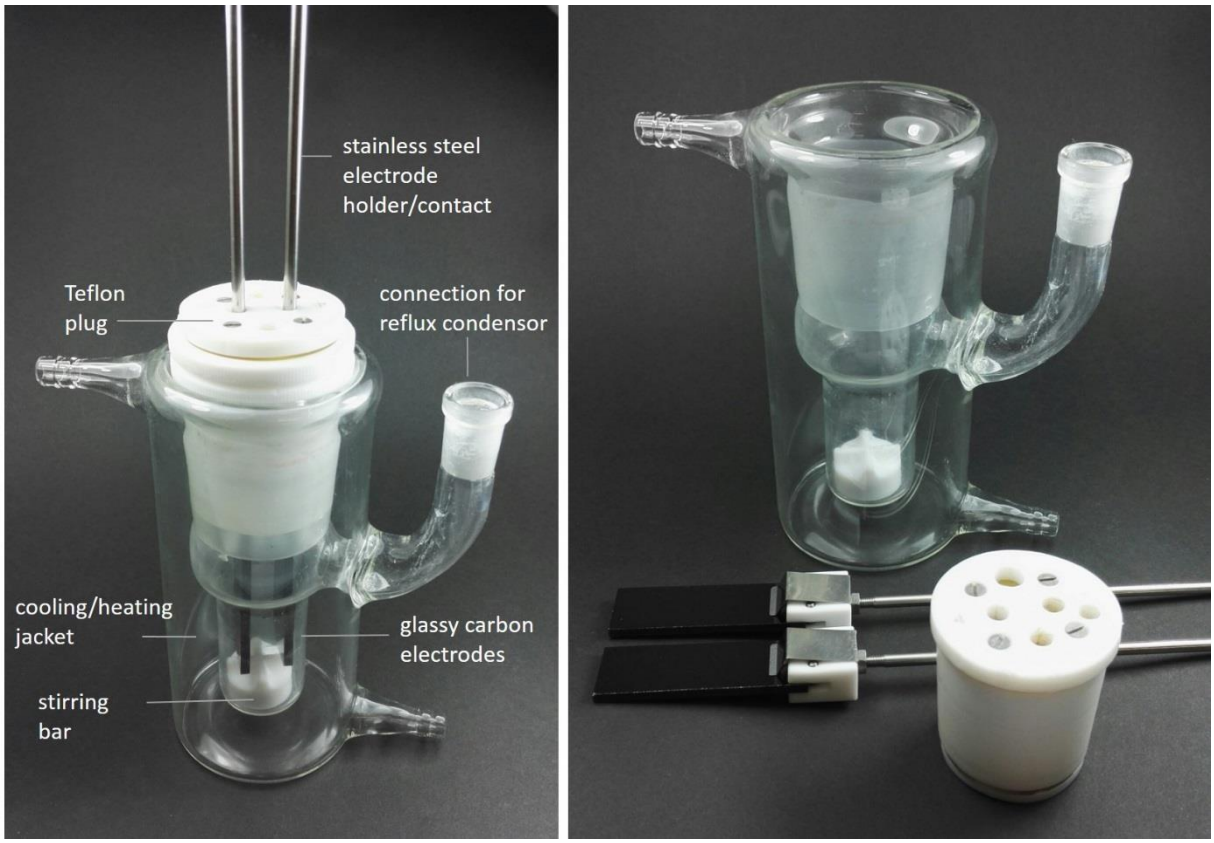

Figure S2: Pictures of an undivided beaker-type electrolysis cell. Essential parts are labeled.[6]

Synthesis of Non-symmetric 2,2‘-Diamidobiphenyls

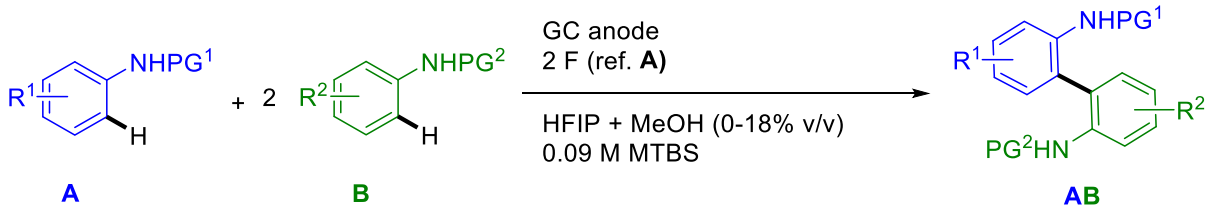

A **B** **AB**

2‘-Benzamido-2-formamido-5‘-methyl-4,4‘,5-trimethoxybiphenyl (1)

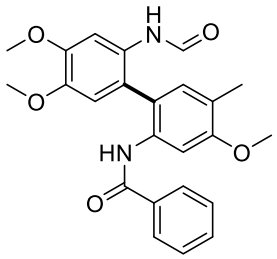

According to the general protocol **B3**, 340 mg (1.9 mmol, 1.0 eq) *N*-(3,4-dimethoxyphenyl)formamide **14**, 902 mg (3.8 mmol, 2.0 eq) *N*-(3-methoxy-4-methylphenyl)formamide and 770 mg MTBS were dissolved in 25 mL HFIP. After electrolysis, the solvent was recovered by distillation. Column chromatography of the residue (cyclohexane/ethyl acetate = 1:1 → 0:1) yielded the desired product as an off-white powder (yield: 56%, 439 mg, 1.0 mmol).

R_f (cyclohexane/ethyl acetate = 0:1) = 0.77; m.p. 200–202 °C; The NMR shows a 2*:1 mixture of two rotamers (rotation of the *N*-formyl group), rotameric mixture: ^{1}H NMR (400 MHz, d_6-DMSO): δ (ppm) = 9.66/9.32 (s, 1 H), 8.94 (d, *J* = 11.2 Hz)/8.86 (s, 1 H), 8.17/8.09 (d, *J* = 11.2/1.9 Hz, 1 H), 7.77–7.72/7.71–7.65 (m, 2 H), 7.57/6.84 (s, 1 H), 7.56–7.29/7.48–7.39 (m, 3 H), 7.31/7.12 (s, 1 H), 7.02/7.00 (s, 1 H), 6.80/6.71 (s, 1 H), 3.83/3.83 (s, 3 H), 3.74/3.73 (s, 3 H), 3.64/3.63 (s, 3 H), 2.18/2.17 (s, 3 H); ^{13}C NMR (101 MHz, d_6-DMSO): δ (ppm) = 165.77, 165.51*, 164.43*, 160.47*, 156.85*, 156.59, 148.17, 147.66*, 145.93, 145.35*, 134.83*, 134.77, 134.50*, 134.36, 132.47, 132.31*, 131.50*, 2x128.38*, 2x128.19*, 128.15, 2x127.34, 2x127.23*, 127.08, 125.14*, 124.42, 123.80, 123.21*, 123.12*, 114.21, 113.88*, 109.64, 108.41*, 108.08, 107.42*, 55.58, 55.55*, 55.49*, 55.45, 2x15.75*; HRMS for $C_{24}H_{24}N_2O_5$ (ESI+) $[M+H]^+$: calc.: 421.1758; found: 421.1746; $[M+Na]^+$: calc.: 443.1577; found: 443.1568; Elemental anal. for $C_{24}H_{24}N_2O_5$ calc.: C: 68.56%, H: 5.75%, N: 6.66%, found: C: 68.41%, H: 5.73%, N: 6.63%.

^{1}H NMR spectra at 353 K and 373 K and ^{13}C NMR spectra at 373 K can be found in the attachment.

5-Acetamido-6-(4‘,5‘-dimethoxy-2‘-formamidophenyl)benzo-1,3-dioxole (2)

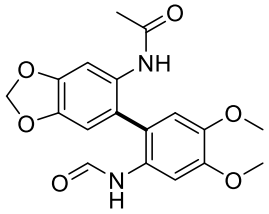

According to the general protocol **B3**, 350 mg (1.9 mmol, 1.0 eq) 5-acetamidobenzo-1,3-dioxole, 700 mg (3.8 mmol, 2.0 eq) *N*-(3,4-dimethoxyphenyl)formamide **14** and 770 mg MTBS were dissolved in 25 mL HFIP. After electrolysis, the solvent was recovered by distillation. Column chromatography of the residue (cyclohexane/ethyl acetate = 1:1 → 0:1) yielded the desired product as an off-white powder (yield: 52%, 317 mg, 1.0 mmol).

R_f (cyclohexane/ethyl acetate = 0:1) = 0.20; m.p. 209–211 °C; The NMR shows a 2.5*:1 mixture of two rotamers (rotation of the *N*-formyl group), rotameric mixture: ^{1}H NMR (400 MHz, d_6-DMSO): δ (ppm) = 8.99 (d, *J* = 11.2 Hz)/8.84/8.70 (s, 2 H), 8.16–8.08 (m)/8.04 (d, *J* = 1.9 Hz, 1 H), 7.57/6.88 (s, 1 H), 7.14/7.06 (s, 1 H), 6.80–6.68 (m, 2 H), 6.05 (s, 2 H), 3.76/3.72/3.71 (s, 6 H), 1.81/1.79 (s, 3 H); ^{13}C NMR (101 MHz, d_6-DMSO): δ (ppm) = 168.85, 168.78*, 164.12*, 163.94, 160.28, 160.17*, 148.07, 147.82*, 146.67*, 146.28, 145.43*, 145.39, 130.11*, 129.90, 128.89, 128.24*, 125.49*, 124.59, 122.62*, 121.36, 114.15, 113.84*, 110.25, 110.18*, 107.48, 107.45*, 107.12, 106.95*, 101.48, 101.42*, 55.68*, 55.59, 55.55, 55.51*, 23.04*, 22.96; HRMS for $C_{18}H_{18}N_2O_6$ (ESI+) $[M+Na]^+$: calc.: 381.1057; found: 381.1045.

5-(2’-Acetamido-4‘,5‘-dimethoxyphenyl)-6-formamidobenzo-1,3-dioxole (3)

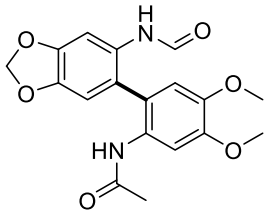

According to the general protocol **B3**, 307 mg (1.9 mmol, 1.0 eq) 5-formamidobenzo-1,3-dioxole **15**, 679 mg (3.8 mmol, 2.0 eq) *N*-(3,4-dimethoxyphenyl)acetamide and 770 mg MTBS were dissolved in 25 mL HFIP. After electrolysis, the solvent was recovered by distillation. Column chromatography of the residue (cyclohexane/ethyl acetate = 1:1 → 0:1) yielded the desired product as an off-white powder (yield: 17%, 116 mg, 0.3 mmol).

R_f (cyclohexane/ethyl acetate = 0:1) = 0.18; m.p. 188–190 °C; The NMR shows a 3*:1 mixture of two rotamers (rotation of the *N*-formyl group), rotameric mixture: ^{1}H NMR (400 MHz, d_6-DMSO): δ (ppm) = 8.96/8.78/8.74 (s)/8.86 (d, *J* = 11.1 Hz, 2 H), 8.07/8.01 (d, *J* = 11.1/1.9 Hz), 7.48/7.17/7.08/6.93 (s, 2 H), 6.69–6.67 (m, 2 H), 6.07/6.02 (s, 2 H), 3.75/3.73/3.71 (s, 6 H), 1.83/1.80 (s, 3 H); ^{13}C NMR (101 MHz, d_6-DMSO): δ (ppm) = 168.75, 168.65*, 163.83, 160.23*, 148.13*, 147.97, 147.01, 146.38, 146.34*, 146.22*, 144.82, 143.81*, 129.37, 129.14*, 129.02*, 128.94, 126.13, 125.76, 124.30*, 123.98*, 114.02, 113.84*, 110.40, 110.35, 110.21*, 110.07*, 105.07, 104.23*, 101.55, 101.35*, 2x55.69, 55.64*, 55.56*, 23.05*, 22.99; HRMS for $C_{18}H_{18}N_2O_6$ (ESI+) $[M+Na]^+$: calc.: 381.1057; found: 381.1048.

5-Formamido-6-(2'-formamido-4',5'-dimethoxyphenyl)benzo-1,3-dioxole (4)

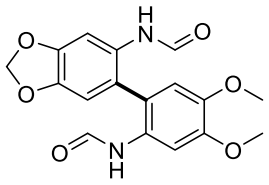

According to the general protocol **B3**, 308 mg (1.9 mmol, 1.0 eq) 5-formamidobenzo-1,3-dioxole **15**, 679 mg (3.8 mmol, 2.0 eq) *N*-(3,4-dimethoxyphenyl)formamide **14** and 770 mg MTBS were dissolved in 25 mL HFIP. After electrolysis, the solvent was recovered by distillation. Column chromatography of the residue (cyclohexane/ethyl acetate = 1:1 → 0:1) yielded the desired product as an off-white powder (yield: 25%, 162 mg, 0.5 mmol).

R_f (cyclohexane/ethyl acetate = 0:1) = 0.41; m.p. 217–219 °C; The NMR shows a 7*:2.5:2.5:1 mixture of four rotamers (rotation of the *N*-formyl groups), NMR-data for rotameric mixture: ^{1}H NMR (400 MHz, d_6-DMSO): δ (ppm) = 9.13–8.76 (m, 2 H), 8.13–8.03 (m, 2 H), 7.77–7.53/7.00–6.89 (m, 2 H), 6.79–6.63 (m, 2 H), 6.09/6.06/6.04 (s, 2 H), 3.81/3.80/3.77/3.76/3.73/3.72 (s, 6 H); The minor rotamer cannot be seen in the ^{13}C NMR, ^{13}C NMR (101 MHz, $CDCl_3$): δ (ppm) = 163.92*, 2x163.77, 160.32*, 160.27, 160.18*, 160.13, 148.85, 148.15*, 147.95, 147.43, 146.76, 146.62, 146.51, 145.47*, 145.12, 2x143.86, 143.82*, 129.88, 129.72*, 129.37, 128.87*, 128.73, 128.52, 125.28, 123.74, 123.62, 122.55*, 122.29, 121.27*, 2x114.36, 114.01*, 110.69, 110.65, 110.43*, 2x108.68, 107.13*, 105.38, 104.00, 103.91*, 2x101.65, 101.42*, 2x55.76, 55.73, 55.68, 55.65*, 55.52*; HRMS for $C_{17}H_{16}N_2O_6$ (ESI+) $[M+Na]^+$: calc.: 367.0901; found: 367.0906; Elemental anal. for $C_{17}H_{16}N_2O_6$ calc.: C: 59.30%, H: 4.68%, N: 8.14%, found: C: 59.07%, H: 4.70%, N: 8.17%.

^{1}H NMR spectra at 353 K and 373 K can be found in the attachment.

5-(2'-Acetamido-4'-methoxy-5'-methylphenyl)-6-formamidobenzo-1,3-dioxole (5)

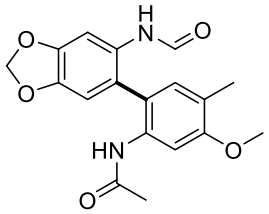

According to the general protocol **B3**, 310 mg (1.9 mmol, 1.0 eq) 5-formamidobenzo-1,3-dioxole **15**, 670 mg (3.8 mmol, 2.0 eq) *N*-(3-methoxy-4-methylphenyl)acetamide and 770 mg MTBS were dissolved in 25 mL HFIP. After electrolysis, the solvent was recovered by distillation. Column chromatography of the residue (cyclohexane/ethyl acetate = 4:1 → 1:1) yielded the desired product as an off-white powder (yield: 51%, 327 mg, 1.0 mmol).

R_f (cyclohexane/ethyl acetate = 1:1) = 0.11; m.p. 195–197 °C; The NMR shows a 3*:1 mixture of two rotamers (rotation of the *N*-formyl group), rotameric mixture: ^{1}H NMR (400 MHz, d_6-DMSO): δ (ppm) = 8.96–8.56 (m, 2 H), 8.07/8.00 (d, *J* = 11.2/1.9 Hz, 1 H), 7.45/7.17 (s, 1 H), 7.28 (s, 1 H), 6.92/6.90/6.65/6.64 (s, 2 H), 6.06/6.03 (s, 2 H) 3.78 (s, 3 H), 2.13/2.11 (s, 3 H), 1.85/1.82 (s, 3 H); ^{13}C NMR (101 MHz, d_6-DMSO): δ (ppm) = 168.67, 168.57*, 163.74, 160.21*, 156.74*, 156.56, 146.97, 146.32*, 144.85, 143.94*, 135.00*, 134.82, 132.44, 132.29*, 129.38, 128.99*, 124.79, 123.94*, 123.56, 123.30*, 122.71, 122.39*, 110.48, 110.25*, 107.84, 107.38*, 104.96, 104.36*, 101.52, 101.34*, 55.29*, 55.25, 23.27*, 23.18, 2x15.65*; HRMS for

$C_{18}H_{18}N_2O_5$ (ESI+) $[M+H]^+$: calc.: 343.1288; found: 343.1287; Elemental anal. for $C_{18}H_{18}N_2O_5$ calc.: C: 63.15%, H: 5.30%, N: 8.18%, found: C: 63.29%, H: 5.28%, N: 8.16%.

2-Acetamido-3-chloro-4‘,5‘-dimethoxy-2‘-formamido-4-hydroxy-5-methylbiphenyl (6)

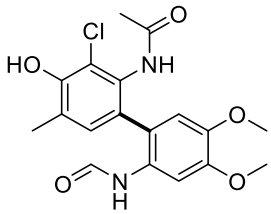

According to the general protocol **B3**, 376 mg (1.9 mmol, 1.0 eq) *N*-(2-chloro-3-hydroxy-4-methylphenyl)formamide, 679 mg (3.8 mmol, 2.0 eq) *N*-(3,4-dimethoxyphenyl)formamide **14** and 770 mg MTBS were dissolved in 25 mL HFIP. After electrolysis, the solvent was recovered by distillation. Column chromatography of the residue (cyclohexane/ethyl acetate = 1:1 → 0:1) yielded the desired product as an off-white powder (yield: 50%, 359 mg, 1.0 mmol).

R_f (cyclohexane/ethyl acetate = 0:1) = 0.19; m.p. 244–246 °C; The NMR shows a 2*:1 mixture of two rotamers (rotation of the *N*-formyl group), rotameric mixture: ^{1}H NMR (400 MHz, d_6-DMSO): δ (ppm) = 9.39–9.18 (m, 1 H), 8.90/8.67 (bs, 1 H), 8.09 (s)/8.05 (d, *J* = 1.9 Hz, 1 H), 7.66/6.90/6.89/6.85 (s, 2 H), 6.69/6.62 (s, 1 H), 3.78/3.75 (s, 3 H), 3.68/3.66 (s, 3 H), 2.22/2.20 (s, 3 H), 1.80/1.79 (s, 3 H); ^{13}C NMR (101 MHz, d_6-DMSO): δ (ppm) = 169.10, 168.99*, 2x164.34*, 2x160.16*, 150.97*, 150.64, 148.29, 147.52*, 145.95, 144.81*, 132.32*, 132.25, 130.39*, 130.35, 129.69, 128.63*, 128.21*, 127.98, 125.29, 125.19*, 122.64*, 120.67, 113.90, 113.57*, 108.13, 106.71*, 2x55.65, 55.55*, 55.48*, 2x22.35*, 2x16.69*; HRMS for $C_{18}H_{19}{}^{35}ClN_2O_5$ (ESI+) $[M+Na]^+$: calc.: 401.0875; found: 401.0875.

^{1}H NMR spectra at 353 K and 373 K and ^{13}C NMR spectra at 373 K can be found in the attachment.

2’-Acetamido-3-chloro-4‘,5‘-dimethoxy-2-formamido-4-hydroxy-5-methylbiphenyl (7)

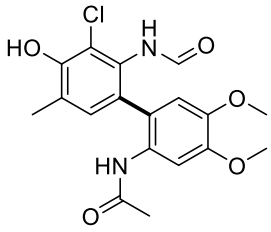

According to the general protocol **B3**, 348 mg (1.9 mmol, 1.0 eq) *N*-(2-chloro-3-hydroxy-4-methylphenyl)formamide **16**, 749 mg (3.8 mmol, 2.0 eq) *N*-(3,4-dimethoxyphenyl)acetamide and 770 mg MTBS were dissolved in 25 mL HFIP. After electrolysis, the solvent was recovered by distillation. Column chromatography of the residue (cyclohexane/ethyl acetate = 1:1 → 0:1) yielded the desired product as an off-white powder (yield: 38%, 270 mg, 0.7 mmol).

R_f (cyclohexane/ethyl acetate = 0:1) = 0.19; m.p. 244–245 °C; The NMR shows a 1.5*:1 mixture of two rotamers (rotation of the *N*-formyl group), rotameric mixture: ^{1}H NMR (400 MHz, d_6-DMSO): δ (ppm) = 9.38/9.28 (s)/9.13 (d, *J* = 11.2 Hz, 2 H), 8.88/8.47 (s, 1 H), 8.01/7.82 (d, *J* = 1.6, 11.2 Hz, 1 H), 7.21/7.10 (s, 1 H), 6.92/6.88 (s, 1 H), 6.67/6.60 (s, 1 H), 3.74/3.73 (s, 3 H), 3.70/3.67 (s, 3 H), 2.22/2.21 (s, 3 H), 1.82/1.81 (s, 3 H); ^{13}C NMR (101 MHz, d_6-DMSO): δ (ppm) = 168.98, 168.86*, 165.01, 161.06*, 151.25*, 151.23, 148.20*, 148.17, 146.57,

145.93*, 131.48, 131.12*, 130.97, 130.64*, 129.56*, 129.38, 129.29*, 128.61, 125.73, 125.65*, 125.22, 125.08*, 120.33*, 119.36, 114.62, 113.99*, 110.51*, 109.55, 56.14, 56.02*, 55.99*, 55.95, 23.73*, 23.49, 17.09*, 17.04; HRMS for $C_{18}H_{19}{}^{35}ClN_2O_5$ (ESI+) $[M+Na]^+$: calc.: 401.0875; found: 401.0860; Elemental anal. for $C_{18}H_{19}ClN_2O_5$ calc.: C: 57,07%, H: 5.06%, N: 7.40%, found: C: 56.71%, H: 5,08%, N: 7,37%.

3-Chloro-4‘,5‘-dimethoxy-2,2’-formamido-4-hydroxy-5-methylbiphenyl (8)

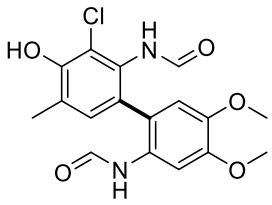

According to the general protocol **B3**, 348 mg (1.9 mmol, 1.0 eq) *N*-(2-chloro-3-hydroxy-4-methylphenyl)formamide **16**, 680 mg (3.8 mmol, 2.0 eq) *N*-(3,4-dimethoxyphenyl)formamide **14** and 770 mg MTBS were dissolved in 25 mL HFIP. After electrolysis, the solvent was recovered by distillation. Column chromatography of the residue (cyclohexane/ethyl acetate = 1:1 → 0:1) yielded the desired product as an off-white powder (yield: 21%, 145 mg, 0.4 mmol).

R_f (cyclohexane/ethyl acetate = 0:1) = 0.53; m.p. 246–247 °C; The NMR shows a 4*:2:2:1 mixture of four rotamers (rotation of the *N*-formyl groups), rotameric mixture: ^{1}H NMR (400 MHz, d_6-DMSO): δ (ppm) = 9.49–9.45/9.38–9.34/9.20–9.10 (m)/9.31 (s, 2 H), 8.39/8.90/8.87/8.72 (s, 1 H), 8.19/8.16/8.11/8.08 (s, 1 H), 8.04/8.00/7.97/6.96 (d, *J* = 1.5 Hz, 1 H), 7.83/7.81/7.77/7.66 (s, 1 H), 6.91/6.87 (s, 1 H), 6.73/6.68/6.67/6.61 (s, 1 H), 3.80/3.78/3.75/3.74 (s, 3 H), 3.71/3.70/3.68/3.66 (s, 3 H), 2.23/2.21 (s, 3 H); The minor rotamer cannot be seen in the ^{13}C NMR, ^{13}C NMR (101 MHz, $CDCl_3$): δ (ppm) = 164.40, 164.24*, 164.22, 160.49, 160.25*, 160.18*, 160.04, 151.24, 151.07*, 150.77, 148.43, 147.77, 147.67*, 146.33, 146.00, 145.21, 144.84*, 131.45, 130.93*, 130.83, 130.47*, 129.44, 128.50*, 128.32, 128.26*, 127.99, 127.53, 125.53, 125.42*, 125.13, 124.72, 122.59*, 122.16, 120.03*, 119.25, 114.84, 114.38, 114.10, 113.75*, 108.20, 108.08, 106.73*, 55.69, 55.67, 55.65, 55.57*, 55.52*, 55.49, 16.69*, 2x16.65; HRMS for $C_{17}H_{17}{}^{35}ClN_2O_5$ (ESI+) $[M+Na]^+$: calc.: 387.0718; found: 387.0700; Elemental anal. for $C_{17}H_{17}ClN_2O_5$ calc.: C: 55.98%, H: 4.70%, N: 7.68%, found: C: 55.88%, H: 4,69%, N: 7.71%.

^{1}H NMR spectra at 353 K and 373 K and ^{13}C NMR spectra at 373 K can be found in the attachment.

Synthesis of Symmetric 2,2‘-Diformamidobiphenyls

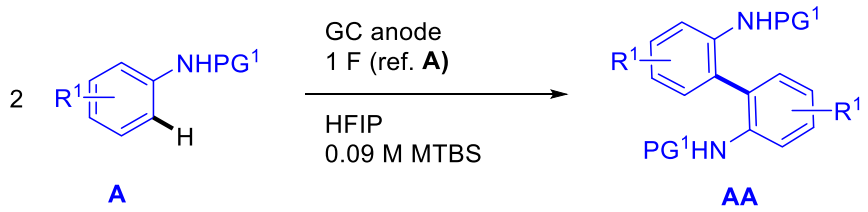

2,2‘-Diformamido-3,3‘-diiodo-4,4‘-dimethoxybiphenyl (9)

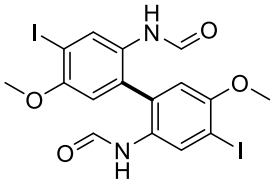

According to the general protocol **B4**, 660 mg (2.38 mmol, 2.0 eq) *N*-(3-iodo-4-methoxyphenyl)formamide **19** and 450 mg MTBS were dissolved in 16 mL HFIP. After electrolysis, the solvent was recovered by distillation. Column chromatography of the residue (cyclohexane/ethyl acetate = 1:1 → 0:1) yielded the desired product as a brown oil (yield: 30%, 197 mg, 0.36 mmol).

R_f (cyclohexane/ethyl acetate = 0:1) = 0.46; m.p. 100–102 °C (decomposition); The NMR shows a 6*:3:1 mixture of three rotamers (rotation of the *N*-formyl groups), rotameric mixture: ^{1}H NMR (400 MHz, d_6-DMSO): δ (ppm) = 9.73/9.67 (s)/9.59 (d, *J* = 10.7 Hz, 1 H), 8.60 (d, *J* = 1.7 Hz, 1H), 8.32 (s, 1 H), 8.16 (s)/8.13/8.05 (d, *J* = 1.7 Hz, 1 H), 7.82/7.76/7.70/7.68 (d, *J* = 2.6 Hz, 1 H), 7.26 (dd, *J* = 8.8, 2.7 Hz)/7.22–7.12/7.05–6.90 (m, 3 H), 3.88/3.86/3.81/3.80/3.78/3.76 (s, 6 H); ^{13}C NMR (101 MHz, d_6-DMSO): δ (ppm) = 162.26*, 162.07, 159.94*, 159.89, 156.23*, 155.72, 154.86, 134.94, 134.76*, 134.19, 133.23*, 132.86, 132.25, 130.67, 129.19, 112.07, 111.59*, 110.93, 86.34*, 85.76, 85.23, 56.85, 56.68*, 56.55.; HRMS for $C_{16}H_{14}I_2N_2O_4$ (ESI+) $[M+Na]^+$: calc.: 574.8935; found: 574.8931.

2,2‘-Diformamido-3,3‘,4,4‘-tetramethylbiphenyl (10)

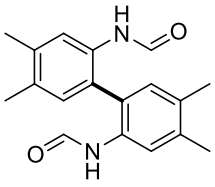

According to the general protocol **B4**, 559 mg (3.8 mmol, 2.0 eq) *N*-(3,4-dimethylphenyl)formamide **17** and 770 mg MTBS were dissolved in 25 mL HFIP. After electrolysis, the solvent was recovered by distillation. Column chromatography of the residue (cyclohexane/ethyl acetate = 4:1 → 1:1) yielded the desired product as an off-white powder (yield: 47%, 256 mg, 0.86 mmol).

R_f (cyclohexane/ethyl acetate = 1:1) = 0.27; m.p. 211–213 °C; The NMR shows a 6*:2.5:2.5:1 mixture of four rotamers (rotation of the *N*-formyl groups), rotameric mixture: ^{1}H NMR (400 MHz, d_6-DMSO): δ (ppm) = 9.14/9.02 (d, *J* = 11.1 Hz)/8.87/8.76 (s, 2 H), 8.12 (d, *J* =

11.1 Hz)/8.06–8.0* (m, 2 H), 7.83/7.78/7.10/7.07 (s, 2 H), 6.97/6.94/6.90/6.88 (s, 2 H), 2.26/2.24/2.24 (s, 6 H), 2.21/2.20/2.19 (s, 6 H); The minor rotamer cannot be seen in the ^{13}C NMR, ^{13}C NMR (101 MHz, d_6-DMSO): δ (ppm) = 163.91, 163.84, 160.66*, 160.62, 137.30, 136.47*, 136.33, 133.97, 133.64, 133.44*, 133.16, 132.85, 132.75*, 132.70, 132.25, 132.08*, 129.58, 128.44, 127.66*, 125.08, 124.23*, 19.87*, 19.83, 19.54, 19.33, 19.33*, 19.21; HRMS for $C_{18}H_{20}N_2O_2$ (ESI+) $[M+H]^+$: calc.: 297.1598; found: 297.1595; Elemental anal. for $C_{18}H_{20}N_2O_2$ calc.: C: 72.95%, H: 6.80%, N: 9.45%, found: C: 72.93%, H: 6,78%, N: 9.43%.

6,6‘-Diformamido-5,5’-bis(benzo-1,3-dioxolyl) (11)

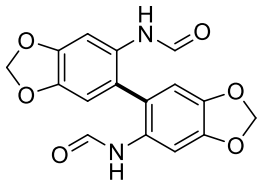

According to the general protocol **B4**, 617 mg (3.8 mmol, 2.0 eq) 4-formamidobenzo-1,3-dioxole **15** and 770 mg MTBS were dissolved in 25 mL HFIP. After electrolysis, the solvent was recovered by distillation. Column chromatography of the residue (cyclohexane/ethyl acetate = 1:1 → 0:1) yielded the desired product as an off-white powder (yield: 41%, 250 mg, 0.76 mmol).

R_f (cyclohexane/ethyl acetate = 0:1) = 0.64; m.p. 228–229 °C; The NMR shows a 9*:3:3:1 mixture of four rotamers (rotation of the *N*-formyl groups), rotameric mixture: ^{1}H NMR (400 MHz, d_6-DMSO): δ (ppm) = 9.12/9.04 (d, *J* = 11 Hz)/8.96/8.89 (s, 2 H), 8.11/8.08 (s)/8.06–8.00 (m, 2 H), 7.61/7.55/6.98/6.96/6.75/6.71/6.68/6.66 (s, 4 H), 6.08/6.06/6.04/6.03 (s, 2 H); ^{13}C NMR (101 MHz, d_6-DMSO): δ (ppm) = 163.79, 163.75, 160.22*, 160.19, 147.54, 147.27, 146.87*, 146.62, 145.16, 145.08, 143.89, 143.89*, 129.92, 129.76*, 129.59, 129.41, 125.47, 125.01, 123.39, 122.39*, 110.96, 110.62, 110.57, 110.32*, 105.39, 105.22, 103.97*, 103.97, 101.68, 101.65, 101.45*, 101.45; HRMS for $C_{16}H_{12}$N2O6 (ESI+) $[M+H]^+$: calc.: 329.0768; found: 329.0768; $[M+Na]^+$: calc.: 351.0588; found: 351.0576; Elemental anal. for $C_{16}H_{12}$N2O6 calc.: C: 58.54%, H: 3.68%, N: 8.53%, found: C: 58.28%, H: 3.70%, N: 8.54%.

^{1}H NMR spectra at 353 K and 373 K and ^{13}C NMR spectra at 373 K can be found in the attachment.

2,2‘-Diformamido-4,4‘,5,5‘-tetramethoxybiphenyl (12)

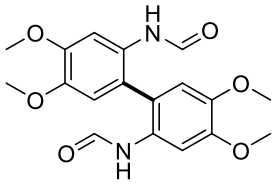

According to the general protocol **B4**, 678 mg (3.8 mmol, 2.0 eq) *N*-(3,4-dimethoxyphenyl)formamide **14** and 770 mg MTBS were dissolved in 25 mL HFIP. After electrolysis, the solvent was recovered by distillation. Column chromatography of the residue (cyclohexane/ethyl acetate = 1:1 → 0:1) yielded the desired product as an off-white powder (yield: 16%, 108 mg, 0.30 mmol).

R_f (cyclohexane/ethyl acetate = 0:1) = 0.50; m.p. 263–265 °C; The NMR shows a 6*:2.5:2.5:1 mixture of four rotamers (rotation of the *N*-formyl groups), rotameric mixture: ^{1}H NMR

(400 MHz, d_6-DMSO): δ (ppm) = 9.12/9.05 (d, *J* = 11.0 Hz)/8.92/8.84 (d, *J* = 2.0 Hz, 2 H), 8.11/8.06 (d, *J* = 11.0/2.0 Hz), 7.75/7.67/6.94/6.91/6.77/6.75/6.71/6.70 (s, 4 H), 3.82/3.81/3.78/3.77/3.74/3.73 (s, 12 H); The minor rotamer cannot be seen in the ^{13}C NMR, ^{13}C NMR (101 MHz, $CDCl_3$): δ (ppm) = 163.92, 160.26*, 160.19, 148.75, 148.55, 148.05*, 147.85, 145.40, 145.37*, 128.87*, 128.71, 128.53, 123.96, 122.50, 121.34*, 114.84, 114.44, 114.10*, 108.70, 107.20, 107.11*, 55.78, 55.75, 55.71, 55.69, 55.66*, 55.54*; HRMS for $C_{18}H_{20}N_2O_6$ (ESI+) $[M+Na]^+$: calc.: 383.1214; found: 383.1209.

2,2'-Diformamido-4,4',6,6'-tetramethylbiphenyl (13a)

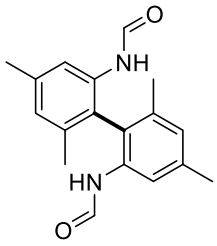

According to the general protocol **B4**, 562 mg (3.8 mmol, 2.0 eq) *N*-(3,5-dimethylphenyl)formamide **18** and 770 mg MTBS were dissolved in 25 mL HFIP. After electrolysis, the solvent was recovered by distillation. Column chromatography of the residue (cyclohexane/ethyl acetate = 1:1 → 0:1) yielded the three following products (**13a**: brown oil, yield: 7%, 40 mg, 0.13 mmol; **13b**: off-white powder, yield: 28%, 158 mg, 0.53 mmol; **13c**: off-white powder, yield: 20%, 109 mg, 0.37 mmol).

13a: R_f (cyclohexane/ethyl acetate = 0:1) = 0.72; The NMR shows a 2.5*:1 mixture of two rotamers (rotation of the *N*-formyl groups), rotameric mixture: ^{1}H NMR (400 MHz, d_6-DMSO): δ (ppm) = 8,86–8.73 (m, 1 H), 8.54 (s, 1 H), 8.29–8.15 (m)/8.05 (d, *J* = 2,0 Hz)/8.04 (s, 2 H), 7.86/7.73/7.03/7.02/6.95 (s, 4 H), 2.32/2.31 (s, 6 H), 1.80/1.76 (s, 6 H); ^{13}C NMR (101 MHz, d_6-DMSO): δ (ppm) = 163.21, 162.90*, 160.63, 160.51*, 137.60, 137.17*, 136.80*, 136.57, 135.91, 135.79*, 127.20, 126.98*, 120.78, 120.28*, 21.11*, 20.98, 19.61, 19.47*; HRMS for $C_{18}H_{20}N_2O_2$ (ESI+) $[M+Na]^+$: calc.: 319.1417; found: 319.1414.

2,4'-Diformamido-4,4',2',6'-tetramethylbiphenyl (13b)

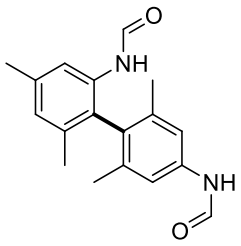

See **13a**; off-white powder, yield: 28%, 158 mg, 0.53 mmol.

13b: R_f (cyclohexane/ethyl acetate = 0:1) = 0.47; m.p. 194–196 °C; The NMR shows a 3*:1 mixture of two rotamers (rotation of the *N*-formyl groups), rotameric mixture: ^{1}H NMR (400 MHz, d_6-DMSO): δ (ppm) = 10.20–10.05 (m, 1 H), 8.90–8.76 (m, 1 H), 8.52–8.41 (m)/8.05/7.85/7.42/7.38 (s, 4 H), 8.29/8.20 (d, *J* = 2.0/11.0 Hz, 1 H), 2.31/2.30 (s, 3 H), 1.80/1.77 (s, 9 H); ^{13}C NMR (101 MHz, d_6-DMSO): δ (ppm) = 162.94, 162.37, 160.39*, 159.51*, 137.58*, 137.41*, 136.86*, 136.68*, 136.43, 136.38, 135.83*, 135.83, 135.08, 134.92*, 130.91, 130.86*, 127.92, 127.29, 126.62, 126.59*, 119.91, 119.85*, 118.39*, 118.23, 116.63*, 116.48,

21.04, 19.81*, 19.73, 19.40*; HRMS for $C_{18}H_{20}N_2O_2$ (ESI+) $[M+Na]^+$: calc.: 319.1417; found: 319.1414.

4,4‘-Diformamido-2,2‘,6,6‘-tetramethylbiphenyl (13c)

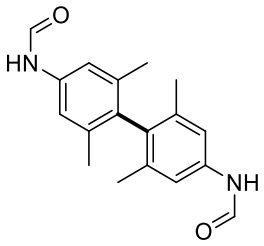

See **13a**; off-white powder, yield: 20%, 109 mg, 0.37 mmol.

13c: R_f (cyclohexane/ethyl acetate = 0:1) = 0.56; m.p. 245–247 °C; The NMR shows a 2.5*:1 mixture of two rotamers (rotation of the *N*-formyl groups), rotameric mixture: ^{1}H NMR (400 MHz, d_6-DMSO): δ (ppm) = 10.07/10.04 (s, 2 H), 8.80/8.26 (d, *J* = 11.0 Hz/1.9 Hz), 7.38/6.99 (s, 4 H), 1.80 (s, 12 H); ^{13}C NMR (101 MHz, d_6-DMSO): δ (ppm) = 162.38, 159.45*, 136.87*, 136.45*, 135.72*, 134.50, 134.33, 134.33, 118.25*, 116.57, 19.70*, 19.64; HRMS for $C_{18}H_{20}N_2O_2$ (ESI+) $[M+Na]^+$: calc.: 319.1417; found: 319.1409; Elemental anal. for $C_{18}H_{20}N_2O_2$ calc.: C: 72.95%, H: 6.80%, N: 9.45%, found: C: 72.86%, H: 6.78%, N: 9.42%.

Preparation of Protected Aniline Derivatives

Preparation of other than formyl-protected anilines can be found in our previous work.[5]

_N_-(3,4-Dimethoxyphenyl)formamide (14)

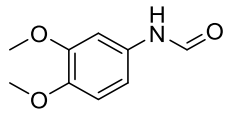

According to the general protocol **A**, 7.00 g (46 mmol, 1.0 eq) 3,4-dimethoxyaniline were dissolved in formic acid (98%, 17 mL, 10.0 eq) and heated at 80 °C overnight to obtain a purple powder (quant. yield, 8.33 g, 46 mmol).

R_f (cyclohexane/ethyl acetate = 1:1) = 0.19; m.p. 86–87 °C; The NMR shows a 3:1 mixture of two rotamers (rotation of the *N*-formyl group), rotameric mixture: ^{1}H NMR (400 MHz, d_6-DMSO): δ (ppm) = 10.01 (bs)/9.91 (d, *J* = 11.1 Hz, 1 H), 8.65/8.20 (d, *J* = 11.1/2.0 Hz, 1 H), 7.29/6.83 (d, *J* = 2.4 Hz, 1 H), 7.08/6.67 (dd, *J* = 8.6 Hz, 2.4 Hz, 1 H), 6.89 (d, *J* = 8.6 Hz, 1 H), 3.74/3.72 (s, 3 H), 3.71/3.71 (s, 3 H).

All analytic data are in agreement with reported data.[4]

5-Formamidobenzo-1,3-dioxole (15)

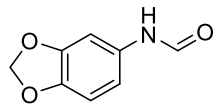

According to the general protocol **A**, 5.00 g (36 mmol, 1.0 eq) 5-aminobenzo-1,3-dioxole were dissolved in formic acid (98%, 14 mL, 10.0 eq) and heated at 90 °C overnight to obtain a purple powder (quant. yield, 5.95 g, 36 mmol).

R_f (cyclohexane/ethyl acetate = 1:1) = 0.41; m.p. 80–81 °C; The NMR shows a 3:1 mixture of two rotamers (rotation of the *N*-formyl group), rotameric mixture: ^{1}H NMR (400 MHz, d_6-DMSO): δ (ppm) = 10.08 (bs)/9.97 (d, *J* = 11.0 Hz, 1 H), 8.60/8.19 (d, *J* = 11.0/2.0 Hz, 1 H), 7.29/6.87 (d, *J* = 2.1 Hz, 1 H), 6.96/6.60 (dd, *J* = 8.4 Hz, 2.1 Hz, 1 H), 6.85 (d, *J* = 8.4 Hz, 1 H), 5.99/5.98 (s, 2 H).

All analytic data are in agreement with reported data.[5]

_N_-(2-Chloro-3-hydroxy-4-methylphenyl)formamide (16)

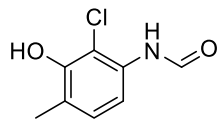

According to the general protocol **A**, 5.00 g (32 mmol, 1.0 eq) 3-amino2-chloro-6-methylphenol were dissolved in formic acid (98%, 9 mL, 7.0 eq) and heated at 80 °C overnight to obtain a reddish-brown powder (yield: 91%, 5.40 g, 29 mmol).

R_f (cyclohexane/ethyl acetate = 1:1) = 0.51; m.p. 165–167 °C; The NMR shows a 4*:1 mixture of two rotamers (rotation of the *N*-formyl group), rotameric mixture: ^{1}H NMR (400 MHz, d_6-

DMSO): δ (ppm) = 9.69 (bs, 1 H), 9.30/9.21 (bs, 1 H), 8.37 (d, *J* = 10.8 Hz)/8.30 (s, 1 H), 7.48/6.80 (d, *J* = 8.1 Hz, 1 H), 7.01 (d, *J* = 8.1 Hz, 1 H), 2.17 (s, 3 H); ^{13}C NMR (101 MHz, $CDCl_3$): δ (ppm) = 163.44, 160.18*, 151.65, 151.11*, 133.45, 132.88*, 128.68, 128.31*, 123.58, 122.34*, 114.06, 113.82*, 112.30, 112.30*, 16.46, 16.46*; HRMS for $C_8H_8{}^{35}ClNO_2$ (ESI+) $[M+H]^+$: calc.: 186.0316; found: 186.0314.

***N*-(3,4-Dimethylphenyl)formamide (17)**

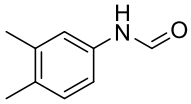

According to the general protocol **A**, 5.60 g (46 mmol, 1.0 eq) 3,4-dimethylaniline were dissolved in formic acid (98%, 10 mL, 6.0 eq) and heated at 90 °C overnight to obtain an off-white powder (quant. yield, 6.86 g, 46 mmol).

R_f (cyclohexane/ethyl acetate = 1:1) = 0.49; m.p. 70–72 °C; The NMR shows a 3:1 mixture of two rotamers (rotation of the *N*-formyl group), rotameric mixture: ^{1}H NMR (400 MHz, d_6-DMSO): δ (ppm) = 9.99/9.97 (bs, 1 H), 8.69/8.21 (d, *J* = 11.1/2.0 Hz, 1 H), 7.36/6.97 (d, *J* = 2.2 Hz, 1 H) 7.30/6.89 (dd, *J* = 8.1 Hz, 2.2 Hz, 1 H), 7.05 (d, *J* = 8.1 Hz, 1 H), 2.18 (s, 3 H), 2.15 (s, 3 H).

All analytic data are in agreement with reported data.[4]

***N*-(3,5-Dimethylphenyl)formamide (18)**

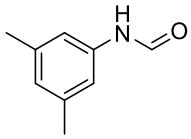

According to the general protocol **A**, 1.00 g (8 mmol, 1.0 eq) 3,5-dimethylaniline were dissolved in formic acid (98%, 1 mL, 3.0 eq) and heated at 90 °C overnight to obtain an off-white powder (quant. yield, 1.19 g, 8 mmol).

R_f (cyclohexane/ethyl acetate = 1:1) = 0.51; m.p. 165–167 °C; The NMR shows a 2:1 mixture of two rotamers (rotation of the *N*-formyl group), rotameric mixture: ^{1}H NMR (400 MHz, d_6-DMSO): δ (ppm) = 10.01 (bs, 1 H), 8.74/8.23 (d, *J* = 11.0/2.0 Hz, 1 H), 7.21/6.80 (s, 2 H), 6.75–6.68 (m, 1 H), 2.22 (s, 6 H).

All analytic data are in agreement with reported data.[5]

***N*-(3-Iodo-4-methoxyphenyl)formamide (19)**

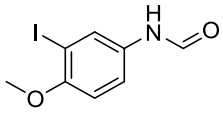

According to the general protocol **A**, 1.00 g (4 mmol, 1.0 eq) 3-iodo-4-methoxyaniline were dissolved in formic acid (98%, 0.75 mL, 5.0 eq) and heated at 90 °C overnight to obtain an off-white powder (quant. yield, 1.11 g, 4 mmol).

R_f (cyclohexane/ethyl acetate = 1:1) = 0.35; m.p. 99-100 °C; The NMR shows a 4*:1 mixture of two rotamers (rotation of the *N*-formyl group), rotameric mixture: ^{1}H NMR (400 MHz, d_6-DMSO): δ (ppm) = 10.10 (s)/9.97 (d, *J* = 11.1 Hz, 1 H), 8.62/8.20 (d, *J* = 11.1/1.9 Hz, 1 H), 8.09/7.59 (d, *J* = 2.5 Hz, 1 H), 7.52/7.21 (dd, *J* = 8.9, 2.5 Hz, 1 H), 6.97/6.96 (d, *J* = 8.9 Hz, 1 H), 3.78 (s, 3 H); ^{13}C NMR (101 MHz, d_6-DMSO): δ (ppm) = 162.57, 159.28*, 154.55, 154.06*, 132.72, 132.70*, 129.60*, 128.53, 120.44*, 119.19, 111.99, 111.51*, 86.49, 85.63*, 56.59, 56.50*; HRMS for $C_8H_8INO_2$ (ESI+) $[M+H]^+$: calc.: 277.9672; found: 277.9668.

References

[1] W. L. F. Armarego, *Purification of laboratory chemicals,* 7. Aufl., Butterworth-Heinemann, Oxford, Waltham, MA, **2013**.

[2] C. Gütz, B. Klöckner, S. R. Waldvogel, *Org. Process Res. Dev.* **2015**, *20*, 26–32.

[3] A. Kirste, G. Schnakenburg, F. Stecker, A. Fischer, S. R. Waldvogel, *Angew. Chem. Int. Ed.* **2010**, *49*, 971–975; Angew. Chem. **2010**, *122*, 983–987.

[4] Y. Qin, Y. Cheng, X. Luo, M. Li, Y. Xie, Y. Gao, *Synlett* **2015**, *26*, 1900–1904.

[5] K.-H. Chiang, S.-H. Lu, W.-P. Yen, N. Uramaru, W.-S. Tseng, T.-W. Chang, F. F. Wong, *Heteroatom Chem.* **2016**, *27*, 235–242.

[6] L. Schulz, M. Enders, B. Elsler, D. Schollmeyer, K. M. Dyballa, R. Franke, S. R. Waldvogel, *Angew. Chem. Int. Ed.* **2017**, *56*, 4877–4881; Angew. Chem. **2017**, *129*, 4955–4959.

Spectra

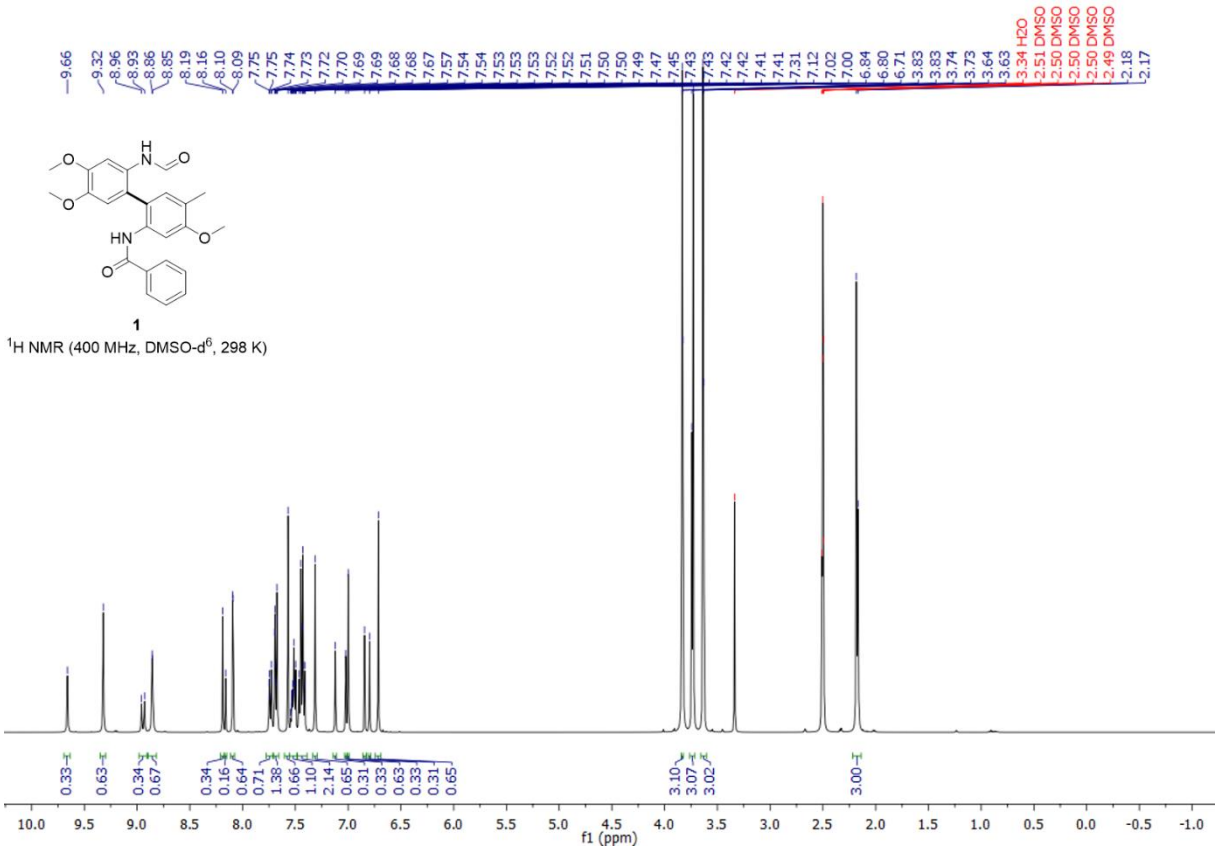
1
1H NMR (400 MHz, DMSO-d6, 298 K)
f1 (ppm)

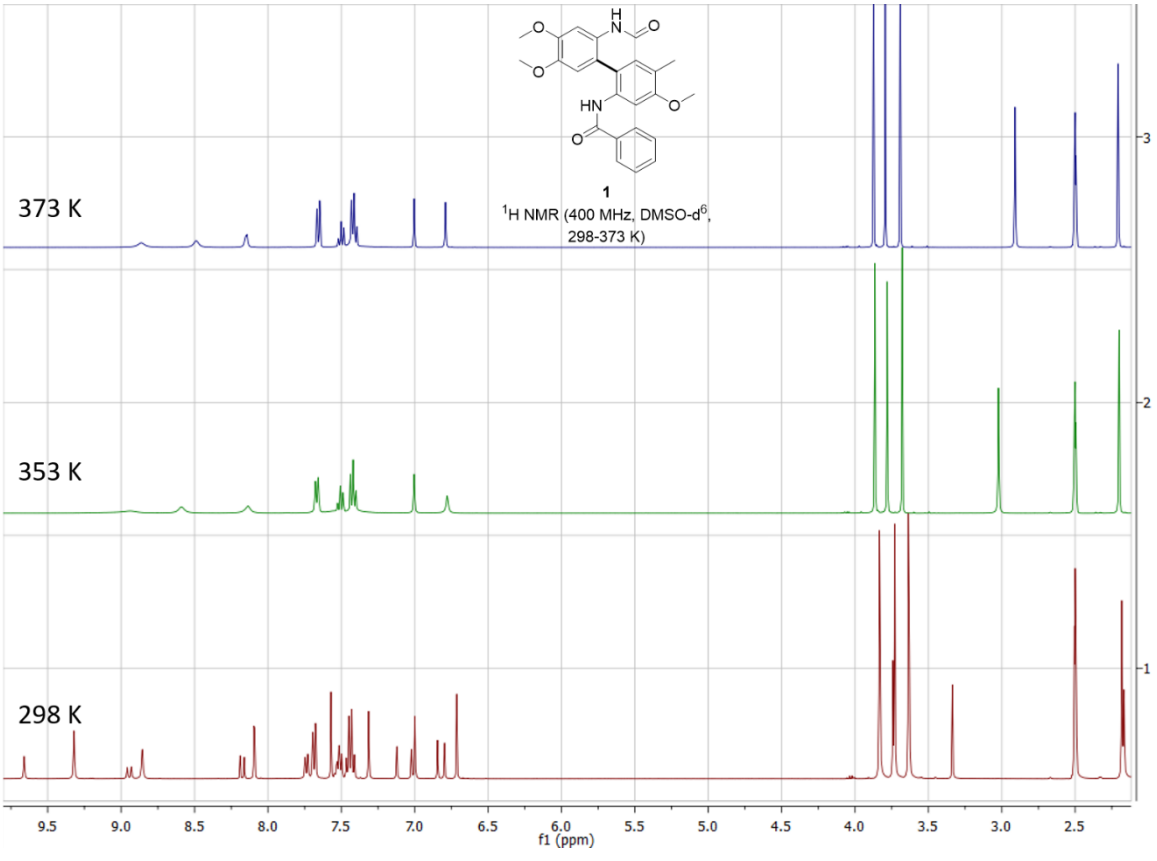
373 K
353 K
298 K
1
1H NMR (400 MHz, DMSO-d6, 298-373 K)
f1 (ppm)

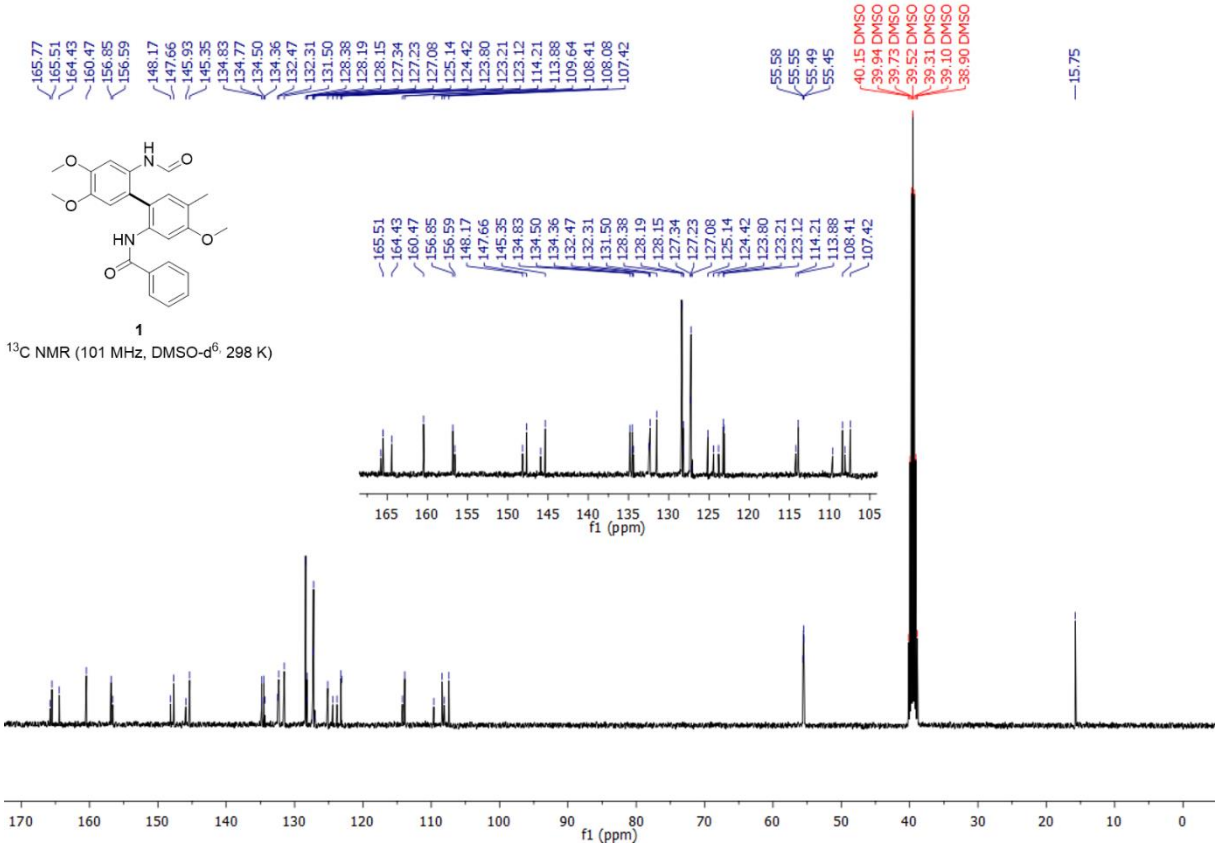
165.77
165.51
164.43
160.47
156.85
156.59
148.17
147.66
145.93
145.35
134.83
134.77
134.50
134.36
132.47
132.31
131.50
128.38
128.19
128.15
127.34
127.23
127.08
125.14
124.42
123.80
123.21
123.12
114.21
113.88
109.64
108.41
108.08
107.42
55.58
55.55
55.49
55.45
40.15 DMSO
39.94 DMSO
39.73 DMSO
39.52 DMSO
39.31 DMSO
39.10 DMSO
38.90 DMSO
15.75
1
13C NMR (101 MHz, DMSO-d6, 298 K)
f1 (ppm)

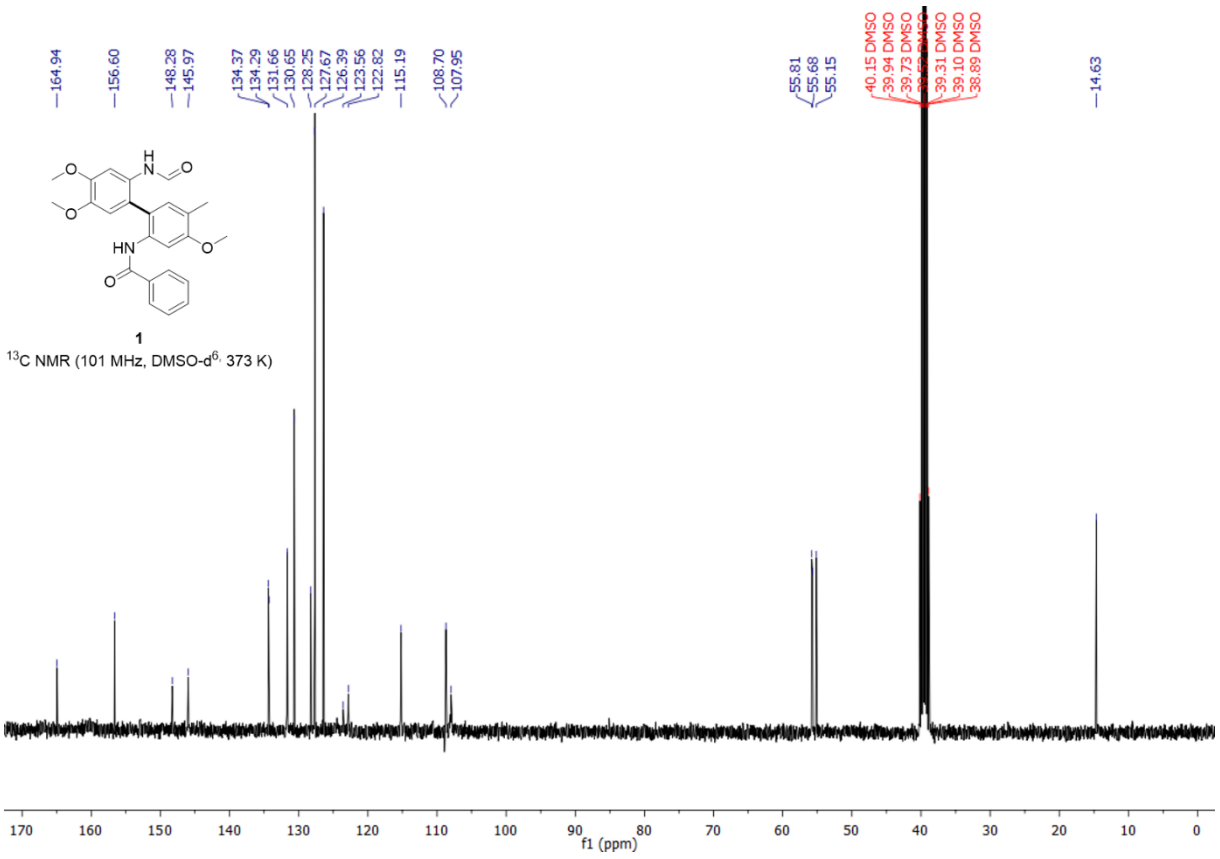
164.94
156.60
148.28
145.97
134.37
134.29
131.66
130.65
128.25
127.67
126.39
123.56
122.82
115.19
108.70
107.95
55.81
55.68
55.15
40.15 DMSO
39.94 DMSO
39.73 DMSO
39.31 DMSO
39.10 DMSO
38.89 DMSO
14.63
1
13C NMR (101 MHz, DMSO-d6, 373 K)
f1 (ppm)

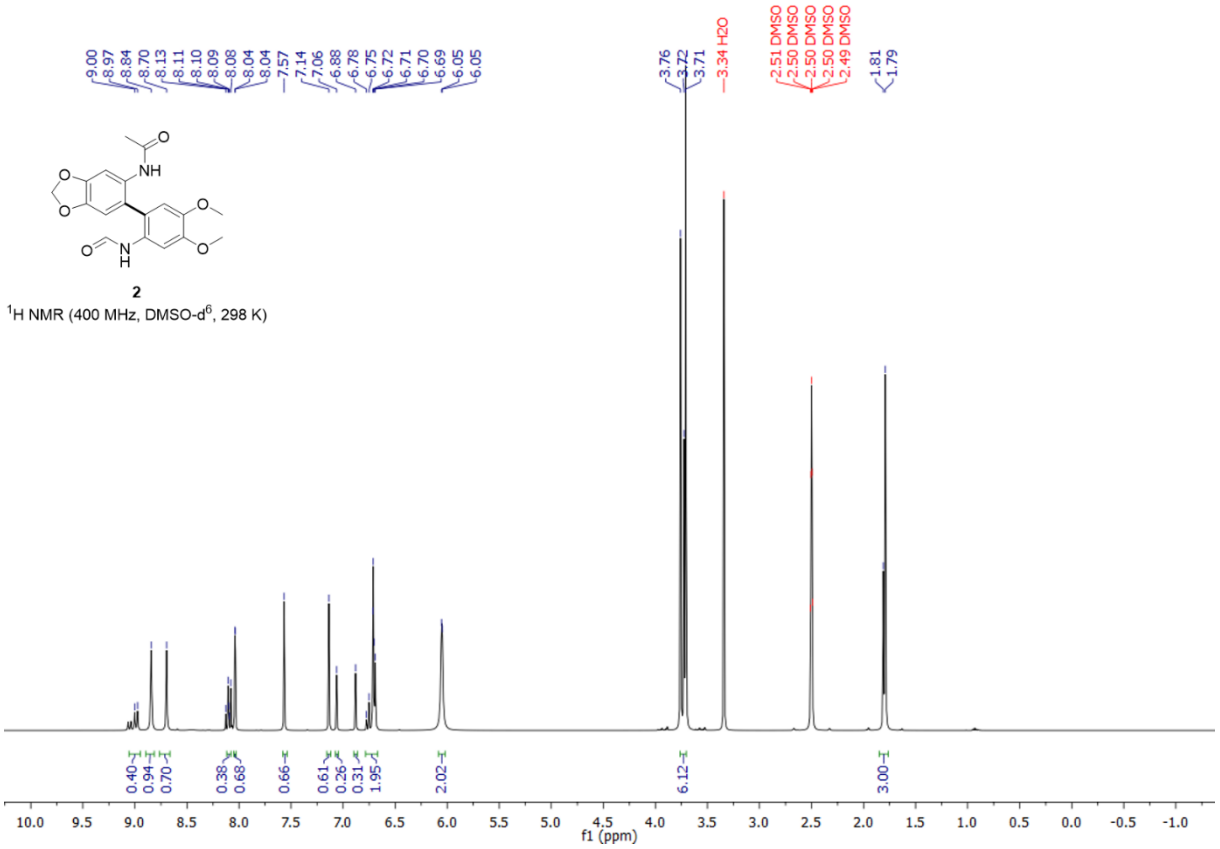

2

^{1}H NMR (400 MHz, DMSO-d^{6}, 298 K)

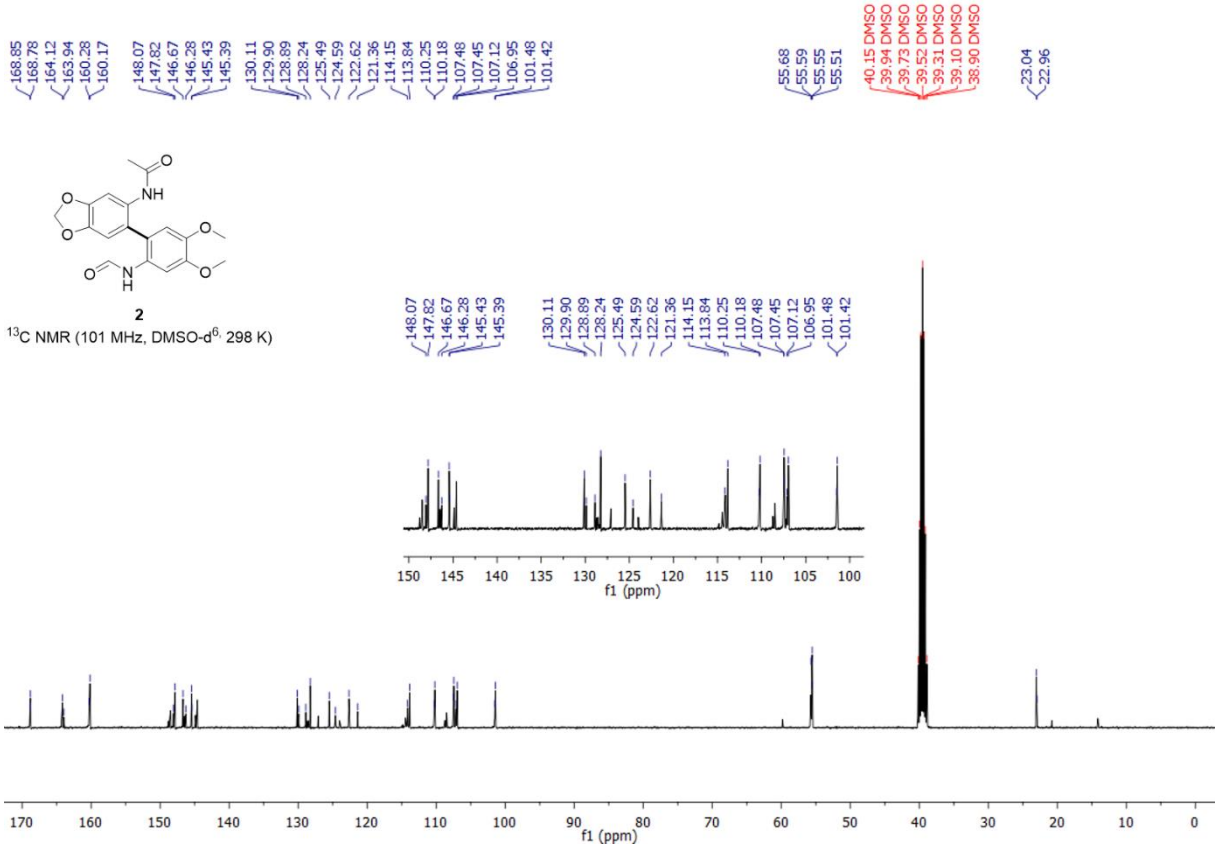

2

^{13}C NMR (101 MHz, DMSO-d^{6}, 298 K)

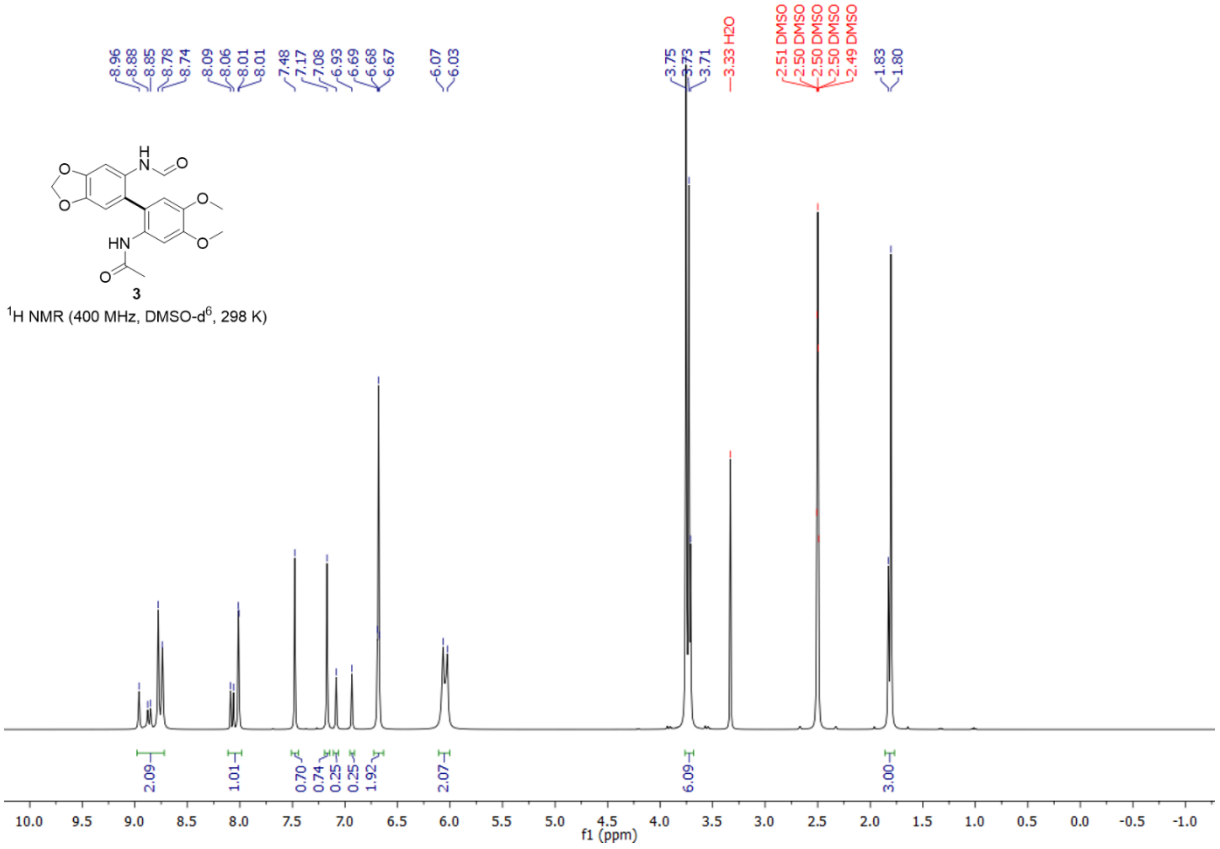

3

^{1}H NMR (400 MHz, DMSO-d^{6}, 298 K)

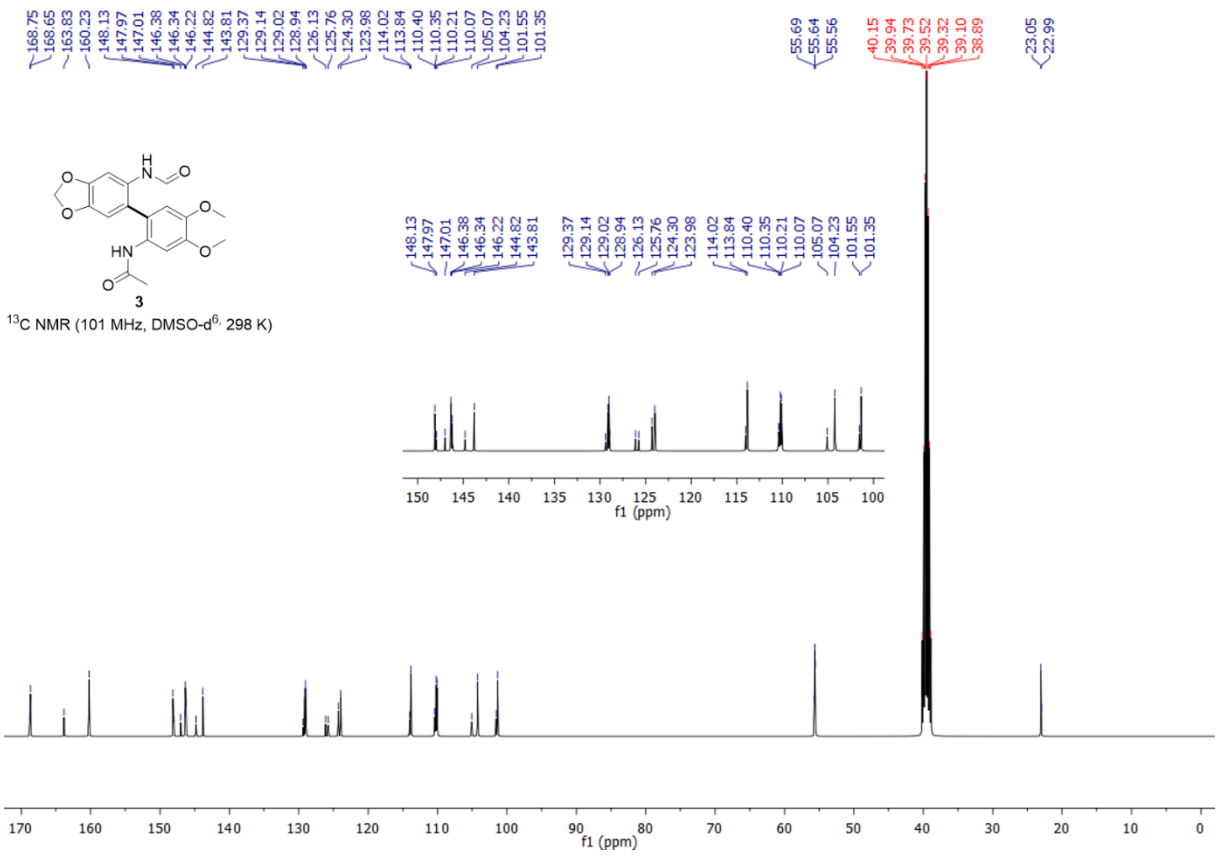

3

^{13}C NMR (101 MHz, DMSO-d^{6}, 298 K)

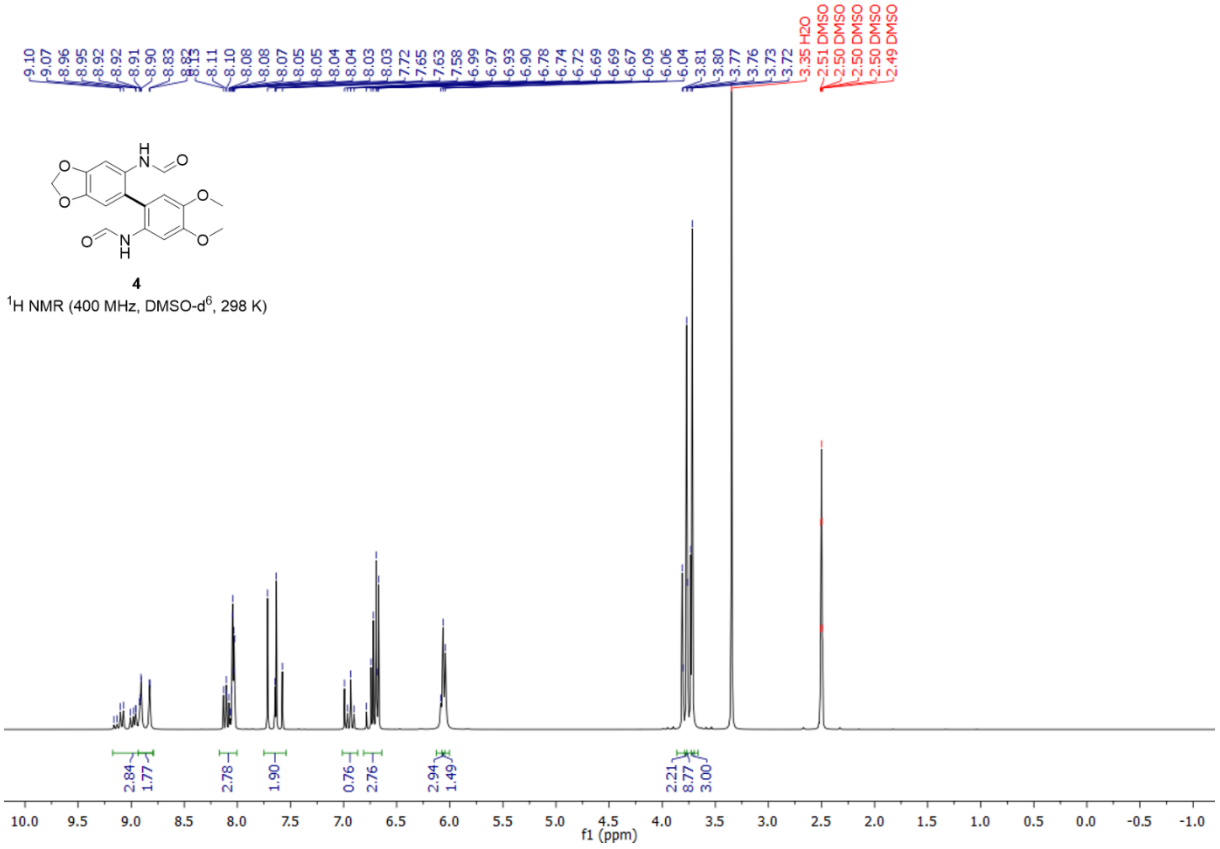
4
^{1}H NMR (400 MHz, DMSO-d^6, 298 K)
f1 (ppm)

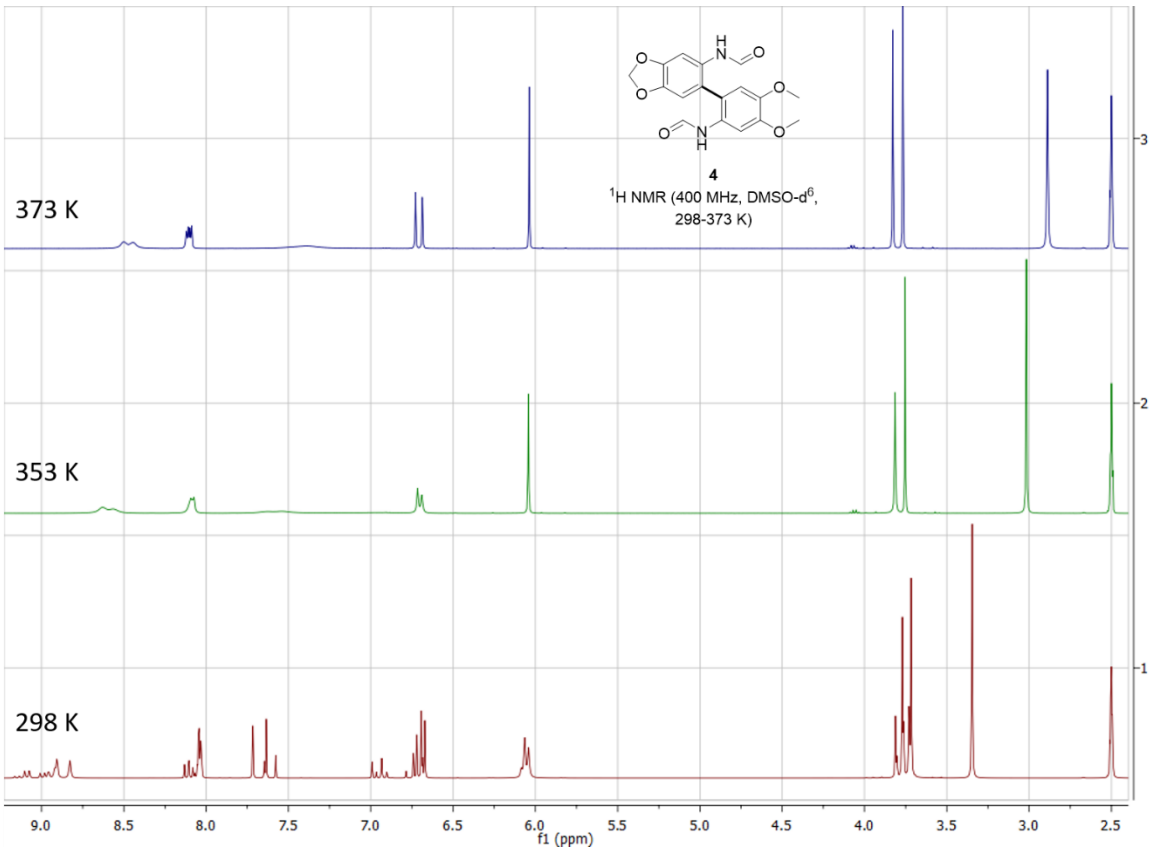
373 K
353 K
298 K
4
^{1}H NMR (400 MHz, DMSO-d^6, 298-373 K)
f1 (ppm)

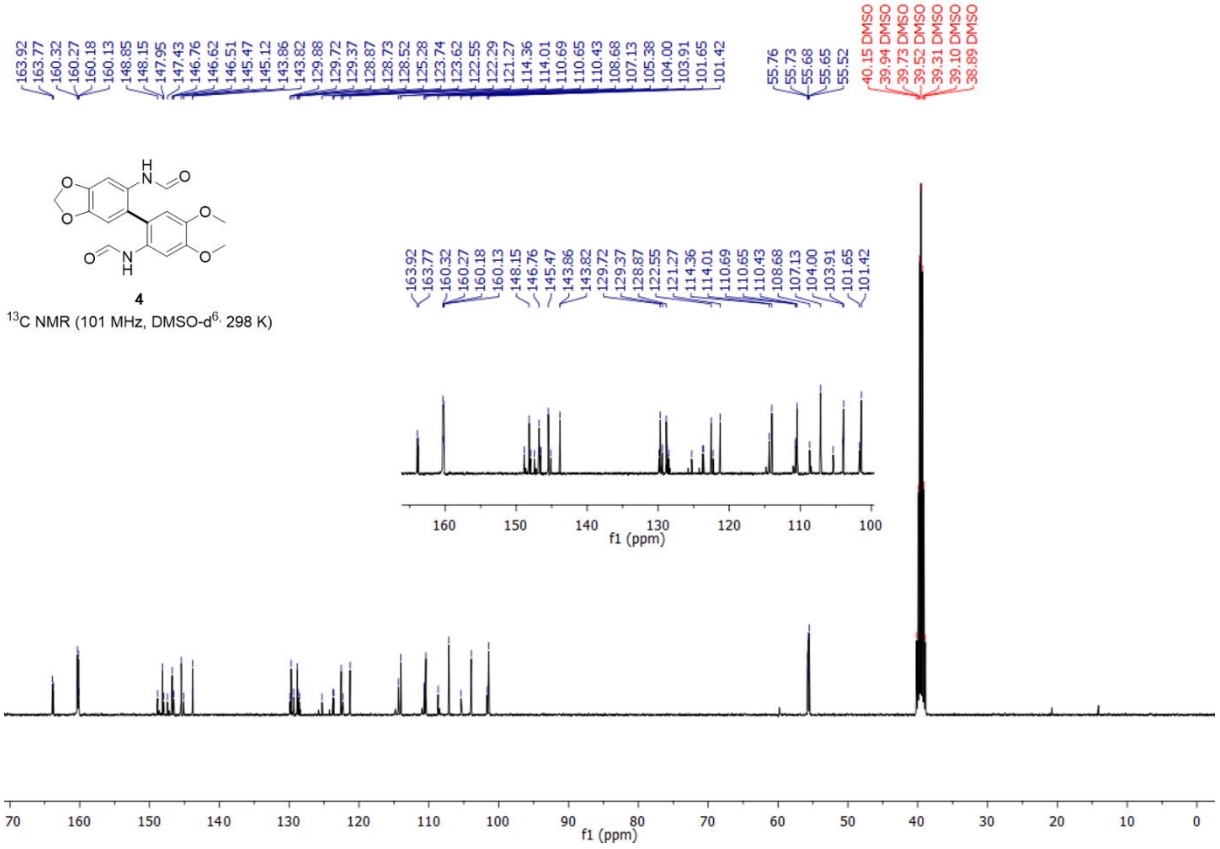
163.92
163.77
160.32
160.27
160.18
160.13
148.85
148.15
147.95
147.43
146.76
146.62
146.51
145.47
145.12
143.86
143.82
129.88
129.72
129.37
128.87
128.73
128.52
125.28
123.74
123.62
122.55
122.29
121.27
114.36
114.01
110.69
110.65
110.43
108.68
107.13
105.38
104.00
103.91
101.65
101.42
55.76
55.73
55.68
55.65
55.52
40.15 DMSO
39.94 DMSO
39.73 DMSO
39.52 DMSO
39.31 DMSO
39.10 DMSO
38.89 DMSO
4
13C NMR (101 MHz, DMSO-d6, 298 K)
f1 (ppm)
f1 (ppm)

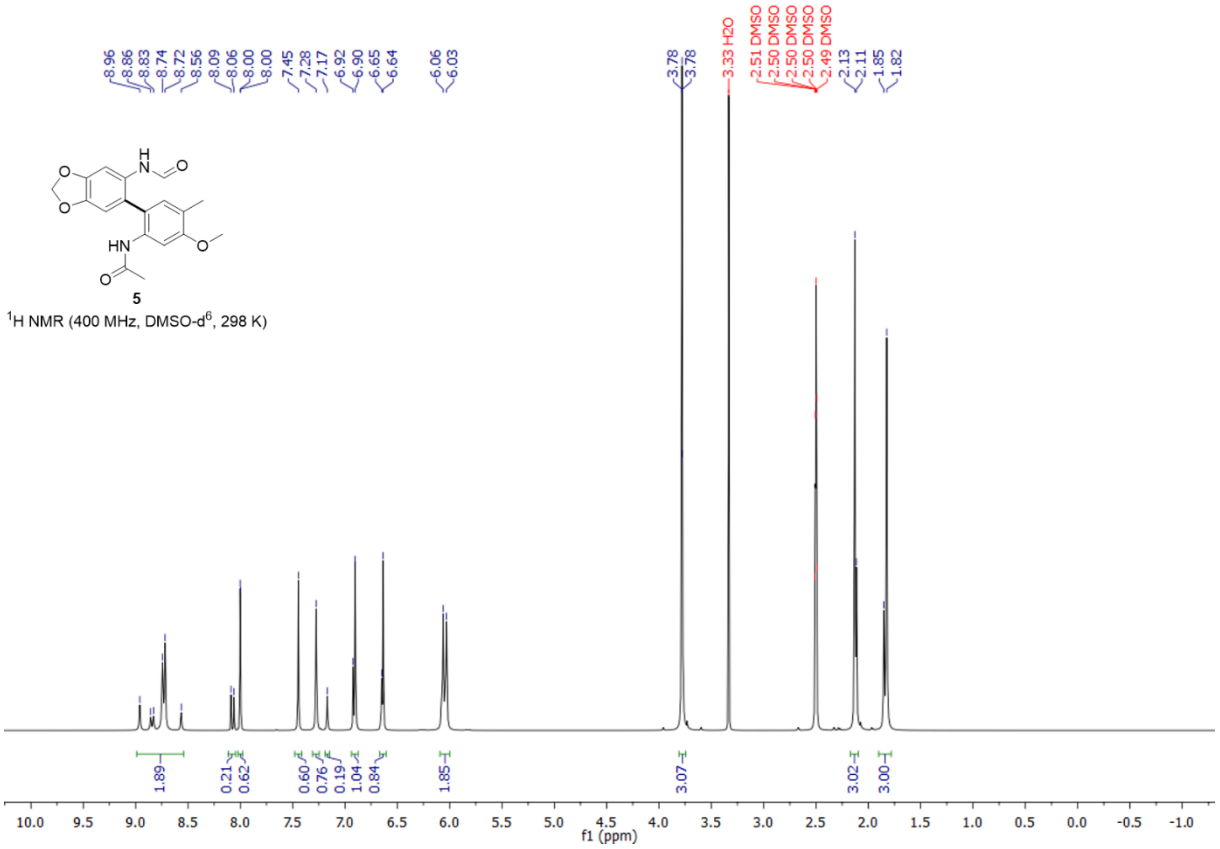

5

^{1}H NMR (400 MHz, DMSO-d^{6}, 298 K)

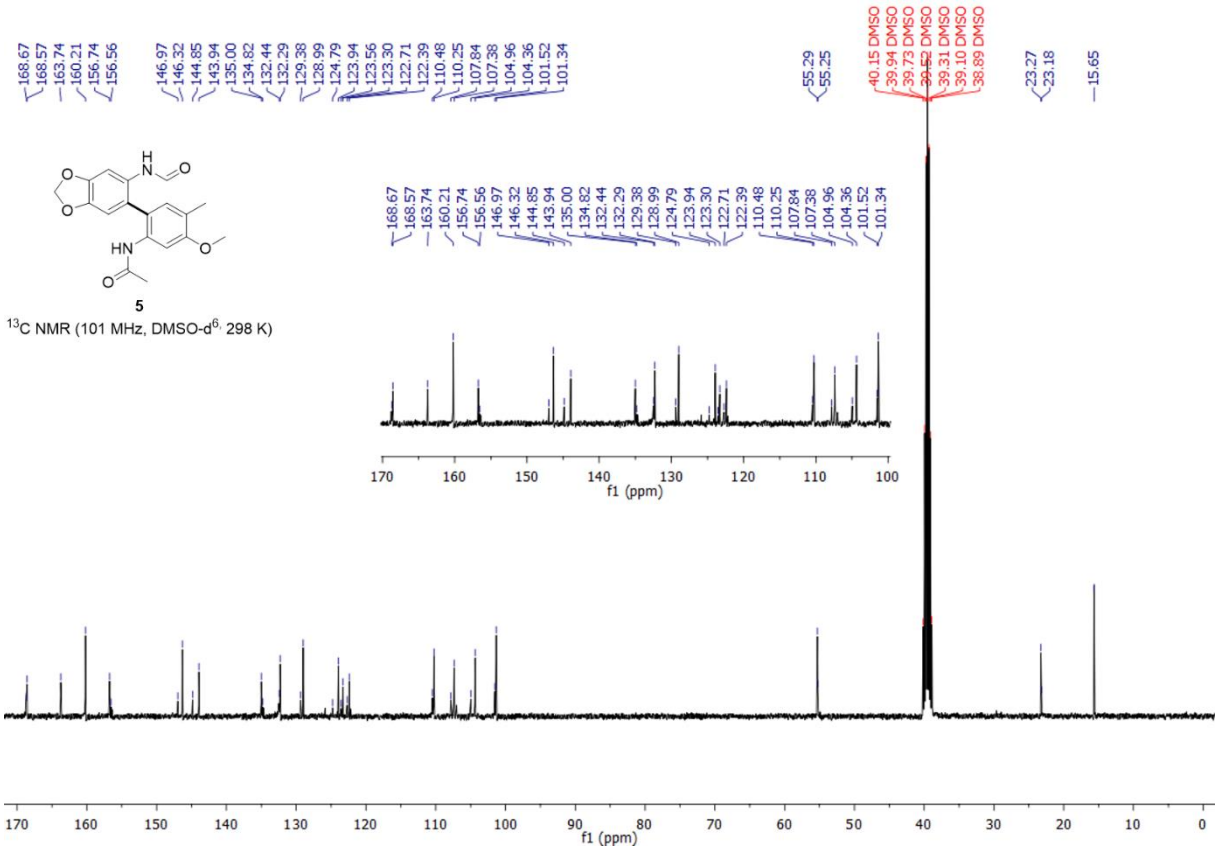

5

^{13}C NMR (101 MHz, DMSO-d^{6}, 298 K)

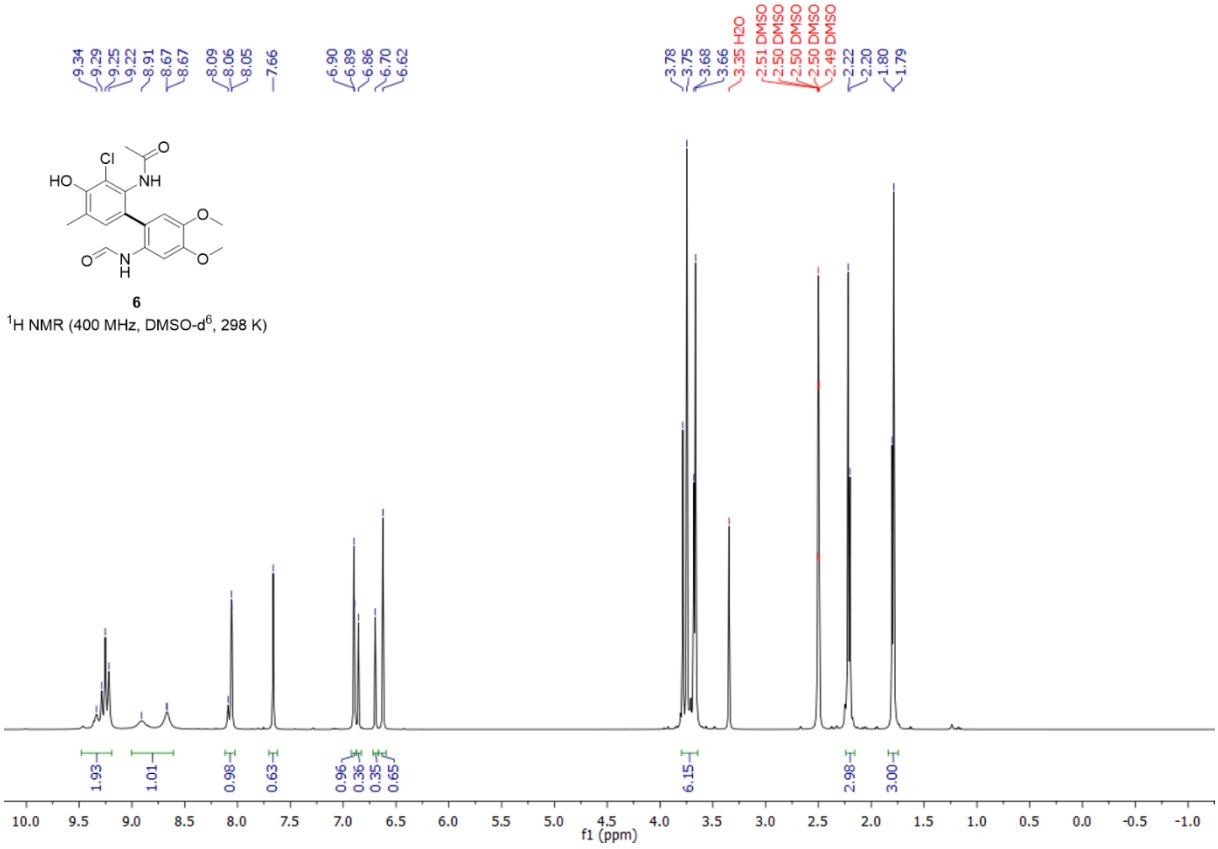
9.34
9.29
9.25
9.22
8.91
8.67
8.67
8.09
8.06
8.05
7.66
6.90
6.89
6.86
6.70
6.62
3.78
3.75
3.68
3.66
3.35 H2O
2.51 DMSO
2.50 DMSO
2.50 DMSO
2.50 DMSO
2.49 DMSO
2.22
2.20
1.80
1.79
Cl
HO
NH
O
O
O
N
H
6
1H NMR (400 MHz, DMSO-d6, 298 K)
1.93
1.01
0.98
0.63
0.96
0.36
0.35
0.65
6.15
2.98
3.00
10.0 9.5 9.0 8.5 8.0 7.5 7.0 6.5 6.0 5.5 5.0 4.5 4.0 3.5 3.0 2.5 2.0 1.5 1.0 0.5 0.0 -0.5 -1.0
f1 (ppm)

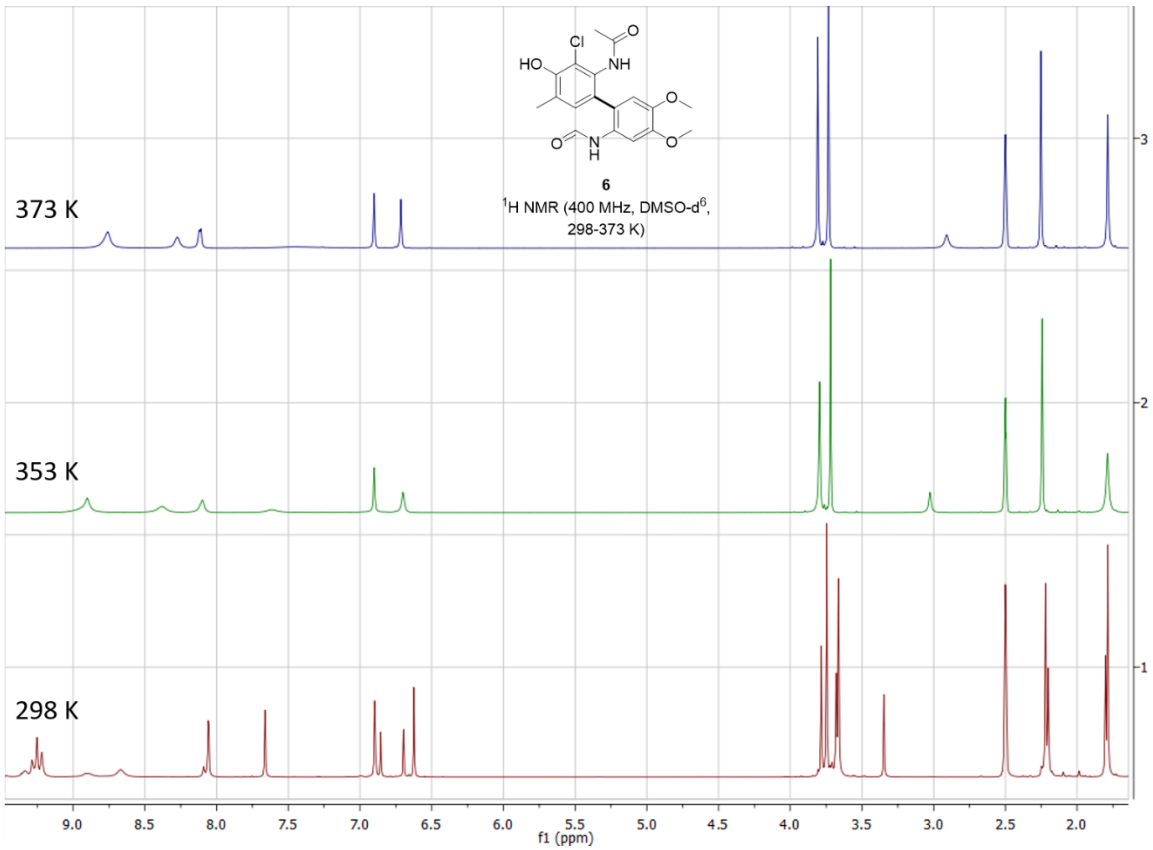
Cl
HO
NH
O
O
O
N
H
6
1H NMR (400 MHz, DMSO-d6, 298-373 K)
373 K
353 K
298 K
3
2
1
9.0 8.5 8.0 7.5 7.0 6.5 6.0 5.5 5.0 4.5 4.0 3.5 3.0 2.5 2.0
f1 (ppm)

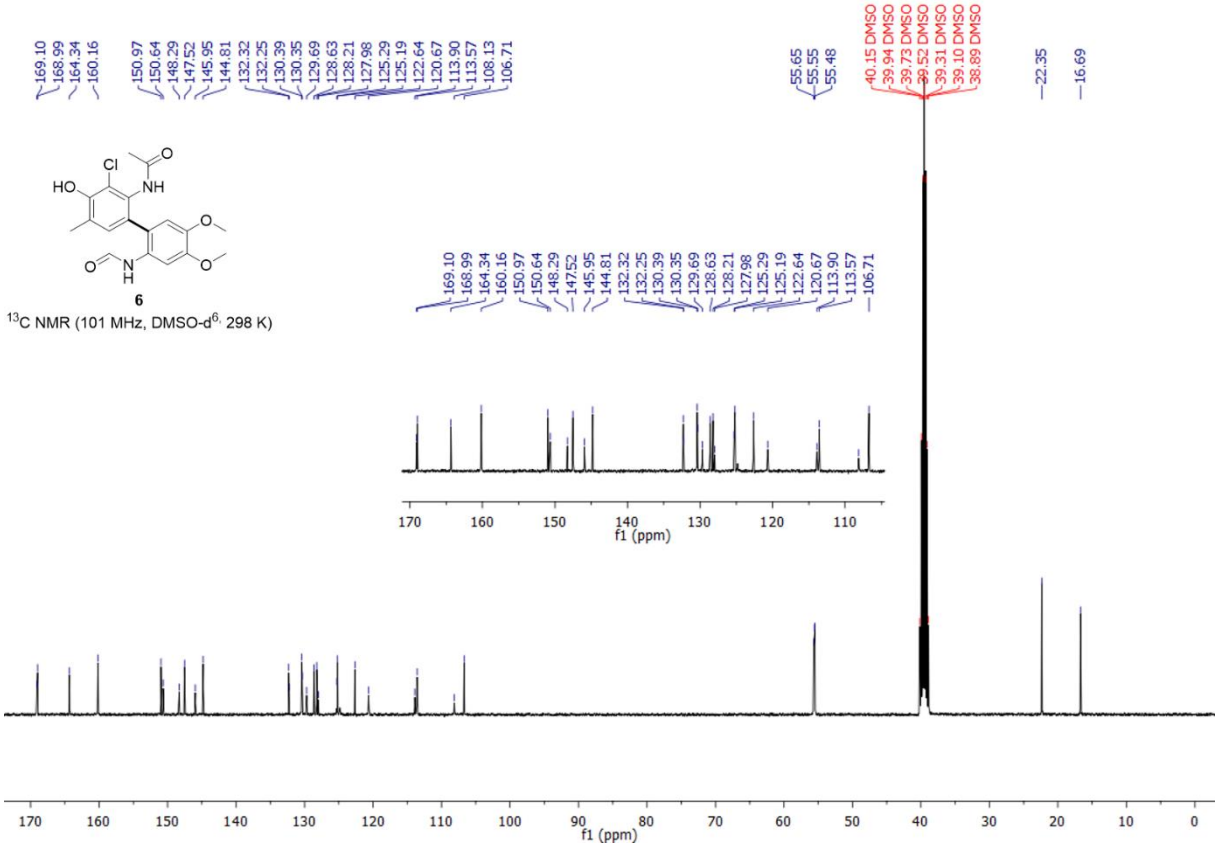

^{13}C NMR (101 MHz, DMSO-d^{6}, 298 K)

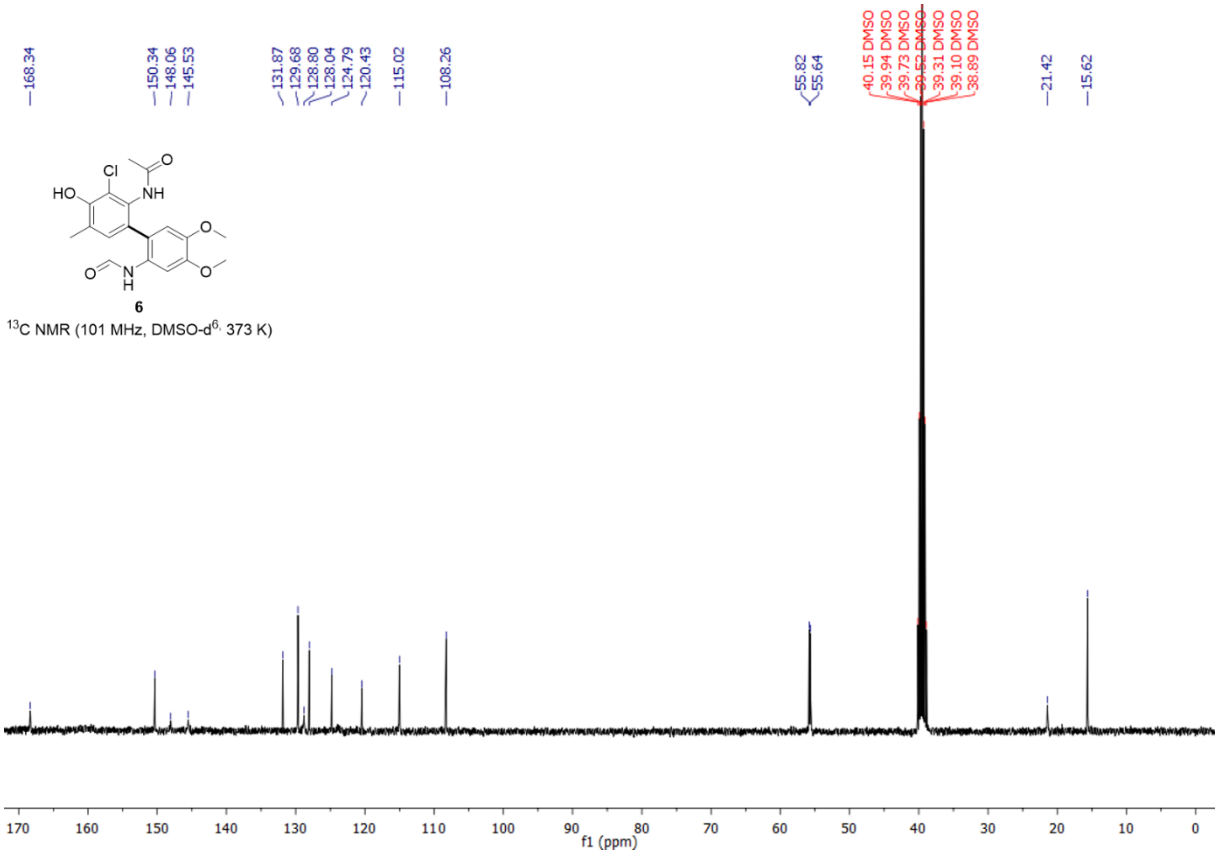

^{13}C NMR (101 MHz, DMSO-d^{6}, 373 K)

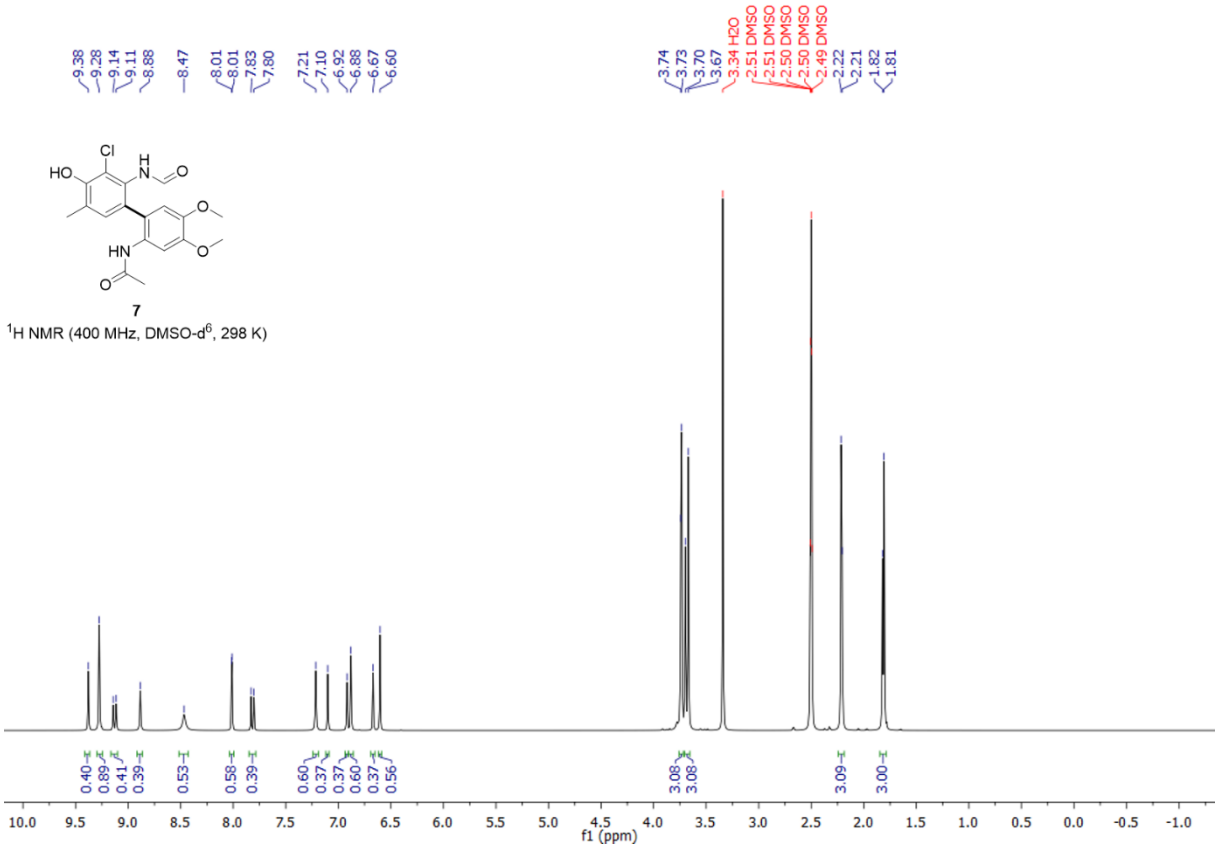

7

^{1}H NMR (400 MHz, DMSO-d^{6}, 298 K)

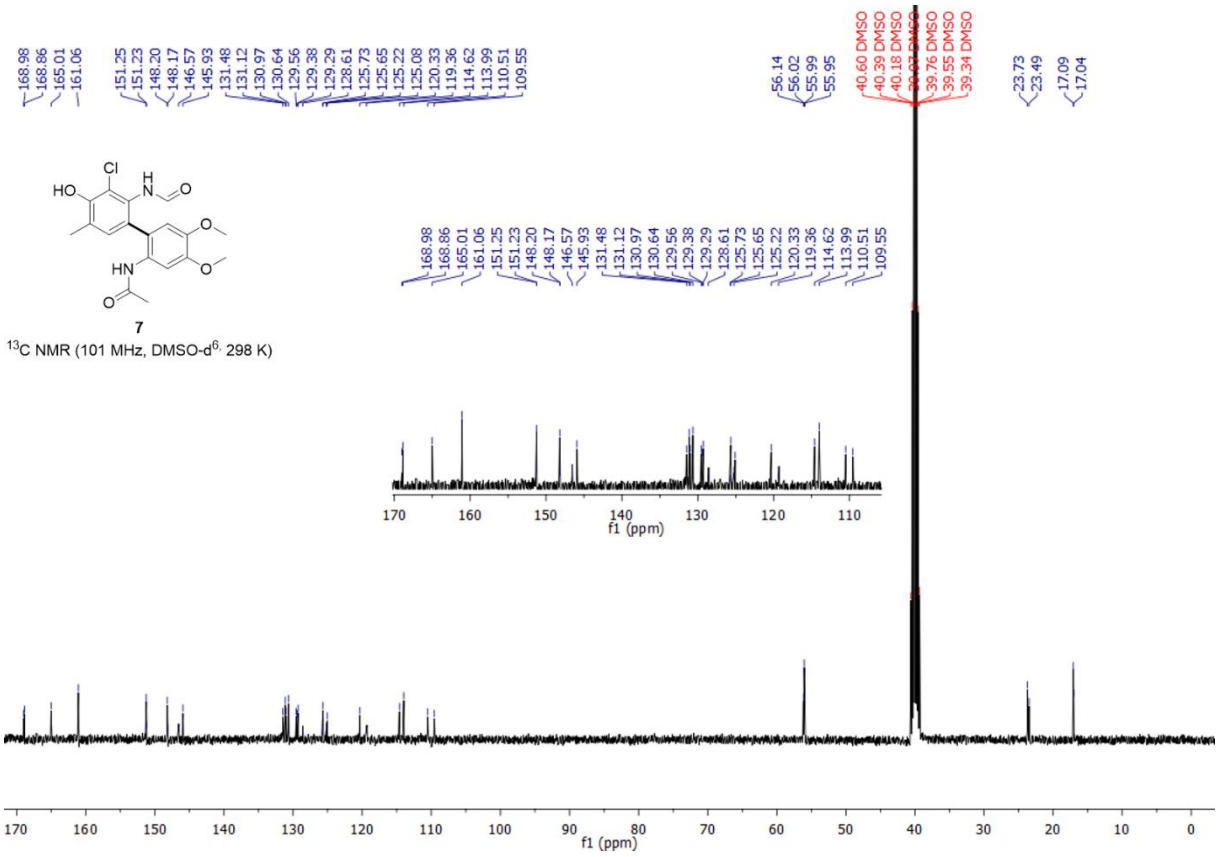

7

^{13}C NMR (101 MHz, DMSO-d^{6}, 298 K)

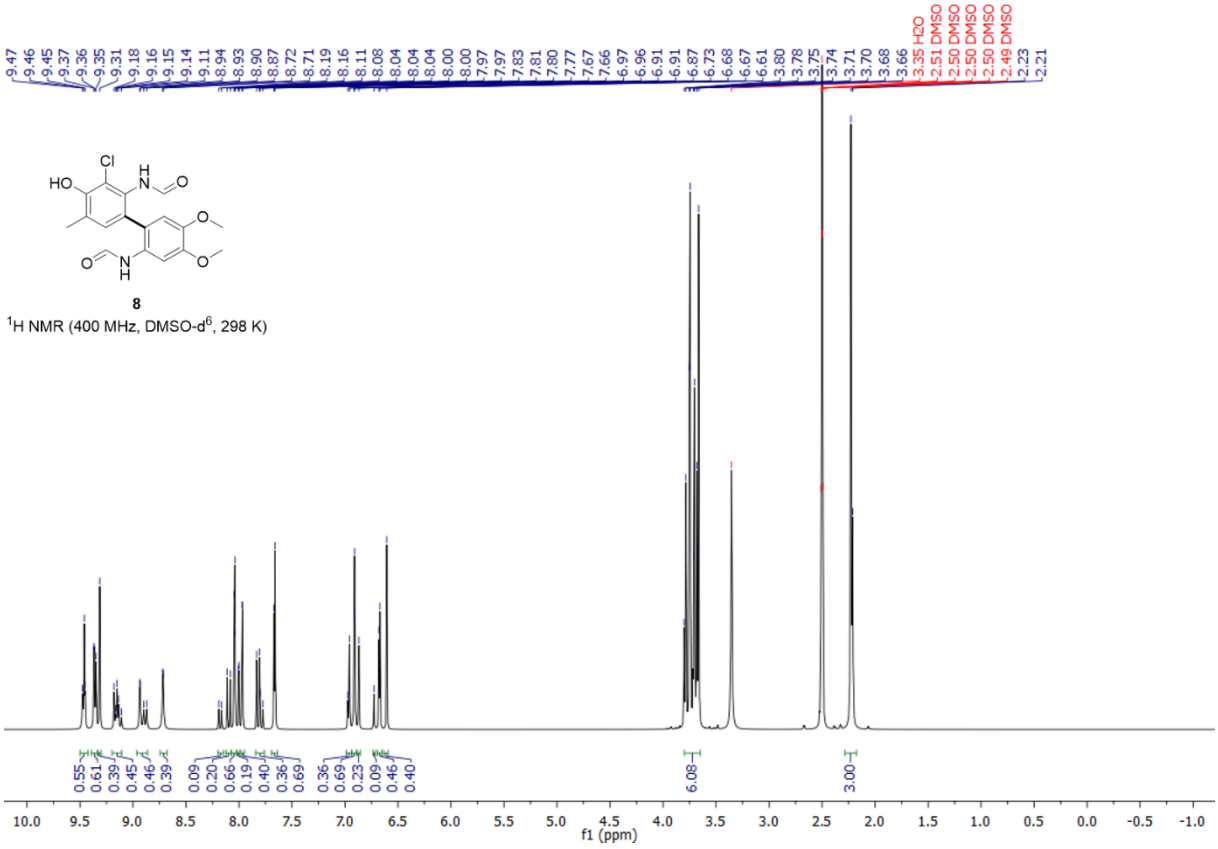
8
1H NMR (400 MHz, DMSO-d6, 298 K)
f1 (ppm)

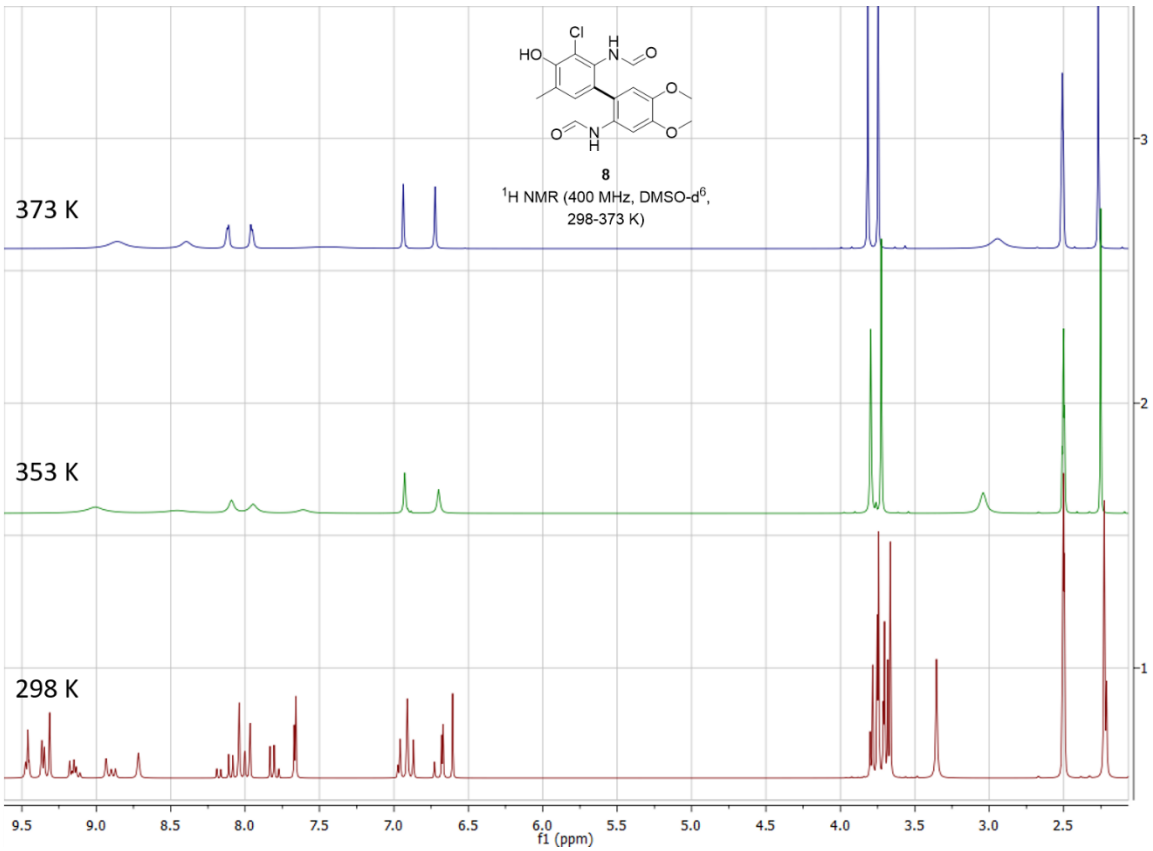
373 K
353 K
298 K
8
1H NMR (400 MHz, DMSO-d6, 298-373 K)
f1 (ppm)

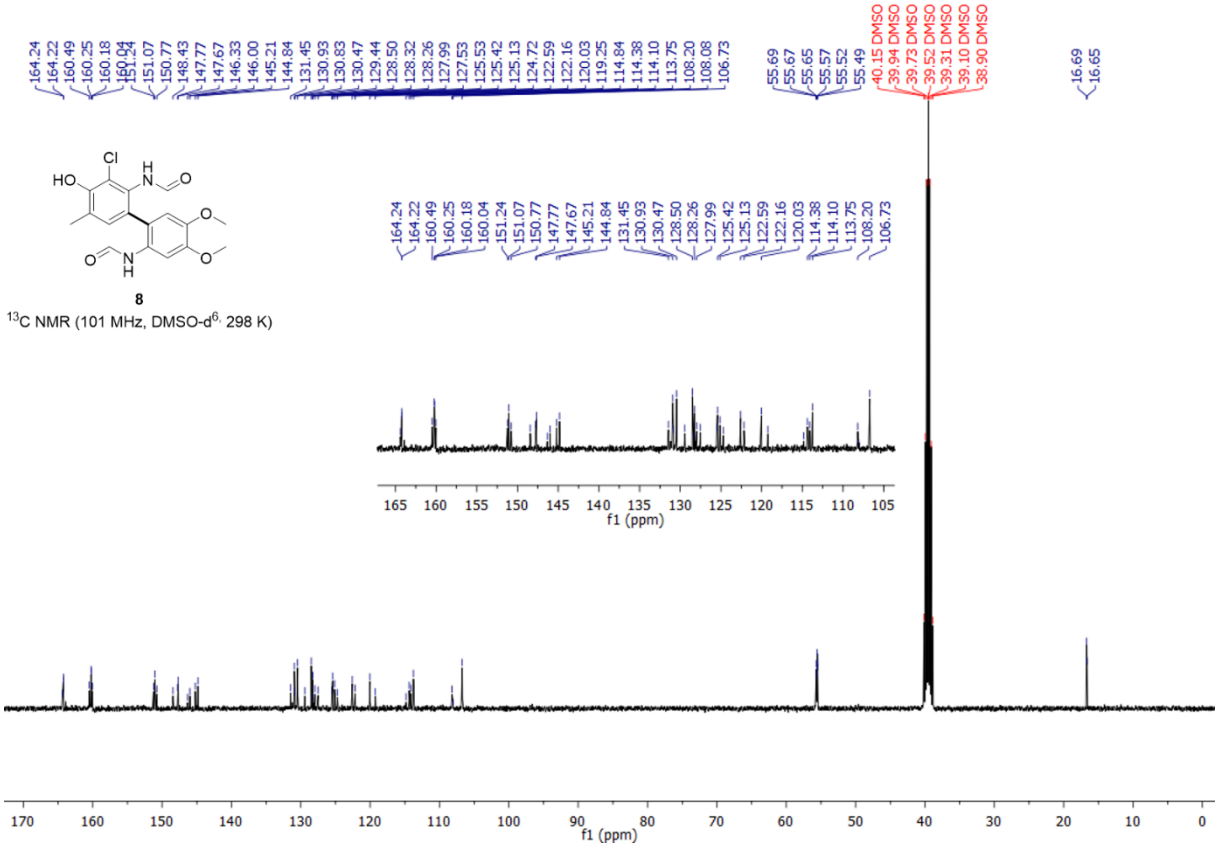
8
13C NMR (101 MHz, DMSO-d6, 298 K)
f1 (ppm)

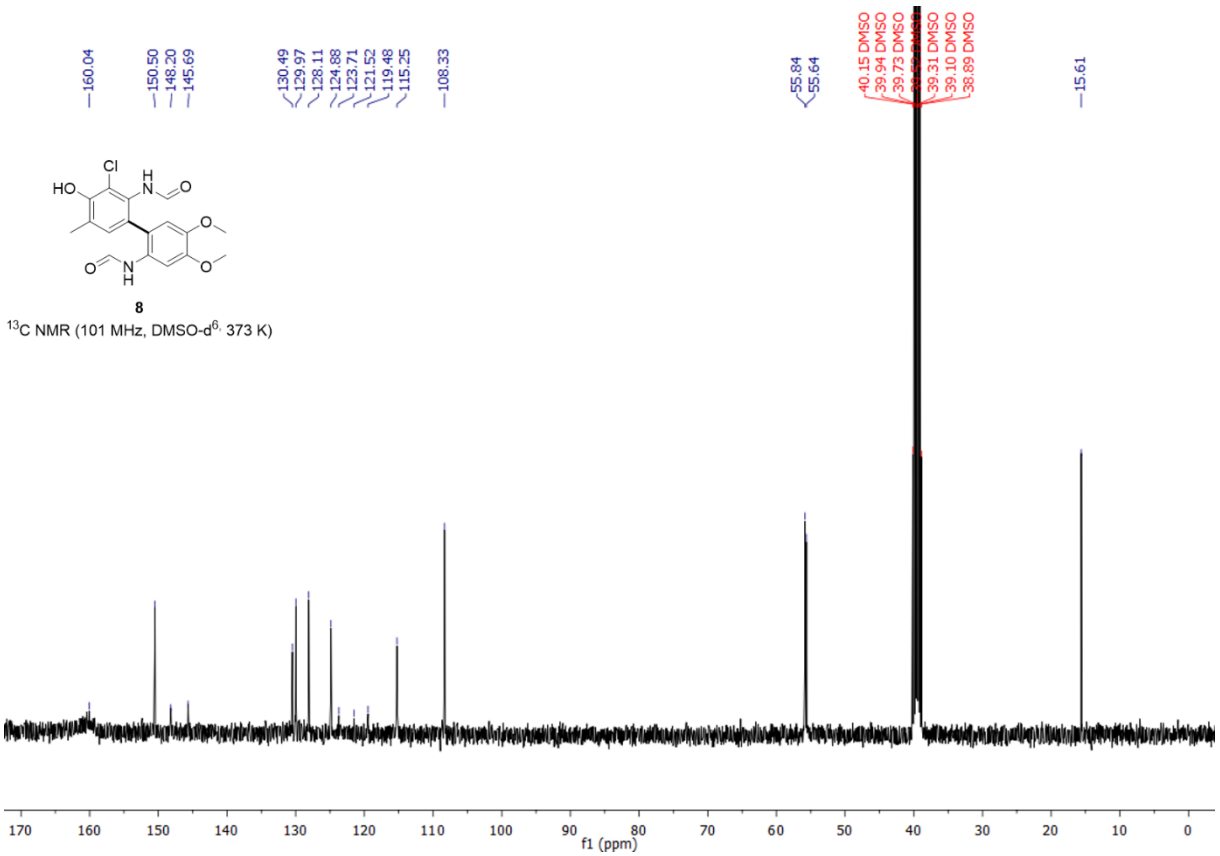
8
13C NMR (101 MHz, DMSO-d6, 373 K)
f1 (ppm)

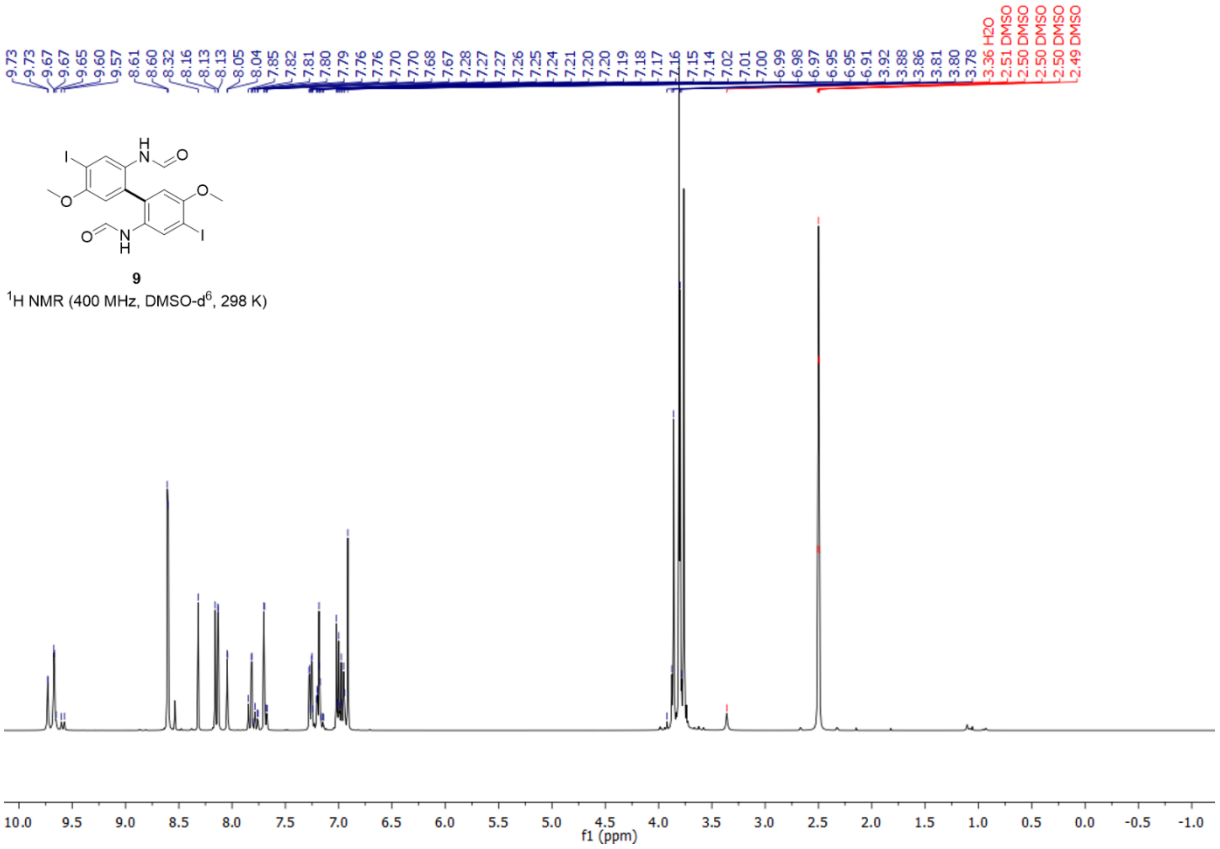
9.73 9.73 9.67 9.67 9.65 9.60 9.57 8.61 8.60 8.32 8.16 8.13 8.13 8.05 8.04 7.85 7.82 7.81 7.80 7.79 7.76 7.76 7.70 7.70 7.68 7.67 7.28 7.27 7.27 7.26 7.25 7.24 7.21 7.20 7.20 7.19 7.18 7.17 7.16 7.15 7.14 7.02 7.01 7.00 6.99 6.98 6.97 6.95 6.95 6.91 3.92 3.88 3.86 3.81 3.80 3.78 3.36 H2O 2.51 DMSO 2.50 DMSO 2.50 DMSO 2.50 DMSO 2.49 DMSO
9
1H NMR (400 MHz, DMSO-d6, 298 K)
f1 (ppm)

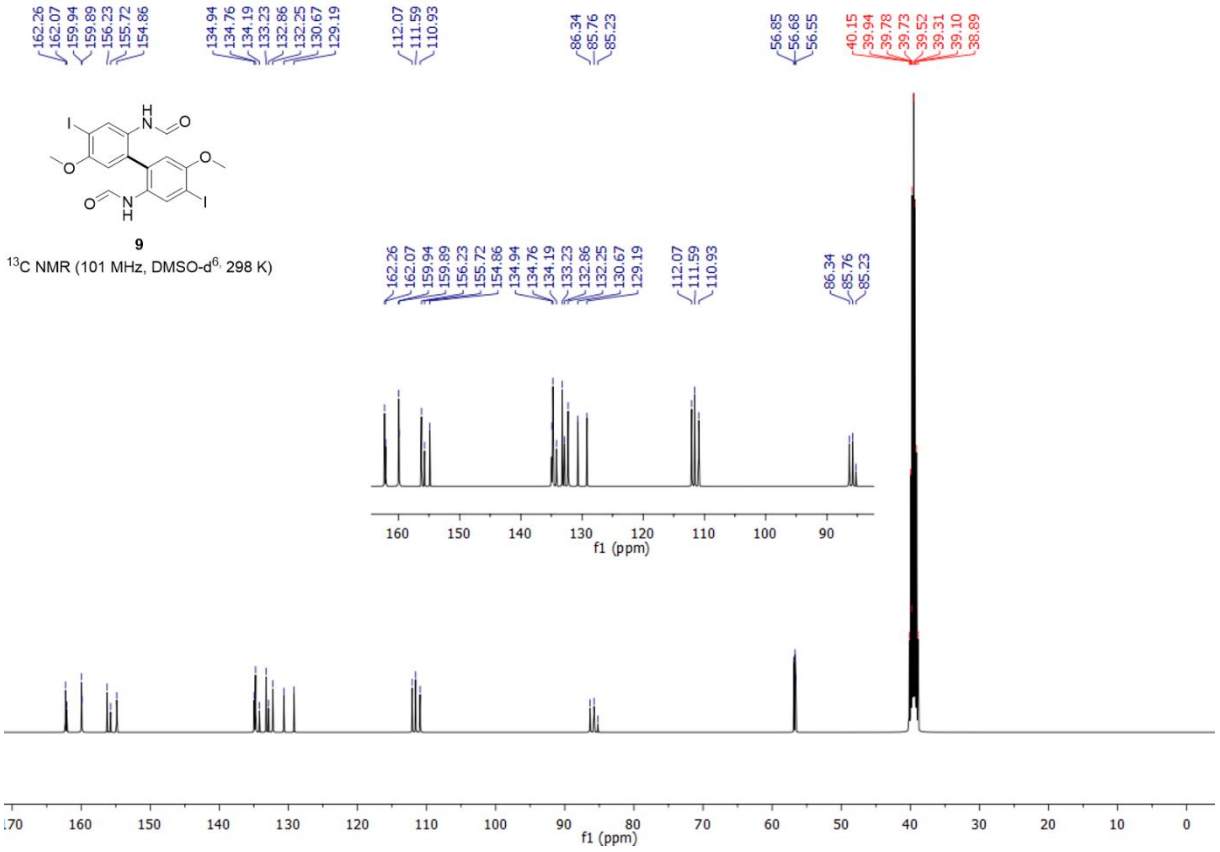
162.26 162.07 159.94 159.89 156.23 155.72 154.86 134.94 134.76 134.19 133.23 132.86 132.25 130.67 129.19 112.07 111.59 110.93 86.34 85.76 85.23 56.85 56.68 56.55 40.15 39.94 39.78 39.73 39.52 39.31 39.10 38.89
9
13C NMR (101 MHz, DMSO-d6, 298 K)
f1 (ppm)

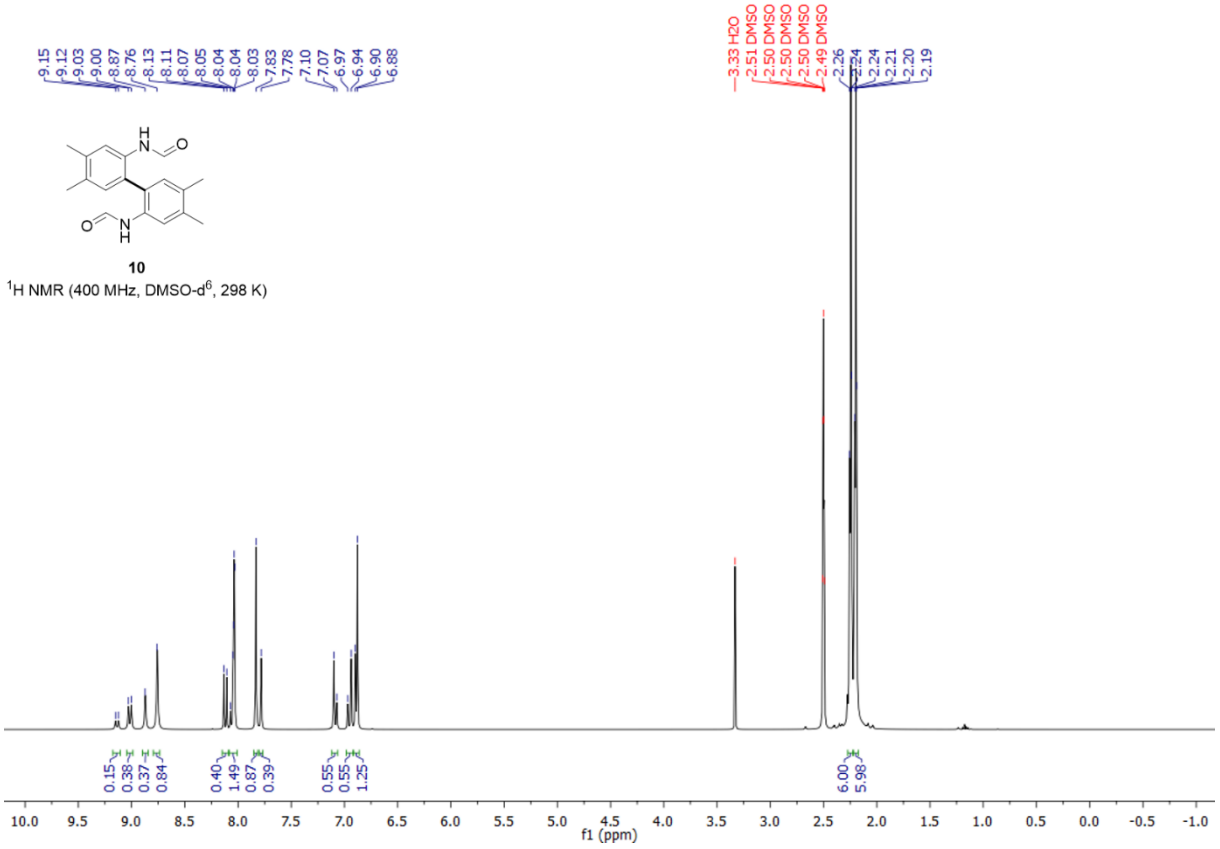

10

^{1}H NMR (400 MHz, DMSO-d^{6}, 298 K)

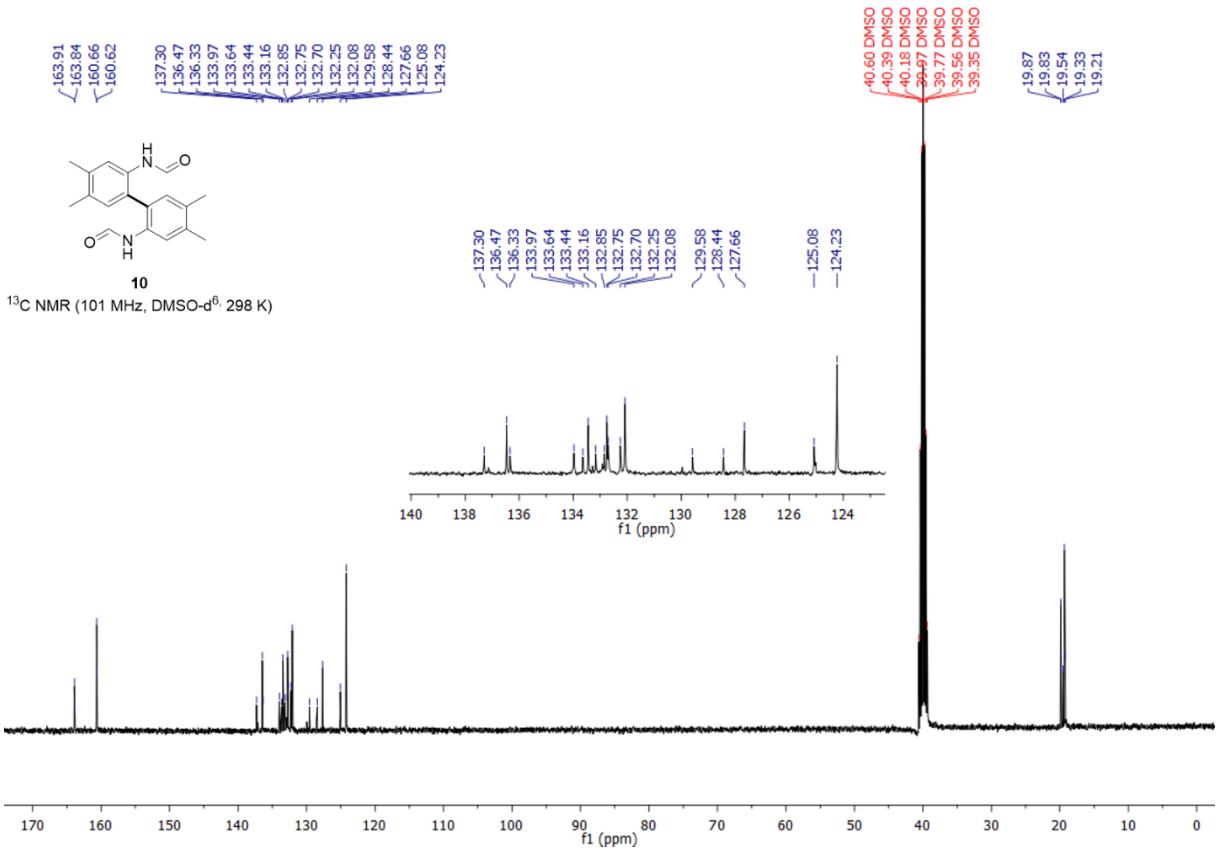

10

^{13}C NMR (101 MHz, DMSO-d^{6}, 298 K)

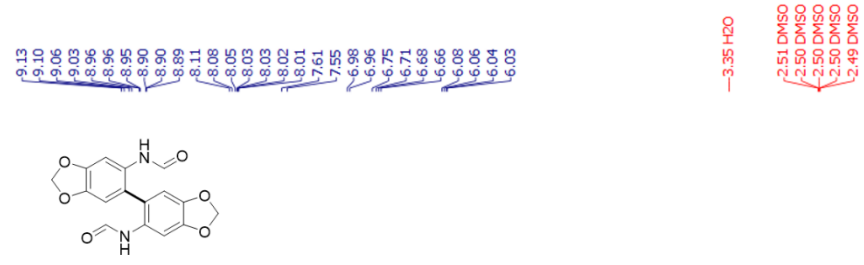

11

^{1}H NMR (400 MHz, DMSO-d^{6}, 298 K)

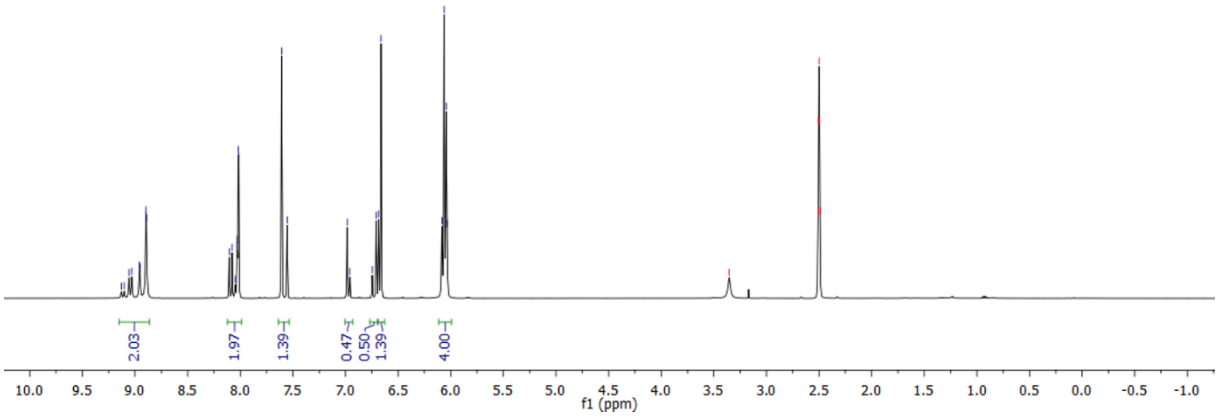

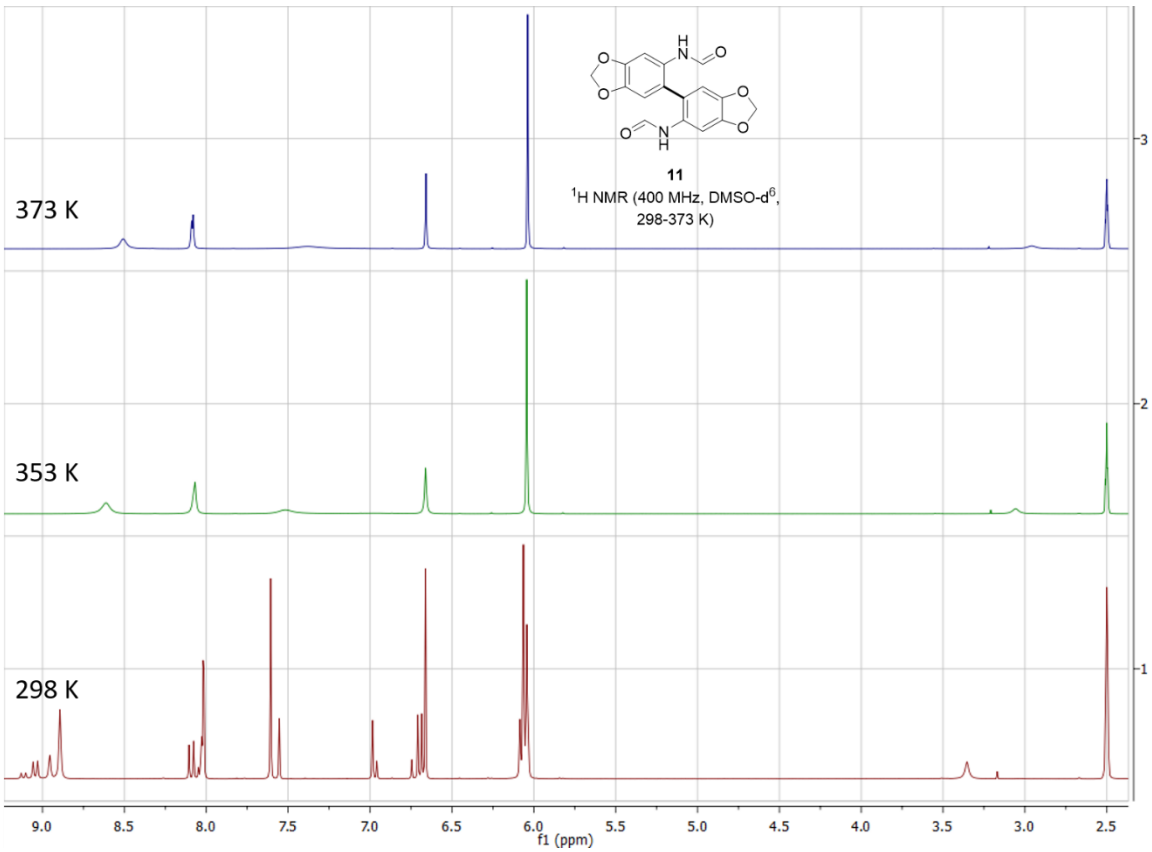

11

^{1}H NMR (400 MHz, DMSO-d^{6}, 298-373 K)

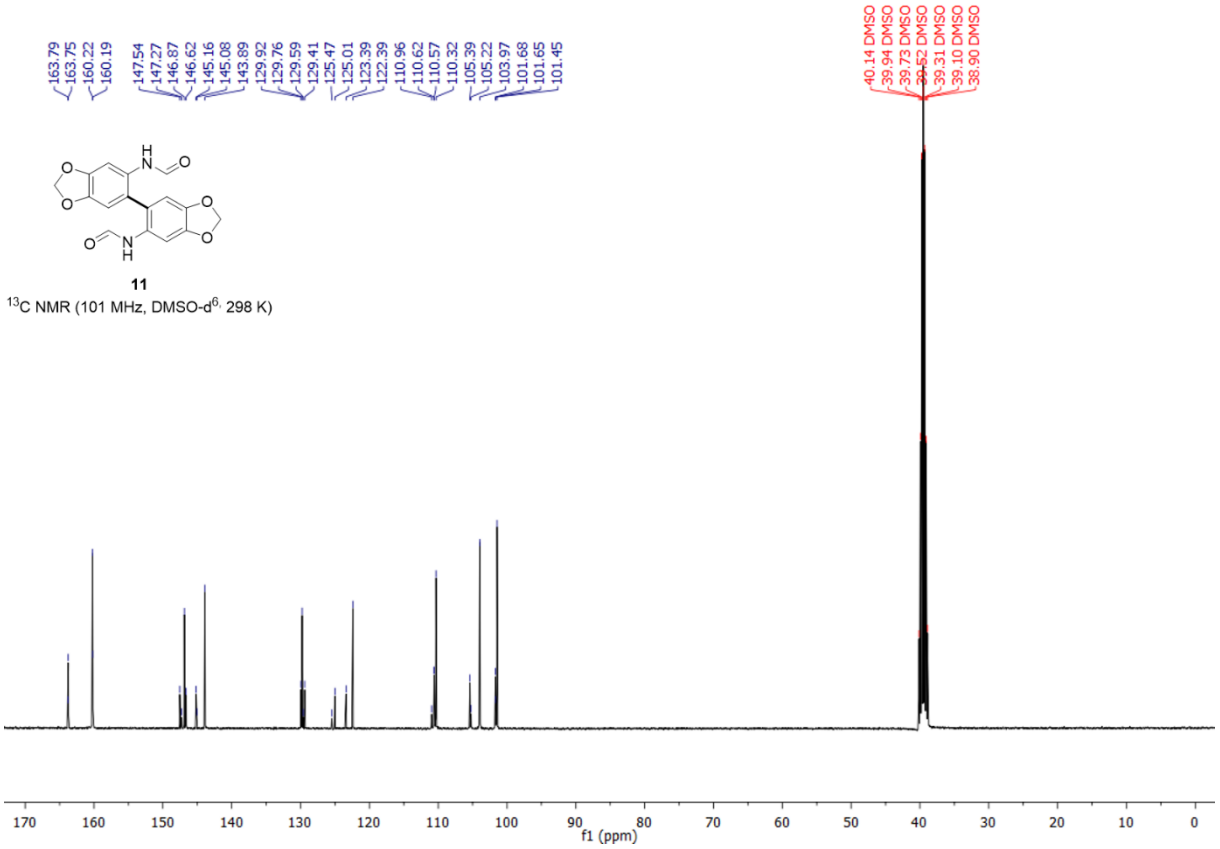
163.79
163.75
160.22
160.19
147.54
147.27
146.87
146.62
145.16
145.08
143.89
129.92
129.76
129.59
129.41
125.47
125.01
123.39
122.39
110.96
110.62
110.57
110.32
105.39
105.22
103.97
101.68
101.65
101.45
40.14 DMSO
39.94 DMSO
39.73 DMSO
39.52 DMSO
39.31 DMSO
39.10 DMSO
38.90 DMSO
11
13C NMR (101 MHz, DMSO-d6, 298 K)
f1 (ppm)

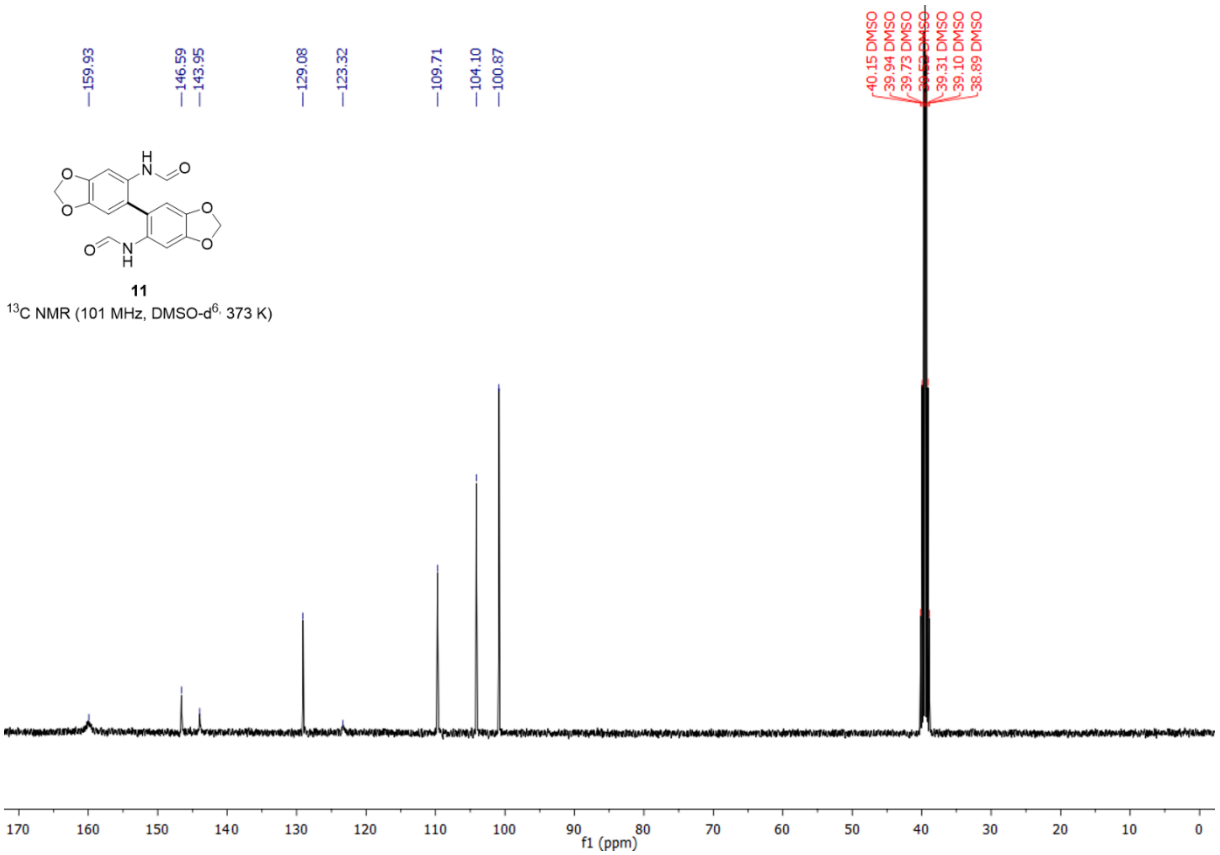
159.93
146.59
143.95
129.08
123.32
109.71
104.10
100.87
40.15 DMSO
39.94 DMSO
39.73 DMSO
39.52 DMSO
39.31 DMSO
39.10 DMSO
38.89 DMSO
11
13C NMR (101 MHz, DMSO-d6, 373 K)
f1 (ppm)

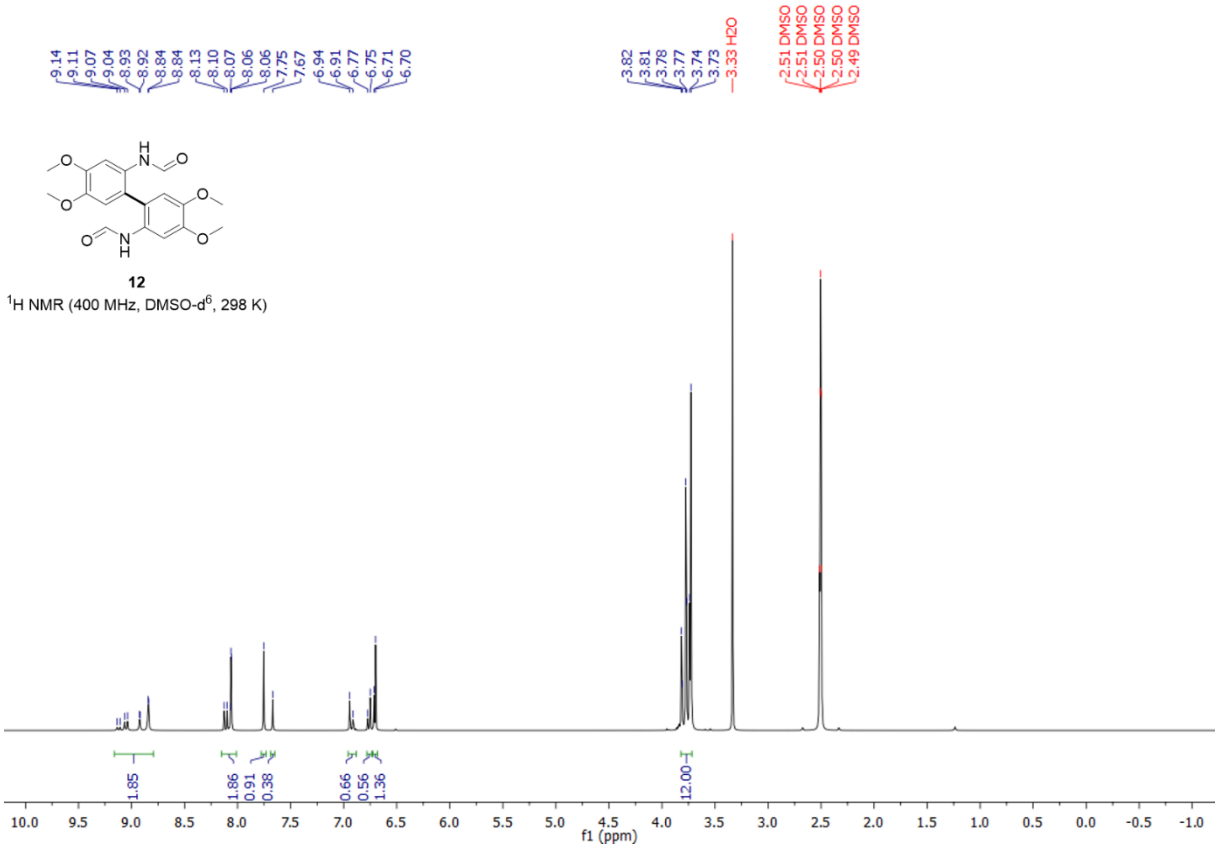
9.14
9.11
9.07
9.04
8.93
8.92
8.84
8.84
8.13
8.10
8.07
8.06
8.06
7.75
7.67
6.94
6.91
6.77
6.75
6.71
6.70
3.82
3.81
3.78
3.77
3.74
3.73
3.33 H2O
2.51 DMSO
2.51 DMSO
2.50 DMSO
2.50 DMSO
2.49 DMSO
12
1H NMR (400 MHz, DMSO-d6, 298 K)
1.85
1.86
0.91
0.38
0.66
0.56
1.36
12.00
f1 (ppm)

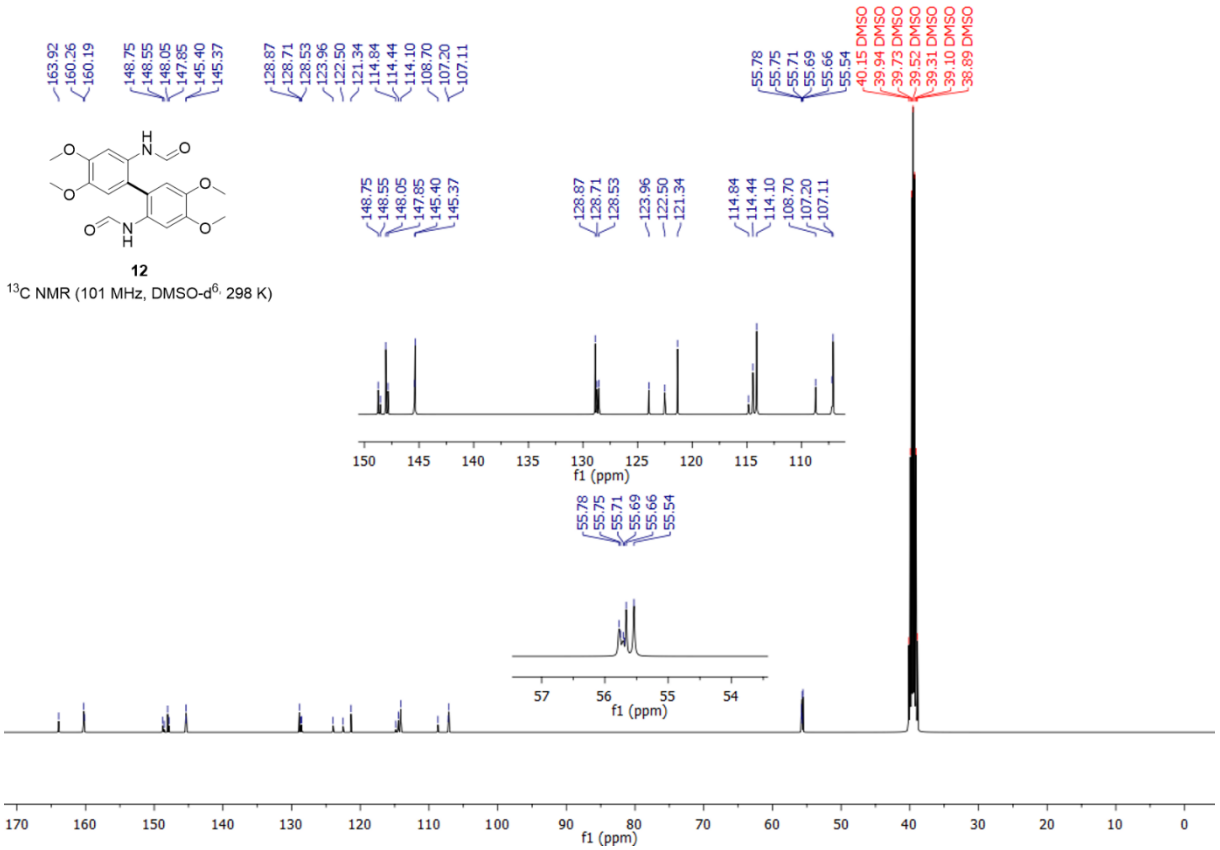
163.92
160.26
160.19
148.75
148.55
148.05
147.85
145.40
145.37
128.87
128.71
128.53
123.96
122.50
121.34
114.84
114.44
114.10
108.70
107.20
107.11
55.78
55.75
55.71
55.69
55.66
55.54
40.15 DMSO
39.94 DMSO
39.73 DMSO
39.52 DMSO
39.31 DMSO
39.10 DMSO
38.89 DMSO
12
13C NMR (101 MHz, DMSO-d6, 298 K)
f1 (ppm)
f1 (ppm)
f1 (ppm)

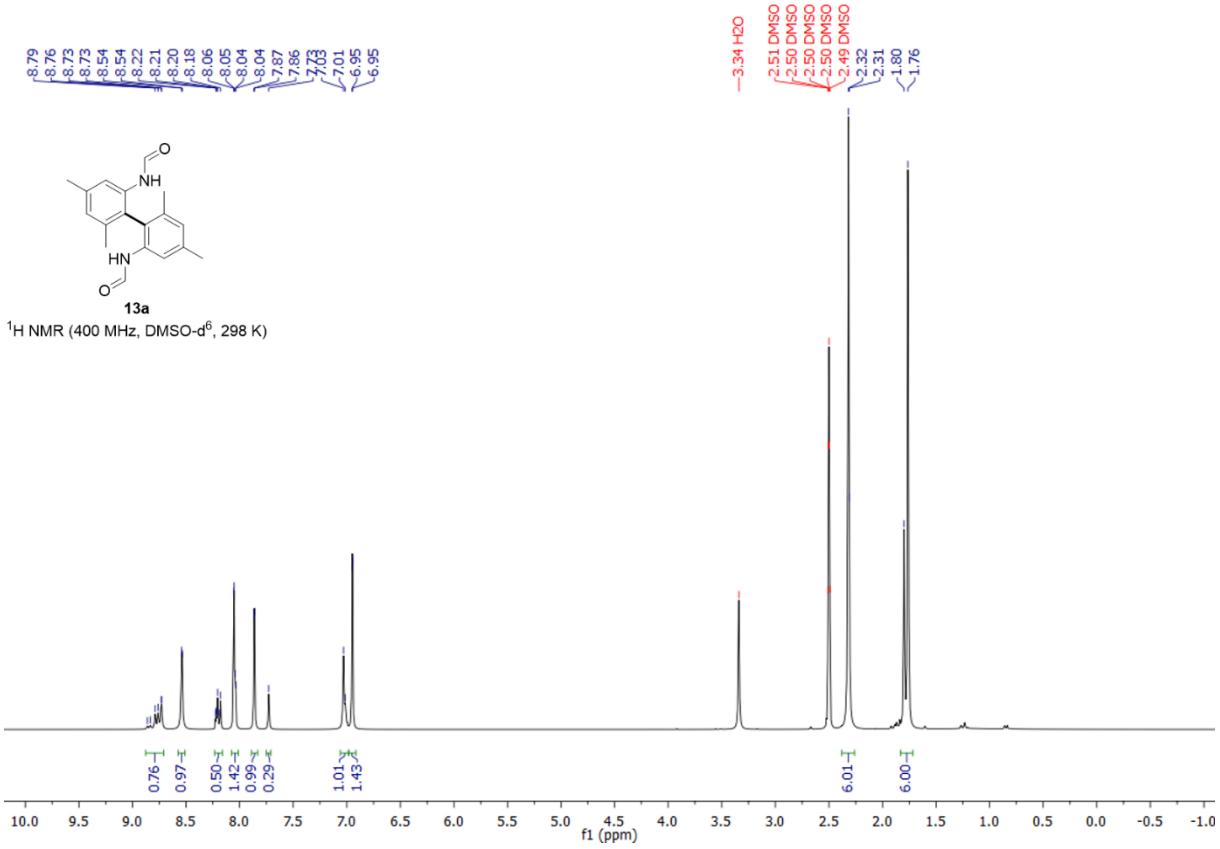

13a

^{1}H NMR (400 MHz, DMSO-d^{6}, 298 K)

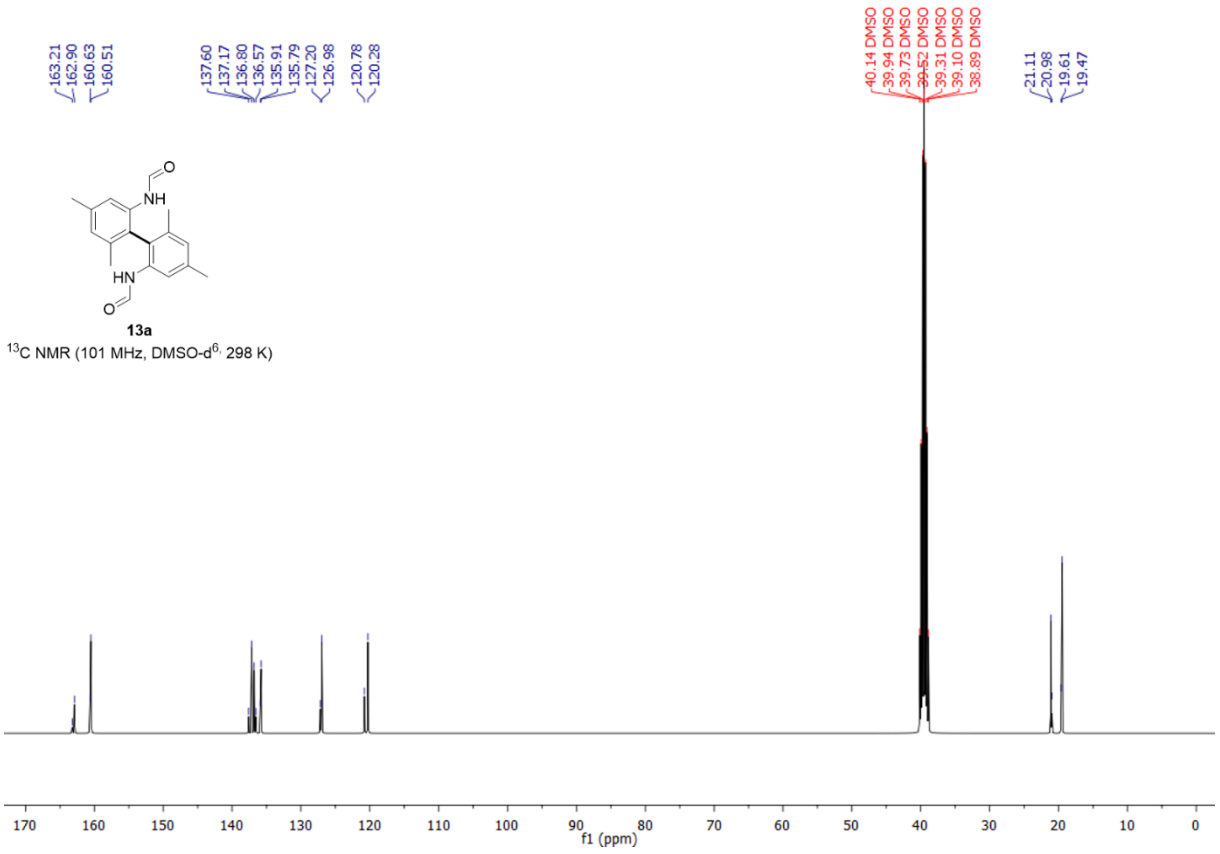

13a

^{13}C NMR (101 MHz, DMSO-d^{6}, 298 K)

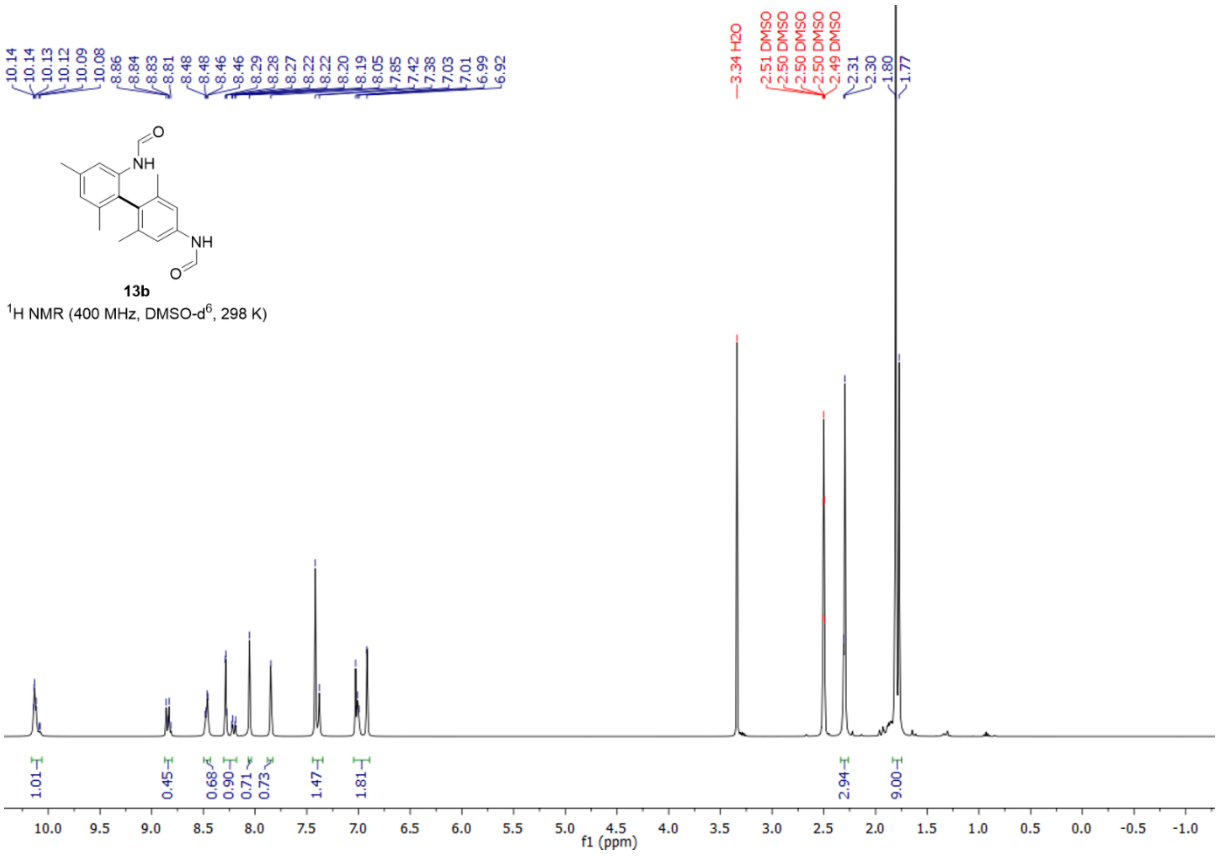
10.14
10.14
10.13
10.12
10.09
10.08
8.86
8.84
8.83
8.81
8.48
8.48
8.46
8.46
8.29
8.28
8.27
8.22
8.22
8.20
8.19
8.05
7.85
7.42
7.38
7.03
7.01
6.99
6.92
3.34 H2O
2.51 DMSO
2.50 DMSO
2.50 DMSO
2.50 DMSO
2.49 DMSO
2.31
2.30
1.80
1.77
NH
NH
O
O
13b
1H NMR (400 MHz, DMSO-d6, 298 K)
1.01
0.45
0.68
0.90
0.71
0.73
1.47
1.81
2.94
9.00
f1 (ppm)

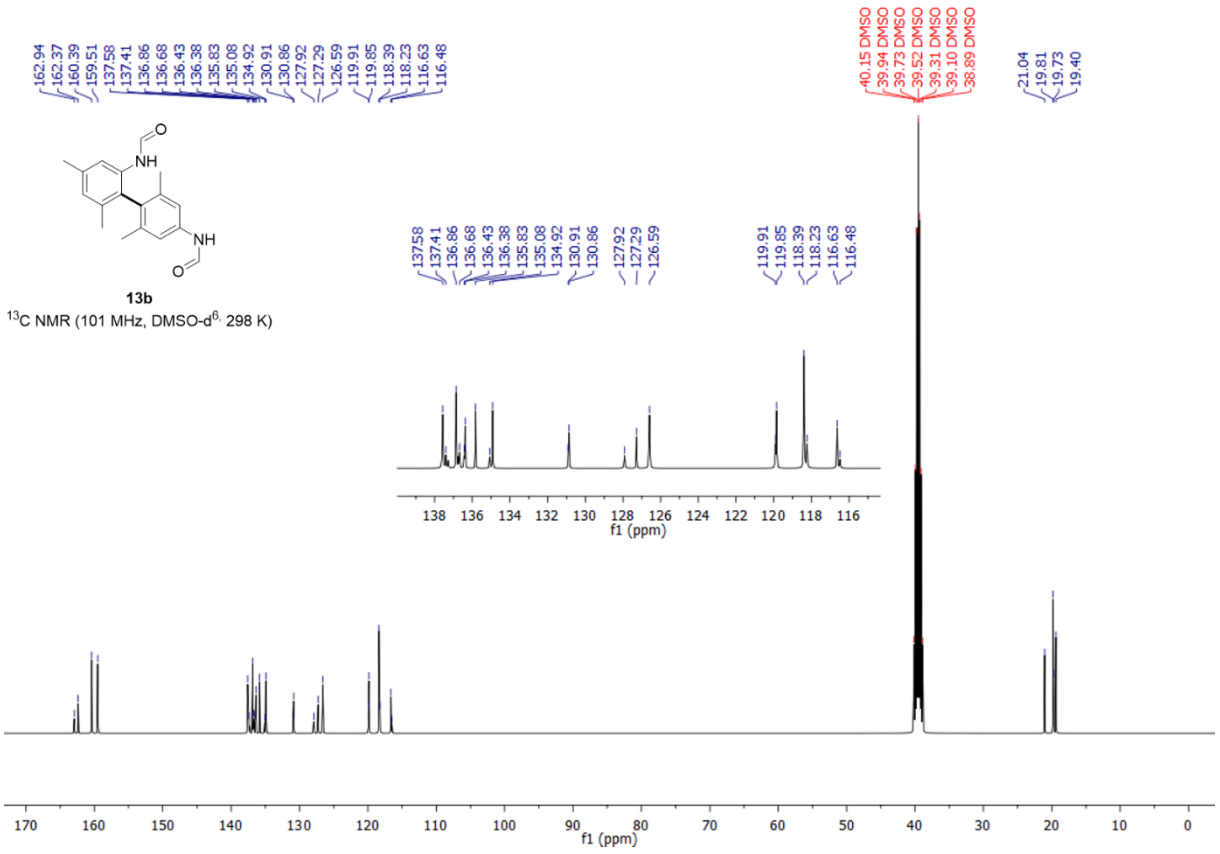
162.94
162.37
160.39
159.51
137.58
137.41
136.86
136.68
136.43
136.38
135.83
135.08
134.92
130.91
130.86
127.92
127.29
126.59
119.91
119.85
118.39
118.23
116.63
116.48
40.15 DMSO
39.94 DMSO
39.73 DMSO
39.52 DMSO
39.31 DMSO
39.10 DMSO
38.89 DMSO
21.04
19.81
19.73
19.40
NH
NH
O
O
13b
13C NMR (101 MHz, DMSO-d6, 298 K)
f1 (ppm)

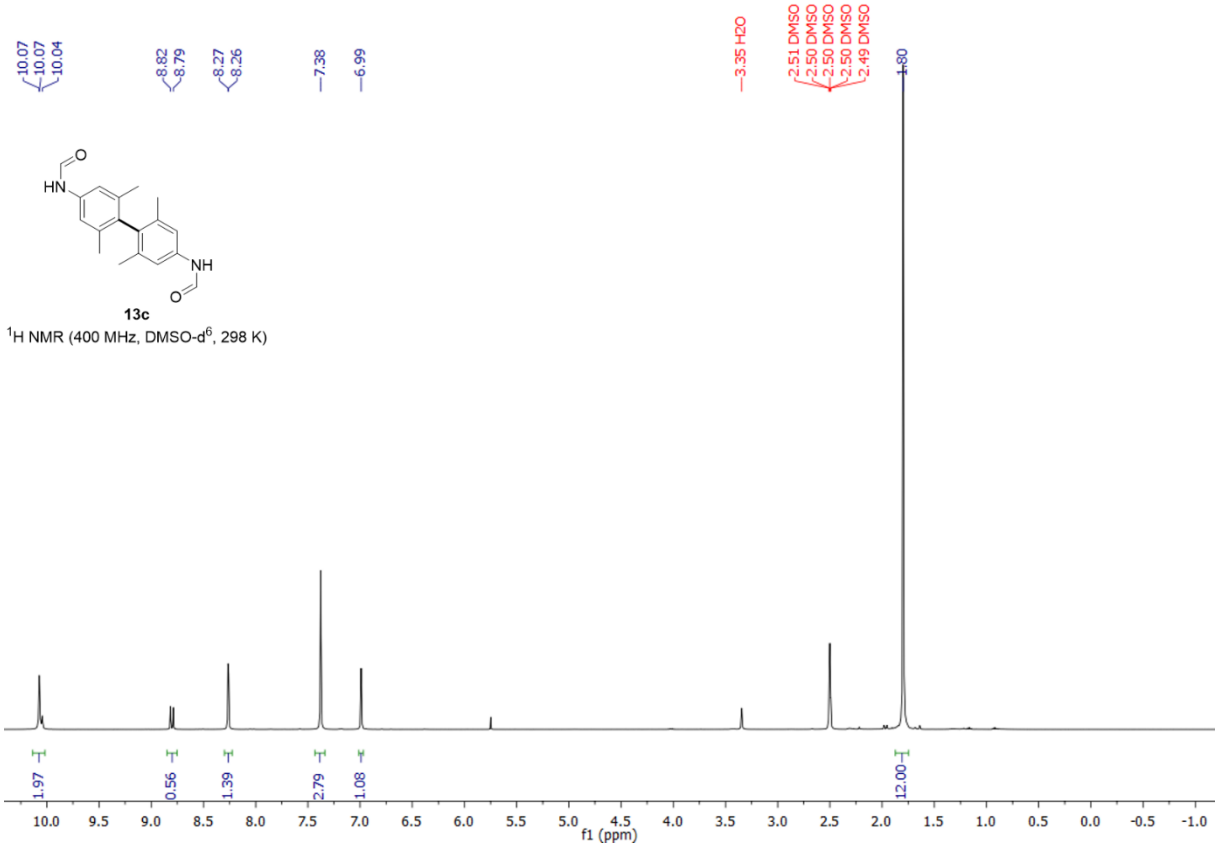
10.07
10.07
10.04
8.82
8.79
8.27
8.26
7.38
6.99
3.35 H2O
2.51 DMSO
2.50 DMSO
2.50 DMSO
2.50 DMSO
2.49 DMSO
1.80
HN
NH
O
O
13c
1H NMR (400 MHz, DMSO-d6, 298 K)
1.97
0.56
1.39
2.79
1.08
12.00
f1 (ppm)

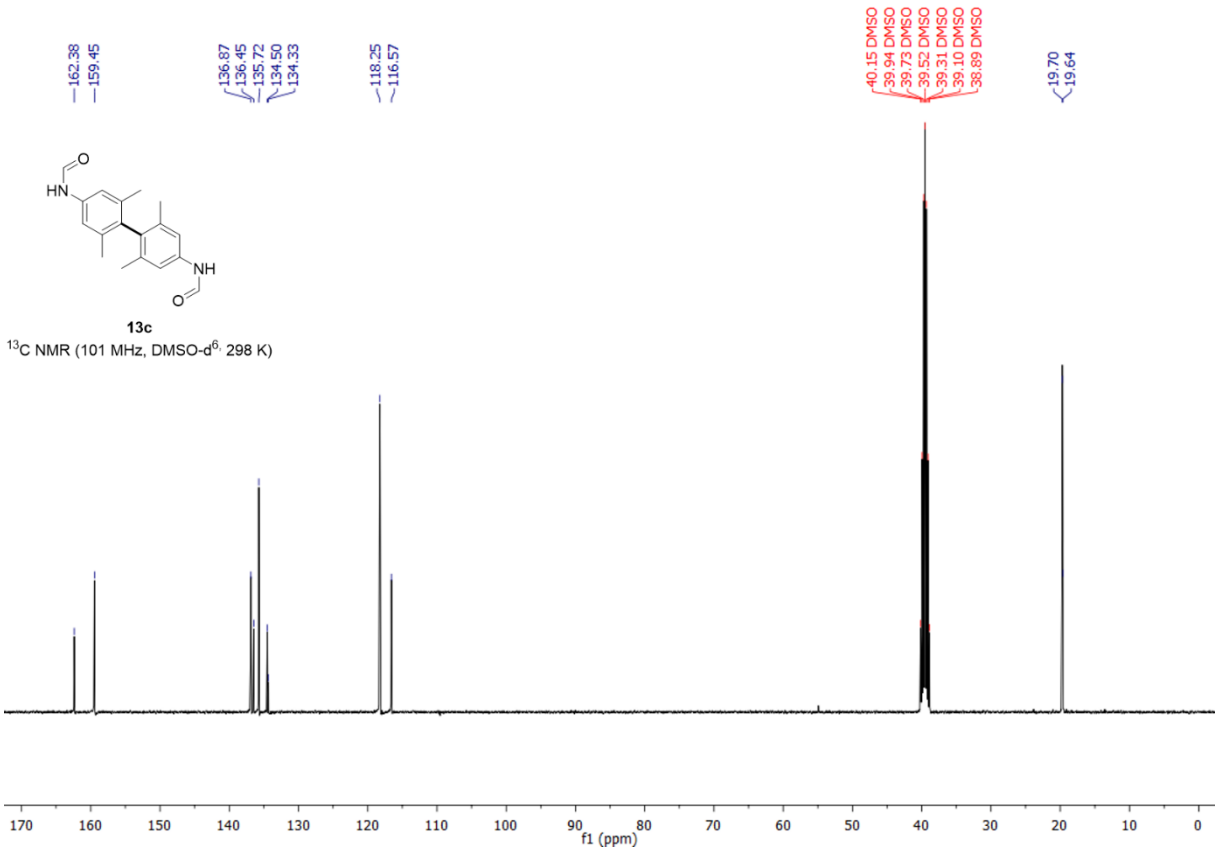
162.38
159.45
136.87
136.45
135.72
134.50
134.33
118.25
116.57
40.15 DMSO
39.94 DMSO
39.73 DMSO
39.52 DMSO
39.31 DMSO
39.10 DMSO
38.89 DMSO
19.70
19.64
HN
NH
O
O
13c
13C NMR (101 MHz, DMSO-d6, 298 K)
f1 (ppm)

Synlett L. Schulz, S. R. Waldvogel THIEME OPEN ACCESS Account

Solvent Control in Electro-Organic Synthesis

Lara Schulz
Siegfried R. Waldvogel*

Institut für Organische Chemie, Johannes Gutenberg-Universität Mainz, Duesbergweg 10–14, 55128 Mainz, Germany
waldvogel@uni-mainz.de

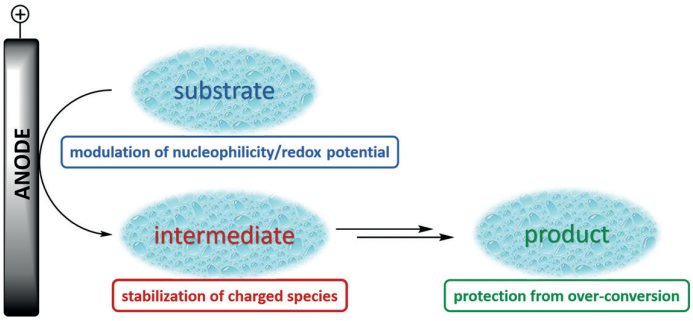

Received: 03.09.2018
Accepted after revision: 17.09.2018
Published online: 13.12.2018
DOI: 10.1055/s-0037-1610303; Art ID: st-2018-a0569-a

Abstract Exploiting the solvent control within electro-organic conversions is a far underestimated parameter in prep-scale electrolysis. The beneficial application in several transformations is outlined and in particular discussed for the dehydrogenative coupling of arenes and heteroarenes. This simple electrolytic strategy in fluorinated solvents allows the modulation of the substrate's nucleophilicity and the stabilization of the intermediates as well as of the final product from over-oxidation.

Key words C–C coupling, electrochemical fluorination, electrosynthesis, Kolbe electrolysis, N–C coupling, solvent effect, 1,1,1,3,3,3-hexafluoropropan-2-ol

1 Introduction

Usually, the electrode material and the applied potential represent the most important parameters in electrochemistry because different reaction courses are often pursued.[1] However, the electrolysis can only occur at the boundary between electrode and a medium being conductive for the electric current. Such media are called electrolytes and can also influence the reaction pathway in a significant way.[2] This parameter is often neglected. The electrolytes typically consist of a solvent and a supporting electrolyte to ensure sufficient electric conductivity. In most studies, focus and attention to the nature of the supporting electrolyte is given, because of the ionic charges and the structuring close to the electrode. However, solvents can play a decisive role in the reaction pathways being populated.[3] Important factors for these solvents are the exploitable potential range, proton activity, dielectric constant, ability to dissolve and dissociate supporting electrolytes, solubility of substrates and intermediates, accessible temperature range, vapor pressure, viscosity, toxicity and, of course, the costs. Solvents for electrochemistry can be divided into two major groups – protic and aprotic solvents. Common protic solvents are sulfuric acid, trifluoroacetic acid (TFA), acetic acid, water, methanol (MeOH), 1,1,1,3,3,3-hexafluoropropan-2-ol (HFIP), or ammonia. Except sulfuric acid most of them are not strong electrolytes and therefore supporting electrolytes are required. Examples for the aprotic systems are acetonitrile (MeCN), dimethylformamide (DMF), hexamethylphosphoramide (HMPA), pyridine, dimethyl sulfoxide (DMSO), propylene carbonate (PC), and various ethers.[4] Nitromethane is also frequently used for anodic oxidative coupling.[5]

The used solvent is able to severely affect the reaction outcome as will be outlined in the next paragraphs. For example, nucleophilicity and redox potentials can be distinctly altered by different solvation and intermediates can be solvated more or less and thus, different reaction pathways can be pursued. Furthermore, the product can be protected from over-conversion and the selectivity and yield can be distinctly improved by choosing a suitable solvent system (Figure 1).

2 Solvent Effects in Kolbe Electrolysis and Anodic Fluorination

There are several well-known electro-organic syntheses in which the solvent employed has a significant impact on the reaction outcome.[6,7] Probably, the most famous exam-

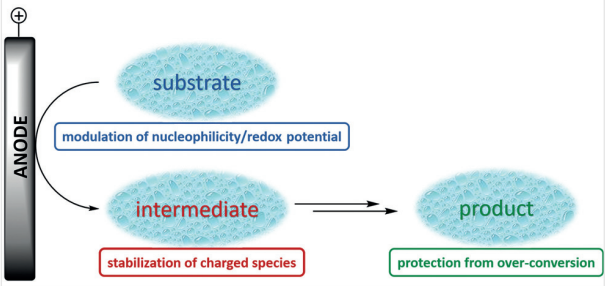

Figure 1 Visualization wherein solvents can influence electrochemical reaction pathways by solvation effects

ple is represented by the oxidation of carboxylic acids, known as Kolbe electrolysis. Usually, aqueous solutions of methanol, DMF, or acetonitrile serve as the solvents.[8] Best results are commonly obtained when the acid is neutralized by an alkali metal hydroxide or trialkylamine to an extent of 2–5%. Figure 2 schematically displays the impact of different classes of solvents [water (W), protic solvents (P), and dipolar aprotic solvents (DA)] on the formation of two different reactive intermediates (cation R^+ and radical $R^{\cdot}$) and thus, four typical reaction pathways, which are Kolbe dimerization (blue), substitution (yellow), rearrangement (green), and alkene formation (red).[4]

Kolbe dimerization is favored in acidic, protic solvents as well as in neutral–water and protic–water mixtures, whereas the two-electron non-Kolbe process is preferred in basic and dipolar aprotic solvents. For example, the electrolysis of cyclopropane carboxylic acids leads to different products by using different solvent systems. In a mixture of pyridine–H_2O–Et_3N at the platinum electrodes, the Kolbe

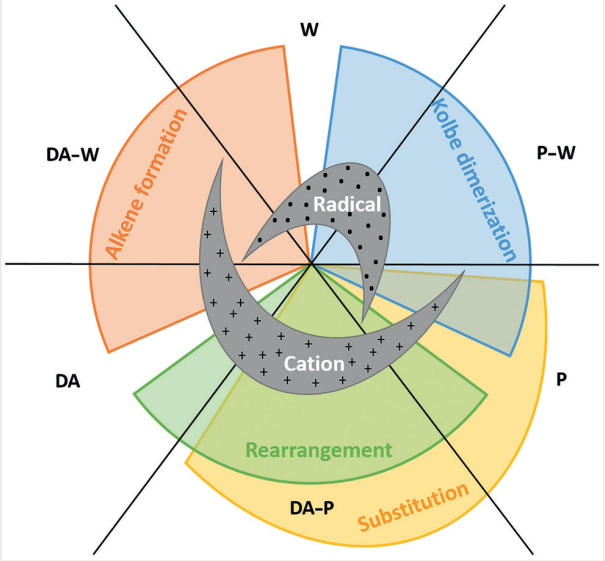

Figure 2 Interrelation between solvent, reactive intermediate, and reaction type. W: water, P: protic solvent, DA: dipolar aprotic solvent such as acetone or DMF

dimer is predominantly formed. However, in a methanol–NaOMe solvent mixture, cyclopropane is mainly generated by a hydrogen atom abstraction (Scheme 1).[9]

Another electrochemical synthesis of wide interest, in which the used solvent system can have a severe influence onto the product selectivity, is the anodic fluorination.[7] Usually, organic solvents such as acetonitrile containing the ionic liquid $Et_4NF{\cdot}HF$ are used for the direct electrochemical fluorination.[10]

Biographical Sketches

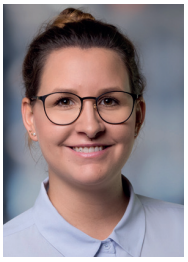

Lara Schulz was born in Frankenthal (Pfalz), Germany in 1991. She studied chemistry at the Johannes Gutenberg University Mainz, where she obtained her B.Sc. in 2014 and her M.Sc. in chemistry in 2016. Currently, she is a Ph.D. student under the supervision of Prof. Dr. S. R. Waldvogel, investigating anodic C–C cross- and homo-coupling reactions.

Siegfried R. Waldvogel was born in 1969 in Konstanz, Germany. He studied chemistry at the University of Konstanz and received his Ph.D. in 1996 from the University of Bochum/Max Planck Institute for Coal Research under the supervision of Prof. Dr. M. T. Reetz. After postdoctoral research at the Scripps Research Institute in La Jolla, California (Prof. Dr. J. Rebek, Jr.) he began his habilitation in 1998 at the University of Münster. In 2004, he moved to the University of Bonn as a professor of Organic Chemistry. In 2010, he became full professor at the Johannes Gutenberg University Mainz. His main research interests are dedicated to organic electrochemistry, oxidative coupling reactions with Mo^V reagents, and supramolecular sensing.

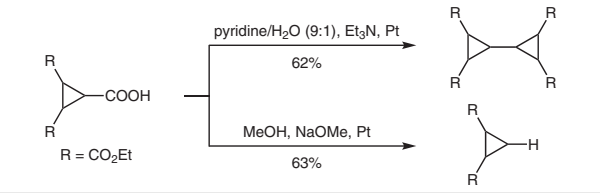

Scheme 1 Solvent effect in Kolbe electrolysis

To avoid the use of flammable organic solvents and circumvent anode passivation as well as side reactions such as acetoamidation, progress has been made by using ionic liquids as the solvent in anodic fluorination reactions.[11] By using the imidazolium ionic liquid [EMIM][OTf], anodic fluorodesulfurization of 3-phenylthiophthalide was exclusively achieved, whereas in DME, α-fluorination proceeded predominantly and desulfurization became the side reaction (Scheme 2).[12] It is noteworthy, that [EMIM][OTf] seems to destabilize the anodically generated radical cation intermediate similarly to CH_2Cl_2 to trigger the desulfurization process.

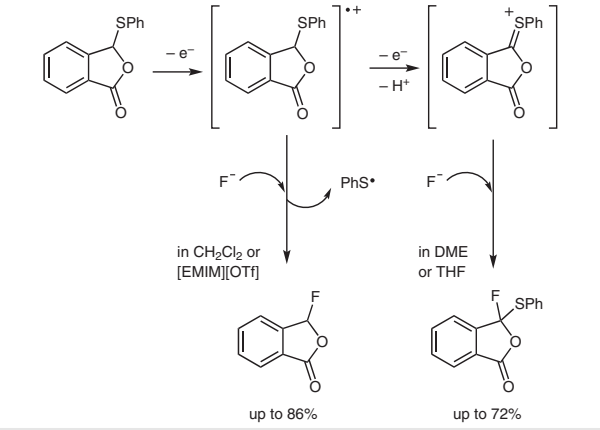

Scheme 2 Solvent effect onto anodic fluorination of 3-phenylsulfanylphthalide

3 Unique Solvent Effects of 1,1,1,3,3,3-Hexa-fluoropropan-2-ol (HFIP)

Seminal studies were conducted by the late Eberson, wherein the significantly enhanced stability of the radical cations was observed in 1,1,1,3,3,3-hexafluoropropan-2-ol (HFIP) in comparison to trifluoroacetic acid.[13] Its beneficial effect is well documented in metal catalysis and oxidation reactions.[14,15,16] However, no rationale could be given at that time for the exceptional behavior of this solvent. In our group, the outstanding features of HFIP as a solvent in electrochemistry have been utilized since 2009.[17]

Recently, we investigated in close collaboration with Kirchner et al. catalytically active mixtures of HFIP and aqueous H_2O_2 by specific molecular dynamics simulations. It was observed that HFIP develops a microheterogeneous structure, which is due to the separation of the hydroxyl groups from the fluorinated alkyl moieties. Thus, large domains are formed which cover significant areas of the system, whereas macroscopically the liquid is still homogeneous. The hydroxyl groups are connected by hydrogen bonding, whereas the fluorine atoms, despite their electronegativity, are not participating in the hydrogen bonding network but cluster together.[14] Figure 4 displays the segregation of the polar, nonpolar, and fluorous phases of the TEFDDOL (**1**, Figure 3).[18]

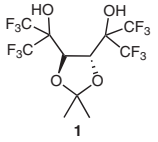

Figure 3 Structure of TEFDDOL (**1**)

This highly fluorinated analogue of the tartrate-derived TADDOLs[19] shows the same behavior as HFIP and also exhibits a distinct separation of the three different domains. A long ribbon-kind structure is formed by hydrogen bonding of the hydroxyl groups, which are coated by the fluorous domains, held together by attractive dispersion interaction of the CF_3 moieties (Figure 4).[16,20]

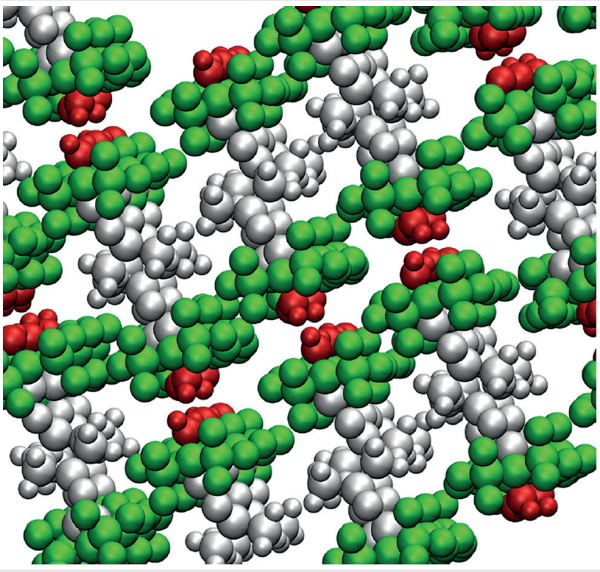

Figure 4 Segregation of polar (hydroxyl groups, red), nonpolar (CH_3 units and the rings, gray), and fluorous (CF_3–C–CF_3 units, green) phases in the crystal structure of **1**. Reprinted with permission from ref. 14. Copyright 2017 American Chemical Society

Radial distribution functions (RDFs) of the hydrogen bonds between the hydrogen bond donor and acceptor molecules in the investigated systems indicate that in pure HFIP, the hydroxyl group acts as a hydrogen bond donor

and acceptor. As mentioned before, the fluorine atoms are excluded from the hydrogen bonding network and instead, cluster together. Hereby two different domains result, one with fluorous and the other with a polar character. The fluorinated moieties form a continuous microphase, whereas the smaller hydroxyl substituents form small clusters of about 10 hydroxyl groups. If water is added, the number of HFIP–HFIP hydrogen bonds decreases, because water is a stronger hydrogen bonding acceptor than HFIP. Unexpectedly, the water–water interplay exhibits the lowest peak in the RDFs, which means that the occurrence of hydrogen bonds between the water molecules is the merest. This is probably due to the very high hydrogen bonding acceptor feature of HFIP. In consequence of the occupation of the hydrogen bonding acceptor sites of the water, only the HFIP's oxygen atoms are left as acceptors. The fluorous domains show no change in size compared to pure HFIP but the number of individual polar domains decreases, which is due to an increased clustering of the polar groups. Furthermore, the addition of water results in an accelerated movement of the HFIP molecules by a factor of 5. This finding might be explained by a more flexible hydrogen bonding network in the presence of water. If another component, e.g. a nonpolar hydrocarbon such as cyclooctene, is added to the HFIP/water mixture, the hydrogen bonding network changes once more and the diffusion constants of all components increase. In Figure 5 it is clearly visible that the cyclooctene molecules form small clusters, which are surrounded by the fluorous moieties.[14] If a polar component such as a phenol or an aniline is added to an HFIP/water mixture instead of a nonpolar one, it is most likely that these polar molecules are also embedded into the hydrogen bonding network and will be part of the polar clusters. Thus, the starting molecules of recently reported anodic C–C and N–N coupling reactions, radical intermediates, as well as products, formed throughout electrolysis, are to a certain degree protected from over-oxidation, side reactions, and mineralization by these HFIP clusters. As a result, many selective and highly innovative reactions become possible, as outlined in the next paragraphs.

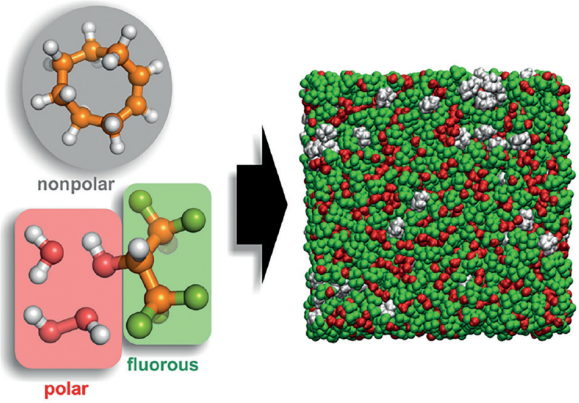

Figure 5 Definition of the subsets that form domains (left) and a snapshot of the simulation box of the HFIP–water/H_2O_2–cyclooctene system with the domain subsets colored accordingly (right).[14] Reprinted with permission from ref. 14. Copyright 2017 American Chemical Society.

4 Anodic Dehydrogenative Coupling Reactions with Use of HFIP as the Solvent

Electrochemical dehydrogenative coupling reactions by direct oxidative C–H and N–H conversion are often challenging because oligomerization or even mineralization of the substrates or the just-built products often occur. In particular, C–H/C–H cross-couplings of two different arenes are demanding, because one coupling partner has to be selectively oxidized. Without any encouragement, homo- and cross-coupling products will arise statistically without any selectivity. There are many electrochemical approaches to push the reaction in the desired direction, e.g. the extremely elegant "radical cation pool method" by Yoshida and coworkers.[21] This strategy is based on the separation of the oxidation and the coupling events in time and space to prevent homo-coupling and over-oxidation. However, the need of low temperatures and the exclusive applicability on a small scale (0.1 mmol) make this method less suitable for scalable synthesis. The easiest way to determine the reaction outcome would be the application of an electrolyte system that is able to control the oxidation potential and nucleophilicity of the distinct coupling partners. With HFIP, such a solvent was discovered as the following will show.

In the beginning of investigations regarding the anodic homo-coupling of 2,4-dimethylphenol, a boron-based template strategy was developed. This process can be performed on a multi-kg scale and gave the homo-coupling product in excellent selectivity, but a multi-step sequence is required.[22] However, the direct electrolysis of 2,4-dimethylphenol is usually challenging because several by-products are formed. Besides the desired biphenol **3**, Pummerer's ketone **4** is typically the major product and dehydrotrimers with pentacyclic scaffolds (e.g. **5**, Scheme 3) are obtained in significant amounts.[23] Testing different electrode materials, Waldvogel et al. surprisingly found that on boron-doped diamond electrodes (BDD) no other by-product than traces of **4** were observed.[24] BDD electrodes are commonly used for total oxidation and mineralization of organic pollution in waste water,[25] which makes this finding even more surprising.

An initial screening of additives showed significantly better results in the homo-coupling of 2,4-dimethylphenol when HFIP was used as an additive. Other primary alcohols with fluorous moieties in the β position, such as 2,2,3,3-tetrafluoropropanol, 2,2,2-trifluoroethanol, or 2,2,3,3,4,4,5,5-octafluoropentanol could also be applied but gave minor yields compared to HFIP. Trifluoroacetic acid

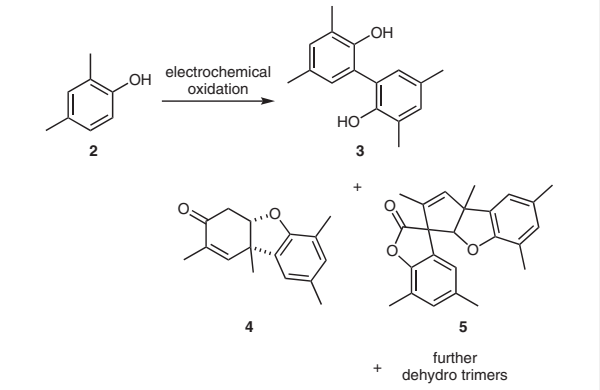

Scheme 3 Product diversity (major components) from the electrochemical oxidation of 2,4-dimethylphenol **2**

and the respective carboxamide gave significantly inferior results, revealing that the Brønsted behavior of HFIP is not the reason for the good conversion of 2,4-dimethylphenol.[17] The application of the optimized parameters for the homo-coupling of 2,4-dimethylphenol could be extended to guaiacol derivatives. By serendipity, it was found that 4-methylguaiacol (**6**) gave the nonsymmetric *ortho-meta* coupled biphenol **7** after electrolysis as the sole product (Scheme 4). This led to the assumption that the biphenol products are not generated by radical recombination because otherwise, only symmetric biphenols would be formed. Thus, an oxidation of the phenol followed by a nucleophilic attack of another phenol and a subsequent second oxidation step is more likely (cf. mechanistic rationale, Scheme 5).

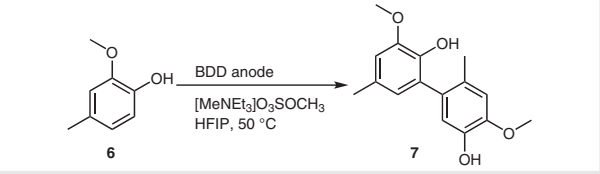

Scheme 4 Electrochemical oxidation of 4-methylguaiacol (**6**) on BDD in HFIP gives the nonsymmetric *ortho-meta* coupled product, which represents the first anodic phenol–phenol cross-coupling reaction in HFIP.

Anodic treatment of other guaiacol derivatives led to the finding that, depending on the steric demand of the substituent in position 4, either a symmetric or nonsymmetrical biphenol was obtained.[26] After this lucky finding, the idea arose to extend this exceptional synthesis to various phenol–phenol cross-couplings as well as phenol–arene cross-coupling reactions.[27] In general, it was observed that the addition of HFIP significantly reduces the oxidative degradation of the substrates and products.

Throughout the investigations considering HFIP-based electrolytes for electrochemical double layer capacitors, studies on the electrochemical stability of HFIP were conducted. Cyclic voltammetry experiments with HFIP as the solvent and tetrabutylammonium perchlorate (TBAPC) as supporting electrolyte showed an excellent stability of the electrolyte (see Table 1).[28] Since the solvent contains active protons, the ideally polarizable regime is limited on platinum because of the onset of hydrogen evolution at +0.25 V vs. Ag/AgCl (Table 1, black line). However, the cathodic limit on glassy carbon is distinctly increased towards more negative values because of the high overpotential of glassy carbon towards the reduction of protons (red line). This results in a potential window of 4.6 V, which is remarkable for an alcohol and is comparable to aprotic solvents with the same supporting salt.[28]

Table 1 Cyclic Voltammograms of 0.1 M HFIP-Based Electrolytes Measured on Glassy Carbon and Pt Electrodes; Scan Rate: 10 mVs^{-1}; RE: Ag/AgCl in sat. LiCl/EtOH.[28] Reprinted from ref. 28, with Permission from Elsevier.

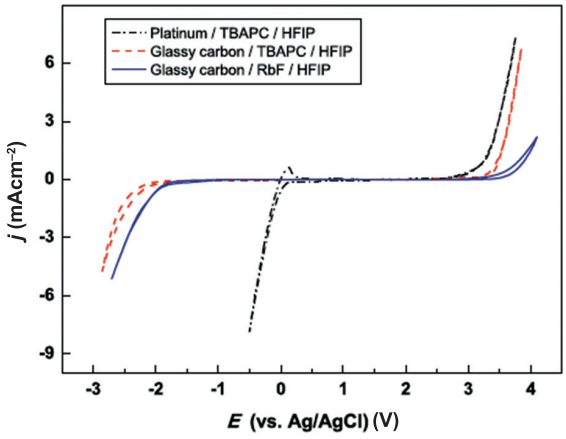

Working electrode	Electrolyte	Cathodic limit (V)	Anodic limit (V)	Potential window (V)
Pt	TBAPC/HFIP	0.6	2.7	2.1
Glassy carbon	TBAPC/HFIP	−1.75	2.85	4.6
Glassy carbon	RbF/HFIP	−1.3	3.2	4.5

Because of its extraordinary stability, HFIP can almost quantitatively be recycled and reused after electrolysis.[29] Exactly this recycling of HFIP led Waldvogel et al. to another important finding – the beneficial role of protic additives such as water or methanol. In the beginning, phenol–arene cross-coupling reactions were carried out in highly pure HFIP. In this case, the desired cross-coupling product **8ab** was only formed as a minor product. The major side reaction was the undesired formation of homo-coupling product **8bb** (Table 2, entry 1). By using recycled HFIP, the yield of the cross-coupling product as well as the selectivity improved distinctly. ^{1}H NMR data of such recycled HFIP indicated traces of water and methanol; thus a systematic study

with different amounts of these additives in the electrolyte was conducted (Table 2, entries 2–12). For easier work-up on a preparative scale, **8ab** was acylated.[30]

Table 2 Influence of Protic Additives onto Anodic Phenol–Arene Cross-Coupling Reaction.[a,30] Adapted with Permission from ref. 30. Copyright 2012 American Chemical Society.

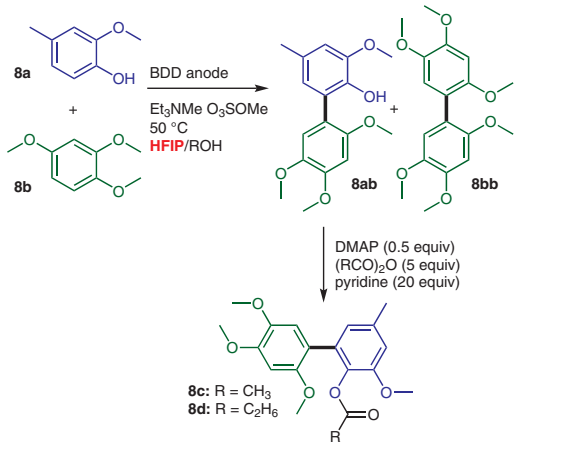

Entry	Ratio **8a**/**8b**	HFIP/ROH (mL/mL)	Yield (%)[b]	Ratio **8ab**/**8bb**[c]
1	1:5	30–	21 (**8d**)	1:3
2	1:5	32/1 (H_2O)	47 (**8d**)	1.5:1
3	1:5	31/2 (H_2O)	68 (**8d**)	8:1
4	1:5	30/3 (H_2O)	67 (**8d**)	85:1
5	1:5	28/5 (H_2O)	41 (**8d**)	>100:1[d]
6	1:5	31/2 (MeOH)	56 (**8d**)	2:1
7	1:5	31/2 (MeOH)	66 (**8c**)	6:1
8	1:5	31/2 (MeOH)	64 (**8d**)	11:1
9	1:5	31/2 (MeOH)	66 (**8d**)	10:1
10	1:5	31/2 (MeOH)	69 (**8d**)	90:1
11	1:5	31/2 (MeOH)	55 (**8d**)	22:1
12	1:7	31/2 (MeOH)	58 (**8d**)	45:1
13	1:3	31/2 (MeOH)	69 (**8d**)	>100:1[d]
14	1:2	31/2 (MeOH)	55 (**8d**)	45:1

[a] Electrolytic conditions: 50 °C, constant current (j = 2.8 mA/cm²), BDD anode, nickel cathode, undivided cell, 2 F/mol (ref. phenol), 0.68 g $Et_3NMe\ O_3SOMe$.
[b] Isolated yield of homo-coupling product.
[c] Determined by GC.
[d] Homo-coupling product **8bb** was not detected.

Distinctly superior results could be obtained by using 9 vol% H_2O and 18 vol% MeOH, respectively. It is noteworthy, that this corresponds to the same molar amount of additive. The yield could be increased to 67% and the selectivity increased to 85:1 (9 vol% H_2O, entry 4). Even better results were obtained by the addition of 18 vol% MeOH; the desired cross-coupling product was obtained in 69% yield and a slightly better selectivity of 90:1 (entry 10). Further improvements were made by varying the excess of the arene compound from 5 to 7, 3, and 2 equivalents, respectively (entries 12, 13, and 14). Best results were obtained by using a molar ratio **8a**/**8b** = 1:3 (entry 13) and the cross-coupling product could be isolated in 69% yield with exclusive selectivity. Furthermore, the oligomerization during electrolysis was decreased. These optimized reaction conditions set the stage for a broad variety of phenol–arene couplings. In all examples studied, the selectivity was clearly enhanced and the yield was often increased. In addition, the scope was extended because several new biaryls could be accessed.[30]

Driven by curiosity why no homo-coupling product **8aa** was observed after electrolysis, the reaction of 4-methylguaiacol **8a** with trimethoxybenzene **8b** was further investigated.[31] When two aromatic components **A** and **B** are directly electrolyzed, the expected major products are the respective cross-coupling products **AA** and **BB** because the reaction outcome is determined by the electron density and therefore the nucleophilicity of the individual substrates. The compound with a higher electron density exhibits a lower oxidation potential and should therefore be preferentially oxidized at the anode. Electron density and nucleophilicity are directly linked, thus the same compound will enter the reaction sequence for a nucleophilic attack. This way, only homo-coupling products would be expected. Surprisingly, in the electrolysis of 4-methylguaiacol **8a** and trimethoxybenzene **8b** no homo-coupling of component **8a**

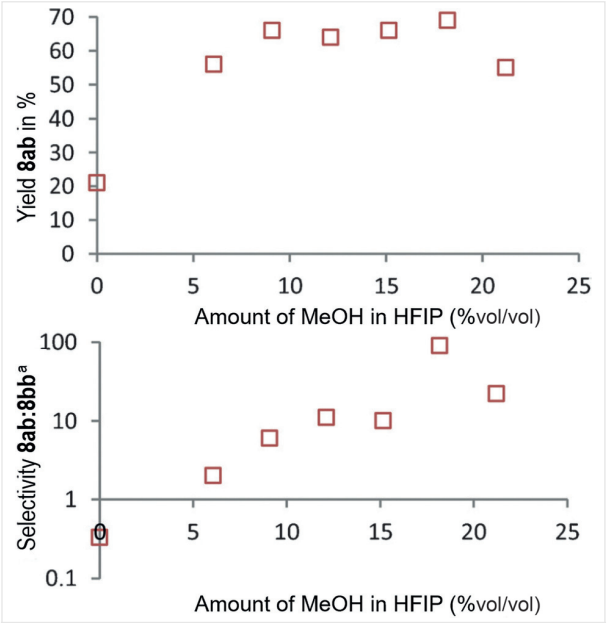

Figure 6 Yield and selectivity of **8ab** formed as a function of the amount of MeOH in HFIP. [a] Selectivity was determined by gas chromatopgraphy.[31] Adapted from ref. 31, with permission from John Wiley and Sons.

occurred. Instead, the cross-coupling product **8ab** and the homo-coupling product **8bb** were obtained, but almost without selectivity. By adding different amounts of MeOH to the electrolyte, the reaction outcome could drastically be changed (Figure 6).

The addition of methanol not just improved **8ab**'s yield distinctly but also enhanced the selectivity regarding the cross-coupling product immensely. Best results were obtained by using 18 vol% MeOH in HFIP, and **8ab** was obtained in 69% yield and exclusive selectivity. To find an explanation for these unusual findings, cyclic voltammetry experiments were conducted. These investigations indicated a clear shift of oxidation potentials in HFIP when MeOH is added to the electrolyte (Figure 7). In pure HFIP, **8b** exhibits a lower oxidation potential and should be preferentially oxidized at the anode, which is consistent with the preparative electrolysis. By addition of methanol, the oxidation potential of **8b** subsequently increases while **8a**'s potential decreases. This engenders a reversal of the oxidation potentials – **8a** now exhibits the lower oxidation potential. Nevertheless, even at 18 vol% MeOH in the electrolyte, no homo-coupling of component **8a** was observed, clearly indicating that the used solvent system must also influence the nucleophilicity of the employed substrates.

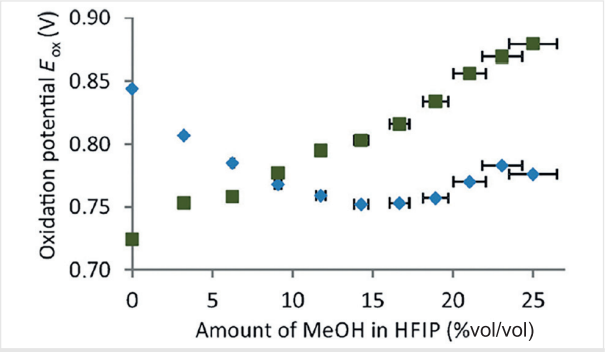

Figure 7 Shift of oxidation potentials with increasing amount of MeOH in HFIP. Blue diamonds: **8a**, green squares: **8b**. WE: glassy carbon electrode tip, 2 mm diameter; CE: glassy carbon rod; RE: Ag/AgCl in sat. LiCl/EtOH. Solvent: HFIP + 0–25 vol% MeOH. Criteria for oxidation: j = 0.1 mA/cm²; v = 50 mV/s; T = 20 °C. Stirring conditions during measurement. c(substrate) =151 mM; supporting electrolyte: 0.09 M Bu_3NMeO_3SOMe.[31] Reprinted from ref. 31, with permission from John Wiley and Sons.

According to our proposed mechanism, component **8a** is, after shifting the oxidation potentials, selectively oxidized at the anode to give phenoxyl radicals (step I, Scheme 5). Now, the solvent system prevents the nucleophilic attack of the same component in step II and thus, inhibits formation of the phenol homo-coupling product. Instead, arene component **8b** enters the reaction sequence to form the intermediate which gives, after a second oxidation step (step III) and aromatization, the desired cross-coupling product **8ab**. Needless to say that the following question came up: How is the solvent system able to keep phenol **8a** off from entering the reaction sequence in step II to form the homo-coupling product?

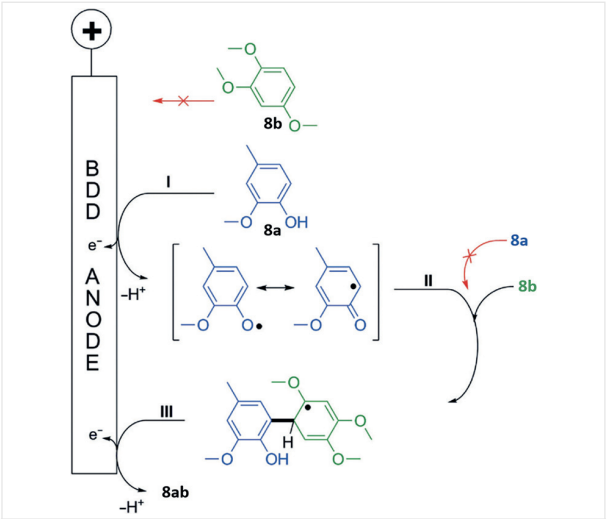

Scheme 5 Proposed mechanism for the anodic phenol–arene cross-coupling with 18 vol% MeOH in HFIP.[31] Adapted from ref. 31, with permission from John Wiley and Sons.

A possible explanation is that in polar solvents such as HFIP, phenols are stronger solvated than arenes. This applies not only to phenols but also to every substrate that is able to participate in the hydrogen bonding network mentioned before, e.g. anilides. In the present case, 1,2,4-trimethoxybenzene (**B**, Scheme 7) exhibits a lower oxidation potential in pure HFIP and is therefore oxidized at the anode. Because of its strong solvation, 4-methylguaiacol (**A**, Scheme 7) is strongly shielded by HFIP, which prevents nucleophilic attack on the radical cation of the arene. Thus, the more electron-rich arene undergoes homo-coupling. Added methanol acts like a weak base when added to the electrolyte and weakens the solvate of the phenol and simultaneously facilitates its deprotonation by interacting through hydrogen bonding. Because of the shifted potentials, phenol **A** is now oxidized at the anode and the less-shielded arene can start a nucleophilic attack – the cross-coupling product **B** is selectively formed. Thus, a decoupling of the oxidation potential from the nucleophilicity is achieved by using this unique electrolyte.[31]

Since then, many different substance classes could be utilized in the direct anodic cross-coupling reaction. By using this simple electrolysis protocol, many different product classes became easily accessible because no leaving functionalities or additional oxidizers are needed. Thus, many synthetic steps for preparing starting materials or a time- and wasteful work-up become superfluous. Furthermore, the shown anodic transformations are inherently safe and easily scalable with similar yield and selectivity.[32,33] There-

fore, the presented electrosyntheses are definitely technically relevant.[34] For example, partially protected biphenols, which formerly had to be synthesized in a multi-step process, are now accessible through a one-pot electrosynthesis (Scheme 6).[32]

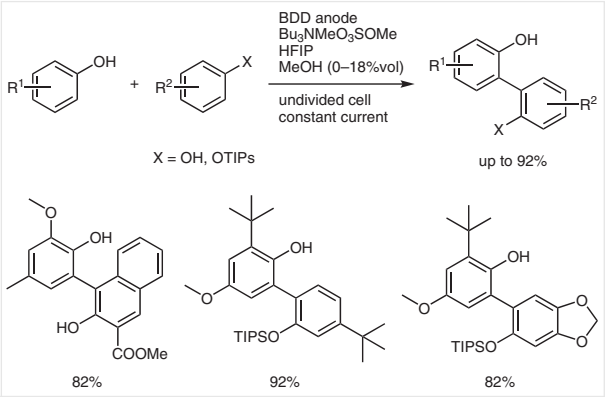

Scheme 6 Anodic formation of nonsymmetric biphenols and nonsymmetric, partially protected biphenols[32,35]

Moreover, many aniline derivatives could be applied in various cross- and homo-coupling reactions to form valuable 2,2'-diaminobiaryls, which are hardly available in classic organic synthesis because of the anilines' predisposition for polymerization.[36–38] Besides the already mentioned phenol–arene[27,30] and phenol–phenol[39] cross-couplings, a broad variety of biphenols could be synthesized (Scheme 6).[32,35] Comparison of the electrochemical approach with the same products synthesized by using chemical oxidizers demonstrated that the developed electrochemical protocol can easily compete with conventional methods.[35] Another improvement in the phenol–phenol cross-coupling could be achieved by installing a TIPS group in one of the substrates. This strategy allows the construction of partially protected biphenols, which formerly had to be synthesized in an effortful multi-step process. Moreover, the cross-coupling yield was distinctly improved. A possible explanation is the twist of the partially protected biphenol because of the bulky TIPS group and thus better stabilization by solvation in HFIP that protects the just-built product from overoxidation.[32] Additionally, the solvation features of this outstanding solvent system allow the electrosyntheses to be conducted at high as well as at lower current densities, just as needed. Several of the C–C cross-coupling reactions performed by using this technique showed an unexpected high robustness towards high current densities, which could be altered in the range of two orders of magnitude without decreasing selectivity or product yield. This extraordinary effect is yet unknown for electrochemical synthesis of products with similar oxidation potentials as the starting materials.[40]

Figure 8 shows three representative cross-coupling products, which could be synthesized by using a current density of j = 7.2 mA/cm² and j = 35 mA/cm². In the case of the *m*-terphenyl-2,2''-diol, the yield was even increased from 28 to 58% by using a higher current density.

Recent studies extended the applicability of this process to the electrochemical synthesis of protected symmetric and nonsymmetric bianiline derivatives,[36,37] *N*,*O*-biaryl structures and biaryl ethers by coupling reactions of naphthylamines with phenols[41] (Scheme 8), (2-hydroxyphenyl)benzofurans,[43] *m*-terphenyl-2,2''-diols by two-fold C–C cross-coupling,[42] and the single and two-fold C–C cross-coupling of phenols with thiophenes (Scheme 9) and benzothiophenes.[33,44]

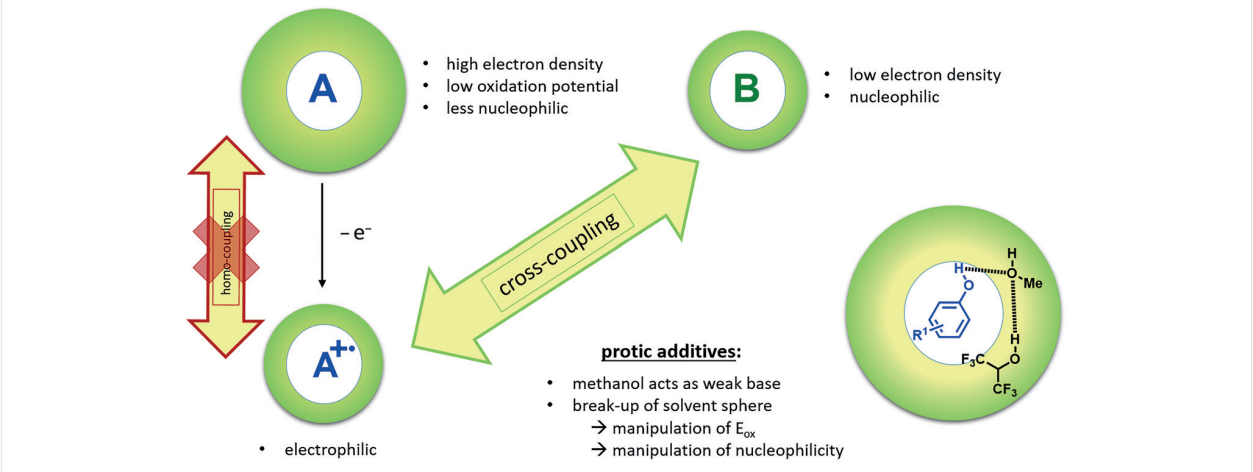

Scheme 7 Source of the selectivity in anodic cross-coupling reactions of different aryls by the solvent effect of HFIP. The color indicates the density of the solvation sphere.[30,31]

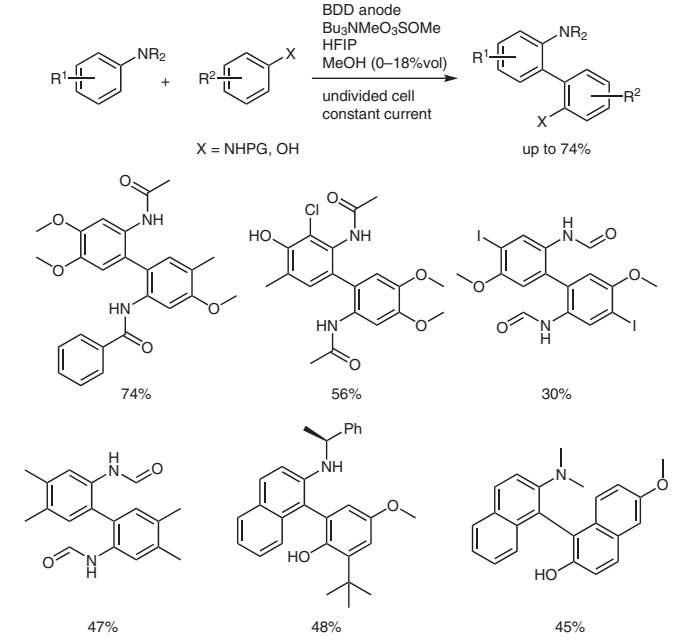

Scheme 8 Electrochemical synthesis of protected symmetric and nonsymmetric bianiline derivatives (middle row) and synthesis of *N*,*O*-biaryl structures by coupling of naphthylamines with phenols (bottom row)[36,37,41]

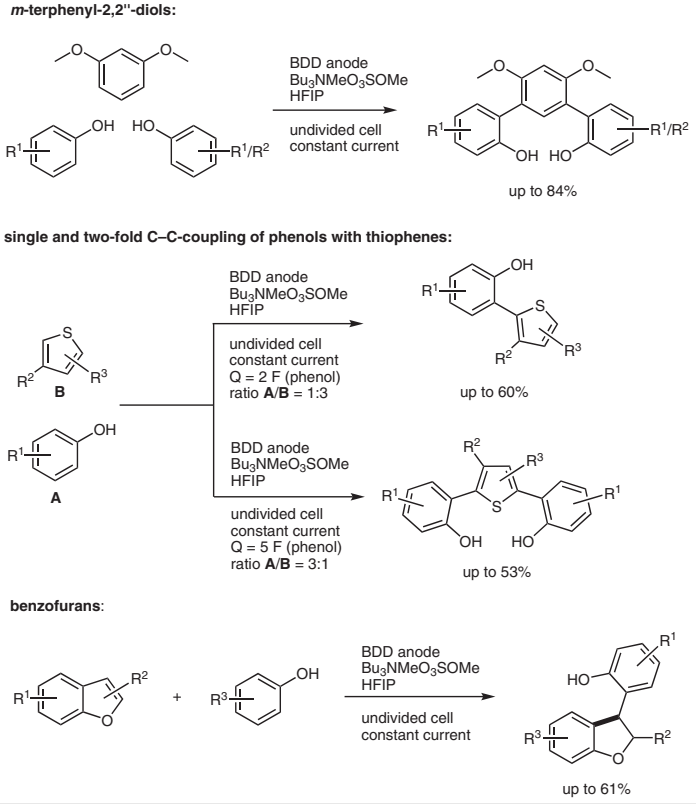

Scheme 9 Electrochemical synthesis of symmetric and nonsymmetric *m*-terphenyl-2,2''-diols (upper row), single and two-fold coupling of phenols with thiophenes (middle row), and benzofuran synthesis through metathesis (bottom row).[33,42,43]

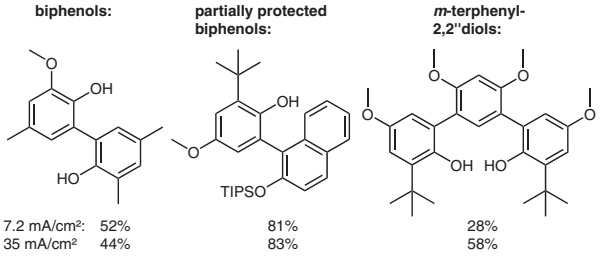

Figure 8 Comparison of C–C cross-coupling reactions at different current densities (j = 7.2 mA/cm² and 35 mA/cm²)

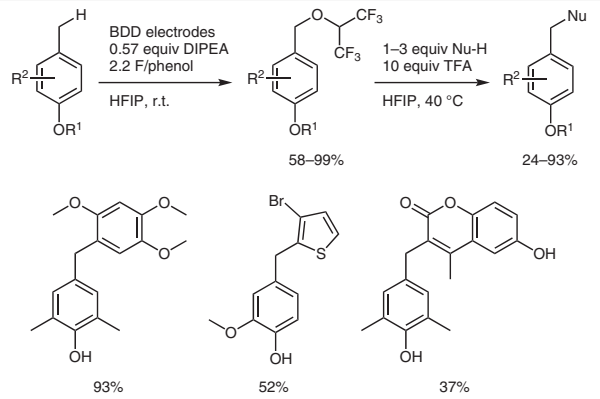

Scheme 10 Anodic benzylic functionalization of a phenol with HFIP and subsequent coupling to a nucleophile[45]

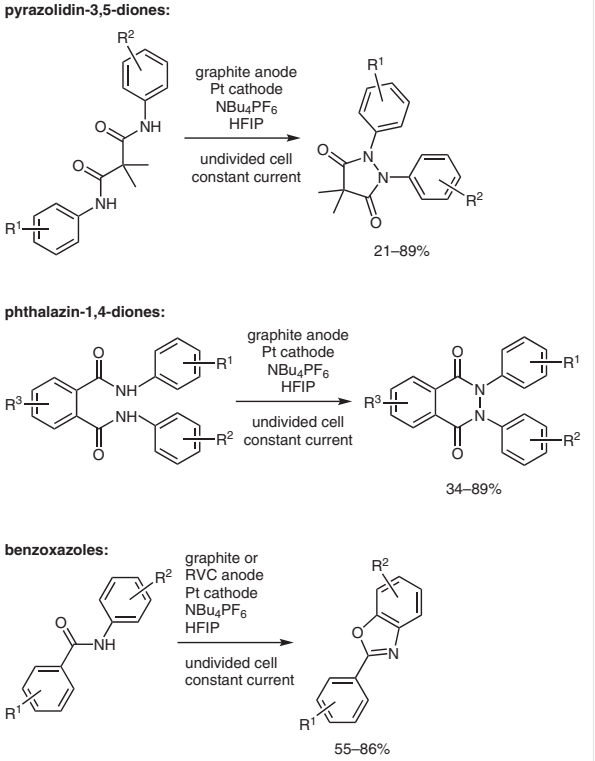

Scheme 11 Anodic synthesis of pyrazolidin-3,5-diones and phthalazin-1,4-diones and benzoxazoles through intramolecular coupling in HFIP.[46–49]

Very recently, a formal benzyl–aryl cross-coupling through an electro-generated masked benzylic cation was reported. In this conversion HFIP acts, despite its low nucleophilicity, as a nucleophile to form HFIP ethers. This method can also be used for late-stage functionalization of natural products and biologically active compounds (Scheme 10).[45]

Another emphasis of the Waldvogel group exists in the intramolecular N–N coupling through anodically generated amidyl radicals to form pyrazolidin-3,5-diones and phthalazin-1,4-diones.[46,47,49] These electro-conversions of malonic acid dianilides were only feasible in HFIP; other solvents failed or only gave traces of the desired compounds. This again underlines the exceptional, radical-stabilizing properties of HFIP. If the N–N bond formation of dianilides proceeds too slowly, a competing C–O bond formation takes place, resulting in benzoxazoles (Scheme 11).[48]

5 Conclusion

The control of the reaction pathway by suitable solvents is an efficient and effective strategy. This has been demonstrated in anodic conversions on prep-scale electrosyntheses. One of the most powerful methods implies the use of 1,1,1,3,3,3-hexafluoropropan-2-ol (HFIP) as the solvent for electrolytes. This particular medium can modulate the nucleophilicity of the substrates and is able to stabilize intermediates as well as the final product from over-oxidation. This concept and electrolytic approach will be inevitable for future electro-synthetic applications.

Funding Information

S.R.W thanks the DFG Wa1276/17-1 for financial support. The authors highly appreciate the financial support by the Center for INnovative and Emerging MAterials (CINEMA) and the support by BMBF-EPSYLON (FKZ 13XP5016D).

References

(1) (a) Fuchigami, T.; Atobe, M.; Inagi, S. *Fundamentals and Applications of Organic Electrochemistry. Synthesis Materials Devices*; John Wiley & Sons: Chichester, **2015**. (b) Möhle, S.; Zirbes, M.; Rodrigo, E.; Gieshoff, T.; Wiebe, A.; Waldvogel, S. R. *Angew. Chem. Int. Ed.* **2018**, *57*, 6018.
(2) Wiebe, A.; Gieshoff, T.; Möhle, S.; Rodrigo, E.; Zirbes, M.; Waldvogel, S. R. *Angew. Chem. Int. Ed.* **2018**, *57*, 5594.
(3) Grimshaw, J. *Electrochemical Reactions and Mechanisms in Organic Chemistry*; Elsevier: Amsterdam and New York, **2000**.

(4) *Organic Electrochemistry*; Hammerich, O.; Speiser, B., Ed.; CRC Press: Boca Raton, **2016**.
(5) (a) Chiba, K.; Kim, S. *Electrochemistry* **2009**, *77*, 21. (b) Shoji, T.; Haraya, S.; Kim, S.; Chiba, K. *Electrochim. Acta* **2016**, *200*, 290.
(6) Heinze, J.; Steckhan, E. *Top. Curr. Chem*; Springer: Berlin, **1990**, Vol. 152.
(7) Fuchigami, T.; Inagi, S. *Chem. Commun.* **2011**, *47*, 10211.
(8) Renaud, R. N.; Sullivan, D. E. *Can. J. Chem.* **1973**, *51*, 772.
(9) Kimura, K.; Horie, S.; Minato, I.; Odaira, Y. *Chem. Lett.* **1973**, *2*, 1209.
(10) (a) Rozhkov, I. N. *Russ. Chem. Rev.* **1976**, *45*, 615. (b) Laurent, E.; Marquet, B.; Tardivel, R.; Thiebault, H. *Tetrahedron Lett.* **1987**, *28*, 2359.
(11) (a) Meurs, J. H. H.; Eilenberg, W. *Tetrahedron* **1991**, *47*, 705. (b) Lee, S. M.; Roseman, J. M.; Blair Zartman, C.; Morrison, E. P.; Harrison, S. J.; Stankiewicz, C. A.; Middleton, W. J. *J. Fluorine Chem.* **1996**, *77*, 65. (c) Suryanarayanan, V.; Noel, M. *J. Fluorine Chem.* **1998**, *92*, 177.
(12) Hasegawa, M.; Ishii, H.; Fuchigami, T. *Green Chem.* **2003**, *5*, 512.
(13) (a) Eberson, L.; Hartshorn, M. P.; Persson, O. *J. Chem. Soc., Chem. Commun.* **1995**, 1131. (b) Eberson, L.; Persson, O.; Hartshorn, M. P. *Angew. Chem. Int. Ed.* **1995**, *34*, 2268.
(14) Hollóczki, O.; Berkessel, A.; Mars, J.; Mezger, M.; Wiebe, A.; Waldvogel, S. R.; Kirchner, B. *ACS Catal.* **2017**, *7*, 1846.
(15) (a) Berkessel, A.; Adrio, J. A.; Hüttenhain, D.; Neudörfl, J. M. *J. Am. Chem. Soc.* **2006**, *128*, 8421. (b) Shuklov, I.; Dubrovina, N.; Börner, A. *Synthesis* **2007**, 2925.
(16) Berkessel, A.; Adrio, J. A. *J. Am. Chem. Soc.* **2006**, *128*, 13412.
(17) Kirste, A.; Nieger, M.; Malkowsky, I. M.; Stecker, F.; Fischer, A.; Waldvogel, S. R. *Chem. Eur. J.* **2009**, *15*, 2273.
(18) Berkessel, A.; Vormittag, S. S.; Schlörer, N. E.; Neudörfl, J.-M. *J. Org. Chem.* **2012**, *77*, 10145.
(19) Seebach, D.; Beck, A. K.; Heckel, A. *Angew. Chem. Int. Ed.* **2001**, *40*, 92.
(20) Wagner, J. P.; Schreiner, P. R. *Angew. Chem. Int. Ed.* **2015**, *54*, 12274.
(21) Morofuji, T.; Shimizu, A.; Yoshida, J.-i. *Angew. Chem. Int. Ed.* **2012**, *51*, 7259.
(22) Malkowsky, I. M.; Rommel, C. E.; Fröhlich, R.; Griesbach, U.; Pütter, H.; Waldvogel, S. R. *Chem. Eur. J.* **2006**, *12*, 7482.
(23) (a) Malkowsky, I. M.; Rommel, C. E.; Wedeking, K.; Fröhlich, R.; Bergander, K.; Nieger, M.; Quaiser, C.; Griesbach, U.; Pütter, H.; Waldvogel, S. R. *Eur. J. Org. Chem.* **2006**, 241. (b) Barjau, J.; Königs, P.; Kataeva, O.; Waldvogel, S. *Synlett* **2008**, 2309. (c) Barjau, J.; Schnakenburg, G.; Waldvogel, S. R. *Angew. Chem. Int. Ed.* **2011**, *50*, 1415.
(24) Malkowsky, I. M.; Griesbach, U.; Pütter, H.; Waldvogel, S. R. *Eur. J. Org. Chem.* **2006**, 4569.
(25) (a) Montilla, F.; Michaud, P. A.; Morallón, E.; Vázquez, J. L.; Comninellis, C. *Electrochim. Acta* **2002**, *47*, 3509. (b) Morão, A.; Lopes, A.; Pessoa de Amorim, M. T.; Gonçalves, I. C. *Electrochim. Acta* **2004**, *49*, 1587.
(26) Kirste, A.; Schnakenburg, G.; Waldvogel, S. R. *Org. Lett.* **2011**, *13*, 3126.
(27) Kirste, A.; Schnakenburg, G.; Stecker, F.; Fischer, A.; Waldvogel, S. R. *Angew. Chem. Int. Ed.* **2010**, *49*, 971.
(28) Francke, R.; Cericola, D.; Kötz, R.; Weingarth, D.; Waldvogel, S. R. *Electrochim. Acta* **2012**, *62*, 372.
(29) Colomer, I.; Chamberlain, A. E. R.; Haughey, M. B.; Donohoe, T. J. *Nat. Rev. Chem.* **2017**, *1*, 88.
(30) Kirste, A.; Elsler, B.; Schnakenburg, G.; Waldvogel, S. R. *J. Am. Chem. Soc.* **2012**, *134*, 3571.
(31) Elsler, B.; Wiebe, A.; Schollmeyer, D.; Dyballa, K. M.; Franke, R.; Waldvogel, S. R. *Chem. Eur. J.* **2015**, *21*, 12321.
(32) Wiebe, A.; Schollmeyer, D.; Dyballa, K. M.; Franke, R.; Waldvogel, S. R. *Angew. Chem. Int. Ed.* **2016**, *55*, 11801.
(33) Wiebe, A.; Lips, S.; Schollmeyer, D.; Franke, R.; Waldvogel, S. R. *Angew. Chem. Int. Ed.* **2017**, *56*, 14727.
(34) Selection of patents submitted by Waldvogel et al.: (a) Dyballa, K. M.; Franke, R.; Fridag, D.; Waldvogel, S. R.; Elsler, B. PCT Int. Appl. WO 2014135236 A1 20140912, Ger. Offen. 2014 DE 102013203865 A1 20140911, US Patent 9,879,353, **2014**. (b) Dyballa, K. M.; Franke, R.; Fridag, D.; Waldvogel, S. R.; Elsler, B. PCT Int. Appl. WO 2014135405 A1 20140912, Ger. Offen. 2014 DE 102013203867 A1 20140911, **2014**. (c) Dyballa, K. M.; Franke, R.; Fridag, D.; Waldvogel, S. R.; Elsler, B. PCT Int. Appl WO 2014135237 A1 20140912, Ger. Offen. DE 102013203866 A1 20140911, **2014**. (d) Dyballa, K. M.; Franke, R.; Fridag, D.; Waldvogel, S. R.; Elsler, B.; Enders, M. PCT Int. Appl , WO 2016034332 A1 20160310, **2016**. (e) Dyballa, K. M.; Franke, R.; Fridag, D.; Waldvogel, S. R.; Elsler, B.; Enders, M. PCT Int. Appl WO 2016034330 A1 20160310, **2016**. (f) Dyballa, K. M.; Franke, R.; Fridag, D.; Waldvogel, S. R.; Elsler, B.; Enders, M. PCT Int. Appl WO 2016034327, **2016**. (g) Dyballa, K. M.; Franke, R.; Fridag, D.; Waldvogel, S. R.; Elsler, B.; Enders, M. PCT Int. Appl WO 2016034328 A1 20160310, **2016**. (h) Dyballa, K. M.; Franke, R.; Fridag, D.; Waldvogel, S. R.; Elsler, B.; Wiebe, A. Ger. Offen DE 102015207280 A1 20160303, **2016**. (i) Dyballa, K. M.; Franke, R.; Fridag, D.; Waldvogel, S. R.; Elsler, B.; Enders, M. Ger. Offen. DE 102014217537 A1 20160303, **2016**. (j) Dyballa, K. M.; Franke, R.; Fridag, D.; Waldvogel, S. R.; Elsler, B.; Wiebe, A. Eur. Pat. Appl EP 3133054 A1 20170222, **2017**. (k) Dyballa, K. M.; Franke, R.; Fridag, D.; Waldvogel, S. R.; Elsler, B.; Wiebe, A. Ger. Offen DE 102015215995 A1 20170223, **2017**. (l) Dyballa, K. M.; Franke, R.; Fridag, D.; Waldvogel, S. R.; Elsler, B.; Wiebe, A. Ger. Offen. DE 102015215997 A1 20170223, **2017**. (m) Dyballa, K. M.; Franke, R.; Fridag, D.; Waldvogel, S. R.; Elsler, B.; Wiebe, A. Ger. Offen DE 102015215998 A1 20170223, **2017**. (n) Dyballa, K. M.; Franke, R.; Fridag, D.; Waldvogel, S. R.; Elsler, B.; Wiebe, A.; Lips, S. Eur. Pat. Appl. EP 3133189 A1 20170222, **2017**. (o) Dyballa, K. M.; Franke, R.; Fridag, D.; Dahms, B.; Waldvogel, S. R. Eur. Pat. Appl EP 3252033 A1 20171206, **2017**. (p) Waldvogel, S. R.; Dahms, B.; Franke, R. Eur. Pat. Appl. EP 17203772.3, **2018**. (q) Waldvogel, S. R.; Frontana-Uribe, B. A.; Wiebe, A.; Lips, S.; Franke, R. Eur. Pat. Appl EP 17203773.1, **2018**.
(35) Riehl, B.; Dyballa, K.; Franke, R.; Waldvogel, S. *Synthesis* **2016**, *49*, 252.
(36) Schulz, L.; Enders, M.; Elsler, B.; Schollmeyer, D.; Dyballa, K. M.; Franke, R.; Waldvogel, S. R. *Angew. Chem. Int. Ed.* **2017**, *56*, 4877.
(37) Schulz, L.; Franke, R.; Waldvogel, S. R. *ChemElectroChem* **2018**, *5*, 2069.
(38) Mohilner, D. M.; Adams, R. N.; Argersinger, W. J. *J. Am. Chem. Soc.* **1962**, *84*, 3618.
(39) Elsler, B.; Schollmeyer, D.; Dyballa, K. M.; Franke, R.; Waldvogel, S. R. *Angew. Chem. Int. Ed.* **2014**, *53*, 5210.
(40) Wiebe, A.; Riehl, B.; Lips, S.; Franke, R.; Waldvogel, S. R. *Science Advances* **2017**, *3*, eaao3920/1.
(41) Dahms, B.; Franke, R.; Waldvogel, S. R. *ChemElectroChem* **2018**, *5*, 1249.
(42) Lips, S.; Wiebe, A.; Elsler, B.; Schollmeyer, D.; Dyballa, K. M.; Franke, R.; Waldvogel, S. R. *Angew. Chem. Int. Ed.* **2016**, *55*, 10872.
(43) Lips, S.; Frontana-Uribe, B. A.; Dörr, M.; Schollmeyer, D.; Franke, R.; Waldvogel, S. R. *Chem. Eur. J.* **2018**, *24*, 6057.

(44) Lips, S.; Schollmeyer, D.; Franke, R.; Waldvogel, S. R. *Angew. Chem. Int. Ed.* **2018**, *57*, 13325.
(45) Imada, Y.; Röckl, J. L.; Wiebe, A.; Gieshoff, T.; Schollmeyer, D.; Chiba, K.; Franke, R.; Waldvogel, S. R. *Angew. Chem. Int. Ed.* **2018**, *57*, 12136.
(46) Gieshoff, T.; Schollmeyer, D.; Waldvogel, S. R. *Angew. Chem. Int. Ed.* **2016**, *55*, 9437.
(47) Kehl, A.; Gieshoff, T.; Schollmeyer, D.; Waldvogel, S. R. *Chem. Eur. J.* **2018**, *24*, 590.
(48) Gieshoff, T.; Kehl, A.; Schollmeyer, D.; Moeller, K. D.; Waldvogel, S. R. *Chem. Commun.* **2017**, *53*, 2974.
(49) Gieshoff, T.; Kehl, A.; Schollmeyer, D.; Moeller, K. D.; Waldvogel, S. R. *J. Am. Chem. Soc.* **2017**, *139*, 12317.

Outstandingly robust anodic dehydrogenative aniline coupling reaction

Lara Schulz,[1] Jan-Åke Husmann,[1] Siegfried R. Waldvogel*[1]

* Corresponding author: waldvogel@uni-mainz.de

[1] Institute of Organic Chemistry, Johannes Gutenberg University Mainz, Duesbergweg 10-14, 55128 Mainz, Germany

Abstract

Oxidative treatment of anilines usually leads to the formation of black polymers, often referred to as “aniline black”. This overoxidation is hardly controllable and also a challenging task in the anodic conversion of anilines. Here, a quick and efficient access to valuable building blocks by anodic cross- and homo-coupling of aniline and benzidine derivatives is reported. This electrosynthesis is easily performed in a simple undivided cell using constant current conditions. The key to the observed outstanding performance and robustness of this system is attributed to the used solvent 1,1,1,3,3,3-hexafluoroisopropanol. The extraordinary performance over a broad range of current density is unprecedented for reactions involving extremely oxidation labile substrates such as anilines and their derivatives.

anilines ● anode ● current density ● electrolysis ● oxidative coupling

TOC:

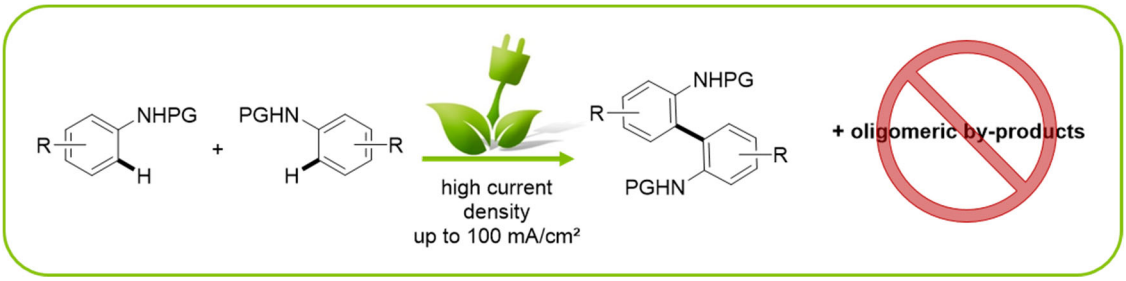

1

1. Introduction

In recent years, electrochemistry has again gained significant importance, in research as well as in industrial processes. Especially, electrosynthetic transformations became more and more popular in developing green and sustainable processes for synthesizing a broad variety of substance classes [1,2]. Because of the mild reaction conditions, electrochemistry benefits from its high functional group tolerance and chemoselective transformations. Furthermore, electrochemistry exhibits a better atom economy than conventional organic synthesis and is therefore remarkably progressive in terms of avoiding reagent waste. In particular, in times of advancing climate change and dwindling resources, it is becoming increasingly important to strive for alternatives to existing, often polluting and outdated processes for a more sustainable use of existing resources. However, renewable energy production from wind power or photovoltaics often generate large surplus electricity, which requires storage in order to compensate a higher demand at a later point.

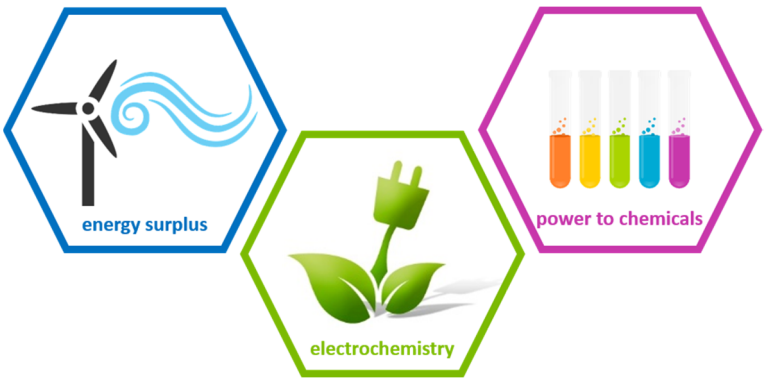

Figure 1: Power to chemicals by electrochemistry – a sustainable and straightforward approach to exploit energy surplus caused by renewable energy resources.

This requires more efficient energy storage in order to compensate the differing supply and demand for electricity. In addition to large mechanical storage devices, such as pumped hydro

power plants, the storage of electrical energy in chemical bonds is also feasible. The energy is therefore stored in substances that can later serve as energy sources or chemicals. In this context, the electrolysis of water to hydrogen and oxygen is often mentioned. However, the direct use of surplus electricity for the production of basic or fine chemicals is also an attractive method for energy valorization [3,4]. In particular, the electrochemical C,C bond formation between aromatic subunits is an attractive method for the preparation of valuable fine chemicals.

Though constant-potential experiments exhibit a high selectivity by specifically addressing one substrate's electric potential, the major drawback is the continuously decreasing current because of depletion of the starting material in the course of conversion. This leads to a prolonged electrolysis, if a complete conversion is desired. If the electrosynthesis is conducted in a constant-current mode, only a simple two-electrode setup is needed. In this case, no expensive reference electrode and sophisticated electronic periphery is required. In addition, large quantities of starting material can be converted in a decent time scale. Especially for technical applications, the basic cell design with an affordable current source and the use of high current densities is highly attractive. Usually, the majority of electrosynthetic processes are rather limited to low current densities of 0.5 to 5 mA/cm² or less and are restricted to a rather small current density window [5–7]. Exceeding this window leads to emerging side reactions or no desired conversion at all. High current density is only used for conversions where electrochemically resilient products are formed like in the Kolbe electrolysis or Monsanto's Baizer process [8,9]. Future applications of electrosynthesis for energy storage will need robust transformations that can easily digest fluctuations in the lectric power used.

In our group it was found that the electrosyntheses of (partially protected) biphenols and *m*-terphenyl-2,2''-diols is unexpectedly robust and can be conducted in a broad range of current density [10]. Other attempts to use high electric currents are e.g. the use of macroporous electrodes to maximize the available electrode surface, [11–15] electrolysis in biphasic systems [16] or utilization of mediating systems in equimolar quantity [17]. Here we report the extraordinary electrochemical synthesis of 2,2'-diaminobiaryls and *meta*-terphenyl amines by anodic coupling of aniline and benzidine derivatives. Such amino-substituted bi- or teraryls are highly valuable building blocks for organocatalysts, ligands, functionalized materials or biologically active molecules. [18–20] In conventional chemistry these substance classes are synthesized via complicated multi-step or transition metal-catalyzed processes that have a poor atom economy and generate large amounts of reagent waste [21–25]. The electrochemical protocol provides the desired products in good yields and selectivity without the need of pre-functionalized substrates and is therefore remarkably advanced in sustainability.

2. Experimental

2.1. Experimental Procedure for Electroorganic Homo-Coupling Reaction

If not stated otherwise, the following standard reaction parameters were employed in the electrolyses:

For each reaction, the respective substrate **A** (0.75 mmol) and methyltributylammonium methyl sulfate (MTBS, 0,5 mmol, 154 mg) were dissolved in HFIP (5.0 mL). Undivided Teflon electrolysis cells (self-made [26] or purchased from IKA-Werke GmbH & Co KG, Staufen,

Germany) equipped with glassy carbon (Sigradur® G, obtained from HTW Hochtemperaturwerkstoffe GmbH, Thierhaupten, Germany), boron-doped diamond (Diachem®, 15 µm boron-doped diamond layer on 3 mm silicon support, obtained from Condias GmbH, Itzehoe, Germany), isostatic graphite (SIGRAFINE® V2100, SGL Carbon, Bonn-Bad Godesberg, Germany) or platinum electrodes (99.9% Pt, Ögussa Ges.mbH, Vienna, Austria) were used. The electrodes (10x70x3 mm) were immersed into the electrolyte and a constant current electrolysis with a current density of 1.0 F per aniline **A** was performed at 50 °C. After electrolysis, the residual mixture was analyzed by GC and GC/MS using 3,3',5,5'-tetramethyl2,2'-biphenol as internal standard. The scale-up protocol can be found within the supporting information.

2.2. Experimental Procedure for Electroorganic Cross-Coupling Reaction

For each reaction, the respective protected benzidine compound **A** (0.375 mmol), protected aniline compound **B** (1.125 mmol, 3 eq.) and methyltributylammonium methyl sulfate (MTBS, 0,5 mmol, 154 mg) were dissolved in HFIP (5.0 mL). Undivided Teflon electrolysis cells (self-made [26] or purchased from IKA-Werke GmbH & Co KG, Staufen, Germany) equipped with glassy carbon electrodes (Sigradur® G, obtained from HTW Hochtemperaturwerkstoffe GmbH, Thierhaupten, Germany). The electrodes (10x70x3 mm) were immersed into the electrolyte and a constant current electrolysis with a current density of 4.0 F per benzidine **A** was performed at 50 °C. After electrolysis, the solvent mixture was recovered *in vacuo* (50 °C, 200–70 mbar). The crude coupling products were purified by column chromatography (SiO_2, cyclohexane/ethyl acetate).

2.3. Characterization

The spectral data for purified compounds were recorded on a multi nuclear magnetic resonance spectrometer of the type AV II 400 (Bruker, analytic measuring technique, Karlsruhe, Germany). The chemical shifts were referenced on δ-value in ppm of the residue signal of the deuterated solvent ($CDCl_3$: ^{1}H = 7.26 ppm, ^{13}C = 77.2 ppm; d_6-DMSO: ^{1}H = 2.50 ppm, ^{13}C = 39.520 ppm).

Reaction mixtures and purified products were analyzed *via* gas chromatography, for which a GC-2010 (Shimadzu, Japan) was used. The column was a quartz capillary column ZB-5 (length: 30 m, inner diameter: 0.25 mm, layer thickness of the stationary phase: 0.25 µm, carrier gas: hydrogen, stationary phase: (5% phenyl)-methylpolysiloxane, Phenomenex, USA). The detector was a flame ionization detector (FID) with a temperature of 310 °C. The injector temperature was 250 °C with a linear carrier gas rate of 45.5 $cm \cdot s^{-1}$. Further gas-chromatographic mass spectra (GC-MS) were recorded using a GC-2010 combined with a mass detector GCMS-QP2010 (Shimadzu, Japan). It had a similar quartz capillary column ZB-5 (length: 30 m, inner diameter: 0.25 mm, layer thickness of the stationary phase: 0.25 µm, carrier gas: hydrogen, stationary phase: ((5% phenyl)-methylpolysiloxane, Phenomenex, USA), whereas the ion source had a temperature of 200 °C. The method "hart" (starting temperature: 50 °C, heating rate: 15 °C/min, end temperature: 290 °C for 8 min) was used for the GC-spectra measurements.

For high-resolution electrospray ionization (ESI) mass spectrometry measurements, an Agilent 6545 Q-ToF MS was utilized.

For standard liquid chromatography separation silica gel 60 M (0.040- 0.063 mm Macherey-Nagel GmbH & Co., Düren, Germany) was used. An automatic silica flash column chromatography system was used, which consists of a control unit C-620, a fraction collector C-660 and a UV photometer C-635 (Büchi, Flawil, Switzerland). Thin-layer-chromatography was performed using "DC Kieselgel 60 F254" (Merck KGaA, Darmstadt, Germany) on aluminum and a UV lamp (Konrad Benda Laborgeräte, NU-4 KL, λ = 254 nm, Wiesloch, Germany). The resulting retention factors (R_f) are given in relation to the solvent ratio.

3. Results and Discussion

3.1. Optimization of the Homo-Coupling of *N*-(3,4-Dimethylphenyl)formamide

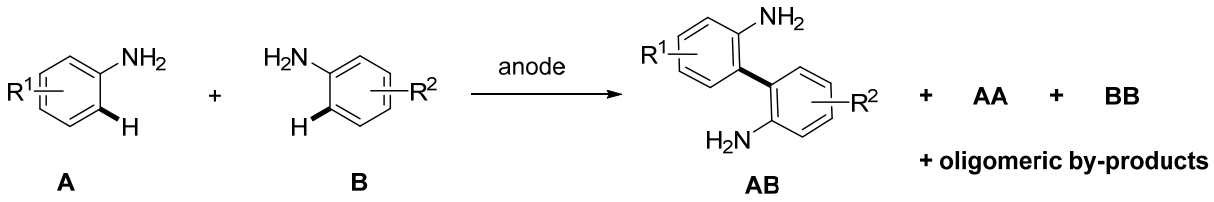

Scheme 1: The direct oxidation of aniline derivatives usually leads to a complex reaction mixture and lots of oligomeric by-products.

The anodic synthesis of symmetric and non-symmetric 2,2'-diaminobiaryls by direct electrolysis of protected anilines as simple starting materials was already established [27,28]. No leaving groups or expensive catalysts are required and only a simple two-electrode arrangement in a beaker-type cell is needed for this exceptional conversion. The best yield and selectivity are obtained in 1,1,1,3,3,3-hexafluoroisopropanol (HFIP). Studies in our group revealed that HFIP has the outstanding ability to not only stabilize ocurring charged intermediates, but also to protect the desired products from over-conversion. This is due to HFIP's special microheterogeneous structure and the distinctly different solvation of the

coupling partners as well as occuring intermediates and the products [29,30]. Thus, side reactions like oligo- and polymerization and for cross-coupling reactions, the formation of homo-coupling products can be diminished (Scheme 1).

In earlier investigations, the anodic coupling of protected anilines was mostly limited to highly electron-rich derivatives [27]. By using the formyl-group to protect the amine function, also less electron-rich anilines like iodo-substituted derivatives or *N*-(3,4-dimethylphenyl)-formamide could successfully be converted [28]. Due to the lower electron density starting material, the used electrolysis parameters can be adjusted and optimized in a broader range than in the coupling of electron-rich substrates, which are very prone to overoxidation and polymerization. Here, we report the optimization of the dehydrogenative homo-coupling of *N*-(3,4-dimethylphenyl)formamide. Scheme 2 shows the previously used standard parameters, with which the homo-coupling product **XX1AA** could be obtained in 47% yield [28].

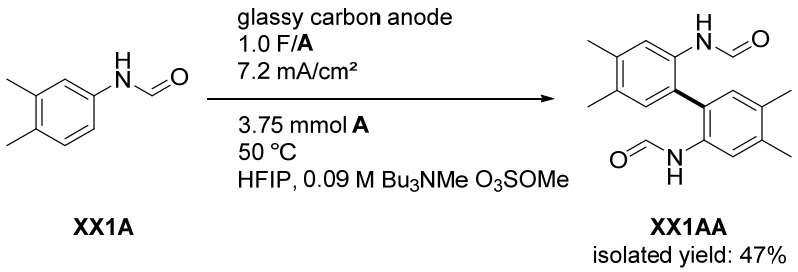

Scheme 2: Standard reaction parameters for the homo-coupling of protected aniline derivatives.

Table 1 summarizes the investigated parameters and in which range they were tested. A complete list of all experiments carried out can be found in the supporting information. In the following, the influence of the current density is discussed exemplarily, which had the most

interesting and unexpected impact on the presented electrochemical reaction. In general, all common electrode materials can be used for this transformation, but it was found that on glassy carbon the least electropolymerization takes place [27].

Table 1: Variation of parameters in the anodic homo-coupling of N-(3,4-dimethylphenyl)formamide. BDD = boron-doped diamond.

Parameter	Investigated range
Substrate concentration	0.15–0.6 mol/L
Amount of charge	1.0–2.0 F/A
Current density	3.9–100 mA/cm²
Additives	MeOH, H_2O
Temperature	30–50 °C
Electrode material	glassy carbon, graphite, BDD, platinum

High current densitities lead to improved space-time yields and are therefore, highly interesting for technical applications. However, high electron densities are associated with an increased rate of heterogeneous electron transfer at the electrodes, which may also promote side reactions. Various phenol couplings in our group have already shown that the anodic coupling process can be performed over a wide range of current densities [10]. Due to the high susceptibility of anilines to overoxidation and polymerization, [31,32] the use of high current densities is rather unusual. The influence of the current density on the homo-coupling of **XX1A** was investigated in the range of 3.9–100 mA/cm². Very high current densities of

250 mA/cm² and more are usually used only for the Kolbe electrolysis, where a high radical density is required to favor the recombination of two alkyl radicals [33]. Electrosynthetical reactions, such as the aniline coupling, which require higher selectivity and are not based on the recombination of two radicals, are usually performed at much lower current densities of 10 mA/cm² and below [27,28]. That is even more surprising that the aniline homo-coupling investigated here gives the desired product in good yields even at a high current density in the range of 50–100 mA/cm² (Figure 2).

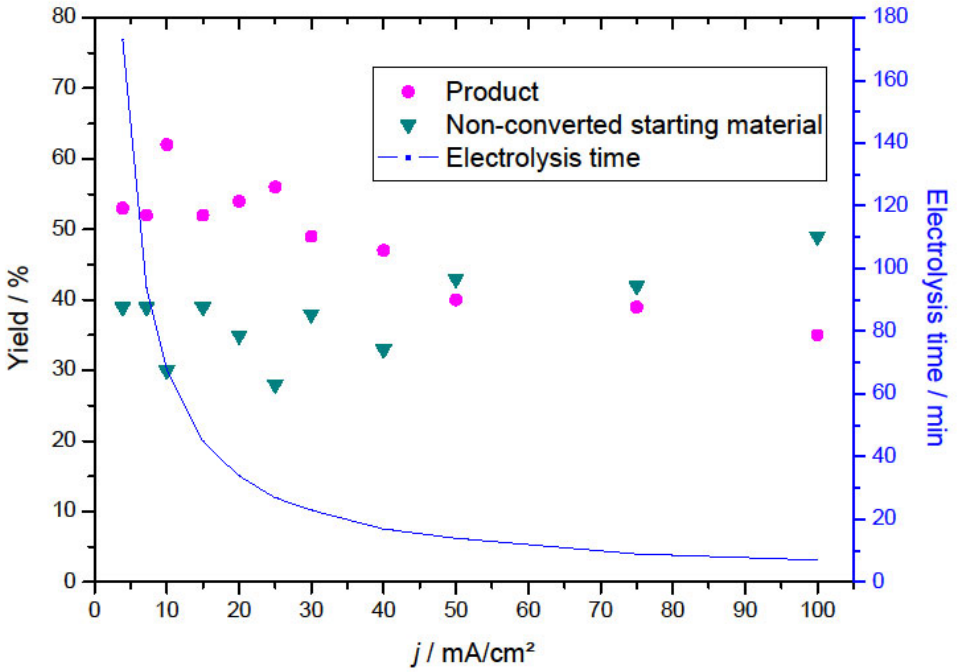

*Figure 2: Influence of the applied current density. Anode/cathode: glassy carbon, Q=1.0 F, j=3.9–100 mA/cm², 0.75 mmol **A**, T=50 °C, solvent: 5 mL HFIP + 0.09 m $Bu_3NMe\ OSO_3Me$. *GC-yield, determined by using 3,3‘,5,5‘-tetramethyl-2,2’-biphenol as internal standard.*

However, the maximum yield is achieved at a current density of 10 mA/cm². The amount of non-converted starting material increases with increasing current density and can thus be recycled after reaction and is not lost to polymerization. Figure 2 illustrates that the reaction is stable over a very wide range of current density. If the screening reaction is carried out at a

current density of 100 mA/cm² instead of the previously used 7.2 mA/cm², the reaction time is shortened from 1.5 h to less than 7 min.

Table 2: Scale-up with combinations of various optimized parameters.

Entry	Current density/ mA/cm²	Applied Charge/ F	*Substrate Concentration*/ mol	Yield XX1AA/%*	Non-converted starting material XX1A/%*
1	10	1.35	0.15	57	17
2	10	1.5	0.15	64	13
3[1]	10	1.5	0.15	63	13
4	25	1.5	0.15	47	16
5[2]	100	1.0	0.15	25	44
6[2]	100	1.5	0.15	29	33

Electrodes: glassy carbon, *T*=40 °C, solvent: 25 mL HFIP + 0.09 M MTBS. *Isolated yield. [1]Electrodes: graphite. [2]Solvent: 5 mL HFIP + 0.09 M MTBS, *T*=20 °C.

Subsequently, some of the optimized parameters were combined in further screening reactions (see supporting information) and the most successful experiments were scaled-up to 3.75 mmol starting material in 25 mL solvent. Table 2 shows the scale-up experiments performed and the corresponding isolated yields. By optimization of the homo-coupling of *N*-(3,4-dimethylphenyl)formamide, the isolated yield could be increased from 47% to 64% (Scheme 3). With current densities of 100 mA/cm², the product could still be isolated in 29% yield.

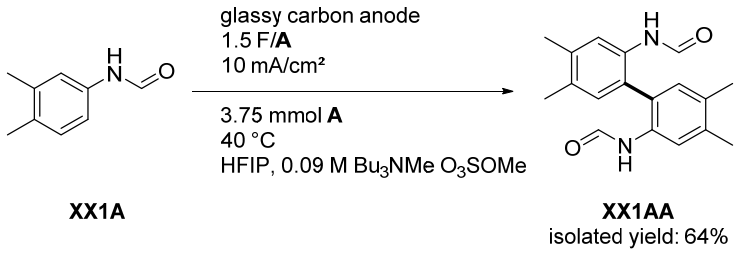

Scheme 3: Optimized conditions for the anodic dehydrogenative homo-coupling of N-(3,4-dimethylphenyl)formamide.

3.2. Cross-Coupling of protected benzidine and aniline derivatives

Besides the optimization of the homo-coupling of less electron-rich derivatives, the first cross-coupling of benzidine derivatives with protected anilines is reported. Using this protocol, amino-substituted terphenyl analogues can easily be synthesized. *Meta*-terphenyl amines have already been tested for their applicability as cyclooxygenase inhibitors, [34] and amino-substituted *para*-terphenyl derivatives can be used as α-helix mimetics. [35]

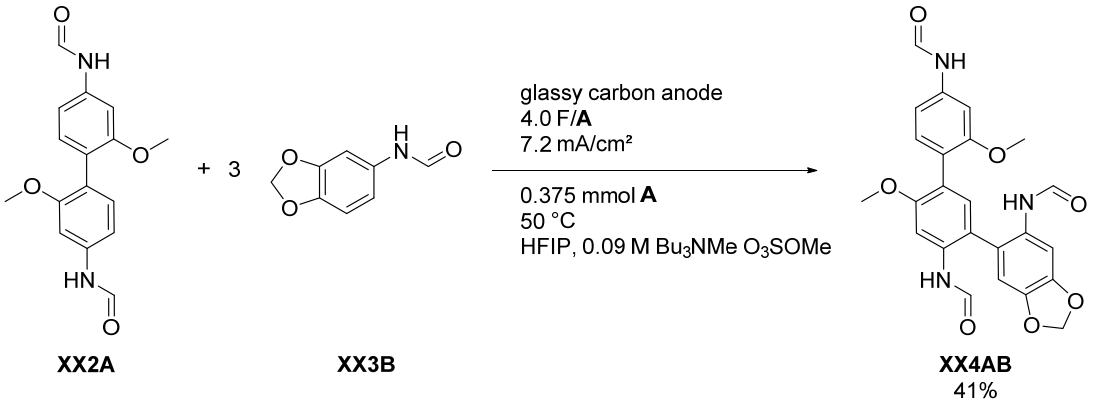

*Scheme 4: Anodic dehydrogenative cross-coupling of benzidine derivative **XX2A** with aniline derivatives.*

Benzidine derivative **XX2A** could succesfully be coupled with protected aniline **XX3B** in 41% yield. The outstanding solvent effect of HFIP is crucial for the selectivity of this reaction and already described for various reactions [29,36]. The formyl groups can easily be removed by

standard procedures which enables the later use of such protected terphenylamines as valuable building blocks in organocatalysts, ligands or functionalized materials. [18–20,37]

4. Conclusions

Using the exceptional solvent properties of HFIP-based electrolytes allows both, the selective cross-coupling of protected benzidine derivatives with anilines and the application of very high electron densities up to 100 mA/cm² for the homo-coupling of *N*-(3,4-dimethylphenyl)formamide. Thanks to HFIP's outstanding performance, the conversion of aniline derivatives is feasible within a broad range of current densities and therefore easily adaptable to existing or lacking energy surplusses caused by renewable energy sources because the electrolyses can easily be turned off and continued later. By using high current densities, the reaction time can enormously be shortened or the used electrolysis set-up scaled-down. Thus, the electrolytic transformation is almost independent from the used equipment and therefore easily realizable for both, academics and industry.

Acknowledgements

S.R.W. thanks the DFG (WA1276/17-1) for funding.

References

[1] A. Wiebe, T. Gieshoff, S. Möhle, E. Rodrigo, M. Zirbes, S.R. Waldvogel, Angew. Chem. Int. Ed. 57 (2018) 5594–5619.

[2] S. Möhle, M. Zirbes, E. Rodrigo, T. Gieshoff, A. Wiebe, S.R. Waldvogel, Angew. Chem. Int. Ed. 57 (2018) 6018–6041.

[3] M. Sterner, I. Stadler (Eds.), Energiespeicher - Bedarf, Technologien, Integration, 2nd ed., Springer, Berlin, Heidelberg, 2017.

[4] A. Sternberg, A. Bardow, Energy Environ. Sci. 8 (2015) 389–400.

[5] T. Gieshoff, D. Schollmeyer, S.R. Waldvogel, Angew. Chem. Int. Ed. 55 (2016) 9437–9440.

[6] Y. Shih, C. Ke, C. Pan, Y. Huang, RSC Adv. 3 (2013) 7330.

[7] H. Salehzadeh, D. Nematollahi, H. Hesari, Green Chem. 15 (2013) 2441.

[8] H.J. Schäfer, C. R. Chim. 14 (2011) 745–765.

[9] O. Hammerich, B. Speiser (Eds.), Organic Electrochemistry, 5th ed., CRC Press, Boca Raton, London, New York, 2016.

[10] A. Wiebe, B. Riehl, S. Lips, R. Franke, S.R. Waldvogel, Sci. Adv. 3 (2017) eaao3920/1-7.

[11] E.J. Horn, B.R. Rosen, Y. Chen, J. Tang, K. Chen, M.D. Eastgate, P.S. Baran, Nature 533 (2016) 77–81.

[12] J. Mihelcic, K.D. Moeller, J. Am. Chem. Soc. 126 (2004) 9106–9111.

[13] T. Morofuji, A. Shimizu, J.-i. Yoshida, J. Am. Chem. Soc. 135 (2013) 5000–5003.

[14] T. Morofuji, A. Shimizu, J.-i. Yoshida, J. Am. Chem. Soc. 136 (2014) 4496–4499.

[15] T. Morofuji, A. Shimizu, J.-i. Yoshida, J. Am. Chem. Soc. 137 (2015) 9816–9819.

[16] P. Krishnan, V.G. Gurjar, J. Appl. Electrochem. 23 (1993).

[17] R. Rastogi, G. Dixit, K. Zutshi, Electrochim. Acta 29 (1984) 1345–1347.

[18] T. Kinzel, Y. Zhang, S.L. Buchwald, J. Am. Chem. Soc. 132 (2010) 14073–14075.

[19] Y. Yang, S.K. Seidlits, M.M. Adams, V.M. Lynch, C.E. Schmidt, E.V. Anslyn, J.B. Shear, J. Am. Chem. Soc. 132 (2010) 13114–13116.

[20] S. Handa, L.M. Slaughter, Angew. Chem. Int. Ed. 51 (2012) 2912–2915.

[21] G.-Q. Li, H. Gao, C. Keene, M. Devonas, D.H. Ess, L. Kürti, J. Am. Chem. Soc. 135 (2013) 7414–7417.

[22] B.-Y. Lim, M.-K. Choi, C.-G. Cho, Tetrahedron Lett. 52 (2011) 6015–6017.

[23] Y.-K. Lim, J.-W. Jung, H. Lee, C.-G. Cho, J. Org. Chem. 69 (2004) 5778–5781.

[24] W. Kalk, H.-S. Bien, K.-H. Schündehütte, Liebigs Ann. Chem. (1977) 329–337.

[25] C. Mei, W. Lu, J. Org. Chem. 83 (2018) 4812–4823.

[26] C. Gütz, B. Klöckner, S.R. Waldvogel, Org. Process Res. Dev. 20 (2015) 26–32.

[27] L. Schulz, M. Enders, B. Elsler, D. Schollmeyer, K.M. Dyballa, R. Franke, S.R. Waldvogel, Angew. Chem. Int. Ed. 56 (2017) 4877–4881.

[28] L. Schulz, R. Franke, S.R. Waldvogel, ChemElectroChem 5 (2018) 2069–2072.

[29] B. Elsler, A. Wiebe, D. Schollmeyer, K.M. Dyballa, R. Franke, S.R. Waldvogel, Chem. Eur. J. 21 (2015) 12321–12325.

[30] O. Hollóczki, A. Berkessel, J. Mars, M. Mezger, A. Wiebe, S.R. Waldvogel, B. Kirchner, ACS Catal. 7 (2017) 1846–1852.

[31] H. Letheby, J. Chem. Soc. 15 (1862) 161–163.

[32] D.M. Mohilner, R.N. Adams, W.J. Argersinger, J. Am. Chem. Soc. 84 (1962) 3618–3622.

[33] J. Heinze, E. Steckhan (Eds.), Electrochemistry IV: Topics in current chemistry, Springer, Berlin, 1990.

[34] J.D. Bauer, M.S. Foster, J.D. Hugdahl, K.L. Burns, S.W. May, S.H. Pollock, H.G. Cutler, S.J. Cutler, Med. Chem. Res. 16 (2007) 119–129.

[35] M. Peters, M. Trobe, H. Tan, R. Kleineweischede, R. Breinbauer, Chem. Eur. J. 19 (2013) 2442–2449.

[36] L. Schulz, S. Waldvogel, Synlett 30 (2019) 275–286.

[37] P.G.M. Wuts, T.W. Greene, Greene's Protective Groups in Organic Synthesis, John Wiley & Sons, Inc, Hoboken, NJ, USA, 2006.

Supporting Information

Outstandingly robust anodic dehydrogenative aniline coupling reaction

Lara Schulz,[1] Jan-Åke Husmann,[1] Siegfried R. Waldvogel*[1]

[1] Institute of Organic Chemistry, Johannes Gutenberg University Mainz, Duesbergweg 10-14, 55128 Mainz, Germany

General Remarks

All reagents were used in analytical grades without further purification. Solvents were purified by standard methods [1]. As supporting electrolyte *N*-methyl-*N,N,N*-tributylammonium methylsulfate was used (MTBS, kindly provided by BASF SE, Ludwigshafen, Germany). For electrochemical reactions glassy carbon (SIGRADUR® G, obtained from HTW Hochtemperaturwerkstoffe GmbH, Thierhaupten, Germany), boron-doped diamond (DIACHEM®, 15 µm boron-doped diamond layer on 3 mm silicon support; obtained from CONDIAS GmbH, Itzehoe, Germany), isostatic graphite (SIGRAFINE® V2100; obtained from SGL Carbon, Bonn-Bad Godesberg, Germany) and platinum electrodes (99.9% Pt, ÖGUSSA GES.mbH, Vienna, Austria) were applied.

Column chromatography was performed on silica gel 60 M (0.040–0.063 mm, Macherey-Nagel GmbH & Co, Düren, Germany) with a maximum pressure of 1.6 bar. As eluents mixtures of cyclohexane and ethyl acetate were used. Silica gel 60 sheets on aluminum (F254, Merck, Darmstadt, Germany) were employed for thin layer chromatography.

Gas chromatography was performed with a Shimadzu GC-2010 (Shimadzu, Japan) using a ZB-5 column (Agilent Technologies, USA; length: 30 m, inner diameter: 0.25 mm, film: 0.25 µm, carrier gas: hydrogen, injection temperature: 250 °C, detection temperature: 310 °C, program: method *hart*: 50 °C starting temperature for 1 min, heating rate: 15 °C/min, 290 °C final temperature for 8 min). GC-MS measurements were carried out on a Shimadzu GC-2010 (Shimadzu, Japan) using a ZB-5 column (Phenomenex, USA; length: 30 m, inner diameter: 0.25 mm, film: 0.25 mm, carrier gas: hydrogen, method *hart*: 50 °C starting temperature for 1 min, heating rate: 15 °C/min, 290 °C final temperature for 8 min). The method was coupled with mass spectrometry on a Shimadzu GCMS-QP2010 (ion source's temperature: 200 °C).

Melting points were determined with a Melting Point Apparatus SMP3 (Stuart Scientific, Staffordshire, U.K.) and are uncorrected. Heating rate: 2 °C/min.

Spectroscopy and spectrometry: ^{1}H NMR, ^{13}C NMR spectra were recorded at 298 K by using a Bruker Avance II 400 (Analytische Messtechnik, Karlsruhe, Germany). Chemical shifts (δ) are reported in parts per million (ppm) relative to TMS as internal standard or traces of $CHCl_3$ or d_5-DMSO in the corresponding deuterated solvent. High resolution mass spectra were obtained by using a QTof Ultima 3 (Waters, Milford, Massachusetts) apparatus employing ESI+.

General protocols for the Synthesis of Substrates

A: General protocol for *N*-formylation:

The aniline (4–46 mmol, 1.0 eq) was dissolved in formic acid (98%, 3.0–10.0 eq, depending on the solubility of the aniline) and heated to 80–90 °C overnight in a pressure tube. The mixture was chilled to room temperature and excess solvent was removed at reduced pressure. The formanilides were used without further purification.

B: General protocol for aniline-aniline coupling reactions:

Beaker-type Teflon cells and beaker-type glass cells were home-made by the local mechanical shop at the university or purchased from IKA-Werke GmbH & Co KG (Staufen, Germany). The undivided cells are briefly described here, whereas more details are found in literature (Figure S1 and S2) [2,3].

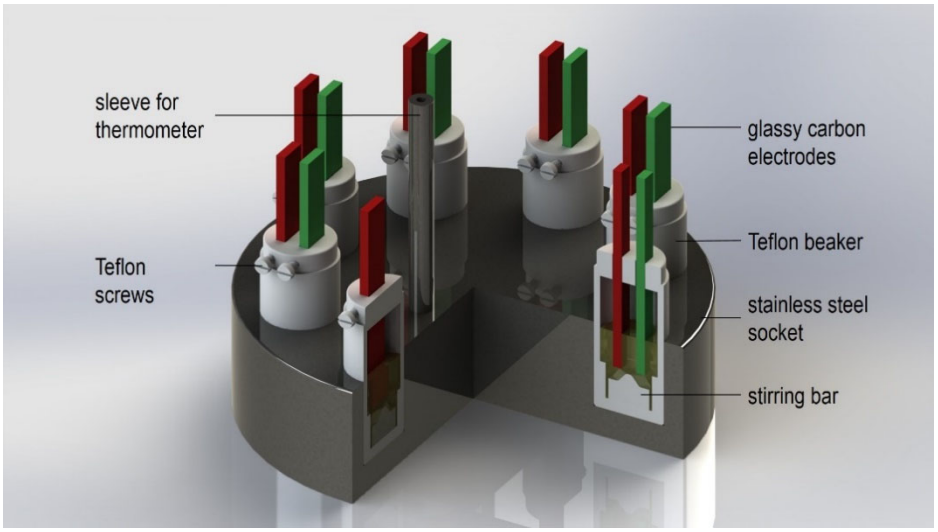

Figure S1: Schematic view of undivided screening cells in a screening arrangement [2].

Recently, the set-up for screening was reported in detail [2]. Dimensions of glassy carbon electrodes are 7.0 x 1.0 x 0.3 cm. Using a 5 mL reaction mixture, electrodes immerse 1.8 cm into solution. This gives an active surface of 1.8 cm².

B1: Screening experiments, homo-coupling reactions (5 mL beaker-type screening cell):

If not stated otherwise, the following standard reaction parameters were used in the electrolyses:

A solution of protected aniline component **A** (0.75 mmol, 2.0 eq) and *N*-methyl-*N,N,N*-tributylammonium methylsulfate (MTBS) (0.154 g, 0.5 mmol) in 5 mL 1,1,1,3,3,3-hexafluoroisopropanol (HFIP) was transferred into a screening cell equipped with glassy carbon electrodes. A constant current electrolysis with a current density of 7.2 mA/cm² was performed at 50 °C. After application of 73 C (1.0 F per aniline A) the electrolysis was stopped and the solvent mixture was recovered in vacuo (50 °C, 200–70 mbar). The residual mixture was analyzed by GC or GC/MS and TLC and, if applicable, the crude coupling products were purified by column chromatography (SiO_2, cyclohexane/ethyl acetate).

B2: Screening experiments, cross-coupling reactions (5 mL beaker-type screening cell):

A solution of protected benzidine component **A** (0.375 mmol, 1.0 eq), protected aniline component **B** (1.125 mmol, 3.0 eq) and *N*-methyl-*N*,*N*,*N*-tributylammonium methylsulfate (MTBS) (0.154 g, 0.5 mmol) in 5 mL 1,1,1,3,3,3-hexafluoroisopropanol (HFIP) was transferred into a screening cell equipped with glassy carbon electrodes. A constant current electrolysis with a current density of 7.2 mA/cm^2 was performed at 50°C. After application of 146 C (4.0 F referred to benzidine **A**) the electrolysis was stopped and the solvent mixture was recovered *in vacuo* (50 °C, 200–70 mbar). The residual mixture was analyzed by GC or GC/MS, and TLC and, if applicable, the crude coupling products were purified by column chromatography (SiO_2, cyclohexane/ethyl acetate).

B3: Scale up experiments, homo-coupling reactions (25 mL beaker-type cell):

If not stated otherwise, the following standard reaction parameters were used in the electrolyses:

A solution of protected aniline component A (3.8 mmol, 2.0 eq) and N-methyl-N,N,N-tributylammonium methylsulfate (MTBS) (770 mg, 2.3 mmol) in 25 mL 1,1,1,3,3,3-hexafluoroisopropanol (HFIP) was transferred into an undivided beaker-type electrolysis cell equipped with glassy carbon electrodes. A constant current electrolysis with a current density of 7.2 mA/cm² was performed at 50 °C. After application of 363 C (1.0 F per aniline A) the electrolysis was stopped and the solvent mixture was recovered in vacuo (50 °C, 200–70 mbar). The crude coupling products were purified by column chromatography (SiO2, cyclohexane/ethyl acetate).

The beaker-type cell (25 mL) consists of a simple glass beaker with cooling jacket, covered with a Teflon plug. This cap allows precise location of the glassy carbon electrodes (Figure S2). Usually, a single glassy carbon electrode has upon immersion into the electrolyte an active surface of 9.0 cm^2 (2.0 cm x 4.5 cm).

Figure S2: Pictures of an undivided beaker-type electrolysis cell. Essential parts are labeled [4].

Optimization of the Homo-Coupling of *N*-(3,4-dimethyl-phenyl)formamide

To achieve a quantification of the screening experiments, 3,3',5,5'-tetramethyl-2,2'-biphenol as an internal standard was used. The homo-coupling product forms up to four rotamers, which show slightly different retention times in the GC chromatogram and are all taken into account in the evaluation.

GC Calibration: Internal Calibration Product

The indicated amount 2,2'-Diformamido-3,3',4,4'-tetramethylbiphenyl (t_R(method „hart")=17.31–17.87 min) and 9 mg (0.037 mmol) 3,3',5,5'-tetramethyl-2,2'-biphenol (t_R(method „hart")=13.05 min) as standard are dissolved in 1 mL ethyl acetate. 12 drops of this solution are filtered through silica gel (0.4 g silica gel 60) with 2.5 mL ethyl acetate and analyzed via gas chromatography. The quotients were calculated from the weight of the biphenyl m_p and the biphenol m_s, as well as from the GC integrals P_p and P_s. With this data, the calibration graph was set up.

Table 1: Masses m_p and m_s and GC integrals P_p and P_s of the product and standard, respectively, as well as their quotients $\frac{m_p}{m_s}$ and $\frac{P_p}{P_s}$.

Entry	m_p/mg	m_s/mg	$\frac{m_p}{m_s}$	P_p	P_s	$\frac{P_p}{P_s}$
1	10.01	9.00	1.11	67000	118000	0.57
2	10.61	9.00	1.18	76000	122000	0.62
3	11.20	9.00	1.24	87000	122000	0.71
4	11.82	9.00	1.31	86000	105000	0.82
5	12.47	9.00	1.39	94000	112000	0.84
6	13.08	9.00	1.45	101000	110000	0.92
7	13.70	9.00	1.52	113000	116000	0.97
8	14.33	9.00	1.59	115000	111000	1.04
9	14.95	9.00	1.66	132000	118000	1.12
10	15.55	9.00	1.73	161000	130000	1.24

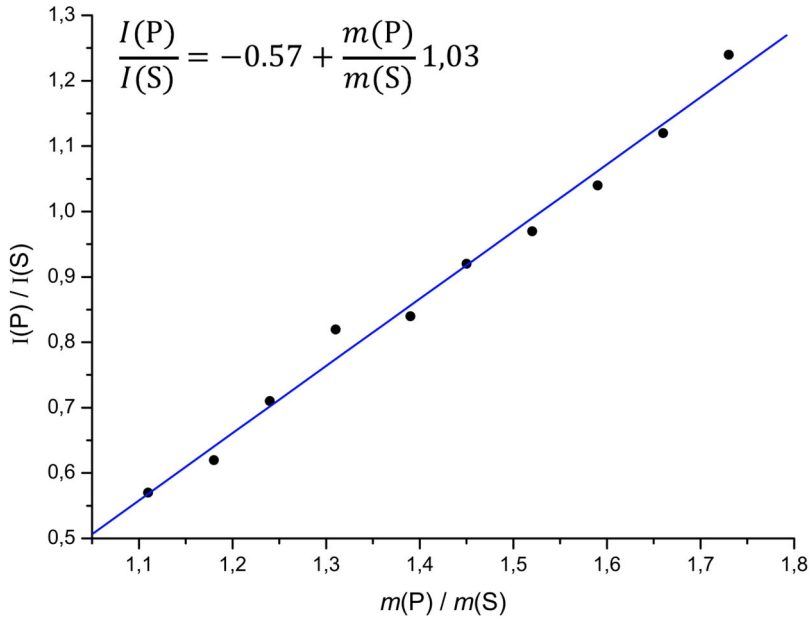

Figure S3: Calibration line for the internal calibration of the product.

GC Calibration: Internal Calibration non-converted Substrate

The indicated amount *N*-(3,4-dimethylphenyl)formamide (t_R(method „hart“)=9.79 min) and 9 mg (0.037 mmol) 3,3’,5,5’-tetramethyl-2,2’-biphenol (t_R(method „hart“)=13.05 min) as standard are dissolved in 5 mL ethyl acetate. 12 drops of this solution are filtered through silica gel (0.4 g silica gel 60) with 2.5 mL ethyl acetate and analyzed via gas chromatography. The quotients were calculated from the weight of the biphenyl m_p and the biphenol m_s, as well as from the GC integrals P_E and P_s. With this data, the calibration graph was set up.

Table 2: Masses m_E and m_s and GC integrals P_E and P_s of the substrate and standard, respectively, as well as their quotients $\frac{m_E}{m_s}$ and $\frac{P_E}{P_s}$.

Entry	m_E/mg	m_s/mg	$\frac{m_E}{m_s}$	P_E	P_s	$\frac{P_E}{P_s}$
1	12.31	9.00	1.37	207142	149686	1.38
2	11.68	9.00	1.30	179811	140972	1.28
3	11.06	9.00	1.23	172869	140445	1.23
4	10.45	9.00	1.16	150111	134800	1.11
5	9.83	9.00	1.09	165885	159404	1.04
6	9.19	9.00	1.02	146296	147014	1.00
7	8.57	9.00	0.95	137111	149964	0.91
8	7.96	9.00	0.88	125006	145355	0.86
9	7.33	9.00	0.81	119537	151954	0.79
10	6.73	9.00	0.75	101686	137809	0.74

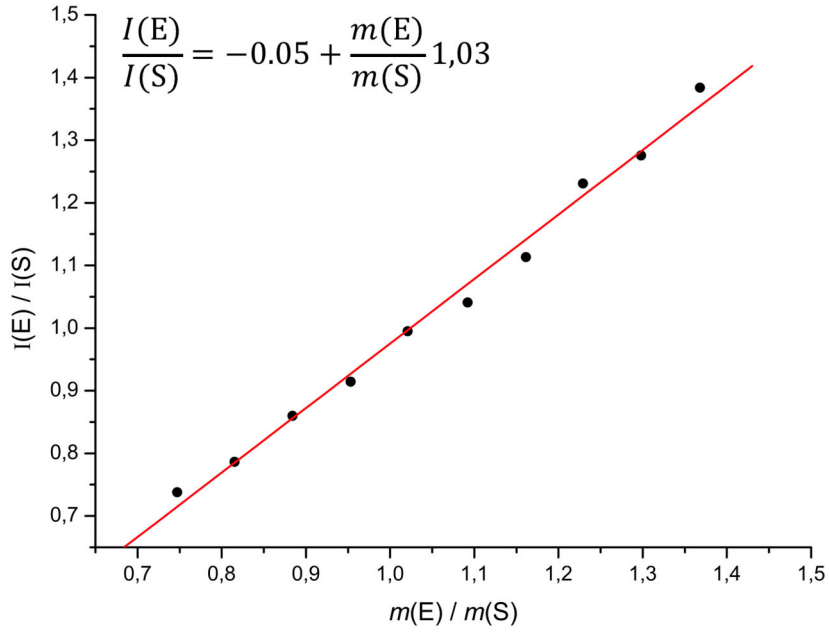

Figure S4: Calibration line for the internal calibration of the non-converted starting material.

Analysis of the elctrolysis

After the electrolysis was finished, the solvent was removed by distillation and 45 mg (0.185 mmol) 3,3',5,5'-tetramethyl-2,2'-biphenol in 5 mL ethyl acetate were added to the residue. 12 drops of this mixture were taken from the cell and filtered through silica gel (0.4 g, silica gel 60) and rinsed with 2.5 mL ethyl acetate. The filtrate was analyzed by GC. With the aid of the calibration line, the mass of the product could then be calculated with equation 1:

$$m_{\mathrm{P}}^{\mathrm{GC}} = \frac{\frac{I_{\mathrm{p}}}{I_{\mathrm{S}}} + 0.57}{1.03} \cdot 45.00\ \mathrm{mg} \tag{1}$$

The GC yield was then calculated using the weighed in mass of the starting material m_{E}, the molar mass of the starting material $M_{\mathrm{E}} = 149{,}19\,\frac{\mathrm{g}}{\mathrm{mol}}$ and the molar mass of the product $M_{\mathrm{P}} = 296{,}37\,\frac{\mathrm{g}}{\mathrm{mol}}$ with equation 2:

$$\mathrm{Yield}_{\mathrm{GC}} = \frac{2 \cdot \frac{m_{\mathrm{P}}^{\mathrm{GC}}}{M_{\mathrm{p}}}}{\frac{m_{\mathrm{E}}}{M_{\mathrm{E}}}} \cdot 100\% \tag{2}$$

The corresponding error was calculated using equation 3, the error of the weighed in starting material was set to $\Delta m_{\mathrm{SM}} = \pm 5\ \mathrm{mg}$.

$$\Delta\text{Yield}_{\text{GC}} = \sqrt{\left(\frac{M_{\text{E}}\Delta m_{\text{P}}^{\text{GC}}}{m_{\text{E}}M_{\text{P}}}\right)^2 + \left(-\frac{m_{\text{P}}^{\text{GC}}M_{\text{E}}\Delta m_{\text{E}}}{m_{\text{E}}^2 M_{\text{P}}}\right)^2} \cdot 100\% \quad (3)$$

To calculate the amount of the non-converted starting material and its corresponding error, the following equations were used:

$$m_{\text{E}}^{\text{GC}} = \frac{\frac{I_{\text{E}}}{I_{\text{S}}} + 0.05}{1.03} \cdot 45.00\ \text{mg} \quad (4)$$

$$\text{Yield}_{\text{GC}} = \frac{m_{\text{E}}^{\text{GC}}}{m_{\text{E}}} \cdot 100\% \quad (5)$$

$$\Delta\text{Yield}_{\text{GC}} = \sqrt{\left(\frac{\Delta m_{\text{E}}^{\text{GC}}}{m_{\text{E}}}\right)^2 + \left(-\frac{m_{\text{E}}^{\text{GC}}\Delta m_{\text{E}}}{m_{\text{E}}^2}\right)^2} \cdot 100\% \quad (6)$$

With this method, only the ratio between formed product and internal standard is taken into account. The occurrence of possible side products during the electrolysis can be neglected, making the results more reliable.

Reaction Optimization

According to general protocol **B1**, the electrolyses were conducted using the standard parameters, if not stated otherwise. The changed reaction parameters are listed in the corresponding tables below.

Optimization of the current density:

Table 3: Optimization of current density.

Entry	Current density / mA·cm^{-2}	GC yield product / %	Non-converted starting material / %
1	3.9	53±2	39±2
2	7.2	52±2	39±2
3	10	62±2	30±2
4	15	52±2	39±2
5	20	54±1	35±2
6	25	56±2	28±2
7	30	49±1	38±2
8	40	47±1	33±2
9	50	40±1	43±2
10	75	39±1	42±2
11	100	35±1	49±2

Addition of Additives:

Table 4: Variation of the solvent mixture.

Entry	Solvent	GC yield product / %	Non-converted starting material / %
1	HFIP	52±2	39±2
2	HFIP + 18 vol.-% MeOH	36±1	50±2
3	HFIP + 14 vol.-% H_2O	23±1	64±2

Optimization of the applied charge:

Table 5: Variation of the applied charge. Theoretically, 1.0 F is needed for a full conversion.

Entry	Applied charge / F	GC yield product / %	Non-converted starting material / %
1	1.0	52±2	39±2
2	1.1	57±1	23±2
3	1.25	63±2	10±2
4	1.35	73±2	15±2
5	1.5	61±2	11±2
6	1.75	56±2	6±2
7	2.0	51±1	4±1

Optimization of the substrate concentration:

Table 6: Optimization of the substrate concentration.

Entry	Substrate concentration / mol·L^{-1}	GC yield product / %	Non-converted starting material / %
1	0.15	52±2	39±2
2	0.225	58±1	21±2
3	0.30	52±1	38±1
4	0.375	41±1	40±2
5	0.45	46±1	38±2
6	0.6	33±1	38±1

Optimization of the electrolysis temperature:

Table 7: Optimization of the electrolysis temperature.

Entry	Electrolysis temperature / °C	GC yield product / %	Non-converted starting material / %
1	50	52±2	39±2
2	40	62±2	36±2
3	30	55±2	28±2

Optimization of the electrode material:

Table 8: Optimization of the used electrode material.

Entry	Substrate concentration / mol·L^{-1}	GC yield product / %	Non-converted starting material / %
1	glassy carbon	54±2	28±2
2	isostatic graphite	59±2	19±2
3	boron-doped diamond	54±2	26±2
4	platinum	48±1	26±2

Combination of different optimized parameters:

Table 9: Combination of different optimized parameters.

Entry	Current density / mA·cm^{-2}	Applied charge / F	Substrate concentration / mol·L^{-1}	GC yield product / %	Non-converted starting material / %
1	10	1.0	0.15	68±2	37±2
2	10	1.25	0.15	73±2	12±2
3	10	1.25	0.225	61±1	21±2
4	10	1.25	0.3	56±1	24±1
5	10	1.5	0.15	71±2	12±2
6	10	1.5	0.225	52±1	16±2
7	10	1.5	0.3	61±1	12±1
8	10	1.5	0.6	55±1	17±1
9	30	1.0	0.15	50±1	35±2
10	30	1.25	0.15	49±1	21±2
11	30	1.25	0.15	57±2	30±2
12	30	1.5	0.15	27±1	52±2
13	30	2.0	0.15	43±1	6±2
14	40	1.0	0.15	24±1	73±2
15	40	1.25	0.15	44±1	24±2
16	40	1.5	0.15	42±1	18±2
17	40	2.0	0.15	44±1	10±2
18	50	1.0	0.15	31±1	47±2
19	75	1.0	0.15	30±1	52±2
20	100	1.0	0.15	26±2	57±2

Scale-ups and isolation of products:

Table 10: Scale-ups with combinations of various optimized parameters and isolation of the product and the non-converted starting material. All given yields are isolated yields. Anode/cathode: glassy carbon, *T*=40 °C, solvent: 25 mL HFIP + 0.09 M MTBS. [1]Anode/cathode: graphite. [2]Solvent: 5 mL HFIP + 0.09 M MTBS, *T*=20 °C.

Entry	*Current density* / mA·cm^{-2}	*Applied charge* / F	*Substrate concentration* / *mol*·L^{-1}	*Isolated yield product* / %	*Isolated amount of non-converted starting material* / %
1	10	1.35	0.15	57	17
2	10	1.5	0.15	64	13
3[1]	10	1.5	0.15	63	13
4	25	1.5	0.15	47	16
5[2]	100	1.0	0.15	25	44
6[2]	100	1.5	0.15	29	33

Synthesis and Characterization

***N*-(3,4-Dimethylphenyl)formamide (XX1A)**

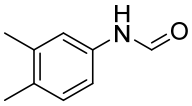

According to the general protocol **A**, 5.60 g (46 mmol, 1.0 eq) 3,4-dimethylaniline were dissolved in formic acid (98%, 10 mL, 6.0 eq) and heated at 90 °C overnight to obtain an off-white powder (quant. yield, 6.86 g, 46 mmol).

The NMR shows a 3:1 mixture of two rotamers (rotation of the *N*-formyl group), rotameric mixture: **^{1}H NMR** (400 MHz, d_6-DMSO): δ (ppm) = 9.99/9.97 (bs, 1 H), 8.69/8.21 (d, *J* = 11.1/2.0 Hz, 1 H), 7.36/6.97 (d, *J* = 2.2 Hz, 1 H) 7.30/6.89 (dd, *J* = 8.1 Hz, 2.2 Hz, 1 H), 7.05 (d, *J* = 8.1 Hz, 1 H), 2.18 (s, 3 H), 2.15 (s, 3 H); **R_f** (cyclohexane/ethyl acetate = 1:1) = 0.49; **m.p.** 70–72 °C.

All analytic data are in agreement with reported data [5].

2,2'-Diformamido-3,3',4,4'-tetramethylbiphenyl (XX1AA)

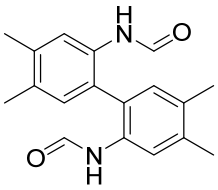

According to the general protocol **B3**, 559 mg (3.75 mmol, 2.0 eq.) *N*-(3,4-dimethylphenyl)formamide and 770 mg MTBS were dissolved in 25 mL HFIP. After electrolysis (543 C, 1.5 F), the solvent was recovered by distillation. Column chromatography of the residue (cyclohexane/ethyl acetate = 4:1 → 1:1) yielded the desired product as an off-white powder (yield: 64%, 335 mg, 1.13 mmol).

The NMR shows a 6*:2.5:2.5:1 mixture of four rotamers (rotation of the *N*-formyl groups), rotameric mixture: **^{1}H NMR** (400 MHz, d_6-DMSO): δ (ppm) = 9.14/9.02 (d, *J* = 11.1 Hz)/8.87/8.76 (s, 2 H), 8.12 (d, *J* = 11.1 Hz)/8.06–8.0* (m, 2 H), 7.83/7.78/7.10/7.07 (s, 2 H), 6.97/6.94/6.90/6.88 (s, 2 H), 2.26/2.24/2.24 (s, 6 H), 2.21/2.20/2.19 (s, 6 H); **HRMS** for $C_{18}H_{20}N_2O_2$ (ESI+) $[M+H]^+$: calc.: 297.1598; found: 297.1595; **R_f** (cyclohexane/ethyl acetate = 1:1) = 0.27; **m.p.** 211–213 °C.

All analytical data are in agreement with reported data [6].

5-Formamidobenzo-1,3-dioxole (XX3B)

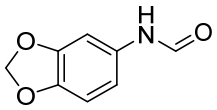

According to the general protocol **A**, 5.00 g (36 mmol, 1.0 eq) 5-aminobenzo[1,3]dioxole were dissolved in formic acid (98%, 14 mL, 10.0 eq) and heated at 90 °C overnight to obtain a purple powder (quant. yield, 5.95 g, 36 mmol).

The NMR shows a 3:1 mixture of two rotamers (rotation of the *N*-formyl group), rotameric mixture: **^{1}H NMR** (400 MHz, d_6-DMSO): δ (ppm) = 10.08 (bs)/9.97 (d, *J* = 11.0 Hz, 1 H), 8.60/8.19 (d, *J* = 11.0/2.0 Hz, 1 H), 7.29/6.87 (d, *J* = 2.1 Hz, 1 H), 6.96/6.60 (dd, *J* = 8.4 Hz, 2.1 Hz, 1 H), 6.85 (d, *J* = 8.4 Hz, 1 H), 5.99/5.98 (s, 2 H); **R_f** (cyclohexane/ethyl acetate = 1:1) = 0.41; **m.p.** 80–81 °C.

All analytic data are in agreement with reported data [7].

2-Iodo-5-nitroanisole (XX5)

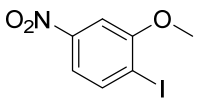

2-Iodo-5-nitroanisole is prepared starting from 2-methoxy-4-nitroaniline following a procedure from literature [8]; (yield: 54% (26.8 g, 96 mmol), yellow powder.

^{1}H NMR (400 MHz, d_6-DMSO): δ (ppm) = 7.96 (d, *J*=8.4 Hz, 1H), 7.61 (m, 2H), 3.99 (s, 1H); **R_f** (cyclohexane/ethyl acetate = 1:1) = 0.63; **m.p.** 127–128 °C.

All analytic data are in agreement with reported data [8].

2,2‘-Dimethoxy-4,4‘-dinitrobiphenyl (XX6)

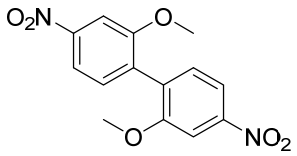

2,2‘-Dimethoxy-4,4‘-dinitrobiphenyl is prepared starting from 2-iodo-5-nitroanisole following a procedure from literature [8]; (yield: 63% (3.5 g, 11.4 mmol), colorless needles.

^{1}H NMR (400 MHz, d_6-DMSO): δ (ppm) = 7.92 (dd, *J*=8.3, 2.1 Hz, 2H), 7.84 (d, *J*=2.1 Hz, 2H), 7.38 (d, J=8.3 Hz, 2H), 3.88 (s, 6H); **R_f** (cyclohexane/ethyl acetate = 1:1) = 0.31; **m.p.** 247–249 °C.

All analytic data are in agreement with reported data [8].

2,2‘-Dimethoxy-4,4‘-diaminobiphenyl (XX7)

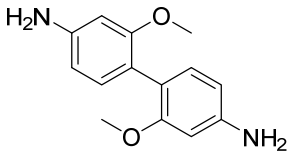

2,2‘-Dimethoxy-4,4‘-diaminobiphenyl is prepared starting from 2,2‘-dimethoxy-4,4‘-dinitrobiphenyl similar to a procedure described by *Knoelker et al.* [9]; (yield: 94% (1.90 g, 7.8 mmol), yellow powder.

^{1}H NMR (400 MHz, d_6-DMSO): δ (ppm) = 6.67 (d, *J*=8.0 Hz, 2H), 6.22 (d, *J*=2.0 Hz, 2H), 6.11 (dd, *J*=8.0, 2.0 Hz, 2H), 4.96 (s, 4H), 3.56 (s, 6H); **R_f** (cyclohexane/ethyl acetate = 0:1) = 0.59; **m.p.** 187–188 °C.

All analytic data are in agreement with reported data [8].

4,4‘-Diformamido-2,2‘-dimethoxybiphenyl (XX2A)

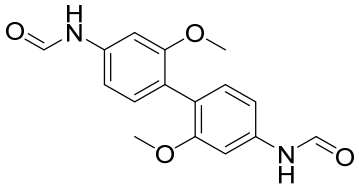

According to the general protocol **A**, 1.00 g (4.1 mmol, 1.0 eq) 2,2‘-dimethoxy-4,4‘-diamino-biphenyl were dissolved in formic acid (98%, 1.6 mL, 10 eq.) and heated at 90 °C overnight to obtain an off-white powder (quant. yield, 1.23 g, 4.1 mmol).

The NMR shows a 2.3:1 mixture of two rotamers (rotation of the *N*-formyl groups), rotameric mixture: **^{1}H NMR** (400 MHz, d_6-DMSO): δ (ppm) = 10.22/10.13 (d, *J*=2.0/11.0 Hz, 2H), 8.85/8.29 (d, *J*=11.0/2.0 Hz, 2H), 7.38/6.89 (d, *J*=2.0 Hz, 2H), 7.13/6.89 (dd, *J*=8.2, 2.0 Hz, 2H), 7.03 (m, 2H), 3.68/3.66 (s, 2H), **^{13}C NMR** (101 MHz, $CDCl_3$): δ (ppm) = 163.12, 160.07, 157.93, 157.32, 139.16, 138.99, 132.17, 131.69, 122.83, 122.71, 111.22, 109.50, 103.10, 101.63, 55.95, 55.74; **HRMS** for $C_{16}H_{16}N_2O_4$ (ESI+) $[M+Na]^+$: ber.: 323,1002; gef.: 323.1010. **R_f** (cyclohexane/ethyl acetate = 0:1) = 0.42; **m.p.** 215–218 °C.

6-Formamideo-5-(4',4''-diformamido-2'',6'-dimethoxy-(1',1''-biphenyl)-3'-yl)-benzo[1,3]dioxole (XX4AB)

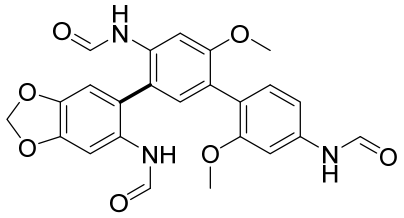

According to the general protocol **B2**, 110 mg (0.375 mmol, 1.0 eq.) 4,4'-diformamido-2,2'-dimethoxybiphenyl **A** and 187 mg (1.125 mmol, 3.0 eq.) 5-formamidobenzo[1,3]dioxole **B** and 154 mg MTBS were dissolved in 5 mL HFIP. After electrolysis (146 C, 4.0 F referred to component **A**), the solvent was recovered by distillation. Column chromatography of the residue (cyclohexane/ethyl acetate = 4:1 → 0:1) yielded the desired product as a yellow oil.

The NMR shows a 2.3:1 mixture of two rotamers (rotation of the *N*-formyl groups), rotameric mixture: **^{1}H NMR** (400 MHz, d_6-DMSO): δ (ppm) = 10.23 (s)/10.14 (d, *J*=11.0 Hz, 1H), 9.26 (m, 1H), 9.18–8.82 (m, 2H), 8.39–8.26 (m, 1H), 8.11 (m, 2H), 7.90 (m)/7.63–7.47 (m, 1H), 7.40 (s, 1H), 7.21–6.70 (m, 5H), 6.19–5.93 (m, 2H), 3.83–3.62 (m, 6H). **^{13}C NMR** (101 MHz, $CDCl_3$): δ (ppm) = 163.85, 163.80, 162.68, 160.58, 160.34, 159.66, 157.53, 156.92, 156.40, 147.47, 146.80, 146.53, 145.24, 144.16, 144.10, 138.68, 135.99, 135.86, 133.75, 133.39, 133.06, 131.84, 131.35, 130.01, 129.67, 129.28, 124.84, 122.96, 122.60, 122.01, 121.74, 120.45, 110.84, 110.61, 110.48, 109.09, 106.42, 105.29, 104.48, 104.43, 102.72, 101.66, 101.45, 101.24, 55.77, 55.55, 55.46, 55.34; **HRMS** for $C_{24}H_{21}N_3O_7$ (ESI+) $[M+Na]^+$: ber.: 486.1277; gef.: 486.1268. $\mathbf{R_f}$ (cyclohexane/ethyl acetate = 0:1) = 0.3.

References

[1] W.L.F. Armarego, Purification of laboratory chemicals, 7th ed., Butterworth-Heinemann, Oxford, Waltham, MA, 2013.

[2] C. Gütz, B. Klöckner, S.R. Waldvogel, Org. Process Res. Dev. 20 (2015) 26–32.

[3] A. Kirste, G. Schnakenburg, F. Stecker, A. Fischer, S.R. Waldvogel, Angew. Chem. Int. Ed. 49 (2010) 971–975.

[4] L. Schulz, M. Enders, B. Elsler, D. Schollmeyer, K.M. Dyballa, R. Franke, S.R. Waldvogel, Angew. Chem. Int. Ed. 56 (2017) 4877–4881.

[5] Y. Qin, Y. Cheng, X. Luo, M. Li, Y. Xie, Y. Gao, Synlett 26 (2015) 1900–1904.

[6] L. Schulz, R. Franke, S.R. Waldvogel, ChemElectroChem 5 (2018) 2069–2072.

[7] K.-H. Chiang, S.-H. Lu, W.-P. Yen, N. Uramaru, W.-S. Tseng, T.-W. Chang, F.F. Wong, Heteroat. Chem. 27 (2016) 235–242.

[8] C. He, P. Liu, P.J. McMullan, A.C. Griffin, phys. stat. sol. (b) 242 (2005) 576–584.

[9] M.P. Krahl, O. Kataeva, A.W. Schmidt, H.-J. Knölker, Eur. J. Org. Chem. 2013 (2013) 59–64.

Appendix: NMR-Spectra

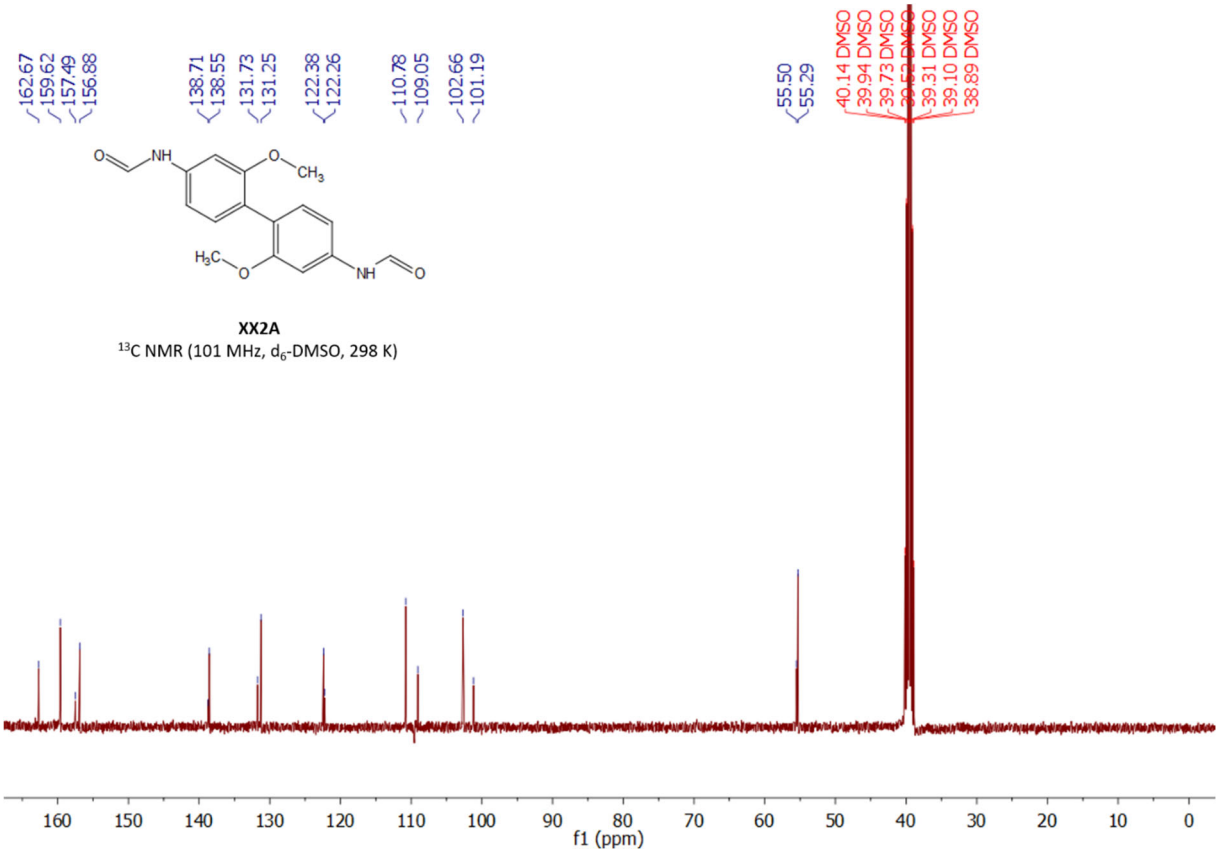

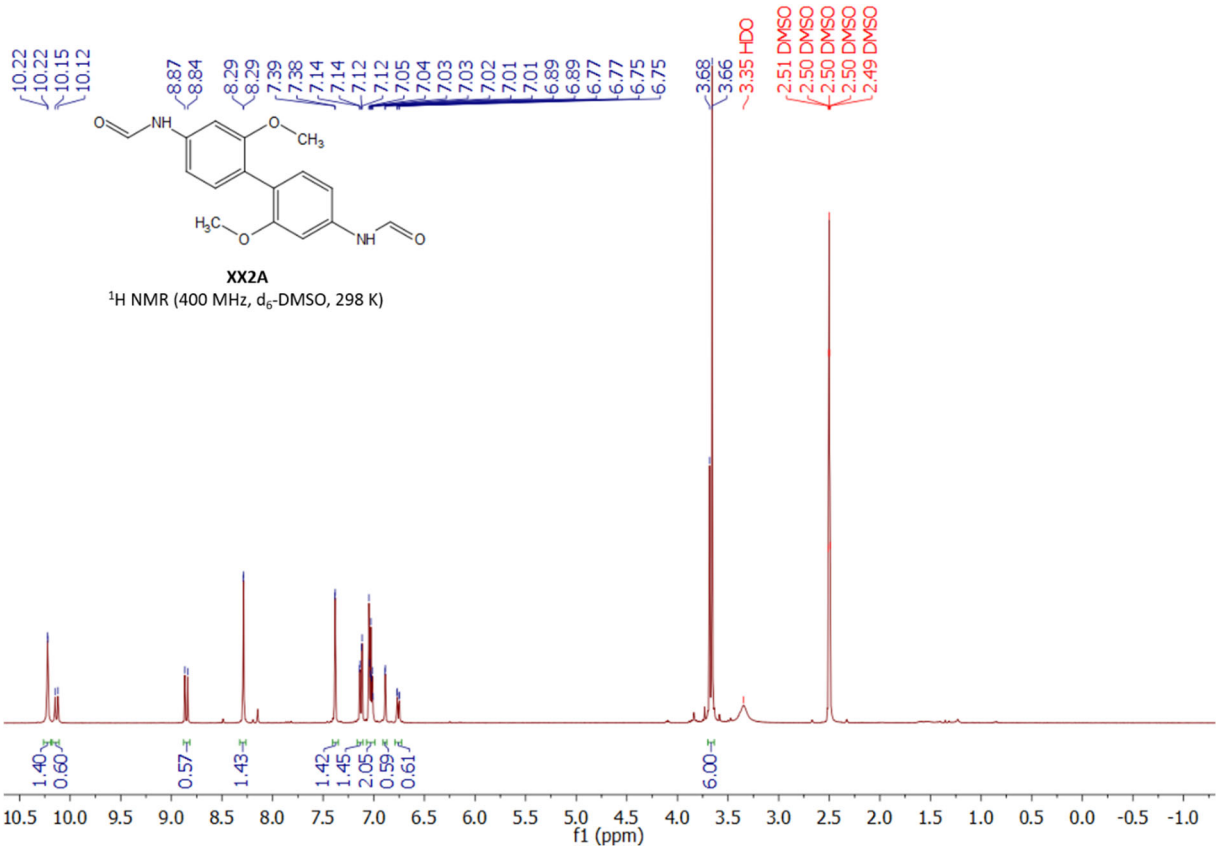

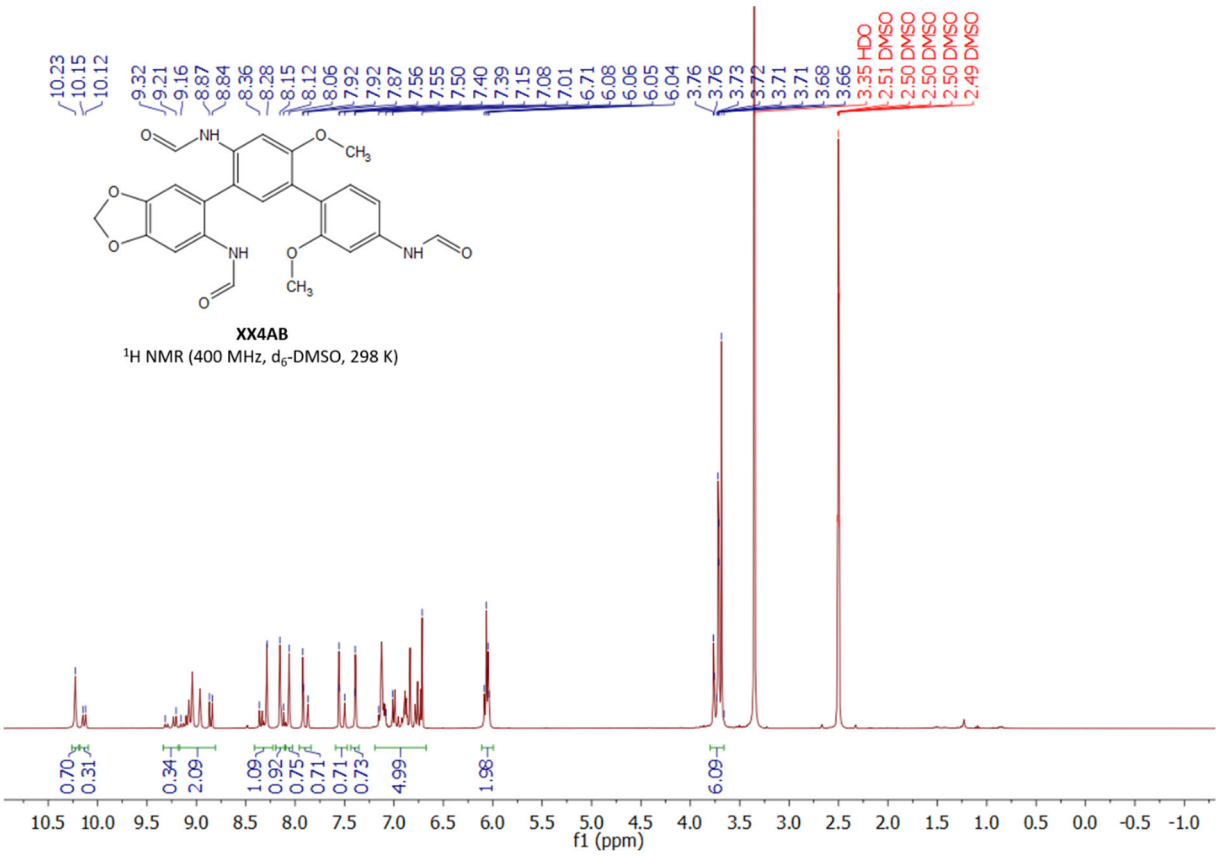
10.23
10.15
10.12
9.32
9.21
9.16
8.87
8.84
8.36
8.28
8.15
8.12
8.06
7.92
7.87
7.56
7.55
7.50
7.40
7.39
7.15
7.08
7.01
6.71
6.08
6.06
6.05
6.04
3.76
3.76
3.73
3.72
3.71
3.71
3.68
3.66
3.35 HDO
2.51 DMSO
2.50 DMSO
2.50 DMSO
2.50 DMSO
2.49 DMSO
NH
O
CH3
XX4AB
1H NMR (400 MHz, d6-DMSO, 298 K)
0.70
0.31
0.34
2.09
1.09
0.92
0.75
0.71
0.71
0.73
4.99
1.98
6.09
f1 (ppm)

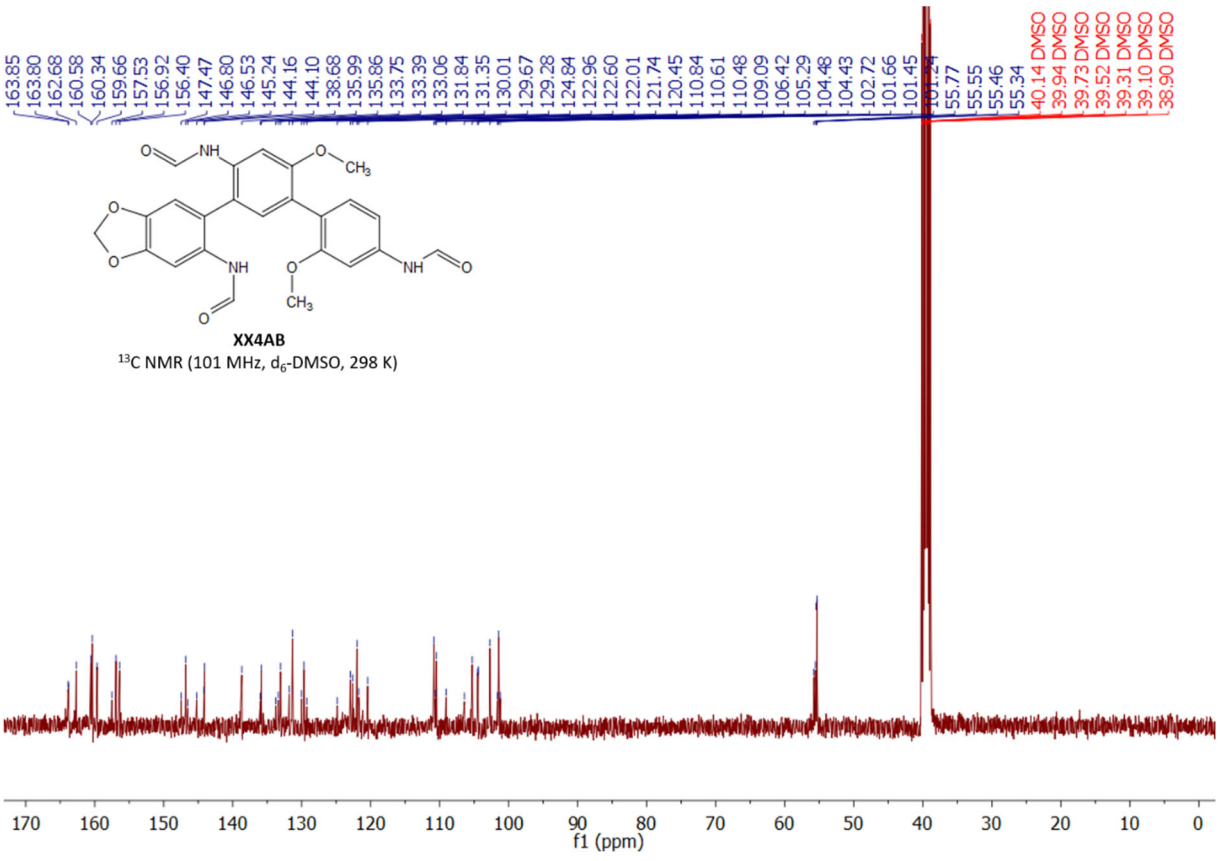
163.85
163.80
162.68
160.58
160.34
159.66
157.53
156.92
156.40
147.47
146.80
146.53
145.24
144.16
144.10
138.68
135.99
135.86
133.75
133.39
133.06
131.84
131.35
130.01
129.67
129.28
124.84
122.96
122.60
122.01
121.74
120.45
110.84
110.61
110.48
109.09
106.42
105.29
104.48
104.43
102.72
101.66
101.45
55.77
55.55
55.46
55.34
40.14 DMSO
39.94 DMSO
39.73 DMSO
39.52 DMSO
39.31 DMSO
39.10 DMSO
38.90 DMSO
NH
O
CH3
XX4AB
13C NMR (101 MHz, d6-DMSO, 298 K)
f1 (ppm)

Active Nickel Electrodes for Anodic Dehydrogenative Arylation Reaction in HFIP and their Unusual Behavior

Sebastian B. Beil,[a,b] Lara Schulz,[a] Manuel Breiner,[a] Aaron Schüll,[a] Timo Müller,[a] Nicole Beiser,[a] Dieter Schollmeyer,[a] Alexander Bomm,[c] Michael Holtkamp,[d] Uwe Karst,[d] Wolfgang Schade,[c] and Siegfried R. Waldvogel*[a,b]

Abstract: Active anodes which are operating in protic media such as 1,1,1,3,3,3-hexafluoro-isopropanol are rare. Nickel forms, within this unique solvent, an active electrode which is superior and less expensive to the reported molybdenum system. This novel active anode allows the efficient dehydrogenative coupling of 4-fluoroveratrole. Surprisingly, a better performance is found when the electrolyte is not stirred during electrolysis. Besides the aryl-aryl coupling, a dehydrogenative arylation reaction of benzylic nitriles was found providing quick access to useful building blocks. The electrolysis can be performed in very simple undivided batch-type cells at constant current conditions enabling a scalable electrolytic transformation.

Organic electro-synthesis evolved most recently to one of the major research areas in the toolbox of organic chemists.[1] Obviously, the development of new chemistry and reactivity requires innovative approaches, such as material science aspects, into this purely synthetic habit. Usually, platinum and carbon allotropes perform most oxidative reactions. In contrast, boron-doped diamond (BDD) facilitates anodic coupling reactions due to the inert behaviour and exploiting inherent reactivity of substrates,[2] such as phenols, arenes, anilines and various heterocycles in high yields.[3] In particular, solvent control enables distinct selectivity, wherein protic media, such as 1,1,1,3,3,3-hexafluoroisopropanol (HFIP), outperform others.[4] To improve the mechanical and chemical stability together with a more reasonable source, we investigated different transition metals and their alloys with regards to their applicability in electrochemical conversions. Leaded bronze enabled the selective and high yielding dehalogenation of cyclopropanes.[5] These active metal electrodes represent elegant alternatives, since the electrocatalytic species remains at the electrode surface. The electrocatalyst (mediator) thereby is immobilized and does not contaminate the electrolyte, which facilitates work-up and down-stream processing (Figure 1).

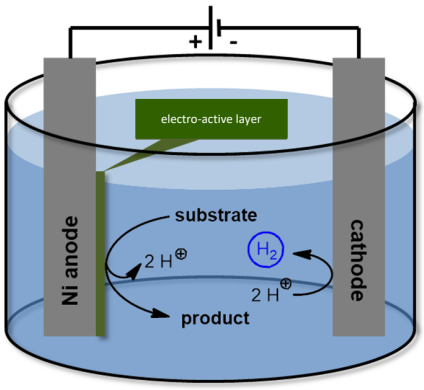

Figure 1: Schematic representation of an active anode within electrolysis.

Combining this elegant approach with the high performance of HFIP-based electrolytes resulted in an active molybdenum anode, which accomplished a variety of dehydrodimerization and oxidative cyclization reactions.[6] Obviously, this results represent only a starting point and more abundant metals are favoured, such as nickel which is advantageous due to its inexpensive nature and various geometries as well as morphologies being commercially available. It is noteworthy, that nickel seems to play an outstanding role as active anode in oxidations within alkaline media and anhydrous HF.[7] In addition, nickel phosphides and other nickel salt coating have been described as electrocatalytically active.[8]

In the previous study,[6c] 4-fluoro veratrole (**1a**) turned out to be a challenging substrate, since the corresponding biaryl **2a** was only obtained in 12% yield (Table 1, Entry 1). Other metal electrodes, such as nickel, were barely superior and the yield of **2a** was only slightly increased (Table 1, Entry 2). Surprisingly, this yield could be drastically improved when stirring was avoided. An isolated yield of 42% was obtained in high purity without dehalogenation processes observed in the undivided cell set-up. During the optimization, various electrolysis parameters were investigated (see SI, Tables S4-S10), but interestingly the previous conditions[6c] matched the best. The charge amount was kept at 3.0 F per mole product **2a**. The substrate concentration was optimal at 0.2 M, and at room temperature the highest yield was detected by GC (for calibration details see SI,

[a] Dr. Sebastian B. Beil, Lara Schulz, Manuel Breiner, Aaron Schüll, Timo Müller, Nicole Beiser, Dr. Dieter Schollmeyer, Prof. Dr. Siegfried R. Waldvogel
Institute of Organic Chemistry
Johannes Gutenberg University Mainz
Duesbergweg 10-14, 55128 Mainz (Germany)
E-mail: waldvogel@uni-mainz.de
[b] Dr. Sebastian B. Beil, Prof. Dr. Siegfried R. Waldvogel
Graduate School of Excellence Material Science in Mainz (MAINZ)
Johannes Gutenberg University Mainz
Staudinger Weg 9, 55128 Mainz (Germany)
[c] Alexander Bomm, Prof. Dr. Wolfgang Schade
Fraunhofer Heinrich-Hertz-Institut
Abteilung Faseroptische Sensorsysteme
Am Stollen 19H, 38640 Goslar (Germany)
[d] Michael Holtkamp, Prof. Dr. Uwe Karst
Institute of Inorganic and Analytical Chemistry
University of Münster
Corrensstr. 30, 48149 Münster (Germany)

Supporting information for this article is given.

Table 1. Optimization of the dehydrogenative coupling of 4-fluoroveratrole (**1a**).

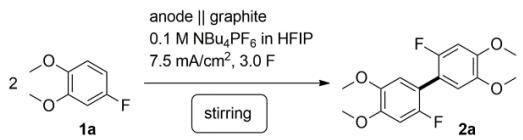

Entry	Anode	Stirring	Yield[a]
1	molybdenum	yes	12
3	nickel	yes	16 (25)
4	nickel	no	42 (55)

[a] Isolated yield, in parenthesis GC yield with internal calibration (see SI). HFIP: 1,1,1,3,3,3-hexafluoroisopropanol.

Tables S1-S3, Figure S4). Again, the use of additives like water or methanol resulted in diminished or no yield.[9]

The distinct effect of electrolysis without stirring on this particular substrate was unanticipated and unprecedented. This inspired us to investigate this finding in detail.

Nickel is a base metal commonly available in several alloys and many geometries.[7b,7d,10] We tested Waspalloy, Ni/Cr, and Inconel as alloys, but surprisingly all resulted in lower product formation compared to pure nickel. All these three alloys exhibit a high content in chromium. However, pure chromium as anode was previously identified for successful dehydrogenative coupling but going along with significant corrosion.[6c] Nevertheless, the combination of high nickel and chromium compositions gave diminished conversions (Table 2, Entries 2-4). A similar low yield of 24% for **2a** was observed when using Hastelloy, which consists mainly of nickel and molybdenum (Table 2, Entry 5). Hence, both metals are applicable in this homocoupling reaction individually, the combination appears to be less favoured. A reversed picture was obtained for Monel alloy, which provides a surprisingly high yield (Table 2, Entry 6). Due to the high copper content a low yield was anticipated, as noticed earlier where no reaction took place at a pure copper anode.[6c] Earlier, laser grafting resulted in an improved yield for the active molybdenum anode, but did not work for nickel. Even a slightly lower yield was observed by GC analysis (Table 2, Entry 7).

This observation is in contrast to our previous study, giving rise to a different reaction pathway for active nickel anodes compared to molybdenum. The surface structuring enables a larger active electrode surface and therefore a higher conversion was anticipated (Figure 2, a and b).

Table 2. Various nickel alloys and geometries in the dehydrogenative coupling of 4-fluoroveratrole (**1a**).

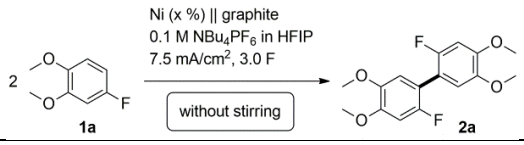

Entry	Anode	Ni content (%)[a]	Yield[b]
1	nickel	99.5	55
2	Waspalloy®	59	31
3	Ni/Cr	75	30
4	Inconel 625®	61	21
5	Hastelloy C276®	57	24
6	Monel® K-500	63	43
7	nickel V8.1[c]	99.5	48

[a] Content of nickel in the anode material/alloy wt%. For details on the nickel composition and morphology see SI. [b] GC yield for **2a** by internal calibration (see SI). [c] Laser grafted surface as shown in Figure 1.

To obtain a better understanding of the electrode surface we applied the same nickel electrode in many consecutive runs (Figure 2, c). During the first three runs, the GC yield was constant at around 55%. Afterwards, the yield eroded constantly down to 10% after nine cycles. A plausible rationale is an in-situ formation of an electro-active layer. Within several cycles it grows leading to a deactivated and therefore diminished active surface. This kind of deactivation is known for NiOOH electrodes, whereby nickelates are formed.[11] Nevertheless, this inactive layer can easily be removed by simple polishing (see SI for details). This active electrode layer acts as a kind of redox-filter, which was observed during CV studies. Always the same redox behaviour was observed and reflects the electrochemical window of the electro-active layer (see SI, Figure S5).

To rationalize the unexpected dependence of stirring on the outcome of the reaction using nickel as anode material, we subjected upon electrolysis the crude electrolyte mixtures to ICP-OES (inductively coupled plasma optical emission spectroscopy) to determine the amount of nickel therein. The nickel content was monitored for **1a** and **1b** as substrates (Table 3). These

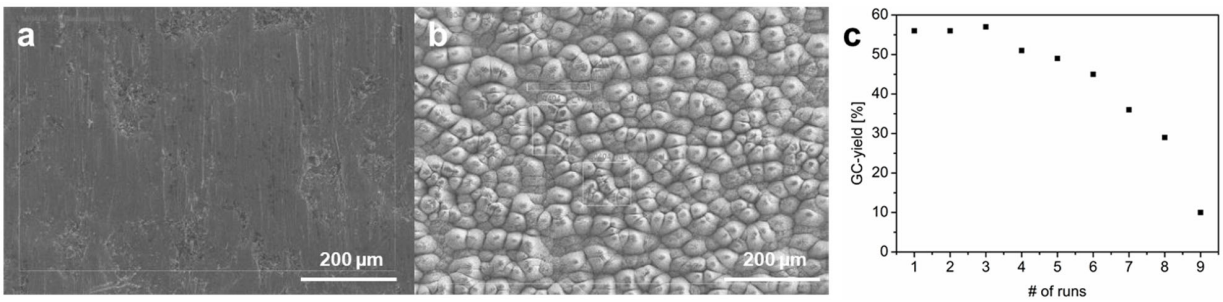

Figure 2: REM images of planar (a) and micro-structured (nickel V8.1) (b) nickel electrodes. c) Long-term deactivation effect of a nickel anode in HFIP. GC yield of **2a** obtained with internal calibration after each electrolysis (see SI).

substrates were subjected to identify influences by halo or alkyl substituents.

Table 3. Determination of nickel content upon electrolysis by ICP-OES.

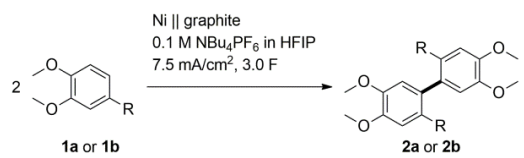

Entry	R[a]	Substrate [GC/%]	Product [GC/%]	Stirring	Ni content [ppm]
1	F	77	19	yes	59.9 ± 1.8
2	F	26	62	no	57.1 ± 5.2
3	Me	4	93	yes	43.0 ± 4.9
4	Me	2	96	no	89.9 ± 6.1

The conversion of **1a** was highly dependent on the stirring (Table 3, Entries 1 and 2), but a constant amount of nickel was found in the electrolysis mixture in both cases. Nevertheless, the amount of about 60 ppm was one order of magnitude lower compared to our previously described protocol employing molybdenum as anode material (c(Mo) = 740 ± 10 ppm).[6c]

In contrast, by GC analysis almost full conversion was found for **2b** either with or without stirring of the reaction mixture (Table 3, Entries c and d). Surprisingly, product **2b** contained the twofold traces of nickel without stirring. When substrates with a low oxidation potential are applied (*e.g.* **1b**) the product formation is fast at the active electrode surface and after consumption of substrate, the nickel surface seems to dissolve without stirring. For halogenated substrates with a higher oxidation potential (e.g. **1a**) the product formation is promoted without stirring. The substrate dependence could also been visually followed by the respective GC solutions (see SI, Figure S3).

With this novel active electrode system and handling, the scope of accessible substrates was evaluated with regards to anisole and veratrole derivatives. Various 2,5-dihalo-substituted anisoles were coupled and the dehydrodimers **2c-g** were obtained in good yields up to 76%. For the first time, we could convert 2,6-substituted anisoles, which gave no conversion at the active molybdenum anode.[6c] Product **2g** was obtained in 31% isolated yield. A small library of 4-substituted veratroles was coupled to achieve good yields up to 76% for **2a-b** and **2h-i**, respectively. Even labile *O*-alkoxycarbonylmethyl protective groups[12] could be applied in the dehydrodimerization in an acceptable yield of 56% (**2j**), in agreement with previous $MoCl_5$-mediated transformations.[13] Again for the first time, a 1,3-dimethoxy arene could be transformed in a synthetically useful yield. 4-Bromo-1,3-dimetoxybenzene (**2ka**) was obtained as a dehydrodimer in 10% yield, together with a by-product, which could be assigned to 4,6-dibromo-1,3-dimethoxybenzene (**2kb**) and was obtained in 31% yield. This halogen scrambling reaction was again unanticipated and is rationalized by the active electrode nature of nickel in HFIP electrolyte. Benzylnitrile **1l** was also applied to the anodic coupling at the active nickel electrodes and resulted in the benzyl-aryl cross-coupled product **2l** in 51% isolated yield.

This observation inspired us to investigate benzylic cross-coupling reactions on nickel anodes of such α-aryl acetonitrile derivatives, which lead to highly substituted nitriles common in pharmaceuticals such as anastrozole or verapamil,[14] or motifs in natural products like cherylline dimethyl ether.[15] Most reported approaches towards such targets apply transition-metal catalysis and require leaving groups.[16] Only few examples described a direct synthesis of α-aryl benzylnitriles.[17] Electrochemical dehydrodimerization of benzylnitriles was described,[18] and with chemical oxidants even dehydrotrimerization reaction was observed.[19] None of them was found in this case. The reasonable stability of benzylic radical intermediates was recently described in polar solvents,[20] and led here to successful benzylic

Scheme 1: Scope obtained by anodic coupling of anisoles and veratroles **1** on an active nickel electrode. Isolated yields are shown for all compounds.

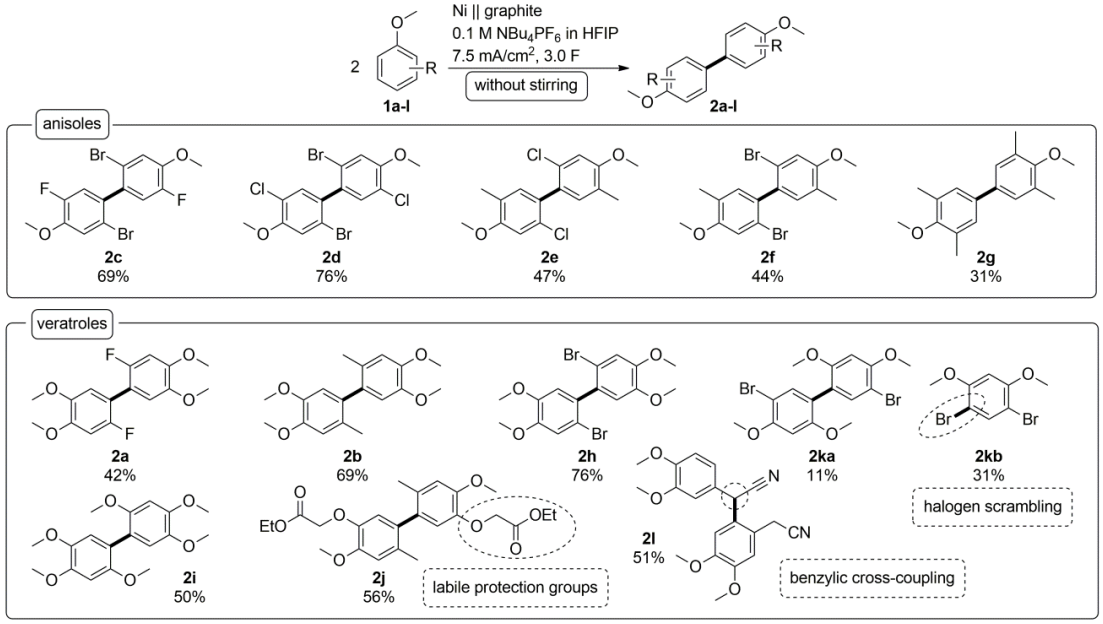

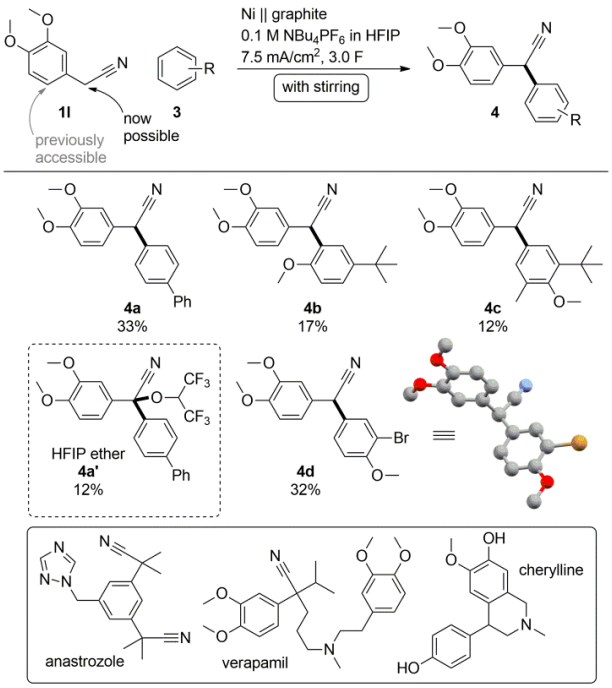

Scheme 2: Benzylic dehydrogenative cross-coupling of 2-aryl acetonitrile (**1l**) and arenes by anodic treatment. Hydrogen atoms of the X-ray single crystal structure of **4d** were removed for simplicity.

cross-coupling on active nickel electrodes. We found, that biphenyl **3a** can be coupled selectively to the benzylic position of **1l** in 33% yield (**4a**, Scheme 2). Anisoles are also possible cross-coupling partners and selective ortho- and para-coupling is accessible in yields up to 32% (**4b** to **4d**). In all cases, stirring was crucial for successful benzylic cross-coupling reactions enabling enhanced convection. In some cases, the formation of additional HFIP ethers was observed, which could be isolated in lower yields of 12% (**4a'**). Single crystals were successfully obtained for derivative **4d** proving the formation of 2,2-biaryl acetonitrile compounds.

In conclusion, an active nickel electrode system, which forms in-situ in HFIP, was found and the successful dehydrodimerization and benzylic cross-coupling of arenes was performed. The nature of this abundant material became obvious when different geometries and alloys were tested, and the crucial effect of stirring was discovered. On the basis of these observations further investigations on the utility of active electrodes on valuable substrates are on-going.

Experimental Section

Supplementary data to this article can be found online.

Acknowledgements

The authors thank the Carl-Zeiss-Stiftung for supporting the ELYSION network. Support by Deutsche Forschungsgemeinschaft is highly appreciated (GSC 266).

Keywords: nickel • electrochemistry • C-H activation • active electrode • 1,1,1,3,3,3-hexafluoroisopropanol

References

[1] a) S. Möhle, M. Zirbes, E. Rodrigo, T. Gieshoff, A. Wiebe, S. R. Waldvogel, *Angew. Chem. Int. Ed.* **2018**, *57*, 6018-6041; b) A. Wiebe, T. Gieshoff, S. Möhle, E. Rodrigo, M. Zirbes, S. R. Waldvogel, *Angew. Chem. Int. Ed.* **2018**, *57*, 5594-5619; c) S. Tang, Y. Liu, A. Lei, *Chem* **2018**, *4*, 27-45; d) M. Yan, Y. Kawamata, P. S. Baran, *Chem. Rev.* **2017**, *117*, 13230-13319; e) M. D. Kärkäs, *Chem. Soc. Rev.* **2018**, *47*, 5786-5865.

[2] a) S. Lips, S. R. Waldvogel, *ChemElectroChem* **2018**, *0*; b) T. A. Ivandini, Y. Einaga, *Chem. Commun.* **2017**, *53*, 1338-1347; c) S. R. Waldvogel, S. Mentizi, A. Kirste, in *Radicals in Synthesis III* (Eds.: M. Heinrich, A. Gansäuer), Springer Berlin Heidelberg, Berlin, Heidelberg, **2012**, pp. 1-31.

[3] a) S. Lips, D. Schollmeyer, R. Franke, S. R. Waldvogel, *Angew. Chem. Int. Ed.* **2018**, *57*, 13325-13329; b) S. Lips, B. A. Frontana-Uribe, M. Dörr, D. Schollmeyer, R. Franke, S. R. Waldvogel, *Chem. Eur. J.* **2018**, *24*, 6057-6061; c) A. Wiebe, S. Lips, D. Schollmeyer, R. Franke, S. R. Waldvogel, *Angew. Chem. Int. Ed.* **2017**, *56*, 14727-14731; d) L. Schulz, M. Enders, B. Elsler, D. Schollmeyer, K. M. Dyballa, R. Franke, S. R. Waldvogel, *Angew. Chem. Int. Ed.* **2017**, *56*, 4877-4881; e) A. Wiebe, D. Schollmeyer, K. M. Dyballa, R. Franke, S. R. Waldvogel, *Angew. Chem. Int. Ed.* **2016**, *55*, 11801-11805.

[4] a) R.-J. Tang, T. Milcent, B. Crousse, *J. Org. Chem.* **2017**; b) I. Colomer, A. E. R. Chamberlain, M. B. Haughey, T. J. Donohoe, *Nat. Rev. Chem.* **2017**, *1*, 0088.

[5] a) V. Grimaudo, P. Moreno-García, A. Riedo, S. Meyer, M. Tulej, M. B. Neuland, M. Mohos, C. Gütz, S. R. Waldvogel, P. Wurz, P. Broekmann, *Anal. Chem.* **2017**, *89*, 1632-1641; b) C. Gütz, M. Bänziger, C. Bucher, T. R. Galvão, S. R. Waldvogel, *Org. Process Res. Dev.* **2015**, *19*, 1428-1433; c) C. Gütz, V. Grimaudo, M. Holtkamp, M. Hartmer, J. Werra, L. Frensemeier, A. Kehl, U. Karst, P. Broekmann, S. R. Waldvogel, *ChemElectroChem* **2018**, *5*, 247-252; d) C. Gütz, M. Selt, M. Bänziger, C. Bucher, C. Römelt, N. Hecken, F. Gallou, T. R. Galvão, S. R. Waldvogel, *Chem. Eur. J.* **2015**, *21*, 13878-13882.

[6] a) S. B. Beil, P. Franzmann, T. Müller, M. M. Hielscher, T. Prenzel, D. Pollok, N. Beiser, D. Schollmeyer, S. R. Waldvogel, *Electrochim. Acta* **2019**, *302*, 310-315; b) S. B. Beil, S. Mohle, P. Enders, S. R. Waldvogel, *Chem. Commun.* **2018**, *54*, 6128-6131; c) S. B. Beil, T. Müller, S. B. Sillart, P. Franzmann, A. Bomm, M. Holtkamp, U. Karst, W. Schade, S. R. Waldvogel, *Angew. Chem. Int. Ed.* **2018**, *57*, 2450-2454.

[7] a) L. Conte, G. Gambaretto, *J. Fluor. Chem.* **2004**, *125*, 139-144; b) M. A. García-Contreras, S. M. Fernández-Valverde, J. R. Vargas-García, *J. Alloys Comp.* **2007**, *434*, 522-524; c) M. Okimoto, K. Ohashi, H. Yamamori, S. Nishikawa, M. Hoshi, T. Yoshida, *Synthesis* **2012**, *44*, 1315-1322; d) F. D. Popp, H. P. Schultz, *Chem. Rev.* **1962**, *62*, 19-40; e) A. B. Sheremetev, B. V. Lyalin, A. M. Kozeev, N. V. Palysaeva, M. I. Struchkova, K. Y. Suponitsky, *RSC Adv.* **2015**, *5*, 37617-37625; f) J. H. Simons, W. J. Harland, *J. Electrochem. Soc.* **1949**, *95*, 55-59.

[8] a) S. Surendran, S. Shanmugapriya, S. Shanmugam, L. Vasylechko, R. Kalai Selvan, *ACS Applied Energy Materials* **2018**, *1*, 78-92; b) F. S. Omar, A. Numan, S. Bashir, N. Duraisamy, R. Vikneswaran,

Y.-L. Loo, K. Ramesh, S. Ramesh, *Electrochim. Acta* **2018**, *273*, 216-228; c) Z. Zhang, S. Liu, J. Xiao, S. Wang, *J. Mat. Chem. A* **2016**, *4*, 9691-9699; d) Y.-L. Shih, C.-L. Wu, T.-Y. Wu, D.-H. Chen, *Nanotechnology* **2019**, *30*, 115601; e) X. X. Liang, W. Weng, D. Gu, W. Xiao, *J. Mat. Chem. A* **2019**, *7*, 10514-10522; f) M. M. Haring, E. G. V. Bosche, *J. Phys. Chem.* **1928**, *33*, 161-178.

[9] A. Kirste, B. Elsler, G. Schnakenburg, S. R. Waldvogel, *J. Am. Chem. Soc.* **2012**, *134*, 3571-3576.

[10] L.-K. Wu, W.-Y. Wu, J. Xia, H.-Z. Cao, G.-Y. Hou, Y.-P. Tang, G.-Q. Zheng, *J. Mat. Chem. A* **2017**, *5*, 10669-10677.

[11] D. S. Hall, D. J. Lockwood, C. Bock, B. R. MacDougall, *Proc. Math. Phys. Eng. Sci.* **2015**, *471*, 20140792.

[12] A. Spurg, S. R. Waldvogel, *Eur. J. Org. Chem.* **2008**, *2008*, 337-342.

[13] B. Kramer, R. Fröhlich, K. Bergander, S. R. Waldvogel, *Synthesis* **2003**, *1*, 0091-0096.

[14] R. Shang, in *New Carbon–Carbon Coupling Reactions Based on Decarboxylation and Iron-Catalyzed C–H Activation*, Springer Singapore, Singapore, **2017**, pp. 107-124.

[15] A. S. Kumar, S. Ghosh, K. Bhima, G. N. Mehta, *Journal of Chemical Research* **2009**, *2009*, 482-484.

[16] a) X. Cheng, H. Lu, Z. Lu, *Nature Comm.* **2019**, *10*, 3549; b) Z. Jiao, K. W. Chee, J. S. Zhou, *J. Am. Chem. Soc.* **2016**, *138*, 16240-16243; c) N. Rad, M. Mąkosza, *Eur. J. Org. Chem.* **2018**, *2018*, 376-380; d) H. M. Refat, A. A. Faddo, E. Biehl, *J. Fluor. Chem.* **1996**, *76*, 99-103; e) R. Shang, D.-S. Ji, L. Chu, Y. Fu, L. Liu, *Angew. Chem. Int. Ed.* **2011**, *50*, 4470-4474; f) G.-H. Yang, M. Liu, N. Li, R. Wu, X. Chen, L.-L. Pan, S. Gao, X. Huang, C. Wang, C.-M. Yu, *Eur. J. Org. Chem.* **2015**, *2015*, 616-624; g) P. Y. Yeung, K. H. Chung, F. Y. Kwong, *Org. Lett.* **2011**, *13*, 2912-2915.

[17] a) A. V. Aksenov, N. A. Aksenov, Z. V. Dzhandigova, D. A. Aksenov, M. Rubin, *RSC Adv.* **2015**, *5*, 106492-106497; b) M. H. Al-Huniti, Z. B. Sullivan, J. L. Stanley, J. A. Carson, I. F. D. Hyatt, A. C. Hairston, M. P. Croatt, *J. Org. Chem.* **2017**, *82*, 11772-11780; c) D. K. Singh, S. S. Prasad, J. Kim, I. Kim, *Organic Chemistry Frontiers* **2019**, *6*, 669-673.

[18] M. N. Elinson, A. I. Ilovaisky, V. M. Merkulova, T. A. Zaimovskaya, P. A. Belyakov, G. I. Nikishin, *Mendeleev Comm.* **2010**, *20*, 207-208.

[19] T. B. Nguyen, P. Retailleau, *J. Org. Chem.* **2019**, *84*, 5907-5912.

[20] J. P. Peterson, A. H. Winter, *J. Am. Chem. Soc.* **2019**, *early view*, DOI: 10.1021/jacs.1029b06576.

COMMUNICATION

Text for Table of Contents

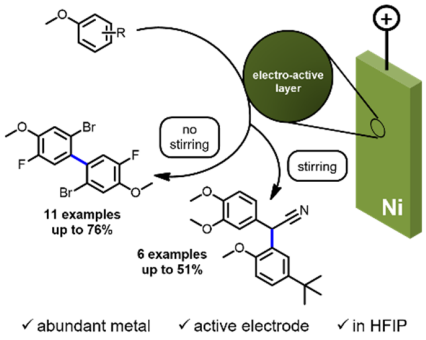

*S. B. Beil, L. Schulz, M. Breiner, A Schüll, T. Müller, N. Beiser, D. Schollmeyer, A. Bomm, M. Holtkamp, U. Karst, W. Schade, S. R. Waldvogel**

Page No. – Page No.

Active Nickel Electrodes for Anodic Dehydrogenative Arylation Reaction in HFIP and their Unusual Behaviour

Supporting Information

DOI:

Active Nickel Electrodes for Anodic Dehydrogenative Arylation Reaction in HFIP and their Unusual Behavior

Sebastian B. Beil, Lara Schulz, Manuel Breiner, Aaron Schüll, Timo Müller, Nicole Beiser, Dieter Schollmeyer, Alexander Bomm, Michael Holtkamp, Uwe Karst, Wolfgang Schade, and Siegfried R. Waldvogel*

Table of Contents

General Remarks

All reagents were purchased from commercial suppliers or synthesized following the given literature. No further purification was required. For standard electrolysis conditions 1,1,1,3,3,3-hexafluoroisopropanol (Fluorochem) and tetra-*n*-butylammonium hexafluorophosphate (ABCR, 98%) were used as received. The following materials were applied as anodes:

Material	**Supplier**	**Purity (%)**
Molybdenum	haines & maassen	99,9
Nickel	IKA-Werke	99,5
Waspalloy®	GOODFELLOW (NI150450)	Ni 59, Cr 19.5, Co 13.5, Mo 4.2, Ti 3, Al 1.2, Fe <2, Mn 0.7, C 0.07
Ni/Cr	GOODFELLOW (NI053250)	Ni 75, Cr 19, Fe 5, Cu 0.5, Si 0.5, Ti 0.4
Inconel 625®	GOODFELLOW (NI040240)	Ni 61, Cr 21.5, Mo 9, Fe <5, Nb+Ta 3.65, Si<0.5, Al 0.25, Mn 0.25, Ti 0.25, C <0.1, S <0.015
Hastelloy C276®	GOODFELLOW (NI140550)	Ni 57, Mo 16-18, Cr 13-17.5, Fe 4.5-7, W 3.7-5.3, C <0.15
Monel® K-500	GOODFELLOW (NE043050)	Ni 63, Cu 30, AL 3, Fe 2, Mn 1.5, Ti 0.5

NMR spectroscopy: For measurements concerning NMR-Spectroscopy a multi nuclear magnetic resonance spectrometer of the type AV II 400 (*Bruker,* analytic measuring technique, Karlsruhe, Germany) was employed. The chemical shifts were referenced on δ-value in ppm of the residue signal of the deuterated solvent ($CDCl_3$: ^1H = 7.26 ppm, ^{13}C = 77.2 ppm; C_6D_6: ^1H = 7.16 ppm, ^{13}C = 128.06 ppm; CD_2Cl_2: ^1H = 5.32 ppm, ^{13}C = 53.84 ppm; DMSO-d_6: ^1H = 2.50 ppm, ^{13}C = 39.52 ppm). ^{19}F signals were referenced to $CFCl_3$.

Gas chromatography: Reaction mixtures and purified products were analysed *via* gas chromatography, for which a GC-2010 (*Shimadzu,* Japan) was used. The column is a quartz capillary column ZB-5 (length: 30 m, inner diameter: 0.25 mm, layer thickness of the stationary phase: 0.25 µm, carrier gas: hydrogen, stationary phase: (5%-phenyl)-methylpolysiloxane, *Phenomenex,* USA). The detector is a flame ionization detector (FID) with a temperature of 310 °C. The injector temperature was 250 °C with a linear carrier gas rate of 45.5 $cm \cdot s^{-1}$. Further gas-chromatographic mass spectra (GC-MS) were taken, using a GC-2010 combined with a mass detector GCMS-QP2010 (*Shimadzu,* Japan). It has a similar quartz capillary column ZB-5 (length: 30 m, inner diameter: 0.25 mm, layer thickness of the stationary phase: 0.25 µm, carrier gas: hydrogen, stationary phase: (5%-phenyl-methlpolysiloxane, *Phenomenex,* USA), whereas the ion source has a temperature of 200 °C. Four different methods were used for the GC-spectra measurements: method "*hart"* (starting temperature: 50 °C, heating rate: 15 °C/min, end temperature: 290 °C for 8 min), method "*hart 16 min"*, which is identical, but leaving out the last 8 minutes. Method "method1langextrahart" (starting temperature: 100 °C, heating rate: 15 °C/min, end temperature: 310 °C for 22 min) and method "method1" (starting temperature: 50 °C, heating rate: 10 °C/min, end temperature: 250 °C for 15 min) were also used.

Mass spectrometry: For high resolution electrospray ionization or atmospheric pressure chemical ionization mass spectrometry measurements, an Agilent 6545 Q-ToF MS was utilized. The field desorption mass spectra (FD) were accomplished with MAT 95 (*Thermo Finnigan*, Bremen).

IR spectroscopy: For IR measurements, a "Bruker Alpha II FTIR" spectrometer (*Bruker Corporation,* Massachusetts, USA) with a Platinum-ATR unit was used.

Melting points: The melting ranges were measured with "Melting Point Apparatus M-565" (*Büchi,* Essen, Germany). Heating rates of 5 °C min^{-1} were used.

Preparative chromatography: For standard liquid chromatography separation silica gel 60 M (0.040-0.063 mm *Macherey-Nagel GmbH & Co.*, Düren, Germany) was used. An automatic silica flash column chromatography system was used, which consists of a control unit C-620, a fraction collector C-660 and a UV photometer C-635 (*Büchi*, Flawil, Switzerland).
Thin-layer-chromatography was performed using "DC Kieselgel 60 F254" (*Merck KGaA,* Darmstadt, Germany) on aluminum and a UV lamp (*Benda*, NU-4 KL, λ = 254 nm, Wiesloch, Germany). The resulting retention factors (R*f*) are given in relation to the solvent ratio.

Electrochemical Setup

Galvanostat: For the electrolysis a self-built eight-channel galvanostat with an integrated coulomb counter of the University Bonn was used.[1]
For electrolysis conditions different cell types were applied. For screening and small scale reactions 5 mL undivided Teflon cells were used (Scheme 1). These can be home-made according to the previous report[1] or purchased from IKA-Werke GmbH & Co KG, Staufen, Germany. For reactions on larger scale 25 mL beaker-type cells were utilized (Scheme 2).

Figure S1: Design of the screening array with eight-channel galvanostatic device (left), 5 mL Teflon cell with two parallel electrodes; size of electrodes: 3 mm x 10 mm x 70 mm (right).

Figure S2: 25 mL beaker-type electrolysis cell; size of electrodes: 3 mm x 20 mm x 60 mm.

Applied electrodes were cut mechanically into the respective size for screening or beaker-type electrolysis cells, with the respective thickness of the metals (Ni: 3 mm). No additional finishing was performed.

ICP-OES (inductively coupled plasma with optical emission spectrometry):

Instrument: ArCos MVII (Spectro GmbH, Kleve, Germany), radial view mode

Plasma conditions: RF-Power: 1200 W; cooling gas (Ar): 13 L/min; aux gas (Ar): 0,8 L/min; nebulizer gas (Ar): 0,8 L/min

Wavelength: Ni (232,003 nm, 221,648 nm, 231,604 nm) and Rh (IS) (343,489 nm)

Single element standards (Ni and Rh) were purchased from SCP-Science (Clark Graham Baie D'Urfé, Quebec, Canada)

GC-solutions of the respective samples showed distinct color depending on the substrate and whether stirring was applied.

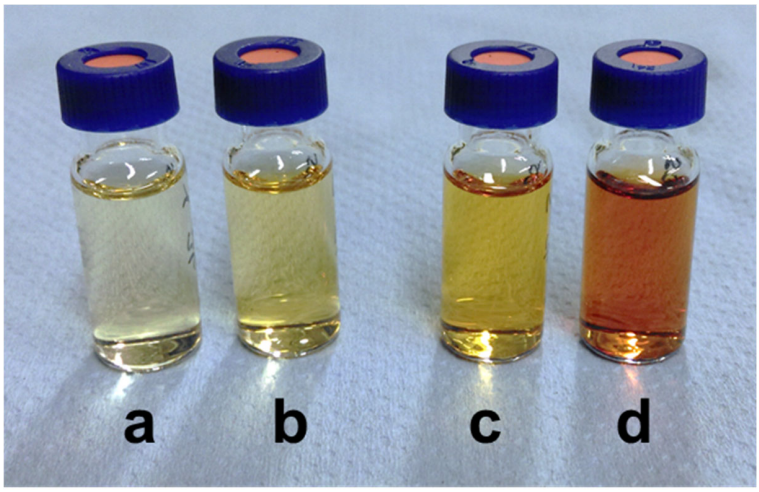

Figure S3: GC solution of samples (0.1 mL was diluted with ethyl acetate and filtered over silica for GC analysis). a) **1b** with stirring, b) **1b** without stirring, c) **1a** with stirring, d) **1a** without stirring.

Surface structuring of Nickel V8.1

Nickel plates with a thickness of 3.0 mm have been cleaned by ultrasonication with acetone and deionized water. For laser microstructuring, an *AMPHOS* 400 Yb:YAG high power laser system at a centre wavelength of λ = 1030 nm has been applied. By a grating compressor, the final pulse length of τ = 0.75 ps has been achieved. A spot diameter of approximately 94 µm (1/e²) after a 420 mm f-theta objective has been used. The average output power of P = 23.7 W in combination with the repetition rate of f = 1 MHz results in a pulse energy of E = 23.7 µJ and a fluence of J = 0.34 Jcm^{-2} per shot. The samples have been processed with a continuous speed of v = 0.05 ms^{-1}. Each spot on the surface has been hit N = 1879 times by the laser beam. Areas of 70 mm x 10 mm have been irradiated with a meandering pattern scan in lines with a distance of D = 5 µm. The chamber has been flooded by a constant airflow of about v = 12 ms^{-1} to provide a clean surface area.

Surface Analysis of Laser Grafted Nickel Surfaces

EDX measurements revealed a high carbon content of 8.31 wt-% and a low oxygen content of 1.75 wt-% on the plane nickel surface. The grafting leads to an inversed picture with decreased carbon content of 2.80 wt-% and largely increased oxygen amount of 12.43 wt-% (for nickel V8.1). This amount corresponds to a nickel to oxygen ratio of 2:1.

GC Calibration

The indicated amount 2,2'-difluor-4,4',5,5'-tetramethoxy-1,1'-biphenyl (t_R(GC 3, "hart")=14.35 min) and 30 mg (0.12 mmol) 3,3',5,5'-tetramethyl-2,2'-biphenol (t_R(GC 3, "hart")=12.67 min) as standard are dissolved in 5 mL of an 0.1 M NBu_4PF_6 solution in HFIP. 0.5 mL of this solution is filtered through silica gel (1.5 g, silica gel 60) with 2.5 mL ethyl acetate and analyzed *via* gas chromatography. The quotients were calculated from the weight of the biphenyl m_p and the biphenol m_s, as well as from the GC integrals P_p and P_s. With this data, the calibration graph was set up.

Table S1: Masses $\boldsymbol{m_p}$ of the product and $\boldsymbol{m_S}$ of the standard as well as quotient $\frac{m_P}{m_S}$ with respective errors.

Entry	$\boldsymbol{m_P}$/mg	$\Delta\boldsymbol{m_P}$/mg	$\boldsymbol{m_S}$/mg	$\Delta\boldsymbol{m_S}$/mg	$\frac{\boldsymbol{m_P}}{\boldsymbol{m_S}}$	$\Delta\frac{\boldsymbol{m_P}}{\boldsymbol{m_S}}$
1	10	±1	30	±1	0.33	±0.03
2	20	±1	30	±1	0.67	±0.04
3	30	±1	30	±1	1.00	±0.05
4	40	±1	30	±1	1.33	±0.06
5	50	±1	30	±1	1.67	±0.06
6	65	±1	30	±1	2.17	±0.08
7	80	±1	30	±1	2.67	±0.09

The error from the analytical balance was used as mass errors. The error of the quotient was calculated by the propagation of errors:

$$\Delta\frac{m_P}{m_S} = \sqrt{\left(\frac{\Delta m_P}{m_S}\right)^2 + \left(\frac{\Delta m_S m_P}{m_S^2}\right)^2} \quad (1)$$

Table S2: GC-Integrals $\boldsymbol{P_p}$ of the product and $\boldsymbol{P_S}$ of the standard as well as quotient $\frac{P_P}{P_S}$ with respective errors.

Entry	$\boldsymbol{P_P}$	$\Delta\boldsymbol{P_P}$	$\boldsymbol{P_S}$	$\Delta\boldsymbol{P_S}$	$\frac{\boldsymbol{P_P}}{\boldsymbol{P_S}}$	$\Delta\frac{\boldsymbol{P_P}}{\boldsymbol{P_S}}$
1	13377	±1149	60532	±391	0.22	±0.02
2	20688	±1149	52429	±391	0.39	±0.02
3	27806	±1149	42627	±391	0.65	±0.03
4	46601	±1149	51288	±391	0.91	±0.02
5	67890	±1149	54730	±391	1.24	±0.02
6	108520	±1149	66270	±391	1.64	±0.02
7	123172	±1149	58682	±391	2.10	±0.02

The integral errors were obtained by measuring the sample **3** three times in a row and calculating the average value and the standard error:

Table S3: Values for the calculation of the Integral errors.

	P_P	P_S
Measurement 1	27806	42627
Measurement 2	26116	42786
Measurement 3	25612	42043
Average $\bar{P}$	26511	42485
Standard error ΔP	$\pm$1149	$\pm$391

$$\bar{P} = \frac{1}{n}\sum_{i=1}^{n} P_i \tag{2}$$

$$\Delta P = \frac{1}{\sqrt{n}}\sqrt{\frac{\sum_{i=1}^{n}(P_i - \bar{P})^2}{n-1}} \tag{3}$$

The error of the quotient was again calculated by the propagation of errors:

$$\Delta\frac{P_P}{P_S} = \sqrt{\left(\frac{\Delta P_P}{P_S}\right)^2 + \left(\frac{\Delta P_S P_P}{P_S^2}\right)^2} \tag{4}$$

The calibration graph was created using the data in table 6.2 and 6.3:

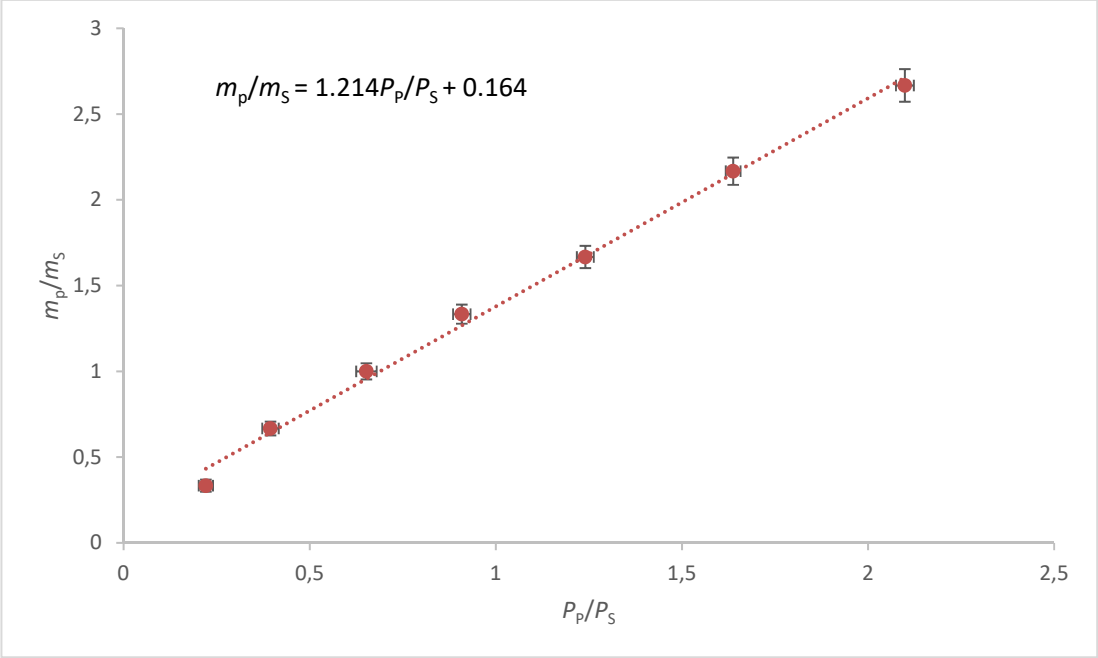

Figure S4: Calibration line for the internal calibration.

Analysis of the electrolysis

After the electrolysis was finished, 30 mg (0.12 mmol) 3,3',5,5'-tetramethyl-2,2'-biphenol was added to the reaction mixture while stirring. 0.5 mL of this mixture was taken from the cell and filtered through silica gel (1.5 g, silica gel 60) and rinsed with 2.5 mL ethyl acetate. The filtrate was analyzed by GC. With the aid of the calibration line, the mass of the product could then be calculated:

$$m_{\mathrm{P}}^{\mathrm{GC}} = 30\ \mathrm{mg} \cdot \left[1.214 \cdot \frac{P_{\mathrm{P}}}{P_{\mathrm{S}}} + 0.164\right] \tag{4}$$

The corresponding error $\Delta m_{\mathrm{P}}^{\mathrm{GC}}$ was calculated by:

$$\Delta m_{\mathrm{P}}^{\mathrm{GC}} = \sqrt{\left[\Delta m_{\mathrm{S}} \cdot \left(1.214 \cdot \frac{P_{\mathrm{P}}}{P_{\mathrm{S}}} + 0.164\right)\right]^2 + \left[1.214 \cdot \Delta\frac{P_{\mathrm{P}}}{P_{\mathrm{S}}} \cdot m_{\mathrm{s}}\right]^2} \tag{5}$$

The GC yield was then calculated using the weighed in mass of the starting material m_{SM}, the molar mass of the starting material $M_{\mathrm{SM}} = 156.15\,\frac{\mathrm{g}}{\mathrm{mol}}$ and the molar mass of the product $M_{\mathrm{P}} = 310.29\,\frac{\mathrm{g}}{\mathrm{mol}}$ with equation 6:

$$\mathrm{Yield}_{\mathrm{GC}} = \frac{\frac{m_{\mathrm{P}}^{\mathrm{GC}}}{M_{\mathrm{p}}}}{0.5 \cdot \frac{m_{\mathrm{SM}}}{M_{\mathrm{SM}}}} \cdot 100\% \tag{6}$$

The corresponding error was calculated using equation 7, the error of the weighed in starting material was set to $\Delta m_{\mathrm{SM}} = \pm 5\ \mathrm{mg}$. In this case, the error is larger than the scale error, as exact the dosing of the liquid starting material is rather difficult.

$$\Delta\mathrm{Yield}_{\mathrm{GC}} = \sqrt{\left(\frac{M_{\mathrm{SM}}\Delta m_{\mathrm{P}}^{\mathrm{GC}}}{m_{\mathrm{SM}} M_{\mathrm{P}}}\right)^2 + \left(\frac{m_{\mathrm{P}}^{\mathrm{GC}} M_{\mathrm{P}} \Delta m_{\mathrm{SM}}}{m_{\mathrm{SM}}^2 M_{\mathrm{P}}}\right)^2} \cdot 100\% \tag{7}$$

With this method, only the ratio between formed product and internal standard is taken into account. The occurrence of possible side products during the electrolysis can be neglected, making the results more reliable.

Reaction Optimization

General protocol for reaction optimization
156 mg (1 mmol) 1,2-dimethoxy-4-fluorobenzene and the corresponding supporting electrolyte (0.1 M) were dissolved in 5 mL HFIP (+additive) in an undivided screening-cell and electrolyzed. After the electrolysis, the reaction mixture was analyzed *via* internal calibration. The individual reaction parameters are listed in the corresponding tables below. As the initial optimization steps with stirring lead to significantly lower yields in all cases, only the optimization without stirring is shown.
Whenever pure Nickel was used as anode material, the electrodes were polished directly before use with fine sandpaper (P400 and P1000) and rinsed with acetone.

Optimization of the current density

Table S4: Optimization of current density. Reaction conditions: Ni anode, graphite cathode, RT, 3 F, 0.1 M NBu_4PF_6, reaction carried out without stirring.

Entry	Current density/$\frac{mA}{cm^2}$	GC-yield/%
1	4	41±1
2	5	47±1
3	6	48±1
4	7	47±1
5	7.5	48±1
6	8	48±1
7	9	45±1
8	10	44±1

Optimization of the supporting electrolyte

Table S5: Optimization of supporting electrolyte (0.1 M). Reaction conditions: Ni anode, graphite cathode, RT, 3 F, 7.5 mA/cm^2, reaction carried out without stirring.

Entry	Supporting electrolyte	GC-yield/%
1	NBu_4PF_6	53±2
2	NBu_4BF_4	49±1
3	NBu_4Br	0
4	NBu_4I	0
5	NBu_4Cl	0
6	NBu_4HSO_4	6±1
7	NBu_4ClO_4	20±1
8	NBu_4Br_3	0

Optimization of the applied charge

Table S6: Optimization of applied charge**.** Reaction conditions: Ni anode, graphite cathode, RT, 7.5 mA/cm^2, 0.1 M NBu_4PF_6, reaction carried out without stirring.

Entry	Applied charge/F	GC-yield/%
1	1.5	42±1
2	2	45±1
3	2.5	48±2
4	3	46±1
5	3.5	46±1
6	4	43±1
7	4.5	34±1
8	5	30±1

Optimization of the substrate concentration

Table S7: Optimization of concentration**.** Reaction conditions: Ni anode, graphite cathode, RT, 7.5 mA/cm^2, 0.1 M NBu_4PF_6, 3.0 F, reaction carried out without stirring.

Entry	Substrate concentration/$\frac{mol}{L}$	GC-yield/%
1	0.05	34±1
2	0.1	48±2
3	0.15	45±1
4	0.2	53±2
5	0.3	57±2
6	0.4	50±2

Entry 5 and 6 showed overoxidation products as well as unconverted substrate, providing double negative properties.

Optimization of the anode material

Table S8: Variation of the anode. Reaction conditions: graphite cathode, RT, 3 F, 0.1 M NBu_4PF_6, 7.5 mA/cm^2, reaction carried out without stirring.

Entry	Anode material	GC-yield/%
1	Ni	47±1
2	Waspalloy	31±1
3	Ni/Cr	30±1
4	Inconel	21±1
5	Hastelloy	24±1
6	Monel	43±1
7	nano V8	40±1
8	Nano V8.1	48±1

Optimization of the reaction temperature

Table S9: Variation of the temperature. Reaction conditions: Ni-anode, graphite cathode, 3 F, 0.1 M NBu_4PF_6, 7.5 mA/cm^2, reaction carried out without stirring.

Entry	Temperature/°C	GC-yield/%
1	10	50±2
2	20	51±1
3	RT (≈25)	55±2
4	30	45±1
5	40	43±1
6	50	39±1

Long term stability test without electrode polishing

Table S10: Long term stability without pretreatment. Reaction conditions: Ni-anode, graphite cathode, 3 F, 0.1 M NBu_4PF_6, 7.5 mA/cm^2, reaction carried out without stirring.

Entry	Electrolysis	GC-yield/%
1	1st	56±2
2	2nd	56±2
3	3rd	57±2
4	4th	51±2
5	5th	49±1
6	6th	45±1
7	7th	36±1
8	8th	29±1
9	9th	10±1

For all reactions, the same electrode was used without polishing between electrolysis.

CV measurements

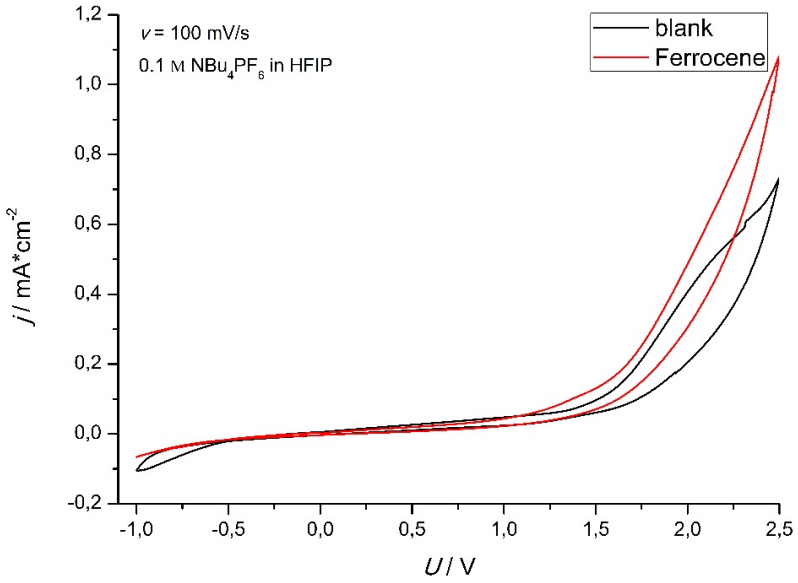

Figure S5: CV measurement of the electrolyte (0.1 M NBu_4PF_6 in HFIP; black line) and Ferrocene in the respective electrolyte (red line). WE: nickel electrode tip, 2 mm diameter; CE: glassy carbon rod; RE: Ag/AgCl in saturated LiCl/EtOH.

Oxidation potentials of the used arenes could not be determined using a nickel electrode tip due to the formation of a passivation layer. Even Ferrocene showed the same behavior without the common oxidation peak. Oxidation potentials of the arenes using other electrodes/electrolyte systems can be found in literature.

Synthesis

General Protocol for Electrolysis

For each reaction the substrate and tetrabutylammonium hexafluorophosphate (0.5 mmol, 194 mg) were dissolved in HFIP (5.0 mL) in an undivided electrolysis cell equipped with a nickel anode[1] and graphite cathode. The electrodes were immersed in the solution and the applied charge was set to 1.5 F. The current density was 7.5 mA/cm². While the reaction was in progress the solution was stirred or not stirred. The reaction mixture was purified by silica flash column chromatography using CH and EA. For analytical purpose the isolated products were further recrystallized from methanol.

2,2'-Dibromo-5,5'-difluoro-4,4'-dimethoxy-1,1'-biphenyl (2c)

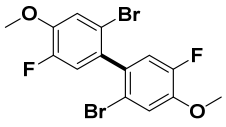

5-Bromo-2-fluoroanisol (201 mg, 1.0 mmol) was treated with 145 C (1.5 F) with stirring. The reaction mixture was purified by silica flash column chromatography (1% → 5% EA in CH) to obtain the product as colorless needles (140 mg, 0.34 mmol, 69%).

^{1}H NMR (400 MHz, $CDCl_3$): δ = 7.22 (d, $^4J_{HF}$ = 8.0 Hz, 2H), 6.98 (d, $^3J_{HF}$ = 11.3 Hz, 2H), 3.93 (s, 6H) ppm. **GCMS:** 13.9 min (method "hart"), *m/z* = 406 (51), 408 (100), 410 (49).
Analytical data are in agreement with previous results.[2]

2,2'-Dibromo-5,5'-dichloro-4,4'-dimethoxy-1,1'-biphenyl (2d)

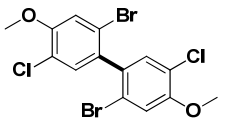

5-Bromo-2-chloroanisol (230 mg, 1.0 mmol) was treated with 145 C (1.5 F) without stirring. The reaction mixture was purified by silica flash column chromatography (10% → 20% EA in CH) to obtain the product as colorless needles (174 mg, 0.38 mmol, 76%).

^{1}H NMR (400 MHz, $CDCl_3$): δ = 7.23 (s, 2H), 7.19 (s, 2H), 3.95 (s, 6H) ppm. **GCMS:** 17.4 min (method "hart"), *m/z* = 441.
Analytical data are in agreement with previous results.[2]

2,2'-Dichloro-4,4'-dimethoxy-5,5'-dimethyl-1,1'-biphenyl (2e)

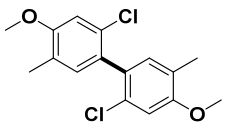

5-Chloro-2-methylanisol (156 mg, 1.0 mmol) was treated with 145 C (1.5 F) with stirring. The reaction mixture was purified by silica flash column chromatography (1% → 5% EA in CH) to obtain the product as yellow needles (72 mg, 0.23 mmol, 47%).

^{1}H NMR (400 MHz, $CDCl_3$): δ = 7.01 (q, ^4J = 0.9 Hz, 2H), 6.91 (s, 2H), 3.93 (s, 6H), 2.20 (s, 6H) ppm. **^{13}C NMR** (101 MHz, $CDCl_3$): δ = 157.7, 133.2, 131.4, 130.0, 125.2, 111.0, 55.7, 15.9 ppm. **HR-MS** (APCI): *m/z* calculated for $C_{16}H_{16}Cl_2O_2$ $[M+H]^+$: 310.0527, found: 310.0525. **GC:** 14.280 min (method "hart"). **GCMS:** 15.2 min (method "hart"), *m/z* = 310 (100), 312 (65), 314 (11). **Mp:** 136.7-138.9 °C. **R_f:** 0.50 (CH:EA, 99:1).

2,2'-Dibromo-4,4'-dimethoxy-5,5'-dimethyl-1,1'-biphenyl (2f)

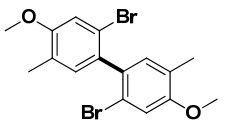

5-Bromo-2-methylanisol (208 mg, 1.0 mmol) was treated with 145 C (1.5 F) without stirring. The reaction mixture was purified by silica flash column chromatography (10% → 15% EA in CH) to obtain the product as colorless needles (92 mg, 0.22 mmol, 44%).

^{1}H NMR (400 MHz, $CDCl_3$): δ = 7.07 (s, 2H), 6.99 (s, 2H), 3.86 (s, 6H), 2.18 (s, 6H) ppm. **GCMS:** 15.9 min (method "hart"), *m/z* = 400.
Analytical data are in agreement with previous results.[2]

[1] After each run the anode was polished with fine sand paper (P400) and rinsed with acetone.

4,4'-Dimethoxy-2,2',6,6'-tetramethyl-1,1'-biphenyl (2g)

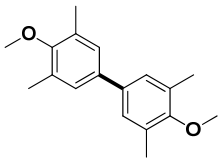

2,6-Dimethylanisol (140 mg, 1.0 mmol) was treated with 145 C (1.5 F) without stirring. The reaction mixture was purified by silica flash column chromatography (10% → 30% EA in CH) to obtain the product as yellow oil (43 mg, 0.16 mmol, 31%).

^{1}H NMR (400 MHz, $CDCl_3$): δ = 7.20 (s, 4H), 3.76 (s, 6H), 2.35 (s, 12H) ppm. **GCMS:** 14.7 min (method "hart"), *m/z* = 270.

Analytical data are in agreement with previous results.[3]

2,2'-Difluoro-4,4',5,5'-tetramethoxy-1,1'-biphenyl (2a)

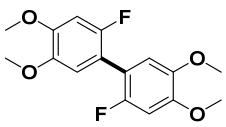

4-Fluoro-1,2-dimethoxy-benzene (156 mg, 1.0 mmol) was treated with 145 C (1.5 F) without stirring. The reaction mixture was purified by silica flash column chromatography (10% → 12% EA in CH) to obtain the product as colorless needles (65 mg, 0.21 mmol, 42%).

^{1}H NMR (400 MHz, $CDCl_3$): δ = 6.85 (m, 2H), 6.73 (m, 2H), 3.90 (s, 6H), 3.88 (s, 6H) ppm. **GCMS:** 14.3 min (method "hart"), *m/z* = 310.

Analytical data are in agreement with previous results.[2]

2,2'-Dibromo-4,4',5,5'-tetramethoxy-1,1'-biphenyl (2b)

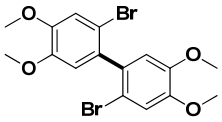

4-Bromo-1,2-dimethoxy-benzene (230 mg, 1.0 mmol) was treated with 145 C (1.5 F) with and without stirring. The reaction mixture was purified by silica flash column chromatography (10% → 30% EA in CH) to obtain the product as colorless needles (with stirring: 114 mg, 0.25 mmol, 50%; without stirring: 168 mg, 0.38 mmol, 76%).

^{1}H NMR (400 MHz, $CDCl_3$): δ = 7.11 (s, 2H), 6.76 (s, 2H), 3.92 (s, 6H), 3.86 (s, 6H) ppm. **GCMS:** 17.3 min (method "hart"), *m/z* = 432.

Analytical data are in agreement with previous results.[2]

4,4',5,5'-Tetramethoxy-2,2'-dimethyl-1,1'-biphenyl (2h)

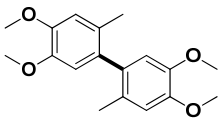

1,2-Dimethoxy-4-methyl-benzene (151 mg, 1.0 mmol) was treated with 145 C (1.5 F) with and without stirring. The reaction mixture was purified by silica flash column chromatography (10% → 30% EA in CH) to obtain the product as colorless needles (with stirring: 79 mg, 0.26 mmol, 52%; without stirring: 111 mg, 0.35 mmol, 69%).

^{1}H NMR (400 MHz, $CDCl_3$): δ = 6.77 (s, 2H), 6.65 (s, 2H), 3.91 (s, 6H), 3.83 (s, 6H), 2.02 (s, 6H) ppm. **GCMS:** 15.1 min (method "hart"), *m/z* = 302.

Analytical data are in agreement with previous results.[2]

2,2',4,4',5,5'-Hexamethoxy-1,1'-biphenyl (2i)

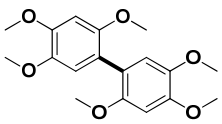

1,2,4-Trimethoxy-benzene (178 mg, 1.0 mmol) was treated with 145 C (1.5 F) with and without stirring. The reaction mixture was purified by silica flash column chromatography (10% → 30% EA in CH) to obtain the product as colorless needles (with stirring: 106 mg, 0.30 mmol, 60%; without stirring: 86 mg, 0.25 mmol, 50%).

^{1}H NMR (400 MHz, $CDCl_3$): δ = 6.82 (s, 2H), 6.63 (s, 2H), 3.93 (s, 6H), 3.84 (s, 6H), 3.76 (s, 6H) ppm. **GCMS:** 16.7 min (method "hart"), *m/z* = 334.

Analytical data are in agreement with previous results.[2]

Diethyl 2,2'-((4,4'-dimethoxy-6,6'-dimethyl-[1,1'-biphenyl]-3,3'-diyl)bis(oxy))diacetate (2j)

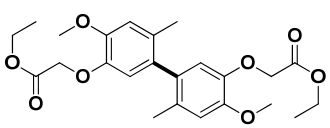

Ethyl 2-(2-methoxy-4-methylphenoxy)acetate (224 mg, 1.0 mmol) was treated with 145 C (1.5 F) without stirring. The reaction mixture was purified by silica flash column chromatography (10% → 20% EA in CH) to obtain the product as colorless needles (125 mg, 0.28 mmol, 56%).

^{1}H NMR (400 MHz, $CDCl_3$): δ = 6.77 (s, 2H), 6.56 (s, 2H), 4.63 (d, 4H), 4.22 (q, ^3J = 8.0 Hz, 4H), 3.90 (s, 6H), 1.98 (s, 6H), 1.25 (t,^3J = 8.0 Hz, 6H) ppm. **^{13}C NMR** (101 MHz, $CDCl_3$): δ = 169.1, 148.4, 144.7, 132.9, 130.1, 115.9, 113.6, 66.7, 61.2, 56.0, 19.4, 14.2 ppm. **HR-MS** (ESI): *m/z* calculated for $C_{24}H_{30}O_8Na$ [M+Na]$^+$: 469.1838, found: 469.1841. **GC:** 17.74 min (method "hart"). **GCMS:** 20.7 min (method "hart"), *m/z* = 446. **Mp:** 62–64 °C. **R_f:** 0.33 (CH:EA, 7:3).

5,5'-Dibromo-2,2',4,4'-tetramethoxy-1,1'-biphenyl (2ka) and 1,5-Dibromo-2,4-dimethoxy-benzene (2kb)

1-Bromo-2,4-dimethoxy-benzene (228 mg, 1.0 mmol) was treated with 145 C (1.5 F) without stirring. The reaction mixture was purified by silica flash column chromatography (10% → 30% EA in CH) to obtain the coupling product as colorless needles (24 mg, 0.06 mmol, 11%).

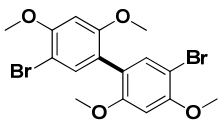

^{1}H NMR (400 MHz, $CDCl_3$): δ = 7.35 (s, 2H), 6.55 (s, 2H), 3.94(s, 6H), 3.79 (s, 6H) ppm. **GC:** 17.38 min (method "hart"). **GCMS:** 18.4 min (method "hart"), *m/z* = 432; and the bromination product as colorless needles (70 mg, 0.16 mmol, 31%). **^{1}H NMR** (400 MHz, $CDCl_3$): δ = 3.90 (s, 6H), 6.49 (s, 1H), 7.66 (s, 1H) ppm. **GCMS:** 11.7 min (method "hart"), *m/z* = 296.

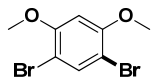

Analytical data are in agreement with previous results.[4]

2-(2-(Cyanomethyl)-4,5-dimethoxyphenyl)-2-(3,4-dimethoxyphenyl)acetonitrile (2l)

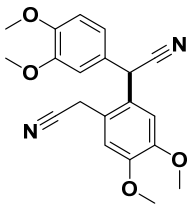

3,4-Dimethoxyphenyl acetonitrile (887 mg, 5.0 mmol) in 25 mL HFIP was treated with 725 C (1.5 F) without stirring. The reaction mixture was purified by silica flash column chromatography (10% → 30% EA in CH) to obtain the product as colorless needles (456 mg, 1.3 mmol, 51%).

^{1}H NMR (400 MHz, $CDCl_3$): δ = 6.96 (s, 1H), 6.94 (s, 1H), 6.82 (d, ^3J = 8.0 Hz. 1H), 6.76 (dd, ^3J = 8.0 Hz, ^4J = 4.0 Hz, 1H), 6.73 (d, ^4J = 4.0 Hz, 1H), 5.20 (s, 1H), 3.92 (s, 3H), 3.88 (s, 3H), 3.86 (s, 3H), 3.82 (s, 3H), 3.55 (q, ^2J = 16.0 Hz, 2H) ppm. **^{13}C NMR** (101 MHz, $CDCl_3$): δ = 149.8, 149.5, 149.4, 149.3, 126.2, 125.3, 120.4, 119.9, 119.1, 117.3, 112.9, 112.7, 111.6, 110.5, 56.3, 56.3, 56.1, 56.1, 39.2, 21.1 ppm. **HR-MS** (ESI): *m/z* calculated for $C_{20}H_{20}N_2O_4Na$ [M+Na]$^+$: 375.1321, found: 375.1321. **GC:** 16.63 min (method "hart"). **GCMS:** 19.0 min (method "hart"), *m/z* = 352. **Mp:** 145–146 °C. **R_f:** 0.15 (CH:EA, 7:3).

2-([1,1'-Biphenyl]-4-yl)-2-(3,4-dimethoxyphenyl)acetonitrile (4a)

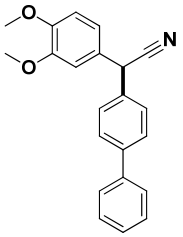

3,4-Dimethoxyphenyl acetonitrile (177 mg, 1.0 mmol) and biphenyl (308 mg, 2.0 mmol, 2.0 eq.) in 5 mL HFIP was treated with 288 C (3.0 F) with stirring. The reaction mixture was purified by silica flash column chromatography (17% → 25% EA in CH) to obtain the product as orange solid (109 mg, 0.33 mmol, 33%).

^{1}H NMR (400 MHz, CD_3CN): δ = 7.68 – 7.59 (m, 4H), 7.51 – 7.42 (m, 4H), 7.39 – 7.34 (m, 1H), 6.99 – 6.91 (m, 3H), 5.35 (s, 1H), 3.78 (s, 6H) ppm. **^{13}C NMR** (101 MHz, CD_3CN): δ = 150.6, 150.1, 141.6, 140.9, 137.2, 129.9, 129.9, 128.9, 128.7, 128.6, 127.9, 121.1, 120.8, 113.0, 112.1, 56.5, 56.4, 42.0 ppm. **HR-MS** (APCI): *m/z* calculated for $C_{22}H_{19}NO_2$ [M]$^+$: 329.1416, found: 329.1402. **GC:** 18.17 min (method "hart"). **GCMS:** 20.00 min (method "hart"), *m/z* = 329. **R_f:** 0.17 (CH:EA, 5:1).

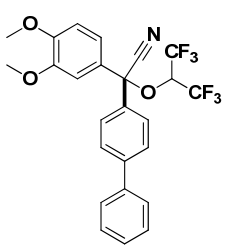

As byproduct a colorless oil was obtained (61 mg, 0,12 mmol, 12%).
^{1}H NMR (400 MHz, CD_3CN): δ = 7.75 (d, ^3J = 8.7 Hz, 2H), 7.69 – 7.65 (m, 2H), 7.59 (d, ^3J = 8.7 Hz, 2H), 7.50 – 7.44 (m, 2H), 7.43 – 7.37 (m, 1H), 7.18 (dd, $^{3,4}J$ = 8.5, 2.3 Hz, 1H), 7.02 (d, ^3J = 8.5 Hz, 1H), 6.94 (d, ^4J = 2.3 Hz, 1H), 5.00 (hept, $^3J_{HF}$ = 5.8 Hz, 1H), 3.84 (s, 3H), 3.73 (s, 3H) ppm. **^{13}C NMR** (101 MHz, CD_3CN): δ = 152.1, 150.5, 143.5, 140.4, 137.4, 130.0, 129.1, 128.5, 128.4, 128.0, 122.1, 118.2, 112.3, 111.8, 84.4, 72.3 (q, J = 32.9 Hz), 56.5, 56.4 ppm.[2] **^{19}F NMR** (376 MHz, CD_3CN): δ = -73.6 (qd, J = 9.8, 6.0 Hz), -73.9 (qd, J = 9.7, 5.6 Hz) ppm. **HR-MS** (APCI): *m/z* calculated for $C_{25}H_{19}F_6NO_3$ $[M]^+$: 495.1269, found: 495.1248. **GC:** 16.17 min (method "hart"). **GCMS:** 17.66 min (method "hart"), *m/z* = 495. **R_f:** 0.40 (CH:EA, 5:1).

2-(5-(tert-Butyl)-2-methoxyphenyl)-2-(3,4-dimethoxyphenyl)acetonitrile (4b)

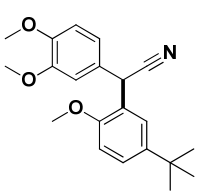

3,4-Dimethoxyphenyl acetonitrile (88.6 mg, 0.5 mmol) and 4-*tert*-butyl anisole (176 mg, 1.3 mmol, 2.6 eq.) in 5 mL HFIP was treated with 144.7 C (3.0 F) with stirring. The reaction mixture was purified by silica flash column chromatography (17% EA in CH) and by reversed phase column chromatography (50% → 0% H_2O in MeCN) to obtain the product as orange oil (29 mg, 0.09 mmol, 17%).
^{1}H NMR (400 MHz, $CDCl_3$): δ = 7.35 (d, ^4J = 2.5 Hz, 1H), 7.31 (dd, $^{3,4}J$ = 8.6, 2.5 Hz, 1H), 6.93 – 6.88 (m, 2H), 6.83 (d, ^3J = 8.6 Hz, 1H), 6.82 (d, ^3J = 8.2 Hz, 1H), 5.48 (s, 1H), 3.86 (s, 3H), 3.85 (s, 3H), 3.83 (s, 3H), 1.27 (s, 9H) ppm. **^{13}C NMR** (101 MHz, $CDCl_3$): δ = 154.0, 149.2, 148.7, 144.0, 128.3, 126.3, 125.9, 124.0, 120.4, 120.1, 111.3, 111.0, 110.7, 56.0, 56.0, 55.8, 36.2, 34.3, 31.6 ppm. **HR-MS** (ESI): *m/z* calculated for $C_{21}H_{26}NO_3$ $[M+H]^+$: 340.1907, found: 340.1906. **GC:** 15.50 min (method "hart"). **GCMS:** 16.94 min (method "hart"), *m/z* = 339. **R_f:** 0.25 (CH/EA, 5:1).

2-(3-(Tert-butyl)-4-methoxy-5-methylphenyl)-2-(3,4-dimethoxyphenyl)acetonitrile (4c)

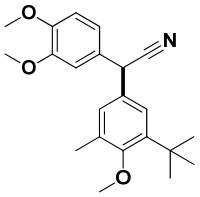

3,4-Dimethoxyphenyl acetonitrile (177 mg, 1.0 mmol) and 2-tert butyl-5-methyl anisole (357 mg, 2.0 mmol, 2.0 eq.) in 5 mL HFIP was treated with 288 C (3.0 F) with stirring. The reaction mixture was purified by silica flash column chromatography (16% → 25% EA in CH) and by high pressure liquid chromatography (60% → 0% H_2O in MeCN in 90 min) to obtain the product as colorless oil (43 mg, 0.12 mmol, 12%).
^{1}H NMR (400 MHz, CD_3CN): δ = 7.20 (d, ^4J = 2.5 Hz, 1H), 7.09 (dt, $^{4,5}J$ = 2.4, 0.7 Hz, 1H), 6.93 (s, 3H), 5.20 (s, 1H), 3.78 (s, 6H), 3.73 (s, 3H), 2.28 (d, ^5J = 0.7 Hz, 3H), 1.35 (s, 9H) ppm. **^{13}C NMR** (101 MHz, CD_3CN): δ = 159.1, 150.5, 150.0, 144.1, 133.4, 132.4, 130.3, 129.7, 125.1, 121.4, 120.6, 113.0, 112.1, 61.3, 56.5, 56.4, 42.0, 35.8, 31.1, 17.5 ppm. **HR-MS** (ESI): *m/z* calculated for $C_{22}H_{27}NO_3Na$ $[M+Na]^+$: 376.1883, found: 376.1886. **GC:** 16.00 min (method "hart"). **GCMS:** 17.48 min (method "hart"), *m/z* = 353. **R_f:** 0.30 (CH:EA, 5:1).

2-(3-Bromo-4-methoxyphenyl)-2-(3,4-dimethoxyphenyl)acetonitrile (4d)

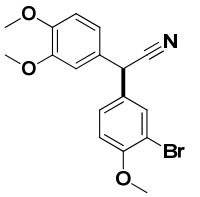

3,4-Dimethoxyphenyl acetonitrile (177 mg, 1.0 mmol) and 2-bromo anisole (374 mg, 2.0 mmol, 2.0 eq.) in 5 mL HFIP was treated with 288 C (3.0 F) with stirring. The reaction mixture was purified by silica flash column chromatography (16% → 25% EA in CH) and by reversed phase column chromatography (50% → 0% H_2O in MeCN) to obtain the product as yellow oil (117 mg, 0.32 mmol, 32%). Recrystallization from MeOH yielded colorless dices.
^{1}H NMR (400 MHz, CD_3CN): δ = 7.54 (dd, $^{4,5}J$ = 2.3, 0.6 Hz, 1H), 7.36 (ddd, $^{3,4,5}J$ = 8.6, 2.4, 0.6 Hz, 1H), 7.03 (d, ^3J = 8.6 Hz, 1H), 6.96-6.88 (m, 3H), 5.24 (s, 1H), 3.86 (s, 3H), 3.79 (s, 3H), 3.77 (s, 3H) ppm. **^{13}C NMR** (101 MHz, CD_3CN): δ = 156.6, 150.6, 150.1, 133.0, 131.4, 129.6, 128.9, 120.9, 120.7, 113.7, 112.9, 112.3, 112.1, 57.0, 56.5, 56.4, 41.1 ppm. **HR-MS** (APCI): *m/z* calculated for $C_{17}H_{16}{}^{79}BrNO_3$ $[M]^+$: 361.0314, found: 361.0294, and calculated for $C_{17}H_{16}{}^{81}BrNO_3$ $[M]^+$:

[2] Two signals are missing: the *C*-1 carbon of the dimethoxyphenyl and the residue signal of CF_3 could not been resolved.

363.0293, found: 363.0275. **GC:** 16.38 min (method “hart”). **GCMS:** 17.91 min (method “hart”), *m/z* = 361 (100), 363 (98). **Mp:** 68 °C. **R_f:** 0.22 (CH:EA, 4:1).

Author Contributions

SBB: lab work, data acquisition, writing draft; **LS**: lab work; **MB**: lab work; **AS**: lab work; **TM**: lab work; **NB**: lab work; **DS**: x-ray single crystal analysis; **AB**: laser surface structuring; **MH**: ICP-OES analysis; **UK**: supervision ICP-OES; **WS**: supervision laser surface structuring; **SRW**: project administration, writing draft.

References

[1] C. Gütz, B. Klöckner, S. R. Waldvogel, *Org. Process Res. Dev.* **2016**, *20*, 26–32.

[2] Beil, S. B., Müller, T., Sillart, S. B., Franzmann, P., Bomm, A., Holtkamp, M., Karst, U., Schade, W., Waldvogel, S. R., *Angew. Chem. Int. Ed.* **2018**, *57*, 2450–2454.

[3] Rathore, R., Bosch, E., Kochi, J. K., *Tetrahedron* **1994**, *50*, 6727–6758.

[4] a) Goto, H., Furusho, Y., Miwa, K., Yashima, E., *J. Am. Chem. Soc.* **2009**, *131*, 4710–4719; b) Shi, C., Miao, Q.; Ma, L., Lu, T., Yang, D., Chen, J., Li, Z., *ChemistrySelect* **2019**, *4*, 6043–6047.

Appendix: NMR spectra

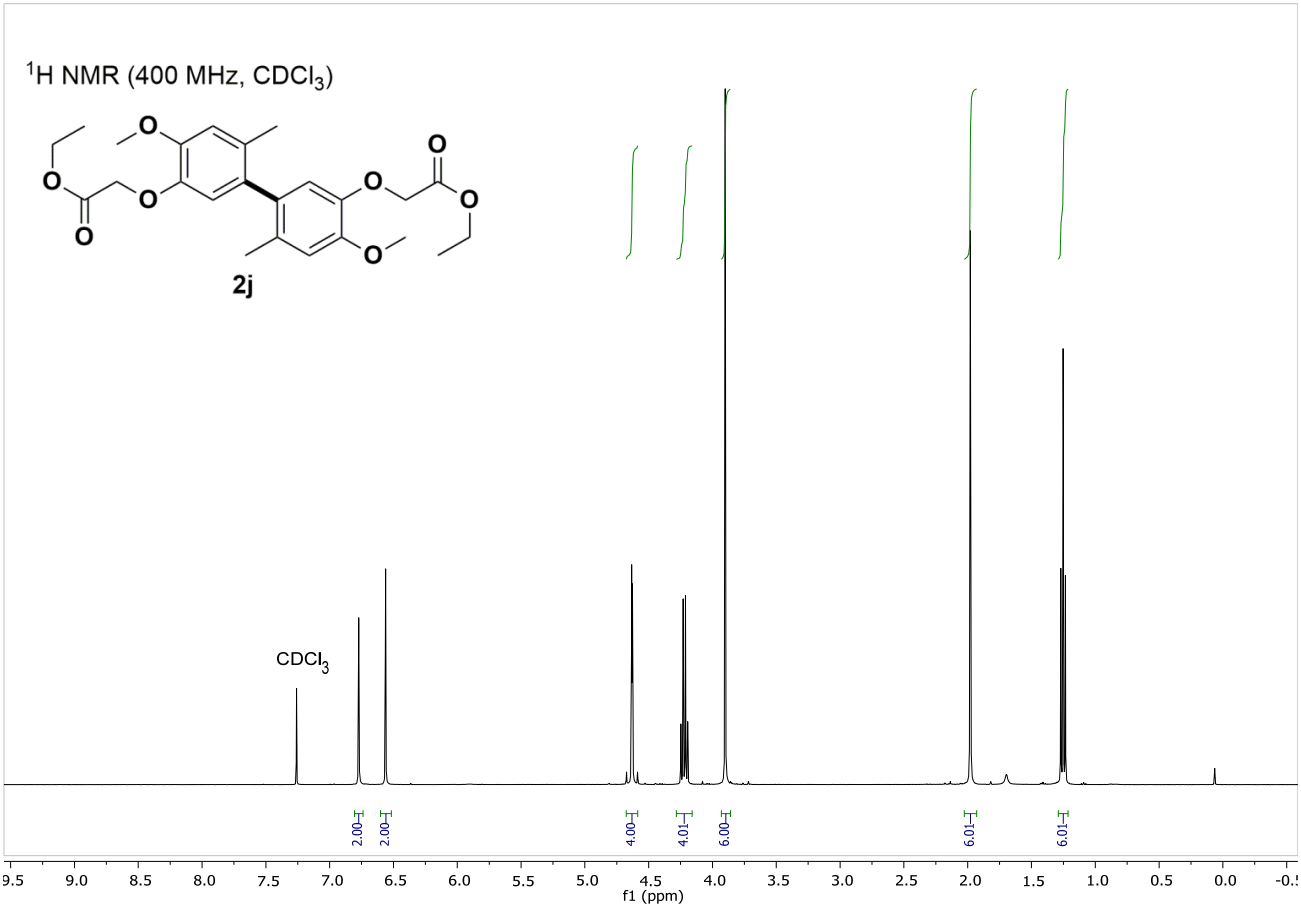

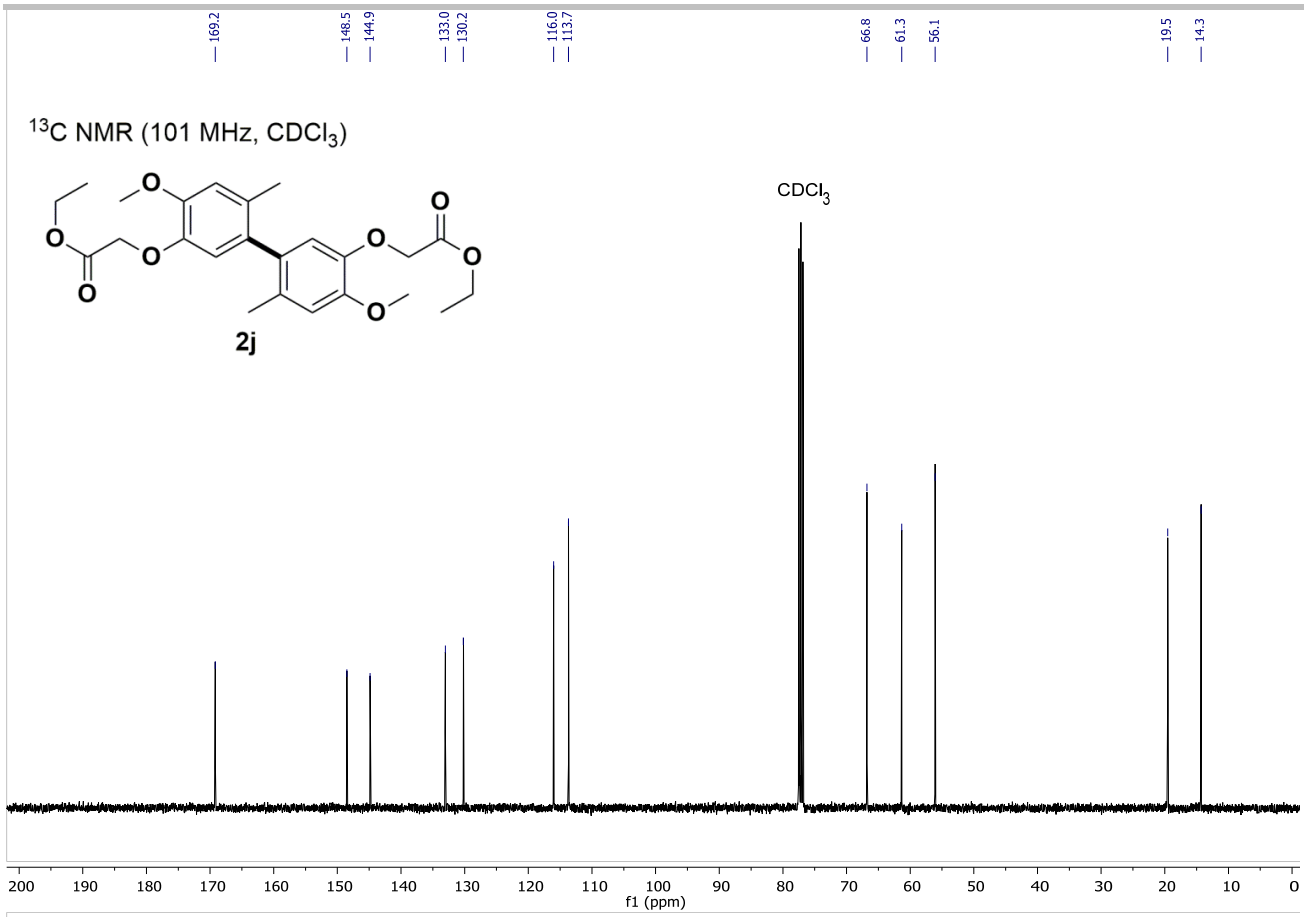
169.2
148.5
144.9
133.0
130.2
116.0
113.7
66.8
61.3
56.1
19.5
14.3
13C NMR (101 MHz, CDCl3)
CDCl3
2j
f1 (ppm)

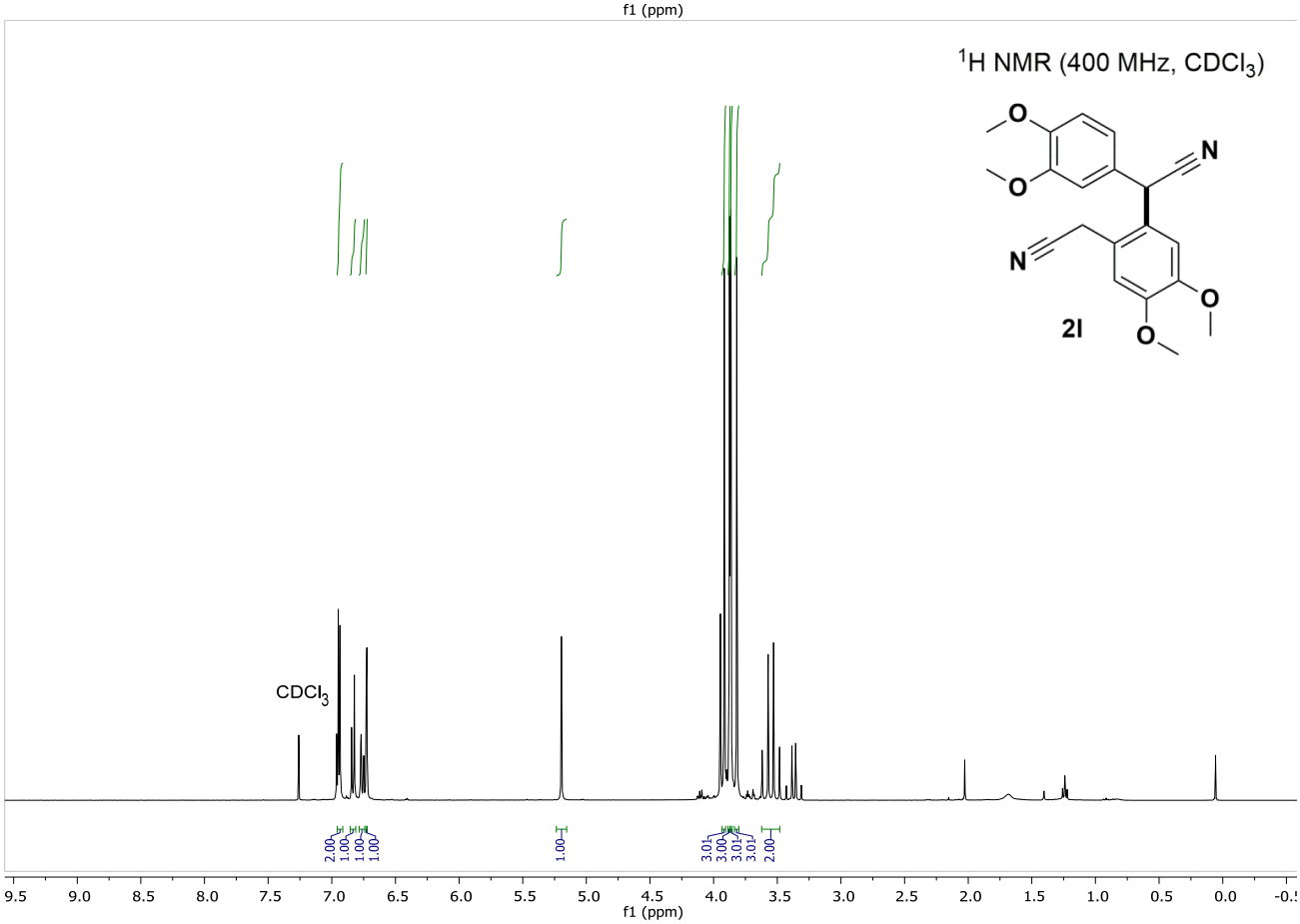
1H NMR (400 MHz, CDCl3)
CDCl3
2l
2.00
1.00
1.00
1.00
1.00
3.01
3.00
3.01
3.01
2.00
f1 (ppm)

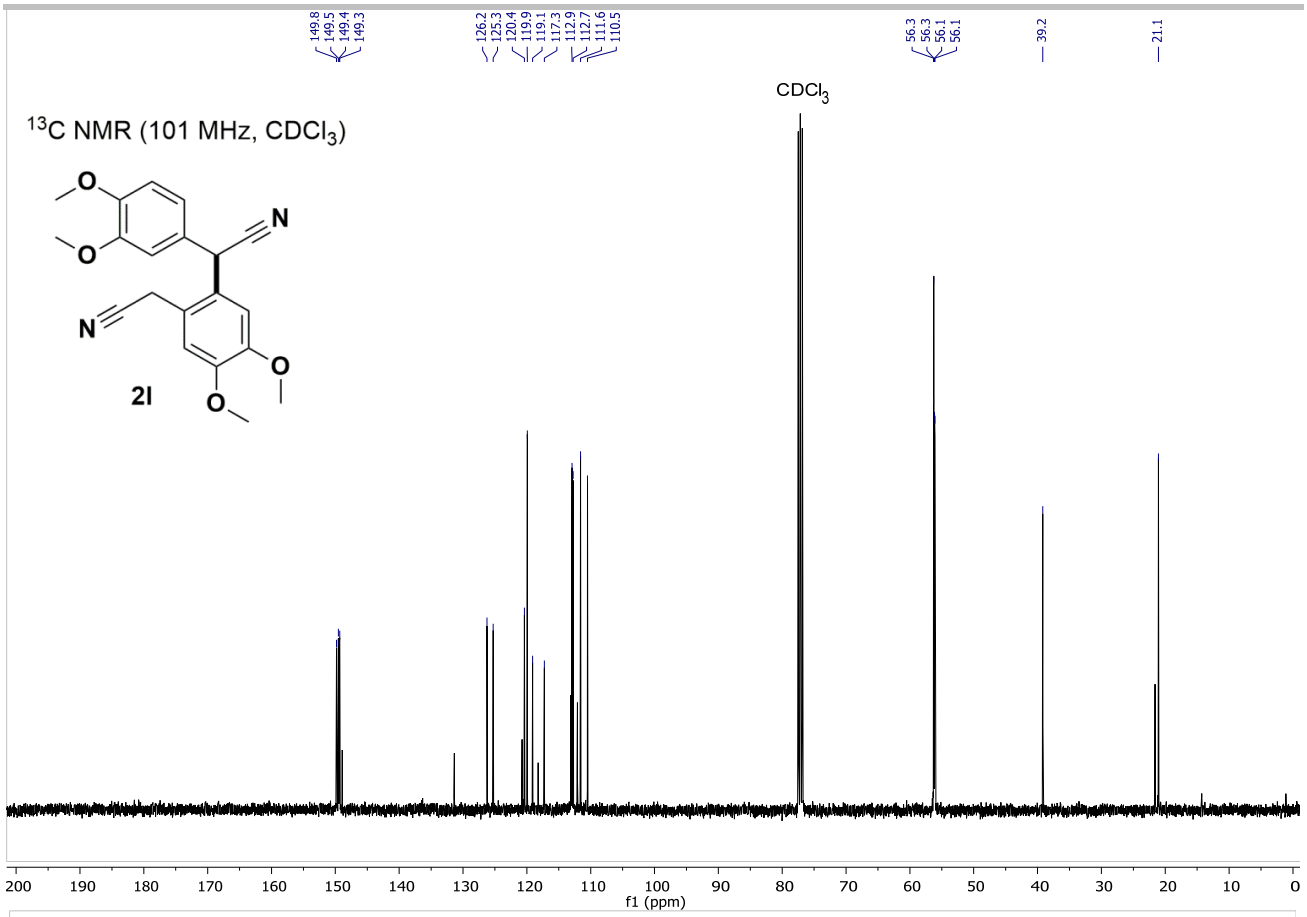
149.8
149.5
149.4
149.3
126.2
125.3
120.4
119.9
119.1
117.3
112.9
112.7
111.6
110.5
56.3
56.3
56.1
56.1
39.2
21.1
CDCl3
13C NMR (101 MHz, CDCl3)
O
O
N
N
O
O
2l
200 190 180 170 160 150 140 130 120 110 100 90 80 70 60 50 40 30 20 10 0
f1 (ppm)

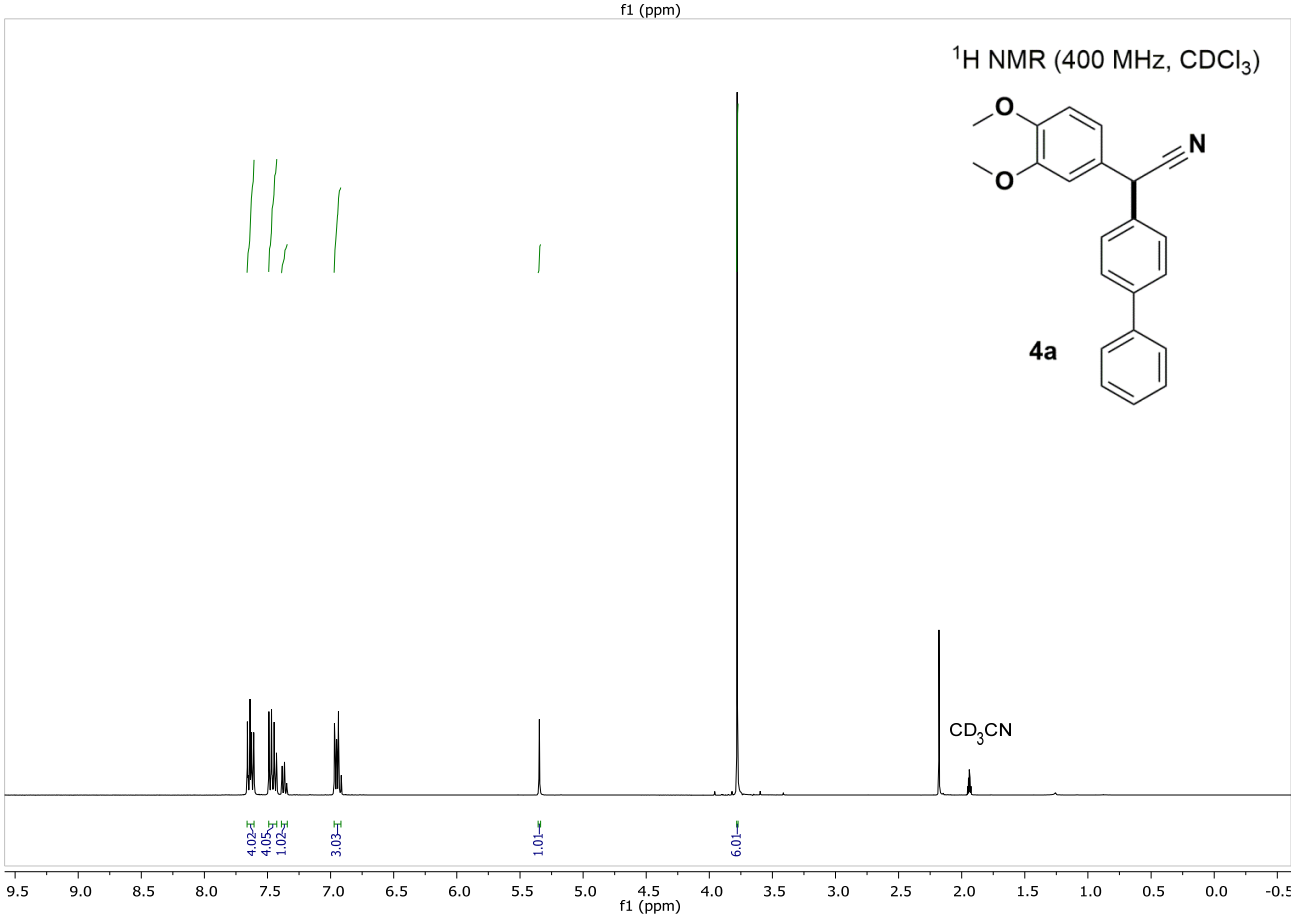
1H NMR (400 MHz, CDCl3)
O
O
N
4a
CD3CN
4.02
4.05
1.02
3.03
1.01
6.01
9.5 9.0 8.5 8.0 7.5 7.0 6.5 6.0 5.5 5.0 4.5 4.0 3.5 3.0 2.5 2.0 1.5 1.0 0.5 0.0 -0.5
f1 (ppm)

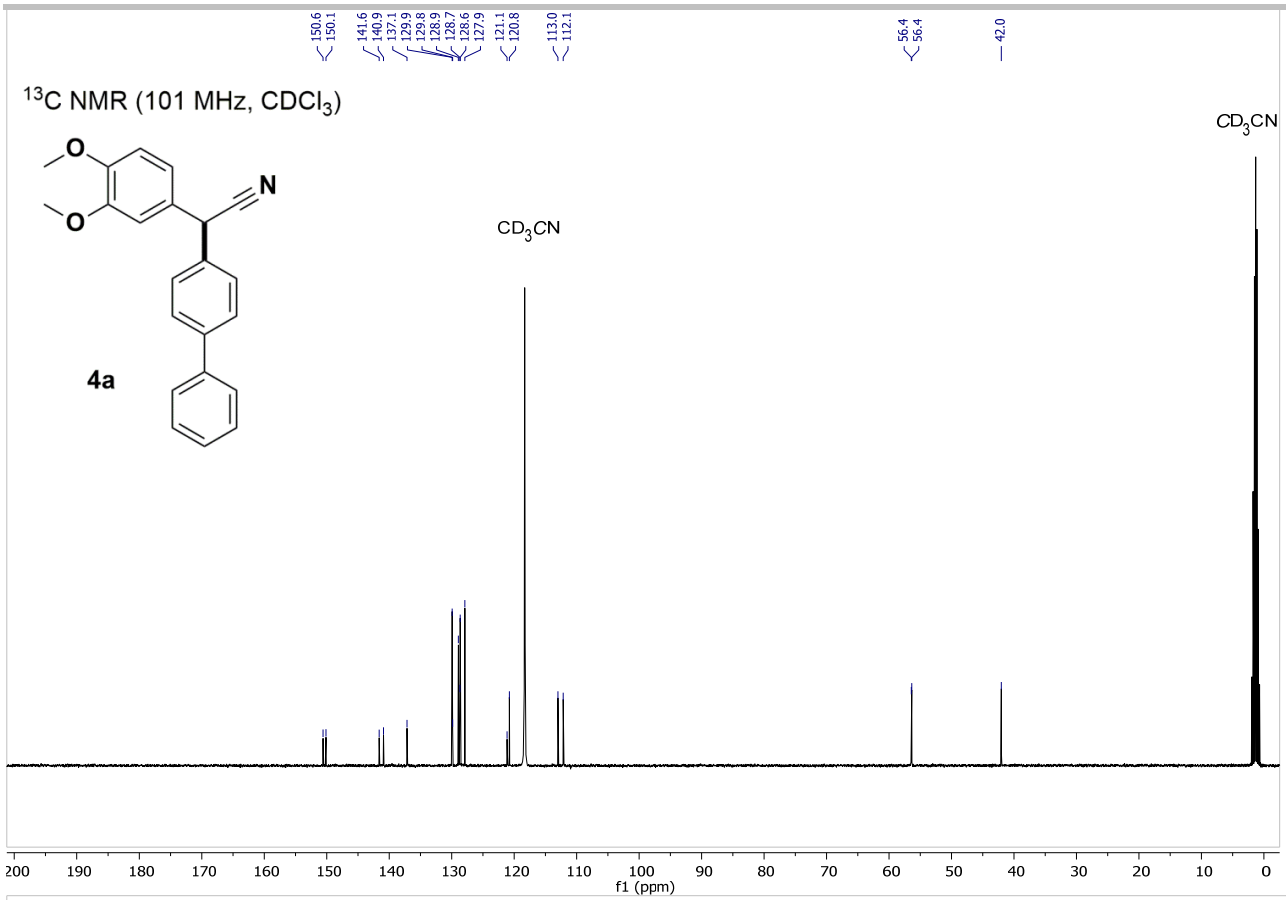
150.6
150.1
141.6
140.9
137.1
129.9
129.8
128.9
128.7
128.6
127.9
121.1
120.8
113.0
112.1
56.4
56.4
42.0
13C NMR (101 MHz, CDCl3)
CD3CN
CD3CN
O
O
N
4a
f1 (ppm)

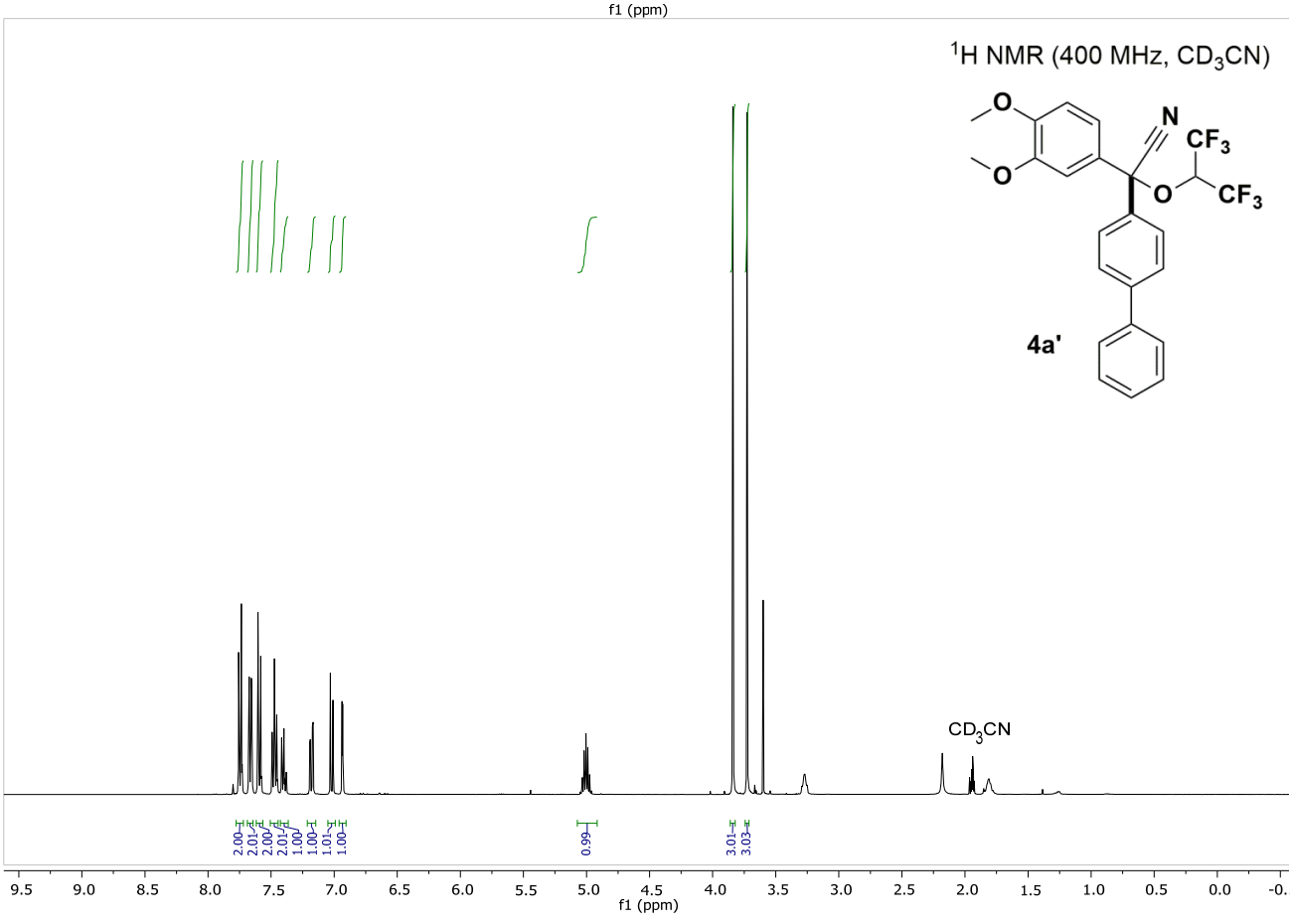
1H NMR (400 MHz, CD3CN)
O
O
N
CF3
CF3
O
4a'
CD3CN
2.00
2.01
2.00
2.01
1.00
1.00
1.01
1.00
0.99
3.01
3.03
f1 (ppm)

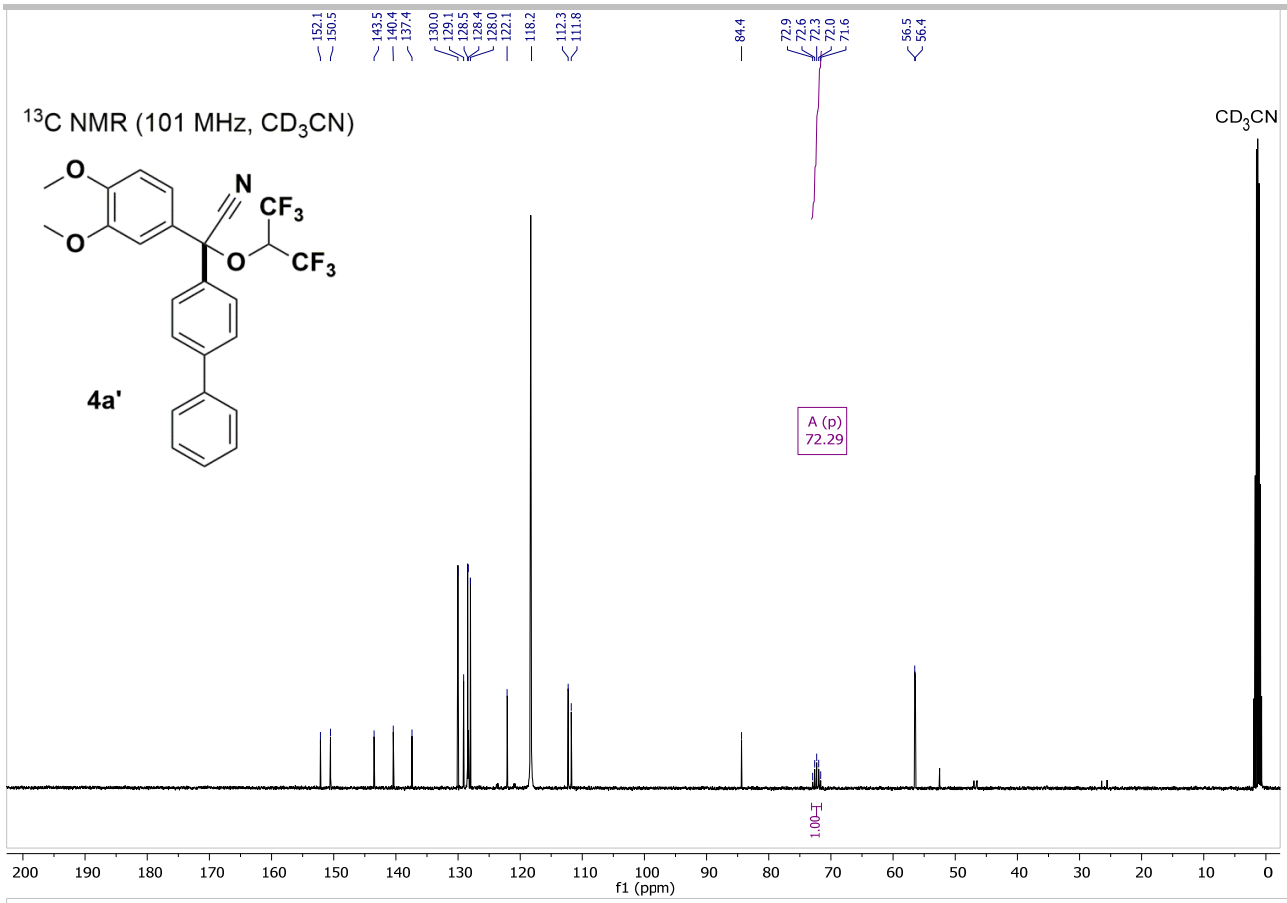
152.1
150.5
143.5
140.4
137.4
130.0
129.1
128.5
128.4
128.0
122.1
118.2
112.3
111.8
84.4
72.9
72.6
72.3
72.0
71.6
56.5
56.4
13C NMR (101 MHz, CD3CN)
CD3CN
4a'
A (p)
72.29
1.00
f1 (ppm)

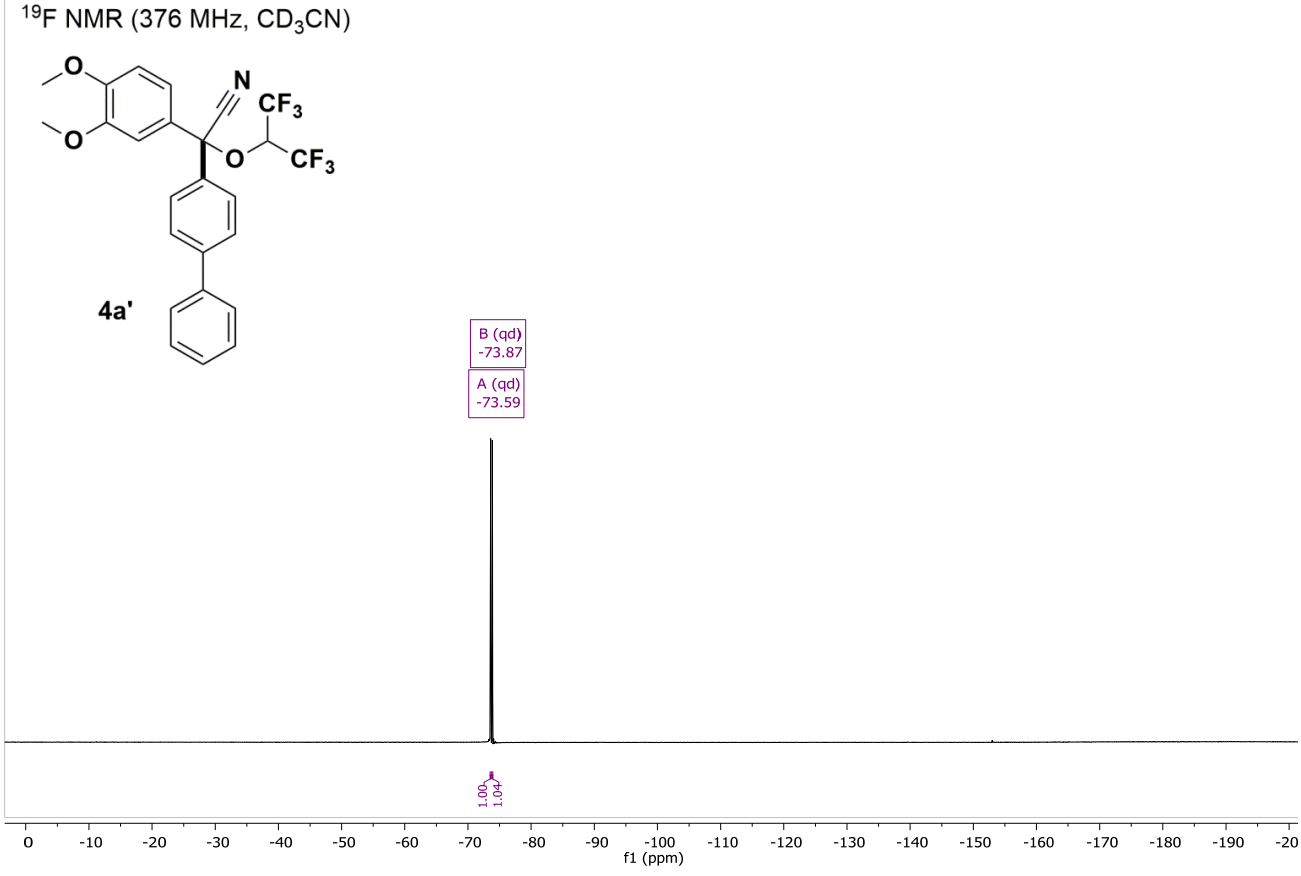
19F NMR (376 MHz, CD3CN)
4a'
B (qd)
-73.87
A (qd)
-73.59
1.00
1.04
f1 (ppm)

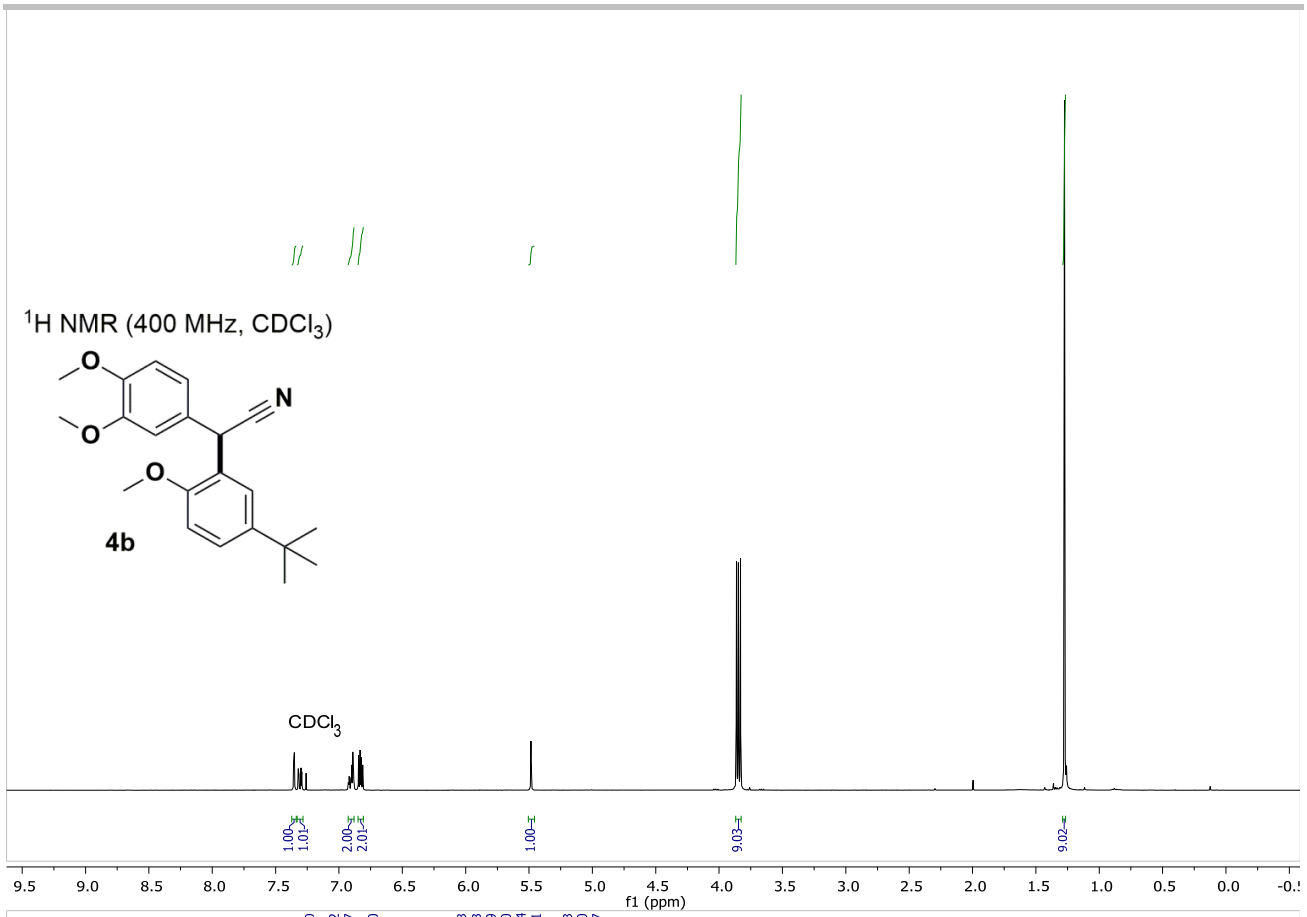
^{1}H NMR (400 MHz, $CDCl_3$)
4b
$CDCl_3$
1.00
1.01
2.00
2.01
1.00
9.03
9.02
f1 (ppm)

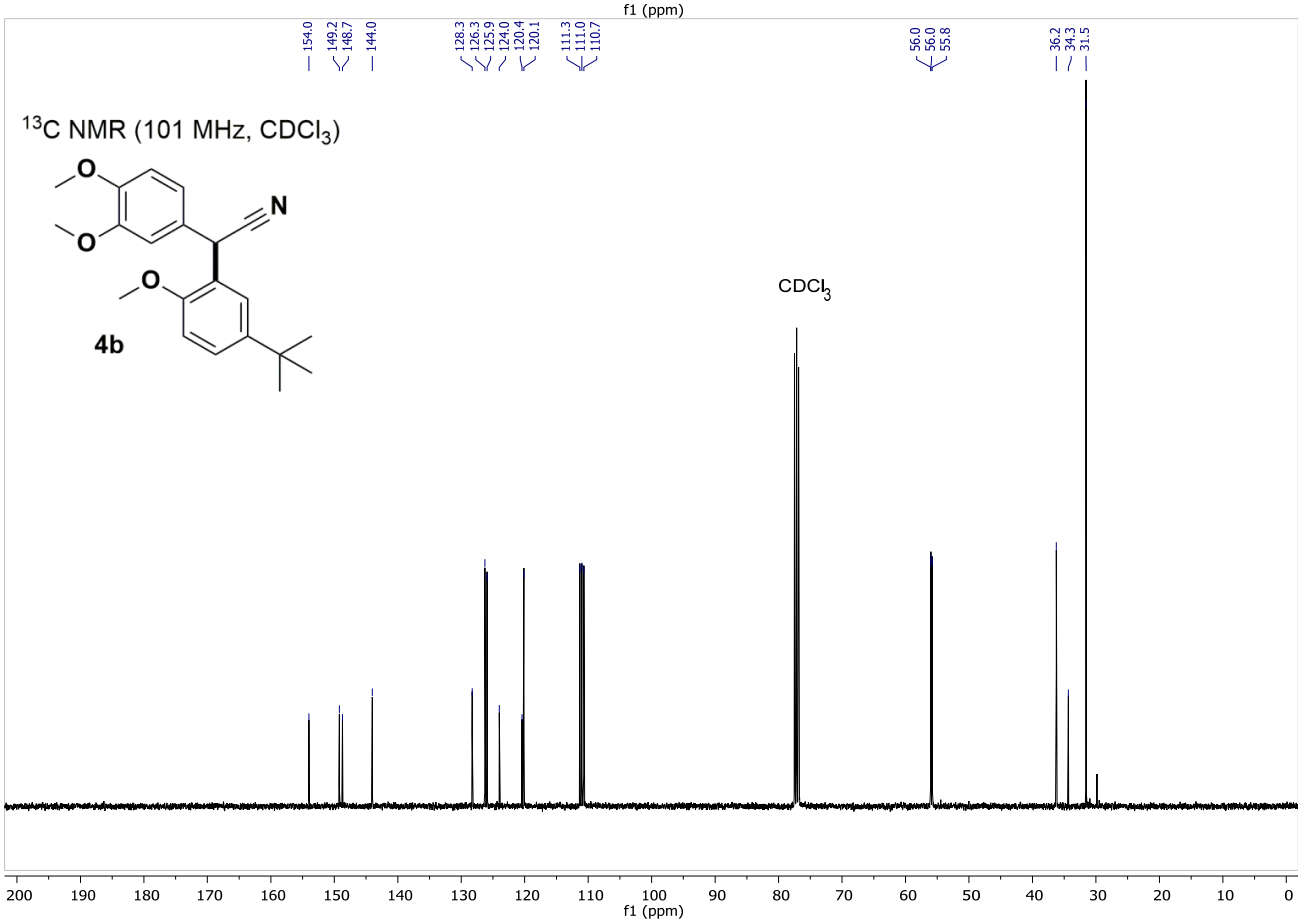
^{13}C NMR (101 MHz, $CDCl_3$)
4b
$CDCl_3$
154.0
149.2
148.7
144.0
128.3
126.3
125.9
124.0
120.4
120.1
111.3
111.0
110.7
56.0
56.0
55.8
36.2
34.3
31.5
f1 (ppm)

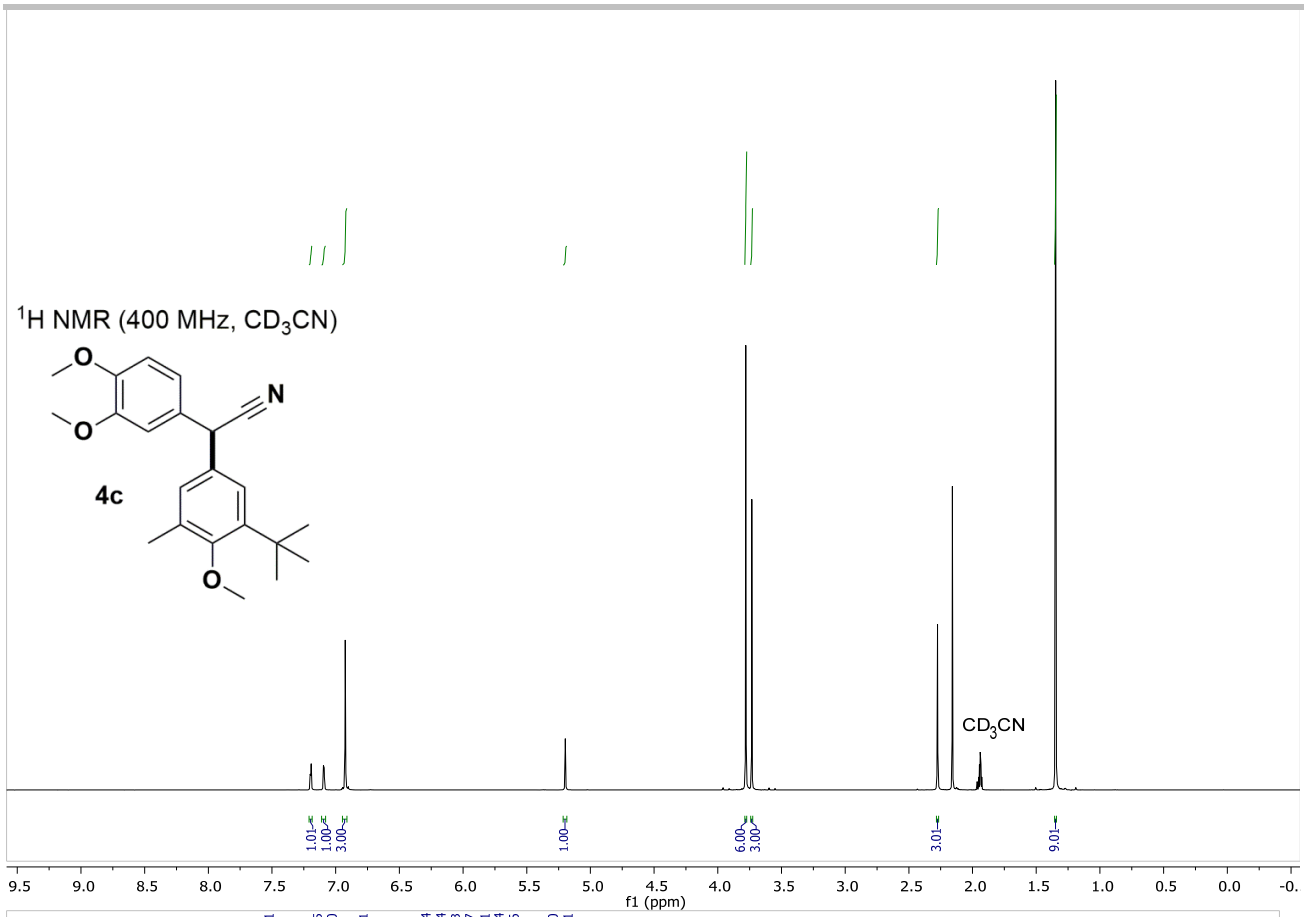
^{1}H NMR (400 MHz, CD_3CN)
4c
CD_3CN
f1 (ppm)

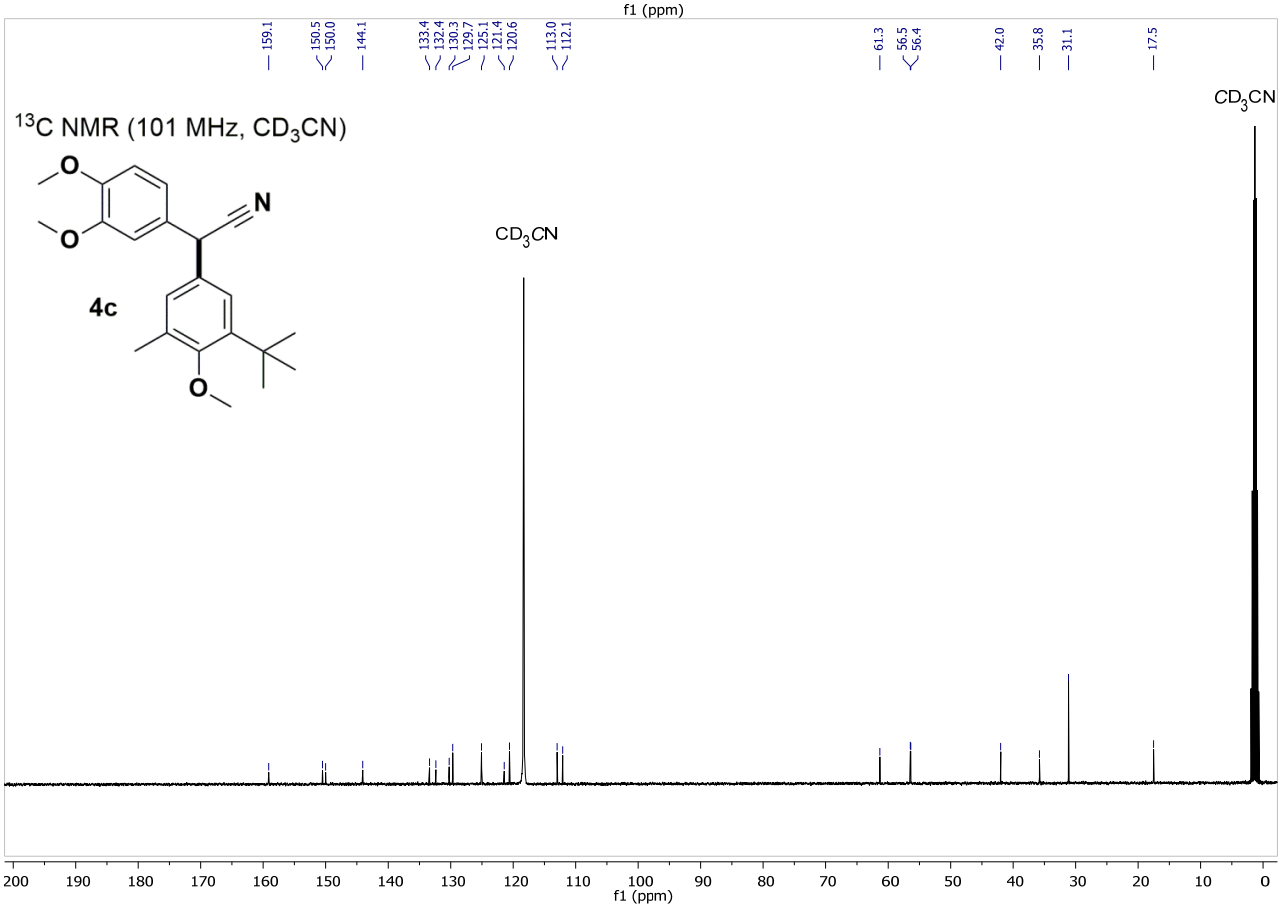
^{13}C NMR (101 MHz, CD_3CN)
4c
CD_3CN
CD_3CN
f1 (ppm)

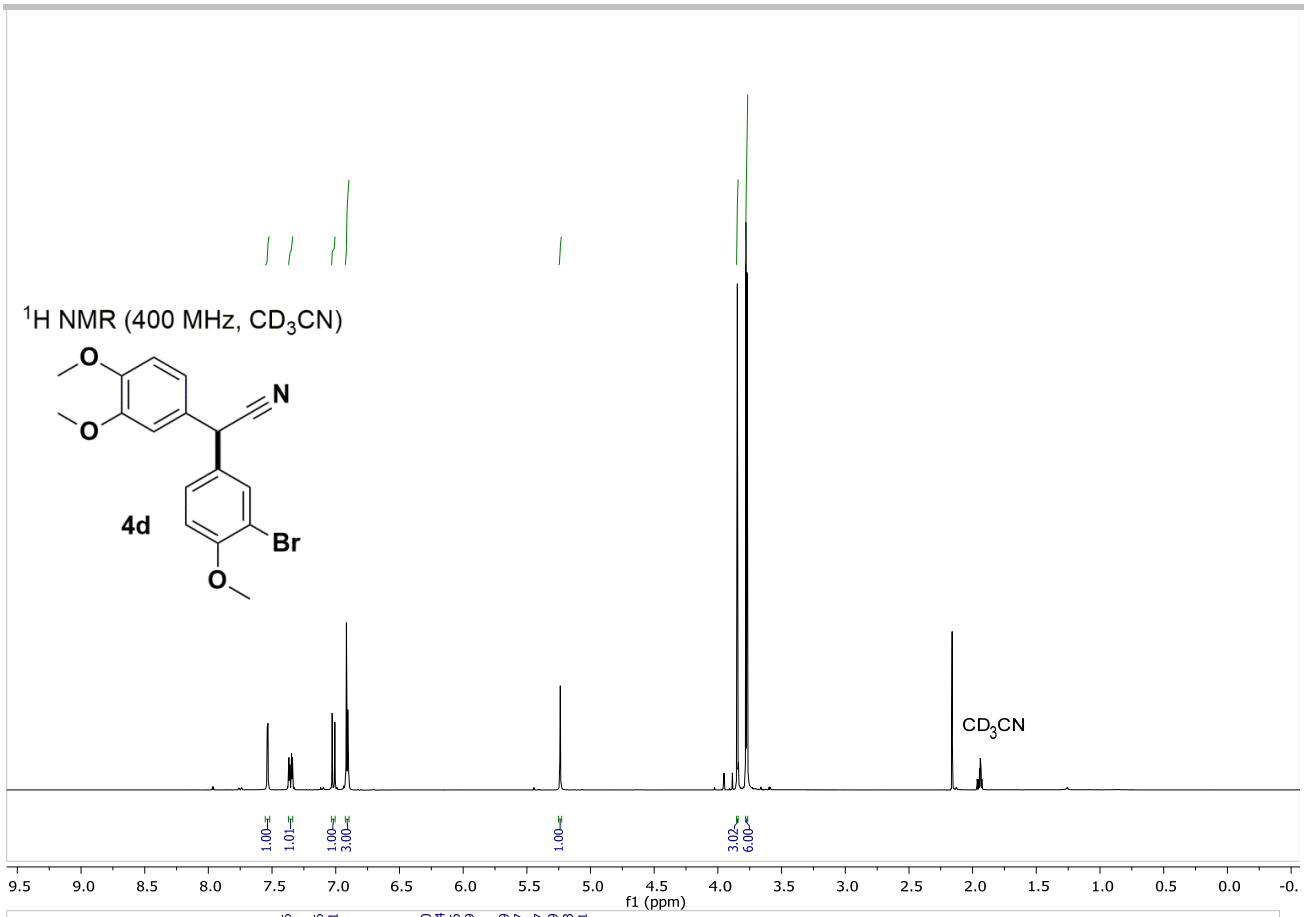
^{1}H NMR (400 MHz, CD_3CN)
4d
Br
N
O
O
O
CD_3CN
1.00
1.01
1.00
3.00
1.00
3.02
6.00
f1 (ppm)

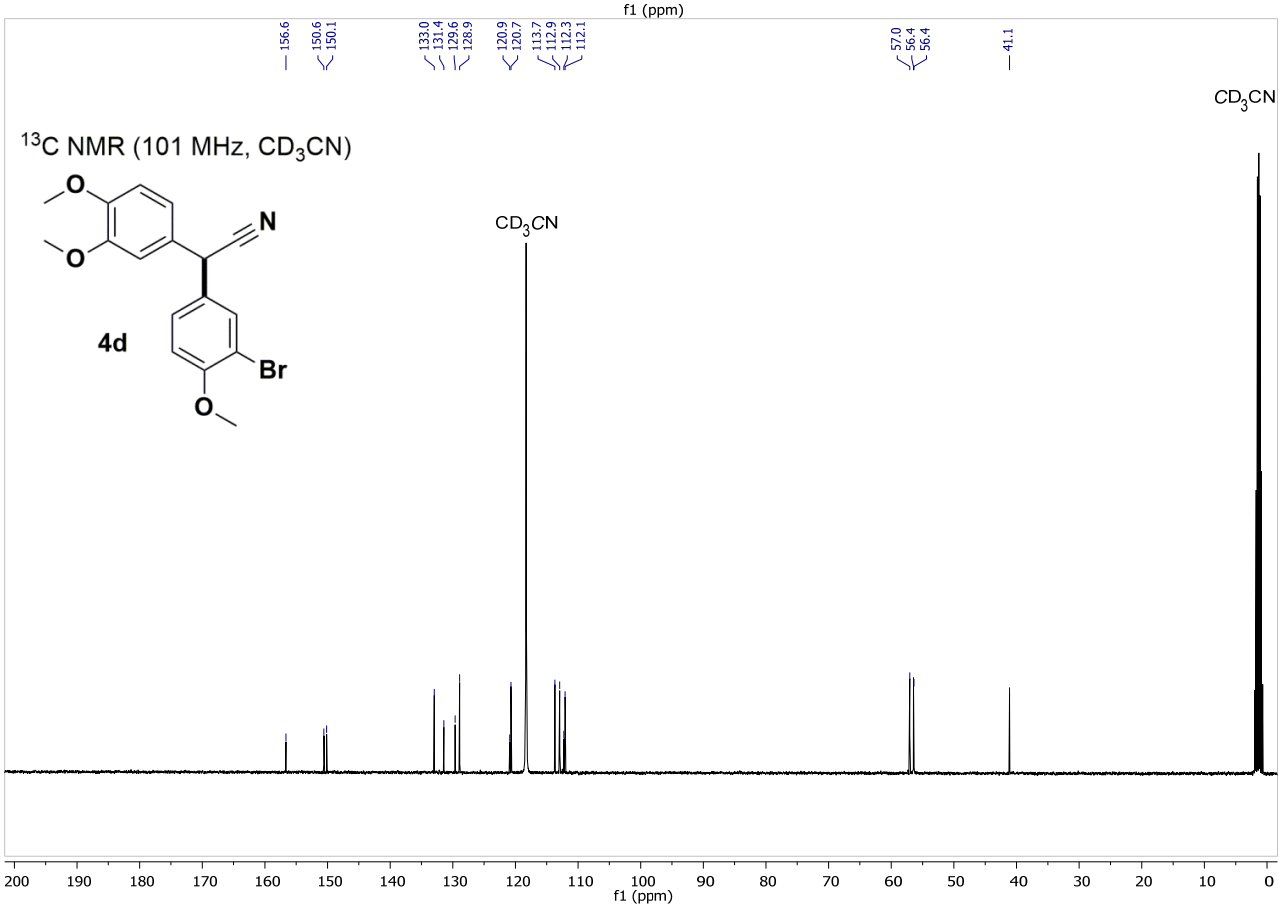
^{13}C NMR (101 MHz, CD_3CN)
4d
Br
N
O
O
O
CD_3CN
CD_3CN
156.6
150.6
150.1
133.0
131.4
129.6
128.9
120.9
120.7
113.7
112.9
112.3
112.1
57.0
56.4
56.4
41.1
f1 (ppm)